NASA Contractor Report 4443

Effects of Cockpit Lateral Stick Characteristics on Handling Qualities and Pilot Dynamics

David G. Mitchell, Bimal L. Aponso,
and David H. Klyde

NASA

NASA Contractor Report 4443

Effects of Cockpit Lateral Stick Characteristics on Handling Qualities and Pilot Dynamics

David G. Mitchell, Bimal L. Aponso,
and David H. Klyde
Systems Technology, Inc.
Hawthorne, California

NASA

National Aeronautics and
Space Administration

Office of Management

Scientific and Technical
Information Program

1992

CONTENTS

ABSTRACT

This report presents the results of analysis of cockpit lateral control feel-system studies. Variations in feel-system natural frequency, damping, and command sensing reference (force and position) were investigated, in combination with variations in the aircraft response characteristics. The primary data for the report were obtained from a flight investigation conducted with a variable-stability airplane, with additional information taken from other flight experiments and ground-based simulations for both airplanes and helicopters. The study consisted of analysis of handling qualities ratings and extraction of open-loop, pilot–vehicle describing functions from sum-of-sines tracking data, including, for a limited subset of these data, the development of pilot models. The study confirms the findings of other investigators that the effects on pilot opinion of cockpit feel-system dynamics are not equivalent to a comparable level of added time delay. The effects on handling qualities ratings are, however, very similar to those of time delay, and until a more comprehensive set of criteria are developed, it is recommended that feel-system dynamics be considered a delay-inducing element in the aircraft response. The best correlation with time-delay requirements was found when the feel-system dynamics were included in the delay measurement, regardless of the command reference. This is a radical departure from past approaches.

NOMENCLATURE

Acronyms

HQR	handling qualities rating
HUD	head-up display
LATHOS	lateral high-order systems
PIO	pilot-induced oscillation
rms	root mean square, deg
SOS	sum of sines
STI	Systems Technology, Inc., Hawthorne, California

Symbols

A_i	forcing function input amplitude, deg
b	stick damping, lb-sec/in.
F_s	stick force, lb
I	stick inertia, slug-ft^2
k	spring gradient, lb/in.
T_R	roll mode time constant, sec
x	stick position, in.
ζ_{FS}	feel system damping ratio

τ_R roll mode time constant, sec (used in figures only)

ω_{FS} feel system natural frequency, rad/sec

ω_i forcing function input frequency, rad/sec

INTRODUCTION

Background

An in-flight research effort investigating various aspects of lateral handling qualities was conducted by Calspan Corporation (now Arvin/Calspan Advanced Technology Center, Buffalo, NY) in 1987 under contract to the U.S. Air Force and supported by NASA Dryden Flight Research Facility (DFRF). The experiment, using the Air Force/Calspan NT-33 variable stability aircraft, investigated lateral handling qualities issues such as stick feel-system dynamics, gradient, and sensing type (force or position), combined with airframe roll mode time constant variations. Evaluation tasks included random (sum-of-sines (SOS)) and discrete head-up display (HUD) tracking tasks, as well as air-to-air tracking and power approach and landing. Experimental results were primarily in the form of pilot ratings. The experiment and its results are presented in reference 1. One objective of the flight tests was to further investigate the effects of time delays and feel-system delays on flying qualities, following the initial work of Smith and Sarrafian (ref. 2).

The structure of the HUD tracking tasks provided the capability of measuring describing functions across various elements in the pilot–vehicle loop; this is usually the primary motivation for using an SOS compensatory tracking task (refs. 3, 4, and 5). Hence, the capability existed to use describing functions to identify pilot–vehicle, open-loop dynamics as well as to verify the actual experimental vehicle and stick dynamics. Open-loop, pilot–vehicle describing functions are presented in reference 1 for a few select cases.

A ground-based simulation, performed by Systems Technology, Inc. (Hawthorne, CA), under the sponsorship of DFRF, was very similar in structure to the reference 1 experiment and was actually designed to provide pre-experimental estimates for, and guidance to, the in-flight experiment (ref. 5). As in the subsequent in-flight experiment (ref. 1), open-loop, pilot–vehicle describing functions were obtained in this experiment, and provide an excellent basis for a ground-based and in-flight simulation comparison of pilot behavior.

This report documents analysis conducted under sponsorship of PRC Inc. (Edwards, CA), of the in-flight data results of reference 1 and the fixed-base simulation results of reference 5. Additional experimental data have been obtained from two more recent flight programs that investigated the effects of lateral control feel-system dynamics on helicopter handling qualities (refs. 6 and 7). Analysis of the references 1 and 2 results consists of handling qualities ratings (HQRs, ref. 8) and pilot–vehicle open-loop describing functions from the SOS tracking tasks. A limited amount of tracking data is available from references 6 and 7, but the bulk of the data from these references consists of HQRs.

2

Scope of the Study

This study was undertaken to examine specific features of the flight data of reference 1. The primary focus of the work was the extraction of open-loop, pilot–vehicle describing functions from the tracking data, and, for a limited subset of these data, the development of pilot models. A second objective of the study was the analysis of the HQRs from the flight experiment, in combination with other available data, in an attempt to define the effects of variations in feel-system dynamics on handling qualities.

The limited funding for this effort precluded indepth analysis of either the pilot models or the pilot ratings, and several unresolved issues remain. It has been possible, however, to get a grasp on the effects of feel-system dynamics (for lateral control operations) on both handling qualities and pilot dynamics. Several recommendations are made in this report for addressing feel-system effects in the specification and determination of handling qualities, and possible future analytical and experimental research subjects are identified to fill in the known gaps in the knowledge base.

Some of the findings reported here are not new and were, in fact, also reported in reference 1. The augmentation of the feel-system database with references 6 and 7 has, however, allowed us to draw observations and conclusions with much more certainty, and some new (and potentially controversial) conclusions will be found in this report.

Organization of the Report

The next section of this report briefly reviews the database considered here, i.e., references 1, 2, 5, 6, and 7. Especially important is the selection of appropriate pilot-rating data from reference 1 based on interpilot and intrapilot rating comparisons.

In "EFFECT OF FEEL-SYSTEM ..." the research of Smith and Sarrafian (ref. 2) is revisited and compared with similar selected data from the reference 1 flight tests. These data, along with related cases from the fixed-base simulation (ref. 5) and helicopter flight research (refs. 6 and 7), are compared to identify the proper method of dealing with feel-system dynamics variations. Discussed also is the effect of force in relation to position (displacement) sensing, again using the relevant pilot rating data from the references cited previously. The final subject of this section is the proper method for dealing with the effects of feel-system dynamics in applying handling qualities requirements and criteria.

"DESIGN CONSIDERATIONS FOR FEEL SYSTEMS" looks at the physical characteristics of cockpit manipulators in terms of their principal features, i.e., damping, gradient, and inertia. In this section some recommendations are given for the practical design of control feel systems.

"ANALYSIS OF PILOT PERFORMANCE ..." presents pilot–vehicle describing functions and pilot models for a selected set of the reference 1 flight data. These data show the effects of feel-system frequency and command sensing on the open-loop pilot dynamics.

A summary of conclusions and recommendations, especially for future work that should be conducted on the general subject of feel-system characteristics follows.

Supporting data generated under this contract are included as appendices. Appendix A summarizes the methods employed in extracting the pilot, vehicle, and feel-system dynamics from the Calspan SOS tracking time history data. Appendix B contains the actual time-histories and extracted pilot–vehicle dynamics for all configurations analyzed in this study. The pilot modeling procedures and extracted pilot models are detailed in Appendix C.

STATEMENT OF THE PROBLEM AND DATA

Governing Dynamics

History—While it has long been recognized that the dynamics of the cockpit feel system are important to the pilot, the impact of such dynamics on the pilot's perceptions of handling qualities is not well understood. This question has evolved primarily in conjunction with the evolution of military handling qualities requirements for fixed-wing aircraft, where advanced, highly augmented aircraft have been forced to resort to *equivalent aircraft* forms for specification compliance. A logical question, therefore, has been: what should be included in the aircraft model when these equivalent dynamics are derived? More specifically, should the cockpit manipulator feel-system characteristics be included or not?

The existence and application of equivalent aircraft approaches for handling qualities started with military specification, MIL-F-8785C (ref. 9), which provided for the use of equivalent classical systems. This specification did not, however, address the particular questions stated above.

The issue was faced in the writing of the proposed draft version of the new military standard and handbook (ref. 10), where equivalent systems were explicitly given and required to be obtained in terms of force control inputs. Discussions associated with this proposed document led to the conclusion by the authors that this was the right answer.

Before the official release of the Air Force's standard, MIL-STD-1797(USAF) (ref. 11), however, the flight experiment reported in reference 2 was performed. These quantitative data, in combination with experiences with force-sensing controllers on the X-29 and F-18, suggested that the impact of the feel system on pilot opinion may have been overrated. Certainly this evidence at least raised questions, sufficiently so that MIL-STD-1797(USAF) required the use of equivalent-system techniques referenced to force and position inputs. The final tri-service document, MIL-STD-1797A (ref. 12), is unchanged in this regard from the Air Force standard.

More recently, this controversy has resurfaced in the rotary-wing world, and the Army's rotorcraft specification (ref. 13)—currently a proposed tri-service standard (ref. 14)—states limits on bandwidth response that, "It is desirable to meet ... for both controller force and position inputs."

Mechanization—Feel systems are either position or force sensing (fig. 1). For position (or displacement) sensing, figure 1(a), the reference point for handling-qualities measurements is very important: all measurements in terms of position do not include the feel-system dynamics, while measurements from force do. For force-sensing controllers, figure 1(b), the feel system is in parallel for force reference

and downstream of the position reference point, and therefore, is not included in either case—i.e., the answer is the same for force-sensing systems.

The issue of what to do with the feel system revolves around philosophies of the pilot's actions in controlling the aircraft: does the pilot sense and respond to control *displacements* or *forces*? The governing equation relating stick force, F, and position, x, is

$$F = I\ddot{x} + b\dot{x} + kx$$

where I is the stick inertia, b is the damping, and k is the spring gradient. Dividing by I, we see that damping and frequency are given by

$$2\zeta_{FS}\omega_{FS} = b/I \text{ and } \omega_{FS}^2 = k/I$$

or

$$\zeta_{FS} = b/\sqrt{4Ik}, \omega_{FS} = \sqrt{k/I}$$

In "DESIGN CONSIDERATIONS FOR FEEL SYSTEMS," the characteristics of feel systems are examined in terms of stick inertia, damping, and spring gradient; throughout the rest of this report the stick dynamics are written in terms of damping ratio and natural frequency.

Data Used in this Report

This report makes use of the data from five references, including the initial study of Smith and Sarrafian (ref. 2). The prime sources of data are the in-flight and ground simulation studies (refs. 1 and 5), supported by the helicopter flight experiments (refs. 6 and 7). Following is a brief review of the salient features of each of these references, especially in terms of their applicability to this study.

Smith and Sarrafian—This AIAA article includes anecdotal information on the feel-system effects on handling qualities for the X-29A and F/A-18 aircraft, description of an informal evaluation on the USAF/Calspan NT-33A, and actual HQRs from a flight investigation with the Calspan in-flight simulator. The pilot rating data were obtained from one pilot, on one flight. These data were consistent with the anecdotal discussions, however, and suggested that the pilot was less sensitive to changes in the feel system than to addition of an equivalent amount of transport delay. The conclusions are based on these data and suggest that, "Better correlation with [MIL-F-8785C] time delay boundaries is obtained when the time delay measurement is referenced to stick position, not force, and the feel system is therefore excluded." Feel systems evaluated were, however, reasonably good in terms of dynamics, with damping ratios of 0.7 and natural frequencies of 26 and 13 rad/sec. A degraded feel system was not included.

Calspan Flight Tests—A portion of the reference 1 program was intended to gather more information on the issues raised by Smith and Sarrafian. Unfortunately, as is shown in the data review in "EFFECT OF FEEL-SYSTEM ...", this portion was not sufficiently complete to fully resolve the issues. The results of all of the reference 1 experiments, however—in conjunction with the other data described in the following—do allow us to make some more definitive statements. The experiment included feel systems at the frequencies evaluated in reference 2 ($\omega_{FS} = 26$ and 13 rad/sec), and added a degraded stick with $\omega_{FS} = 8$ rad/sec.

Since this is the main focus of this report, some effort was devoted to comparing the pilot ratings from the three subject pilots (denoted Pilots A, B, and C). Based on information in reference 1, and following an evaluation of the interpilot rating variations, all of the data for one pilot (Pilot B), and a portion of the data for another (Pilot C), were dropped from this analysis, as described here.

Reference 1 includes an intrapilot rating comparison (pages 74 and 75) that shows reasonable consistency between first-time and repeat evaluations for Pilots A and C. There is, however, a distinct difference in the HQRs from Pilot B between early and later runs—especially before and after Flight 4153. There is no interpilot rating comparison, however, so it is difficult to assess the fidelity of Pilot B's ratings with the other two pilots.

In comparing HQRs between pilots, it is necessary to divide the data of reference 1 into three parts based upon flight groupings as follows:

• <u>Flights 4051-4057</u>: These flights used a low-bandwidth sum-of-sines HUD tracking task, and the ratings for these flights are generally better than for subsequent evaluations—except for Pilot A, who appeared to be able to elicit potential handling qualities problems with the low-bandwidth task. In addition, the up-and-away evaluations by Pilot B during these flights typically did not include formation flying and air-to-air tracking tasks, and hence may be considered incomplete. For Pilots A and C in the early flights these tasks generally drove the overall HQRs more than the HUD-referenced tasks. Therefore, the ratings from Pilots B and C for this group, for the up-and-away evaluations, have been ignored for the interpilot rating comparisons.

• <u>Flights after 4057 and before 4153</u>: These flights used the high-bandwidth sum-of-sines HUD tracking task, but, as noted above, there is a difference in Pilot B's assessments of handling qualities for this set of flights when compared to the next set. This difference will become obvious when the HQRs are reviewed.

• <u>Flights 4153 and later</u>: Pilot C did not participate in this series of flights at NASA, so all ratings in this range come from Pilots A and B.

The interpilot rating comparisons for Pilot B as a function of Pilots A and C are plotted in figure 2. Since every pilot flew repeats of some configurations, there are more data points on the plots than the total number of evaluations. (Suppose, for example, that for a particular configuration Pilot A made two evaluations and assigned HQRs of 2 and 3, and that for the same configuration Pilot B assigned ratings of 4 and 5. For this configuration, there would be four points on the figure—Pilot A's 2 and Pilot B's 4 and 5, and Pilot A's 3 and Pilot B's 4 and 5. For this example, even though each pilot flew the configuration only twice, there would be four data points on fig. 2.)

On figure 2, open symbols denote those cases evaluated by Pilot B in flights prior to 4153, and solid symbols are for cases evaluated by Pilot B in Flight 4153 and later. There is no similar distinction for Pilots A and C; again, the intrapilot rating comparisons in reference 1 do not show any need for such discrimination for these pilots. For the up-and-away (Flight Phase Category A) evaluations (top portion of figure), there is a significant clustering of Pilot B's ratings around HQR = 5: of the 28 solid points on the comparison plot for Pilot A, 22 are within one point of 5 (i.e., 4, 5, or 6). There is no evidence of a similar clustering of ratings by Pilot A.

6

The landing (Category C) rating comparisons (bottom plots on fig. 2) are even more dramatic: Pilot B flew a number of configurations also evaluated by Pilots A and C, both before and after Flight 4153 (including cases before Flight 4057; since the landing task was not significantly changed throughout the program, all of the landing ratings may be used for comparisons). There is a clear separation of Pilot B's ratings: before Flight 4153 (open symbols), Pilot B always assigned HQRs of 2, 3, or 4; after Flight 4153 (solid symbols), the ratings were almost always 4, 5, 6, or 7, with only an occasional better rating. Yet for the identical configurations, Pilots A and C assigned HQRs ranging between 2 and 8. Basically, if the discrimination between flight segments were not made in the landing data in figure 2, the plots would look like pure scatter with no correlation whatsoever.

This change in Pilot B's rating behavior was noted in reference 1, with no discussion on any possible reasons and with no impact on the data analysis. Based on figure 2, however, it seems reasonable to remove Pilot B's ratings from any analysis, since the cause for this rating change—as well as for the relatively small spread in HQRs compared to Pilots A and C—is not known. It is important to emphasize that there is no way of ascertaining that it is Pilot B who assigned the anomalous ratings; perhaps the other two pilots were overly conscious of secondary factors that unduly influenced their assessments. Without much more information, it is impossible to determine the full answer.

Interpilot rating comparisons between Pilots A and C are shown in figure 3. For the up-and-away ratings, only Pilot C's ratings for flights after 4057 have been plotted, as discussed above. There is a small spread in pilot ratings for the up and away tasks in figure 3, but also very few data points. Generally, for the landing Pilot C was much more critical than Pilot A (assigning higher HQRs for the same configuration). This difference between the pilots will become evident when the rating data are plotted against equivalent time delay, and it was noted in reference 1 as possibly resulting from differences in piloting techniques for landing. Unfortunately, since the landing task is relatively unconstrained (when compared with most of the up-and-away tasks), it is difficult to define quantitative measures that will determine any differences in piloting technique. Quantitative analysis could be performed using the time-history data for the landings, but such analysis was beyond the scope and funding of this study. It is recommended that analysis of the time history data be performed, including measures of control activity, peak roll rates, etc., to attempt to quantify any piloting differences for the landing task.

As an overall observation from figures 2 and 3, there is a high amount of scatter in the interpilot ratings, much more than has been found in other similar NT-33A inflight experiments (e.g., refs. 15, 16, and 17). This level of scatter would be reason to cast some doubt on the experimental results—except that, for Pilots A and C, the intrapilot rating variation is quite small (ref. 1). Further, the difference in opinion between these two pilots (fig. 3) happens to be one of the most intriguing results from the experiment, as is shown later in this report.

In summary, the remainder of this report will not use pilot rating data from Pilot B, and will use the following data: Pilot A—all data; Pilot C—all landing data; up-and-away data only for flights after 4057.

STI Fixed-Base Simulation—A fixed-base simulation was conducted prior to the reference 1 flight experiment to investigate similar dynamics. This simulation used two McFadden controllers, a sidestick and a centerstick, with two subjects performing roll SOS tracking. The centerstick configurations were

designed to mimic the physical characteristics of the controllers evaluated in reference 1, including force–deflection and control–response values. Besides HQRs, quantitative performance and tracking measures and pilot–vehicle describing functions were obtained. The results of this fixed-base experiment are directly comparable to a small subset of the reference 1 flight data.

NASA CH-47 Experiments—The NASA/Army CH-47B variable-stability helicopter was used to investigate the effects of stick dynamics on helicopter flying qualities. The operation of a helicopter in hover is quite different from control of a fixed-wing airplane, so the specific results from references 6 and 7 cannot be directly compared with those from reference 1; the overall trends, however, should be similar since the task flown in the CH-47B consisted of SOS tracking. This study is especially valuable, because many of the variations of reference 1 were also performed here, but with a larger number of feel-system variations, including damping ratio. (Spring gradient was held fixed at 1 lb/in., as contrasted with 4 lb/in. for most of refs. 1 and 2.) Both force and position sensing were evaluated, and reference 6 contains HQRs as well as more quantitative tracking performance data. Additional information for this report was provided by the first author of reference 6, Mr. Doug Watson of NASA Ames.

The overall value of these data is mitigated somewhat by the characteristics of the simulator: the NASA/Army CH-47B (now back into operational service) was a large helicopter with limited capability as far as attitudes, rates, and accelerations. The safety system of this helicopter precluded aggressive maneuvering, so the SOS task was relatively benign when compared with the task used in either reference 1 or 5 (as discussed in more detail below).

Canadian Institute for Aerospace Research Feel-System Study With a Bell 205A Helicopter—The Canadian Institute for Aerospace Research conducted a feel-system study using their variable-stability Bell 205A helicopter (ref. 7). As mentioned above, the specific results of this study cannot be directly compared with the fixed-wing data from reference 1, but the data are useful nonetheless in identifying trends. This study used the widest range of feel-system dynamics, including three values of damping ratio, five different natural frequencies, and both displacement and fixed (isometric) sticks. In addition, there is a wealth of HQR data, as two pilots flew eight different tasks (seven low-speed maneuvering tasks plus SOS tracking). Unfortunately, the data are complicated by additional variations in stick gradient, which was increased as feel-system frequency increased, while all of the other references used a single spring gradient. In addition, like the CH-47B the 205A required a relatively low-bandwidth forcing function so the SOS task was more benign than in either reference 1 or 5. Most of the low-speed maneuvering tasks emphasized all axes of control, so the ratings for these tasks are not useful for evaluating changes in roll feel-system properties. The results of the lateral sidestep task are of value, however.

Of the two pilots in the reference 7 experiment, one pilot (Pilot A) tended to rate all of the configurations better than the other (Pilot B). This is confirmed by the interpilot rating plot of figure 4 for the SOS and sidestep tasks. Reference 7 suggests that this rating difference was possibly due to Pilot A's considerably greater experience in helicopters—1400 hours (9800 total flight time) compared to 125 hours (4450 total flight time) for Pilot B. It is noted in reference 7 that Pilot A's ratings do not show any consistent change as the feel-system dynamics were changed, while those for Pilot B reflect the expected changes. In this report, the ratings for both pilots will be used, but emphasis is placed on the ratings of Pilot B.

Comparison of Tasks and Performance Limits

Forcing Function Characteristics—Most of the data (HQRs and quantitative measures) analyzed in this report were obtained from SOS tracking runs. Therefore, it is valuable to consider the characteristics of the forcing function elements and the relative performance criteria used by the pilots in assigning their ratings.

The SOS tracking task involves correction for displayed errors generated by a forcing function of the form

$$F(t) = \sum A_i \sin (\omega_i + \phi) \, t$$

where the amplitudes A_i and frequencies ω_i are adjusted to provide the desired task bandwidth and amplitude. The amplitudes for the SOS tasks from references 1, 5, 6, and 7 are plotted (as relative values, A_i/A_1) in figure 5. As figure 5 indicates, these experiments used similar forcing-function bandwidths; the forcing functions for the references 6 and 7 experiments were, in fact, set based on the reference 5 task.

Noted also on figure 5 are the input disturbance root mean square (rms) values for the four experiments. The rms values for the Calspan study and the STI fixed-base study are almost identical (19.0 compared to 18.6 deg), but those for the helicopter studies are much smaller at 4.4 deg. According to reference 6, this reduced rms was "found to be the largest possible without nuisance control-system disconnects by the research system safety monitoring equipment" on the CH-47B. Reference 7, which mimicked the reference 6 experiment, used the same rms.

Performance Limits—Because of the random-appearing nature of the SOS task, it is impossible to set an absolute limit on desired attitude error; for example, for an input rms of 19 deg, it is reasonable to expect that a 3-σ peak of 57 deg will occur occasionally, so a requirement to keep attitude within, say, 20 deg is guaranteed to be violated. Instead, it is usual to set desired and adequate performance limits based on ability to correct large errors and regulate attitude within a reasonable level.

The performance levels for the four SOS experiments were as follows:

- Calspan study (ref. 1): Desired—attitude maintained within 5 mils (approximately 8 deg bank angle) 50 percent of the task, except immediately following step commands; Adequate—relaxed to 10 mils (16 deg).

- STI fixed-base simulation (ref. 5): Desired—Extended time periods of less than 1 to 2 deg roll error and peak errors during reversals of less than 11 deg; Adequate—Short periods of 1 to 2 deg error and peak errors on reversals of less than 22 deg.

- Helicopter experiments (refs. 6 and 7): For reference 6, "The pilots were instructed to minimize the roll error at all times. Peak roll errors of 11 deg and 22 deg defined desired and adequate performance ..." The performance limits are not given in reference 7 for that experiment, but since it was based on the reference 6 study it is assumed the same limits were used.

While the limits on desired and adequate performance are comparable for the four studies, there is a significant difference nonetheless. Although the Calspan and STI SOS tasks had similar rms values

(19 deg) and similar desired-performance limits (8 and 11 deg), the two helicopter studies—which used much lower-rms forcing functions (4.4 deg)—kept the STI performance limit of 11 deg. Hence, it should have been much easier for the pilots in the references 6 and 7 tasks to achieve desired performance (for example, a 3-σ peak command, 13.2 deg, would barely exceed the desired limit), and therefore, one might expect the HQRs to be better overall, and to show a more gradual degradation as the feel systems are degraded. As the next section of this report indicates, this is precisely the case.

EFFECT OF FEEL-SYSTEM DYNAMICS ON HANDLING QUALITIES

Smith and Sarrafian Revisited

Initial Data—Several of the configurations evaluated in the initial study by Smith and Sarrafian (ref. 2) were repeated on the NT-33 (ref. 1). In addition, the single evaluation pilot for reference 2 was also Pilot A in the reference 1 experiment, and, therefore, a one-to-one comparison of ratings from these two experiments is possible. The evaluation task in reference 2 was precision offset landing, identical to the landing task flown in the reference 1 study.

The configurations evaluated in reference 2 were based on two feel-system frequencies, a fast system at 26 rad/sec and a slow system at 13 rad/sec. The configuration identifiers and HQRs for the six configurations (A through F) are listed in table 1. Listed also are similar configurations from reference 1—or what the equivalent configurations would have been if similar cases were flown in reference 1—along with the HQRs from Pilots A and C. Figure 6, reprinted from reference 1, shows the identification method for the reference 1 configurations. All of the cases in table 1 have a medium value of T_R (0.30 sec); a potentially very important difference between the two experiments, however, is the selection of force–response sensitivity. In the Smith and Sarrafian flight tests, the lateral command gain "was selected to provide satisfactory steady-state roll-rate response." By contrast, in the Calspan tests the response was always fixed at a predetermined value (reflected in the configuration identifiers of table 1: the (5) and (10) indicate steady-state roll-rate per force, p_{ss}/F_{as}, of 5 and 10 deg/sec). It is therefore possible—and in some cases highly likely—that the results of the reference 1 NT-33 tests are heavily influenced by control sensitivity. More is said about this subject later in this report.

The most interesting comparisons from the Smith and Sarrafian study are cases A compared with B and C compared with D. Figure 7 (leftmost plots) shows the pilot ratings from reference 2 as a function of time delay for the feel system included (fig. 7(a)) and excluded (fig. 7(b)).

- Configurations A and B: Configuration B had the slow (13 rad/sec) feel system, resulting in about 0.15 sec of time delay with the feel system included. Configuration A consisted of the fast (26 rad/sec) system, with added time delay to produce an equivalent level of overall equivalent delay. As figure 7 shows, there was no HQR difference between these cases, both of which were level 1 (HQR of 2). Note that with the feel system removed (fig. 7(b)), the overall time delay for configuration A is near the MIL-F-8785C (ref. 9) level 1 limit, yet this case was still considered good.

- Configurations C and D: These are the more interesting cases: Configuration C had the fast feel system and a large added transport delay, resulting in 0.27 sec of total delay when the feel system is included (0.22 sec without the feel system), while configuration D, with the slow feel system and a

lower added delay, also had 0.27 sec including feel system, but only 0.17 sec without the feel system. As figure 7(a) shows, there is a large discrepancy in HQRs between configurations C and D if the feel system is included in overall time delay, while the trend is very smooth if the feel system is excluded (fig. 7(b)). It was this comparison that led Smith and Sarrafian to suggest that the feel system should not be considered a delay-causing element in the total aircraft.

Comparison Cases by the Same Pilot from Reference 1—As mentioned above, the pilot for the Smith and Sarrafian study was also Pilot A in the Calspan study of reference 1, so ratings for Pilot A for the same configurations can be of value. Unfortunately, only three of the six reference 2 cases were evaluated in the reference 1 tests, and even these may be clouded by the use of fixed control–response sensitivity. Further, the two most interesting cases—C and D—were not reevaluated on the NT-33. To augment this discussion, three configurations that were flow for reference 1 but not for reference 2 have been added and assigned one-letter identifiers for simplicity, as listed on table 1: (1) Configuration E'— labeled L201P(5) in reference 1, this case is similar to E from reference 2, except for the fixed sensitivity. (2) Configuration G—L203P(10) from reference 1, with the slowest feel-system frequency (8 rad/sec) to assess the effect of further reducing ω_{FS} below 13 rad/sec. (3) Configuration H—L243P(10) from reference 1, identical to L203P(10) except with an added first-order filter at 40 rad/sec (see fig. 6).

The ratings for Pilot A from the Calspan experiment are shown in the middle plots of figure 7. Note that the configurations identified as A and B now have different HQRs: A received HQRs of 3, 3, 4, and B a single rating of 6. The result is a separation in these cases with feel-system dynamics both included in (fig. 7(a)) and excluded from (fig. 7(b)) the overall time delay. Thus neither answer appears to be right for these configurations.

Comparing the fast (configurations E and E') and slow (G) feel systems, there is very little degradation in HQR (2, 4, and 2; 4 and 4), supporting the exclusion of feel-system dynamics from time-delay calculations. There is, however, a surprising degradation in HQR for the slowest system when the 40-rad/sec filter is added (4 and 4 for configuration G and 8 for H). This filter produces only about 0.023 sec of time delay, so it is doubtful that the entire difference in HQR is because of the filter alone. Pilot comments do not help explain it either:

• Configuration G (L203P(10)): "Could feel some lateral displacement, as if the stick was a bobweight in hand . . . Didn't achieve desired performance on both PA's, therefore overall a 4." "Airplane had some peculiar characteristics that I could notice flying around but not in the task . . . You could get the job done but I have some reservations."

• Configuration H (L243P(10)): "Abrupt, too responsive initially. Not predictable . . . Bursts of PIO when closed loop . . . Controllable but barely."

These ratings represent an enigma from the reference 1 flight experiment that cannot be fully explained without more indepth analysis. The overall observation from figure 7, however, is that there is an offset in HQRs for Pilot A when the feel system is included in time delay (center plot of fig. 7(a)), just as there was for the reference 2 study (left plot). There is, however, a huge difference when the feel system is excluded (fig. 7(b), center plot), where absolutely no correlation between time delay and HQR exists, compared to the reference 2 study (left plot), where a very strong correlation was found. It

11

appears that neither method is totally correct, but that excluding the feel system is more incorrect than including it.

By contrast, the ratings of Pilot C for configurations A, B, E', G, and H from reference 1 are shown in the rightmost plots of figure 7. Pilot C's ratings show exactly the opposite trend: there is a smooth correlation between HQR and τ_e with the feel system included (fig. 7(a)), with every configuration correctly located in the MIL-F-8785C Level, and there is no correlation whatever when the feel system is neglected (fig. 7(b)). For Pilot C it appears that it is incorrect to exclude the feel system and correct to include it—an observation counter to both of Pilot A's sets of ratings.

Resolution of these enigmas will require analysis of the time-history data for all of the landings. It is possible that simple measures of task performance—e.g., peak roll attitudes, rates, and accelerations, as well as peak and rms stick activity—will reveal consistent differences between pilots (and experiments). Such analysis was beyond the scope of this report, but may be the only way to determine the reasons behind the conflicting data. It may further be necessary to repeat the entire experiment, but allow the pilots to select their own control sensitivities.

Should Feel-System Dynamics Be Included in Equivalent Time Delay

The issue of whether feel-system dynamics for position-sensing control systems should be included in computation of equivalent time delay was addressed in reference 2. This has significant implications in applying the equivalent-system time-delay requirements of MIL-STD-1797A (ref. 12), and, in general, in application of most traditional and recent handling qualities criteria. It is important, first, to recognize that the force feel system on any cockpit manipulator is not simply a contributor to overall time delay; what is not yet clearly understood is the impact of the dynamics of the feel system on handling qualities, and what should be done (in terms of handling qualities requirements) to account for these effects. Specifically, there are two questions to be addressed here: (1) does the force feel system, whose dynamics are directly sensed by the pilot, affect the pilot's perceptions of handling qualities; and (2) are the effects of feel systems on the pilot's perception of handling qualities adequately represented by equivalent delay measurements alone. Unfortunately, the results of the reference 1 flight tests do not serve to conclusively answer these questions, and indeed, several new questions are raised. This is where the ground-based simulation data of reference 5, plus the helicopter tests of references 6 and 7, will augment the database considerably.

Force in Relation to Position Reference—Figures 8 and 9 compare the HQRs from Pilots A and C with equivalent-system time delay for the up-and-away (fig. 8) and landing (fig. 9) configurations. The data have been sorted by T_R and by whether the time delay measurements are referenced to force or position, meaning the feel-system dynamics have been treated as follows (discussed previously):

- Position-sensing controllers: Force reference—feel system included in computation of τ_e; Position reference—feel system excluded.

- Force-sensing controllers: Feel system excluded for both force and position reference.

Different symbols are used in figures 8 and 9 for the fast, medium, and slow feel-system dynamics; open symbols are position-sensing and solid symbols are force-sensing cases.

12

Based on the up-and-away ratings, it appears that it is more correct to reference the time-delay measures to force, i.e., to include the feel-system dynamics for position-sensing systems (fig. 8). The trends of degrading pilot opinion with increasing τ_{eq} in figures 8(a), 8(c), and 8(e) are very strong; both pilots show these trends, although the relations for the highest T_R case (0.40 sec) for Pilot A are not quite as strong. (The two force-sensing cases for Pilot A with $T_R = 0.15$ sec and HQRs of 7 are ratchet cases—these are discussed separately later in this section.) Certainly, comparison of parts (c) with (d) and (e) with (f) of figure 8 suggests that it is much better to include feel-system dynamics in the computation of equivalent time delay.

Things are not as clear for the landing configurations (fig. 9), where we see the interpilot differences shown earlier in figure 7. Looking only at Pilot C's ratings, there is a clear relationship between τ_{eq} and HQR in figure 9 when the feel system is included, and this relationship is lost almost entirely when the feel-system dynamics are excluded. Pilot A, on the other hand, does not show as strong a trend, and in fact commonly assigned level 1 or borderline level 2 ratings (HQRs of 2, 3, and 4) for configurations with extremely large values of τ_{eq}—if feel-system dynamics are included. For the lowest T_R (0.20 sec) and highest T_R (0.45 sec), Pilot A rated the force-sensing cases consistent with Pilot C, but gave all of the position-sensing cases good HQRs; this was generally true for $T_R = 0.30$ as well, with only a few exceptions. Therefore, as noted in the discussion of figure 7, for Pilot A it appears better to *exclude* the feel-system dynamics, while for Pilot C the dynamics should be *included*.

Similar rating data from the reference 5 simulation are shown in figure 10. Equivalent-delay numbers are not available for the configurations of reference 5; the time-delay measure plotted in figure 10 is incremental added delay, because of both feel-system and command filters but excluding the vehicle ($T_R = 0.15$ sec, actuator modeled by a 0.033-sec time delay). The feel-system and command filter elements were all second-order, for which incremental time delay may be approximated by

$$\Delta \tau \approx \frac{2\zeta}{\omega_n}$$

In all cases the damping ratio was 0.6 or 0.7. As for figures 8 and 9, the time delay for position reference (fig. 10(a)) excludes the feel system, and the delay for force reference (fig. 10(b)) includes the feel system for the position-sensing cases. Both plots show some trends of degrading HQR with increasing delay, but the trend for position-sensing controllers is stronger in figure 10(b), i.e., when the feel system is included.

Similar trends are found from the SOS tracking experiment using the CH-47 helicopter (ref. 6). Figure 11(a) shows the HQRs for both force and position sensing controllers vs. added time delay because of command filters, i.e., feel system not included; while there is a relationship between HQR and time delay, it is not strong, and ratings range between 2 and 4.5 for zero delay. When the feel system is included, figure 11(b), the relationship is much more pronounced. (It is also noticeable that the degradation in HQR with added delay is much lower in figure 11 than for the fixed-wing data of figure 9; this is primarily because of the lower-amplitude SOS command and more relaxed performance criteria, discussed previously.)

The results of the SOS tracking portion of the Bell 205A flight experiment (ref. 7) are even more dramatic. For this experiment, the only delay-inducing element (besides the stick feel system) was a first-order filter (break frequency of 8.66 rad/sec) that was added for some evaluations. (For data

plotting, it has been assumed that the effective delay of this filter is $T_{CF} = 1/8.66 = 115$ msec. In actuality, a low-order equivalent systems match to the aircraft model with this filter would reflect only about 0.07-0.08 sec of added delay because of the filter.) When the HQRs are plotted against added time delay with the feel system excluded, figure 12(a), there is absolutely no correlation. When the feel system is added to delay for the position-sensing sticks, figure 12(b), there is a strong correlation, even though the degradation of HQR with increasing delay is not strong.

The data of figures 8 through 12 do not answer the question of whether it is correct to represent feel-system effects on pilot rating as a pure time delay; they do indicate, however, that the trend of pilot opinion with delay is stronger when the feel system is included in the delay.

Effects of Force-Sensing Feel Systems—The foregoing discussion assumed the conventional method for addressing feel systems in computing time delay (fig. 1): either exclude them or include them for position sensing (feel system in series), and always exclude them for force sensing (where the feel system is in parallel, and therefore, is not picked up in either force or position referencing). There is, however, an interesting feature of the HQRs for the force-sensing controllers in figures 9, 10, 11, and 12 (solid symbols). In all cases, there can be a wide spread of ratings for a single value of delay. This is because the feel-system dynamics are varying widely, but since these dynamics were not included in the computation of delay, their impact is not reflected. Therefore, it is useful to make one more computation: include the effective delay caused by the feel system for all sensing types—position and force. This is a departure from tradition, and does not follow the convention as described for figure 1. But it is based on an observation from the NT-33 and CH-47 experiments (refs. 1 and 6) and an assumption: the data show that the pilots were sensitive to changes in feel-system frequency even for force sensing controllers, and therefore it may be assumed that the effect of the feel system on pilot opinion is the same regardless of the mechanization of the stick.

The landing data from the NT-33 experiment of reference 1 serve as a good starting point for evaluating this hypothesis. In figure 13, the ratings for Pilots A and C from figure 9 have been condensed for the $T_R = 0.20$ and 0.30 sec configurations into single plots. The equivalent-delay values for position-sensing configurations (open symbols) are identical to those of figures 9(a) and 9(c); for the force-sensing configurations (solid symbols); however, the points in figure 13 also reflect the equivalent delay caused by the feel system. Several major observations can be made by comparing figures 13(a) and 9(a), and figures 13(b) and 9(c):

• Inclusion of the feel system in τ_e has improved the overall trends of HQR with delay; e.g., the bad feel system (natural frequency of 8 rad/sec) received poor ratings whether position or force sensing was used (triangles in fig. 9, double flags in fig. 13), and the ratings for force sensing have been shifted to the right in figure 13.

• There is a better relative concordance between the ratings for the position-sensing and force-sensing data, i.e., the trends are similar in figure 13.

• The ratings are generally better than expected based on the requirements of MIL-F-8785C.

• There is a cluster of ratings from Pilot A that are much better than other configurations with similar time delay. These are the ratings at HQR = 3 to 4 and τ_e = 210-230 msec; they are the enigmatic points discussed previously (fig. 7), and they will be analyzed in more detail in the following.

14

Figure 14 shows the data from the reference 5 fixed-base simulation with the feel system included for both controller sensing types; compared with figure 10(b), however, the trends in figure 14 are not nearly as good, as there appears to be a definite shift in the ratings at any value of time delay. In fact, it appears from these data that it is better to exclude the feel system for force-sensing controllers, i.e., that figure 10(b) is correct. (As will be seen shortly, this is the only set of data for which this observation can be made. The reasons for this are not known at this time, but may reflect the differences between fixed-based simulation and full-motion simulation.)

The two helicopter experiments strongly support the inclusion of feel-system effects for force-sensing controllers. The HQR data for these experiments are shown in figure 15. For the CH-47 study of reference 6, the force-reference plot (fig. 11(b)) shows a group of ratings for force-sensing controllers with HQRs between 2 and 5, but at a constant value of time delay. In figure 15(a), the effect of adding the feel system to overall time delay is to more evenly distribute these ratings with the position-sensing points. The same effect is found for the Bell 205A study of reference 7 (compare fig. 12(b) with fig. 15(b)), with the exception of one configuration that received ratings of 5 from Pilot A and 7 from Pilot B. This was the highest-frequency case evaluated in the reference 7 study, and it is possible that the combination of fixed stick and lack of feel-system filtering of pilot inputs made it possible for the pilots to excite other response modes on the subject helicopter. Nothing is mentioned in reference 7 about this, but it is also feasible that a phenomenon similar to roll ratchet may have occurred with this controller.

With the exceptions of the fixed-base simulation data of reference 5, and the single configuration from reference 7, this analysis of the pilot rating data suggests that it is most appropriate to always include the feel-system dynamics in computing time delay, regardless of the reference used in the mechanization of the feel system itself.

It is important to reiterate that this does not mean that the effect of the feel system on the pilot is identical to the effect of adding a pure time delay; indeed, the manifestation of poor feel-system dynamics is distinctly different from that of large time delay. Rather, the foregoing shows that, in the absence of more concrete, specific requirements on feel-system characteristics, it is possible at least to estimate the effects of the feel system on pilot ratings by considering it to be akin to adding a time delay. In other words, the conservative approach in handling-qualities evaluations is to include the feel system as a delay-inducing element in the equivalent aircraft.

Analysis of the Enigmatic Ratings from Pilot A—Despite the previous analysis, there remains a set of ratings by Pilot A in reference 1 that defies explanation. This set, highlighted in figure 13(b), occurred in the landing evaluations, and generally corroborates Pilot A's earlier ratings of reference 2 (fig. 7). The ratings are considered enigmatic because Pilot A was internally consistent between configurations as well as experiments, yet Pilot A's ratings differed from those of Pilot C and from Pilot A's own evaluations in the up-and-away tasks of reference 1.

This difference in ratings is illustrated in figure 16. The configurations plotted in figure 16 are those for both the up-and-away and landing evaluations with an overall time delay (feel system included) of approximately 210 msec and the medium value of T_R for each task. Since the total delay is the same, the primary difference between these configurations is the source of the delay; HQRs are plotted in figure 16 against incremental added delay.

For the up-and-away data, figure 16(a), the total delay was achieved by use of the slowest feel system (resulting in no added delay), configuration 203P(18); the intermediate feel system with a 26-rad/sec second-order command filter, 212P(18); and the fastest feel system with a 13-rad/sec second-order command filter (221P(18)) and with 110-msec of added delay (201P(18) + 110). Pilot C flew only one configuration, but the three ratings (7, 8, and 10) are in agreement with Pilot A's single rating for that configuration (7). Pilot A flew all of the configurations and gave basically the same HQRs for all of them. Thus Pilot A's up-and-away evaluations concur with the MIL-F-8785C requirements on equivalent time delay (fig. 8(c), cluster of ratings at $\tau_{eq} = 0.21$ sec), and suggest that the source of the delay—sluggish feel system, intermediate feel with a command filter, or fast feel with either command filter or added delay—makes no difference whatsoever on pilot ratings. Again, it must be noted that Pilot A's *opinion*—i.e., comments—shows great disparity between configurations; for example, the slow-feel aircraft has unacceptable ratchet-like oscillations, not at all similar to the effects of high pure time delay. Nevertheless, figure 16(a) indicates that the effect on Pilot A's *ratings* is identical when characterized by equivalent time delay.

The ratings for landing, figure 16(b), show an entirely different story. The configurations plotted here are the enigmatic HQRs for Pilot A (fig. 13(b)). The variations in added dynamics are similar to those for the up-and-away data, and again the equivalent time delay (feel system included) is around 210 msec for all cases. The ratings for Pilot A clearly show that, for position-sensing sticks, the initial delay due to the feel system should be ignored entirely: Pilot A's ratings correlate very well with added delay alone. The single rating for the force-sensing stick suggests further that there may even be some beneficial effect from force sensing, since this configuration has 135 msec of added delay but still received an HQR of 4. The ratings for Pilot C, however, are in total opposition and instead look more like Pilot A's up-and-away ratings of figure 16(a); there is very little variation in HQR across the configurations. Unfortunately, Pilot C did not fly two of the cases with 53-55 msec of added delay, but based on figure 16(b), there is no reason to suspect that Pilot C's ratings for these two cases would have been any different.

The data shown in figure 16 remain a mystery, and there may be no way to explain them without a detailed analysis of the landing time histories for Pilots A and C. Based solely on Pilot A's landing ratings, it would seem appropriate to recommend that the feel system be excluded from estimates of handling qualities criteria.

Pilot A's good ratings in the bad time-delay region of figure 13(b) represent the worst possible scenario for handling qualities criteria. There are three possibilities for correlation of HQRs with criteria: (1) Handling qualities ratings (or at least levels) and criteria levels agree. This is clearly the ideal situation. (2) Bad ratings lie in the good region. This may indicate a failure of the criteria or it may only indicate other, unrelated problems. (3) Good ratings lie in the bad region. This indicates either a failure of the criteria or a failure of the original experiment to expose the handling qualities deficiencies under study. Pilot A's enigmatic ratings fit this category with respect to equivalent time delay (fig. 13(b)), and, while they must be considered valid, there is sufficient other evidence (Pilot C's landing ratings and both pilots' ratings for up-and-away flight) to support the use of the time-delay requirement as recommended here.

Effects of Force and Position Sensing on Pilot Ratings

In the previous subsection, the effects of force and position sensing were evaluated with respect to equivalent time delay. In this subsection, the incremental effects on HQRs of the two mechanizations will be addressed. References 1, 5, and 6 all investigated this issue using identical feel-system dynamics for both position and force sensing.

All of the relevant HQRs from these three references are shown in figure 17. The reference 1 data include both up-and-away and landing configurations; where the same pilot flew both mechanizations, there is a general trend for slightly better ratings when force sensing is employed. In most instances, the HQR difference is one pilot rating or less, and hence is not significant; there are two cases where the improvement is greater, and for the final configurations (L342P(10) and L342F(10)), the ratings actually degrade slightly for force sensing. The fixed-base simulation data of reference 5 show the greatest improvement in HQRs in figure 17: in every case, force sensing received better ratings from at least one of the two pilots, and in most cases the improvement is more than one HQR. The CH-47 flight data from reference 6, also shown in figure 17, has no real difference between position-sensing and force-sensing controllers. This lack of HQR difference from the helicopter SOS tracking task is interesting, because there was a distinct difference in roll error reduction, as shown in figure 18. The errors with force sensing are consistently lower than those for position (displacement) sensing.

Based on the data in figure 17, it appears that there may be some beneficial effect on handling qualities from using force rather than position for control commands. Nevertheless, it is clear that a bad feel system (e.g., the $\omega_{FS} = 8$ rad/sec stick in the reference 1 experiment) is still bad, whether position or force sensing is used, and therefore the dynamics of the feel system cannot be totally ignored just because commands are based on control force. For this reason, the conservative approach taken above is considered to be appropriate, i.e., assume the effect of the feel system on handling qualities is the same regardless of the command pickoff used.

Location of Lags

Included in the experiments of references 1, 5, and 6 was an assessment of the importance of the location of second-order lags. Specifically, the studies all looked at whether a lag in the command path was equivalent to the lag due to the feel system. The evaluations involved swapping of second-order lags between the stick and the command filter, as sketched in figure 19. Figure 19 also shows all relevant rating data from the three references.

For the reference 1 study, there is simply not enough data to make any observations; only two comparisons were conducted, and only Pilot A flew all of the configurations. For the up-and-away comparison (221P(18) and 212P(18)), there is no difference in Pilot A's ratings between the 26-rad/sec stick with a 13-rad/sec filter, and the 13-rad/sec stick with a 26-rad/sec filter. The landing comparison for Pilot A (L221P(10) and L212P(10)) reflects one of the enigmatic ratings discussed above. In the fixed-base simulation of reference 5, two comparisons were conducted with basically no change in HQRs. The CH-47 experiment of reference 6 shows no consistent difference. The largest changes in HQR for the CH-47 data in figure 19 are for the low-frequency, low-damped mode ($\zeta_{FS} = 0.3$, $\omega_{FS} = 5.4$ rad/sec). HQRs degrade by one-half to one point when this mode is placed in the feel system instead

of the command filter. For the mode with similar frequency but higher damping ($\zeta_{FS} = 0.6$, $\omega_{FS} = 4.9$ rad/sec), however, the ratings actually improve slightly when this mode is in the feel system.

Overall, based on figure 19 it appears that there is very little effect on pilot ratings because of the location of second-order lags, and that a bad stick with minimal command filtering is about as bad as a good stick with lots of command filtering.

Roll Ratchet

Roll ratchet was observed in the reference 1 flight program, as it was in the earlier lateral high-order systems (LATHOS) experiment (ref. 17) that generated much of the discussion of this phenomenon in the first place. There are several theories on the origin of roll ratchet, most of them conflicting, and there is no way to fully resolve the issue of roll ratchet without further analysis of the reference 1 data and, possibly, even further testing. A ground simulation study (ref. 4) found a tendency for human pilot neuromuscular peaking around the ratchet frequency for certain combinations of aircraft and feel-system dynamics. This tendency was found to exist in the describing-function data from the reference 1 flight experiment as well, as discussed in a later section of this report. In this section, it is possible to identify some of the contributors to roll ratchet, and hence to define what it takes to alleviate ratchet tendencies. Fortunately, several configurations from reference 1, in combination with the "classic" roll-ratchet source, the LATHOS study (ref. 17), and data from a much older NT-33 experiment (ref. 18), clearly illustrate why roll ratchet occurs on the NT-33 in the first place.

When ratcheting was encountered in the LATHOS experiment, several key elements of the aircraft dynamic system were identified as contributors: a low value of roll mode time constant, T_R (or high $1/T_R$), high control sensitivity (in terms of roll rate per unit stick force), and the use of force-sensing rather than position-sensing commands.

One configuration and its variants from reference 1 helps us see in great detail some of the specific factors involved. The pilot ratings for these variants were included on figure 8(a) (solid circles at $\tau_{eq} = 0.063$ sec) and are repeated on figure 20(a). Configuration 141F(18), with force sensing, fast feel system, and high response sensitivity ($p_{ss}/F_{as} = 18$ deg/sec/lb), was given an HQR of 7 by Pilot A and described as "head knocking ... ratcheting" (extracted pilot comments are given in table 2). Pilot C (in an early evaluation, i.e., with a low-bandwidth SOS forcing function) gave it a 4 and called it "jerky." This configuration is identical to Case 5-2 in LATHOS, which also received solid 7's for ride qualities, but 4's for performance.

Reduction in the control–response sensitivity from $p_{ss}/F_{as} = 18$ to 10 deg/sec/lb did not improve the HQRs much (configuration 141F(10)), still a 7 from Pilot A and a 3 from Pilot C. There is no reference to ratcheting, however (table 2)—only to unacceptable lateral accelerations and abruptness by Pilot A (curiously, Pilot C mentions "sluggishness"). The reduction in sensitivity therefore appears to have reduced the ratchet tendency, if not the excessive accelerations.

A further, dramatic improvement was made simply by changing the stick force–deflection gearing from 4 to 2.75 lb/in. for configuration 141F(10). This case was flown twice by Pilot A and received HQRs of 2 and 3; it was "a good, well-rounded airplane" (table 2). Without changing the feel-system

dynamics, the roll mode time constant, or the mechanization of force-sensing commands, what was an overly abrupt HQR = 7 airplane is now almost perfect. The decrease in control sensitivity, in terms of roll rate per unit stick deflection, is dramatic: from 72 deg/sec/in., to 40, and finally, 25 (fig. 20(a)). A less dramatic but similar improvement in HQRs was found for a landing configuration (shown in figure 20(b)). This configuration had reasonably good handling qualities to begin with, so the changes were not as extreme.

There is strong evidence from reference 18 that the single greatest contributor to ratchet, and the cause of recommendations to avoid short roll mode time constants (e.g., ref. 17), was the use of extremely high levels of roll control sensitivity on the LATHOS program. In the LATHOS study, as in reference 1, fixed values of sensitivity were evaluated (in contrast with other Calspan programs, e.g., references 15, 16, and 18, where the pilots were allowed to select their sensitivities); for the short roll mode, $T_R = 0.15$ sec, sensitivities, measured in terms of p_{ss}/F_{as}, were fixed at 10 and 18 deg/sec/lb. In addition, linear stick command gradients were used with no force breakouts. (Level 3 by the requirements of MIL-STD-1797A) and with stick force-to-deflection gearing of 4 lb/in.

A very similar configuration was evaluated in reference 18, with $T_R = 0.155$ sec, but with position sensing, approximately 1.5-lb stick breakouts, 3.81 lb/in. gearing, and with pilot-selectable control/response sensitivities. For the best systems, the optimum sensitivity was around $L_{\delta as} = 162 - 207$ deg/sec^2/in., corresponding to $p_{ss}/F_{as} = 6.6$-8.4 deg/sec/lb. The very best system (configuration BA-2 with no aileron yaw), was rated a 2 (on the old CAL scale), and had the highest value. Unfortunately, the pilot comments for this case are missing. For the next best system, $PR = 2$-$1/2$, $p_{ss}/F_{as} = 7.4$ deg/sec/lb and the pilot noted that "I would like a higher gear ratio and lighter stick forces but I compromised because the response is too abrupt for rapid inputs with higher gear ratios." This comment, with others, hints at the verge of ratcheting—prevented in every case by selecting a response sensitivity below the lowest value flown in either reference 1 or LATHOS. Even LATHOS evaluations with nonlinear control gearings indicate an improvement in handling qualities with this small fix (ref. 19). HQRs improved from 7 to 4-4.5 with only a slight hitch in the control gradient, corresponding to breakout and desensitization around neutral stick.

The data discussed above suggest that ratcheting can be easily avoided by taking several steps: (1) Keep the control–response sensitivity below about 8 deg/sec/lb, (2) use some nonlinearity in the control gradient, and (3) keep the control force–deflection gearing at a reasonable setting, somewhere below 4 lb/in. (2.75 lb/in., after all, may not be the best setting). These data also suggest that any criteria that place lower limits on T_R, such as the effective roll-mode requirements developed in reference 17 (e.g., fig. 21), are not preventing the problem (excessive sensitivity), but merely preventing the manifestation of it (high roll damping).

DESIGN CONSIDERATIONS FOR FEEL SYSTEMS

Inertia and Gradient Characteristics

In the previous sections of this report, the dynamics of the stick feel system have been addressed in terms of the effective damping and frequency characteristics, i.e., ζ_{FS} and ω_{FS} as defined in the statement of the problem. In this section, the characteristics are examined in terms of the three design

parameters: I, the stick inertia (or mass, in slugs or lbm); b, the stick damping, (lb-sec/in.), and k, the stick gradient (lb/in.).

The acceptability of stick feel-system dynamics is clearly influenced by all of these parameters. For example, the flight experiments of reference 7—as well as experiences with the F-16 sidestick—have demonstrated that very stiff sticks are perfectly acceptable as long as their effective natural frequency is sufficiently high. By contrast, it is common for helicopters to be operated with force-feel removed entirely, corresponding to zero natural frequency. The importance of two of the three design parameters—gradient and inertia—can be examined together by using only those data from references 1, 5, 6, and 7 that have reasonable damping.

Figure 22 is a crossplot of effective inertia, I, and stick natural frequency, shown as $1/\omega_{FS}^2 = I/k$. (This figure is based on the authors' oral presentation of ref. 6.) Summary data from references 1, 5, 6, and 7 are shown on this crossplot. These data represent, in every case, the best possible dynamics (in terms of HQR) for the given combination of stick characteristics. For the two experiments where stick damping was a variable (i.e., refs. 6 and 7), the HQRs given are for the moderately and highly damped sticks only. Included also are the stick dynamics (triangles) for several helicopters and V/STOLs (the UH-60A, CH-47B, and YAV-8B) from reference 6, and for the X-29A from reference 2. Of these aircraft, only the CH-47B has a feel system that is not considered good by the pilots. The higher gradients (greater than about 2 lb/in.) are typical of centersticks in fixed-wing airplanes, while the lower gradients (below 2 lb/in.) are more commonly found in rotorcraft.

In figure 22, the open symbols correspond to level 1 HQRs and the half-filled points correspond to level 2 HQRs. Based on this figure, a level 1 minimum on stick natural frequency may be set at about 10 rad/sec for effective inertias above about 5 lbm. Below 5 lbm, the limited data suggest that stick frequency is no longer important; there are, however, very few data points in the region of low inertia and low frequency, since this requires an extremely low value of gradient (less than about 0.5 lb/in.). This figure also shows that the cure for a stick with low natural frequency is either to greatly reduce the gradient—possibly producing, for fixed-wing applications at least, a stick with much too little force feedback to the pilot—or to increase the gradient, thereby increasing the natural frequency without changing the inertia.

More work is clearly required before the design guidelines of figure 22 can be adopted into a specification. For example, the region of acceptable gradients is probably higher for fixed-wing airplanes than for helicopters, so there may be separate level 1 and level 2 regions for these different aircraft types. The vast majority of the data on figure 22 is from the helicopter experiments; much more testing (and data gathering from operational aircraft) is necessary for fixed-wings.

Damping Characteristics

The final variable in stick design is damping, b (or, equivalently, ζ_{FS}). The helicopter studies of references 6 and 7 evaluated variations in damping; the pilot ratings from these variations are shown in figure 23 on a plot of damping ratio and natural frequency. It is important to note that for the reference 7 data, stick gradient is also varying (as a function of natural frequency), while for the reference 6 data the gradient was fixed at 1 lb/in.

Figure 23 confirms the lower limit on natural frequency from figure 22; there are very few data points with a combination of low damping and high natural frequency, so it is difficult to set a definite limit on damping. Based on the limited data, however, a potential lower limit may be recommended at $\zeta_{FS} = 0.3$.

ANALYSIS OF PILOT PERFORMANCE DATA FROM NT-33 FLIGHT TESTS

Overview

The sum-of-sines HUD tracking task used in the NT-33 flight test evaluations (ref. 1), in addition to being a well constrained closed-loop evaluation task, enabled the measurement of specific pilot performance parameters. The most interesting of these pilot performance measurements are open-loop, pilot–vehicle describing functions that directly quantify pilot behavior as an integral linear element of the pilot–vehicle control loop. Pilot opinion, in particular, and pilot behavior, in general, may be better understood through careful interpretation of these describing functions.

Because of their potential for yielding valuable information on pilot behavior in-flight, the extraction of open-loop, pilot–vehicle $(Y_p Y_c)$ describing functions from the run time history data and a limited pilot model-based analysis of these were integral parts of this research effort. Emphasis was placed on extracting as many describing functions as allowed by the budget on this contract. Analysis of these $Y_p Y_c$ describing functions using pilot models was limited in scope due to budgetary constraints.

A listing of the flight-test runs and configurations for which describing functions were obtained is presented in table 3. The runs shown in table 3 were chosen on the basis of the pilot opinion study presented previously in this report, and the runs provide a means for logically assessing the effect of flight test parameter variations on pilot performance. Evaluation runs by Pilot A were chosen whenever possible to minimize the effect of interpilot variations in performance. The emphasis on Pilot A was based primarily on this pilot's evaluation of a broader cross section of experimental configurations than the other pilots in the experiment.

In addition to open-loop, pilot–vehicle describing functions, describing functions for the feel system (Y_{FS}) and controlled element (Y_c) dynamics were also extracted from the run time history data. These additional describing functions provided a means of verifying the actual tested controlled element and feel-system dynamics. The methods used to transmit and analyze the experimental time history data are presented in Appendix A. Time histories and describing functions for the open-loop, pilot–vehicle system, feel-system, and controlled element dynamics for all the runs evaluated in this effort are presented in Appendix B.

The pilot model analysis, by nature a time consuming and sometimes iterative procedure, was limited in scope by budgetary constraints. This analysis was confined to a brief investigation on in-flight feel-system–human pilot interactions, designed specifically to complement the pilot opinion study undertaken previously in this report. Following a brief introduction to the pilot modeling procedure and the derived pilot models, this section will continue to address some issues of interest in feel-system–human pilot interactions.

Transfer Function Models of the Pilot–Vehicle System

The pilot model analysis was directed toward obtaining a better understanding of pilot and feel-system interactions, especially their effect on the human pilot neuromuscular mode, observed during the reference 1 flight-test evaluations. A matrix of configurations evaluated using pilot models, together with pilot identifiers and ratings, is shown in figure 24. The configurations shown in figure 24 encompassed only roll time constant, feel-system frequency, and command sensing (force and position) variations with all other parameters fixed except for a few configurations that incorporated a 40-rad/sec command filter (see ref. 1). This command filter is well outside the frequency region of piloted control and had no significant effect on pilot performance.

A subject of particular interest from previous studies (refs. 2, 5, and 20, for example) and therefore of primary focus here is the effect of feel-system frequency on pilot performance with position and force sensing. Specifically, it was hoped that this analysis would shed some light on the question of whether the feel-system lag is altered by the pilot by loop closures around the stick itself. There are two current schools of thought on this issue: (1) The feel system is not altered by the pilot, and therefore it should be noticeable in the open-loop describing function essentially unchanged, as suggested in reference 5; and (2) This lag is compensated by internal pilot loop closures and its adverse effects mitigated, as suggested in references 2 and 20. The basis for such an analysis, however, was compromised because of crucial gaps in the test matrix (fig. 24). There was a particular dearth of data for configurations employing the slow feel system and force sensing, where only two runs exist, and one (configuration 343F(18)) was unusable because of a discontinuity in tracking the SOS disturbance signal (Appendix B).

Despite the shortcomings in the test matrix, the configurations in figure 24 were analyzed in an effort to glean as much information as possible out of the pilot–vehicle describing functions. Details of the pilot modeling procedure, including the assumed pilot models, are outlined in Appendix C. The model–data correspondence can also be assessed through model and describing function data comparisons shown in Appendix C.

The general form of the pilot model used to fit the describing function data is shown in figure 25. In addition to a gain, first-order lead, and time delay, allowance is made in the pilot model for two second-order modes corresponding to the limb–manipulator and possible modified feel-system dynamics. The specific origins of these modes were not investigated because of time and budgetary constraints. A single second-order mode (referred to here as the limb–manipulator mode), together with the pilot lead, time delay, and gain terms, was sufficient in most cases for satisfactorily matching the describing function data (i.e., generally provided the best match, either in terms of a mismatch value, or qualitatively, or both).

A matrix of the derived $Y_p Y_c$ transfer function models, corresponding to the matrix of configurations (fig. 24), is shown in figure 26. The transfer functions are separated into the controlled element (Y_c) and pilot (Y_p) dynamics. The controlled element dynamics in figure 26 are measured values from the describing function data, not the design values reported in reference 1. In most cases, the Y_c differed by that given in reference 1 by a pure time delay. In one case (configuration 143F(18)), an extra second-order mode was required to correctly match the describing function data for Y_c. The first-order lead term in the pilot models generally lies near the aircraft roll mode $(1/T_R)$, suggesting the pilots equalized

the roll dynamics. One second-order mode adequately models the limb–manipulator dynamics in all cases except one (configuration 203P(18), with position sensing, $T_R = 0.25$ sec, and slow feel system), where an additional second-order mode was required for the best fit. The feel-system dynamics do not appear explicitly in any of the Y_pY_c models, suggesting that they are modified by loop closures internal to the human pilot.

The effects of the feel-system dynamics seem to be embodied in the limb–manipulator mode. This mode accounts for the amplitude ratio peaks seen in most of the describing functions and dominates the higher frequency dynamics of Y_pY_c. Analysis of the effects of feel-system dynamics and type of sensing used in the control system is, therefore, concentrated on this mode.

Pilot models were also obtained using the open-loop, pilot–vehicle describing functions for four configurations (configurations A_2, B_2, C_2, and F_2) from the similarly structured fixed-base experiment in reference 5. These models were dynamically similar to those evaluated in the reference 1 experiment; they are equivalent to the fast and intermediate feel-system configurations with the low T_R in reference 1 (fig. 24). The resulting pilot models and controlled elements are shown in figure 27. These data enabled a limited evaluation of pilot behavior in the fixed-base and flight environments.

Effect of Feel-System Frequency on Y_pY_c

Position Sensing—The effect of feel-system frequency on the overall pilot–vehicle system was assessed for the intermediate and high T_R configurations using stick position sensing and the models from the describing function data for Pilot A. The locations of the limb–manipulator modes (from fig. 26) for all the configurations analyzed (including those for comparable configurations from the ref. 5 fixed-base simulation) are shown on a complex-plane plot (real and imaginary) in figure 28. Shown also in figure 28 are the open-loop, feel-system dynamics from the reference 1 experiment. For most of the configurations, the frequency and damping of this limb–manipulator mode are comparable to those observed in the fixed-base simulation of reference 5. This mode is also in the region of observed roll ratchet (e.g., ref. 4).

For the position-sensing configurations, figure 28 shows a consistent shift of the limb–manipulator mode to a lower frequency when the slow feel system is included in the configuration. The frequency response comparisons, figures 29 and 30, show that this shift in the limb–manipulator mode to a lower frequency causes additional phase lag at higher frequency (around 10 rad/sec) that is approximately equivalent to the difference in the feel-system phase lags when taken independently. Hence, though the feel-system dynamics are not explicitly present in the Y_pY_c model, their effects seem to be incorporated into the limb–manipulator mode, and thereby affect the open-loop, pilot–vehicle dynamics.

The damping of the limb–manipulator mode is low (fig. 26), and relatively minor variations in the damping ratio cause dramatic differences in the amplitude ratio peaking tendency of the Y_pY_c frequency response (figs. 29 and 30). This peaking is the most probable reason for roll ratchet encountered in this experiment, and will be discussed later.

The additional phase lag caused by the slower feel-system dynamics is evident (figs. 29 and 30) in the higher frequency open-loop, pilot–vehicle transfer characteristics. There is little difference in

the Y_pY_c phase curve in the region of crossover for the different configurations. The added phase lag and associated steeper roll-off of the phase curve at frequencies higher than the crossover frequency will cause the closed-loop performance of the pilot–vehicle system for the slow-feel-system case to be particularly sensitive to pilot gain. Such adverse changes in closed-loop performance, with pilot gain variations that are inevitable during the course of a run, can be expected to degrade pilot opinion.

Based on this limited evidence, the inclusion of the feel-system equivalent time delay in time delay computations for handling qualities evaluation purposes seems to be justified when stick position sensing is employed. The actual delay in the open-loop, pilot–vehicle system is not directly related to the open-loop, feel-system dynamic lag; but the change in characteristics of the limb–manipulator mode with feel-system characteristics seems to have a roughly equivalent effect on the open-loop, Y_pY_c system.

Results for the two equivalent position sensing runs from the fixed-base experiment (ref. 5) are very similar: the limb–manipulator mode migrates to a considerably lower frequency with the equivalent intermediate feel system when compared with the fast feel system (diamond symbols on fig. 28).

Force Sensing—An equivalent comparative evaluation was performed for the force-sensing configurations. Unfortunately, as stated earlier, this evaluation was compromised by the lack of experimental data for force-sensing configurations (fig. 24). The primary comparisons that can be made, at the low and high values of T_R, are shown in figures 31 and 32.

Comparison of the configurations for the high T_R (fig. 31) is complicated by inter-pilot differences. The fast and slow feel-system configurations were evaluated by Pilot B, while the intermediate feel-system configuration was evaluated by Pilot A. The Y_pY_c dynamics for Pilot A differs considerably from those for Pilot B (fig. 31). Interpilot differences such as this merit some investigation, but were not possible in this limited analysis. It is, however, an interesting subject for further study, as there are several configurations that have been evaluated by more than one pilot.

The difference between the Y_pY_c's for the fast and intermediate feel systems at the high T_R (both Pilot A), shown in figure 32, is minor. The frequencies of the limb–manipulator modes for these two configurations are similar (fig. 26). Comparison of the Y_pY_c's for the fast and slow feel systems (both Pilot B) for the low T_R configurations in figure 31 shows a greater phase slope (roll off) at frequencies immediately higher than the -180 deg frequency for the slow feel system. This greater degree of phase roll off is primarily because of the movement of the limb–manipulator mode to a lower frequency for the slow feel system (see fig. 26). The ability to draw any definitive conclusion about the effect, when force sensing is employed, of the feel-system lags on pilot performance is clouded because both evaluations in figure 31 were made by Pilot B, whose ratings show greater variability when compared with the other pilots (discussed previously), and also because the controlled element, as evidenced by the describing function, was considerably different from that reported for that configuration (see Appendix B).

The Y_pY_c for the slow feel-system configuration in figure 31 (also see transfer function in fig. 26) points to the possibility that even though force sensing is employed (theoretically excluding the feel-system dynamics from the loop), the limb-manipulator mode can be adversely affected by slow feel-system dynamics. This effect, caused by the movement of the limb–manipulator mode to a lower frequency with the slow feel system, appears to cause a phase lag in the open-loop, pilot–vehicle

24

system roughly equivalent to that which could be anticipated when position sensing is employed. This effect is possibly caused by the encroachment of the feel-system dynamics on the crossover frequency for the task, near the human pilot neuromuscular dynamics. Further evidence for this hypothesis is the relative indifference of the Y_pY_c's in figure 32, where the intermediate and fast feel systems—both at frequencies considerably greater than either the crossover frequency or the pilot's neuromuscular system frequencies—have little effect on the overall open-loop, pilot–vehicle dynamics.

Results from the two equivalent force sensing runs from the reference 5 fixed-base experiment also show the limb–manipulator mode moving to a lower frequency with the lower frequency (intermediate) feel-system. The mode is not observable for the fast feel-system configuration (fig. 27), and is probably at a greater frequency than that covered by the describing functions.

Effect of Force and Position Sensing on Y_pY_c

It has been generally recognized (e.g., refs. 5 and 6) that the primary advantage of force sensing over position sensing is the absence of the feel-system dynamics in the forward loop. This results in less phase lag in the overall pilot–vehicle loop and, therefore, better closed-loop performance when force sensing is used (ref. 5).

Comparisons of the Y_pY_c models for force as a function of position sensing for the high T_R configurations are shown in figures 33 and 34 for the fast and intermediate feel systems, respectively. Added phase lag is observed at frequencies immediately above crossover for the position sensing configurations in both cases. This added phase lag is caused by the lower frequency of the limb–manipulator mode when position sensing is employed (see fig. 26). The movement of the limb–manipulator mode with changes in the feel-system dynamics has a similar effect, in a limited frequency region of Y_pY_c, to that of the added feel-system dynamics. The effect of this added phase lag on pilot performance and opinion is minimal, because of the relatively high-frequency dynamics of the fast and intermediate feel systems that do not seem to encroach on the neuromuscular dynamics or region of piloted control.

Roll Ratchet

The results of the fixed-base experiment reported in reference 4, using a limited displacement, force sensing stick, suggested that the roll ratchet phenomenon is a closed-loop interaction of the pilot's neuromuscular system with the airframe and manipulator dynamics. Specifically, ratchet tendency was linked to the peaking of the limb–manipulator mode. The flight-test data from reference 1, where roll ratchet was experienced with several configurations (see discussion at the end of section entitled "EFFECTS OF FEEL-SYSTEM DYNAMICS ..."), provides an excellent basis to validate this hypothesis.

A review of the pilot comments for the sum-of-sines HUD tracking task (ref. 1) for all the runs listed in table 2 enabled the majority of those runs to be divided into three groups: (1) Those where roll ratchet is specifically mentioned in the pilot comments, (2) those where mention is made of a PIO, incipient PIO, or probable PIO, and (3) those that received level 1 pilot ratings with no comments related to PIO or ratchet. The actual Y_pY_c describing function data (as opposed to the models for these data, as in previous plots) for the three groups are shown in figures 35, 36, and 37, respectively. Shown also in figures 35 through 37 are amplitude ratio and phase curves drawn through the approximate mean

amplitude ratio and phase values at each frequency. An important factor is that all the runs in figure 35 (ratchet cases) are by Pilot A, while those in figure 36 (PIO cases) are primarily by pilots B and C with only one run by Pilot A (see table 2). The amplitude ratio peaking is clearly greater for the runs where roll ratchet was encountered during the SOS tracking task (fig. 35) when compared with that for runs where no ratchet or PIO was encountered (fig. 37). The greatest differences in the describing functions between runs are in the PIO or probable PIO runs of figure 36. Some of these describing functions have the characteristics of the ratchet describing functions in figure 35, while the rest are similar to the no-PIO, no-ratchet runs in figure 37. These differences in figure 36 may be attributed to differences in pilot interpretation of ratchet and PIO.

Selected 20-sec segments of the stick force time histories for the ratchet configurations of figure 35 are shown in figure 38. The approximate frequencies of the ratchet are also shown in figure 38. The approximate ratchet frequencies correspond to the frequencies of the amplitude ratio peaks in figure 35. Note, in particular, that the higher frequency oscillation (when compared with the other ratchet cases) for configuration 201P(18) + 55 (approximately 12.6 rad/sec) in figure 38 corresponds to the higher frequency amplitude ratio peak seen in figure 35. This correlation between the frequency of the amplitude ratio peaking in $Y_p Y_c$ and the closed-loop ratchet frequency provides strong evidence that the limb–manipulator mode is a primary cause of the roll ratchet observed in this experiment.

None of the describing functions for the ratchet runs in figure 35 show a limiting stability condition, i.e., zero gain and phase margin, which would indicate the presence of a continuous closed-loop limit cycle. As mentioned in reference 1, roll ratchet is a time-varying, nonstationary phenomenon that would be expected to be related to pilot gain and compensation variations during the course of the run. The describing function assumes consistent (stationary) pilot dynamics, and is a measurement of the mean or average pilot behavior throughout the run. As a result, subtle variations in pilot gain and compensation during the course of the run, that could be sufficient to cause ratchet for a time, would not be seen in the averaged pilot behavior over the whole run. Episodes of ratchet in the course of the run would be short in duration, as the pilot would immediately change his control strategy upon encountering ratchet to minimize its effects. Analysis of specific sections of a run to define the variations in pilot behavior throughout the course of the run would shed further light on this subject but was beyond the scope of this study. The significant amplitude ratio peaking caused by the limb–manipulator mode comes through strongly in the describing functions for the ratchet cases, and indicates that this was consistent throughout the run. This, in turn, indicates that there was little the pilot could do to modify this characteristic for these cases.

Fixed-Base and Flight-Data Comparison

Four configurations from the similarly structured fixed-base experiment have directly comparable counterparts in the flight-test experiments of reference 1. These are the low T_R, fast and intermediate feel-system configurations with force and position sensing (configurations A_2, B_2, C_2, and F_2 - ref. 5). There is only a minor difference in the frequencies of the intermediate feel systems (14 rad/sec in ref. 5 and 13 rad/sec in ref. 1). The bandwidths and rms magnitude of the SOS disturbance signals were similar in these two experiments (see the statement of problem). Of the directly comparable flight-test configurations (ref. 1), only two, the fast and intermediate feel systems with force sensing, were evaluated (configurations 141F(18) and 142F(18), fig. 24).

The $Y_p Y_c$ describing functions for the fast and intermediate feel system, low T_R, force-sensing configurations from the flight tests are compared with their fixed-base counterparts in figures 39 and 40. The primary difference between the fixed-base and flight data is the higher crossover frequency achieved in the fixed-base experiment. There is also considerably less amplitude ratio peaking and associated phase lag in the fixed-base data.

The greater peaking of the limb–manipulator mode in the flight tests is probably due to the interaction of the aircraft motion with the limb–manipulator dynamics. The higher gains (and therefore crossover frequency) seen in the fixed-base data are most likely caused by the lower phase margins that could be tolerated on the fixed-base simulation where, as a result of the lack of motion cues, an impending instability is sometimes difficult to distinguish. Overall, the pilots exhibit broadly similar behavior in flight and on the fixed-base simulator for the few cases evaluated here.

CONCLUSIONS AND RECOMMENDATIONS

Effects of Feel-System Dynamics on Handling Qualities

This limited study has reviewed the results of the Calspan flight tests of reference 1, along with other recent feel-system experiments, in an attempt to define the fundamental effects of feel-system dynamic characteristics on handling qualities. Analysis of basic handling qualities ratings (HQRs) and more involved investigation of pilot–vehicle describing-function factors have revealed several important conclusions about the importance of feel systems. Unfortunately, several very large gaps also exist in the database, resulting in areas where more questions have been raised in this study.

Based on the analysis of pilot rating data, the following conclusions can be drawn:

- Only a limited number of cases from the original work by Smith and Sarrafian (ref. 2), involving offset landings with a position-sensing controller, were reevaluated in reference 1. Based on the few cases that were reevaluated and that were flown by the same pilot in both experiments, it appears that the results are more or less consistent, i.e., that the HQRs correlate better with overall time delay if the feel system is not included in the computation of that delay. For a second pilot in the reference 1 experiment, the results are exactly the opposite.

- Reference 1 included a stick with a feel-system frequency well below the two frequencies evaluated in the initial reference 2 study. For both pilots in the reference 1 experiment flying the offset landing task, this feel system had a decidedly degrading effect on their HQRs—an effect that is better represented by equivalent time delay if the feel-system dynamics are included in that delay.

- For up-and-away tasks in reference 1, the HQRs for the two pilots were consistent and generally correlate with equivalent time delay resulting from inclusion of the feel system.

- The HQRs from Pilot A, for offset landings in both the reference 2 flight and the reference 1 NT-33 study, remain an enigma that are not explainable without further analysis of the maneuver data. Pilot A's opinions were clearly consistent across two airplanes and several different configurations, yet these rating trends differ considerably from those of Pilot C in the reference 1 study, from Pilot A's own ratings in the up-and-away evaluations, and from the equivalent-time-delay criteria.

- In general, the best correlation with the time-delay requirements was found when the feel-system dynamics were included in the delay measurement regardless of the command reference. This is a radical departure from past approaches, which have been twofold: (1) Don't include the feel system at all (i.e., reference all time-delay computations to control position only, and since the feel system is in parallel for a force-sensing controller, it is not picked up in the measurement), and (2) Include the feel system only for position-command systems (i.e., reference all time-delay computations to control force, and since the feel system is upstream of the force pickoff for force-sensing controllers, it is not included). In the past, concerns about whether to include or exclude the feel system in evaluations against various handling qualities criteria have been minimized by two major factors: (1) Feel-system dynamics are usually fixed for all evaluations in a particular experiment, and so have a constant effect; and (2) The feel systems for most experiments have typically been very good, with moderate damping and high natural frequencies, so their overall contributions have been minor.

- The effect of feel-system dynamics on pilot opinion are not equivalent to just adding pure time delay; the characteristics of a sluggish feel system bear no resemblance to high time delay. The overall effect on pilot *ratings*, however, is reasonably similar to that caused by an equivalent amount of time delay, and a large value of equivalent delay is a sign of handling qualities problems—but not a sign of the source of those problems.

- The overall effect on pilot opinion of slow feel systems is different for force-sensing than for position-sensing systems. As a result, there are some signs of pilot preference for force-sensing controllers as long as the overall dynamics are acceptable. As a first cut, however, it may be assumed that the effect on handling qualities of the feel system for force-sensing controllers is adequately described by including the dynamics of the controllers in the computation of equivalent time delay.

- The location of second-order lags in the total aircraft system is relatively unimportant in terms of HQRs. That is, switching two second-order filters between the stick and a command element downstream of the stick produces relatively little change in pilot ratings. The data for operation with a very slow stick, however, are limited to the helicopter study of reference 6 and should be repeated on the Calspan NT-33. (In the identification system of reference 1, this would consist of configuration 213F(K) compared with 231F(K) and 213P(K) compared with 231P(K), where it is recommended that the command sensitivity, K, be selected by the pilot.)

- Roll ratchet on the NT-33 is directly related to the use of excessive roll command–response sensitivities (in terms of deg/sec/lb) with highly responsive airplane dynamics. The study of reference 1 used fixed sensitivities for up-and-away evaluations of 10 and 18 deg/sec/lb; in a past study where the pilots were allowed to select their sensitivities (ref. 18), a much lower value was chosen for a similar highly responsive configuration and level 1 HQRs were assigned. Many of the problems attributable to high roll inverse time constant may, in fact, be due much more to the high response sensitivity.

Design Configurations

Based on the data analyzed in this report, an acceptable feel system is attainable as long as the effective stick natural frequency is above 10 rad/sec, or the effective mass is less than 5 lbm, with a stick damping ratio above 0.3. More detailed design guidelines require much more experimental data.

Assessment of Human-Operator Dynamics

An attempt was made in this study to research in depth the fundamental characteristics of the human pilot to explore such issues as command sensing (force as a function of position) and feel-system frequency effects. Unfortunately, this was not entirely possible with the reference 1 data. First, several important combinations of sensing, stick frequency, and airplane dynamics were not evaluated at all (e.g., position sensing with the highest roll mode inverse time constant and force sensing with the intermediate inverse time constant). Second, in some cases, even where a comparison is possible, it is not for the same pilot, thus introducing an additional variable. And third, the use of a low-bandwidth forcing function for the sum-of-sines command in the early flights means that these data cannot be compared with the later flights. The following conclusions and observations are based on the limited data that could be extracted from the reference 1 flights.

• Extraction of describing functions from the sum-of-sines tracking task was feasible, and reasonably good data were obtained. It was possible to get not only pilot–vehicle describing functions but also describing functions to verify the aircraft and feel-system dynamics. This technique should be actively pursued in future flight testing as a method to ensure that the desired configuration has been evaluated.

• Most of the describing functions exhibit a low- to moderately-damped peak in the frequency response, corresponding to the expected limb–manipulator mode seen in fixed-base simulations (e.g., refs. 4 and 5). The frequency of this mode, based on pilot modeling matches to the describing-function data, is generally around 12 rad/sec for the fast and intermediate stick frequencies, reducing to about 8-10 rad/sec for the slowest stick (the 8-rad/sec stick). The best pilot models were obtained when only this one second-order mode was included in the model, thus implying that this mode is indeed a modified stick-arm-neuromuscular mode.

• The reduction in frequency of the limb–manipulator mode for the slowest feel system was observed with both force and position sensing. This reduction in frequency causes added phase lag in the open-loop, pilot–vehicle system that is detrimental to pilot performance and opinion, and is equivalent to the added phase lag of the slow feel system. This suggests that even though the feel system is theoretically a parallel element when force sensing is employed, its dynamics still affect the open-loop, pilot–vehicle dynamics through variations in the frequency and damping of the limb–manipulator mode. This observation is based on the data for only one run for the slow feel system with force sensing; more data are required to enable a definitive conclusion to be drawn.

• When position sensing is used, the added feel-system lag appears in the open-loop, pilot–vehicle through variations in the pilot limb–manipulator mode dynamics. The added lags are not the same as but are equivalent to adding the open-loop feel system to the open-loop, pilot–vehicle system.

• For the few cases where a force and position sensing comparison was possible, there was a consistent reduction in the frequency of the limb–manipulator mode with corresponding added phase lag at lower frequency with position sensing. This effect was minor for the cases that could be compared, and had no significant effect on pilot opinion.

• The describing functions for runs in which roll ratchet was noted by the pilots showed significantly greater peaking at the limb–manipulator mode frequency, when compared with those where no ratchet was noted. The frequency of these peaks corresponded approximately to the frequency of

the closed-loop ratchet observed in the time histories. This provides strong flight evidence that roll ratchet is caused by interactions between the pilot's neuromuscular system and the aircraft–feel-system dynamics, a hypothesis previously constructed based on fixed-base experimental data.

● Comparison of open-loop, pilot–vehicle describing functions for the flight data with those for the similarly structured fixed-base experiment was possible for only two cases (fast and intermediate feel systems). These showed that greater crossover frequencies were achieved in the fixed-base experiment. There was also greater peaking with added phase lag in the flight-test data caused by the limb–manipulator mode.

REFERENCES

1. Bailey, R.E. and L.H. Knotts, *Interactions of Feel System and Flight Control System Dynamics on Lateral Flying Qualities*, NASA CR-179445, 1990.

2. Smith, Rogers E. and Shahan K. Sarrafian, "Effect of Time Delay on Flying Qualities: an Update," *J. Guidance, Control, and Dynamics*, Vol. 9, No. 5, Sept.–Oct. 1986, pp. 578-584.

3. McRuer, D.T. and E.S. Krendel, *Mathematical Models of Human Pilot Behavior*, AGARD AG-188, Jan. 1974.

4. Johnston, D.E. and D.T. McRuer, *Investigation of Interactions Between Limb-Manipulator Dynamics and Effective Vehicle Roll Control Characteristics in Roll Tracking*, NASA CR-3983, 1986.

5. Johnston, Donald E. and Bimal L. Aponso, *Design Considerations of Manipulator and Feel-System Characteristics in Roll Tracking*, NASA CR-4111, 1988.

6. Watson, Douglas C. and Jeffrey A. Schroeder, "Effects of Stick Dynamics on Helicopter Flying Qualities," AIAA-90-3477-CP, presented at the AIAA Guidance, Navigation and Control Conference, Portland, OR, Aug. 1990.

7. Morgan, J. Murray, "An Initial Study Into the Influence of Control Stick Characteristics on the Handling Qualities of a Fly-By-Wire Helicopter," presented at the AGARD Flight Mechanics Panel Symposium on Flying Qualities, Quebec City, Canada, Oct. 1990.

8. Cooper, George E. and Robert P. Harper, Jr., *The Use of Pilot Rating in the Evaluation of Aircraft Handling Qualities*, NASA TN D-5153, 1969.

9. *Military Specification – Flying Qualities of Piloted Airplanes*, MIL-F-8785C, Nov. 1980.

10. Hoh, Roger H., David G. Mitchell, Irving L. Ashkenas, R.H. Klein, R.K. Heffley, and J. Hidgkinson, *Proposed MIL Standard and Handbook – Flying Qualities of Air Vehicles. Volume II: Proposed MIL Handbook*, AFWAL-TR-82-3081, Vol. II, Nov. 1982.

11. *Military Standard, Flying Qualities of Piloted Vehicles*, MIL-STD-1797 (USAF), Mar. 1987.

12. *Military Standard, Flying Qualities of Piloted Vehicles*, MIL-STD-1797A, Jan. 1990.

13. *Handling Qualities Requirements for Military Rotorcraft*, U.S. Army Aeronautical Design Standard, ADS-33C, Aug 1989.

14. *Military Standard, Helicopter Flying and Ground Handling Qualities, General Requirements for*, MIL-STD-XXXX (Proposed), Oct. 1990. (Available through US Army Aviations Systems Command, St. Louis, Missouri.)

15. Neal, T. Peter, and Rogers E. Smith, *An In-Flight Investigation to Develop Control System Design Criteria for Fighter Airplanes*, AFFDL-TR-70-74, Volume I, Dec. 1970.

16. Smith, Rogers E., *Effects of Control System Dynamics on Fighter Approach and Landing Longitudinal Flying Qualities*, Volume I, AFFDL-TR-78-122, Mar. 1978.

17. Monagan, Stephen J., Rogers E. Smith, and Randall E. Bailey, *Lateral Flying Qualities of Highly Augmented Fighter Aircraft*, AFWAL-TR-81-3171, June 1982.

18. Meeker, James I. and G. Warren Hall, *In-Flight Evaluation of Lateral-Directional Handling Qualities for the Fighter Mission*, AFFDL-TR-67-98, Oct. 1967.

19. Mitchell, David G. and Roger H. Hoh, "Influence of Roll Command Augmentation Systems on Flying Qualities of Fighter Aircraft," *J. Guidance, Control, and Dynamics*, Vol. 7, No. 1, Jan.-Feb. 1984, pp. 99-105.

20. Hess, Ronald A., "Analyzing Manipulator and Feel-System Effects in Aircraft Flight Control," *IEEE Transactions on Systems, Man, and Cybernetics*, Vol. 20, No. 4, July/Aug. 1990, pp. 923-931.

APPENDIX A

TRANSFER OF TIME HISTORIES AND EXTRACTION OF DESCRIBING FUNCTIONS FROM CALSPAN DATA

Data Transcription and Reduction

The raw experimental time-history data from the relevant flights of reference A-1 was loaded onto the mainframe computer (the ELXSI) at NASA DFRF by NASA personnel. The data could be read, inspected, and rewritten in whole or in part via the THPLOT and GETDATA (ref. A-2) software available on the ELXSI. Access to the ELXSI was obtained via phone modem through an account setup for STI use. A PC version of GETDATA and THPLOT, also provided to STI by Mr. Richard E. Maine of NASA, proved to be of great value in transcribing the data to a format compatible with STI's frequency domain analysis software.

Following is a brief summary of the procedure for extracting and transmitting the appropriate run-time history data to a PC at STI. Run-time histories were available for a whole flight (consisting of several runs) with 28 signals stored at a 100-Hz sample rate.

1. Use GETDATA on ELXSI to create a binary file of a total flight record at a very low sample rate (1 per second).

2. Transmit this file to a PC at STI using KERMIT data transmission protocol.

3. Examine this file using the PC version of THPLOT, and determine approximate start and end times of runs required for analysis.

4. Use GETDATA on ELXSI to create binary files of the required run time histories (ascertained in (3) above) with the appropriate signals. As a 100-Hz sample rate is a greater accuracy than that required for this analysis, these files were decimated to have an equivalent sample rate of 20 Hz.

5. Transmit these files to a PC at STI, and convert from binary to ASCII using the PC version of GETDATA.

Following conversion to ASCII, these files were read into STI's frequency domain analysis software (ref. A-3), which generated describing functions of various components within the control loop using an advanced fast Fourier transform algorithm.

Example Configuration

An evaluation from Flight 4069 was chosen to illustrate the data extraction methods. Evaluation 3 of Flight 4069 (configuration 141F(10), Pilot A) was selected because of the availability of the open-loop pilot–vehicle describing function from Calspan's analysis of this run in reference A-1.

The compensatory HUD tracking task loop structure is shown in figure A-1, where Y_p represents the pilot dynamics and Y_c represents the controlled element. Shown also in figure A-1 is a list of the

32

signals brought down to STI for analysis. Figure A-2 shows the controlled elements for the configuration being considered.

Time histories of some signals for the SOS tracking run in Flight 4069-3 are shown in figure A-3. The data are continuous with no disruptions or undue noise. The power spectrum of the SOS disturbance input (PHIC) is shown in figure A-4. The 13 sine wave components (shown circled in fig. A-4) of the disturbance input are clearly seen above the residual noise and closely correspond in frequency and shape (bandwidth) to that reported in reference A-1.

The signal-to-noise ratio of the roll rate signal (P) was much better than that of roll attitude (PHI), so open-loop pilot–vehicle (Y_pY_c, fig. A-1) describing functions were extracted using roll rate (i.e., P/PHIE was obtained). Amplitude ratio and phase corrections for a pure integrator were then applied to give the PHI/PHIE describing functions used in this report. The describing function for configuration 141F(10) evaluated at the 13 sine-wave component frequencies is shown in figure A-5 (circles). Shown also in figure A-5 are the equivalent describing function points from reference A-1 (squares). The good agreement between the measured and published describing functions seen in figure A-5 increases confidence in the data transmission and analysis procedure.

There is a slight difference in the frequencies of the 13 sine-wave components obtained from this analysis and those extracted from reference A-1 (fig. A-5). The exact frequencies of the sine-wave components used in the reference A-1 experiment are not published and the frequencies shown in figure A-5 are approximate values extracted from a figure in reference A-1. The sine-wave component frequencies obtained through careful analysis of the disturbance signal PHIC (see fig. A-4) are slightly different from those extracted from reference A-1, but are used throughout this report because of the greater confidence that could be placed in them following the evidence in figure A-4.

Using the time-history data, it is possible to verify that the feel-system dynamics and aircraft dynamics were correctly implemented. The describing function for the stick dynamics shown in figure A-6 agrees very closely with the published stick dynamics for configuration 141F(10) (fig. A-2), shown in figure A-6 as solid lines. The describing function for the controlled element (roll rate–stick force) shown in figure A-7, however, differs from the published controlled element dynamics (fig. A-2), shown by solid lines in figure A-7. A simple, nonoptimized model fit to the controlled element describing function data, shown in figure A-8, shows that the actual model had a roll time constant of approximately 0.1 sec and an overall time delay of approximately 80 msec, as opposed to the reference A-1 values of 0.15 sec and 40 msec, respectively.

References

A-1. Bailey, R.E. and L.H. Knotts, *Interactions of Feel System and Flight Control System Dynamics on Lateral Flying Qualities*, NASA CR-179445, 1990.

A-2. Maine, Richard E., *Manual for GETDATA Version 3.1*, NASA TM-88288, 1987.

A-3. Myers, T.T., B.L. Aponso, D.H. Klyde, et al., *FREDA Version 1.4 User's Guide*, Systems Technology, Inc., 1988.

APPENDIX B

COMPILATION OF RUN TIME HISTORIES AND DESCRIBING FUNCTIONS

This appendix contains the run-time histories and extracted describing functions for all the experimental runs analyzed in this research effort. All the runs analyzed were for the SOS tracking task from the NT-33 flight test experiment (ref. 1). A list of the runs analyzed is provided in table 2 of the main text. Methods of data transmission and describing function extraction are explained in Appendix A.

The data are presented by run sequence. For each run, the data presented consist of 1) experimental time histories, 2) describing function for the controlled element (Y_c), 3) describing function for the feel system (Y_{FS}), and 4) describing function for the open-loop pilot–vehicle (Y_pY_c).

The experimental time-history data have an equivalent sample rate of 20 Hz (see Appendix A). The signals shown on the time history plots are stick position (DAS, in units of in.), stick force (FAS, lb), roll rate (P, deg/sec), roll attitude tracking error (PHIE, deg), and roll sum-of-sines disturbance command (PHIC, deg). The describing functions for the controlled element are roll rate (P, deg/sec) referenced to either stick force (FAS, lb) or stick position (DAS, in.), as appropriate. Describing functions for the feel-system dynamics are stick position (DAS, in.) referenced to stick force (FAS, lb). Describing functions for Y_pY_c are roll attitude (PHI, deg) referenced to roll error (PHIE, deg).

Transfer function model responses for Y_c and Y_{FS} are shown superimposed on the describing functions plots. The transfer functions are also displayed. Transfer functions are shown in shorthand notation, as follows,

$$(a) \equiv (s + a)$$

$$[\zeta; \ \omega] \equiv \left(s^2 + 2\zeta\omega s + \omega^2\right)$$

with time delays represented by second-order Padé approximations. In most cases, these transfer functions for Y_c are the same as those presented in reference 1. In a few cases, the transfer functions have been slightly modified (considerably in the case of run 4154-5) from those presented in reference 1 to better reflect the controlled element dynamics as indicated by the describing functions.

APPENDIX C

PILOT MODELS

A pilot modeling analysis was performed on a selected subset of the open-loop pilot–vehicle (Y_pY_c) describing functions presented in Appendix B and on a few Y_pY_c describing functions from the fixed-base simulation discussed in the main text. A brief description of the modeling process is presented in this appendix together with model–data comparison plots.

The closed-loop pilot–vehicle system was assumed to be of the form shown in figure C-1. The pilot was represented by a dynamic element consisting of a lead-lag, pure gain, pure time delay, and a second-order neuromuscular mode. Open-loop Y_pY_c transfer function models were matched to the describing function data using STI-developed optimization software (Program MFP). All the dynamic elements attributed to the pilot were allowed to vary in the optimizing procedure. An additional unknown element was the feel-system dynamics, that, for the case of position sensing, could appear in the pilot–vehicle model in one of three forms: 1) unchanged (i.e., fixed at the experimental value), 2) modified by loop closures internal to the pilot's neuromuscular system to a new value of damping and frequency, or 3) nonexistent (i.e., the arm and manipulator are effectively a single dynamic element, with the second-order neuromuscular mode in the pilot model representing a combined limb–manipulator mode). These variances represent different points of view on the subject of pilot–feel-system interactions, as discussed in the main text of the report.

Based on these three hypotheses, three forms of transfer-function models were matched to each describing function: 1) feel-system dynamics fixed, 2) feel-system dynamics free, and 3) no feel-system dynamics at all. It was unnecessary in most cases to go through the procedure for all three models, as the results for one would make obvious the possibilities of success using the others. The best fit in terms of mismatch, and visual inspection, was chosen as the representative Y_pY_c model. The highest frequency describing function data point (amplitude ratio and phase) was omitted from consideration in the optimization procedure. This highest frequency data point is adversely affected by noise because of the low input power at that frequency (see input power spectrum in Appendix A). The lowest frequency data point is also adversely affected by noise because of the low power (typically) of the tracking error signal; so, this point is also omitted from the analysis for a few cases.

As stated in the main text of this report, the single limb–manipulator mode pilot model proved to be the best model, in terms of model–data correlation, for all cases considered. The extracted pilot models for the flight-test and fixed-base data are presented in the main text of this report. Model–data correlations of Y_pY_c for the flight-test cases are presented in figures C-2 through C-12, and those for the fixed-base cases are presented in figures C-13 through C-16.

35
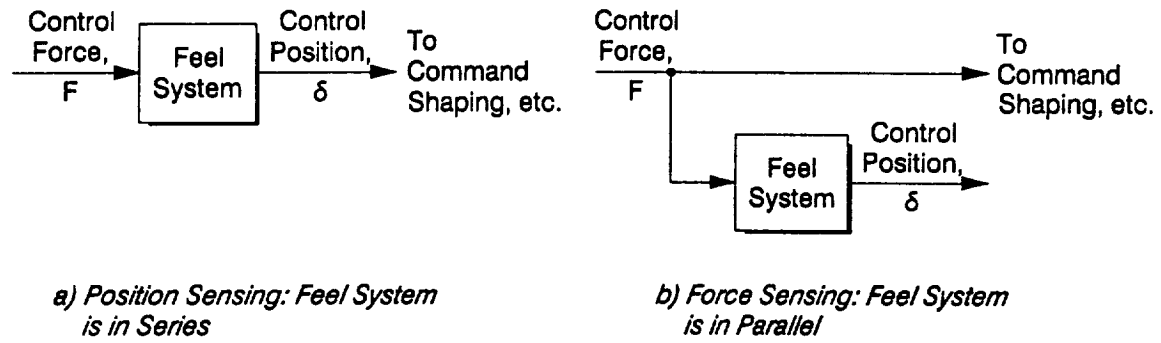
Figure 1. Mechanization of Feel Systems
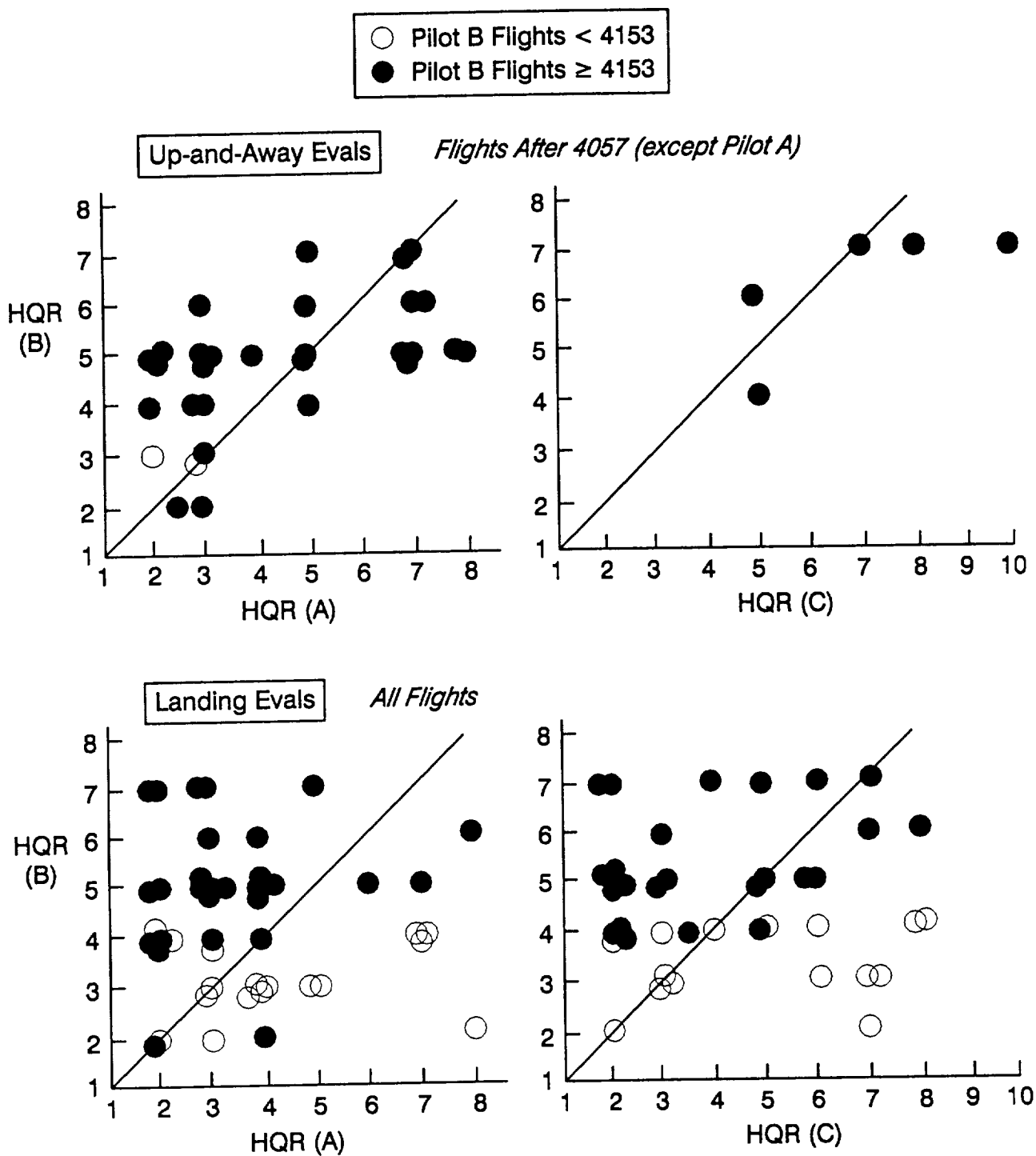
Figure 2. Interpilot Rating Comparison — Pilot B vs. Pilots A and C
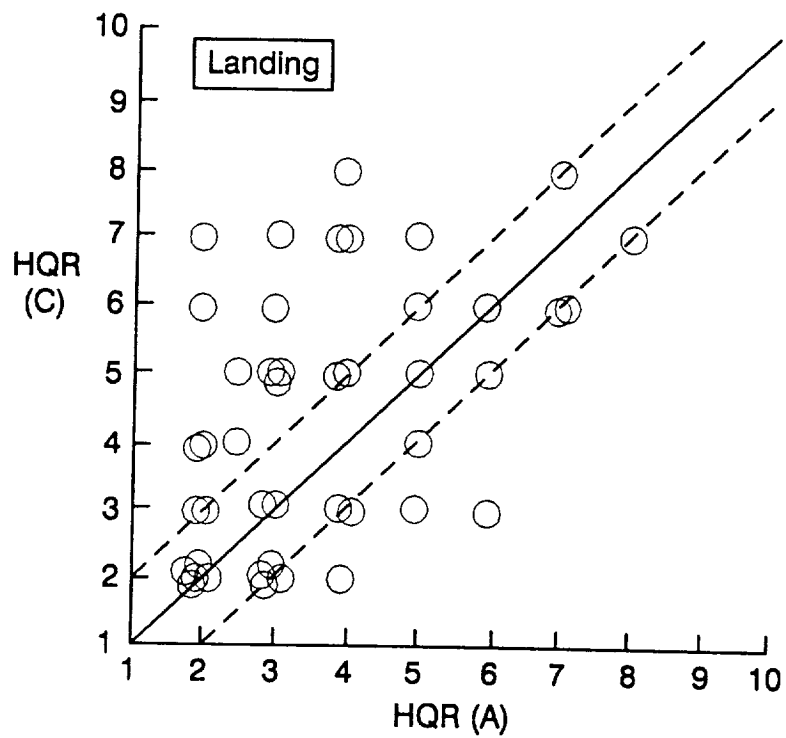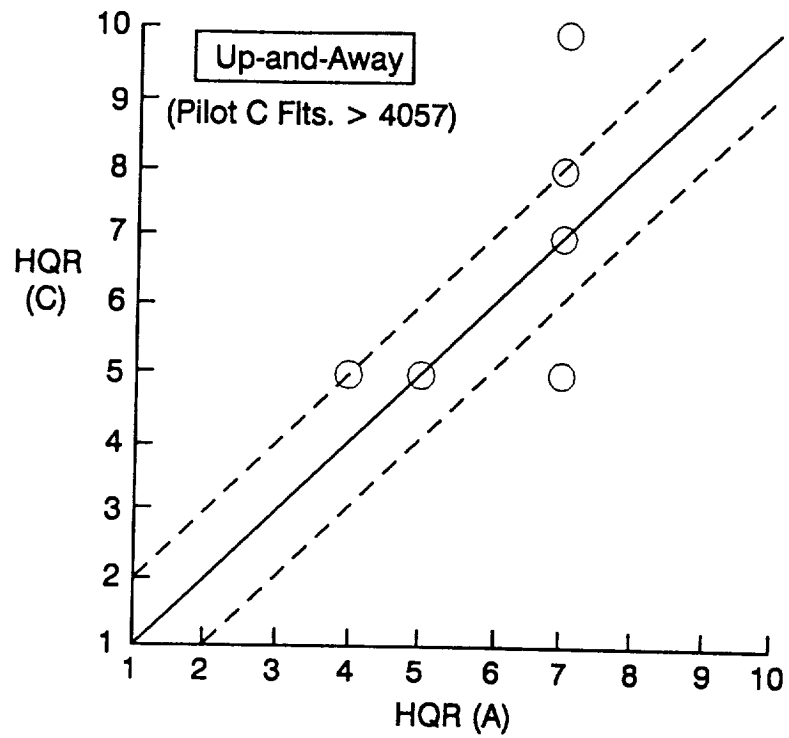
Figure 3. Interpilot Rating Comparison — Pilot A vs. Pilot C
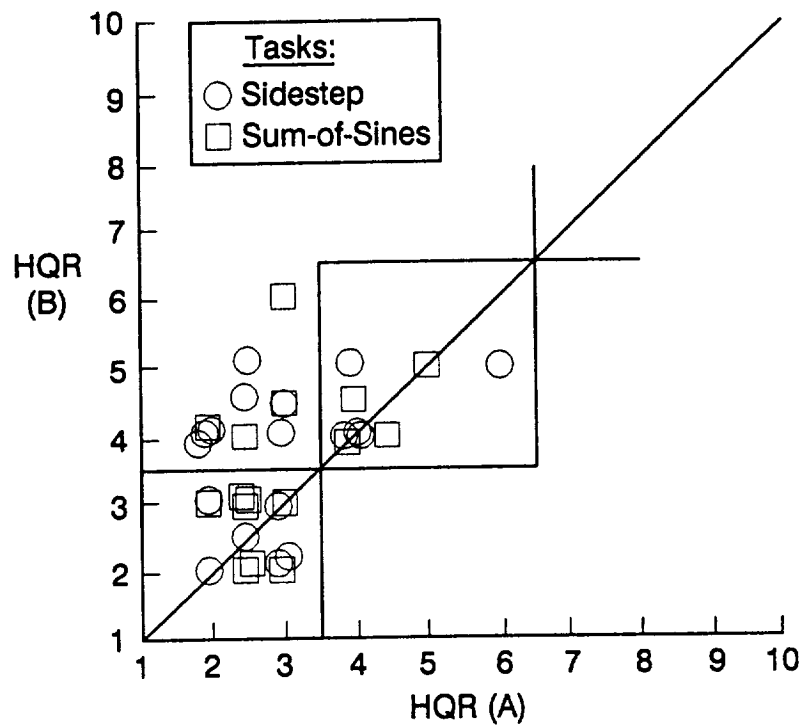
Figure 4. Interpilot Rating Comparisons for Two Tasks
from Ref. 7 Feel System Experiment
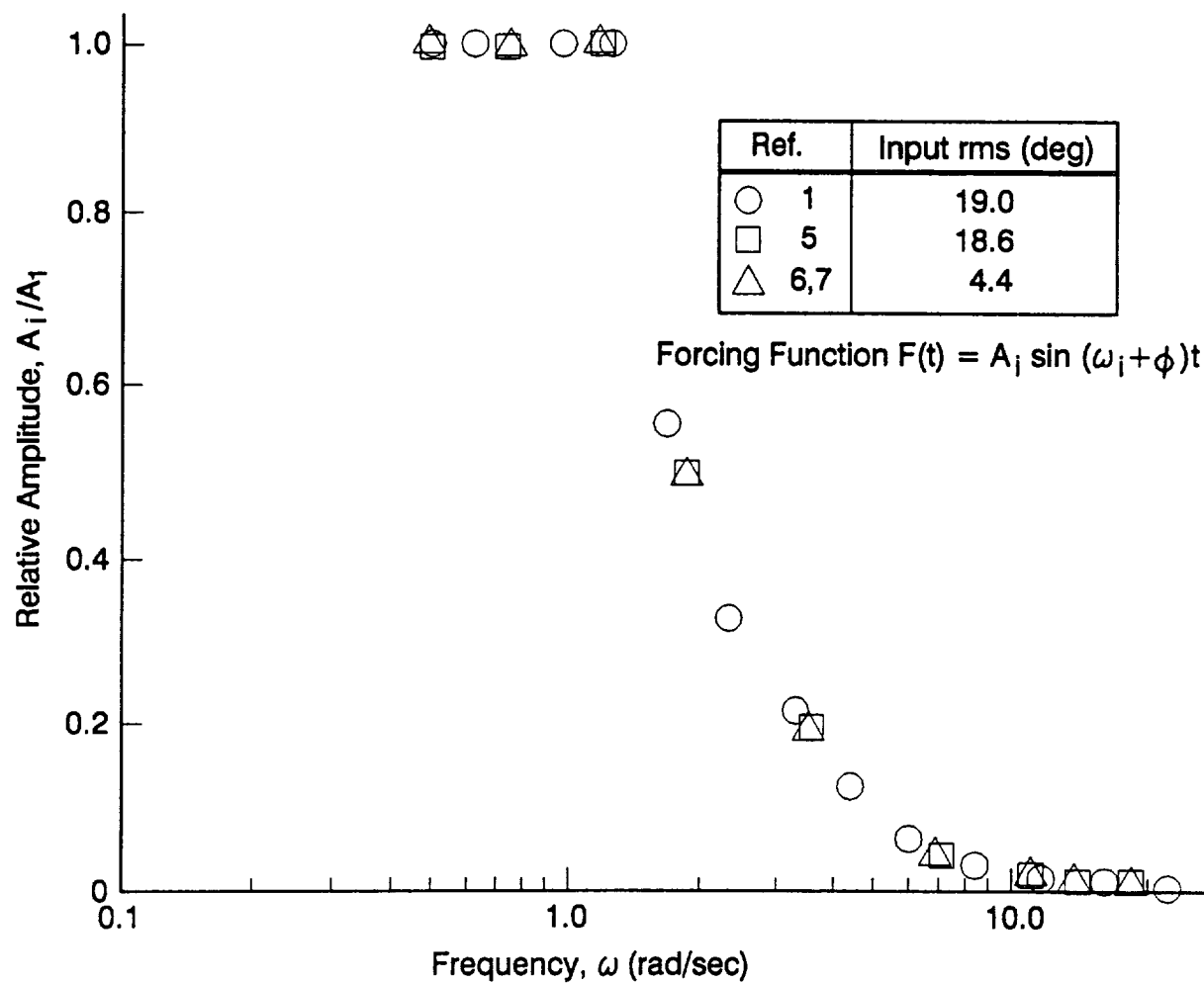
Figure 5. Comparison of Forcing Function Amplitudes
for Roll Sum-of-Sines Tasks

```
                                    ┌──────────────────────┐
                                    │ Added Transport Delay │
                                    │ (ms)                  │
                                    └──────────────────────┘

                    L 1 0 1  P ( ) + τ

                                    ┌──────────────────────┐
                                    │ | p/ Fa|ss = (deg/sec/lbs) │
                                    └──────────────────────┘

                                    ┌─────────────────────────────┐
                                    │ FLIGHT CONTROL SYSTEM TYPE  │
                                    │  (P):  POSITION COMMAND     │
                                    │  (F):  FORCE COMMAND        │
                                    └─────────────────────────────┘
```
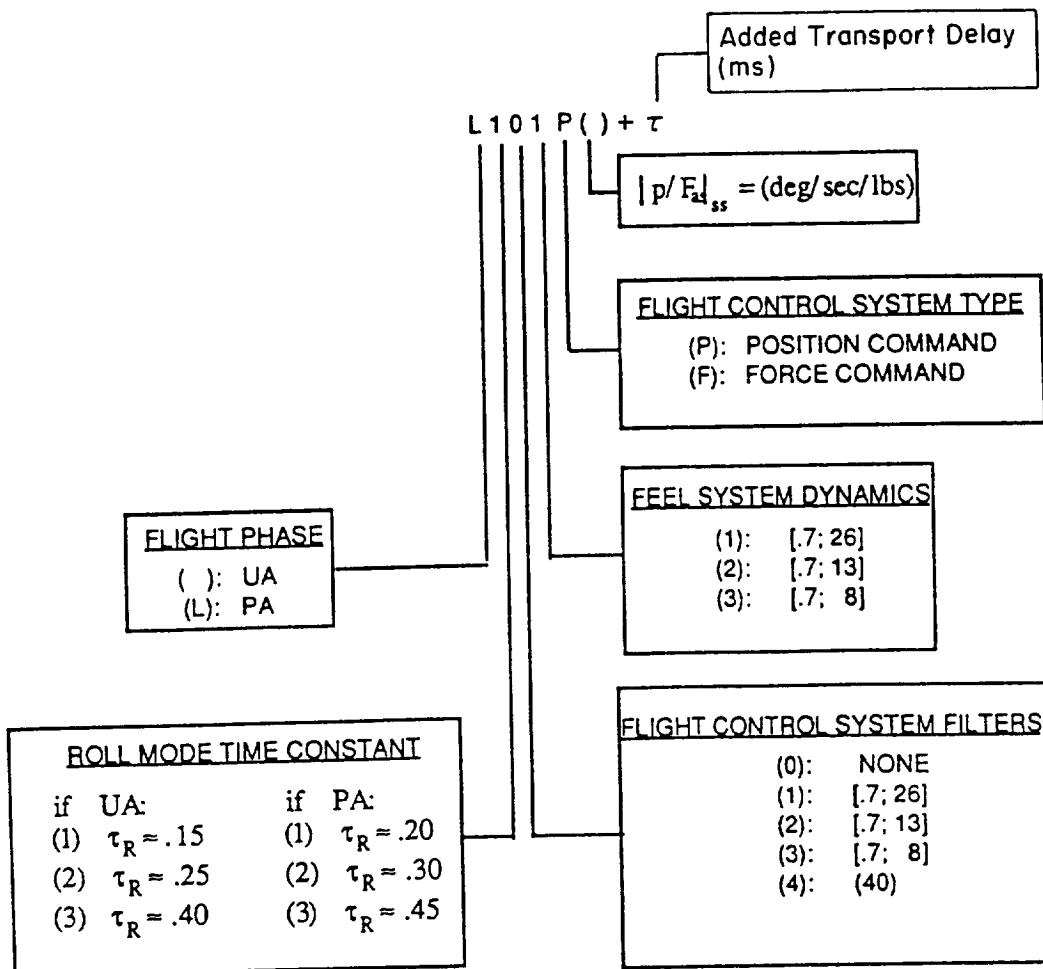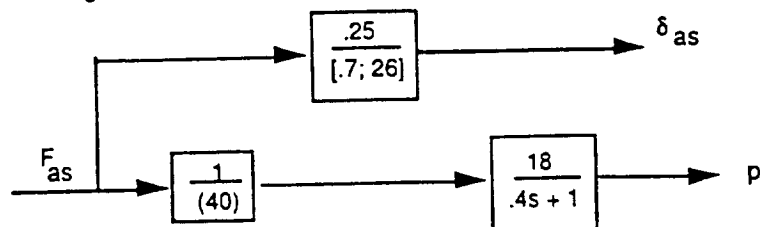

Figure 6. Configuration Identification Scheme
(Reproduced from Ref. 1)

41

a) Feel System Included in Time Delay

b) Feel System Excluded from Time Delay
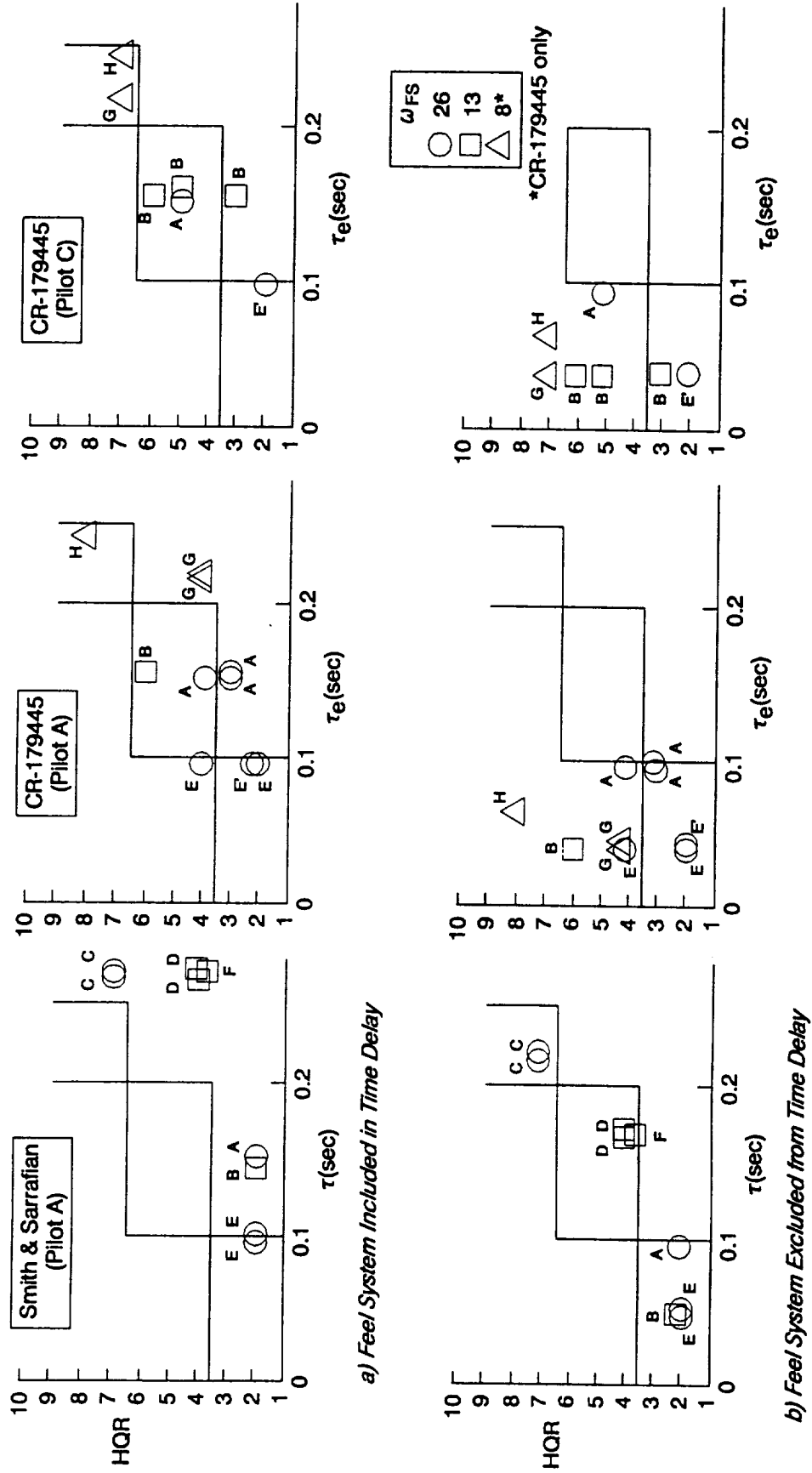
Figure 7. Effect of Feel System on HQRs for Configurations From Study
by Smith and Sarrafian (Position Sensing)
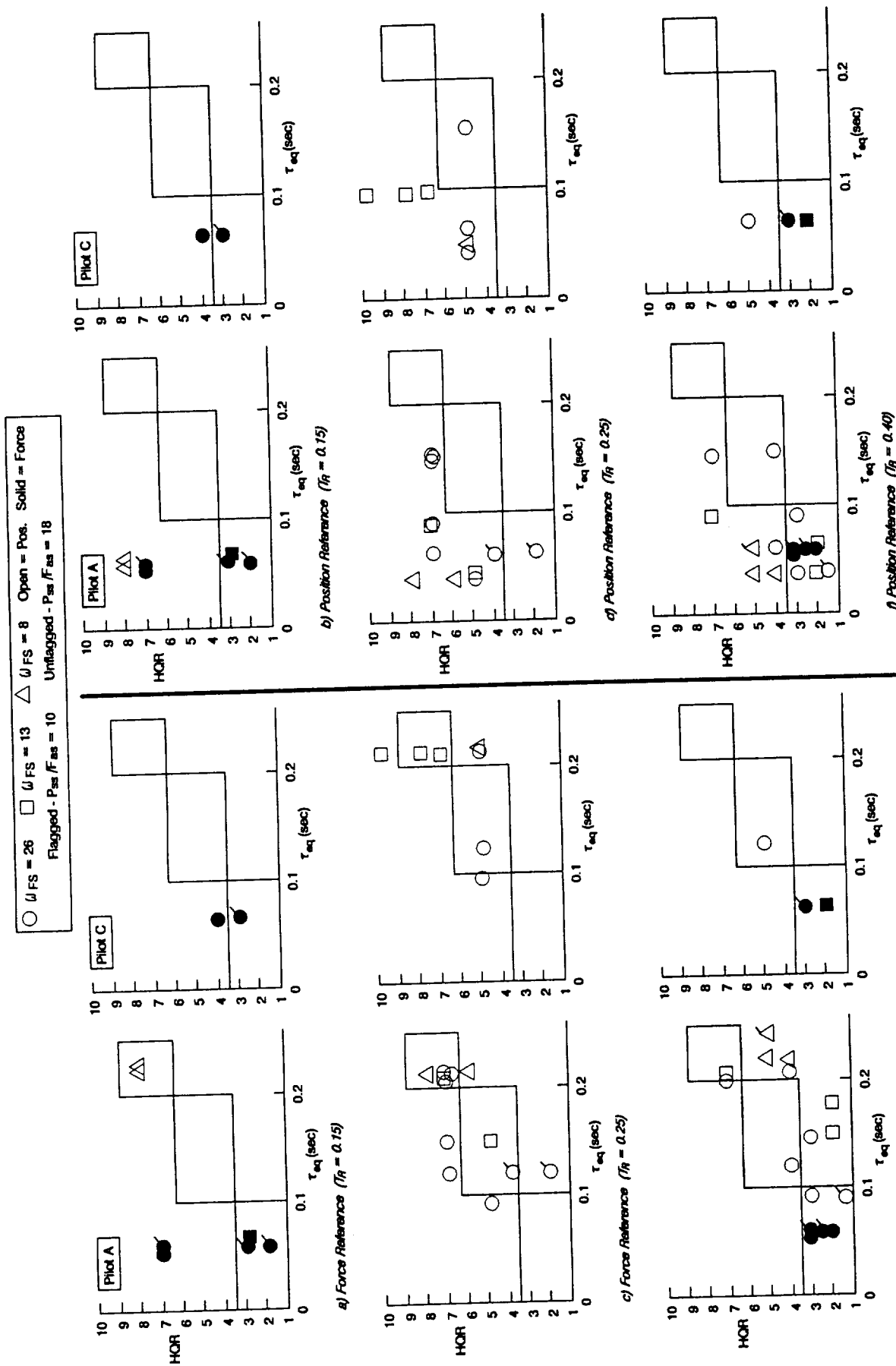
Figure 8. Comparison of HQRs for Up-and-Away Configurations with Equivalent Time Delay

43
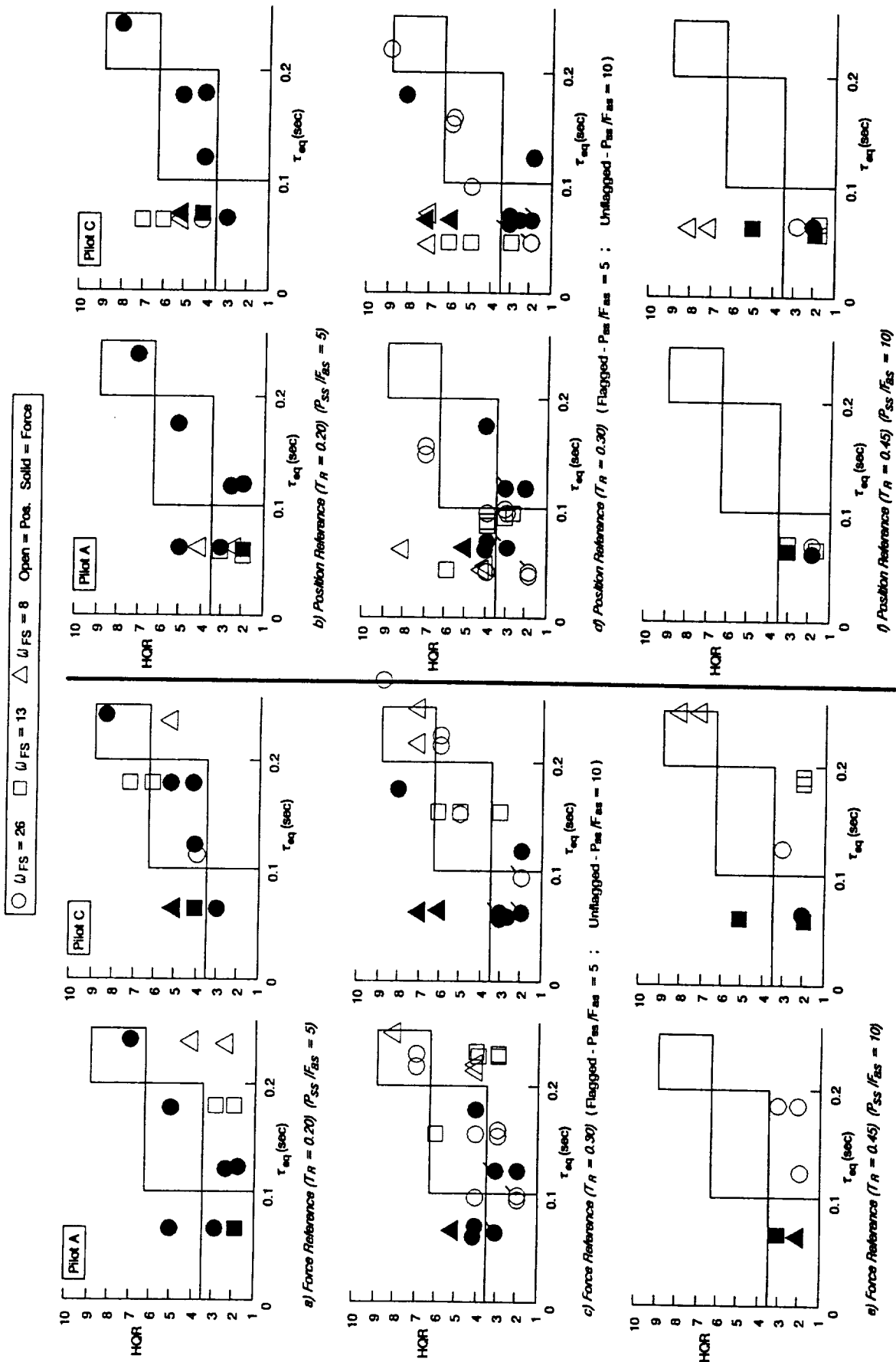
Figure 9. Comparison of HQRs for Landing

44
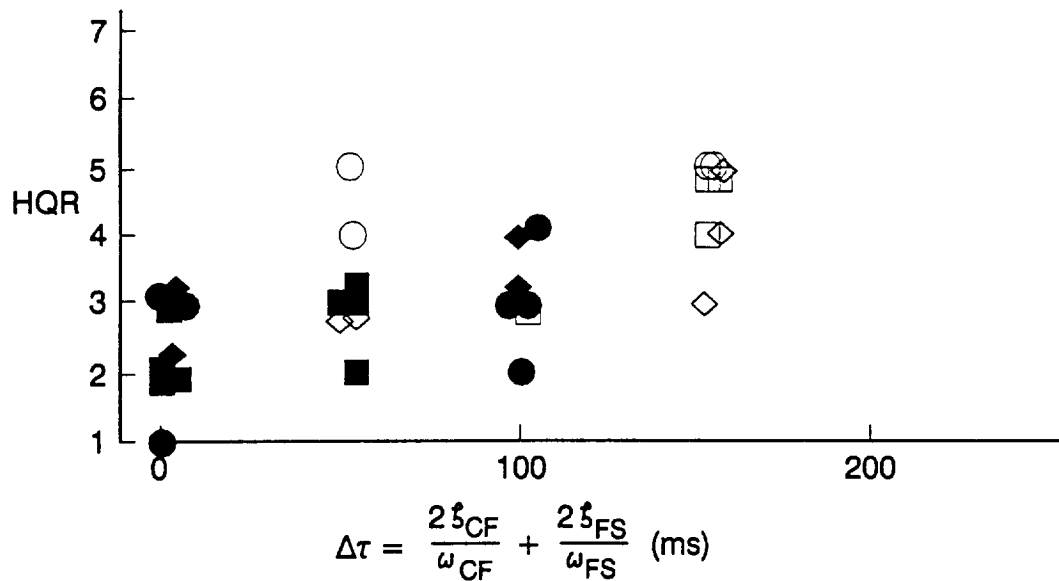
Figure 10. HQR vs. Added Delay for Fixed-Base Simulation Data (Ref. 5)

a) Position Reference

Open = Position Sensing
Solid = Force Sensing

$$\Delta\tau = \frac{2\xi_{CF}}{\omega_{CF}} \ \text{(ms)}$$

b) Force Reference

$$\Delta\tau = \frac{2\xi_{CF}}{\omega_{CF}} + \frac{2\xi_{FS}}{\omega_{FS}} \ \text{(ms)}$$
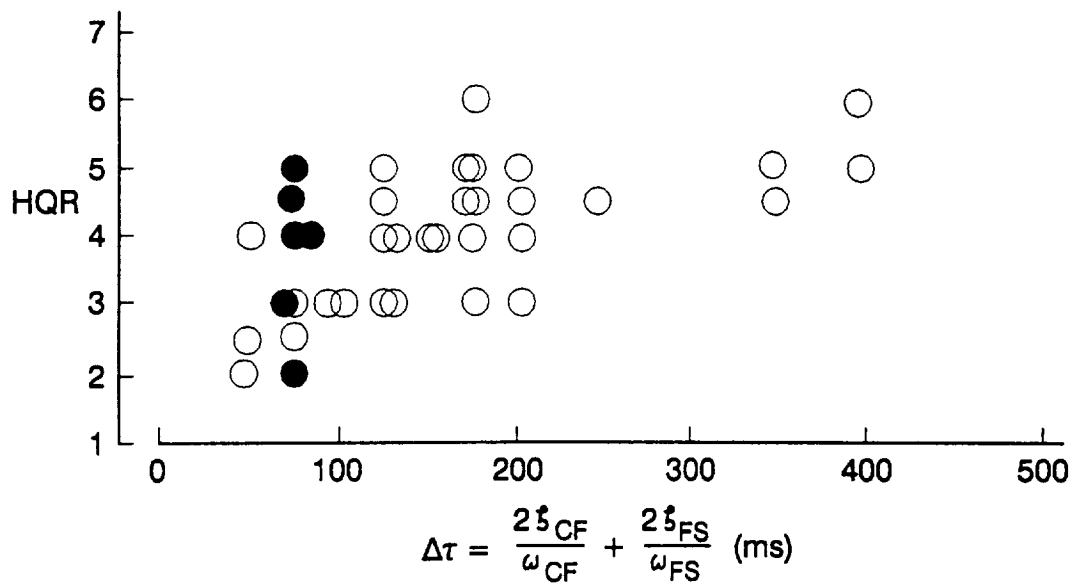
Figure 11. HQR vs. Added Delay for CH-47 SOS Tracking Experiment (Ref. 6)
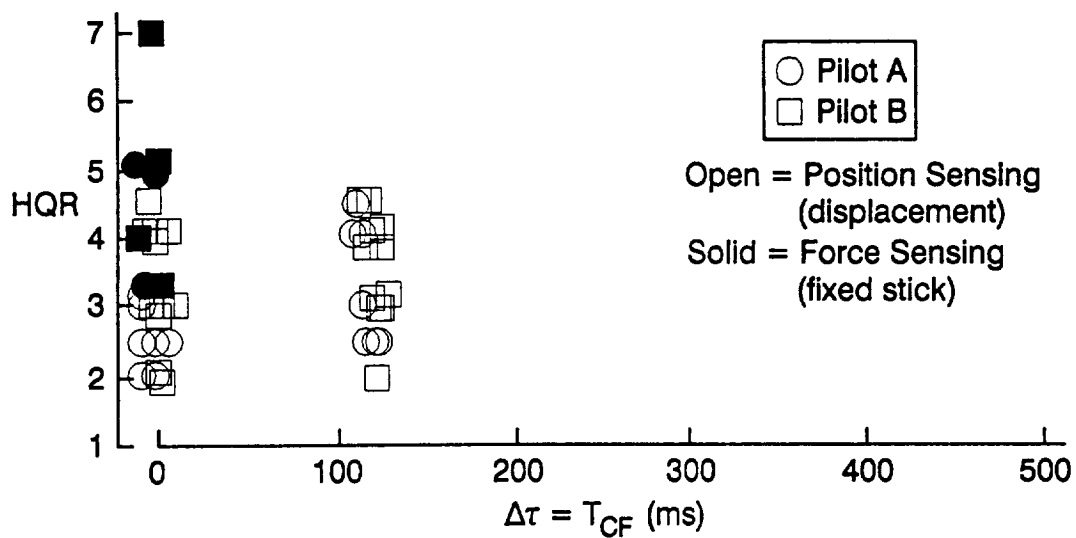
a) Position Reference

b) Force Reference

$$\Delta\tau = \frac{2\zeta_{FS}}{\omega_{FS}} + T_{CF} \ (ms)$$
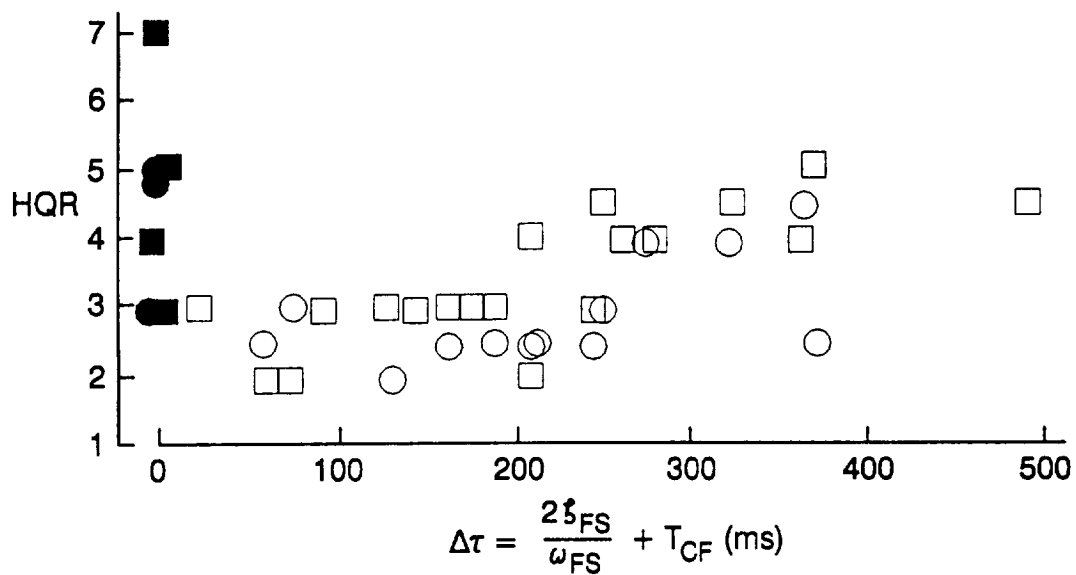
Figure 12. HQR vs. Added delay for SOS Tracking
Task From Bell 205A Experiment (Ref. 7)
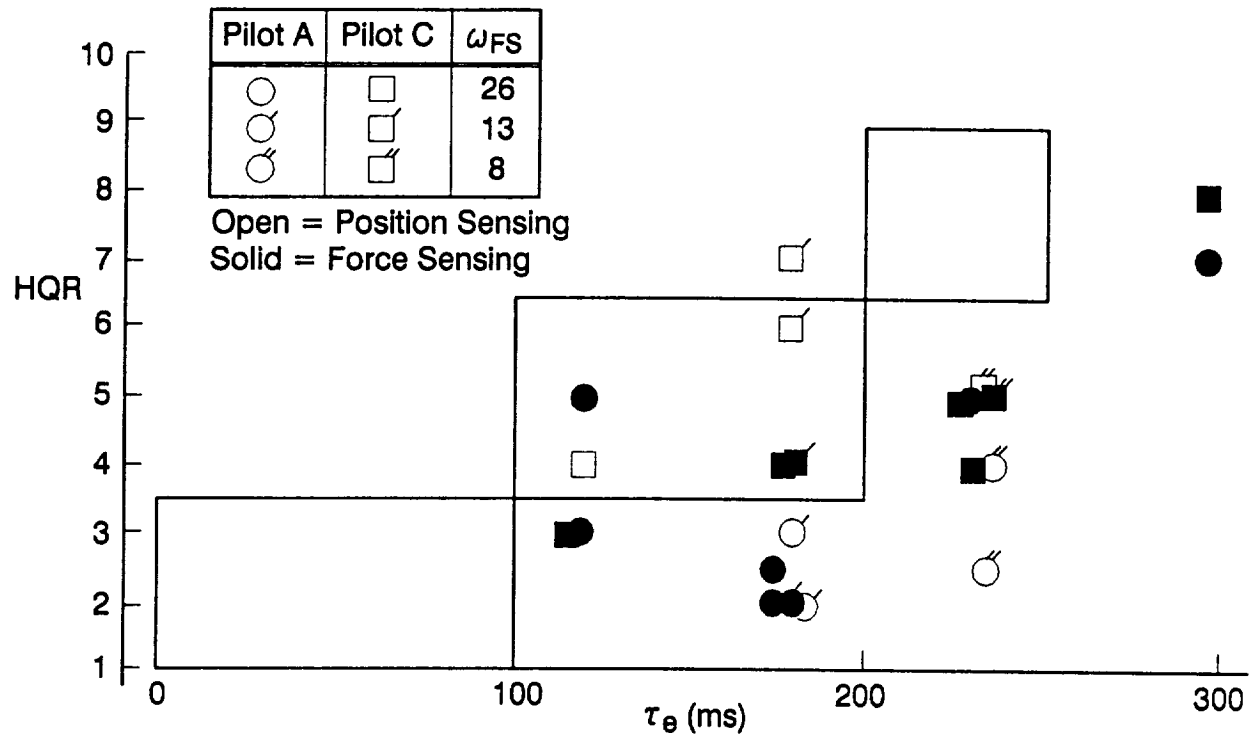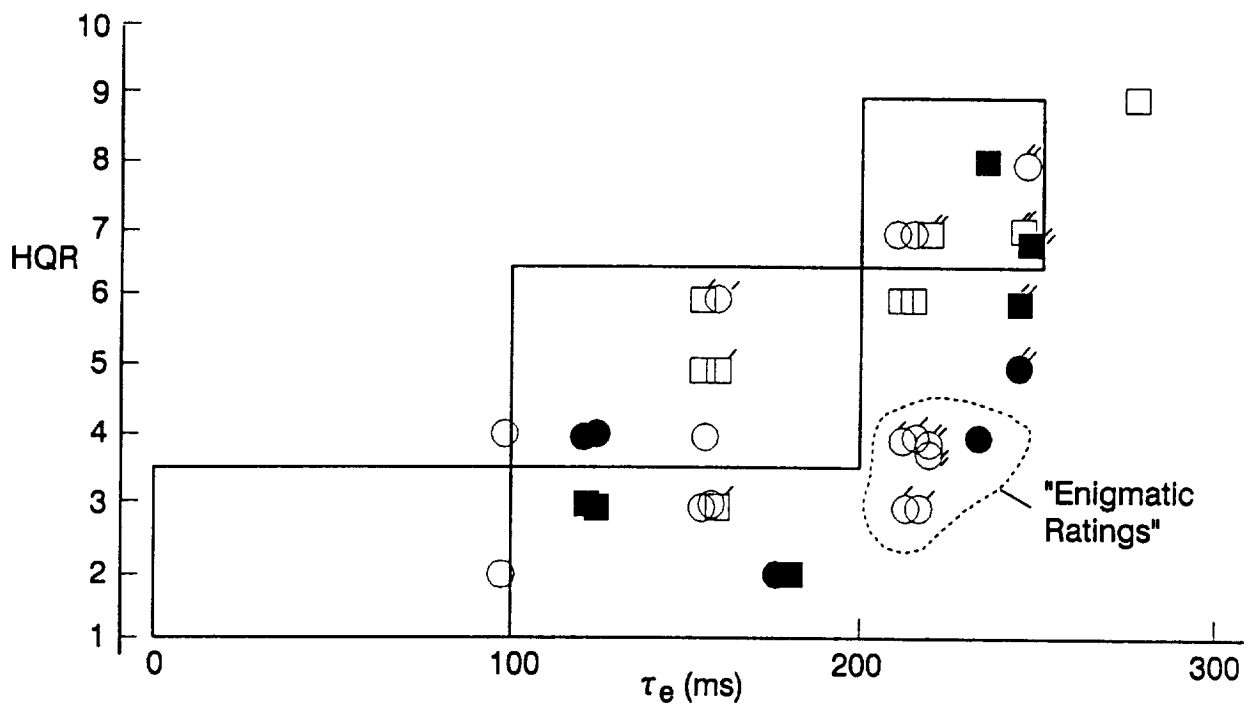
Figure 13. HQR vs. Equivalent Time Delay for Landing Data of Ref. 1 —
Feel System Included for Both Force and Position Sensing

Sensing		ζ_{FS}	ω_{FS}	Controller
Position	Force			
○	●	0.7	26	Centerstick
□	■	0.7	14	(F_{as}/δ_{as} = 4 lb/in.)
◇	◆	0.6	22.4	Sidestick (F_{as}/δ_{as} = 0.65 lb/deg)

Note: P/F_{as} = 20 deg/s/lb

T_R = 0.15 s

$$\Delta\tau = \frac{2\zeta_{CF}}{\omega_{CF}} + \frac{2\zeta_{FS}}{\omega_{FS}} \text{ (ms)}$$
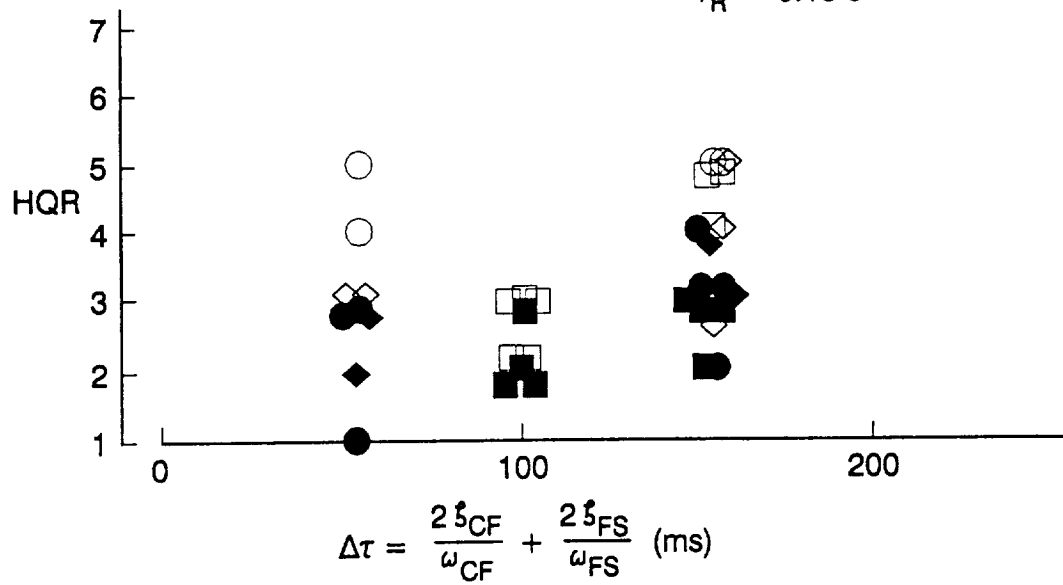
Figure 14. HQR vs. Added Time Delay for Fixed-Base Simulation Data
(Ref.5) — Feel System Included for Both
Force and Position Sensing

49
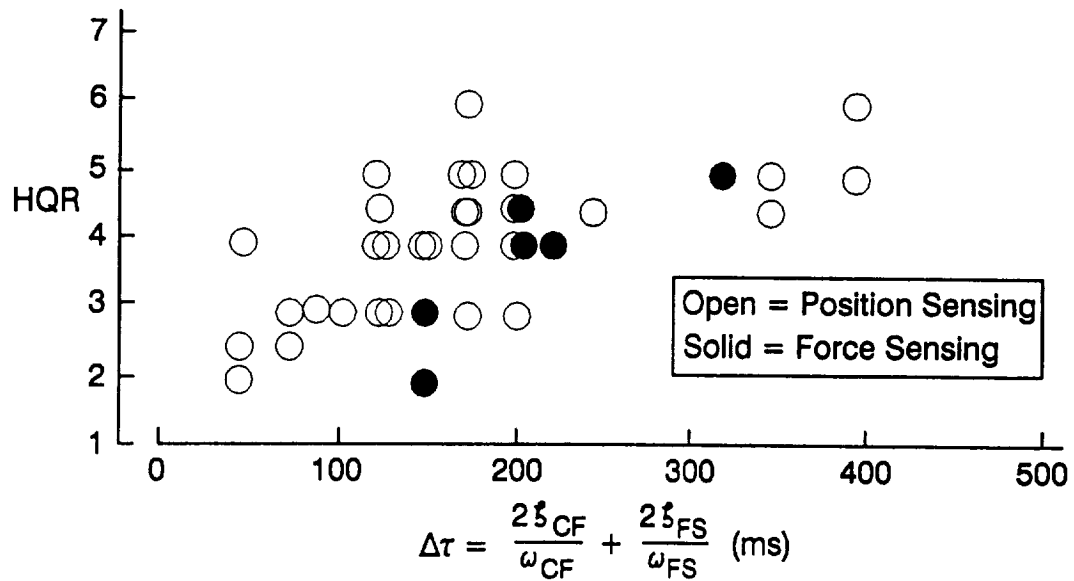
a) CH-47 Experiment (Ref. 6)
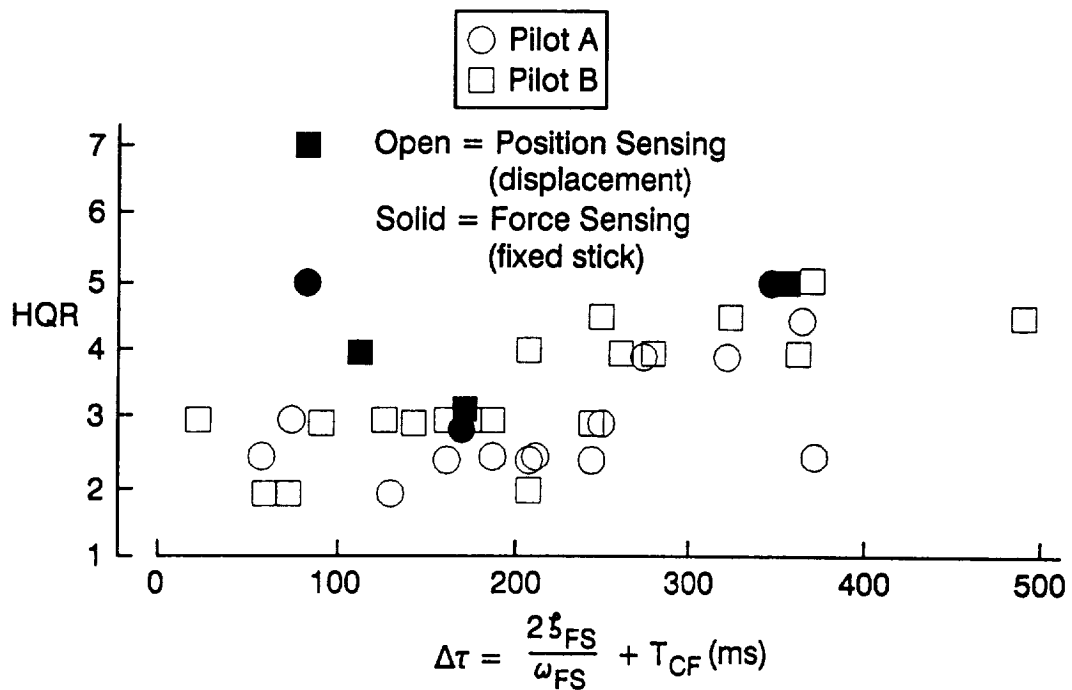
b) Bell 205A Experiment (Ref. 7)

Figure 15. HQR vs. Added Time Delay for SOS Tracking From Helicopter Experiments — Feel System Included for Both Force and Position Sensing
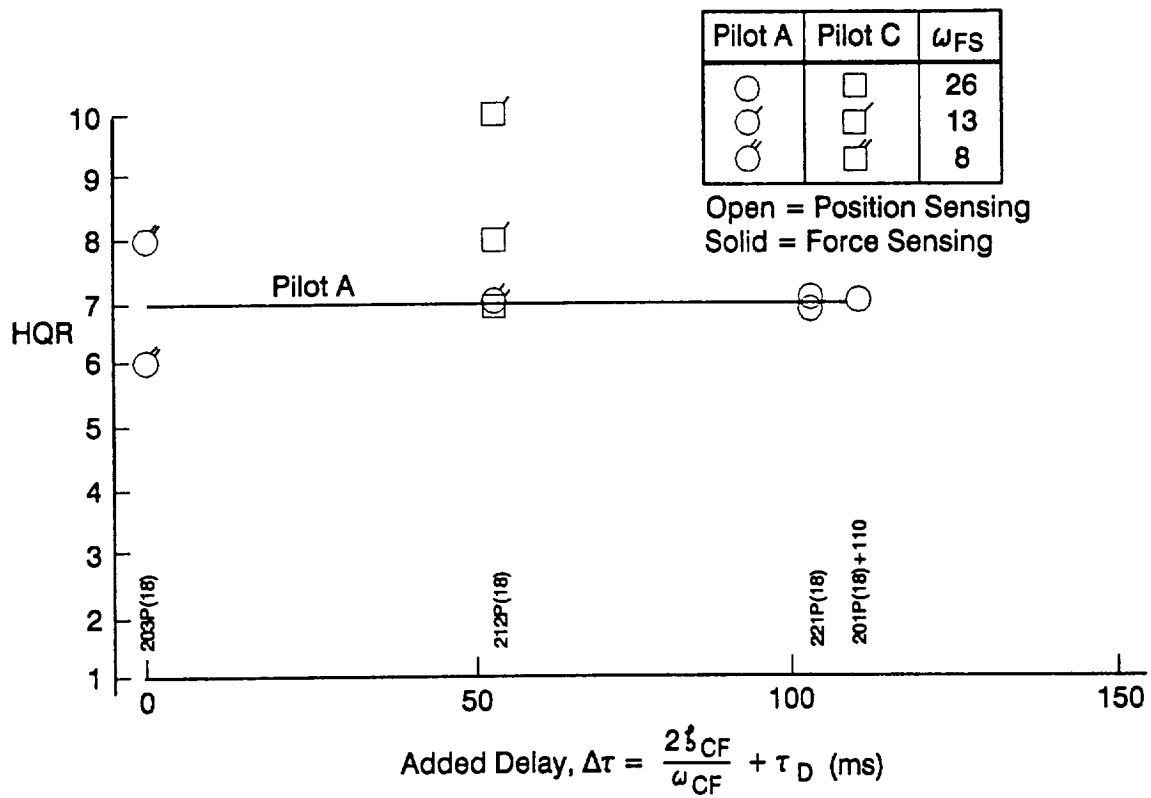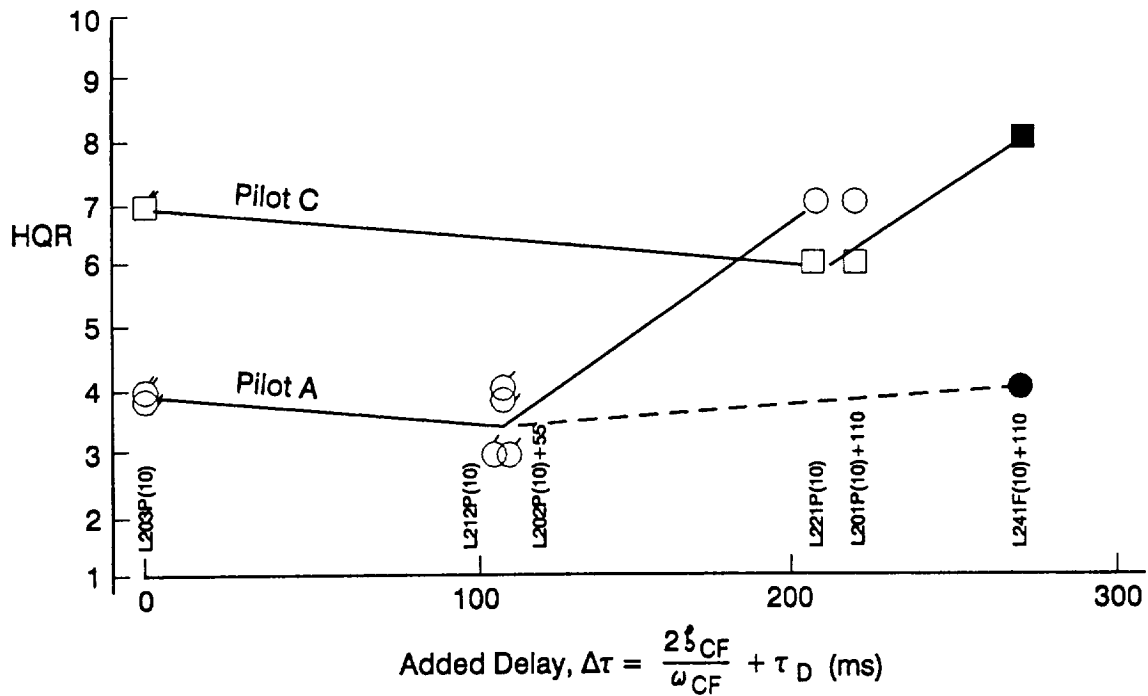
Figure 16. Ratings From Ref. 1 for Medium-T_R Cases with Approximately Equal Time Delay, $\tau_e \doteq 210$ ms (Feel System Included); $\Delta\tau$ Excludes Feel System
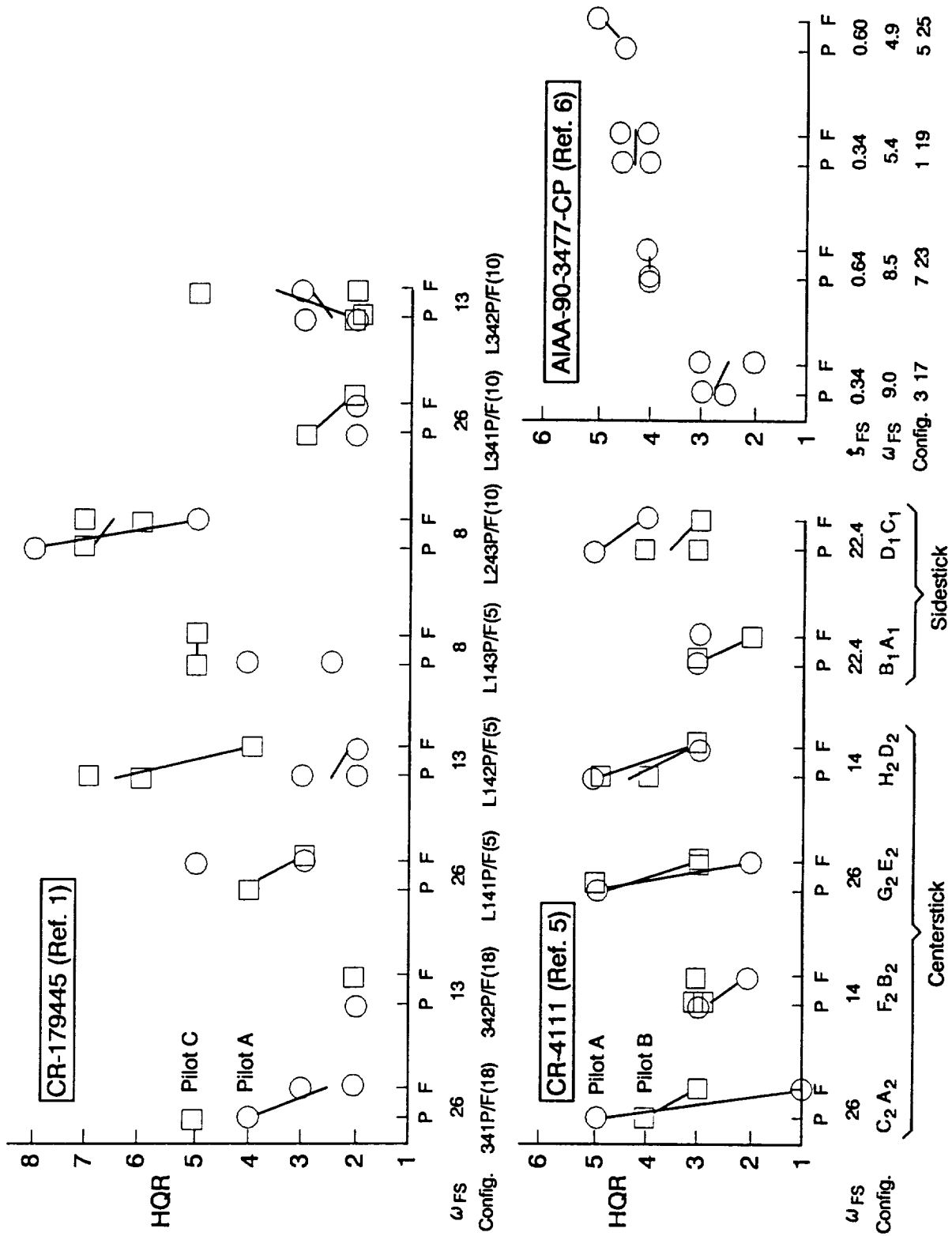
Figure 17. Effect of Force vs. Position Sensing for Otherwise Identical Dynamics
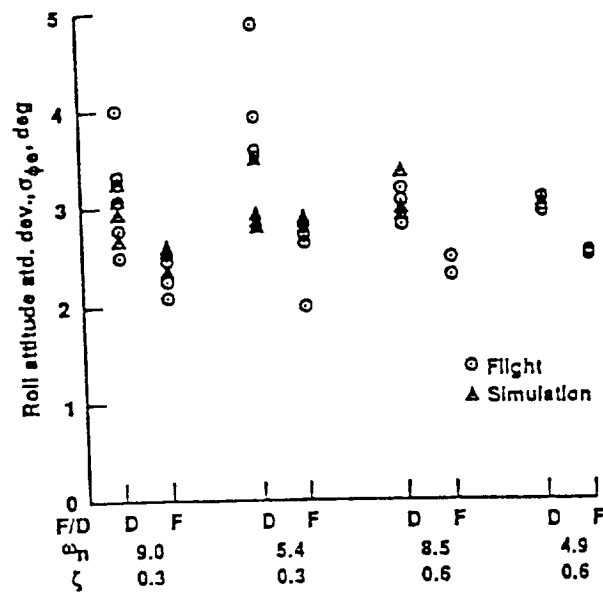
Figure 18. Roll Errors Between Displacement- and Force-Sensing with no Filters
(from Ref. 6)
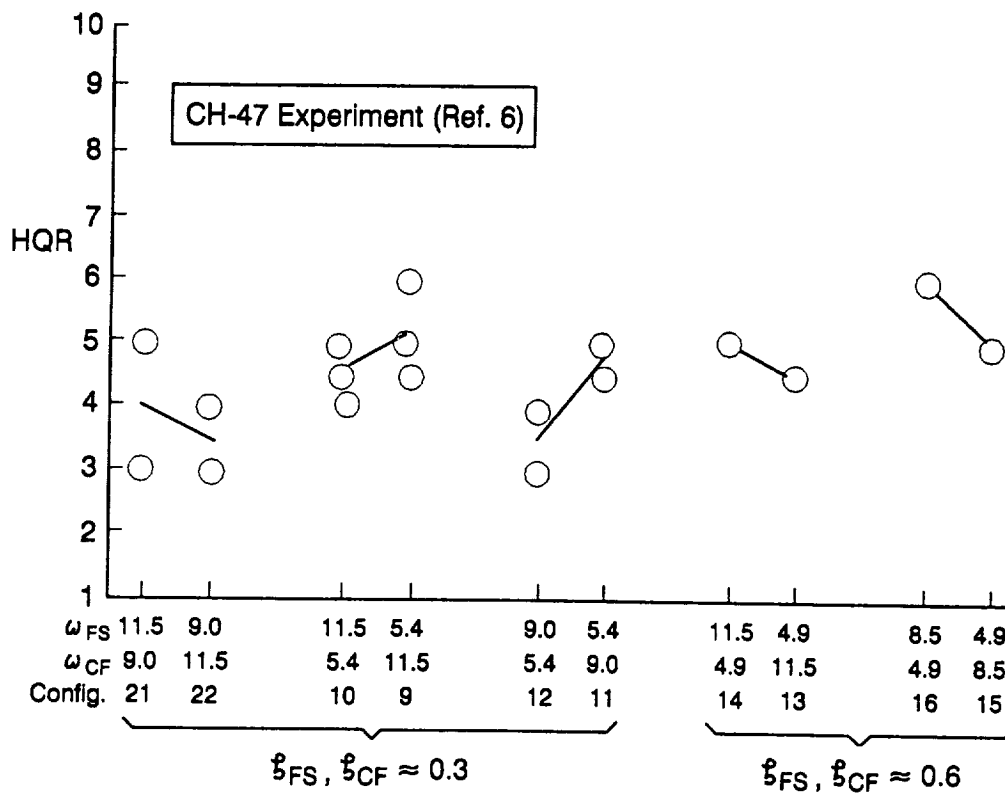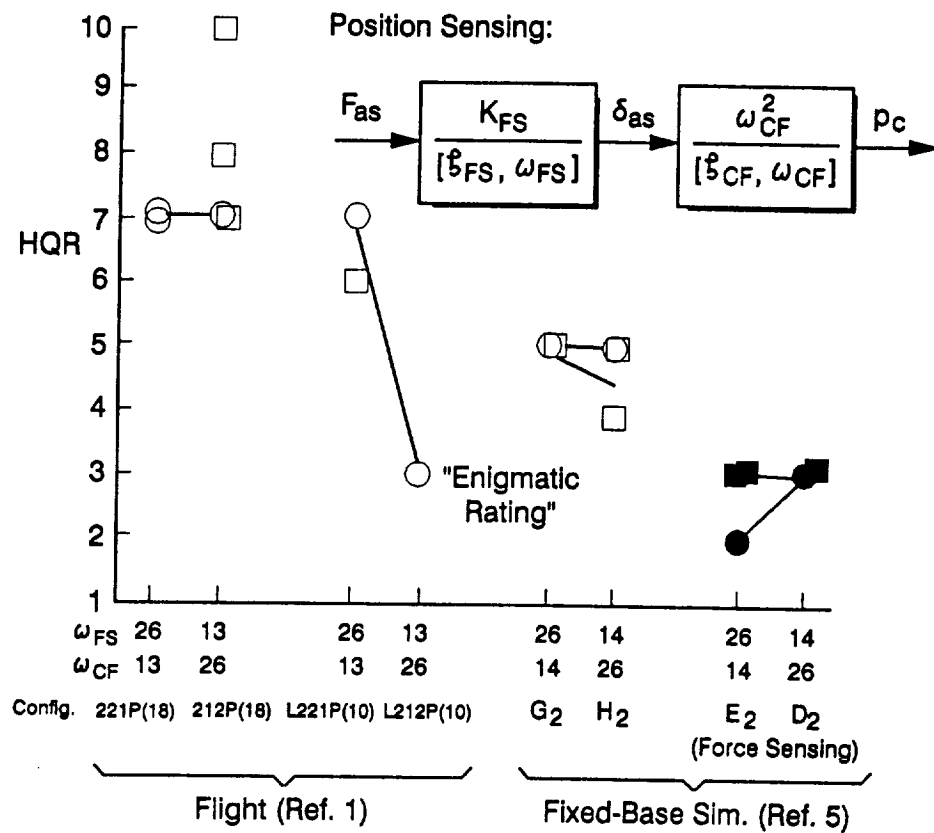
Figure 19. Effect of Location of Lags on HQRs
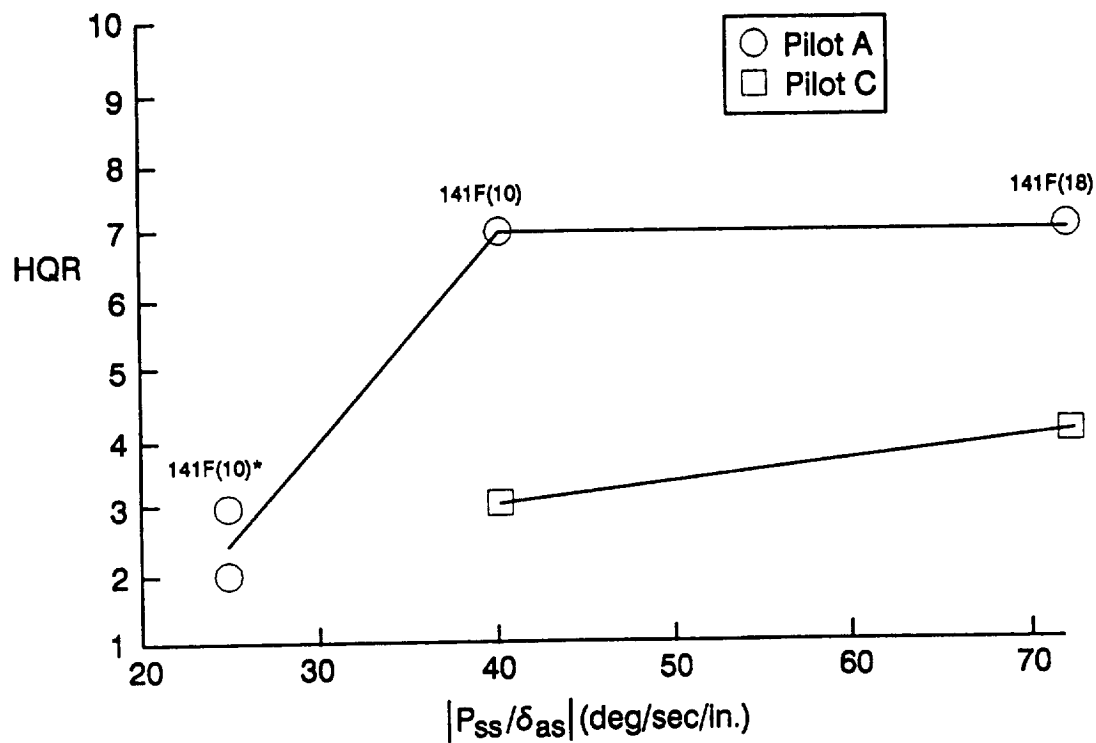
a) Up-and-Away (note: pilot C's evaluations were before flight 4057)
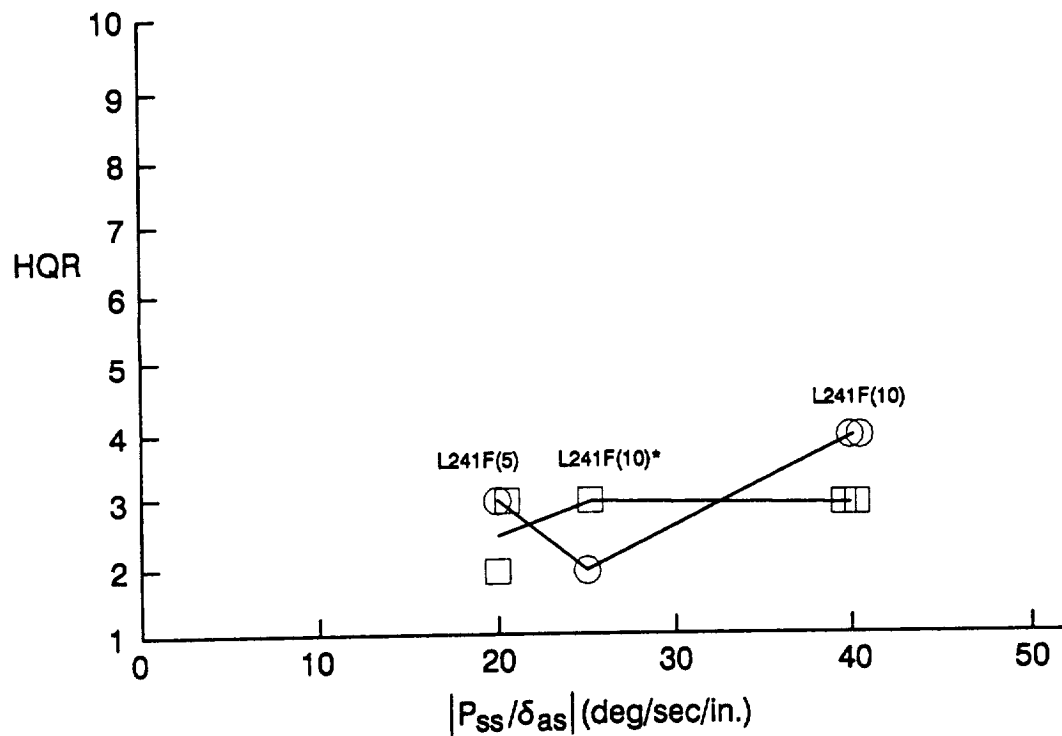
b) Landing

Figure 20. Variation in HQRs with Control Position Sensitivity
for Identical Aircraft Dynamics
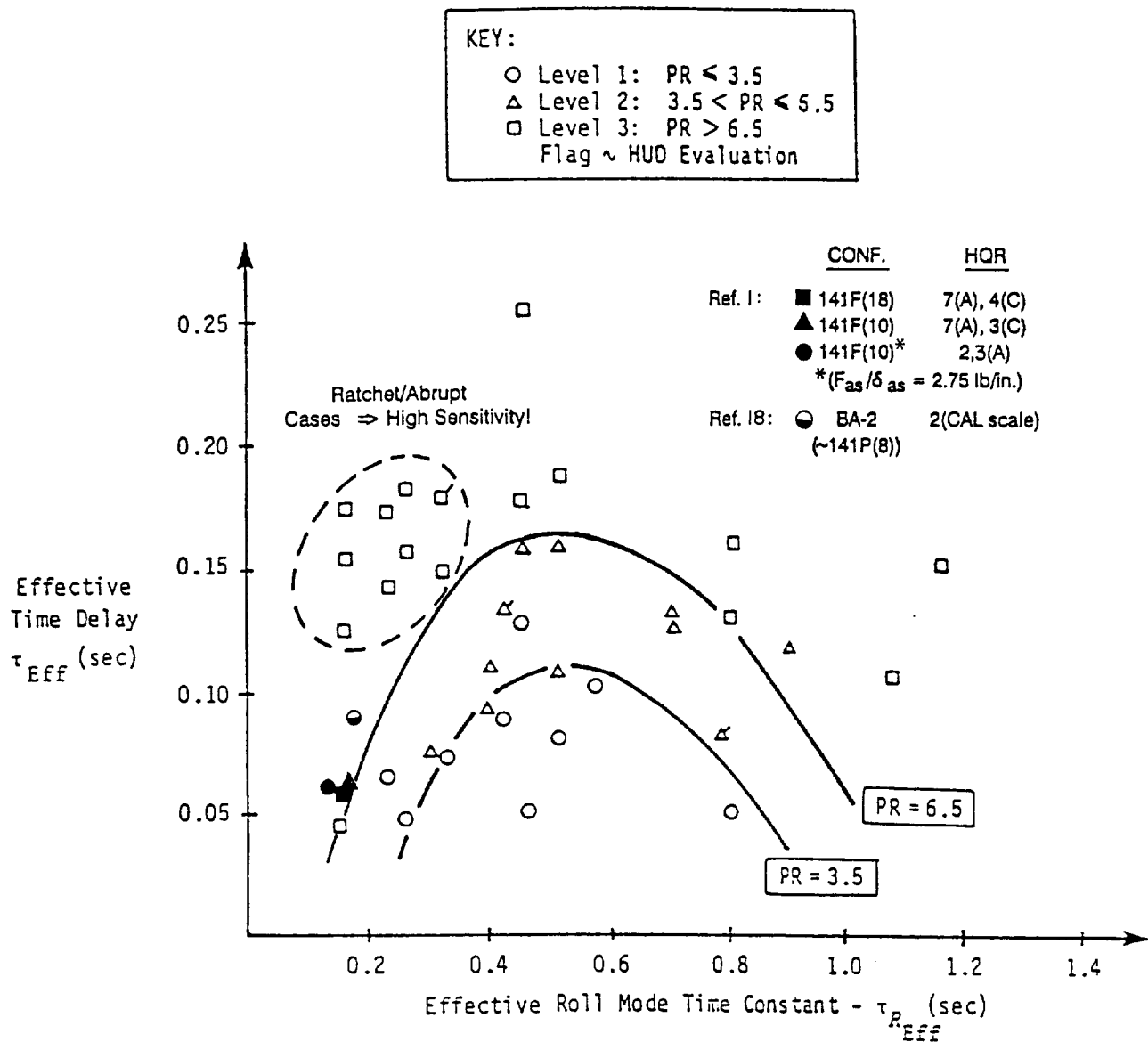
Figure 21. Correlation of Category A Task (TR + AR) Data with τ_{Eff} and $\tau_{R_{Eff}}$ (From Ref. 17)
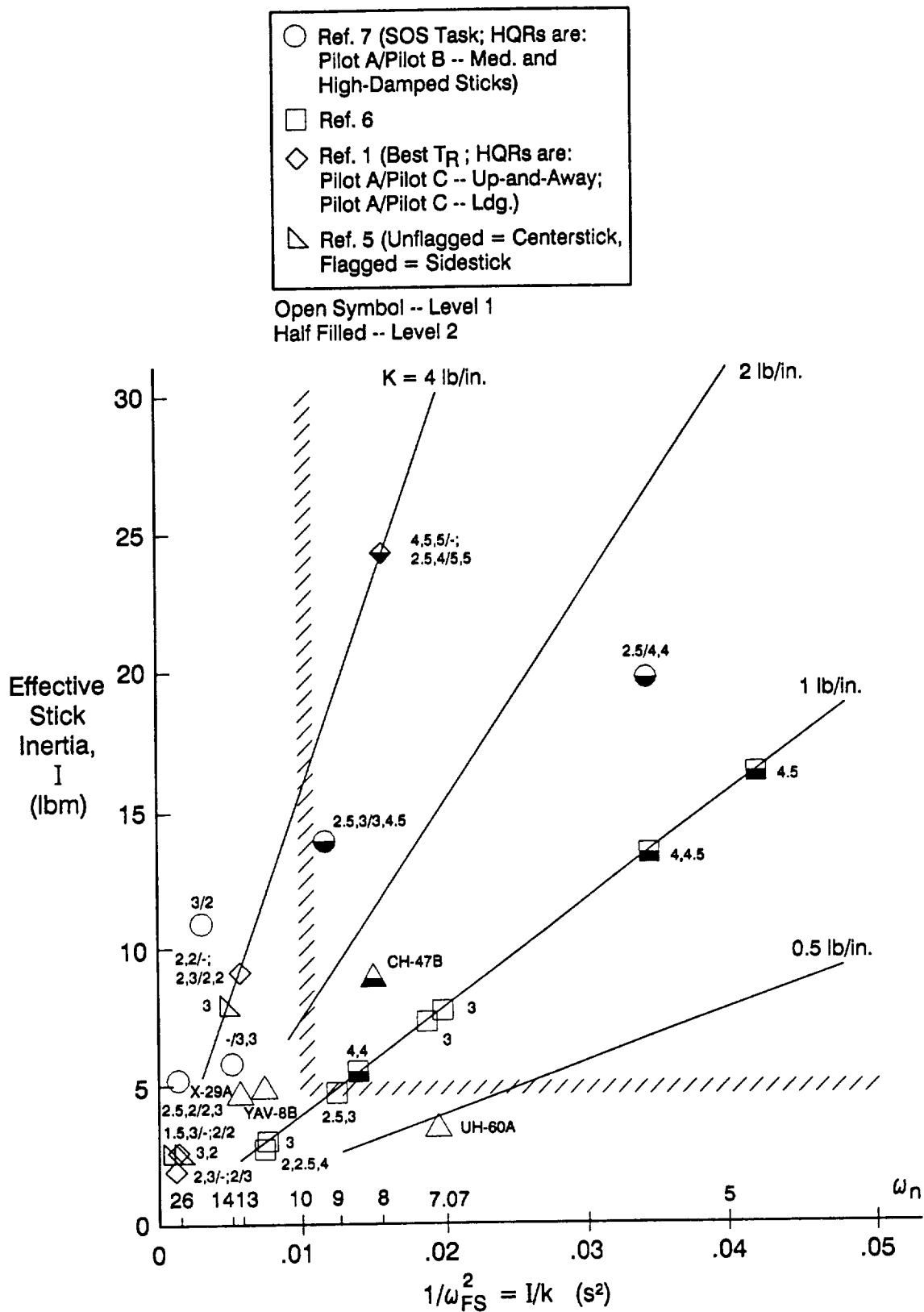
Figure 22. Lateral Stick Inertia vs. Natural Frequency
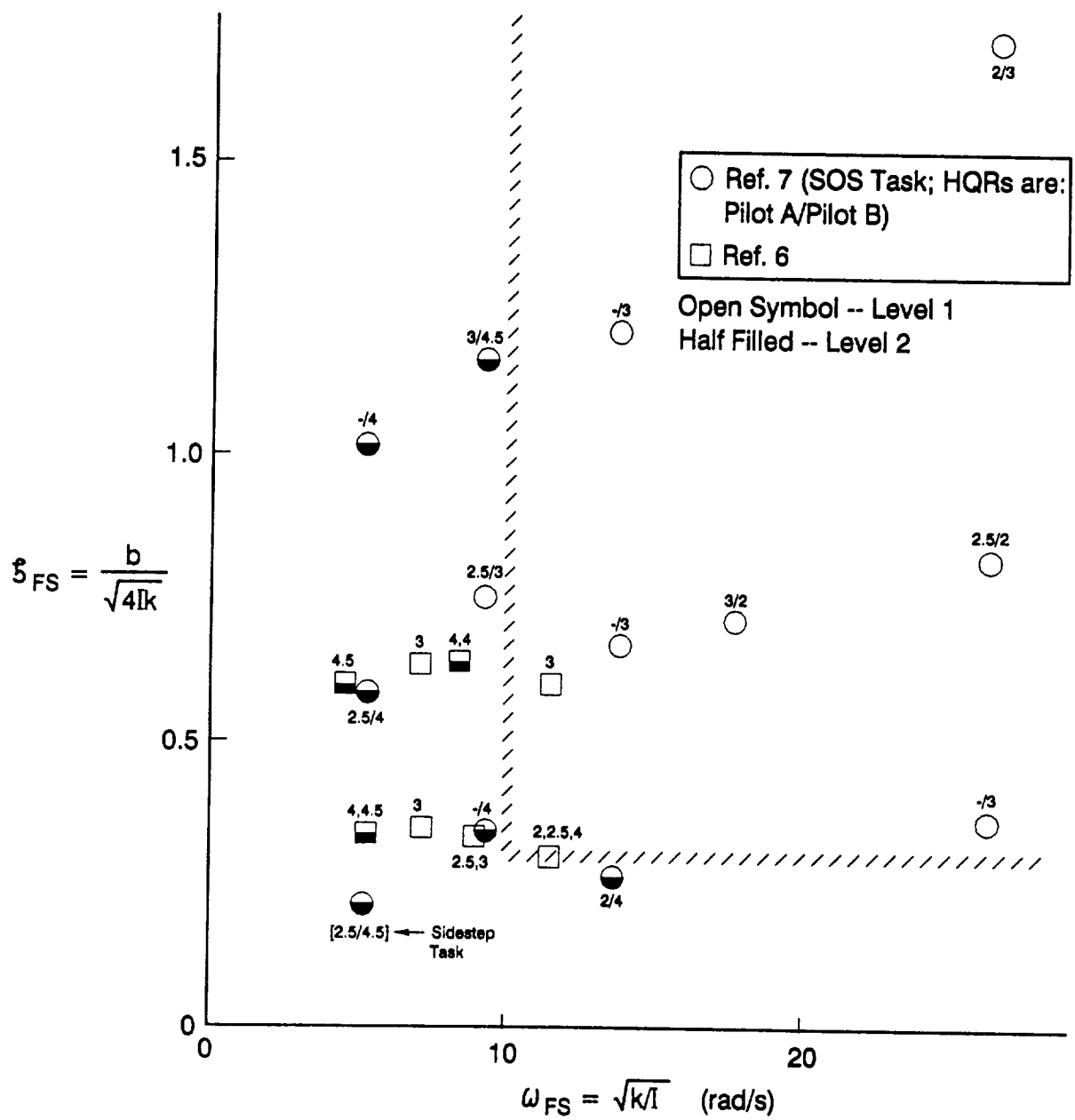
Figure 23. Lateral Stick Damping Ratio vs. Natural Frequency

	FAST [0.7,26]	INTERMEDIATE [0.7,13]	SLOW [0.7,8]
τ_R = 0.15 s — Position	No Evaluations	No Evaluations	143P(18) 4069-4 A 8
τ_R = 0.15 s — Force	Conf. Run 141F(18) 4159-4 Pilot HQR A 5	142F(18) 4160-5 A 5	143F(18) 4154-5 B 7
τ_R = 0.25 s — Position	Not Analyzed	202P(18) 4156-2 A 5	203P(18) 4160-2 A 6
τ_R = 0.25 s — Force	No Evaluations	No Evaluations	No Evaluations
τ_R = 0.40 s — Position	301P(18) 4156-1 A 3	302P(18) 4161-2 A 2	303P(18) 4156-4 A 5
τ_R = 0.40 s — Force	341F(18) 4176-3 A 2	342F(18) 4127-3 C 2	Bad Data

Figure 24. Matrix of Configurations Considered in
the Pilot Modeling Study

$$Y_p$$

$$\frac{K_p(T_{L_1}s + 1)\, e^{-\tau_p s}}{(T_{L_2}s + 1)\,[\zeta_1,\, \omega_1]\,[\zeta_2,\, \omega_2]}$$

$$Y_c$$

$$\frac{K_c\, e^{-\tau_a s}}{s(\tau_R s + 1)}$$

ϕ_e

δ
Force
or
Position

ϕ
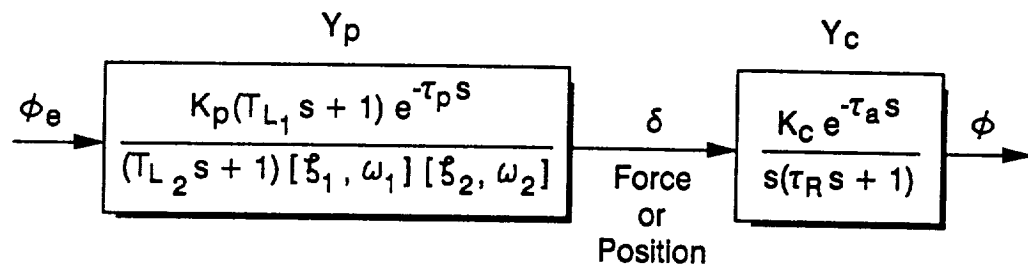
Figure 25. Form of Open-Loop Pilot/Vehicle Model

FEEL SYSTEM

	FAST [0.7, 26]	INTERMEDIATE [0.7, 13]	SLOW [0.7, 8]
τ_R = 0.15 s — Position			
τ_R = 0.15 s — Force	$\underbrace{\dfrac{47040\, e^{-0.04s}}{(0)(6.67)(40)}}_{Y_c}\ \underbrace{\dfrac{e^{-0.123s}}{[0.06,\ 11.3]}}_{Y_p}$	$\underbrace{\dfrac{878\, e^{-0.08s}}{(0)(6.67)}}_{Y_c}\ \underbrace{\dfrac{(3.66)\, e^{-0.287s}}{[0.347,\ 19.1]}}_{Y_p}$	$\underbrace{\dfrac{8070\, e^{-0.04s}}{(0)(6.67)(40)}}_{Y_c}\ \underbrace{\dfrac{(3.85)\, e^{-0.34s}}{[0.08,\ 10.4]}}_{Y_p}$
τ_R = 0.25 s — Position		$\underbrace{\dfrac{221\, e^{-0.04s}}{(0)(4)}}_{Y_c}\ \underbrace{\dfrac{(2.46)\, e^{-0.376s}}{[0.092,\ 9.98]}}_{Y_p}$	$\underbrace{\dfrac{6660000\, e^{-0.025s}}{(0)(6.67)[0.34,\ 16.4](40)}}_{Y_c}\ \underbrace{\dfrac{e^{-0.029s}}{[0.15,\ 9.9]}}_{Y_p}$
τ_R = 0.25 s — Force			$\underbrace{\dfrac{17500\, e^{-0.08s}}{(0)(4)}}_{Y_c}\ \underbrace{\dfrac{(4.23)\, e^{-0.244s}}{[0.0089,\ 8.89][0.148,\ 14.1]}}_{Y_p}$
τ_R = 0.40 s — Position	$\underbrace{\dfrac{117\, e^{-0.08s}}{(0)(2.5)}}_{Y_c}\ \underbrace{\dfrac{(4.69)\, e^{-0.24s}}{[0.053,\ 10.9]}}_{Y_p}$	$\underbrace{\dfrac{153\, e^{-0.04s}}{(0)(2.5)}}_{Y_c}\ \underbrace{\dfrac{(1.85)\, e^{-0.326s}}{[0.128,\ 10.5]}}_{Y_p}$	$\underbrace{\dfrac{91.4\, e^{-0.04s}}{(0)(2.5)}}_{Y_c}\ \underbrace{\dfrac{(2.61)\, e^{-0.33s}}{[0.128,\ 8.54]}}_{Y_p}$
τ_R = 0.40 s — Force	$\underbrace{\dfrac{8680\, e^{-0.08s}}{(0)(2.5)(40)}}_{Y_c}\ \underbrace{\dfrac{(2.43)\, e^{-0.22s}}{[0.206,\ 12.6]}}_{Y_p}$	$\underbrace{\dfrac{9730\, e^{-0.04s}}{(0)(2.5)(40)}}_{Y_c}\ \underbrace{\dfrac{(2.77)\, e^{-0.234s}}{[0.311,\ 12.1]}}_{Y_p}$	

Note: $(a) \equiv (s + a)$; $[\zeta, \omega_n] \equiv [s^2 + 2\zeta\omega_n s + \omega_n^2]$

Figure 26. Open-Loop Pilot/Vehicle Transfer Function Models

FEEL SYSTEM

	Fast [0.7,26]	Intermediate [0.7,14]

Force

$$-1370 \; \underbrace{\frac{e^{-0.033s}}{(0)(6.67)}}_{Y_c} \; \underbrace{\frac{(5.72)e^{-0.284s}}{(-19.0)(19.3)}}_{Y_p}$$

$$83.2 \; \underbrace{\frac{e^{-0.033s}}{(0)(6.67)}}_{Y_c} \; \underbrace{\frac{(27.4)e^{-0.069s}}{[0.21,11.0]}}_{Y_p}$$

$T_R = 0.15 \; s$

Position

$$792 \; \underbrace{\frac{e^{-0.033s}}{(0)(6.67)}}_{Y_c} \; \underbrace{\frac{(4.41)e^{-0.241s}}{[0.18,15.9]}}_{Y_p}$$

$$98.8 \; \underbrace{\frac{e^{-0.033s}}{(0)(6.67)}}_{Y_c} \; \underbrace{\frac{(11.4)e^{-0.041s}}{[0.37,8.11]}}_{Y_p}$$

Figure 27. Open-Loop Pilot/Vehicle Transfer Function Models
From Fixed-Base (Ref. 5) Data
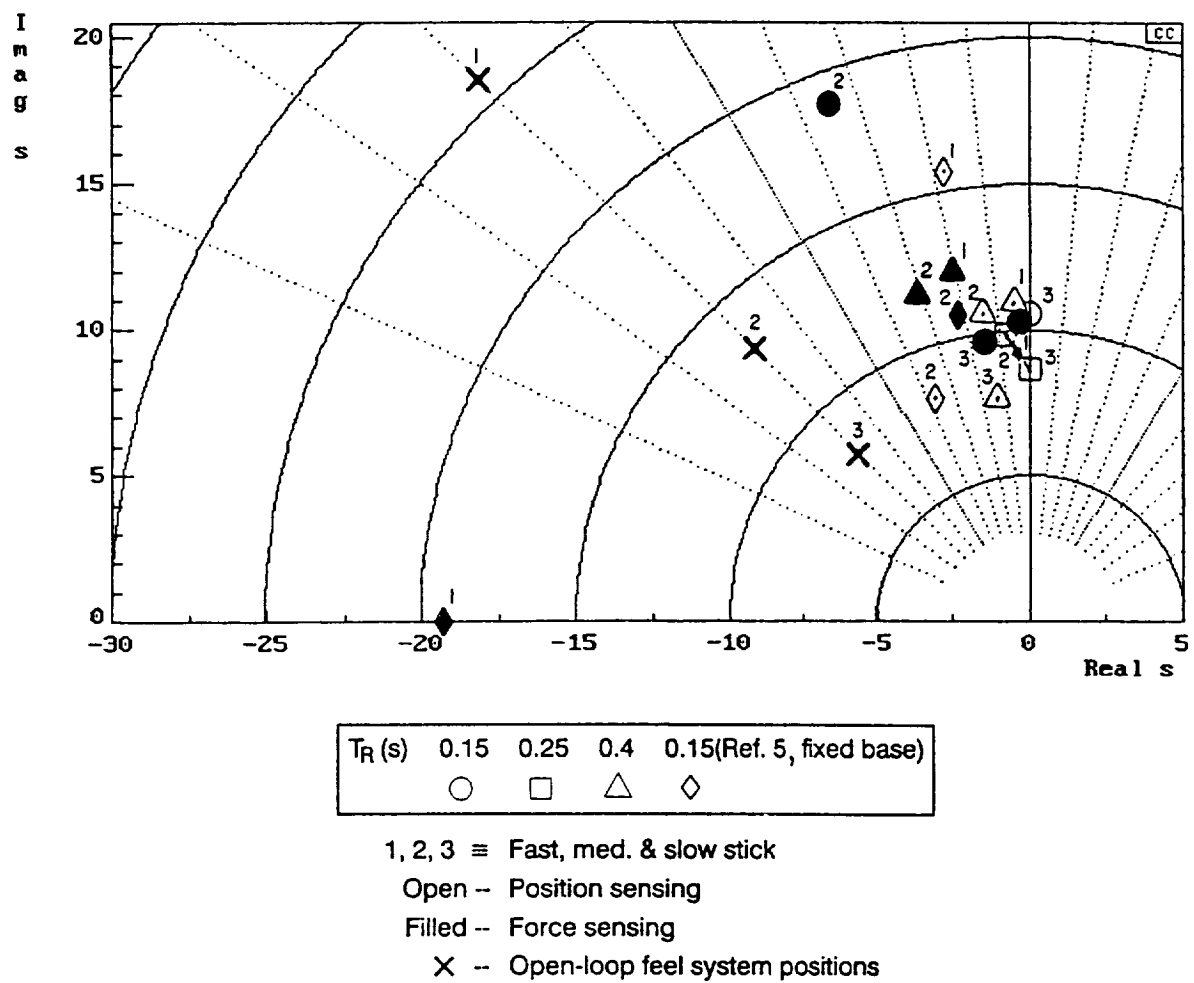
Figure 28. Limb/Manipulator Mode Variation with Configuration
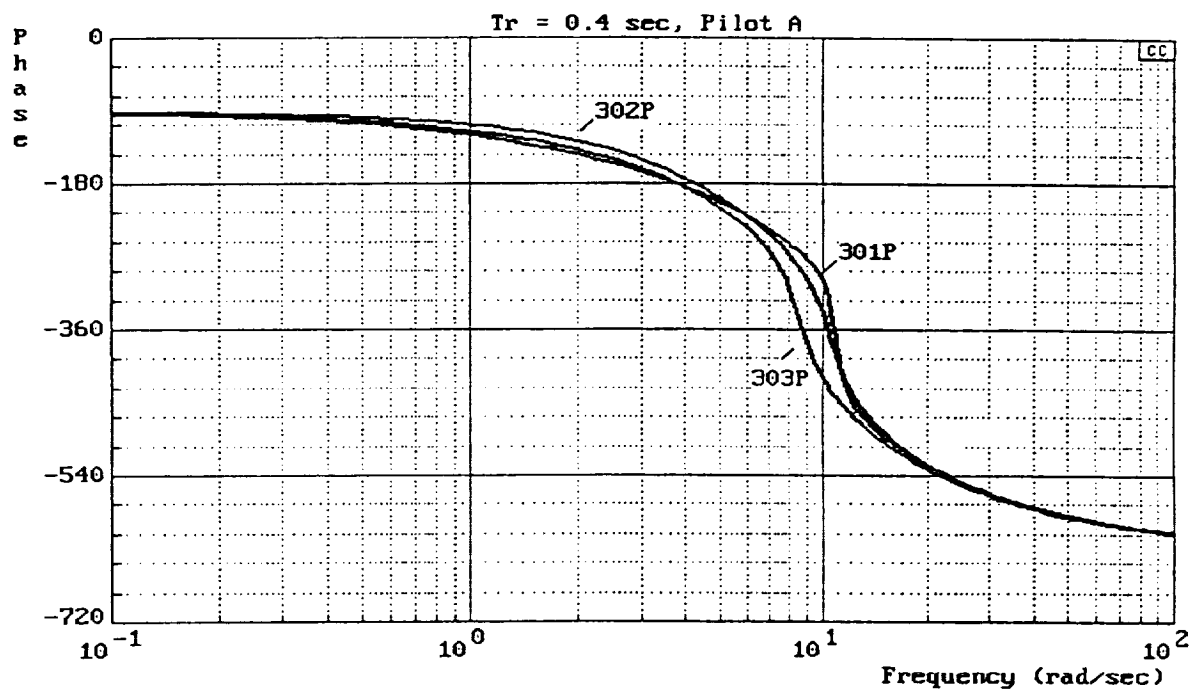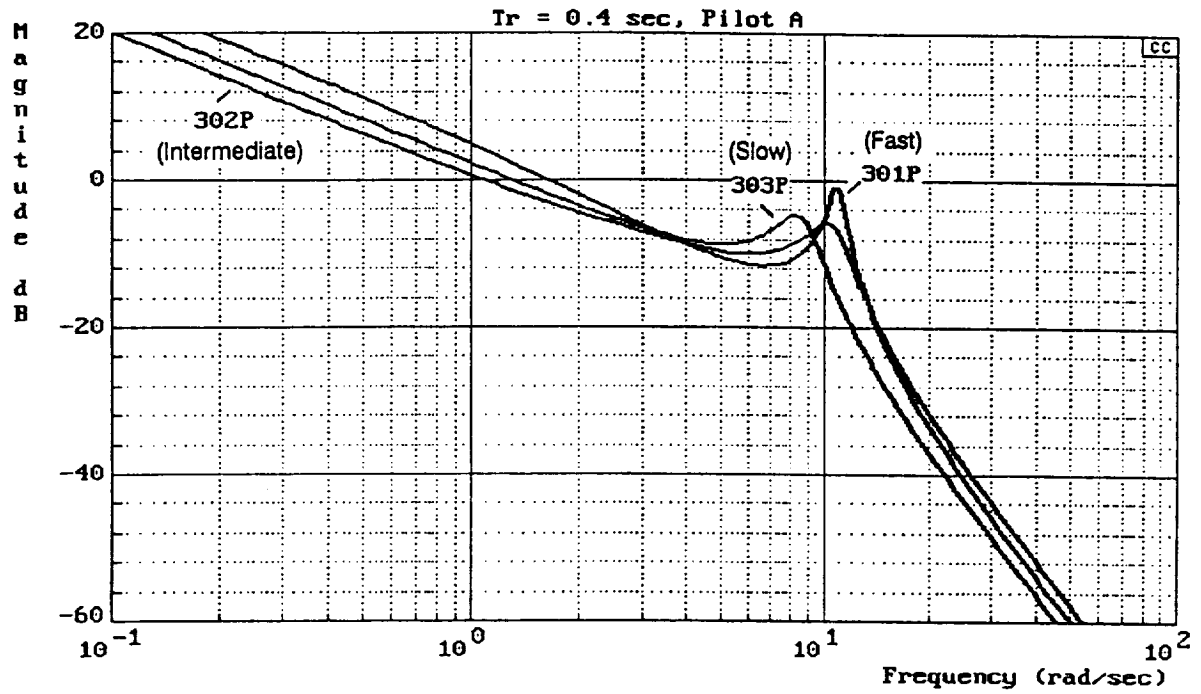
Figure 29. Comparison of Y_pY_c for Position Sensing Configurations, Pilot A $(T_R = 0.4s)$
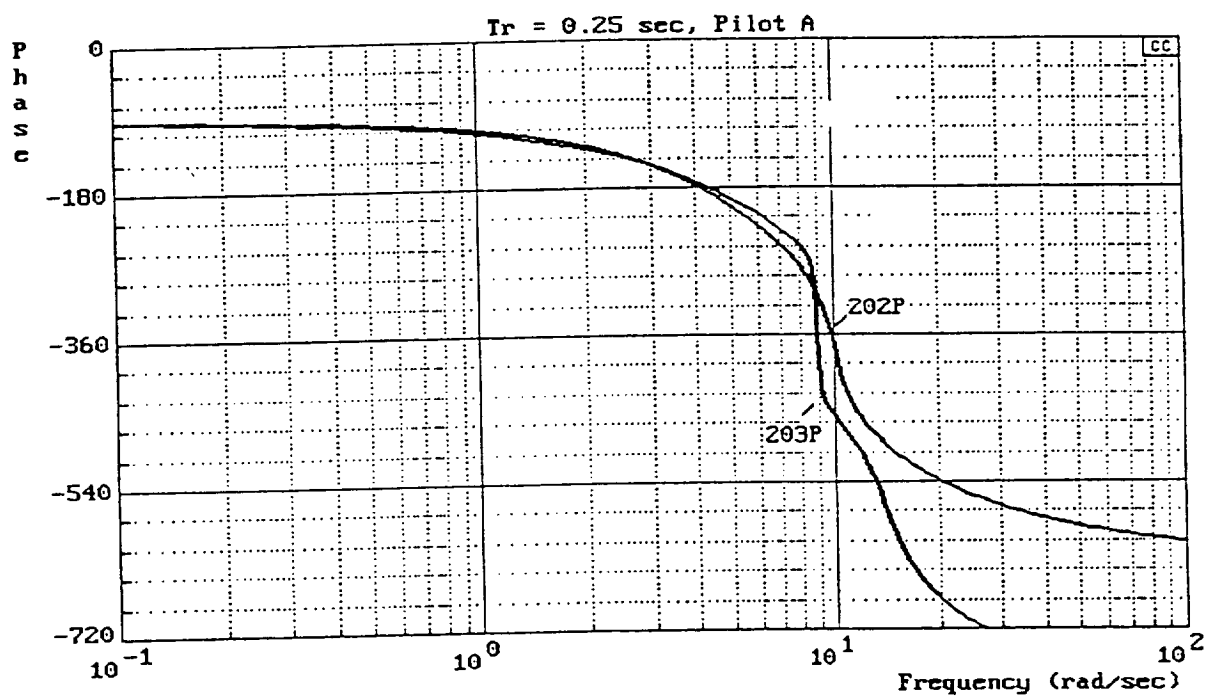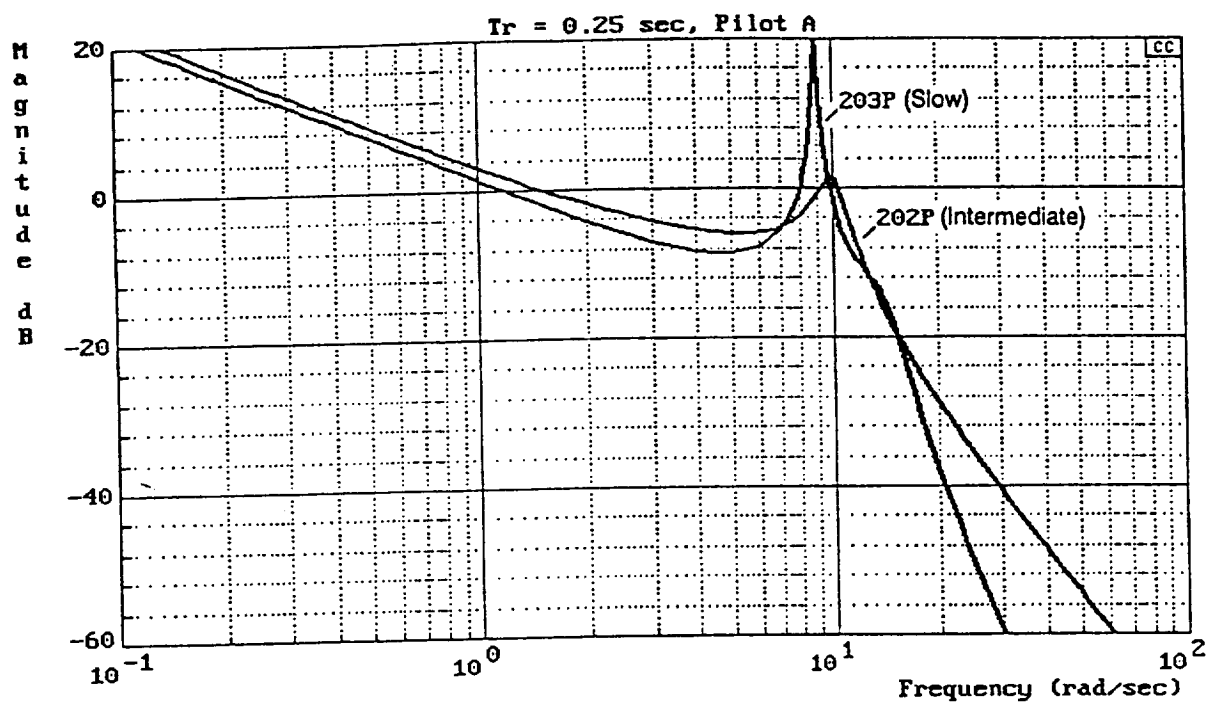
Figure 30. Comparison of Y_pY_c for Position Sensing Configurations, Pilot A $(T_R = 0.25s)$
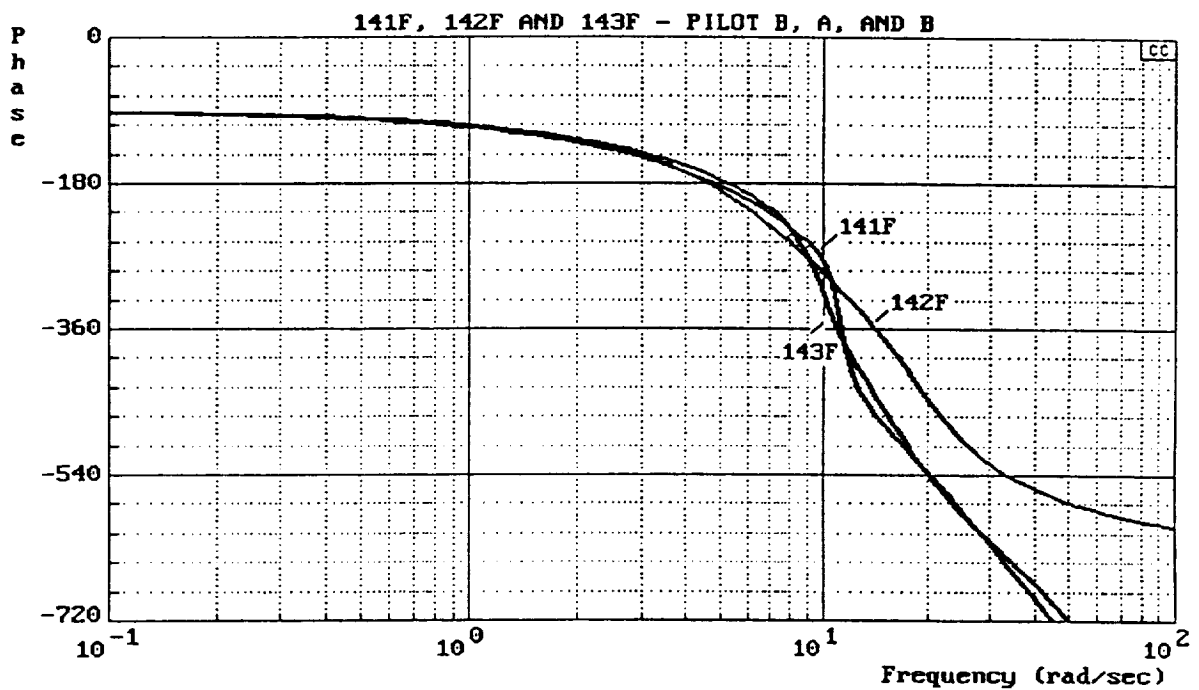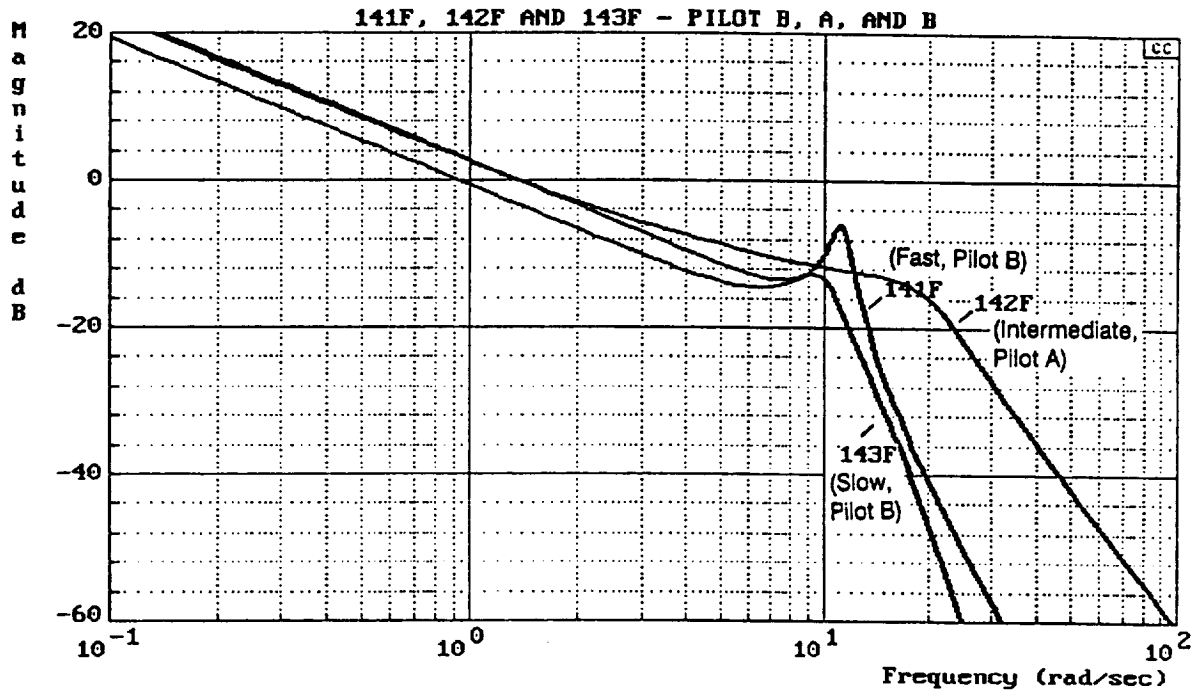
Figure 31. Comparison of $Y_p Y_c$ for Force Sensing Configurations, Pilots A and B (T_R = 0.15s)

TR = 0.4 SEC, FORCE SENS, FAST & MED STICK

342F (Intermediate)

341F (Fast)

TR = 0.4 SEC, FORCE SENS, FAST & MED STICK

342F

341F
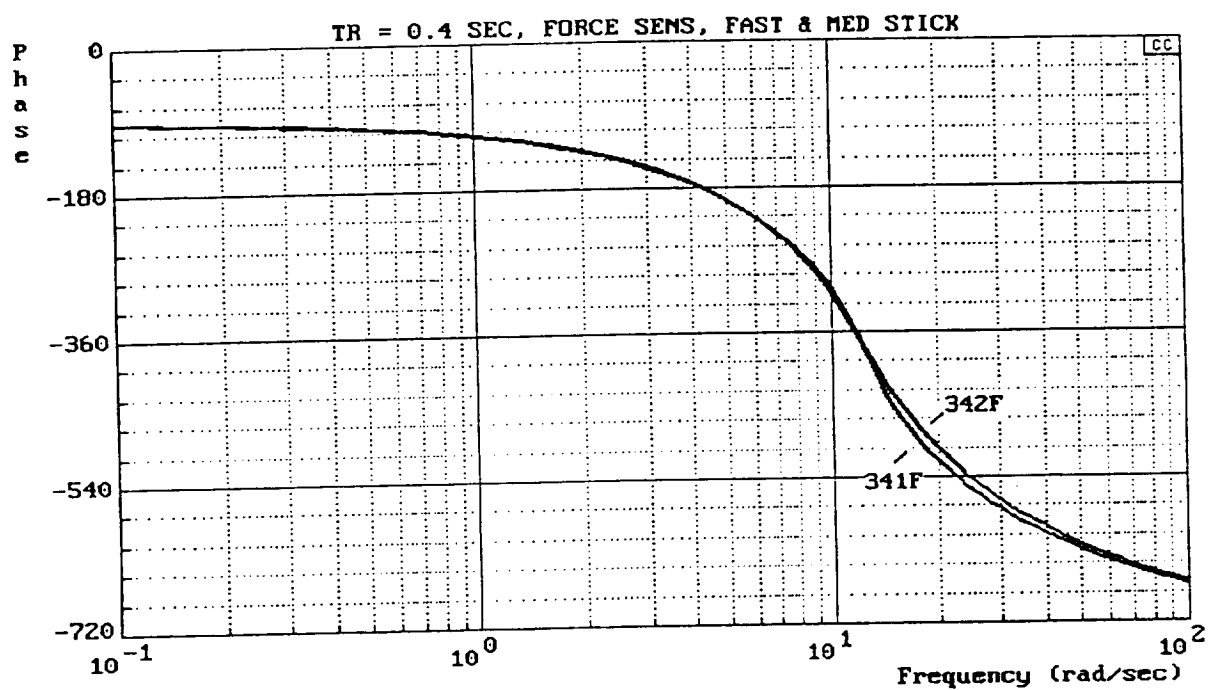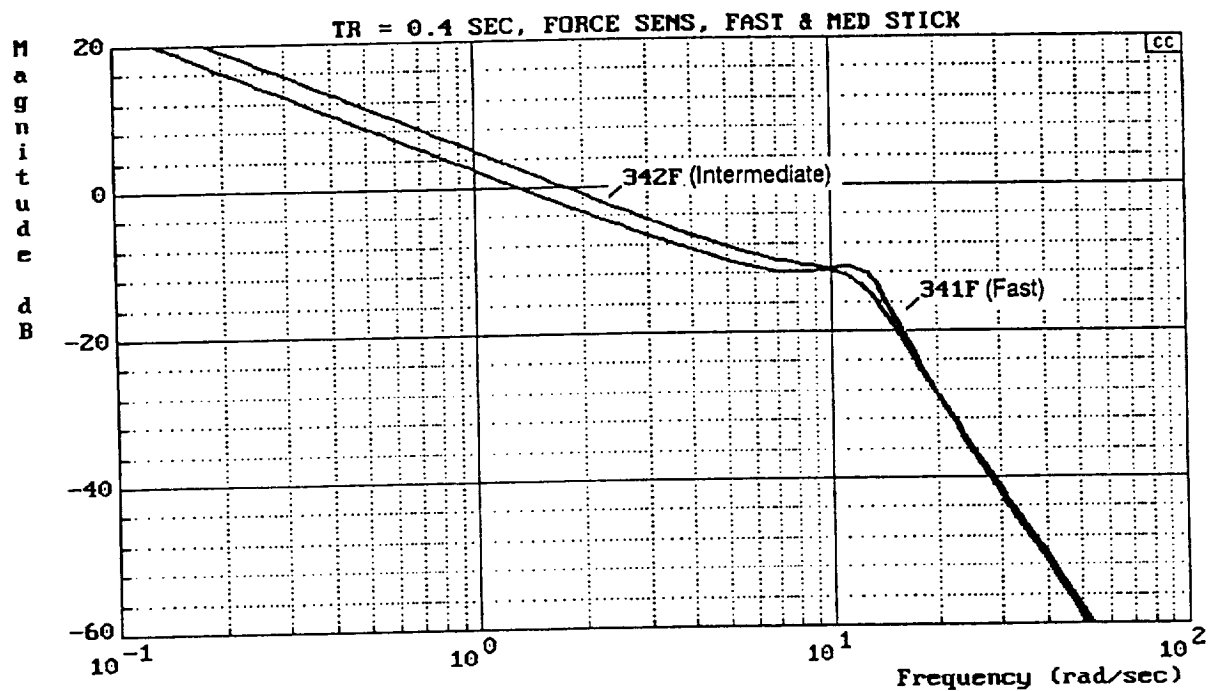
Figure 32. Comparison of $Y_p Y_c$ for Force Sensing Configurations, Pilot A
$(T_R = 0.4s)$
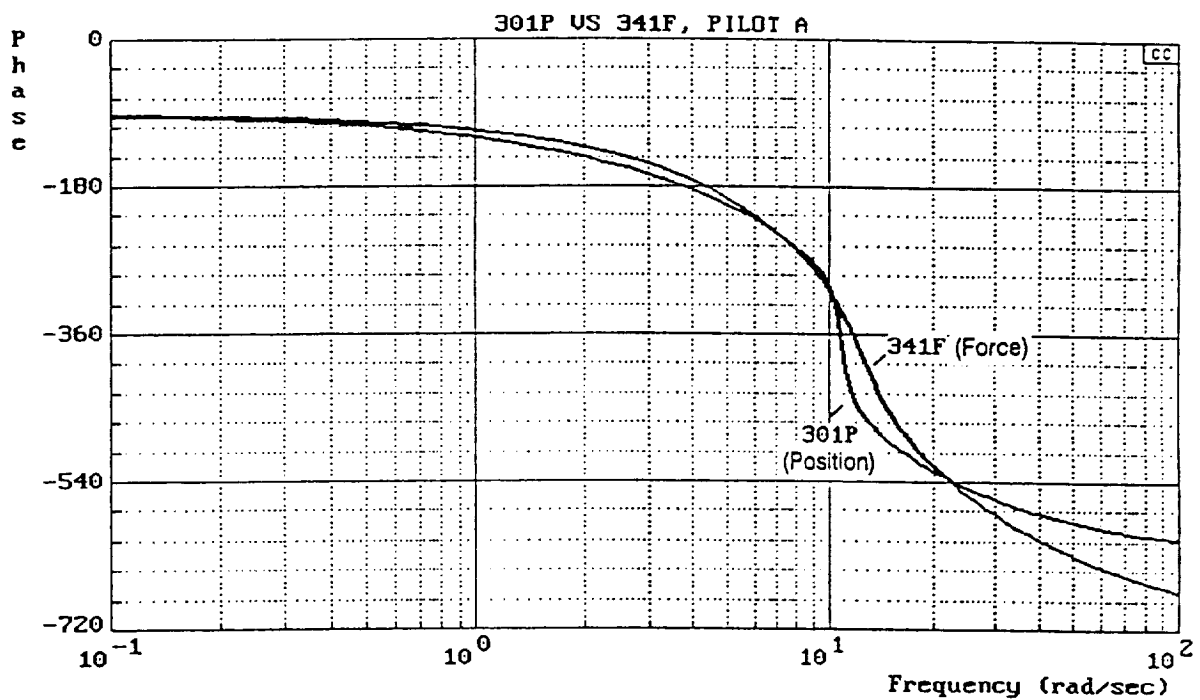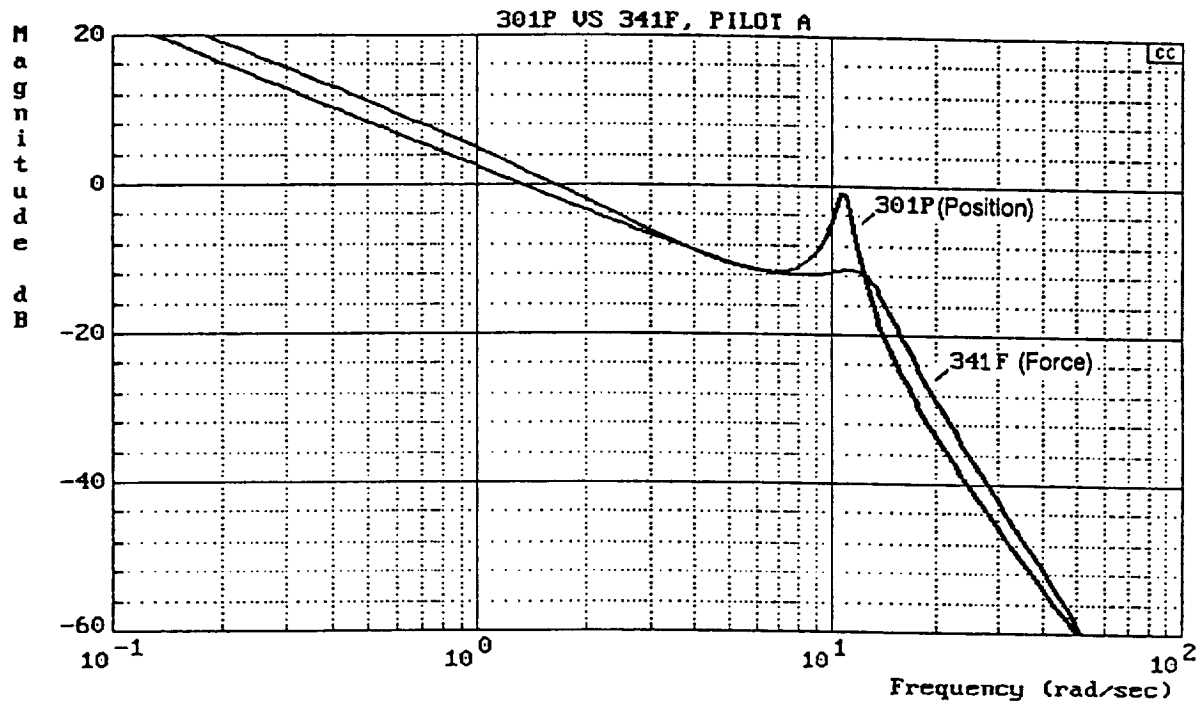
Figure 33. Comparison of $Y_p Y_c$ for Fast Feel System (T_R = 0.45 s)

68
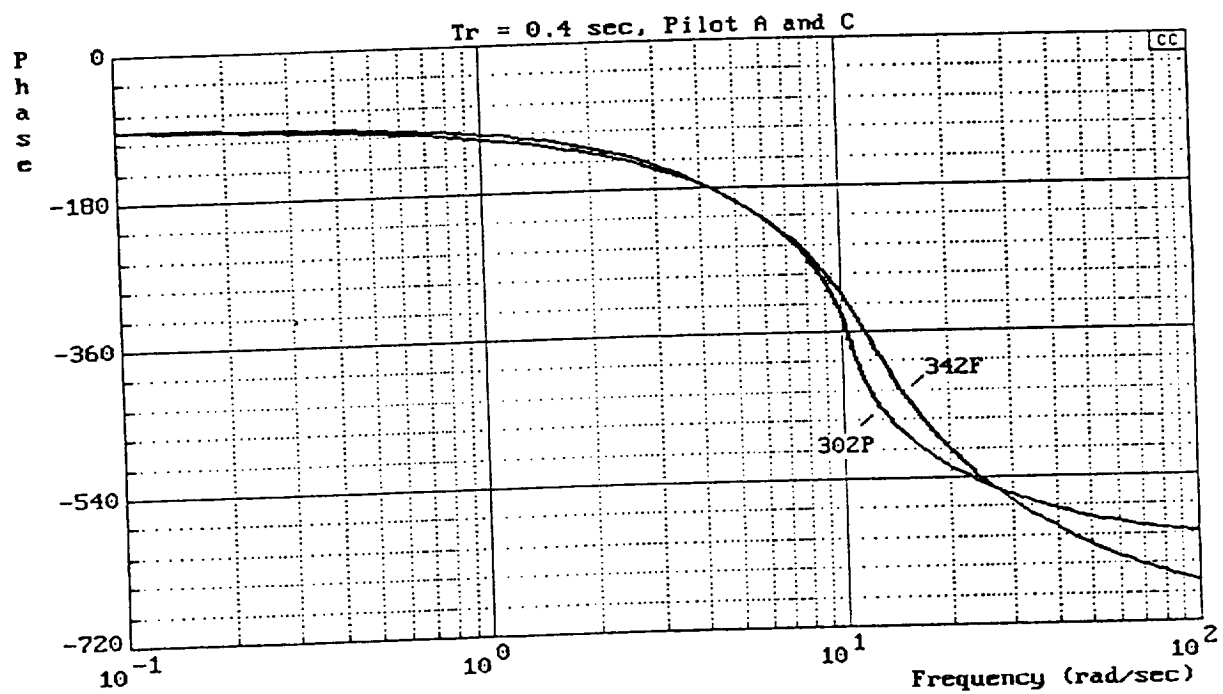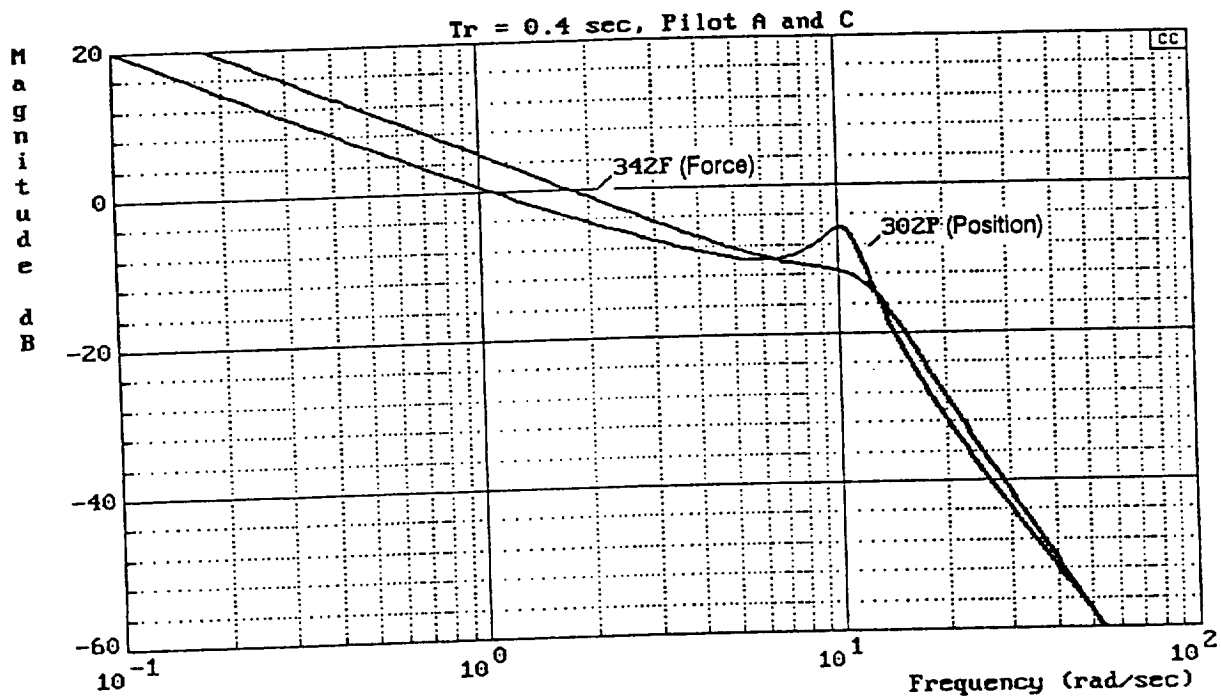
Figure 34. Comparison of Y_pY_c for Intermediate Feel System ($T_R = 0.45$ s)
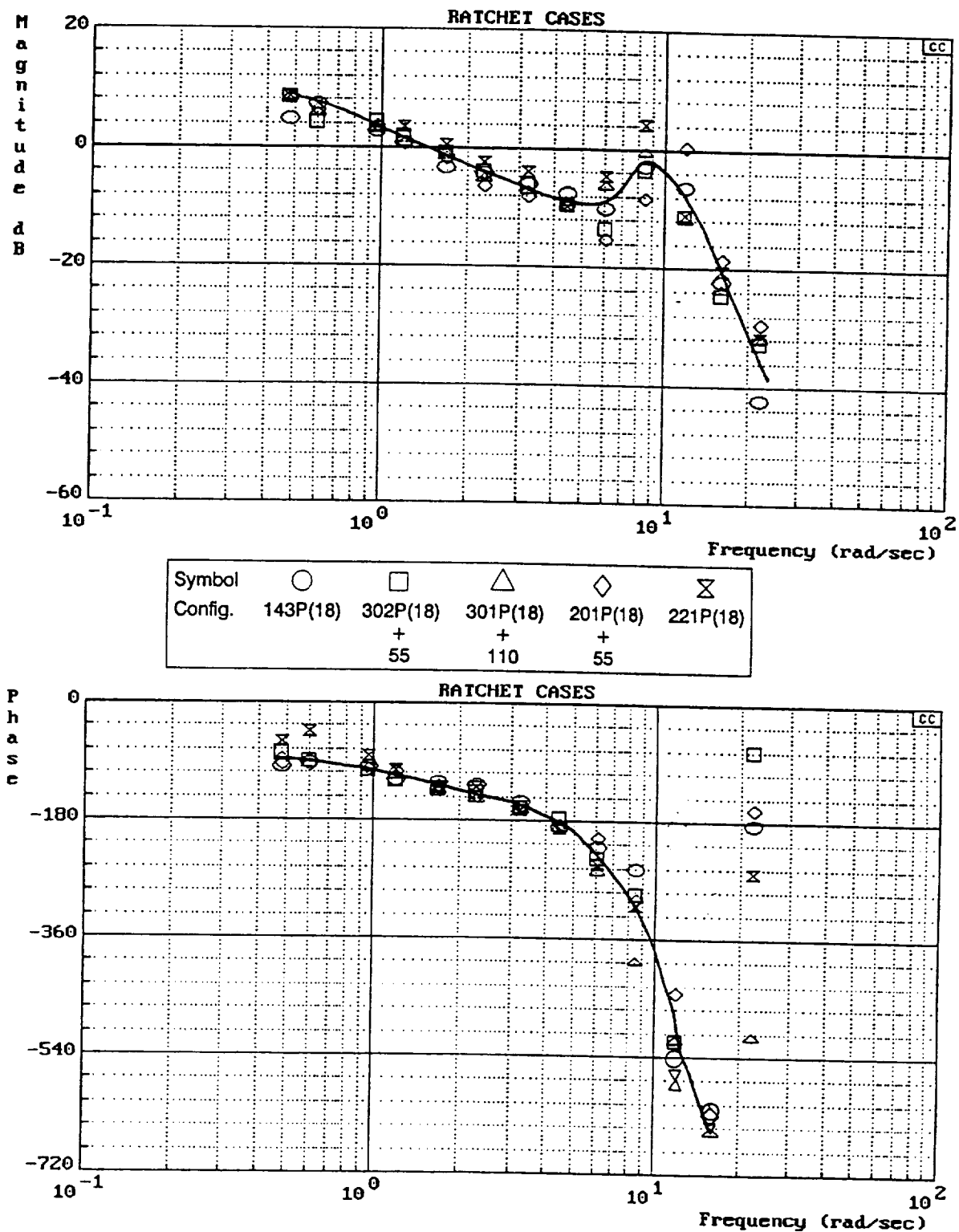
Figure 35. $Y_p Y_c$ Describing Functions for Ratchet Cases
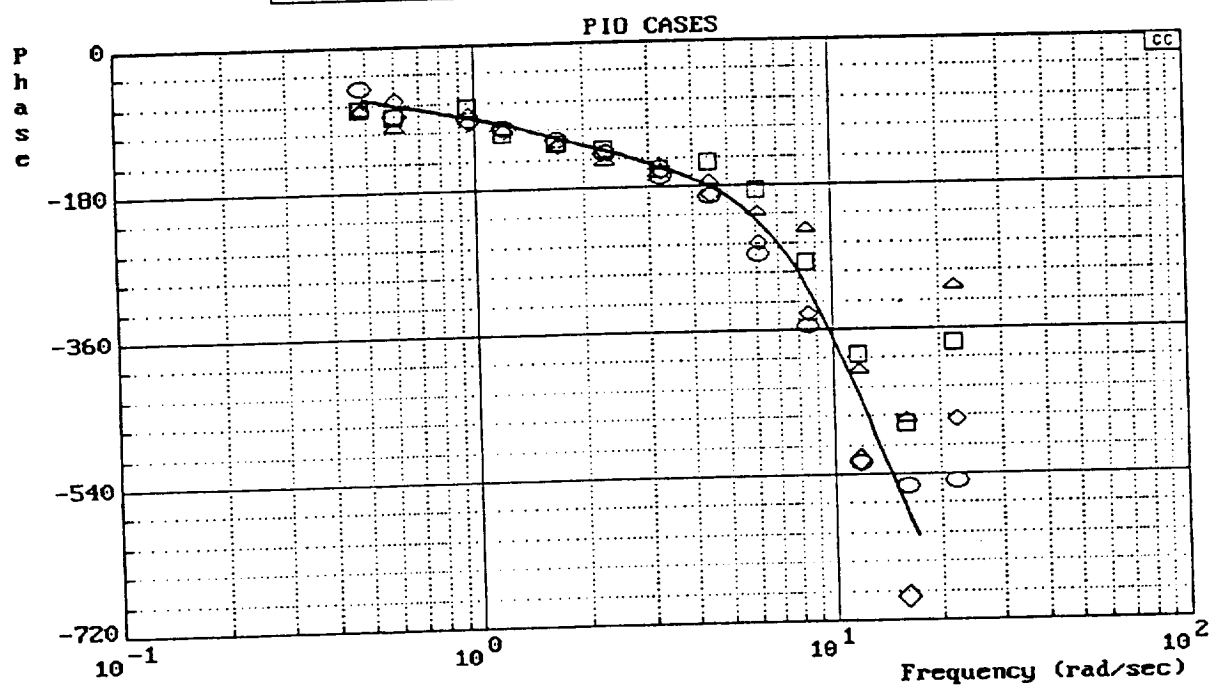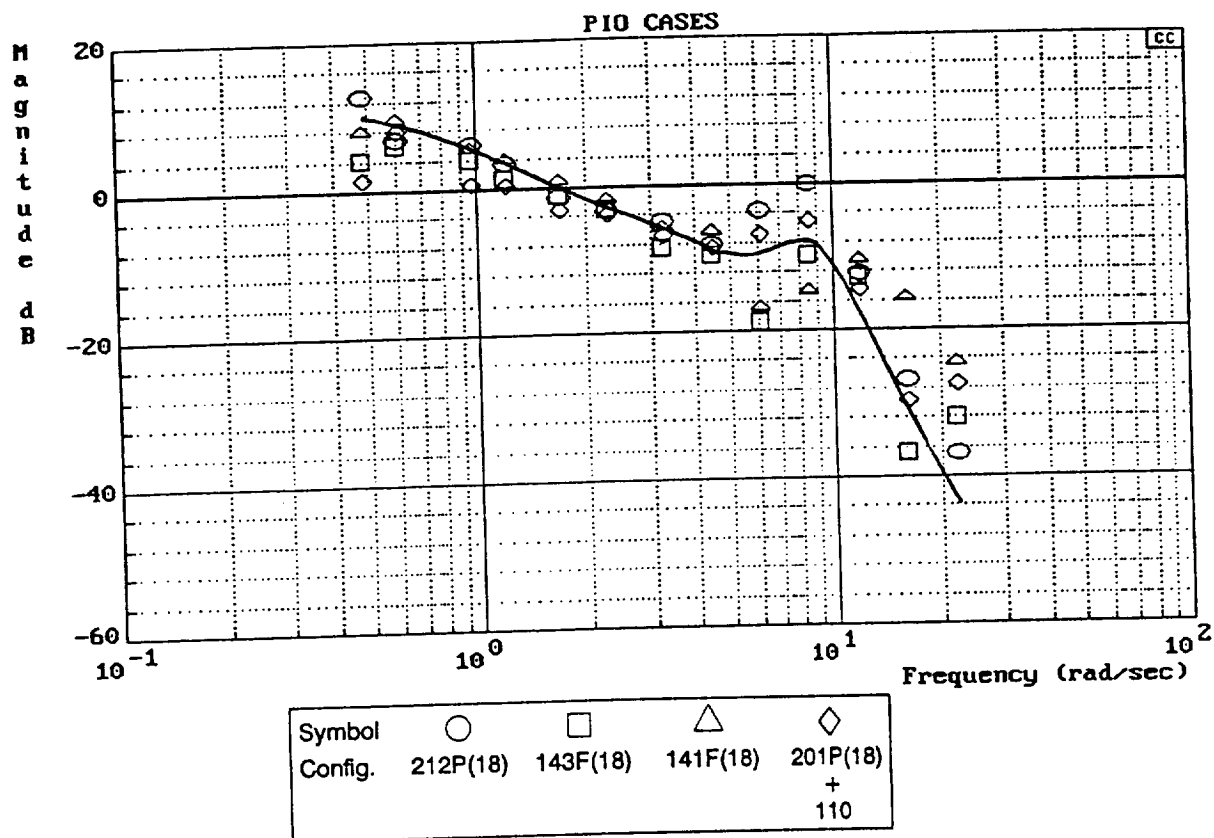
Figure 36. Y_pY_c Describing Functions for PIO Cases
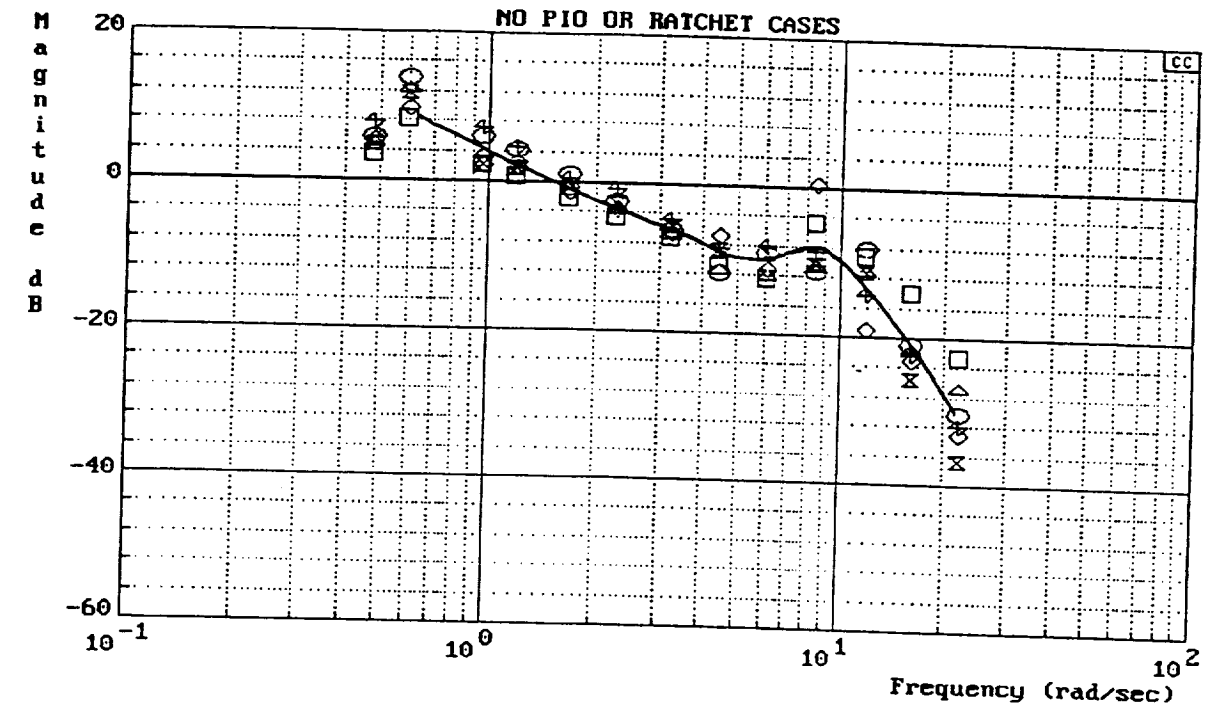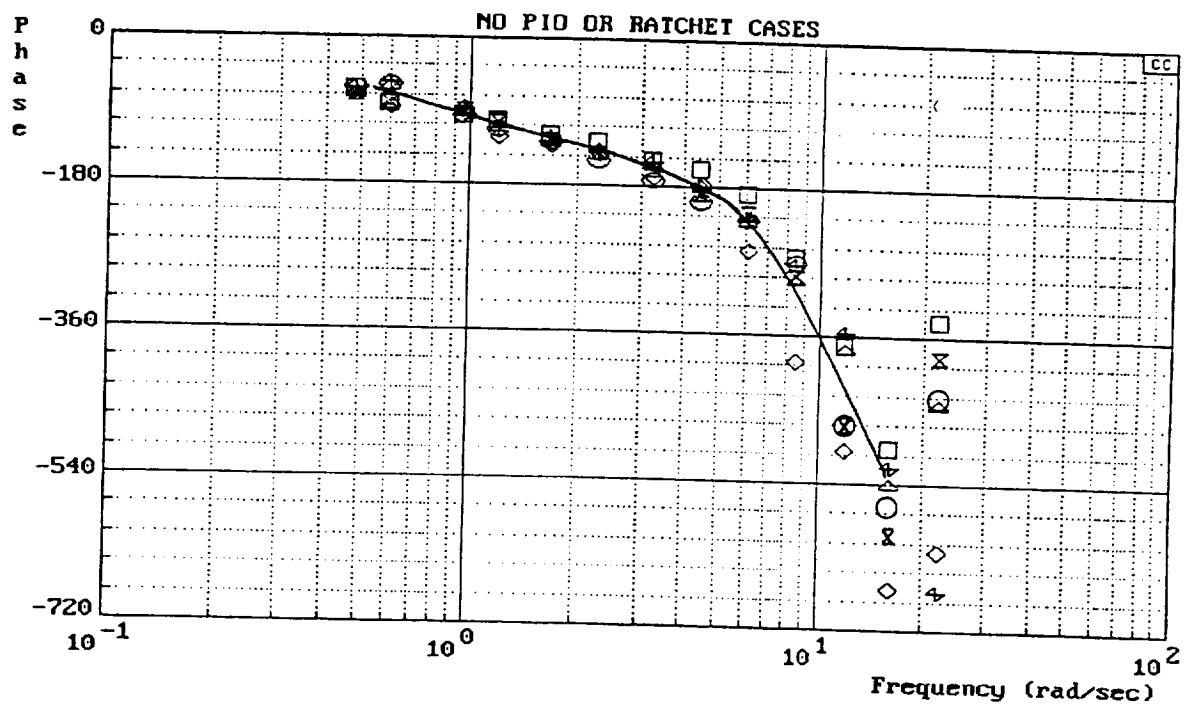
Figure 37. Y_pY_c Describing Functions for Level 1 Cases
(No Ratchet or PIO)
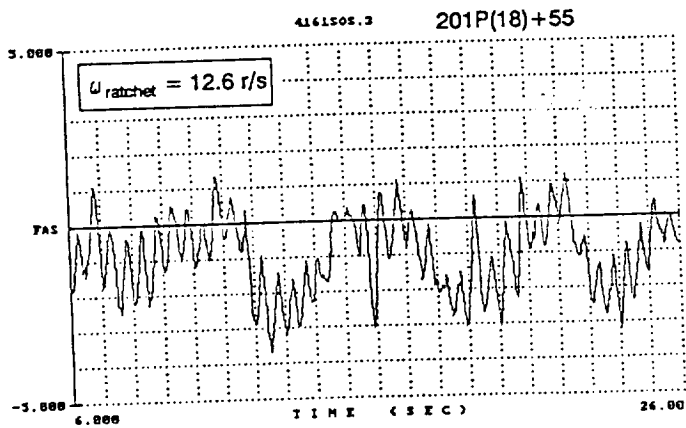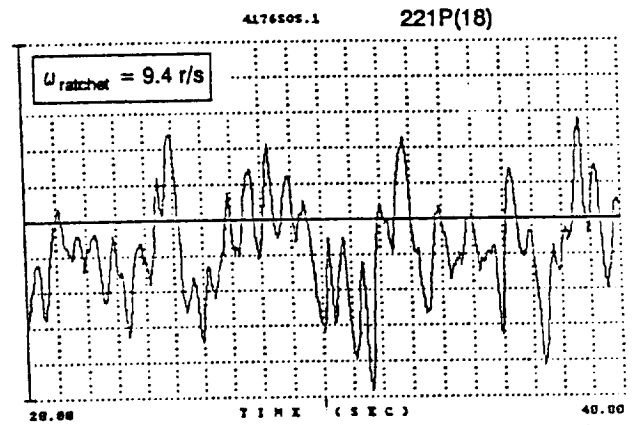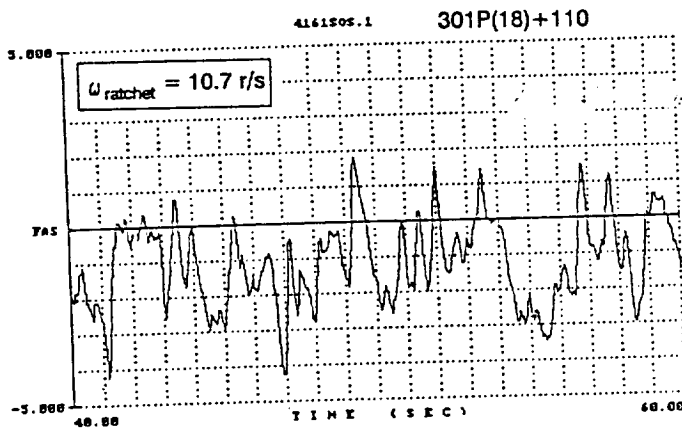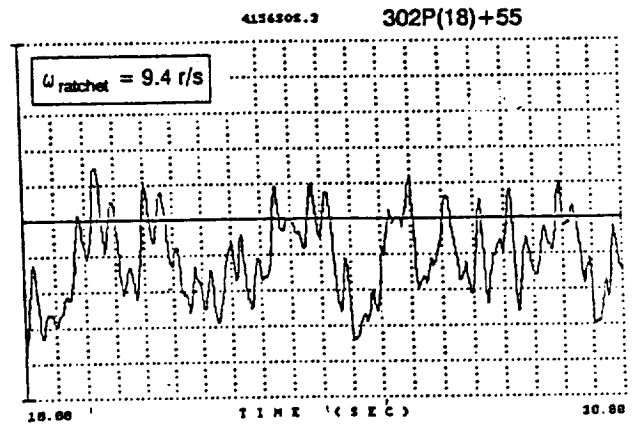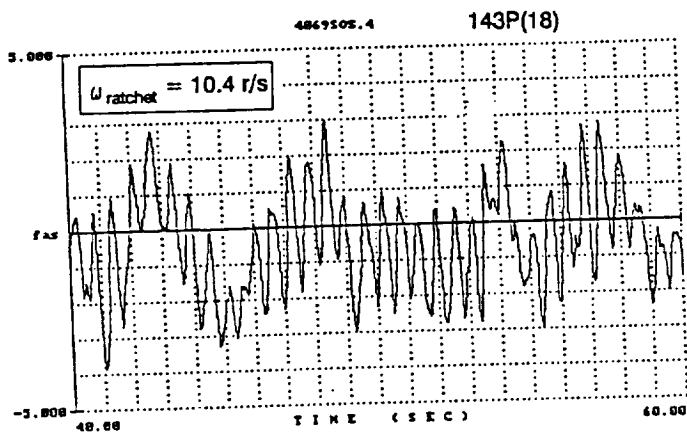
Figure 38. Stick Force Time Histories of Ratchet Incidences

73
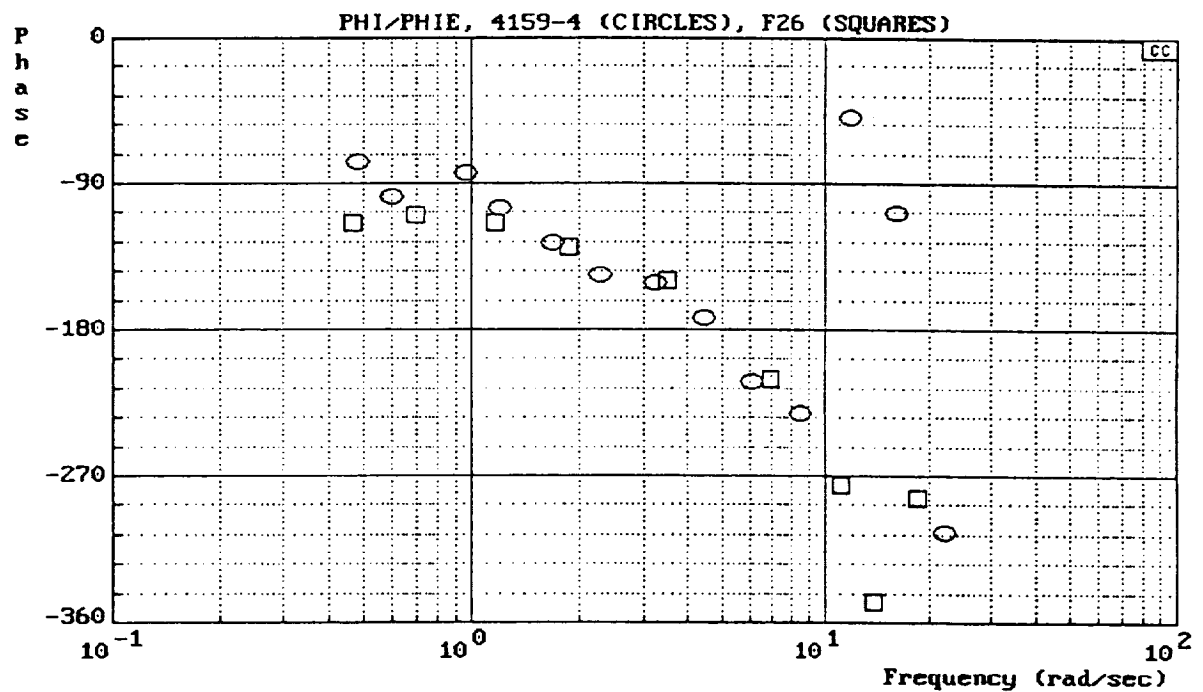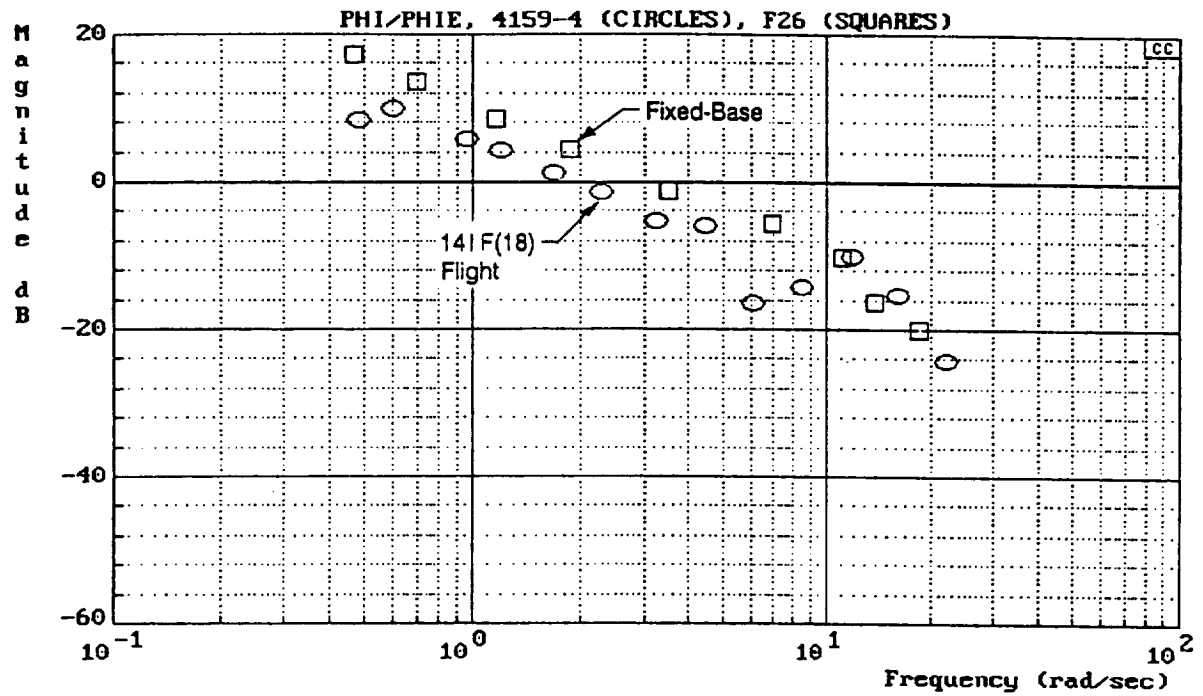
Figure 39. Comparison of Y_pY_c from Fixed-Base Simulation (Ref. 5) and Flight Test (Ref. 1) (Fast Feel System, T_R = 0.15 s)
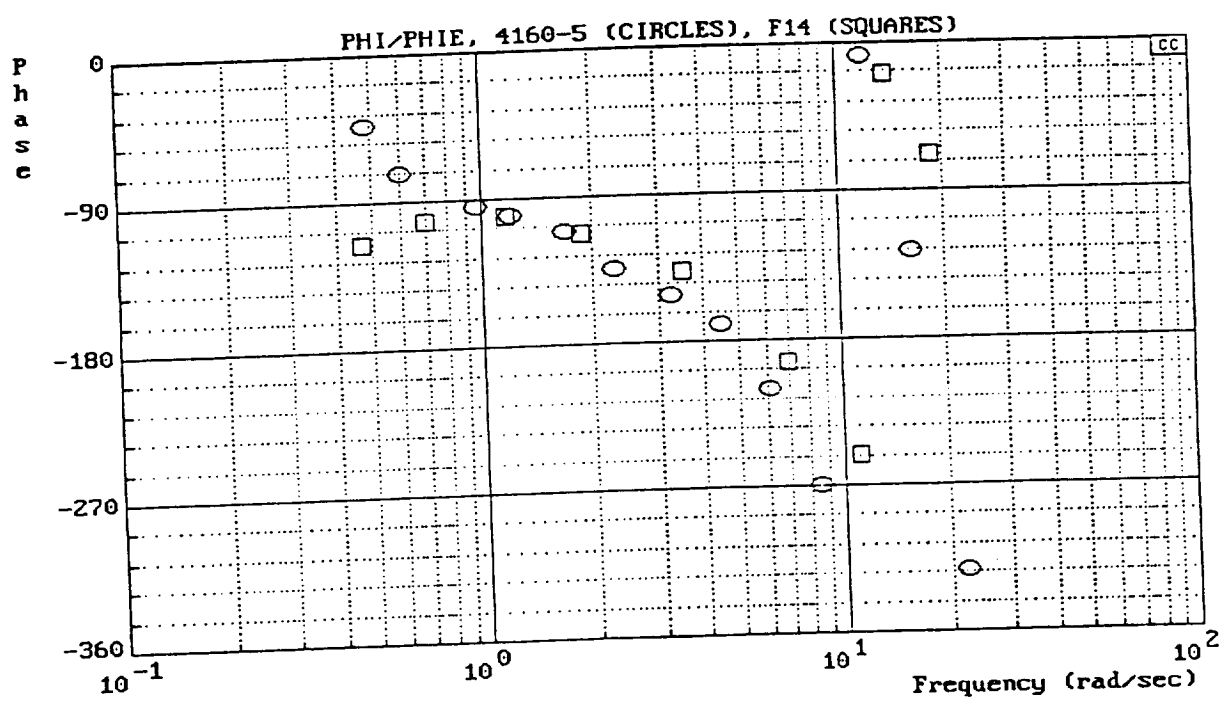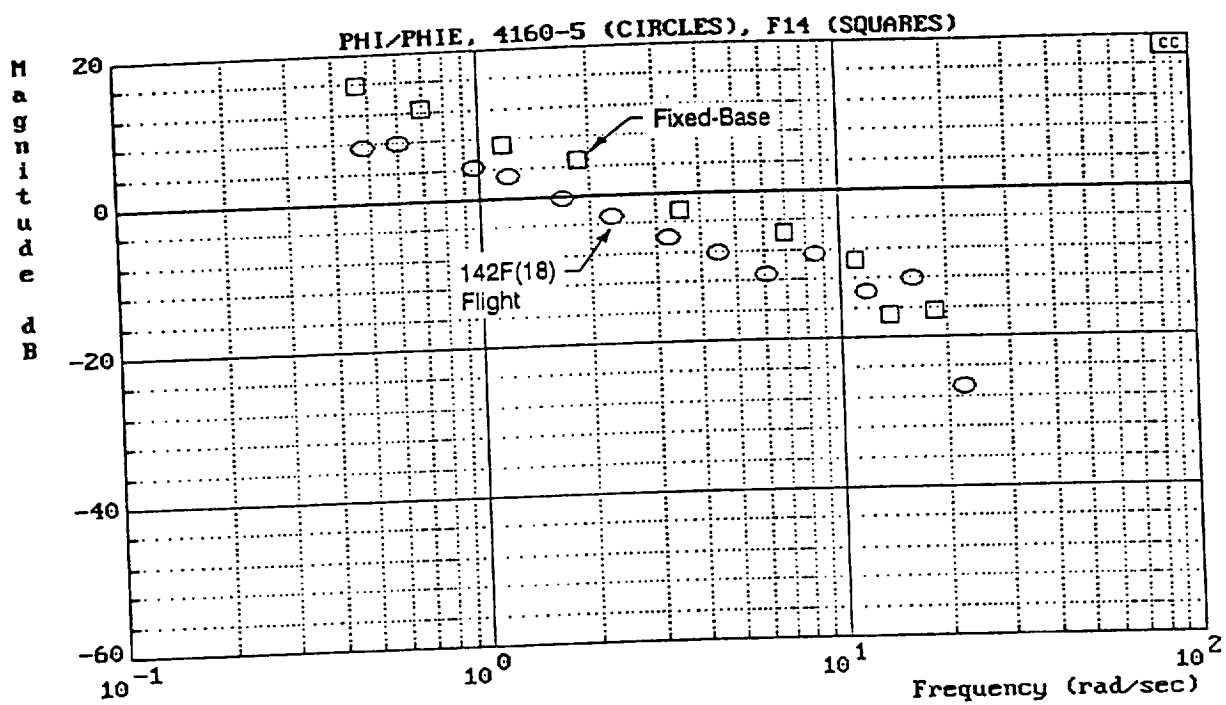
Figure 40. Comparison of Y_pY_c from Fixed-Base Simulation (Ref. 5) and Flight Test (Ref. 1) (Intermediate Feel System, T_R = 0.15 s)
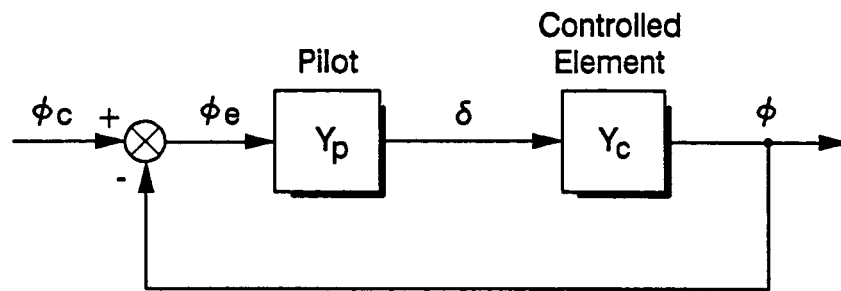
DAS -- Stick Position (in.)

FAS -- Stick Force (lbs)

P -- Roll Rate (deg/s)

PHIC -- Roll Command ϕ_c (deg)

PHIE -- Roll Tracking Error ϕ_e (deg)

PHI -- Roll Attitude ϕ (deg)

Figure A-1. HUD Tracking Task
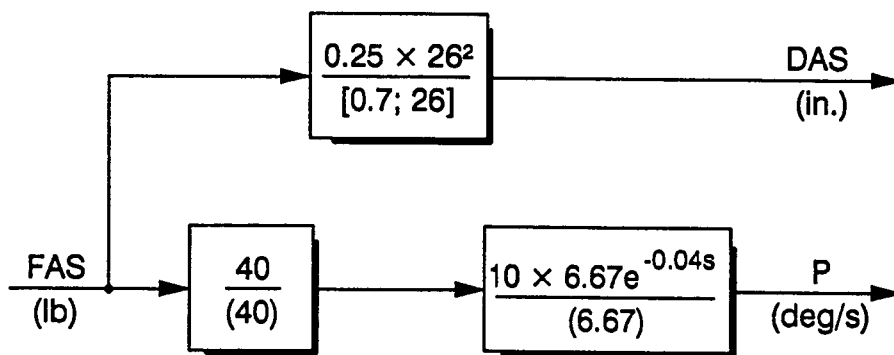
Figure A-2. Evaluated Configuration (141F(10))
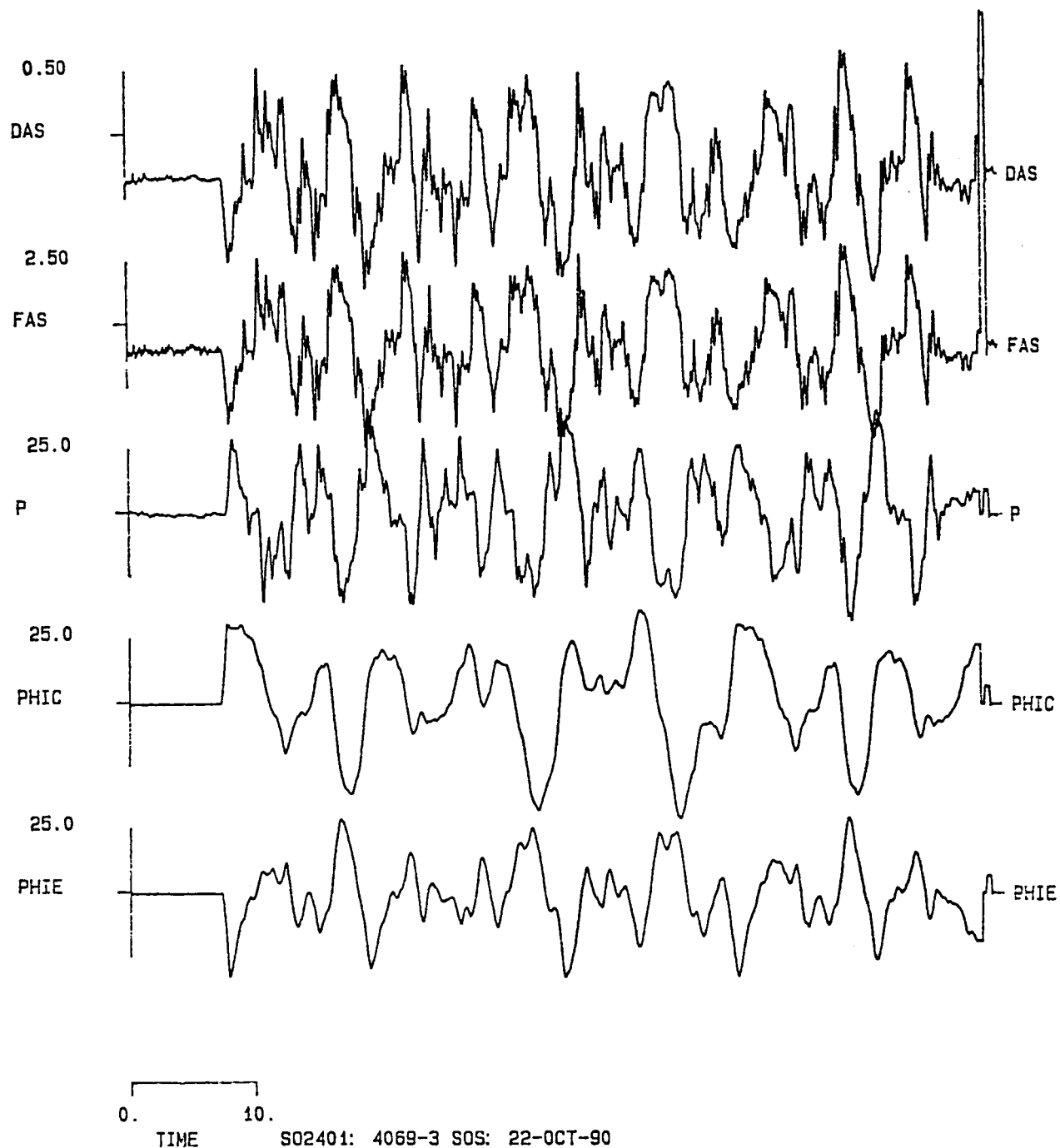
Figure A-3. Time Histories from Sum-of-Sines Tracking Run for Flight 4069-3
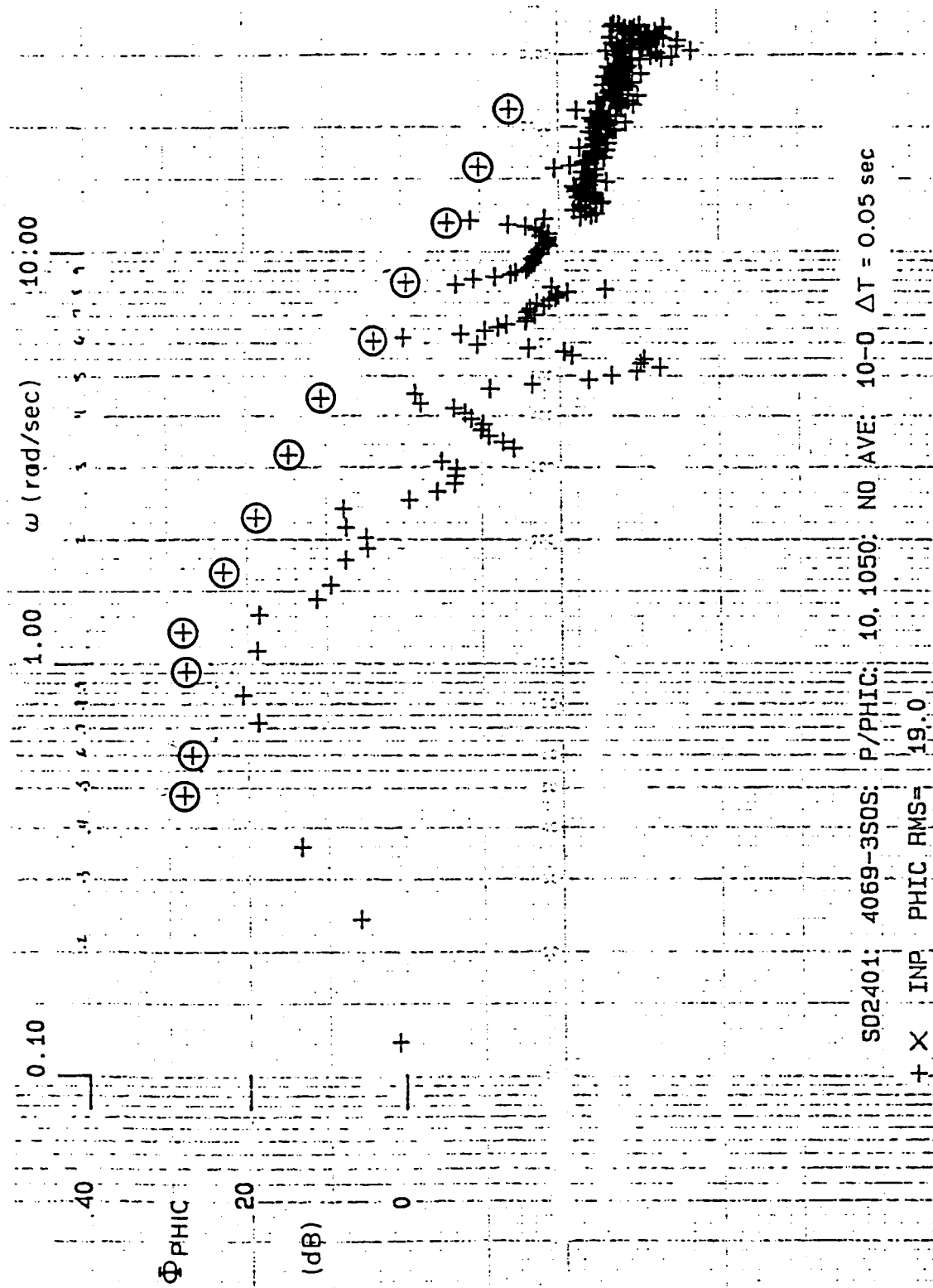
Figure A-4. Power Spectrum of Sum-of-Sines Input Function
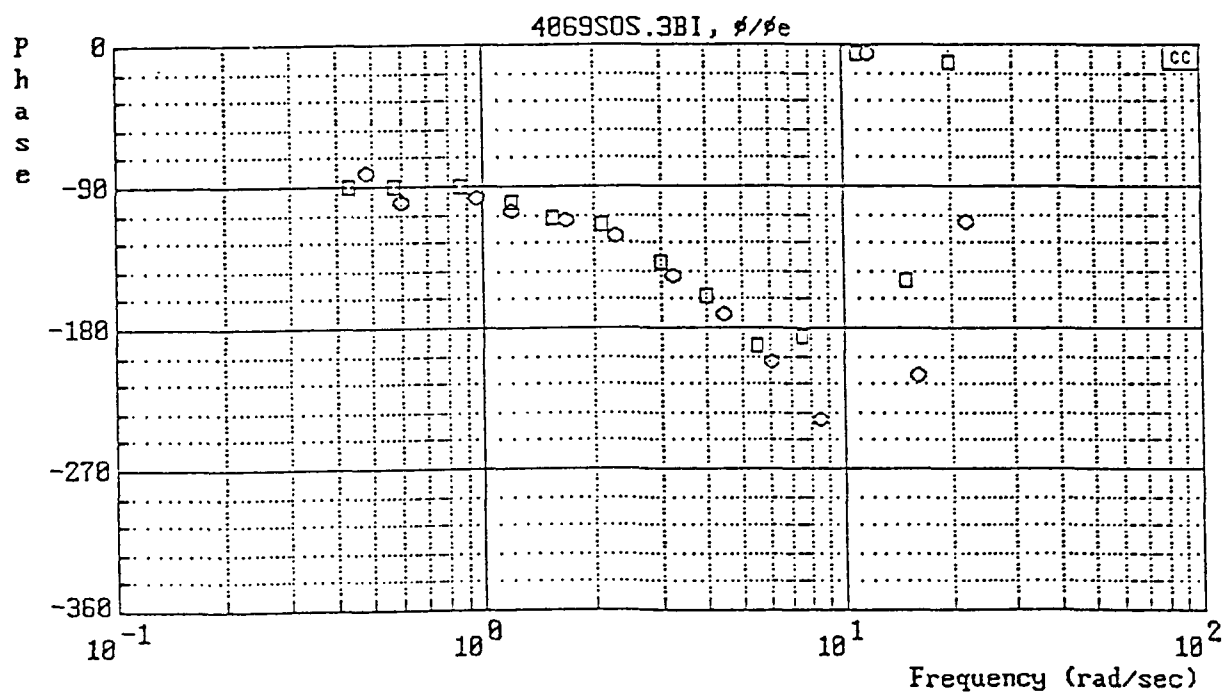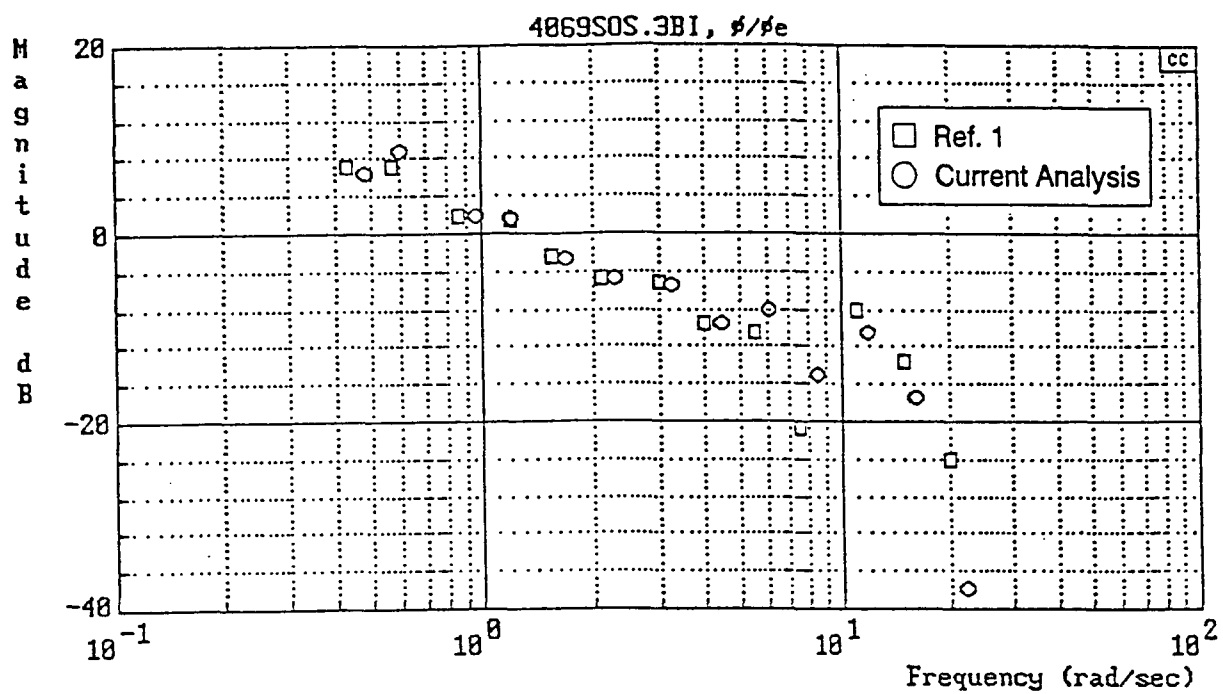
Figure A-5. Open-Loop Pilot/Vehicle Describing Functions,
Configuration 141F(10) — Flight 4069-3
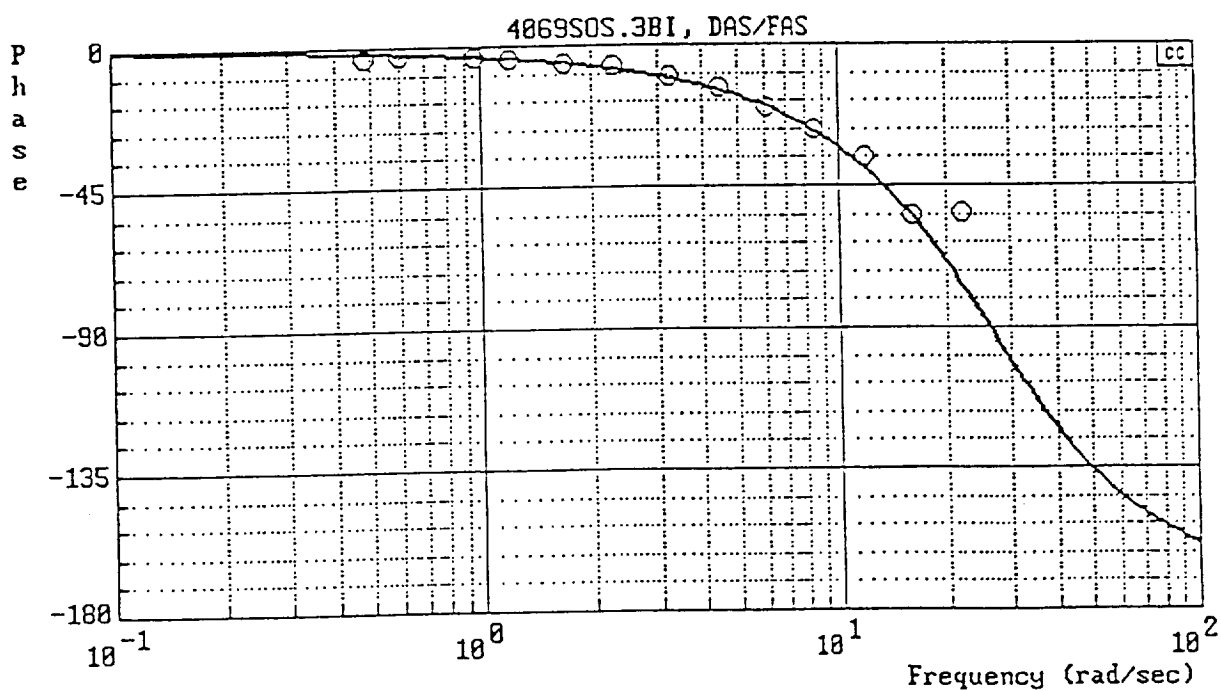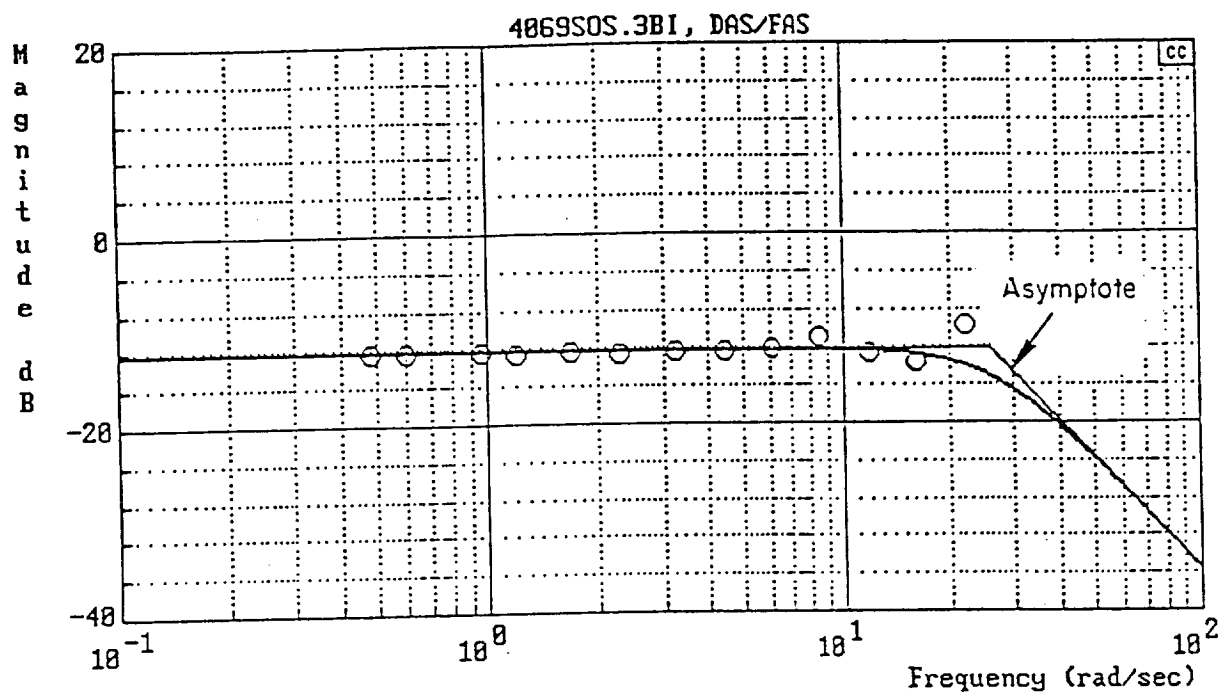
Figure A-6. Stick Dynamics and Describing Function,
Configuration 141F(10)
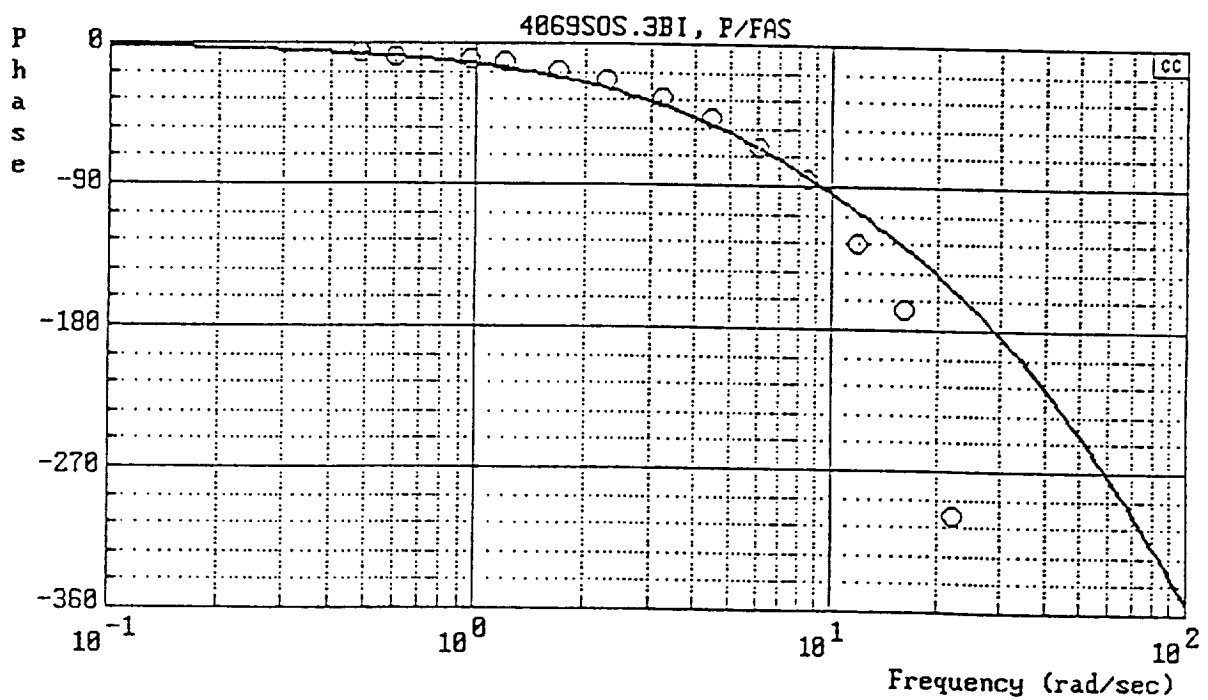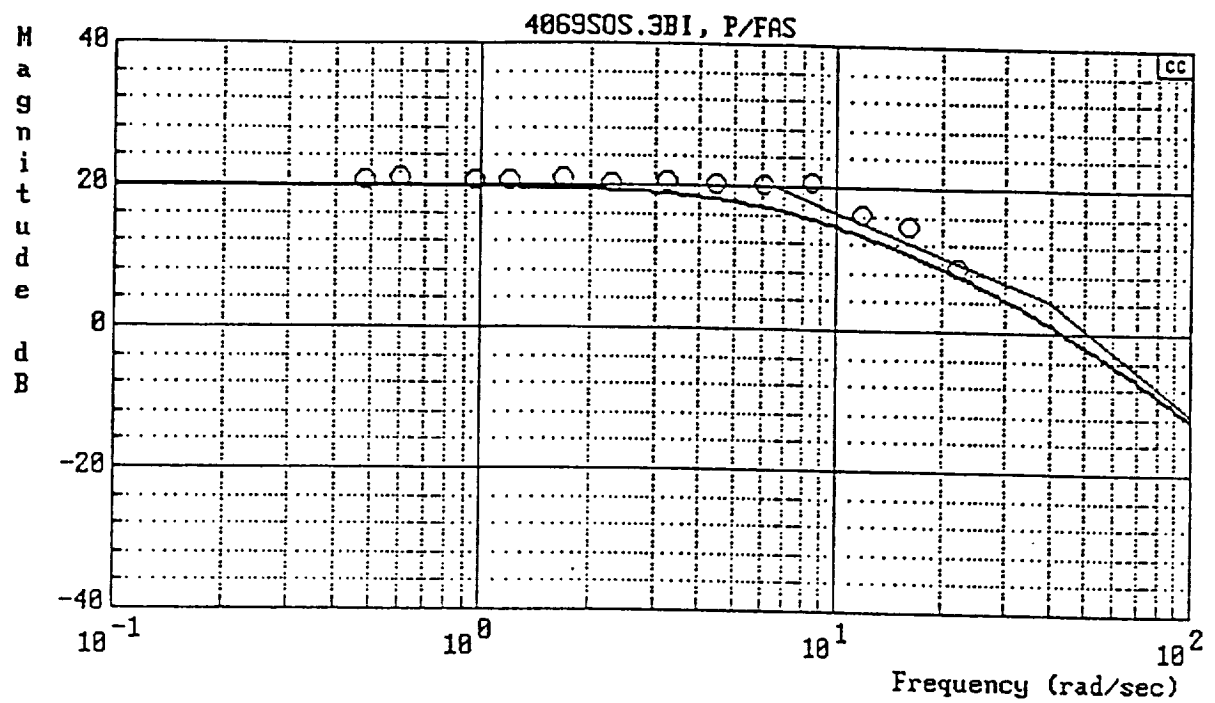
Figure A-7. Controlled Element Dynamics and Describing Function,
Configuration 141F(10)
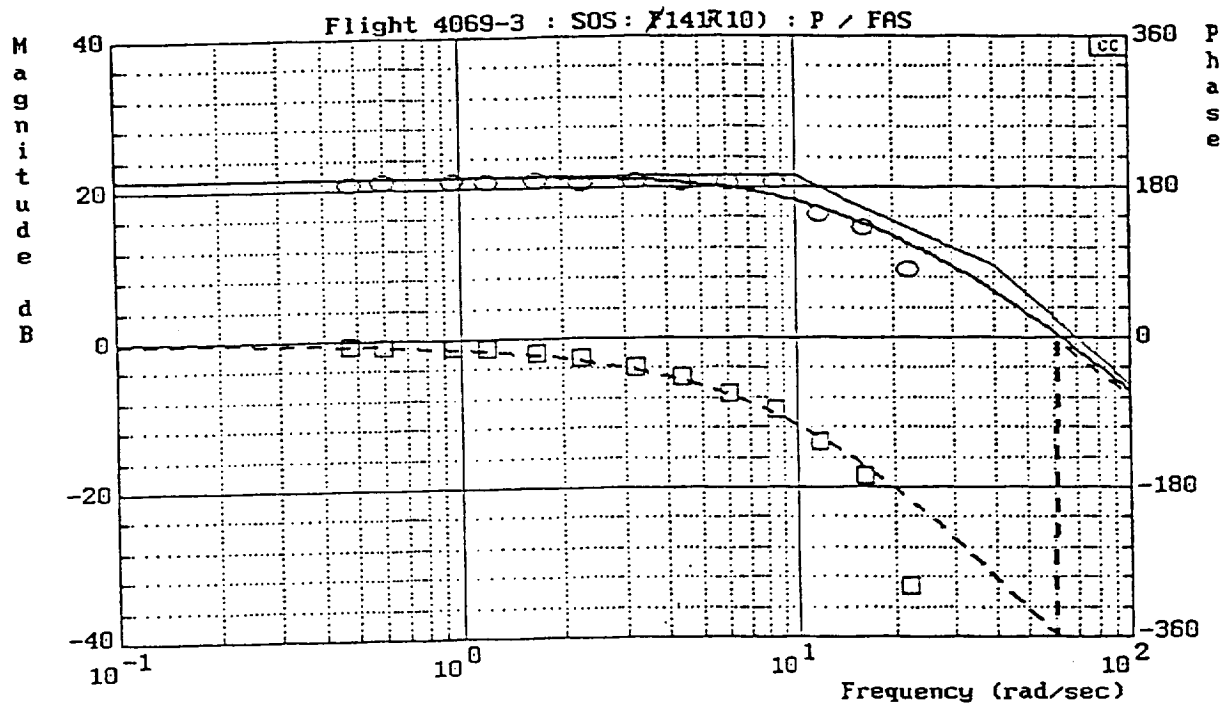
Figure A-8. Model Fit to Controlled Element Describing Function,
Configuration 141F(10)

$$\frac{P}{FAS} = \frac{12 \times 10 \times e^{-0.08s}}{(10)}$$
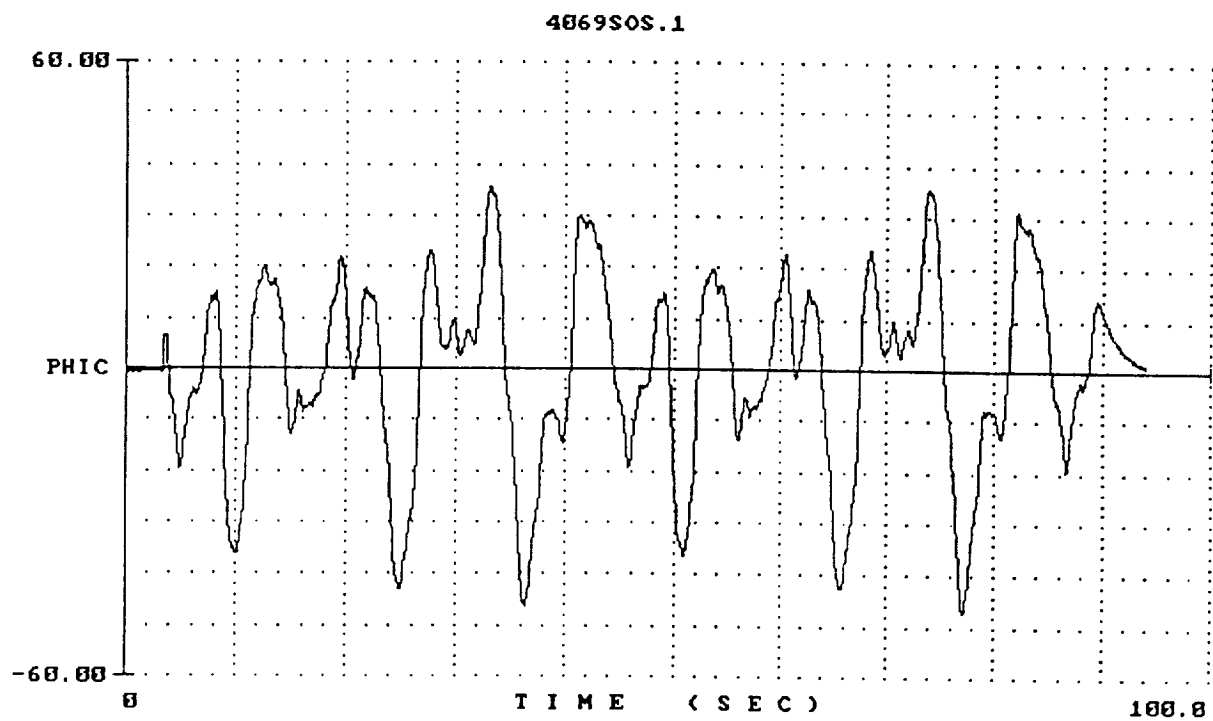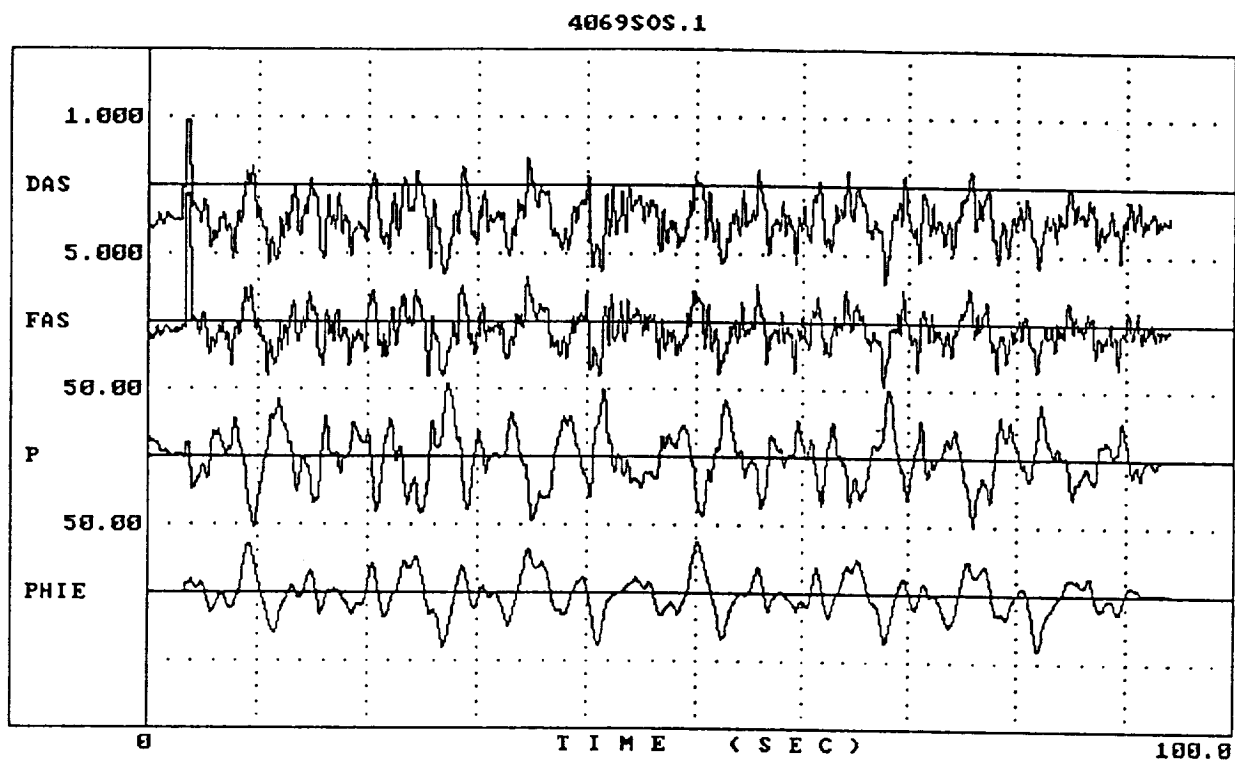
a) Time Histories

Figure B-1. Flight 4069-1

P069.1PD, P/DAS

$$Y_c = \frac{7200[-.8660254, 86.60254]}{(2.5)(40)[.8660254, 86.60254]}$$
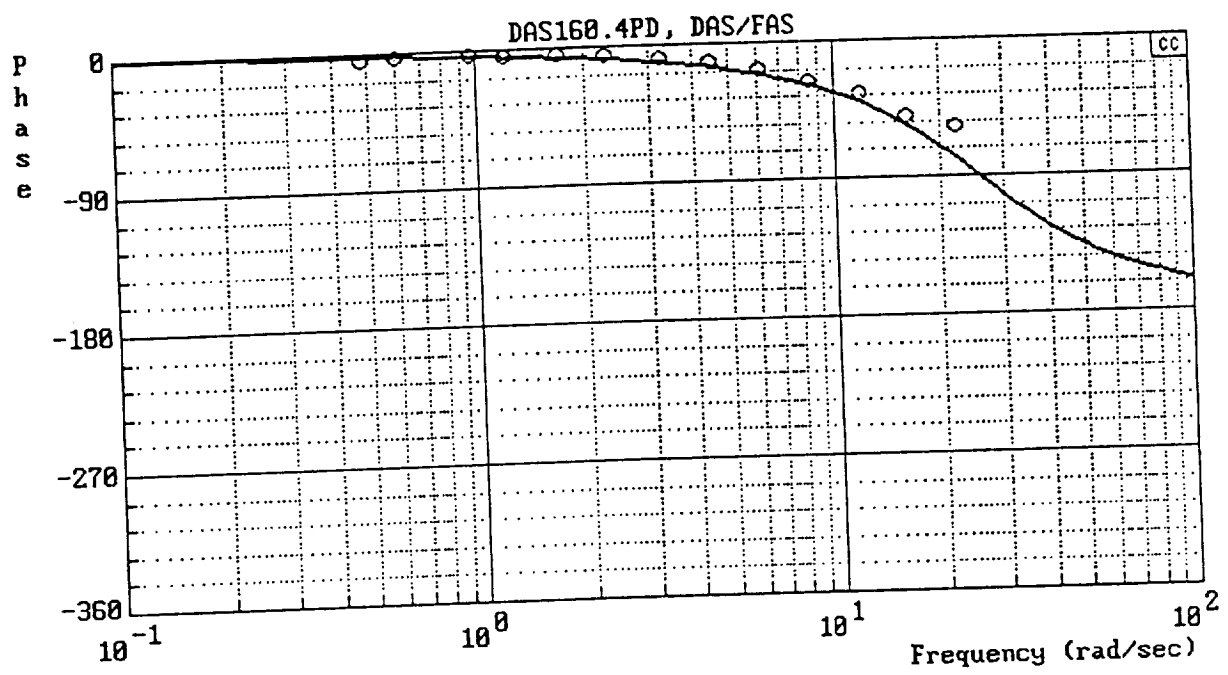

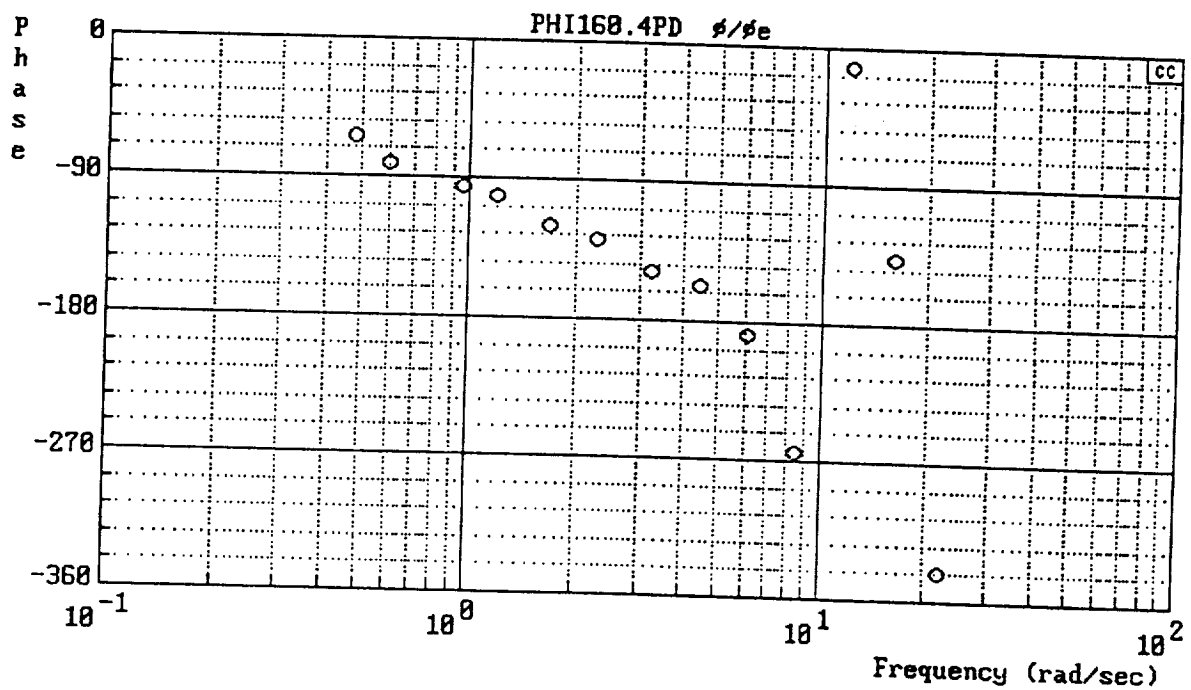P069.1PD, P/DAS
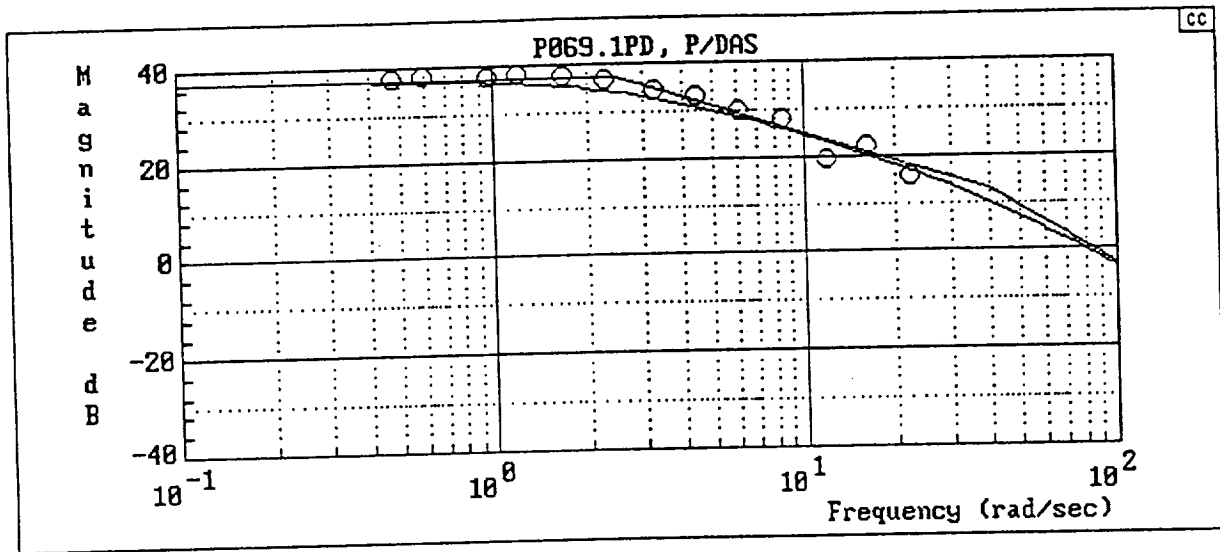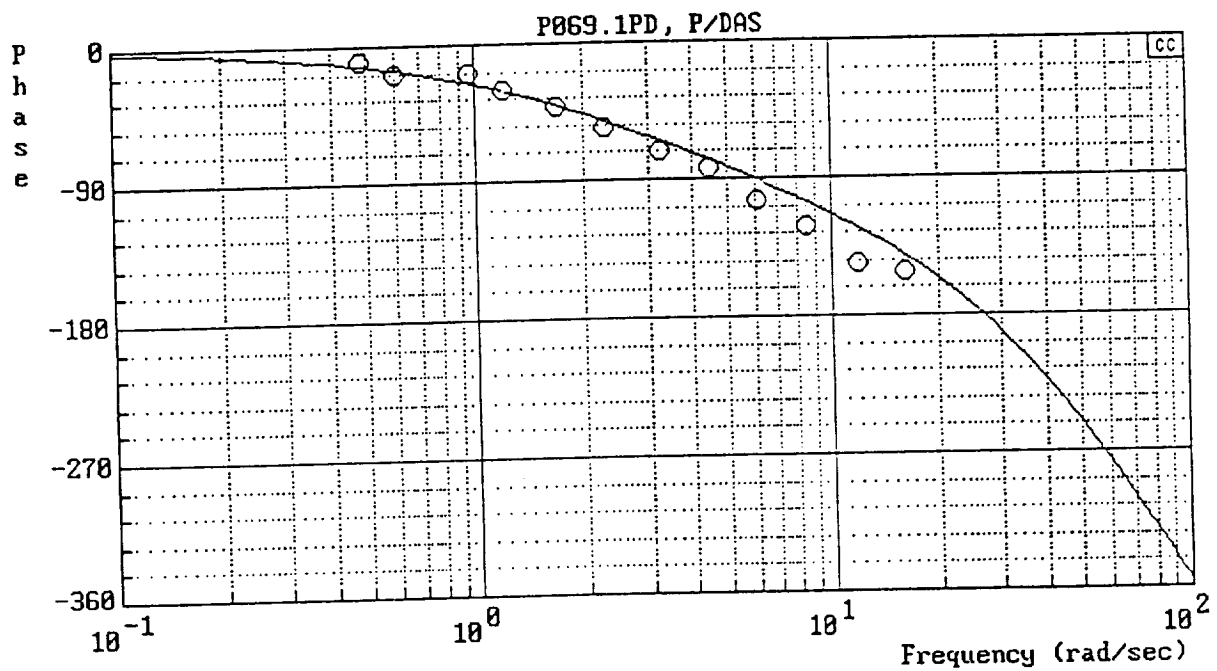
b) Y_c (P/DAS)

Figure B-1. (Continued)
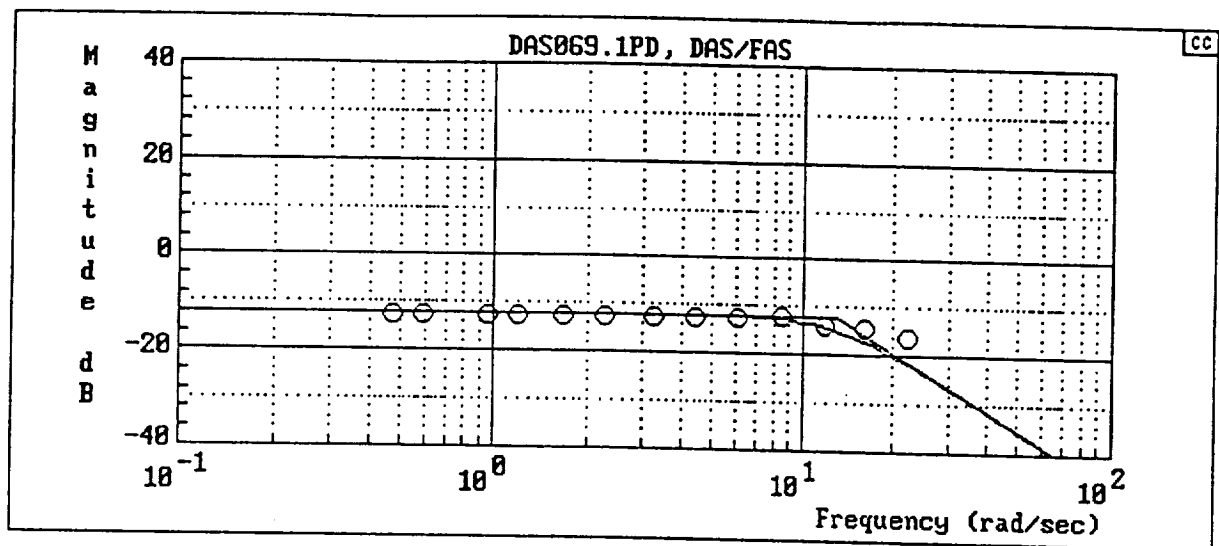
$$Y_{FS} = \frac{42.25}{[\ .7,\ 13]}$$
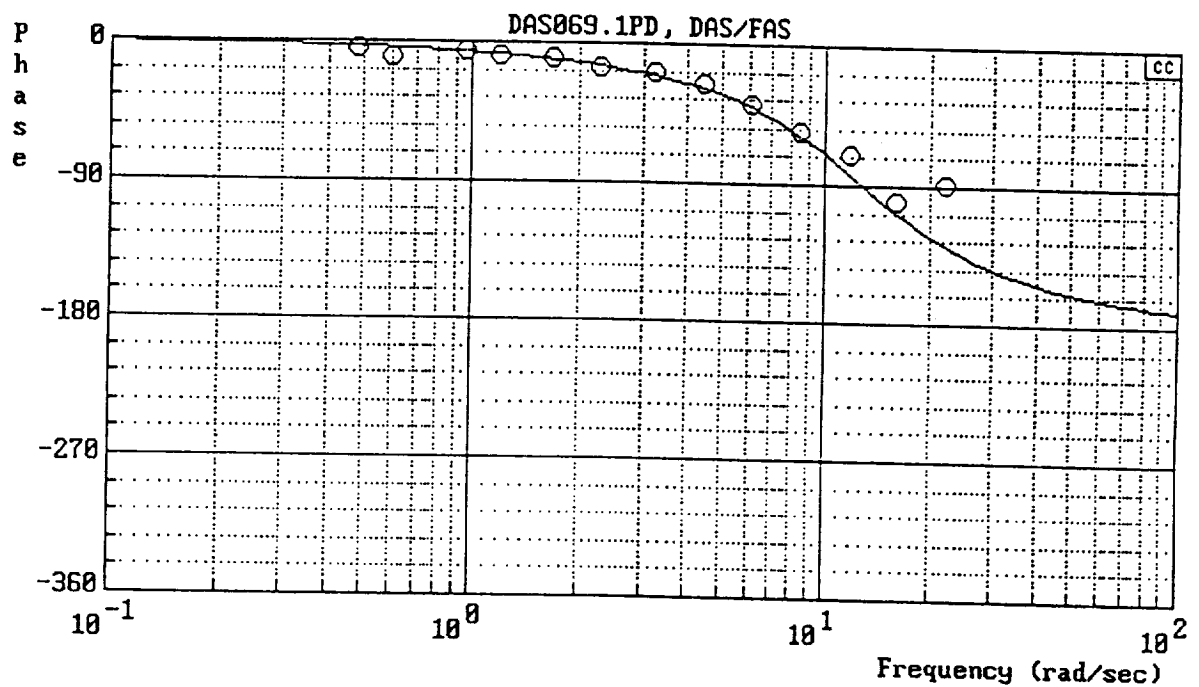
c) Y_{FS} (DAS/FAS)

Figure B-1. (Continued)

PHI069.1PD, ∮/∮e

PHI069.1PD, ∮/∮e
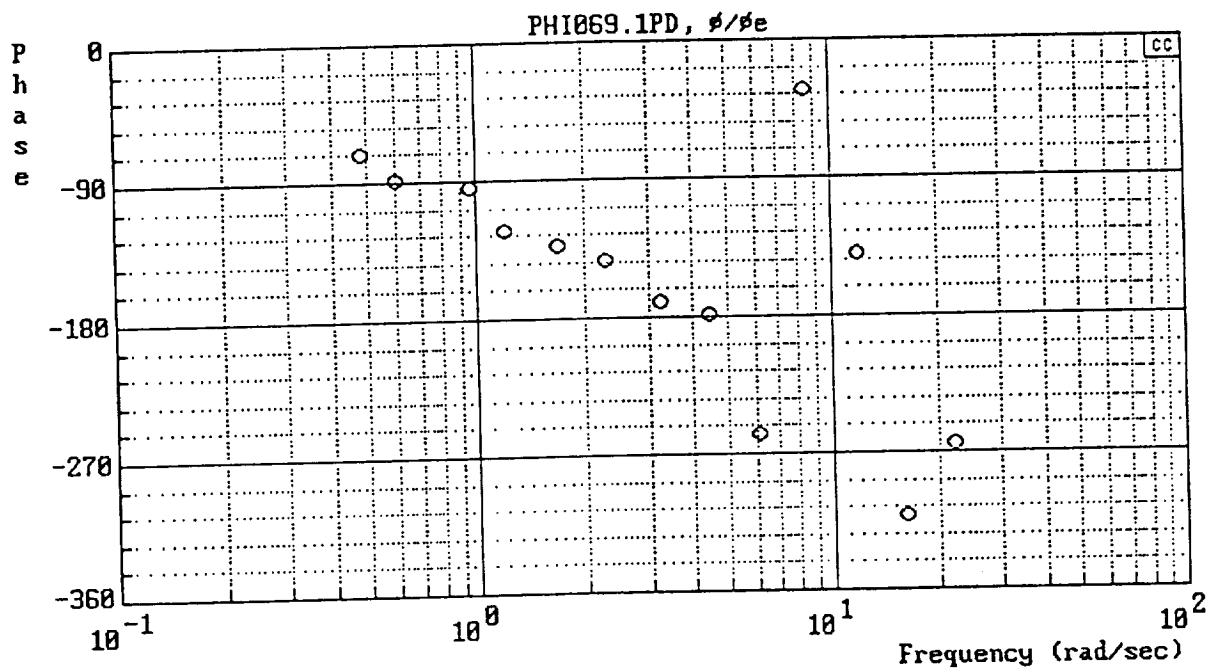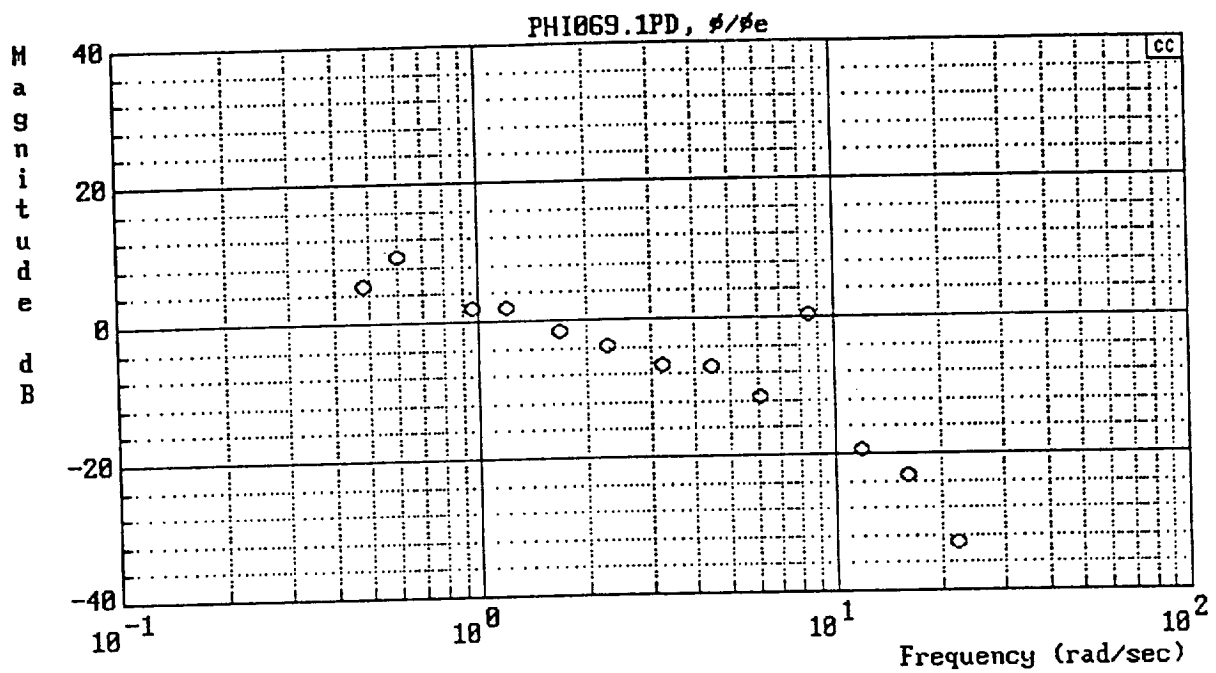
d) $Y_p Y_c$ (PHI/PHIE)

Figure B-1. (Concluded)
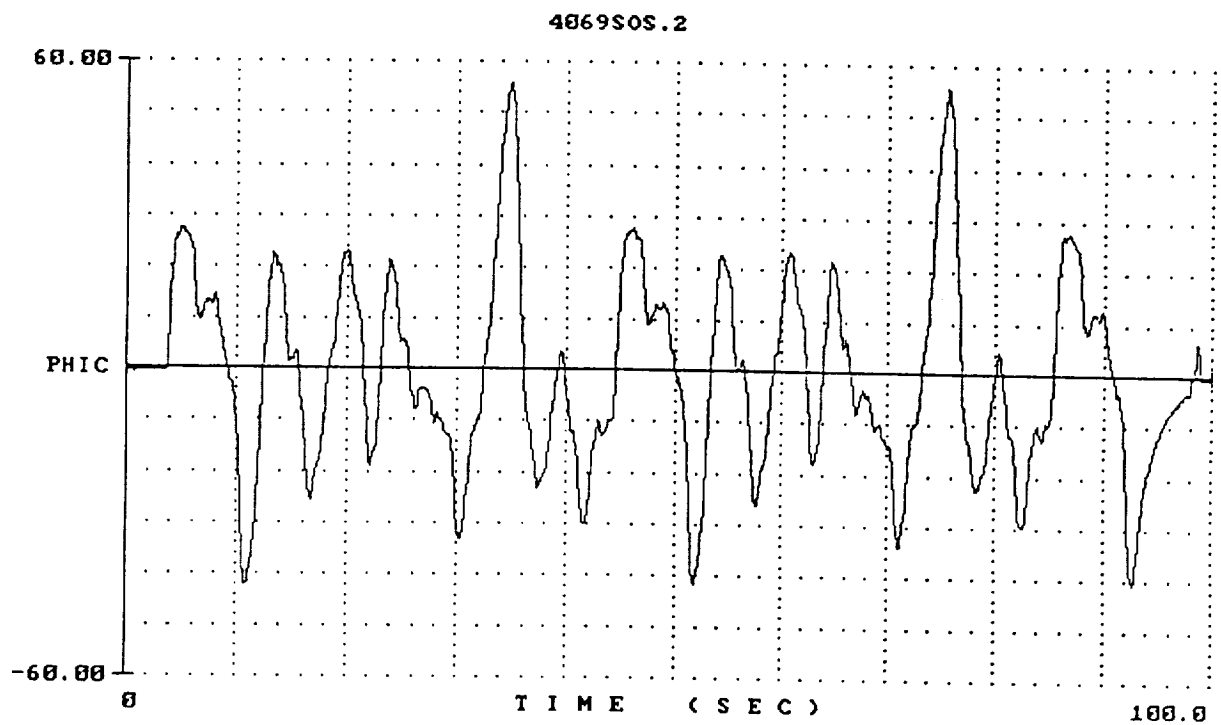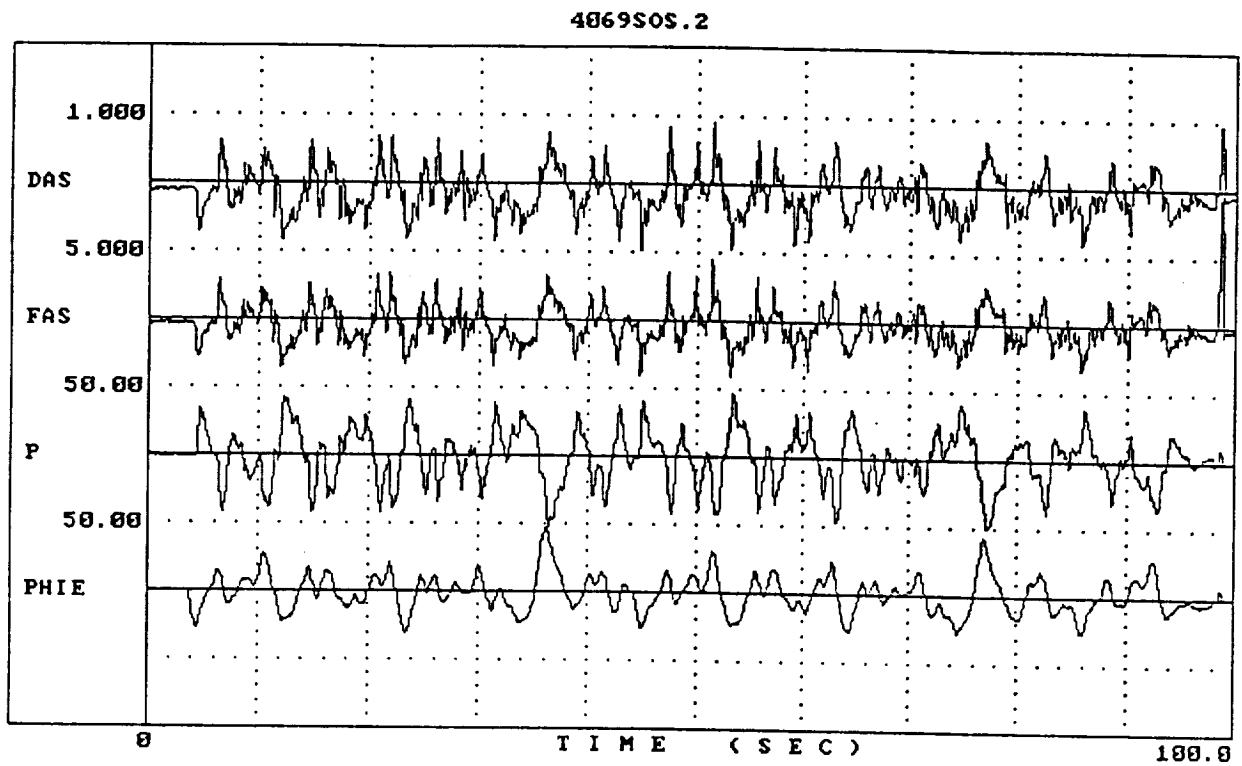
a) Time Histories

Figure B-2. Flight 4069-2

88
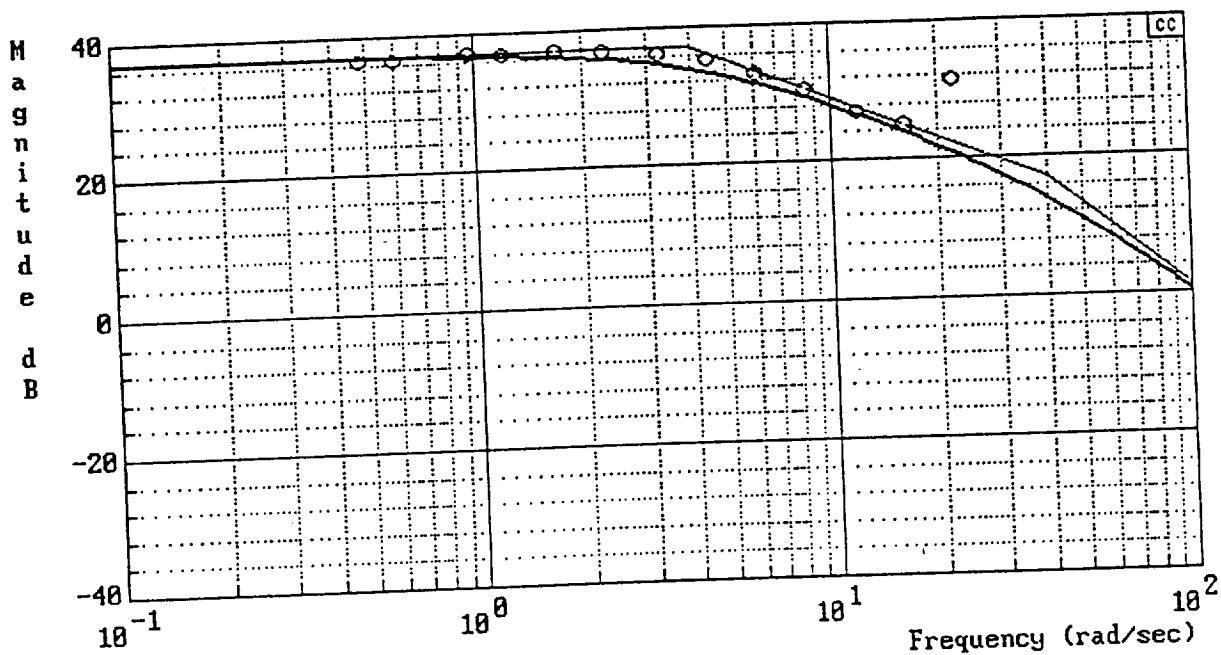
$$Y_c = \frac{40 \times 18 \times 4 \times e^{-.04s}}{.25\,(4)(40)}$$
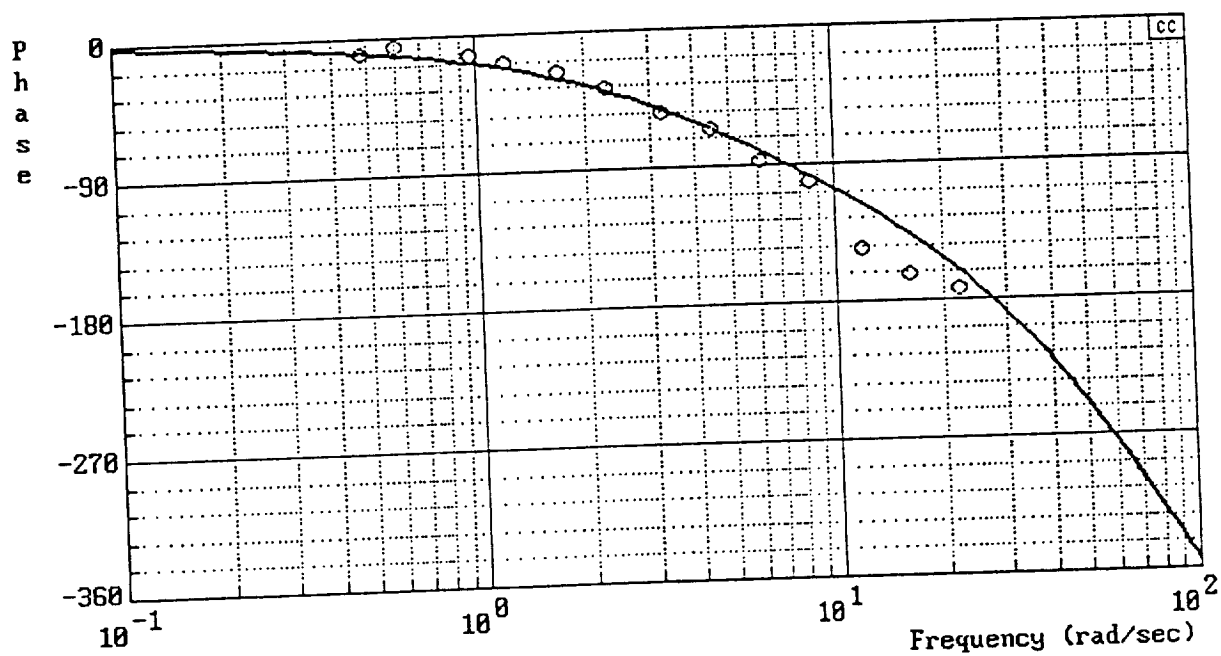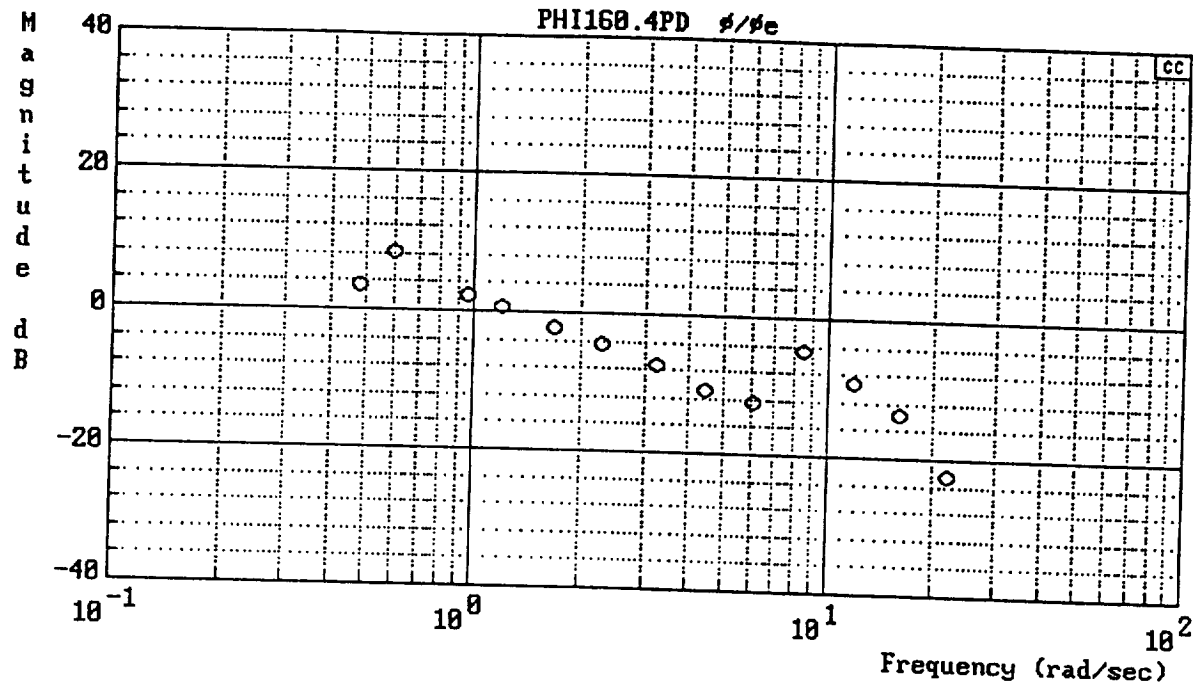

b) Y_c (P/DAS)

Figure B-2. (Continued)
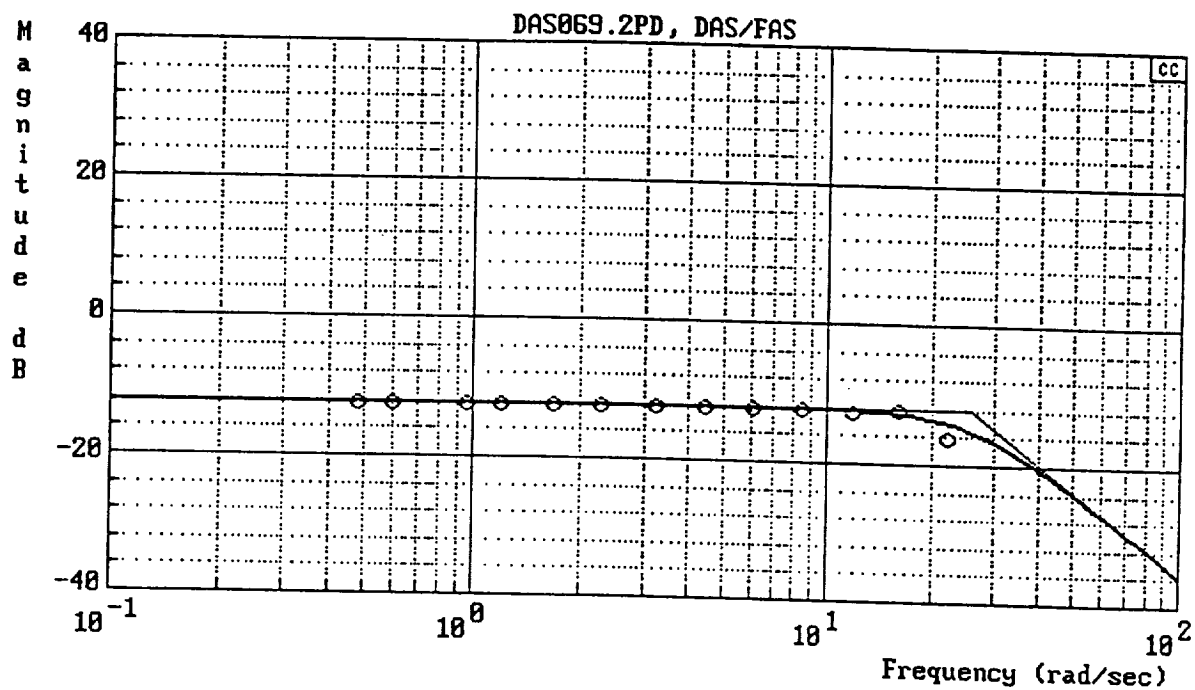
$$Y_{FS} = \frac{169}{[0.7, 26]}$$
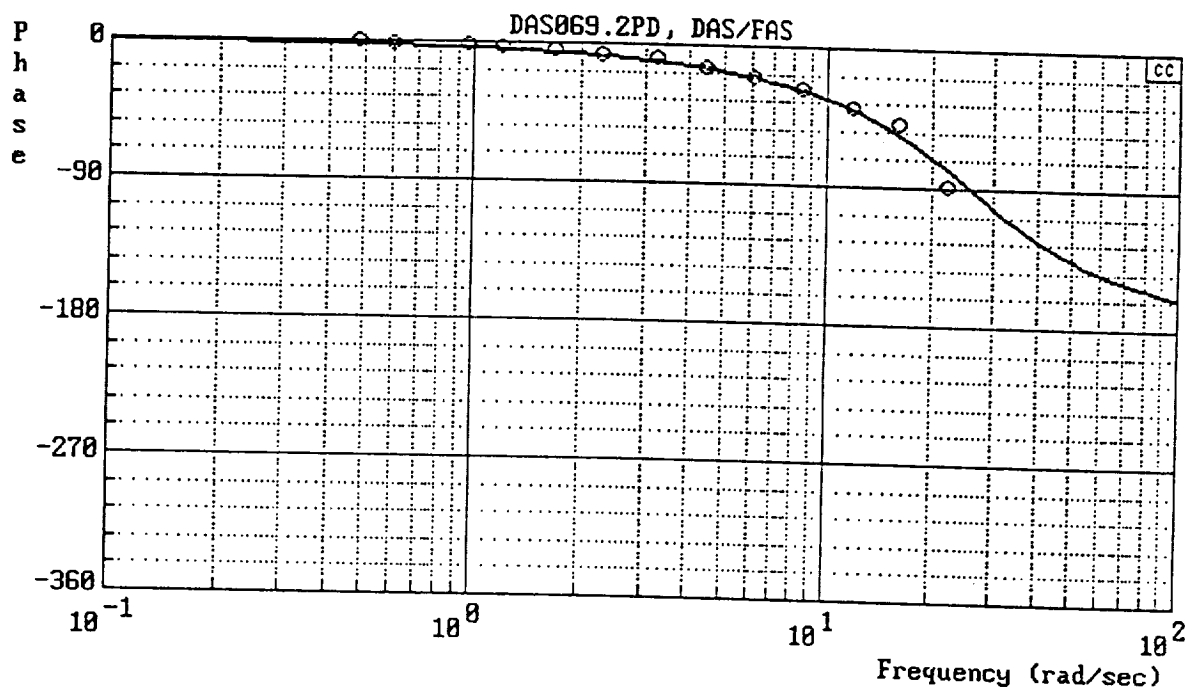
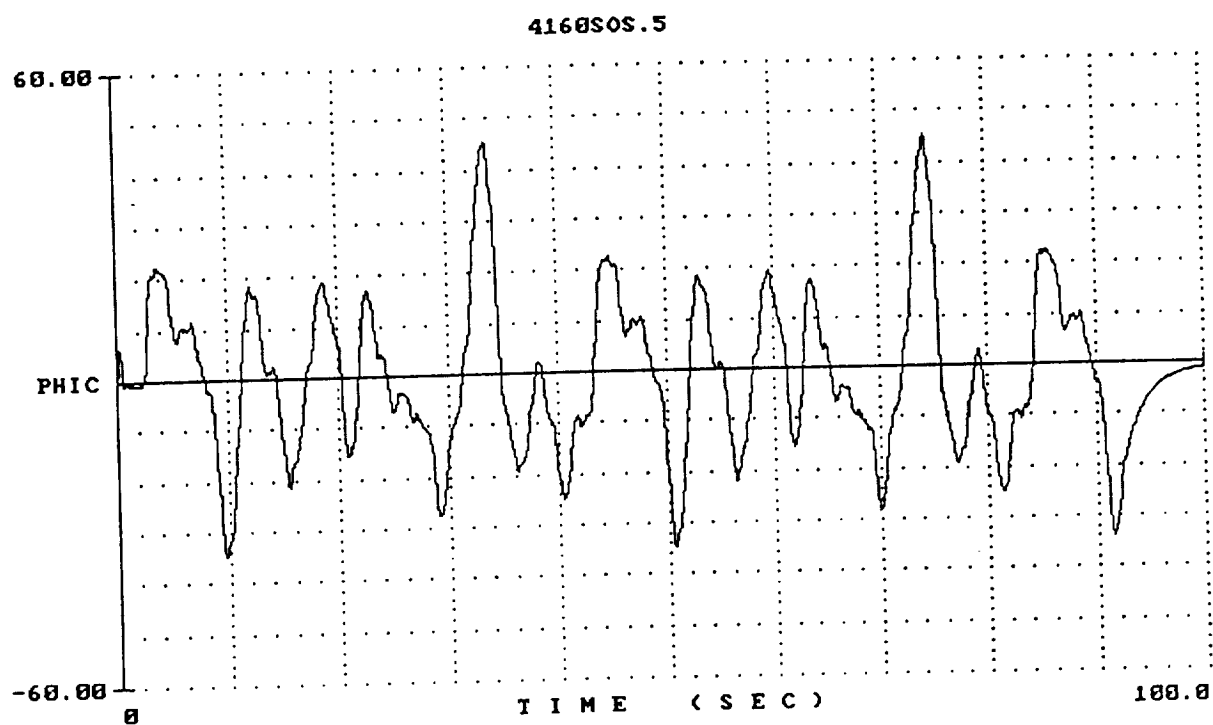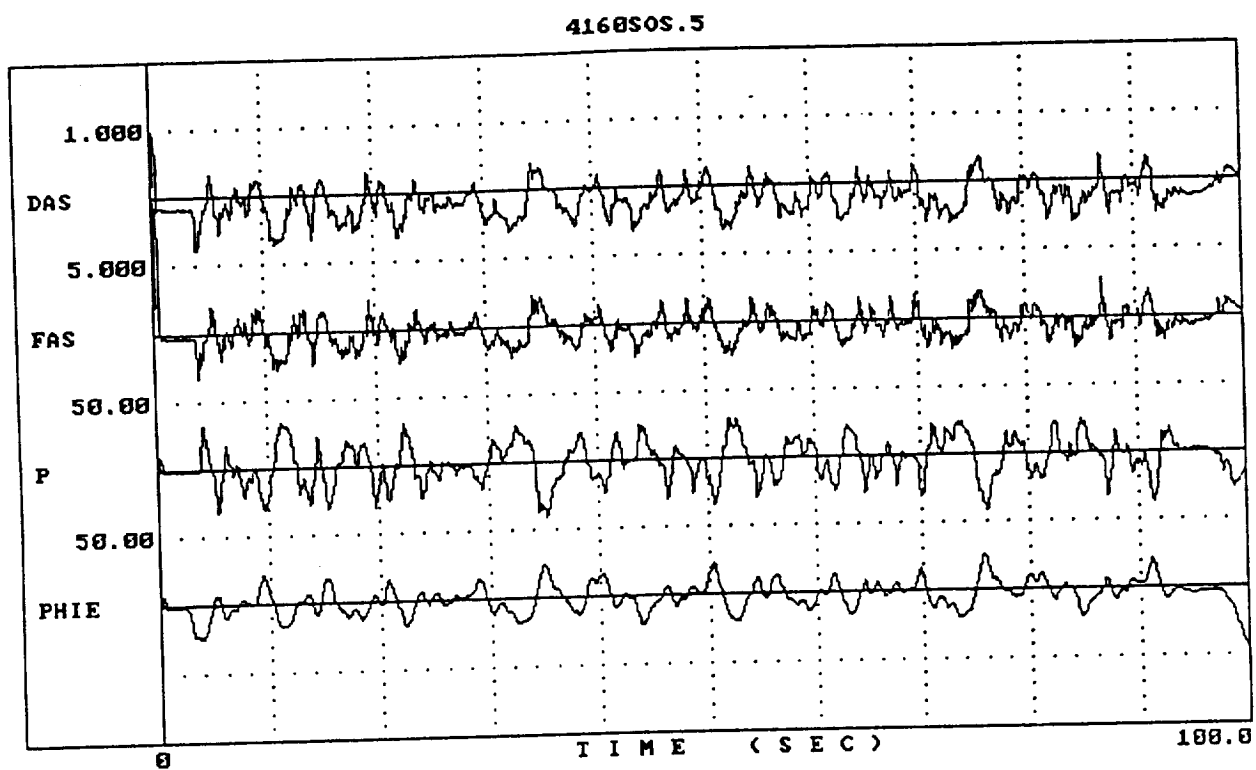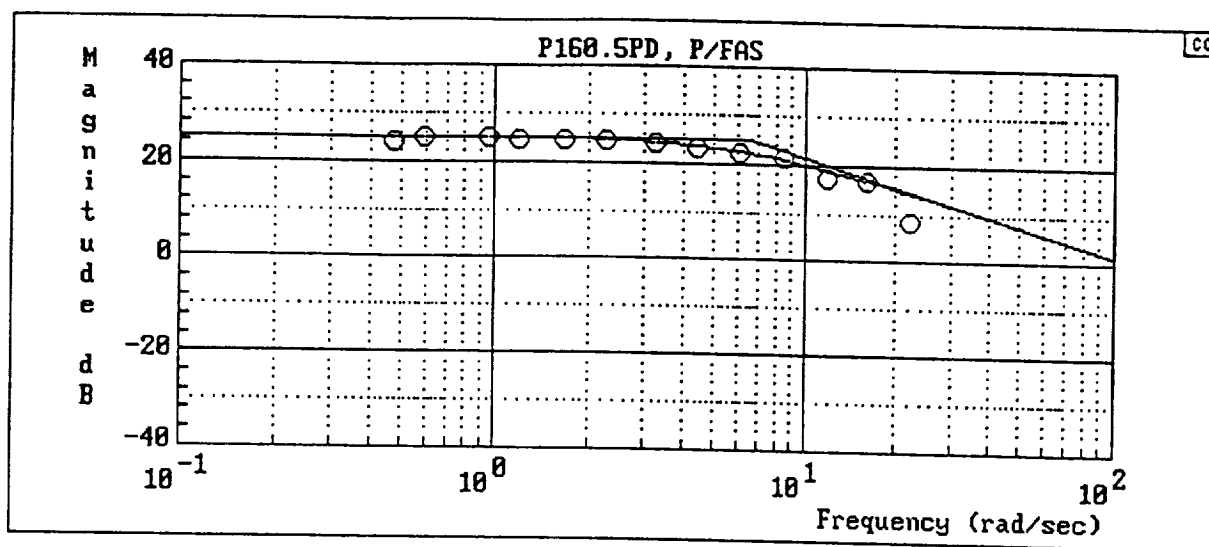c) Y_{FS} (DAS/FAS)

Figure B-2. (Continued)

90
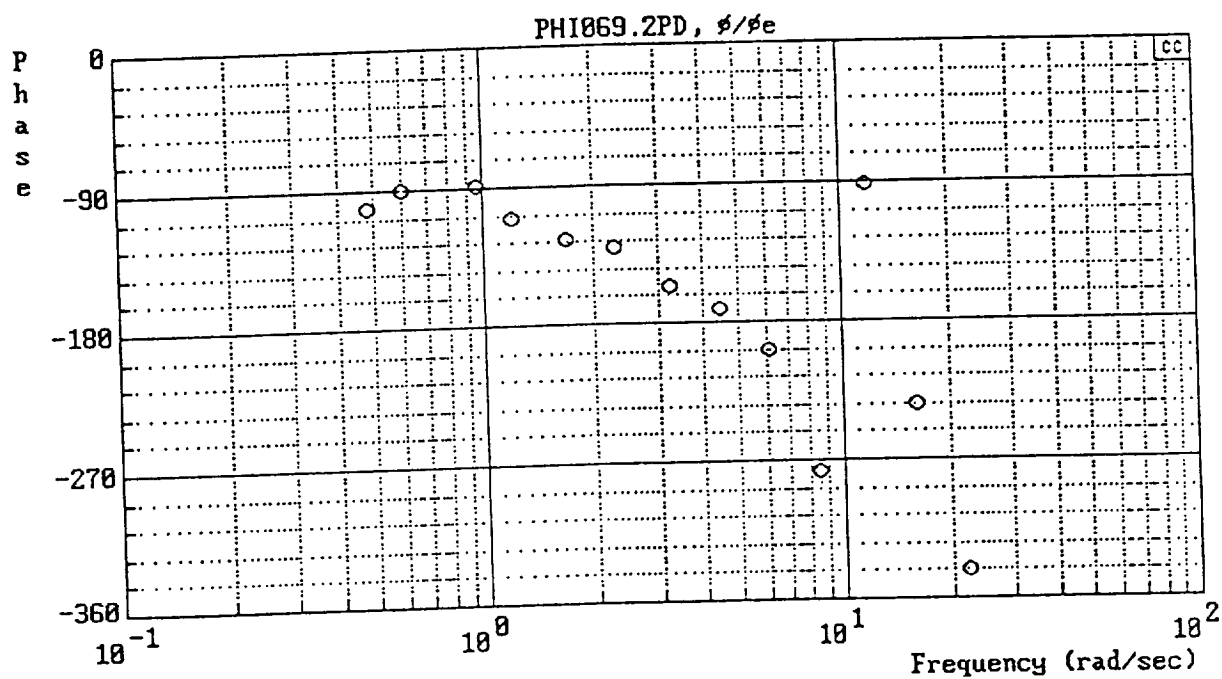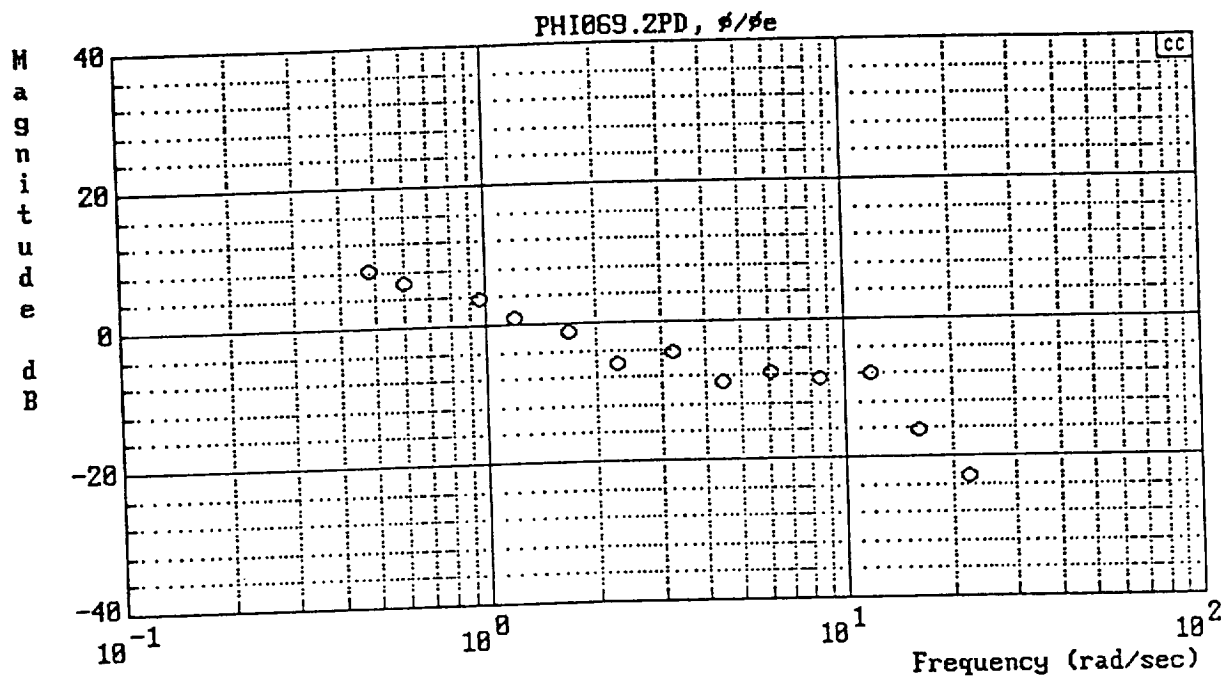
d) Y_pY_c (PHI/PHIE)

Figure B-2. (Concluded)
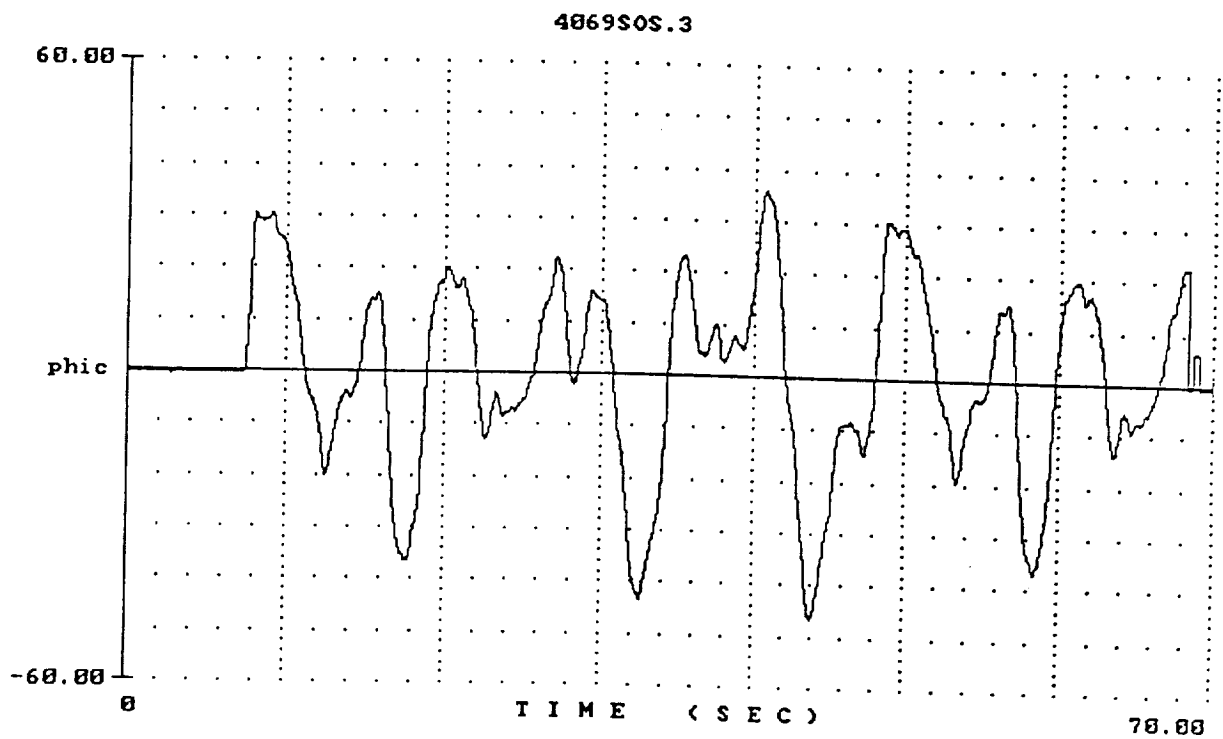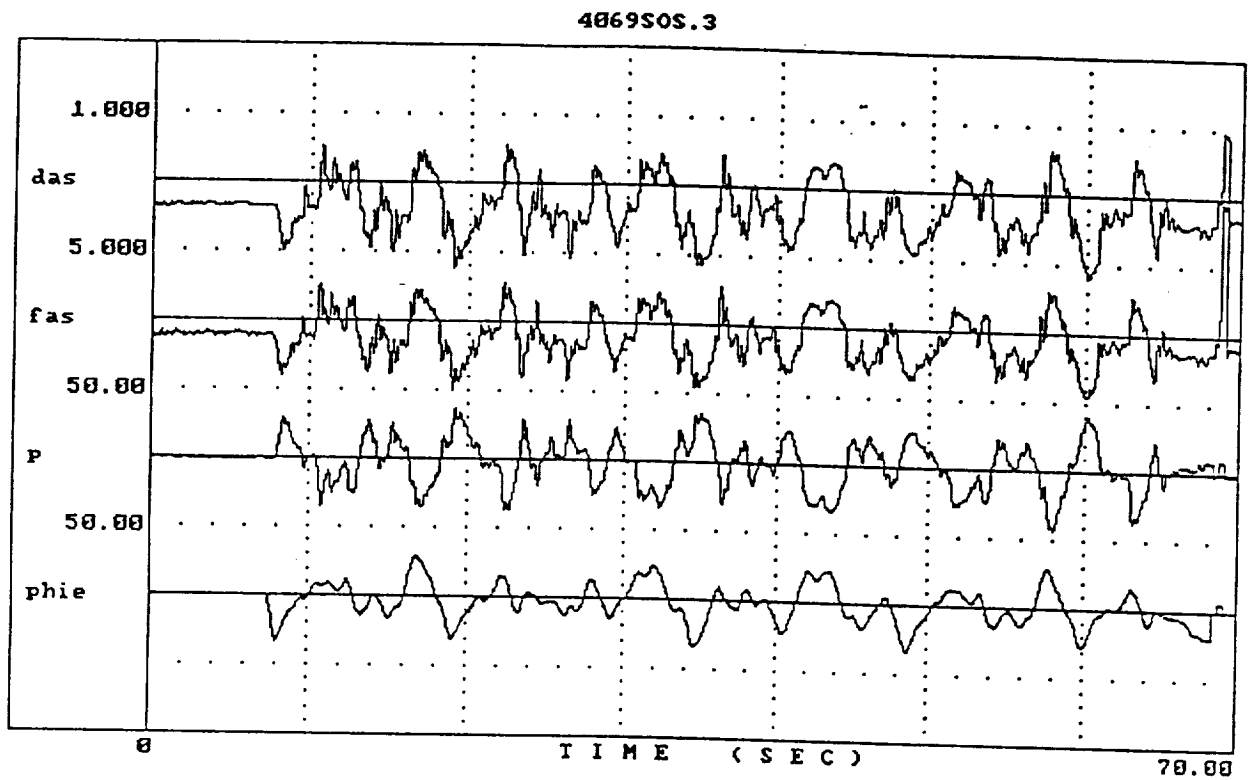
a) Time Histories

Figure B-3. Flight 4069-3

4069SOS.3BI, P/FAS
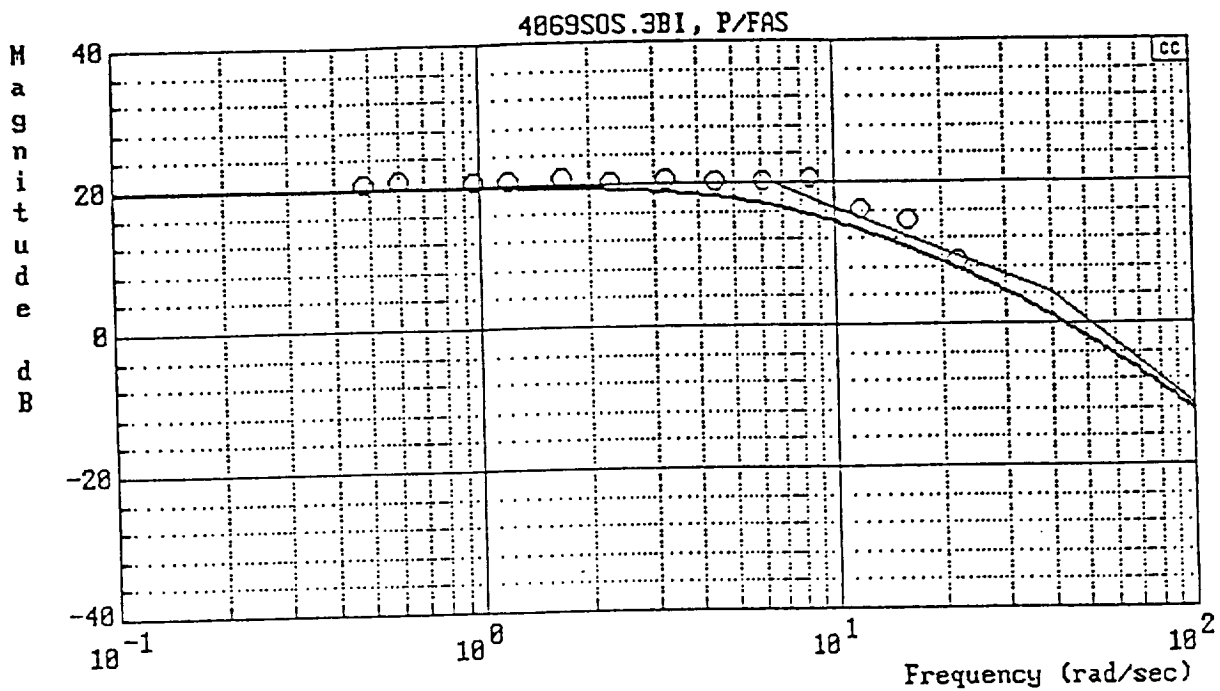
$$Y_C = \frac{10 \times 6.67 \times 40\,e^{-0.04s}}{(6.67)(40)}$$

4069SOS.3BI, P/FAS
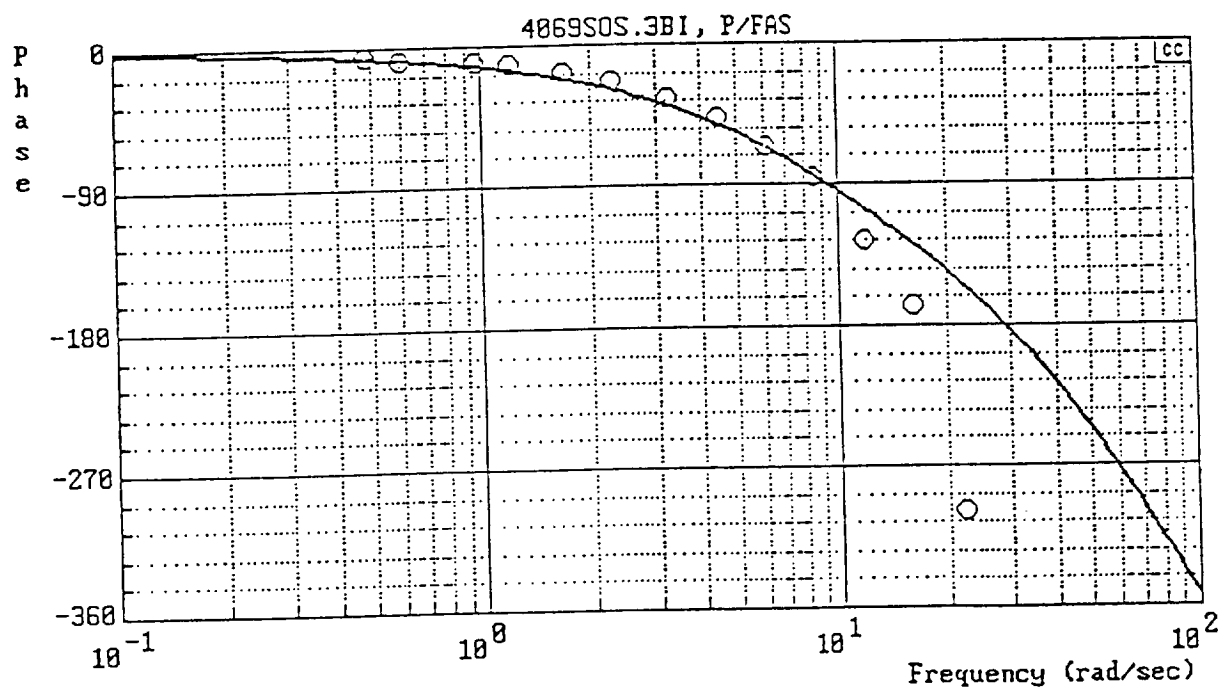
b) Y_c (P/FAS)

Figure B-3. (Continued)

93
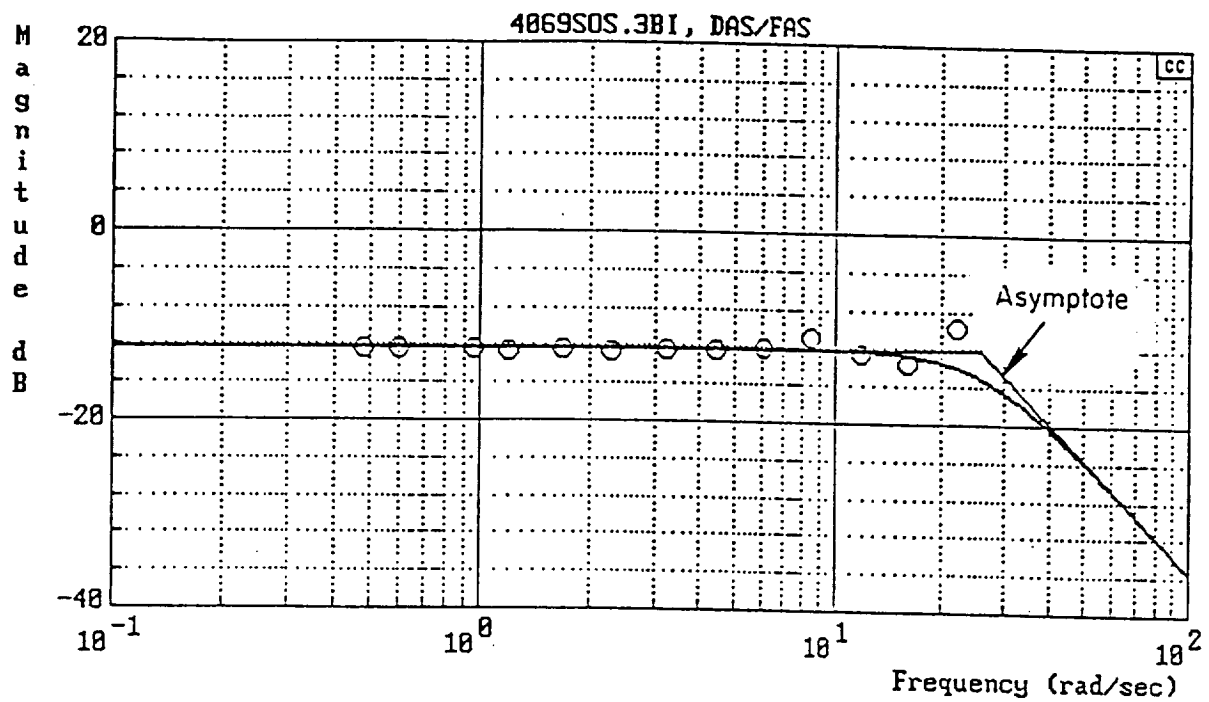
$$Y_{FS} = \frac{169}{[0.7, 26]}$$
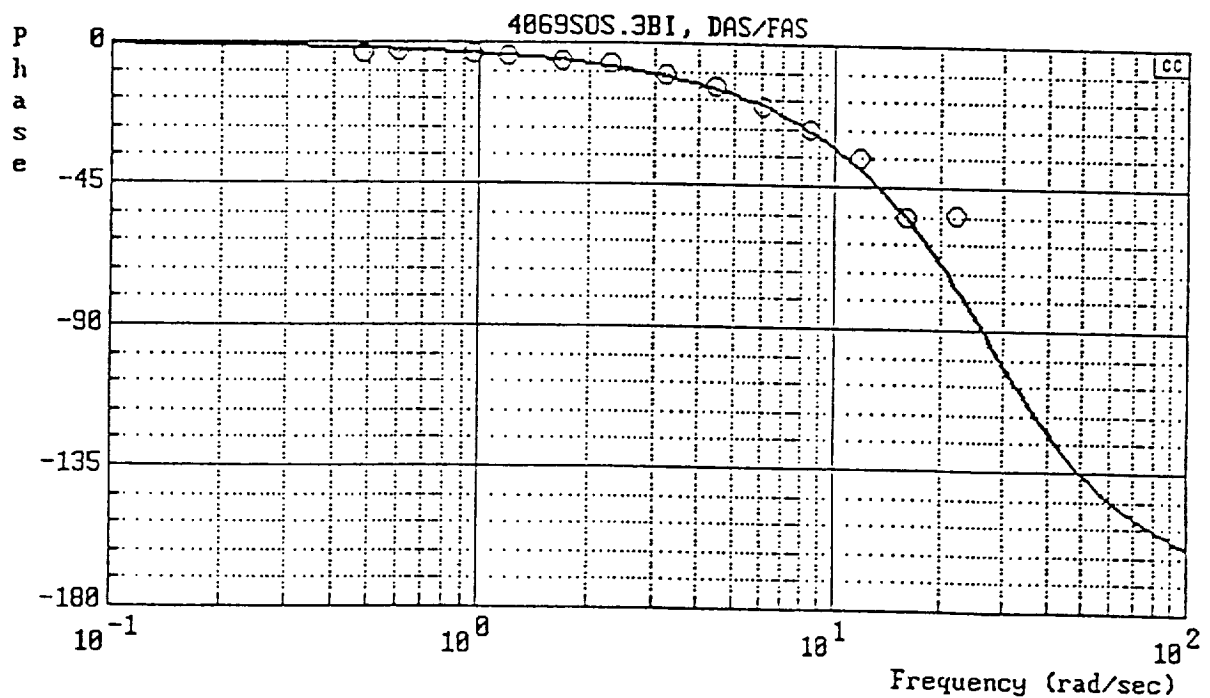
c) Y_{FS} (DAS/FAS)

Figure B-3. (Continued)
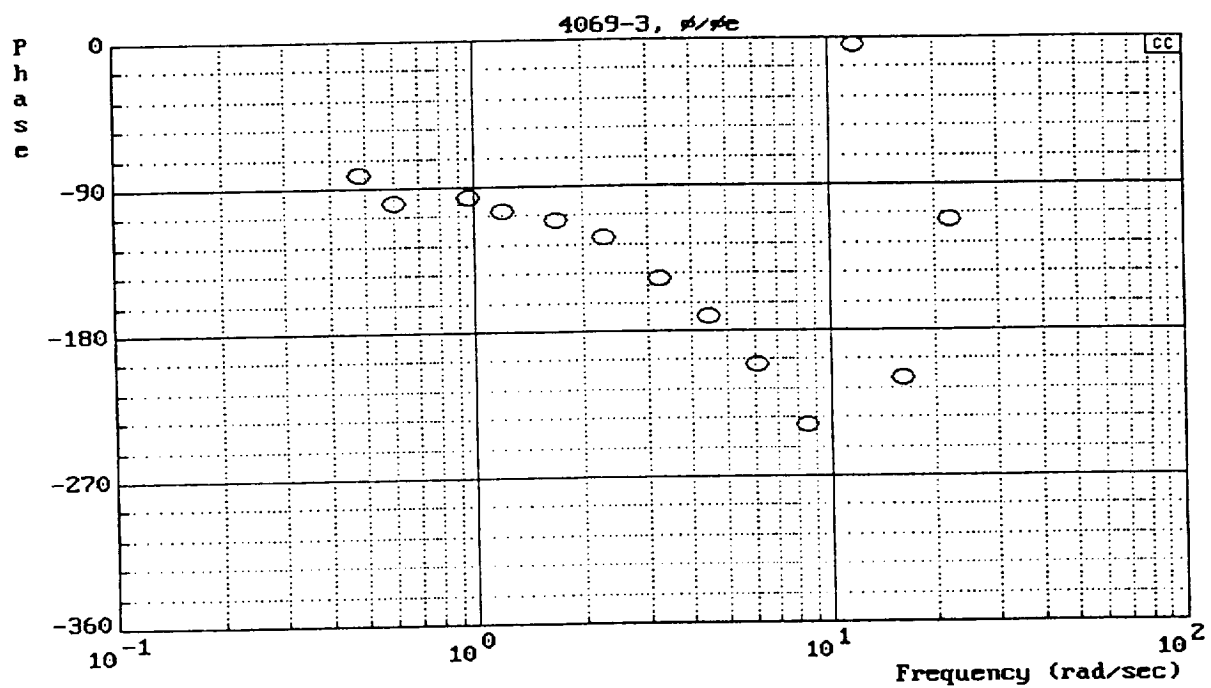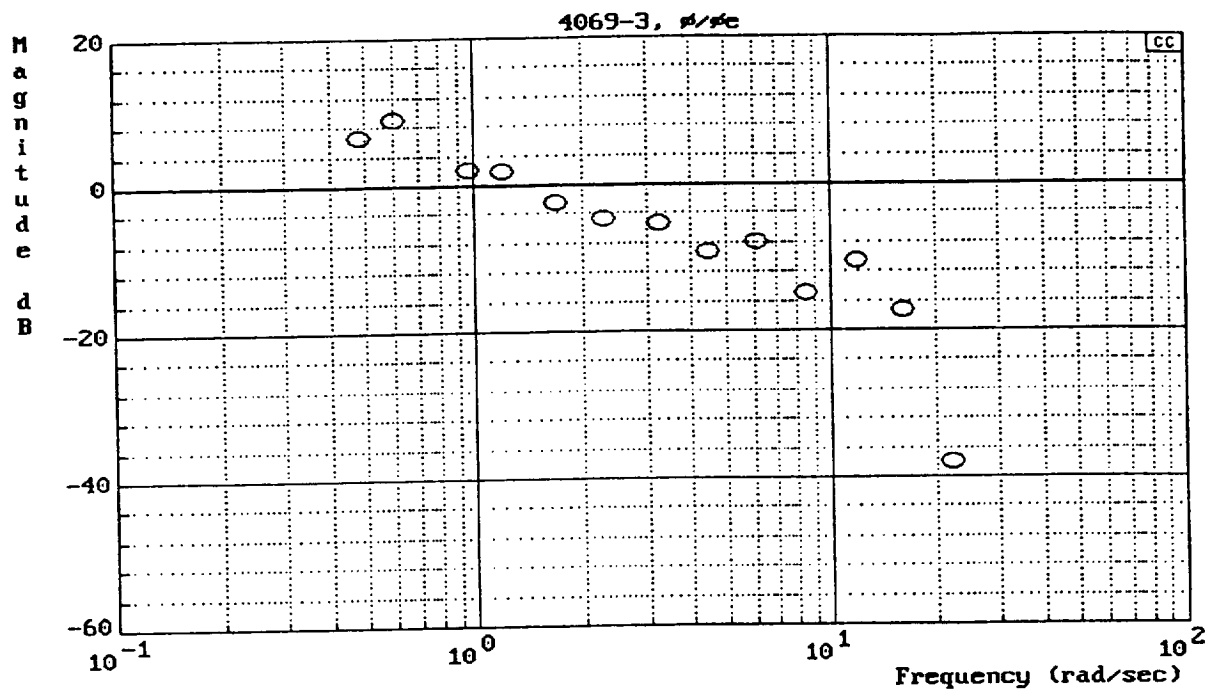
d) Y_pY_c (PHI/PHIE)

Figure B-3. (Concluded)
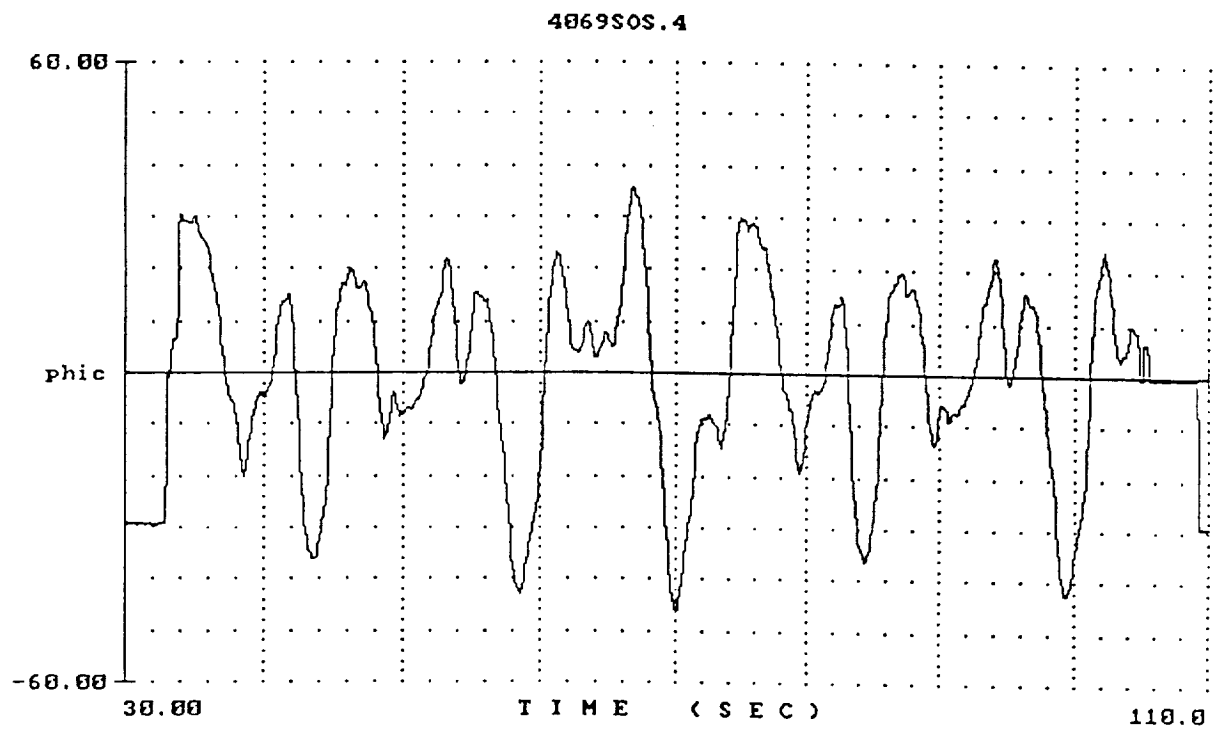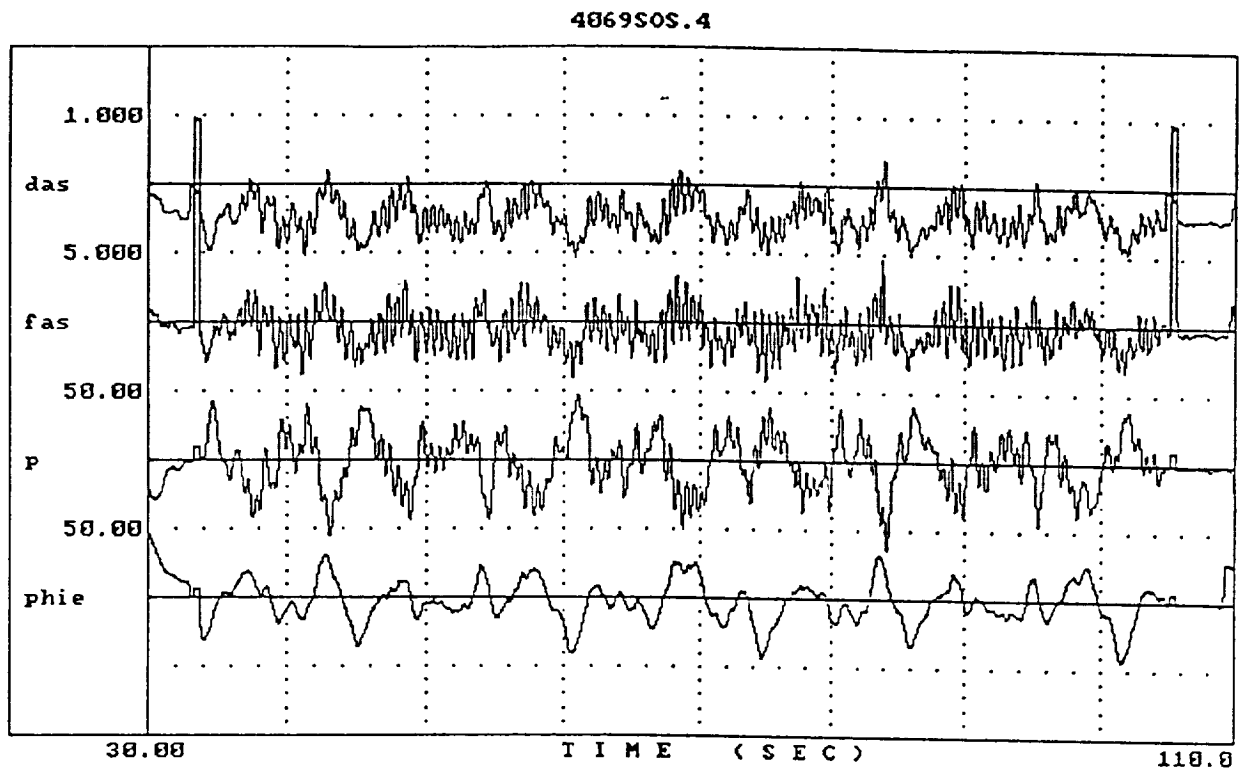
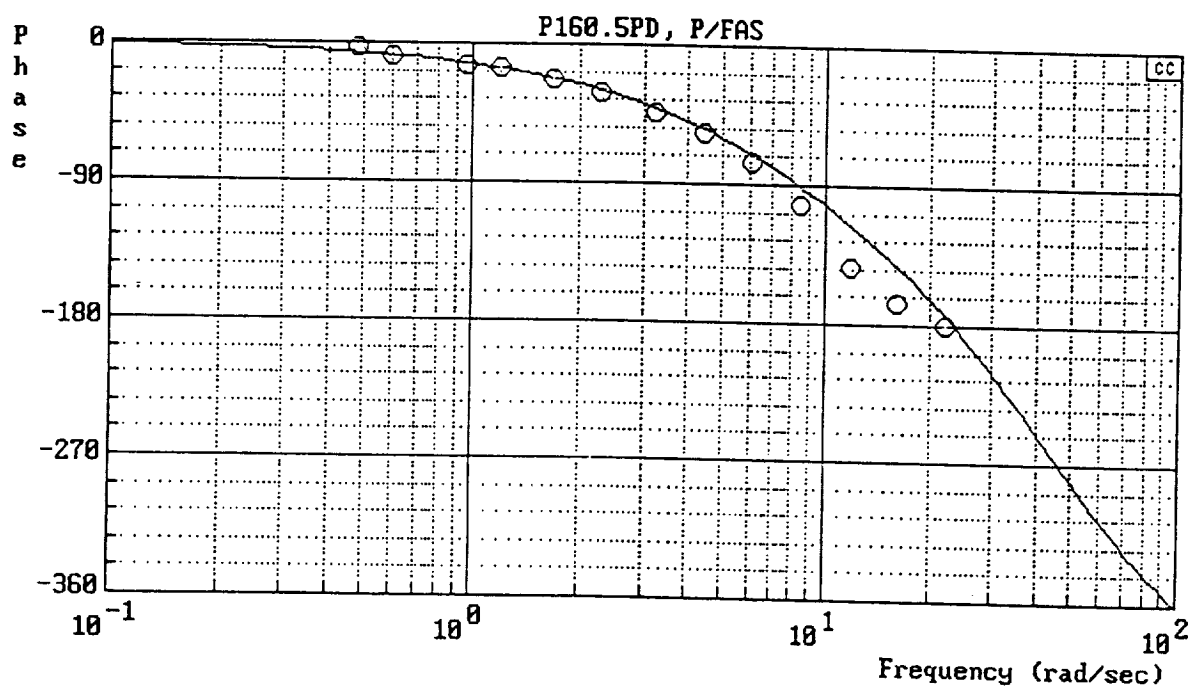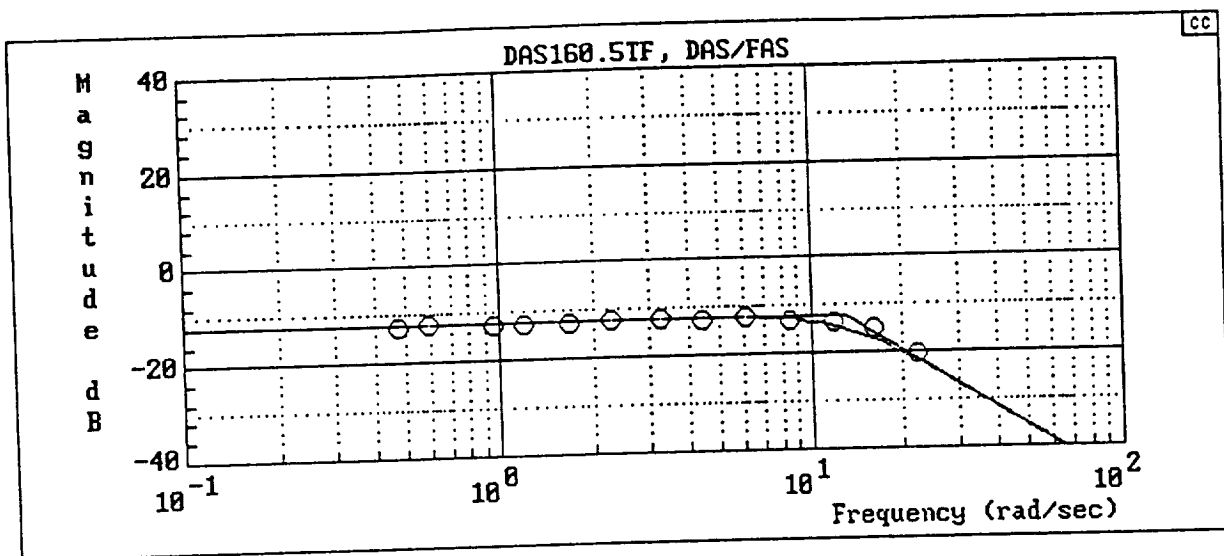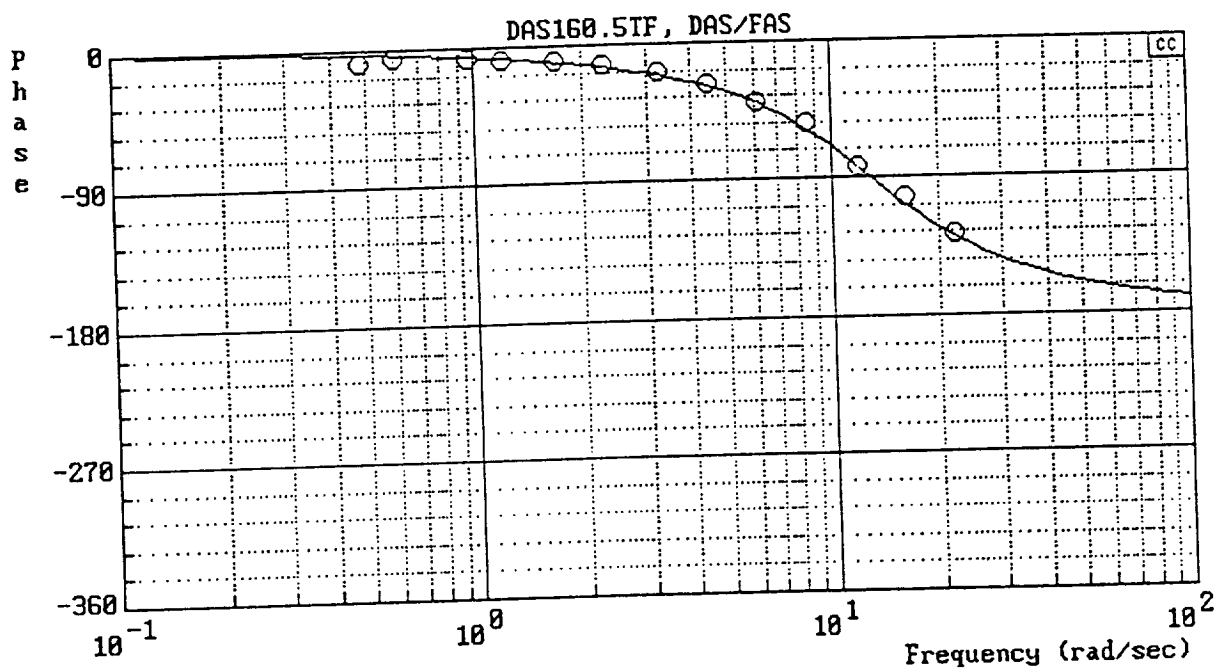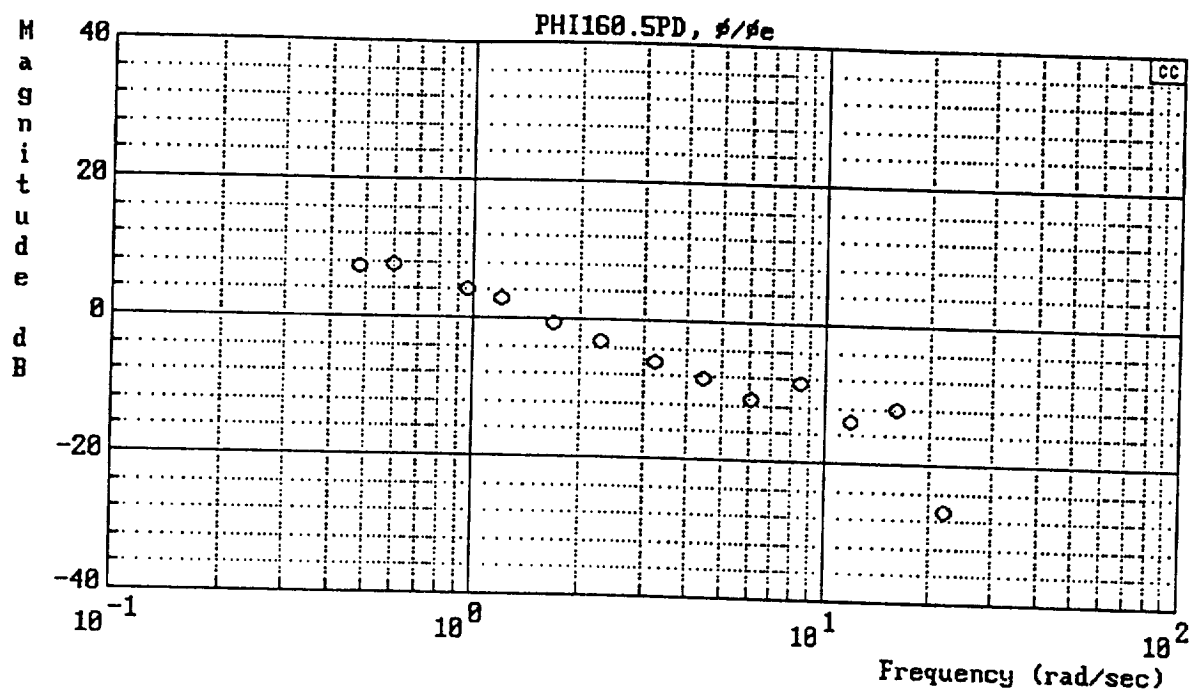a) Time Histories

Figure B-4. Flight 4069-4

4069SOS.4BI, P/FAS
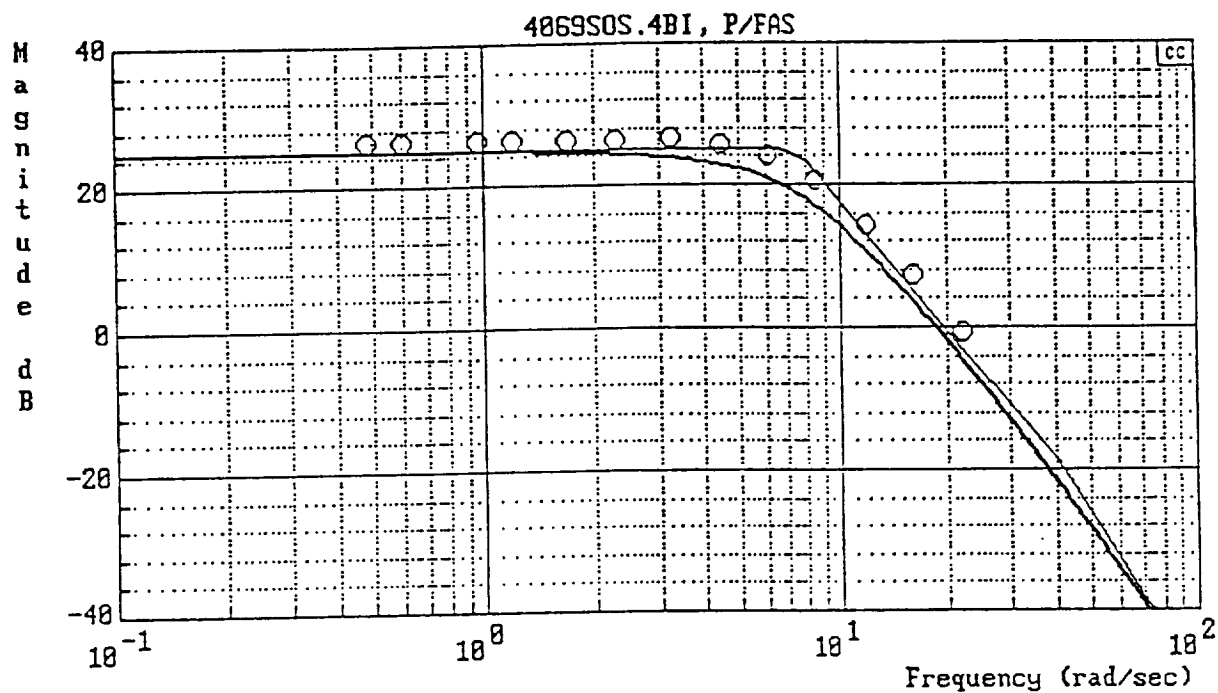
$$Y_c = \frac{18 \times 6.67 e^{-0.04}}{(6.67)} \frac{8^2}{[0.7, 8]}$$

4069SOS.4BI, P/FAS

b) Y_c (P/FAS)

Figure B-4. (Continued)

97

Magnitude dB

20

0

-20

-40

10^{-1} 10^0 10^1 10^2

Frequency (rad/sec)

$$Y_{FS} = \frac{0.25 \times 8^2}{[0.7,8]}$$

4869SOS.4BI, DAS/FAS

Phase

0

-45

-90

-135

-180

10^{-1} 10^0 10^1 10^2

Frequency (rad/sec)
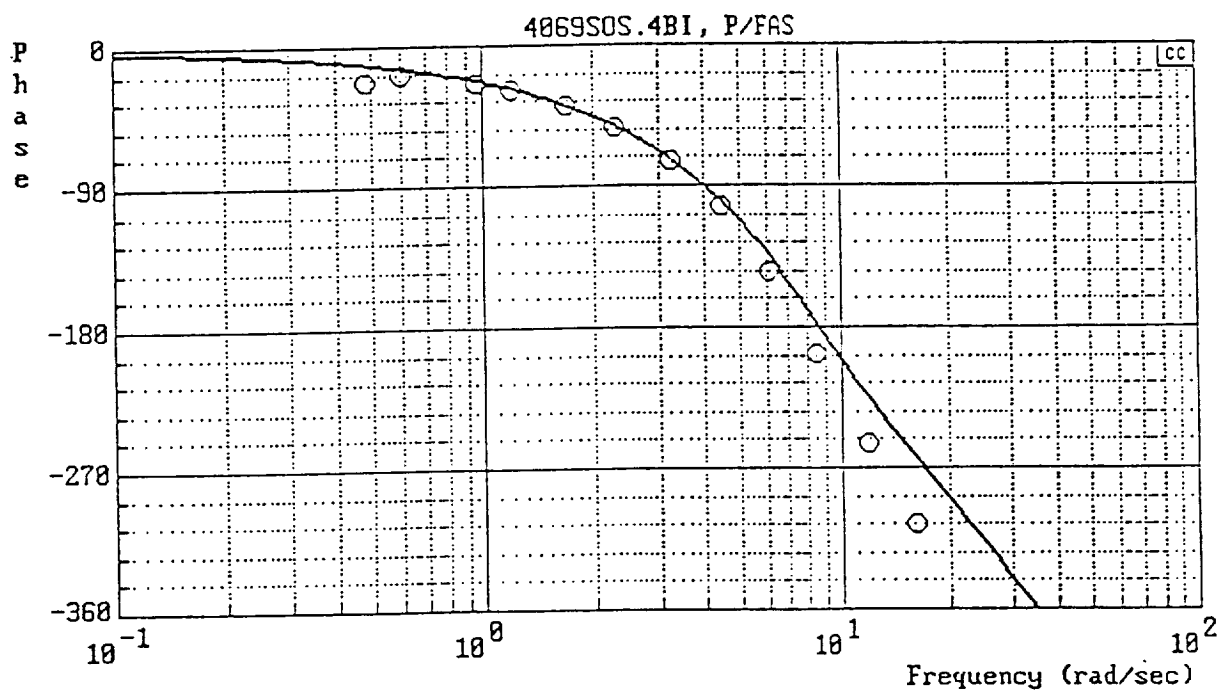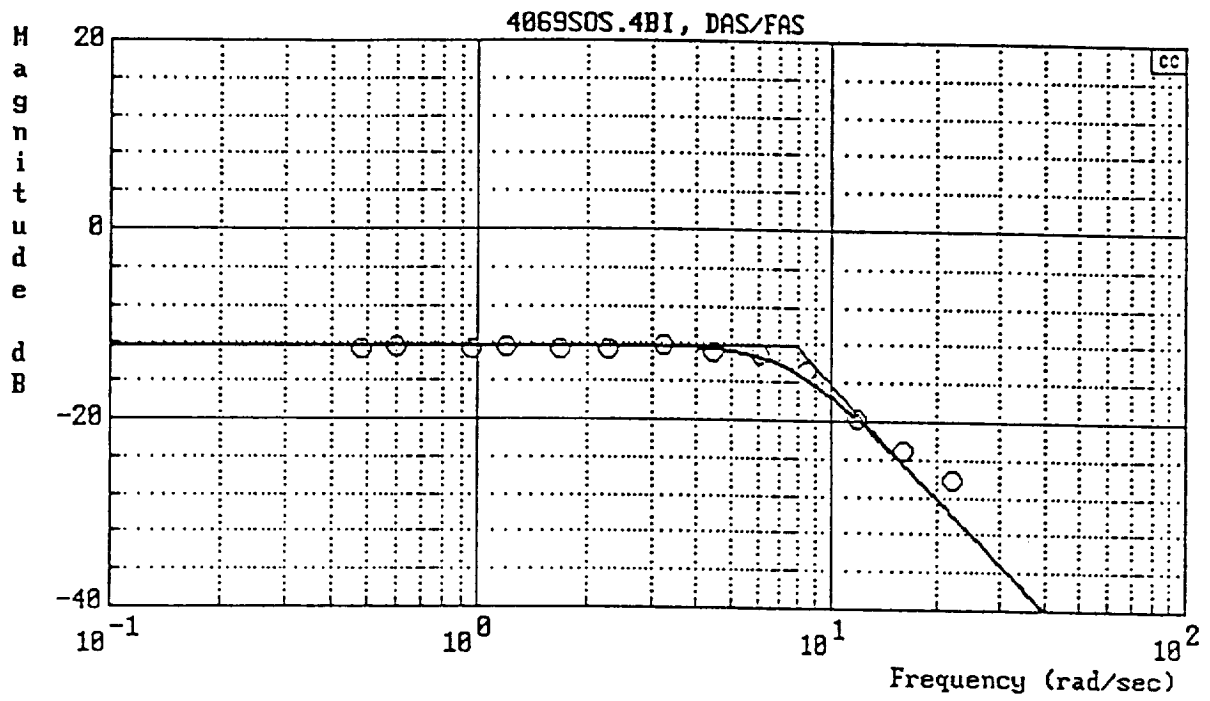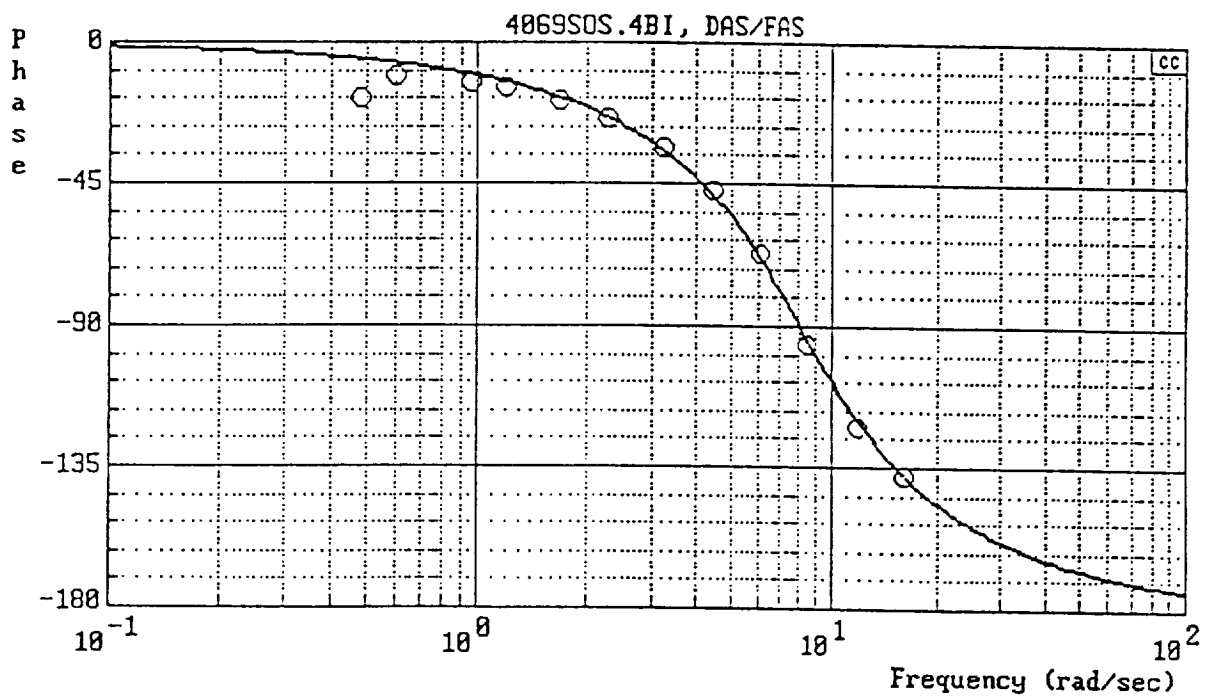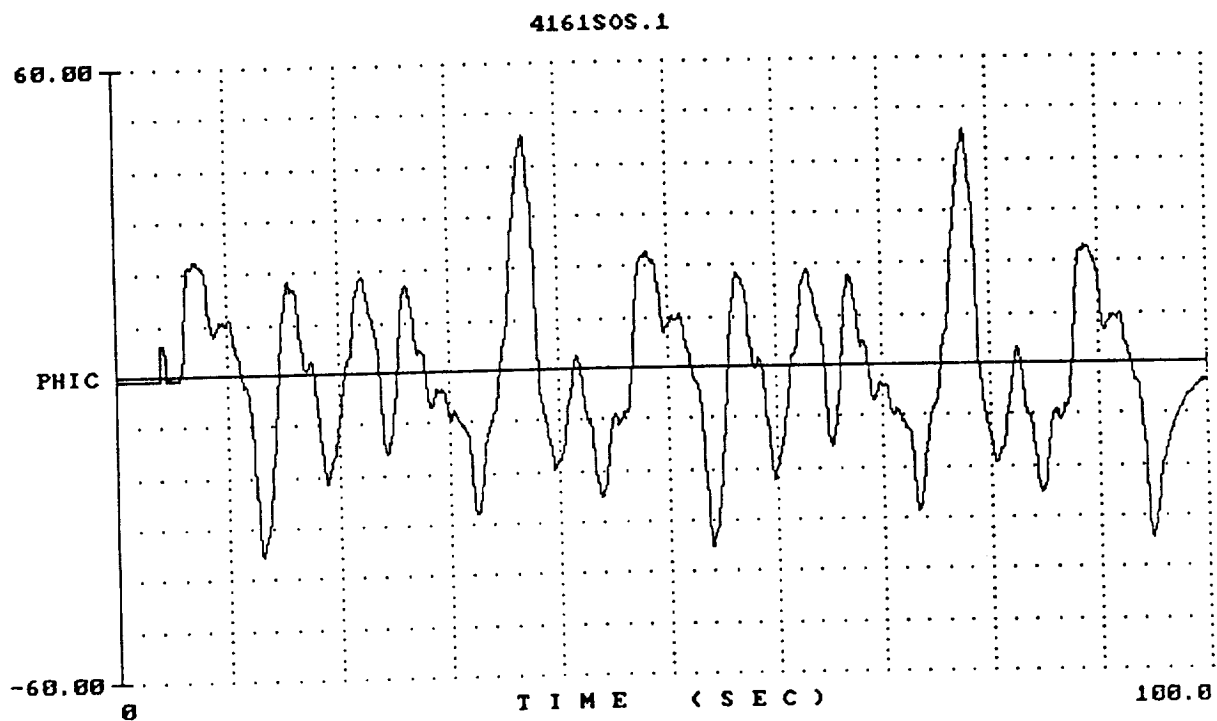
c) Y_{FS} (DAS/FAS)

Figure B-4. (Continued)
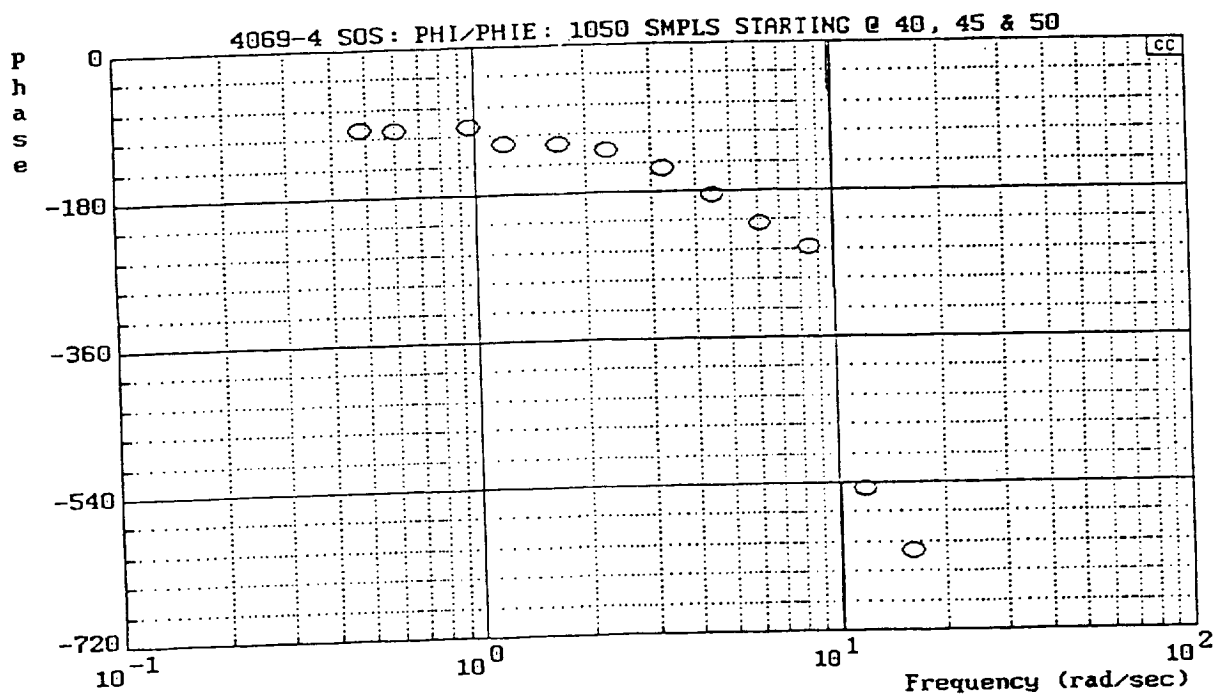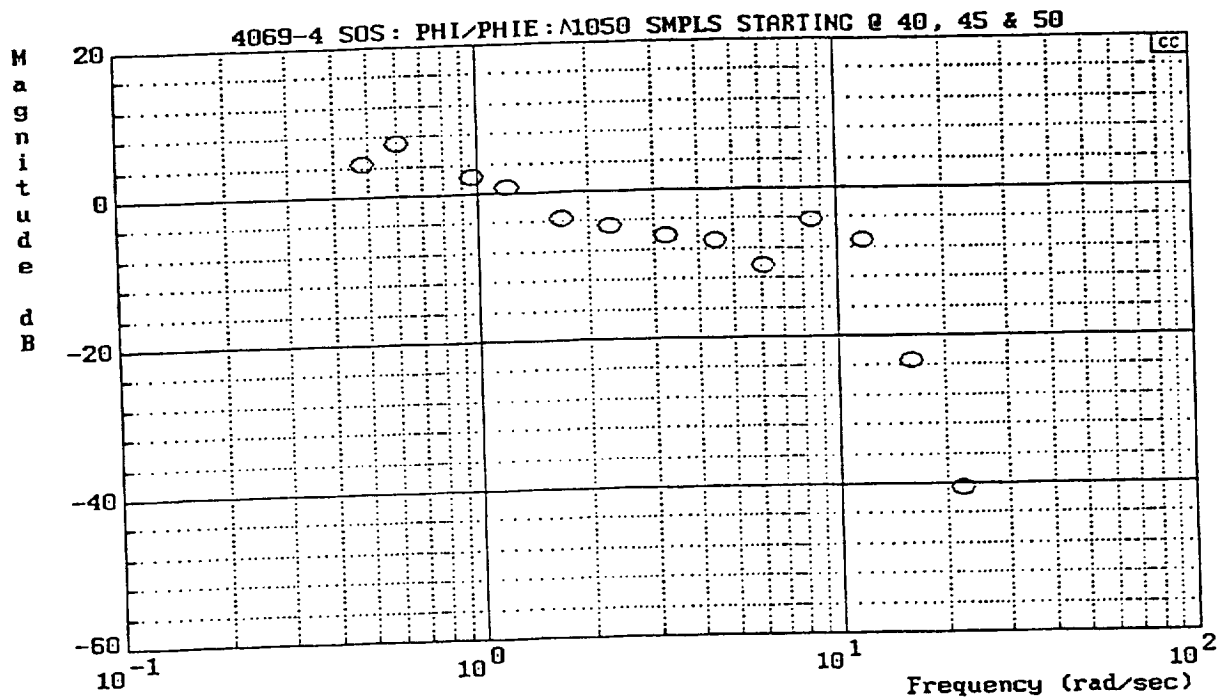
d) Y_pY_c (PHI/PHIE)

Figure B-4 (Concluded)

4079SOS.3

No Tracking

das

1.000

5.000

fas

50.00

P

50.00

phie

0   T I M E   (S E C)   110.0

4079SOS.3

60.00

phic

-60.00

0   T I M E   (S E C)   110.0
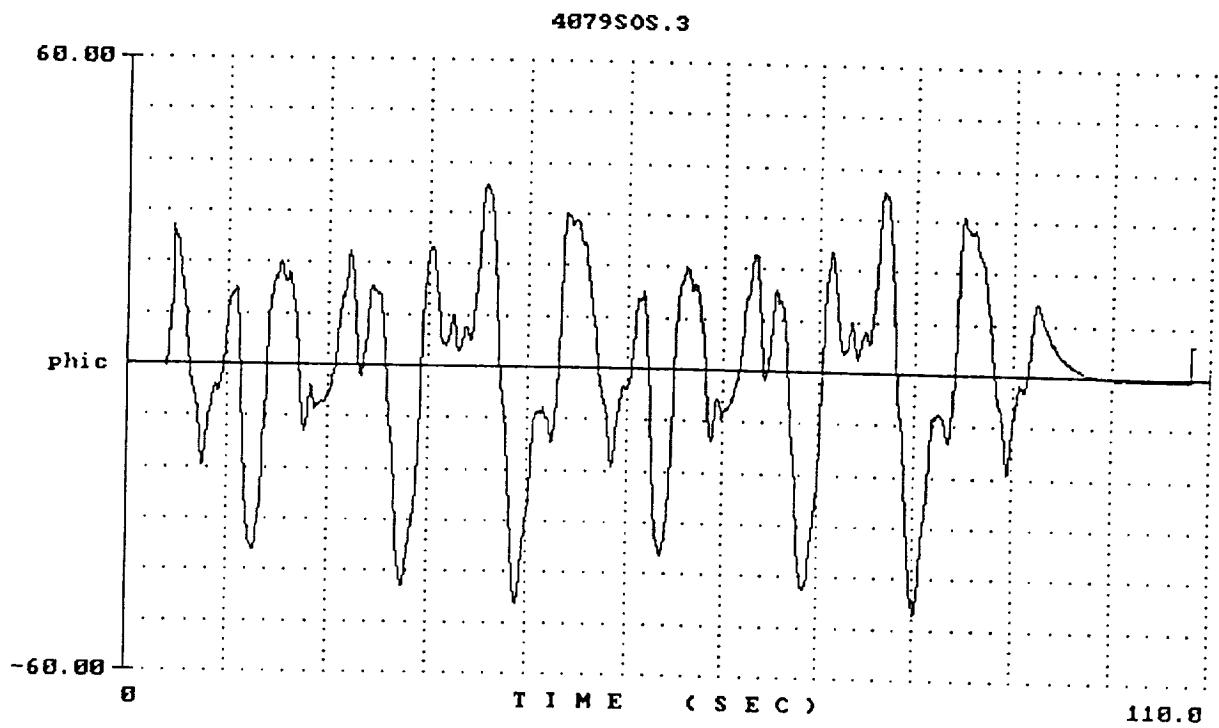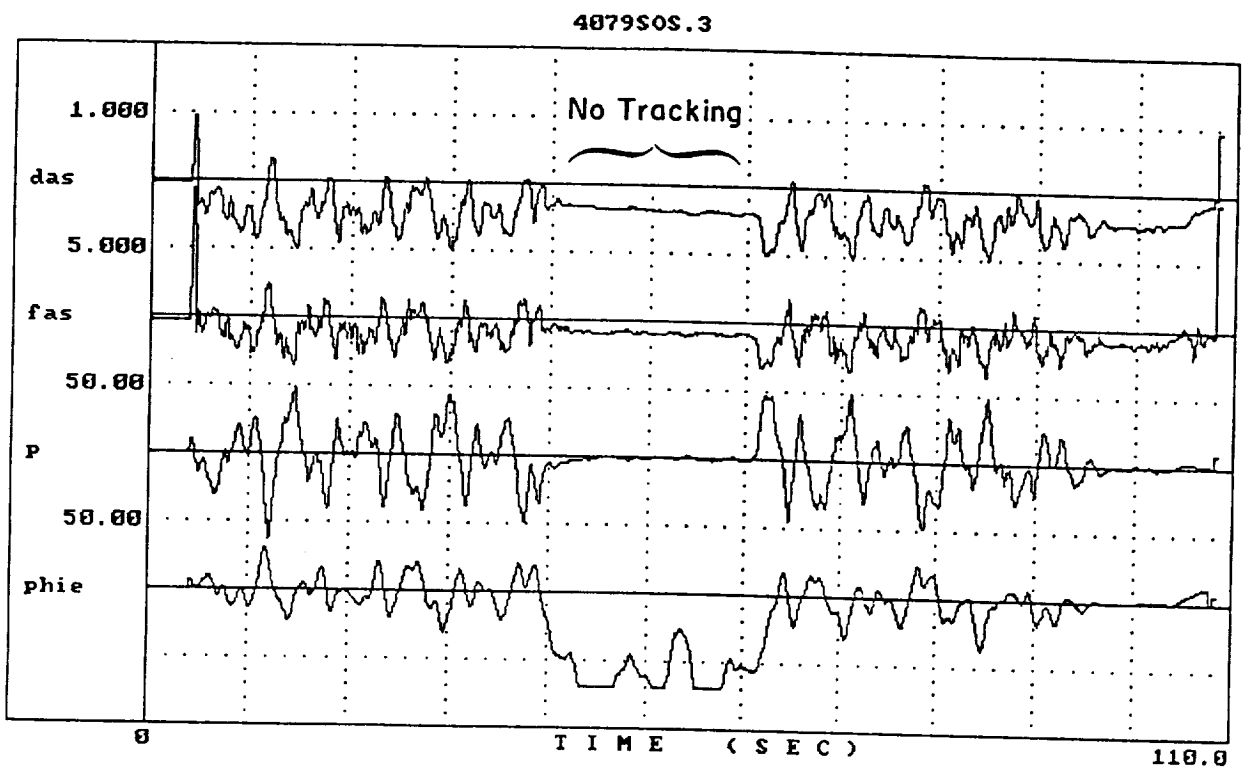
a) Time Histories (not used)

Figure B-5. Flight 4079-3

100
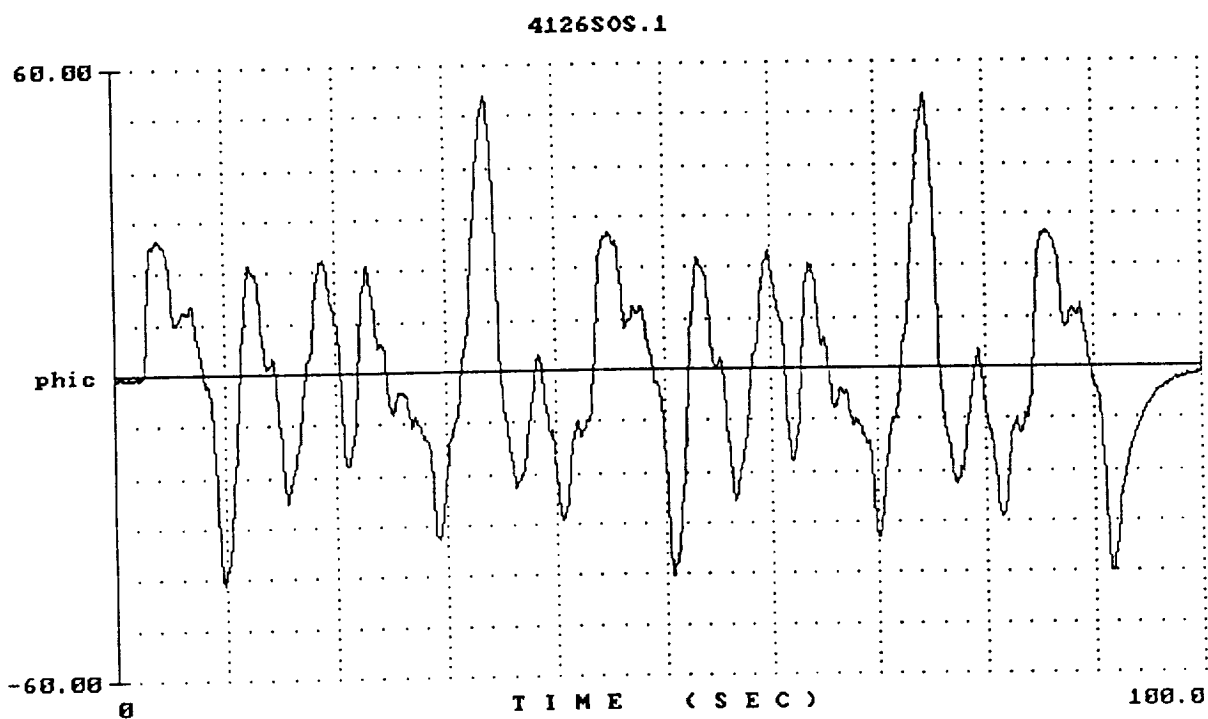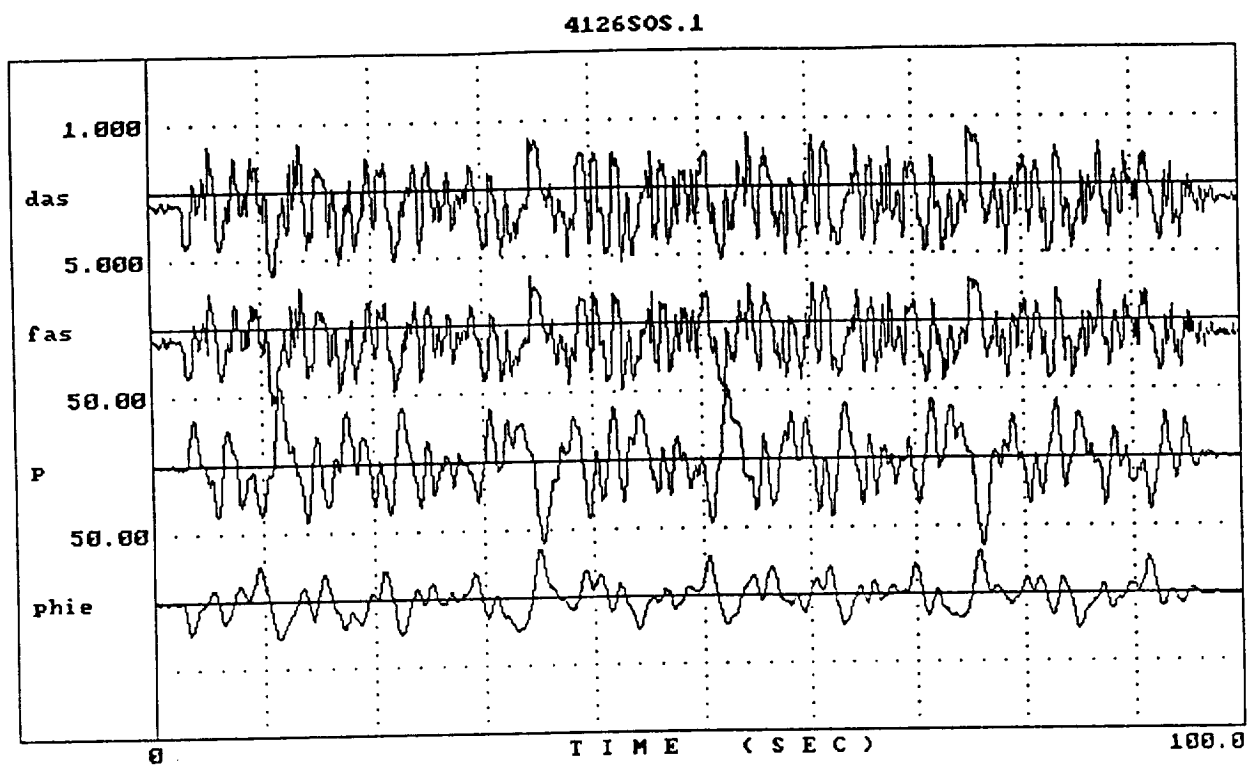
a) Time Histories

Figure B-6. Flight 4126-1
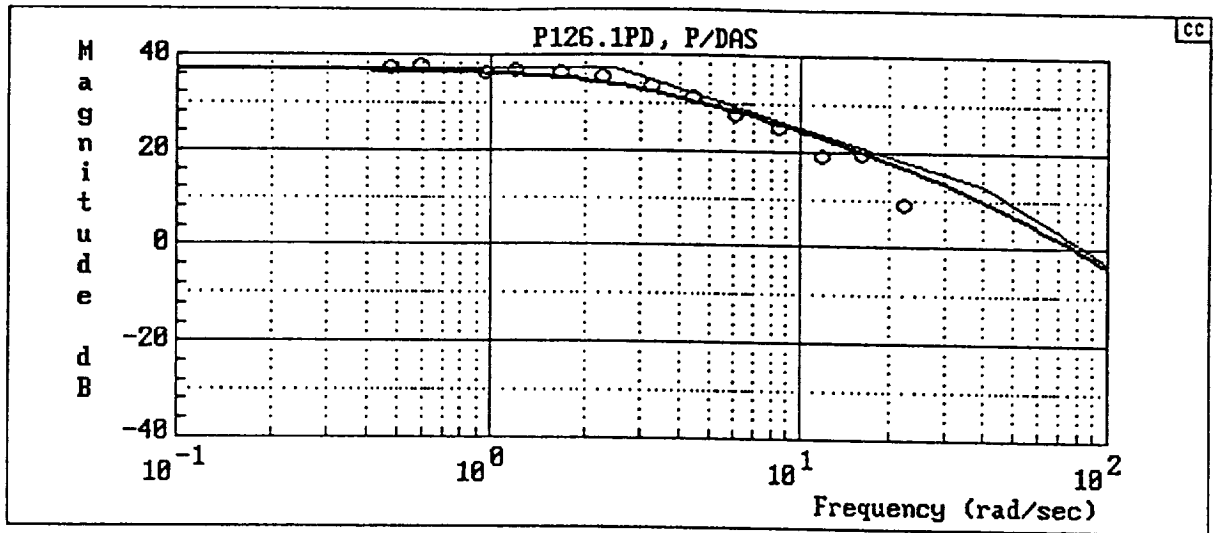
$$Y_c = \frac{7200[-.8660254, 86.60254]}{(2.5)(40)[.8660254, 86.60254]}$$
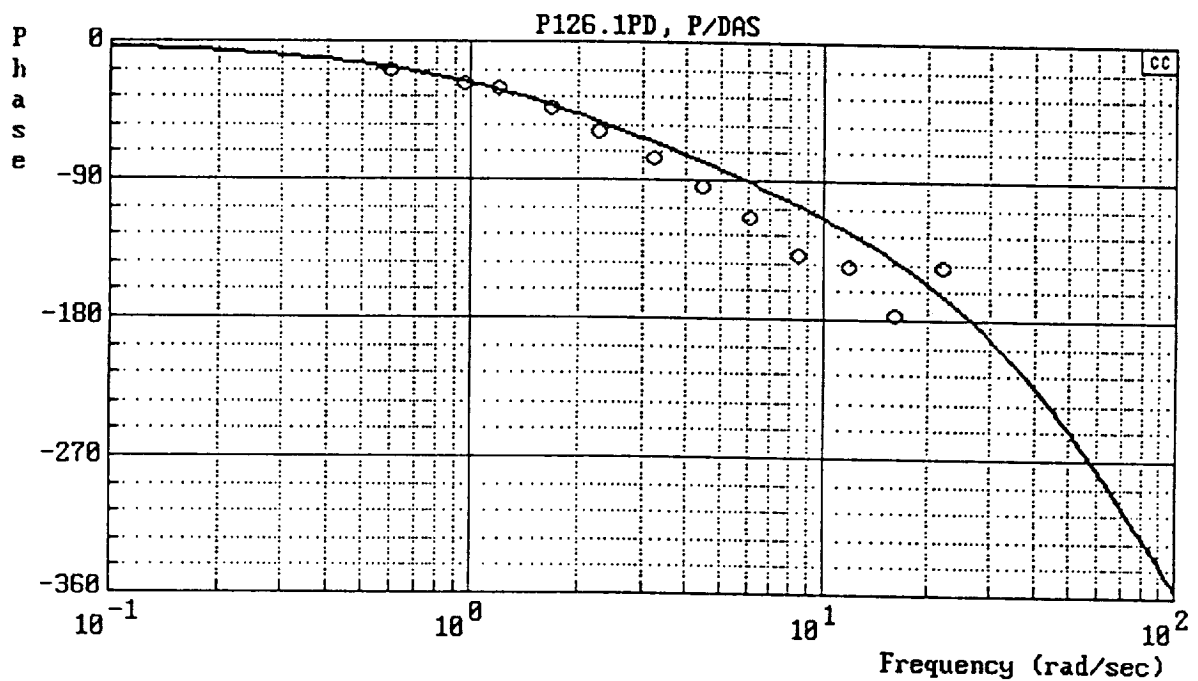
b) Y_c (P/DAS)

Figure B-6. (Continued)

DAS126.1PD, DAS/FAS
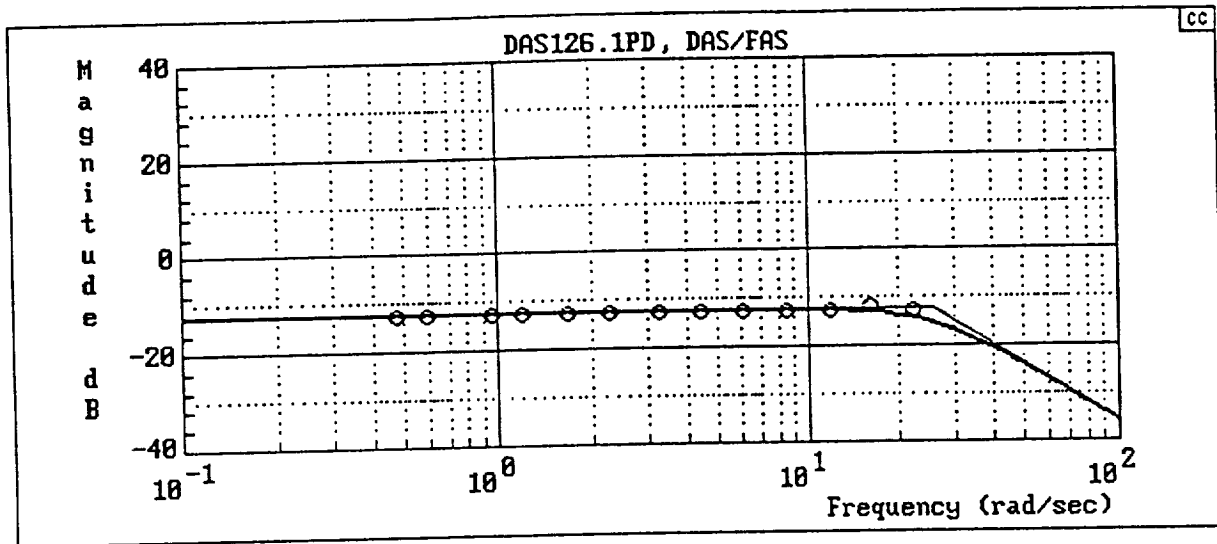
$$Y_{FS} = \frac{169}{[\ .7,\ 26]}$$
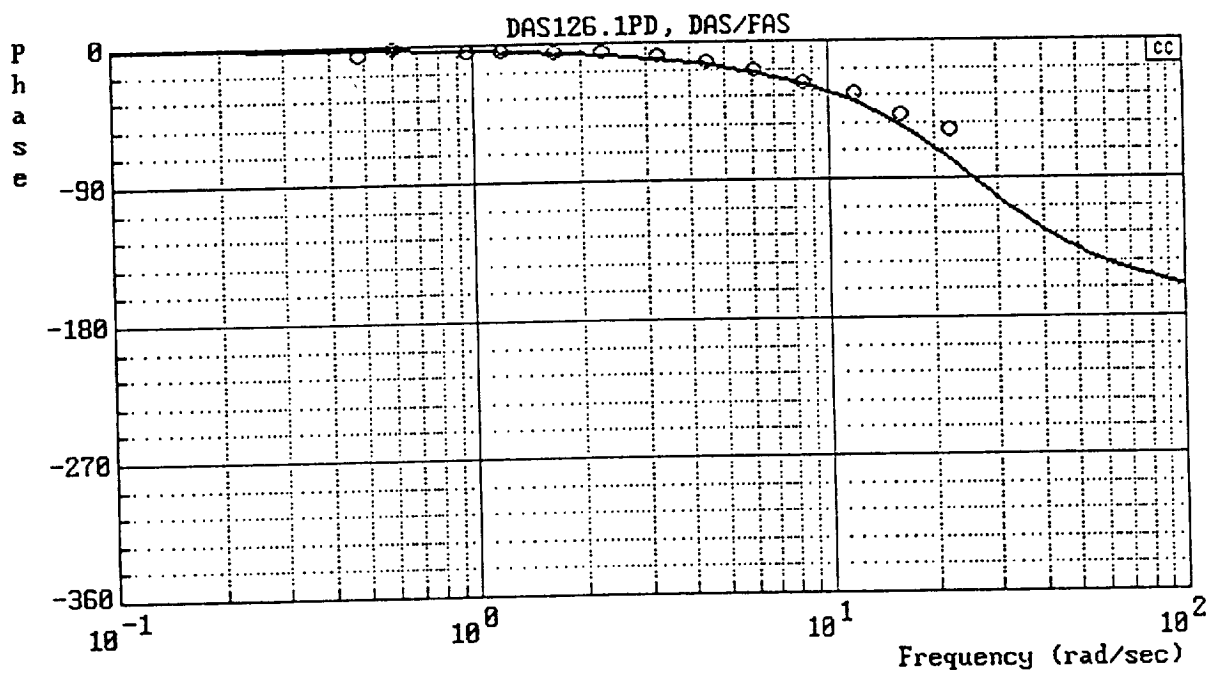
c) Y_{FS} (DAS/FAS)

Figure B-6. (Continued)

PHI126.1PD, φ/φe

PHI126.1PD, φ/φe
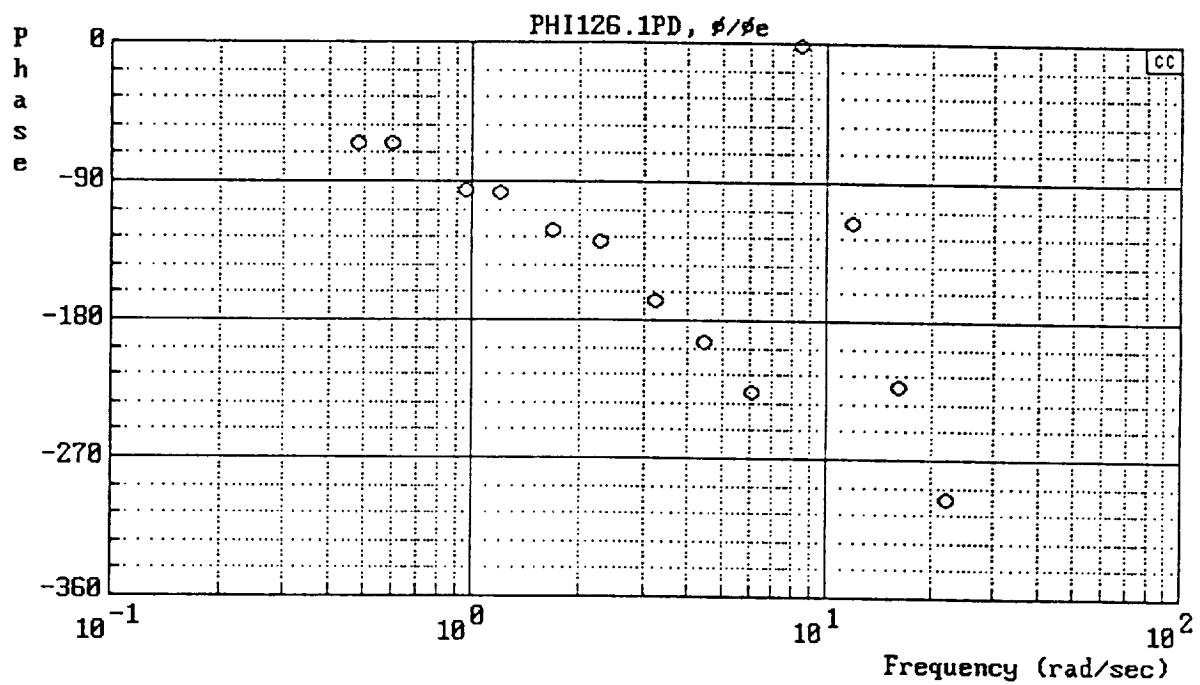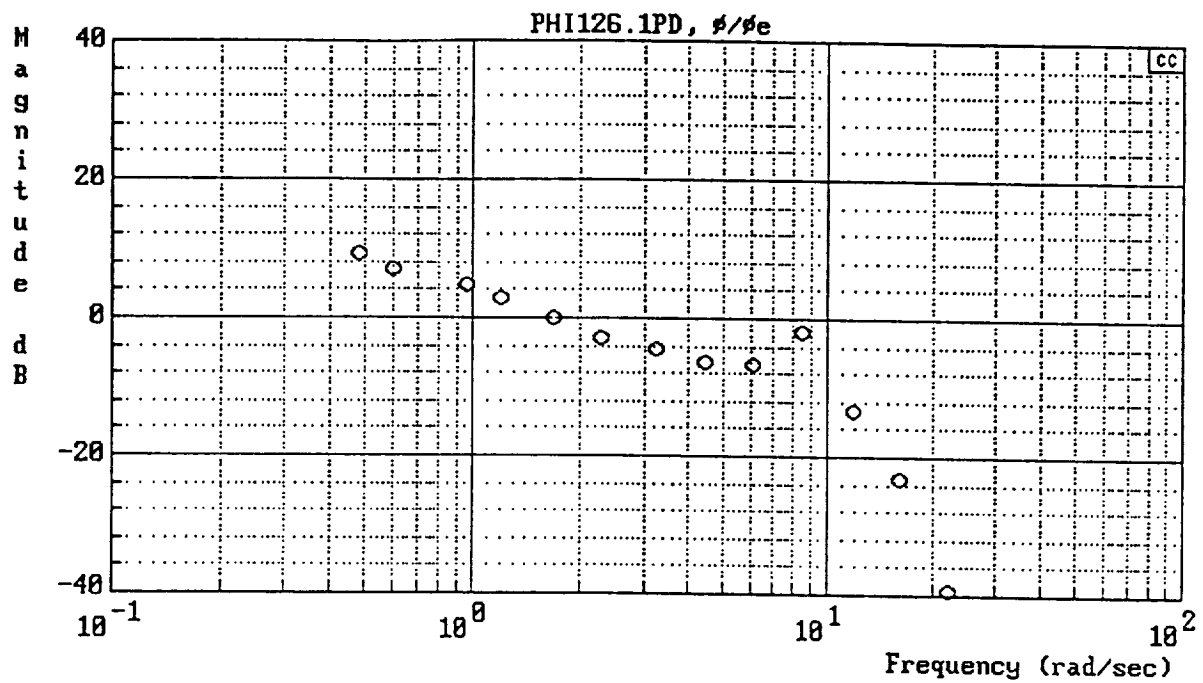
d) $Y_p Y_c$ (PHI/PHIE)

Figure B-6. (Concluded)

104

4126SOS.3

4126SOS.3
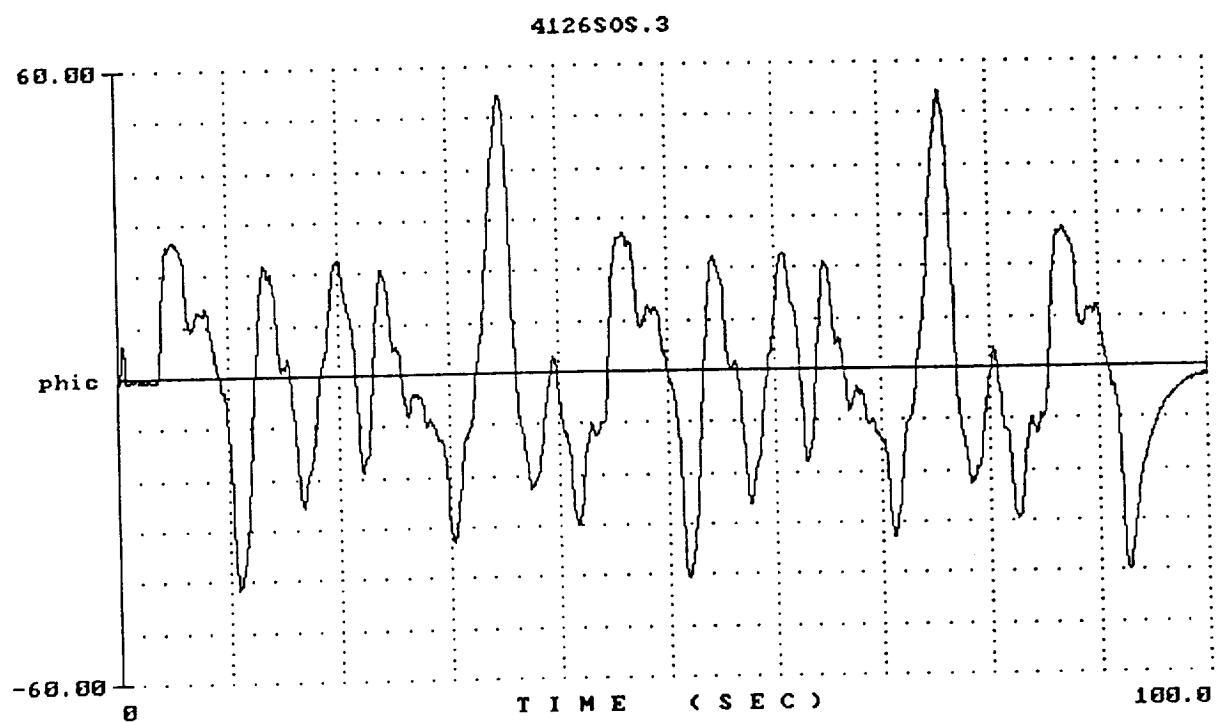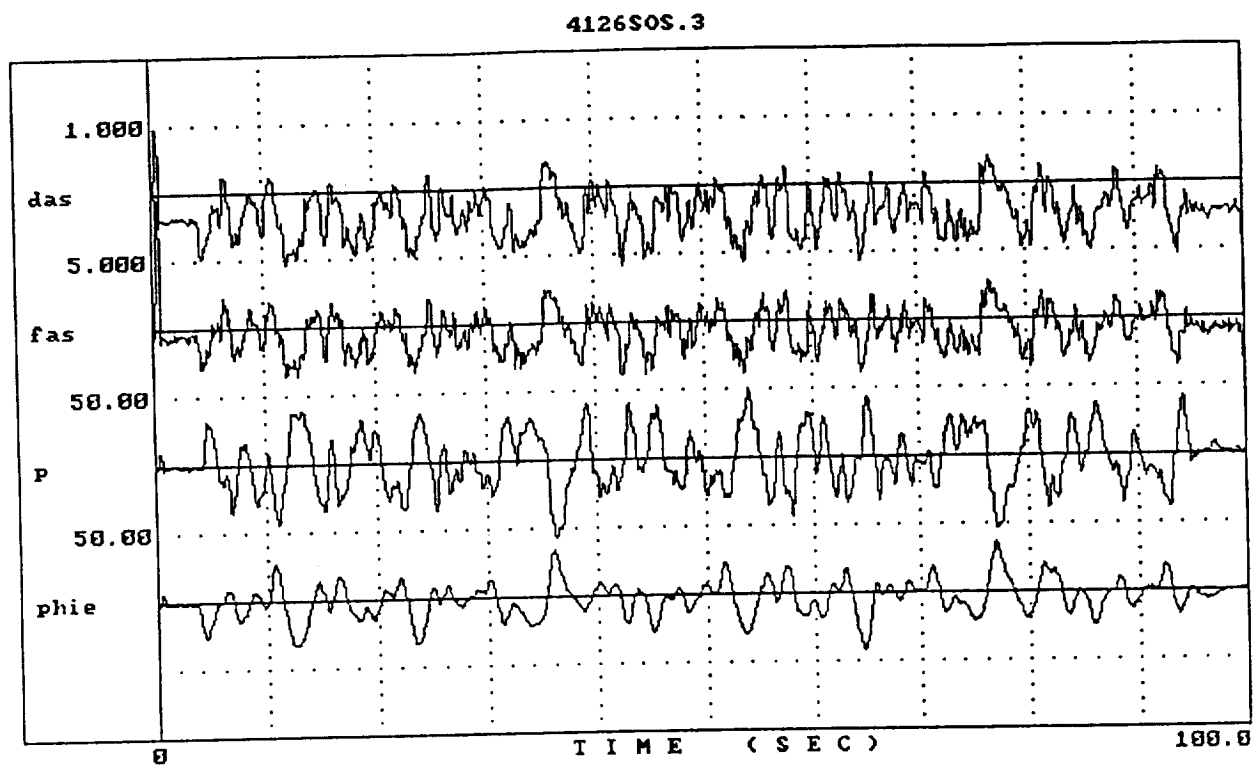
a) Time Histories

Figure B-7. Flight 4126-3

105
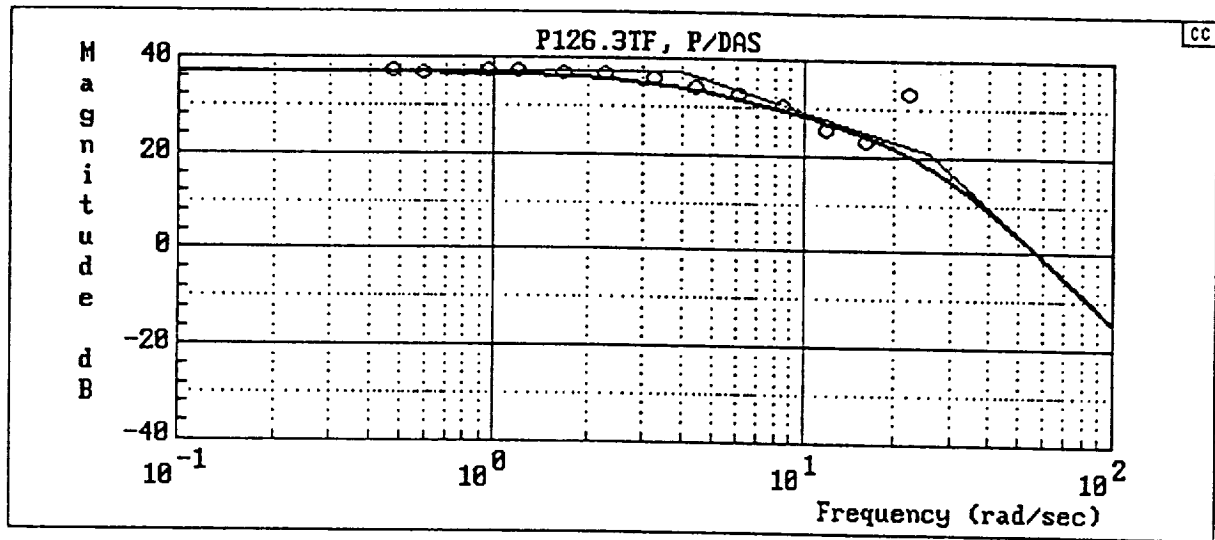
$$Y_C = \frac{194688[-.8660254, 86.60254]}{(4)[.7, 26][.8660254, 86.60254]}$$
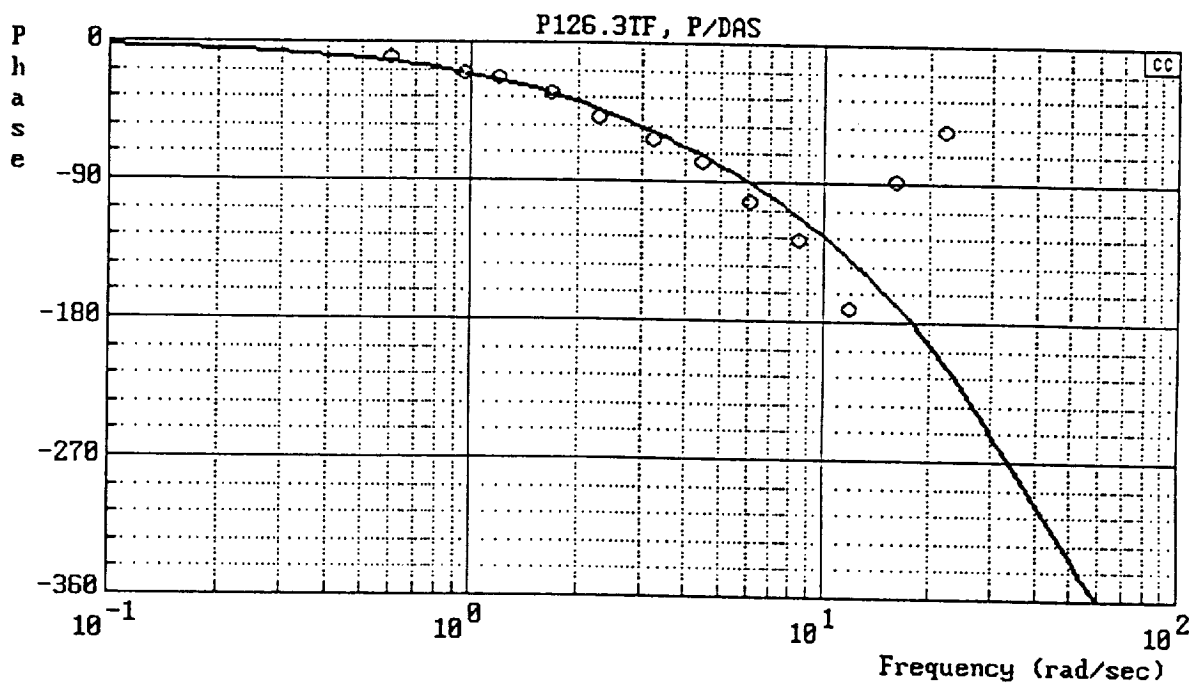
b) Y_p (P/DAS)

Figure B-7. (Continued)
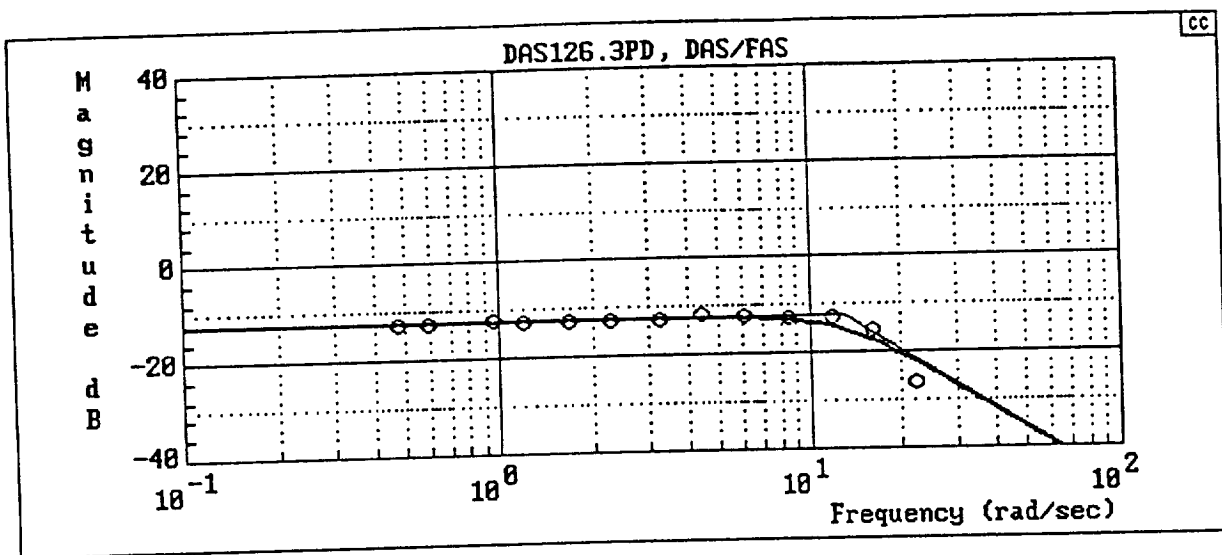
$$Y_{FS} = \frac{42.25}{[\,.7\,,\ 13]}$$
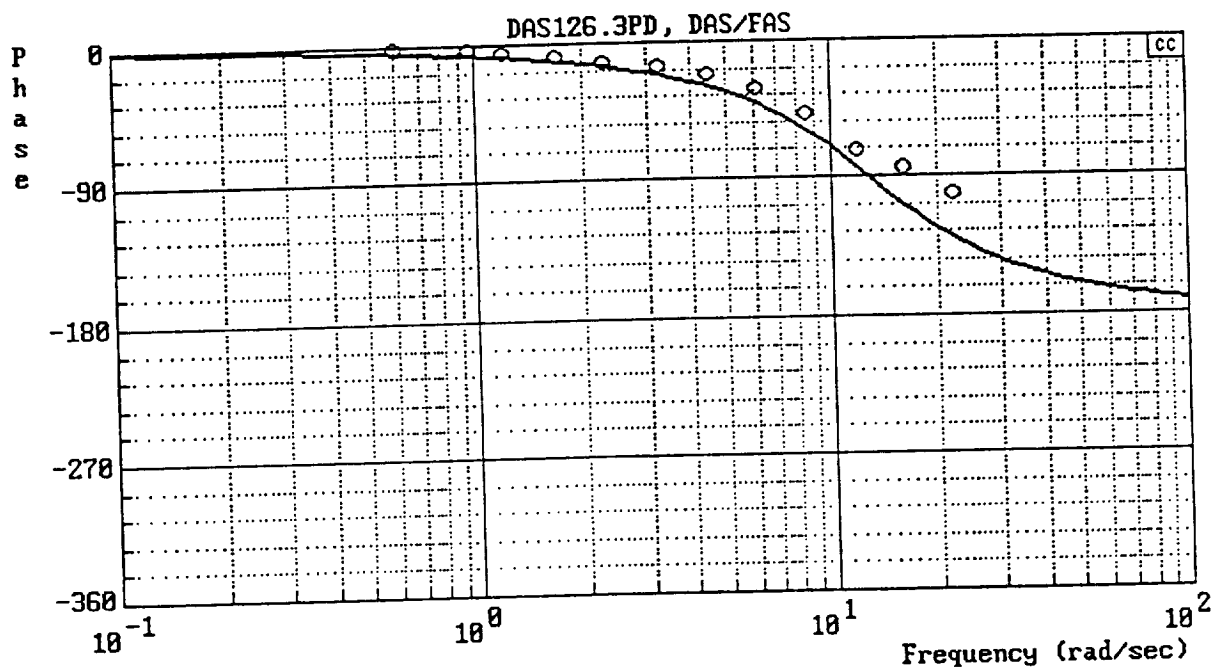
c) Y_{FS} (DAS/FAS)

Figure B-7. (Continued)
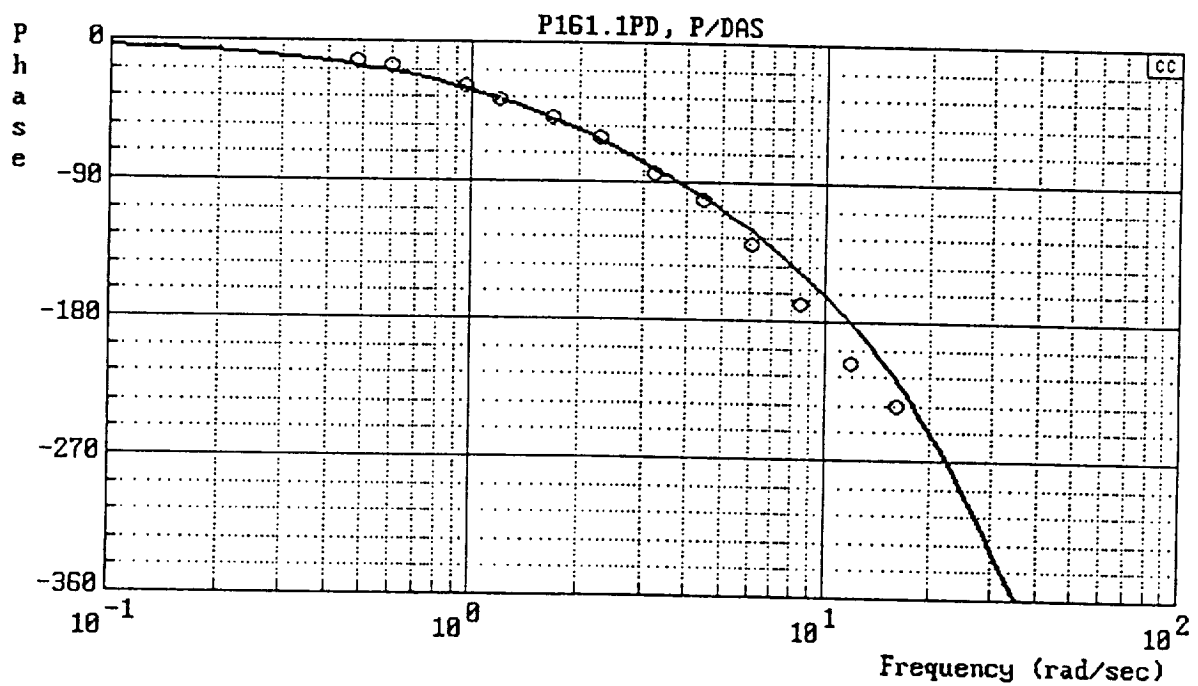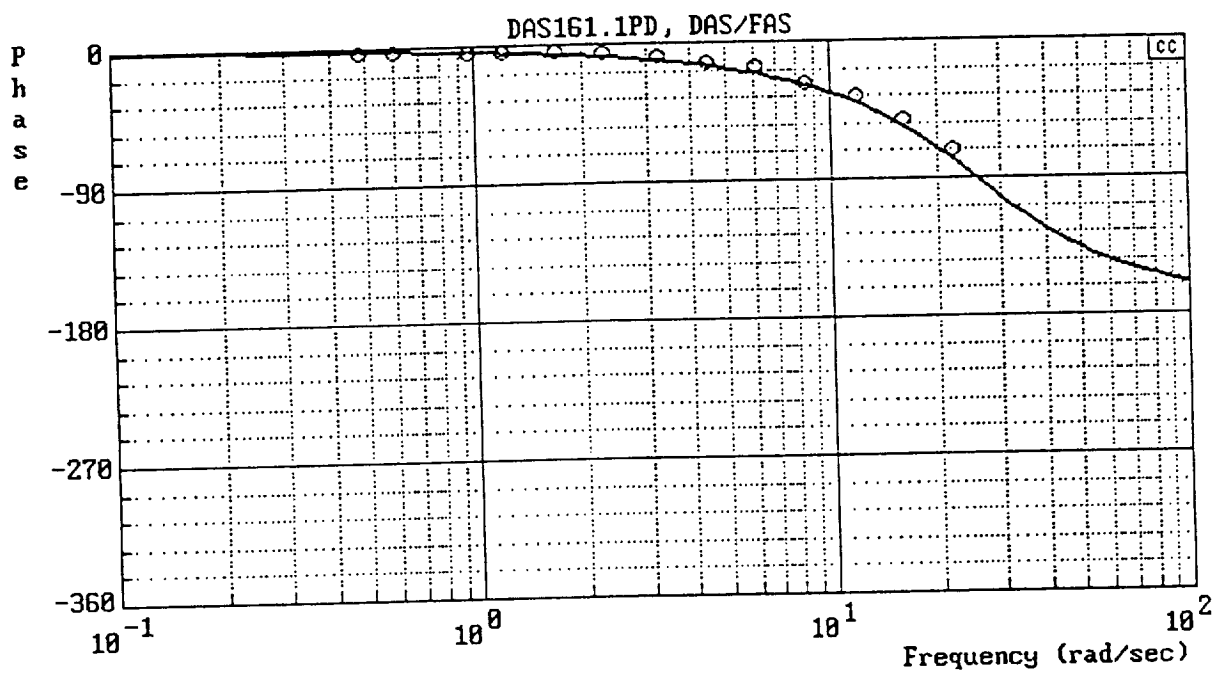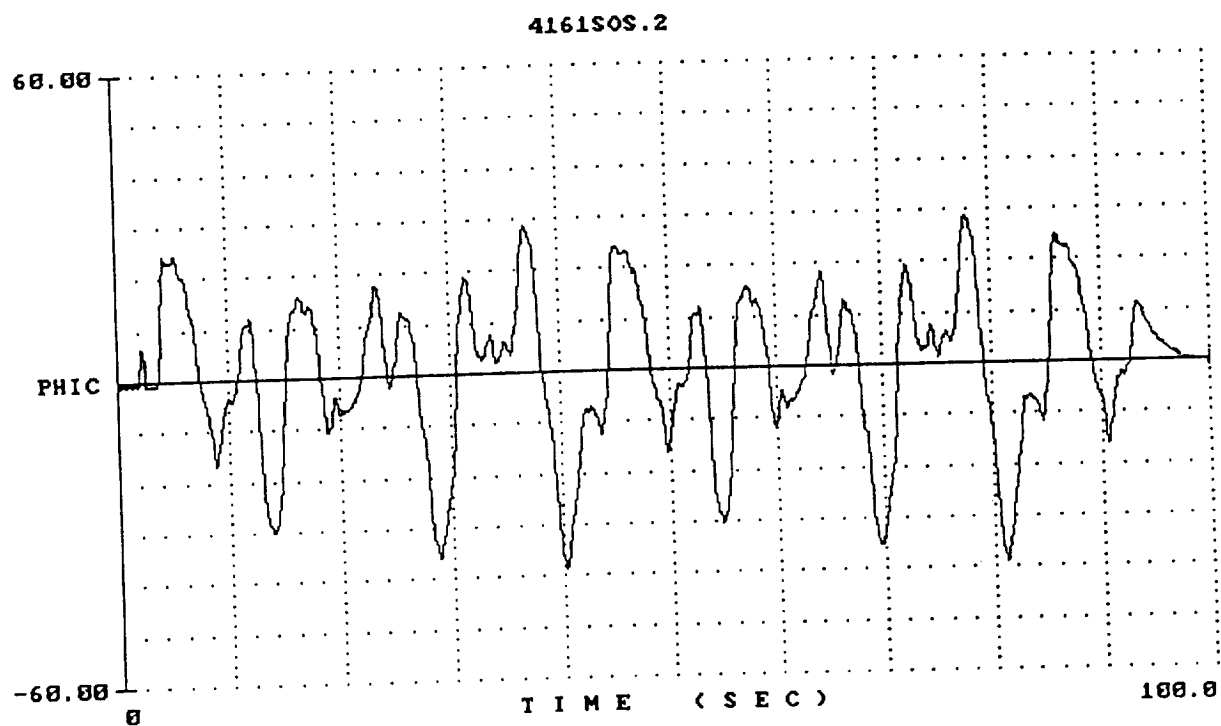
107
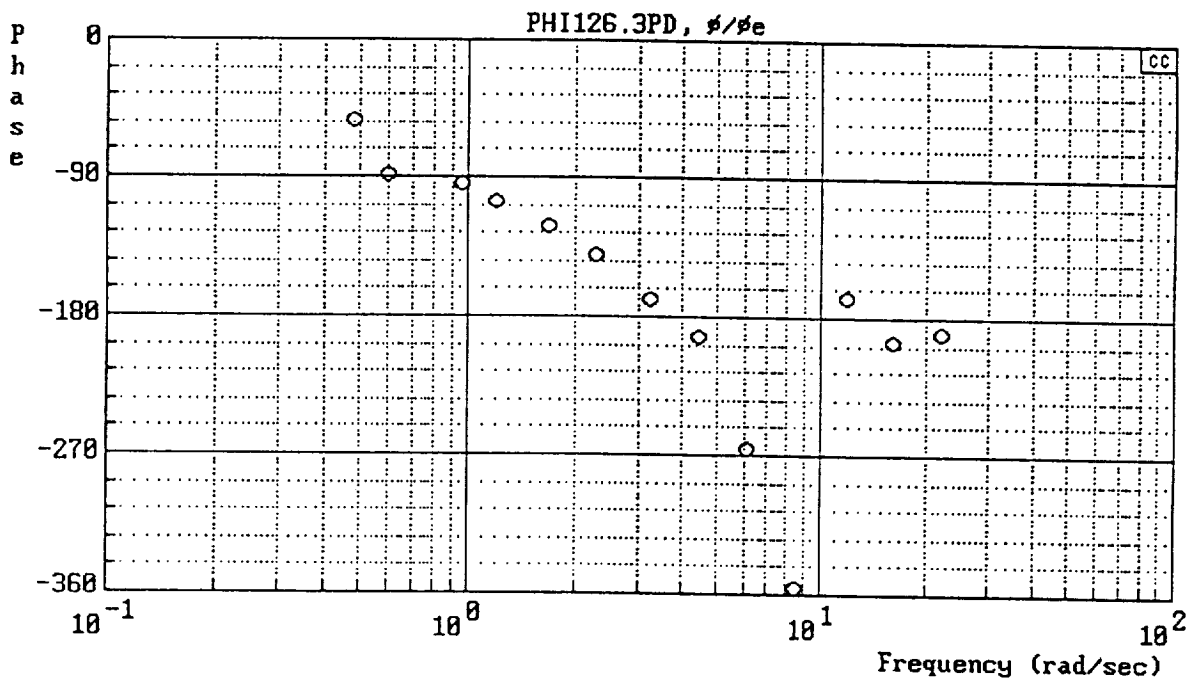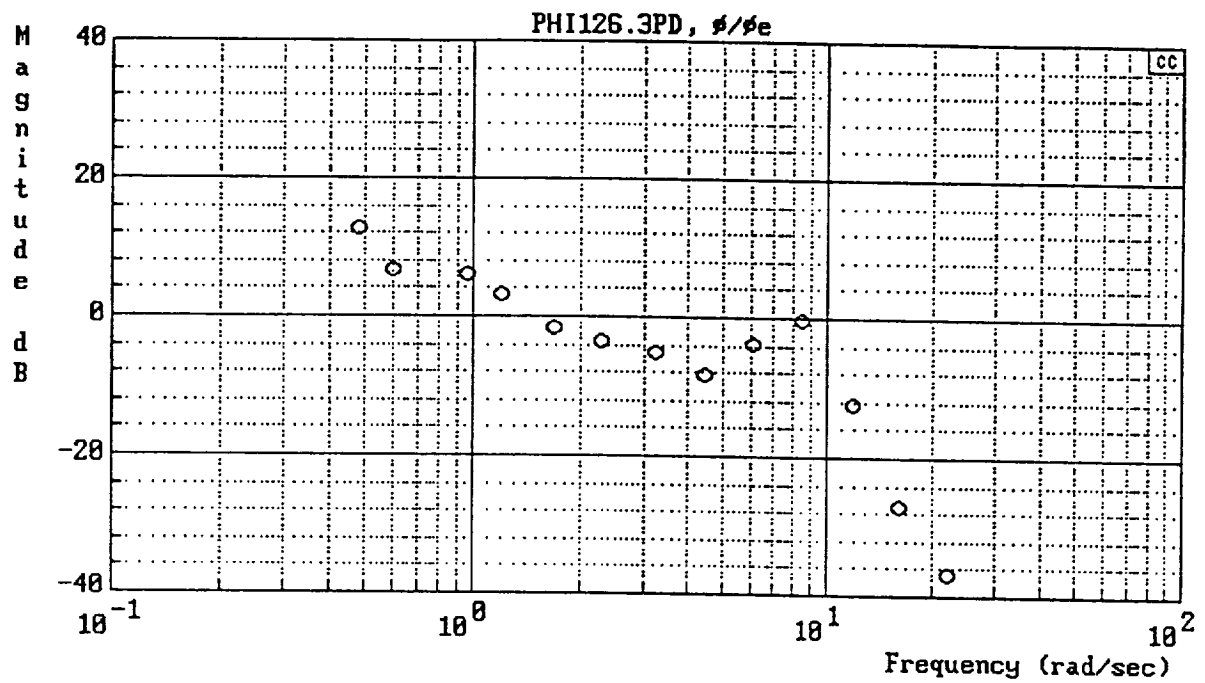
d) Y_pY_c (PHI/PHIE)

Figure B-7. (Concluded)

4127SOS.1B

DAS
FAS
P
PHIE

1.000
5.000
50.00
50.00

0   TIME   (SEC)   100.0

4127SOS.1B

60.00

PHIC

-60.00

0   TIME   (SEC)   100.0
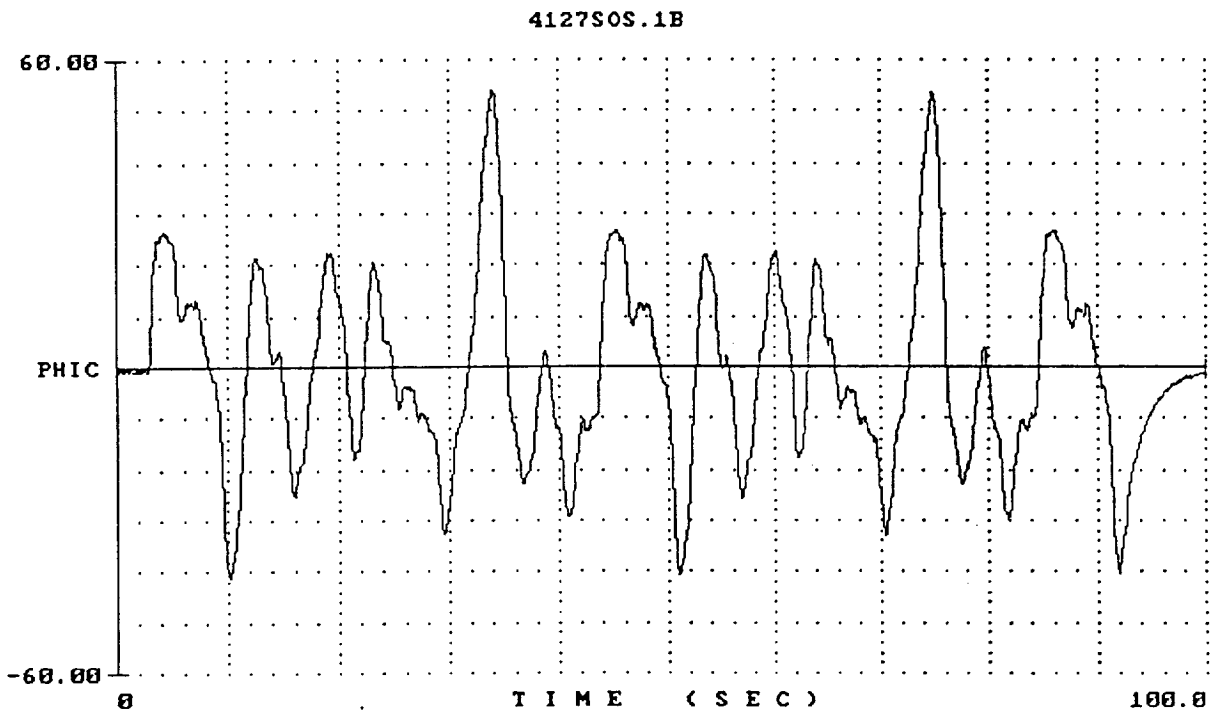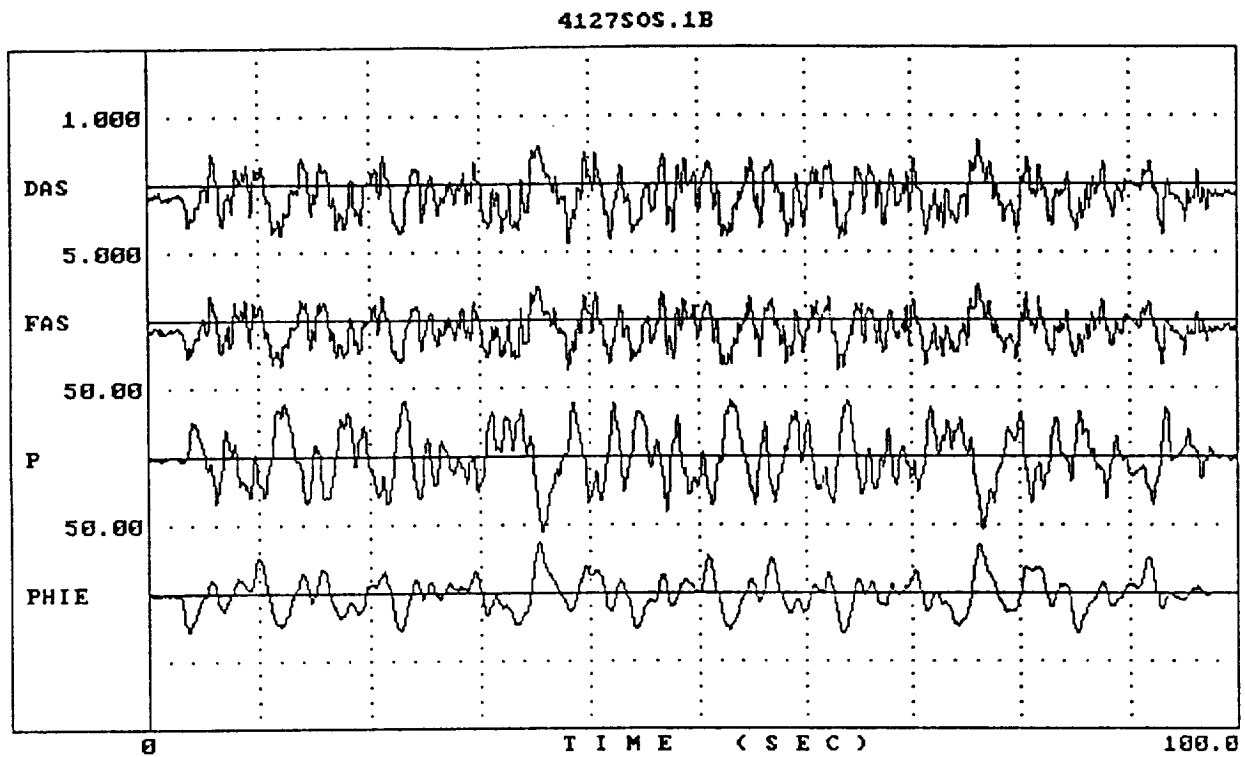
a) Time Histories

Figure B-8. Flight 4127-1
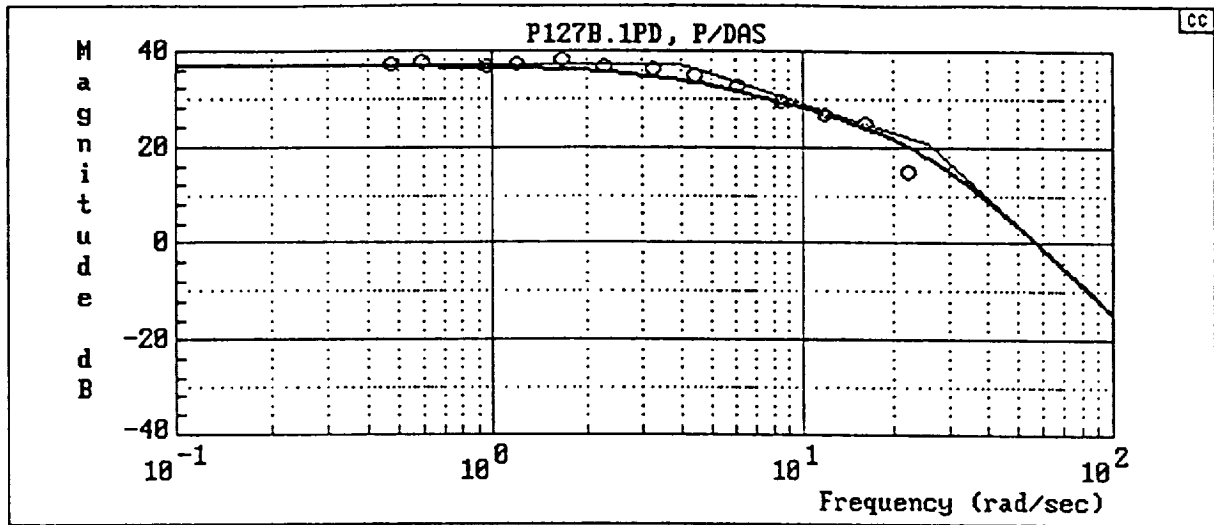
P127B.1PD, P/DAS

$$Y_c = \frac{194688[-.8660254, 86.60254]}{(4)[.7, 26][.8660254, 86.60254]}$$

P127B.1PD, P/DAS

b) Y_c (P/DAS)

Figure B-8. (Continued)

DAS127B.1PD, DAS/FAS

$$Y_{FS} = \frac{42.25}{[\ .7,\ 13]}$$

DAS127B.1PD, DAS/FAS
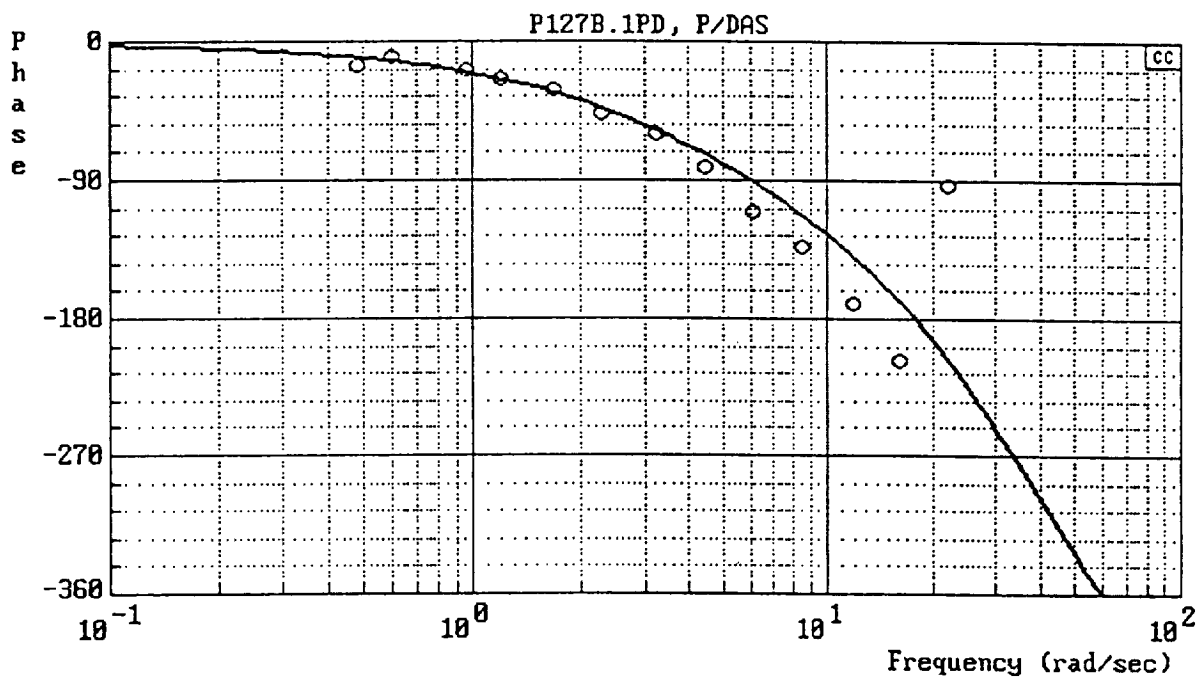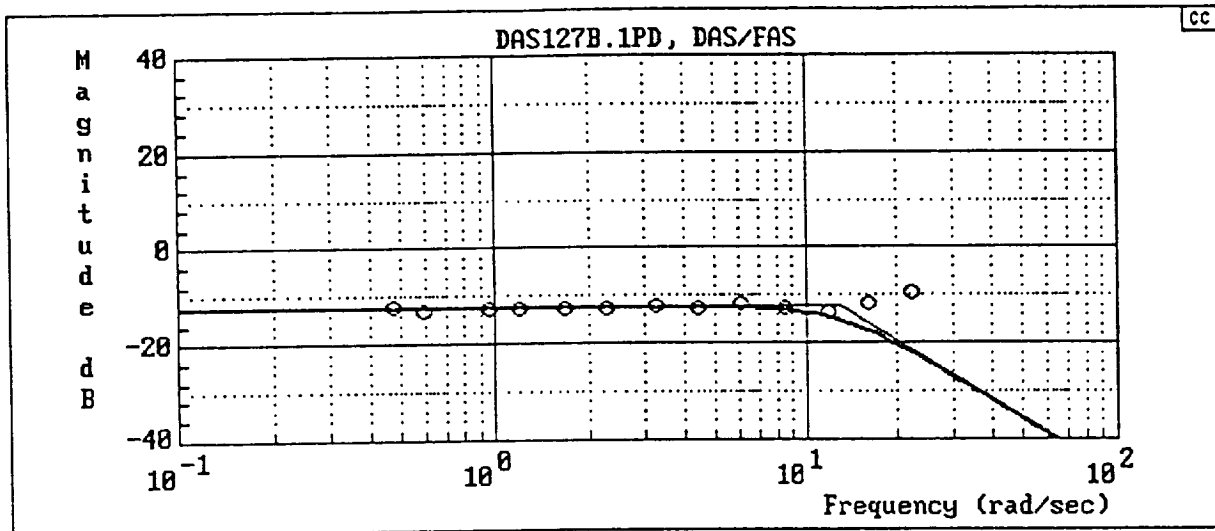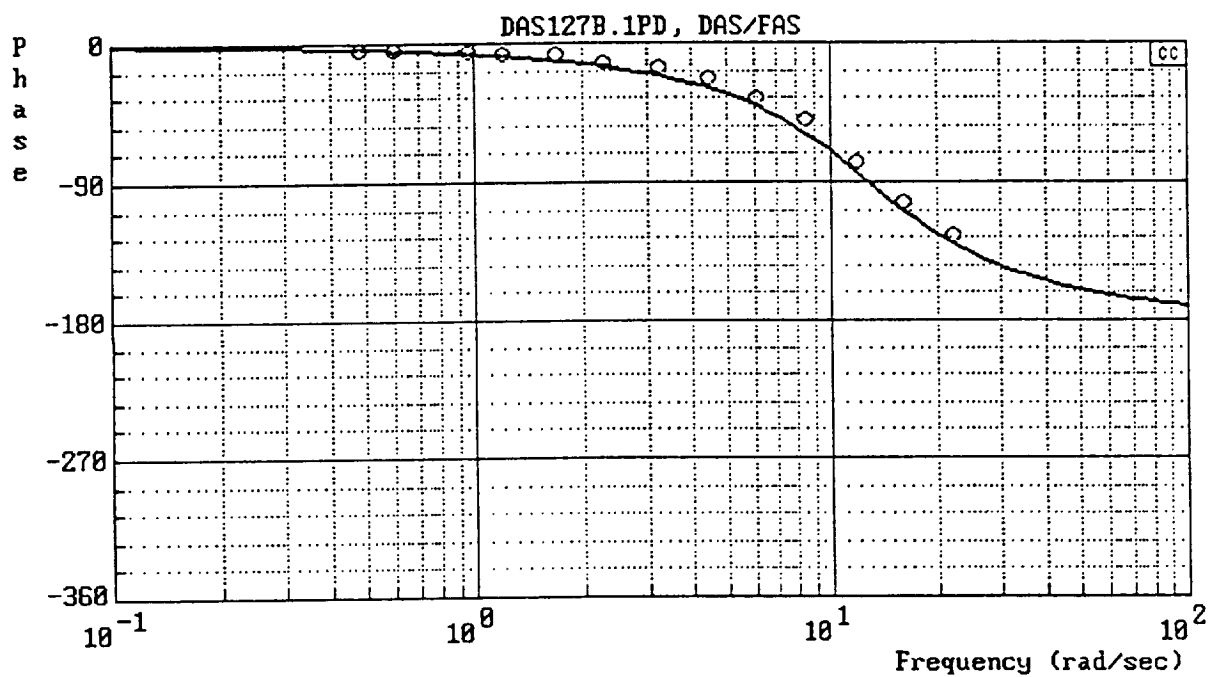
c) Y_{FS} (DAS/FAS)

Figure B-8. (Continued)

PHI127B.1PD, ∮/∮e

PHI127B.1PD, ∮/∮e
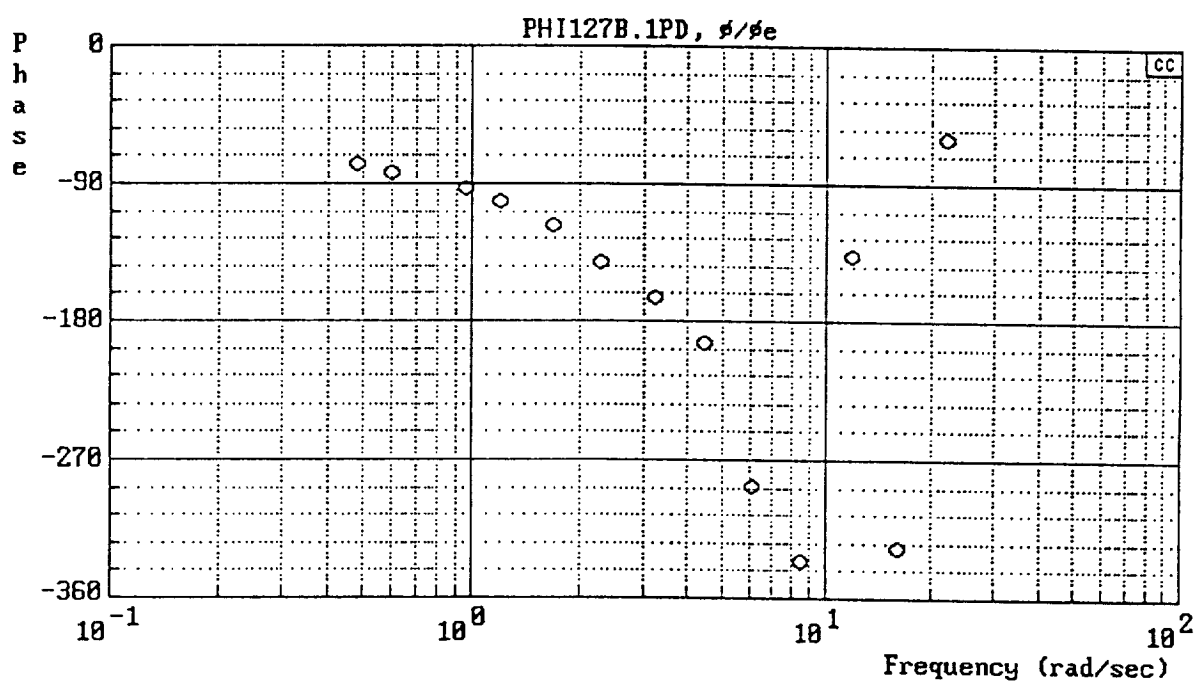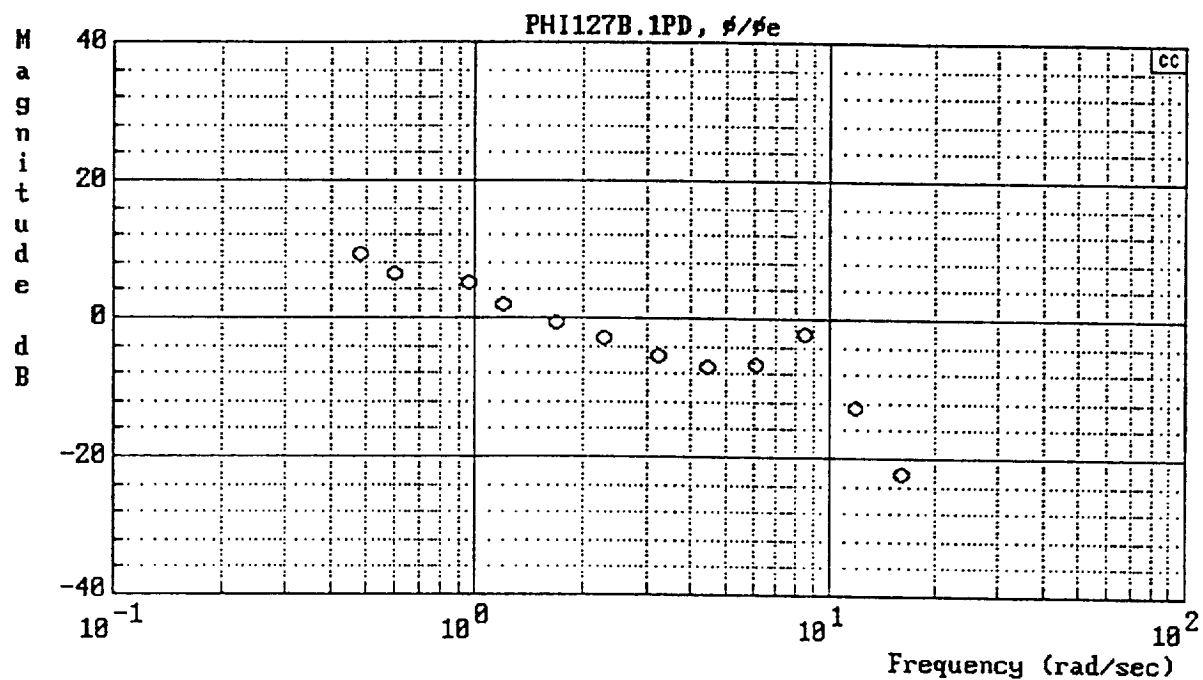
d) $Y_p Y_c$ (PHI/PHIE)

Figure B-8. (Concluded)

112
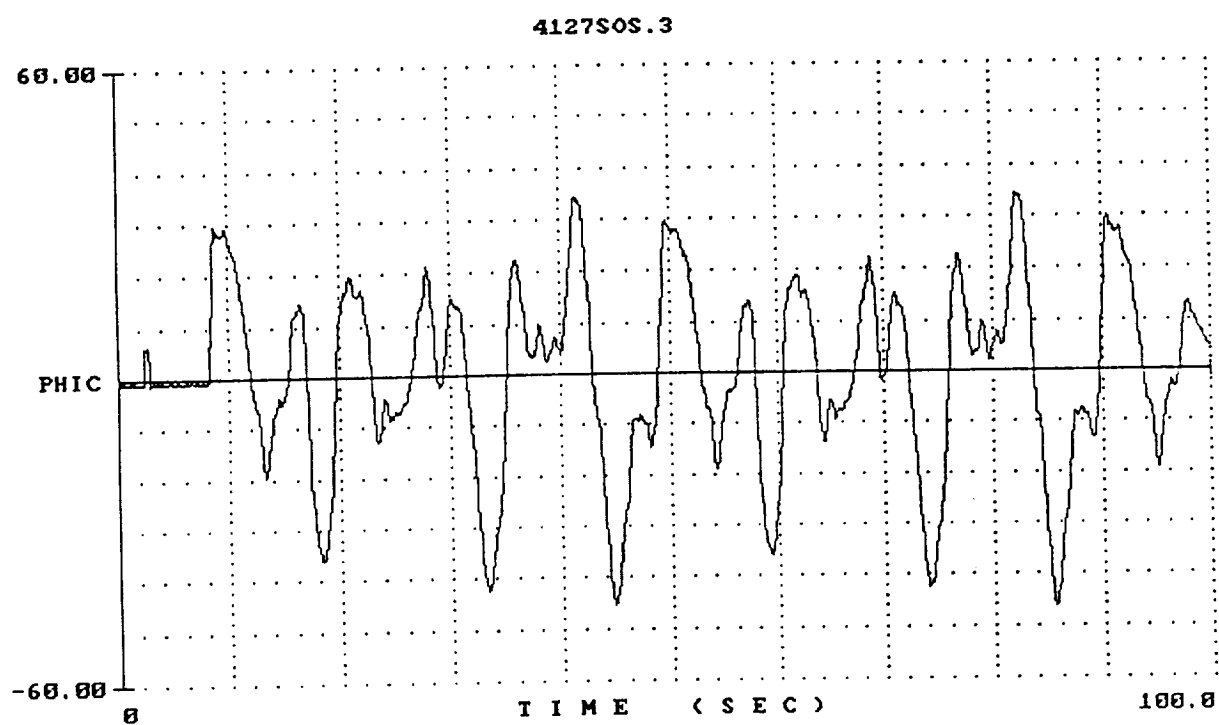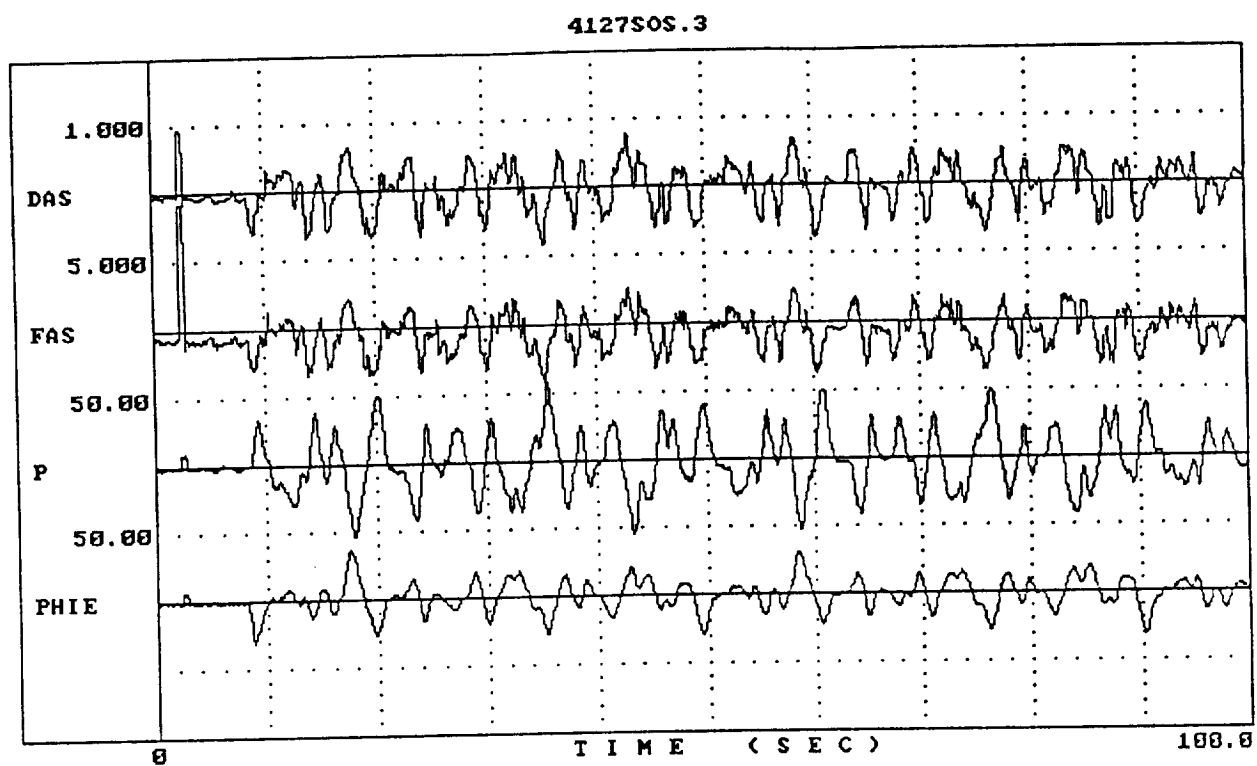
a) Time Histories

Figure B-9. Flight 4127-3
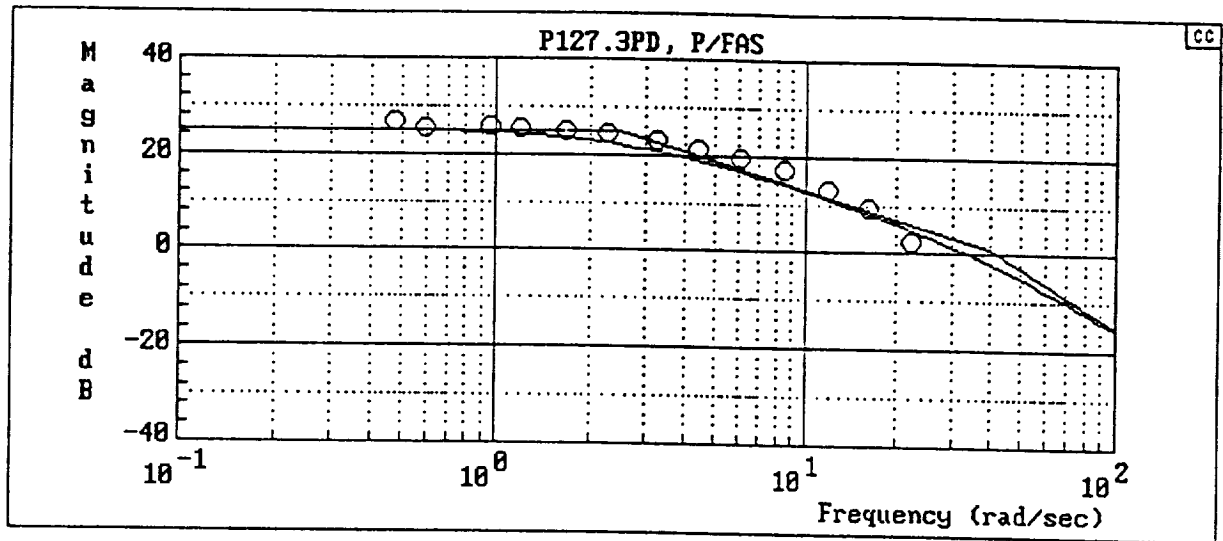
P127.3PD, P/FAS

$$Y_c = \frac{1800[-.8660254, \ 86.60254]}{(2.5)(40)[.8660254, \ 86.60254]}$$

P127.3PD, P/FAS

b) Y_c (P/FAS)

Figure B-9. (Continued)

DAS127.3PD, DAS/FAS

$$Y_{FS} = \frac{42.25}{[\ .7,\ 13]}$$

DAS127.3PD, DAS/FAS
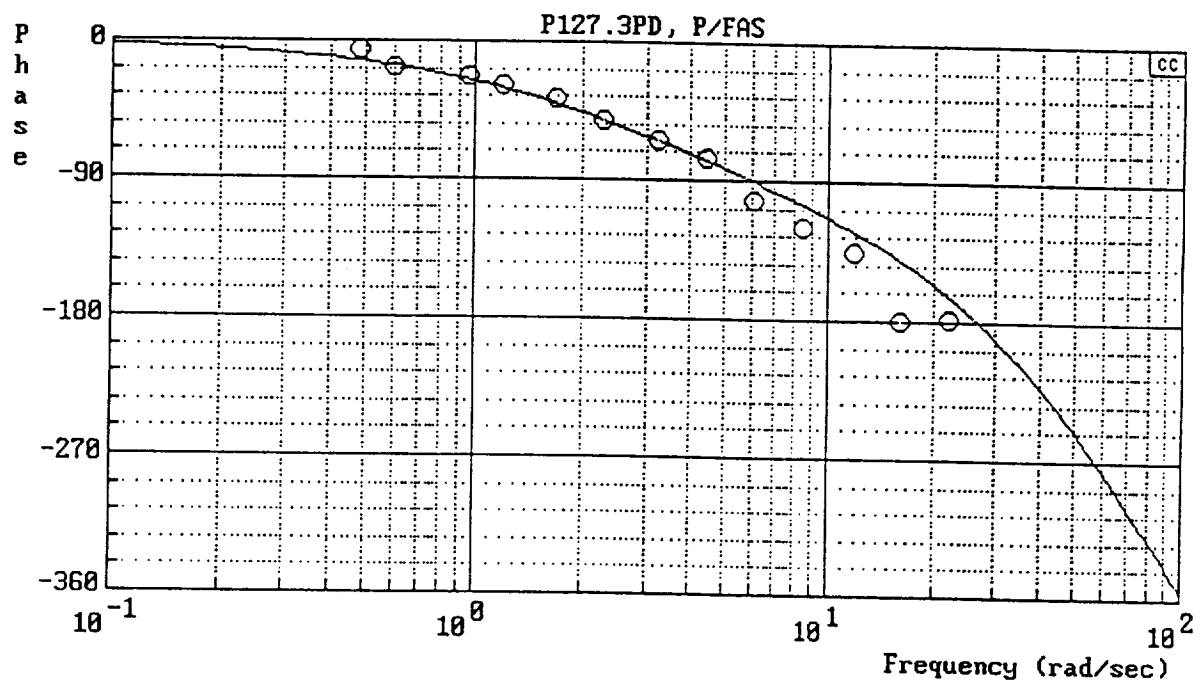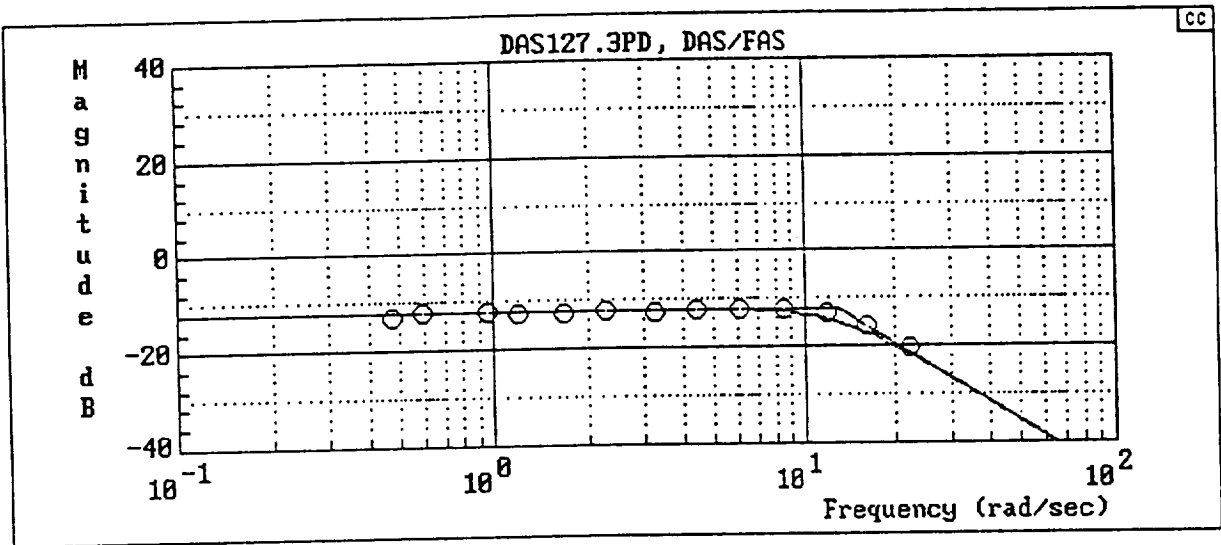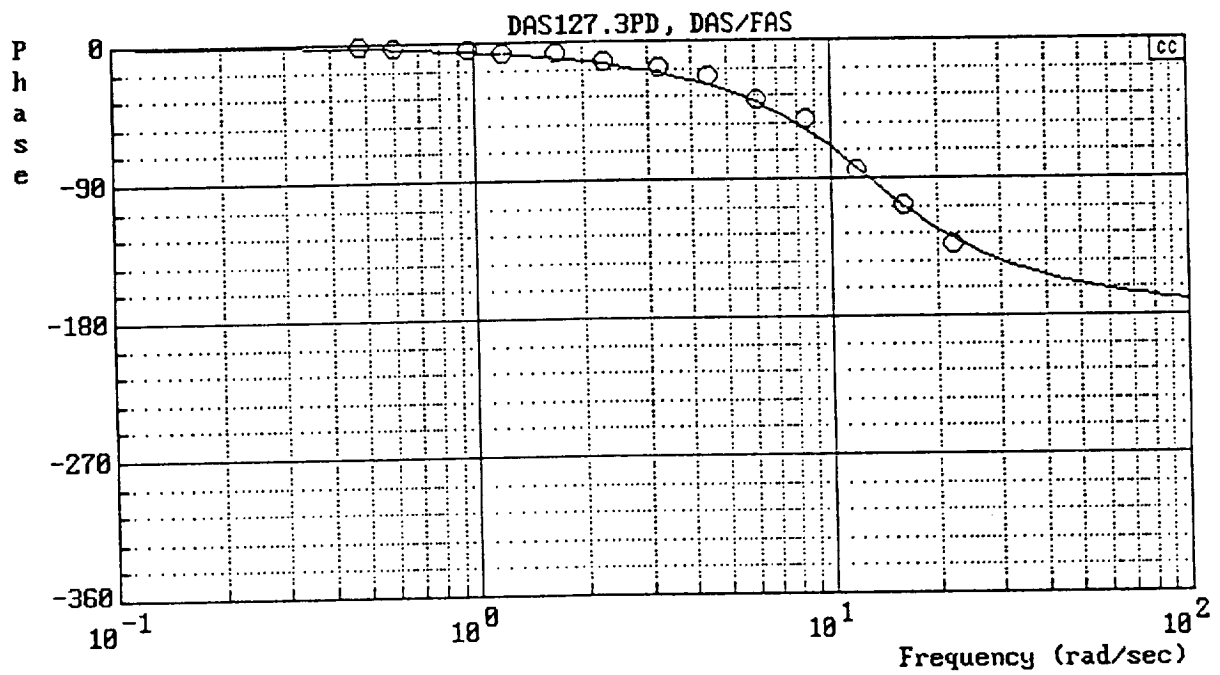
c) Y_{FS} (DAS/FAS)

Figure B-9. (Continued)
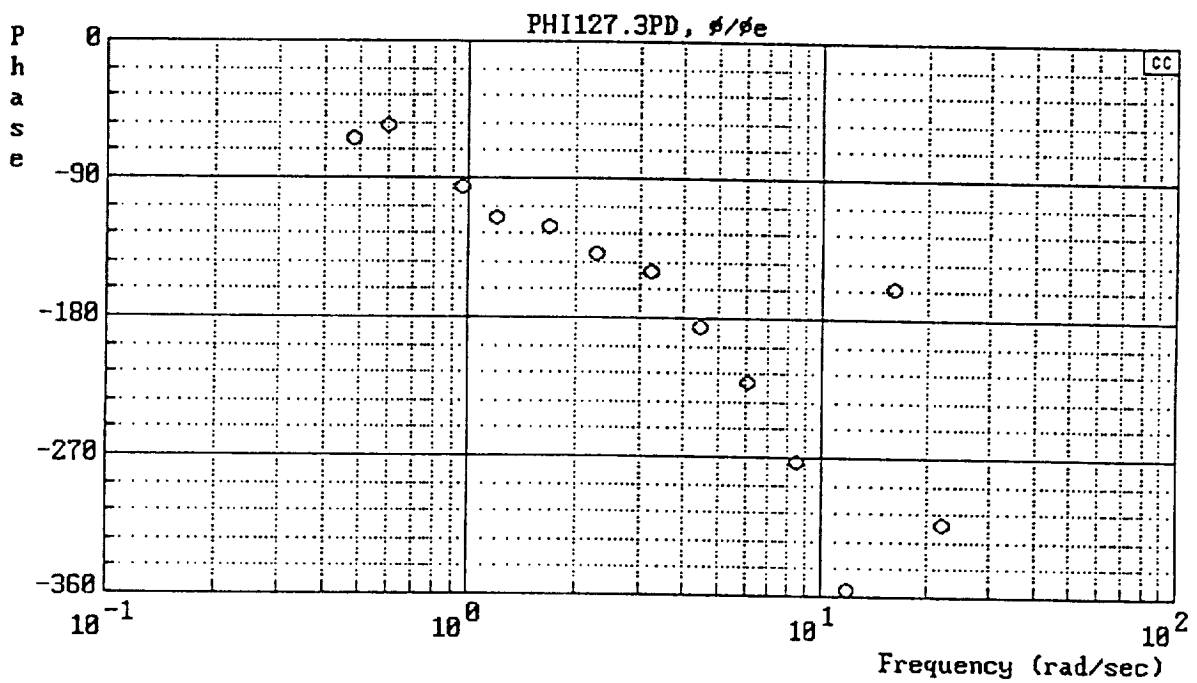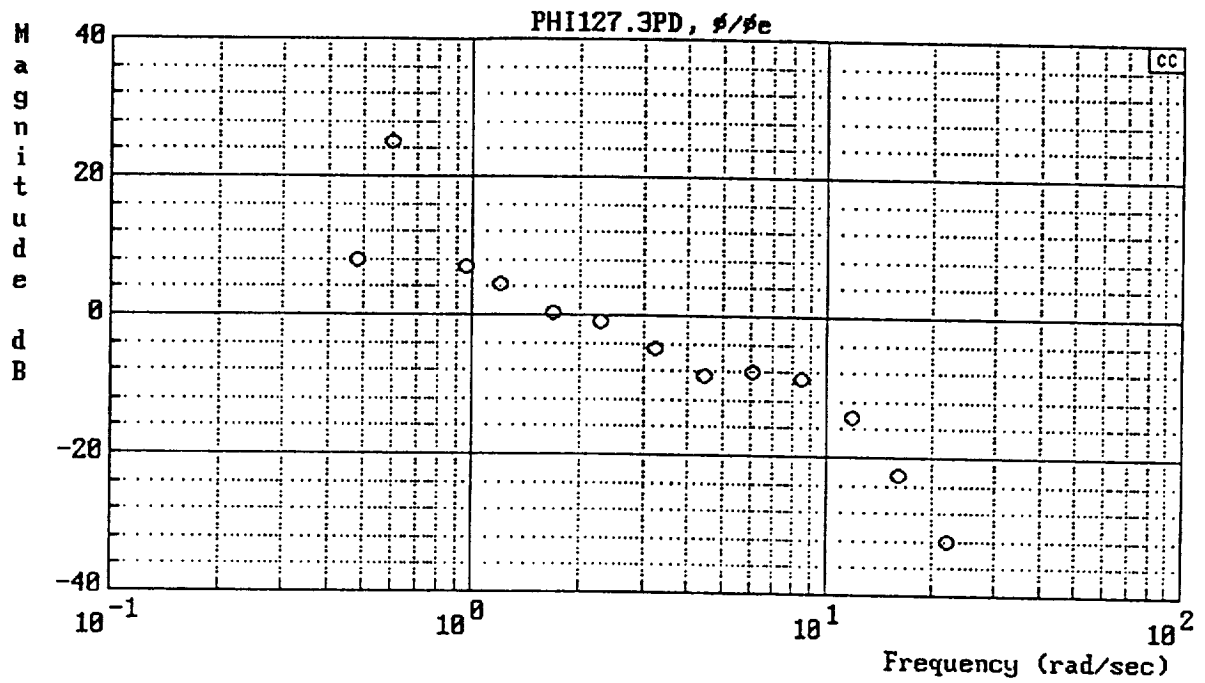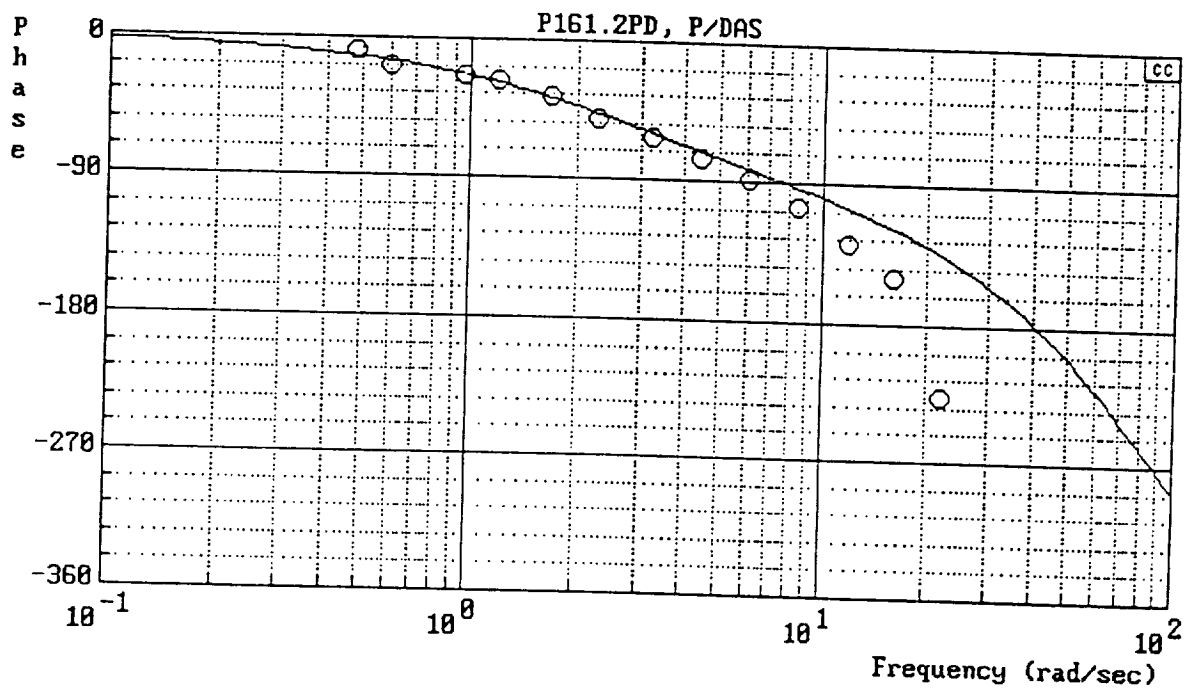
d) $Y_p Y_c$ (PHI/PHIE)

Figure B-9. (Concluded)

4154SOS.5
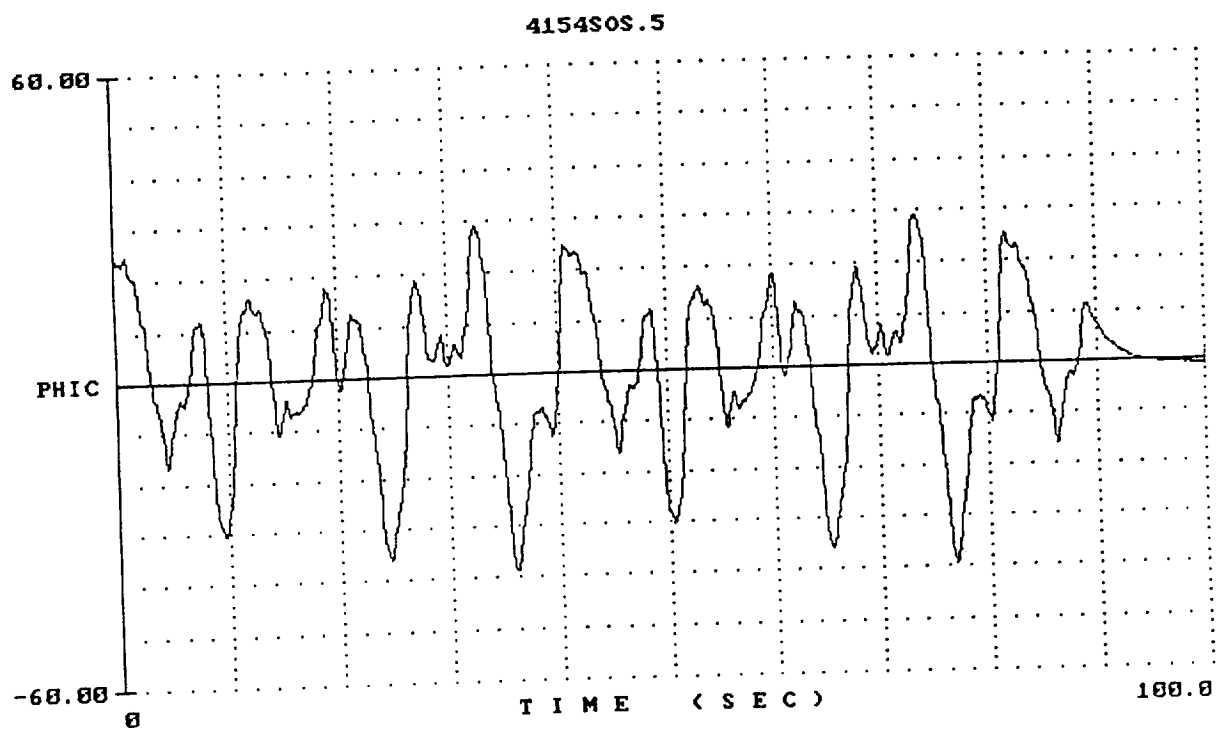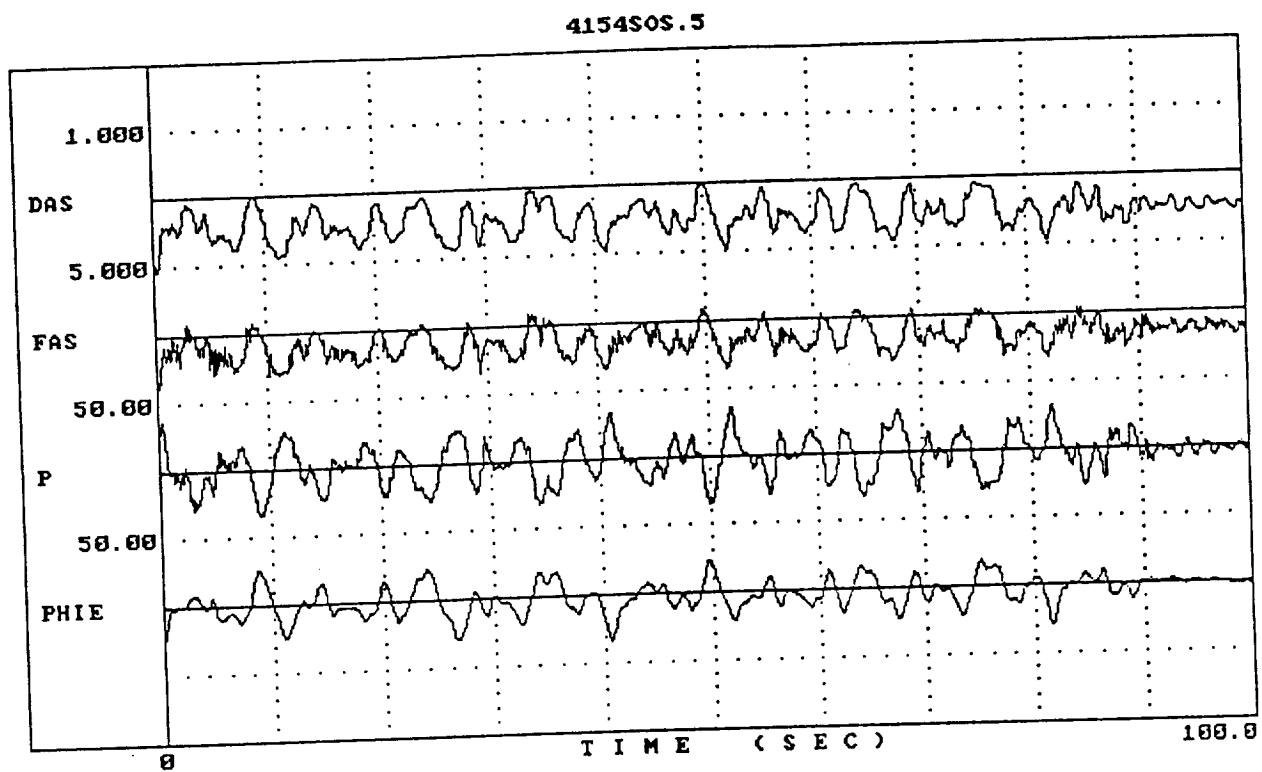
a) Time Histories

Figure B-10. Flight 4154-5
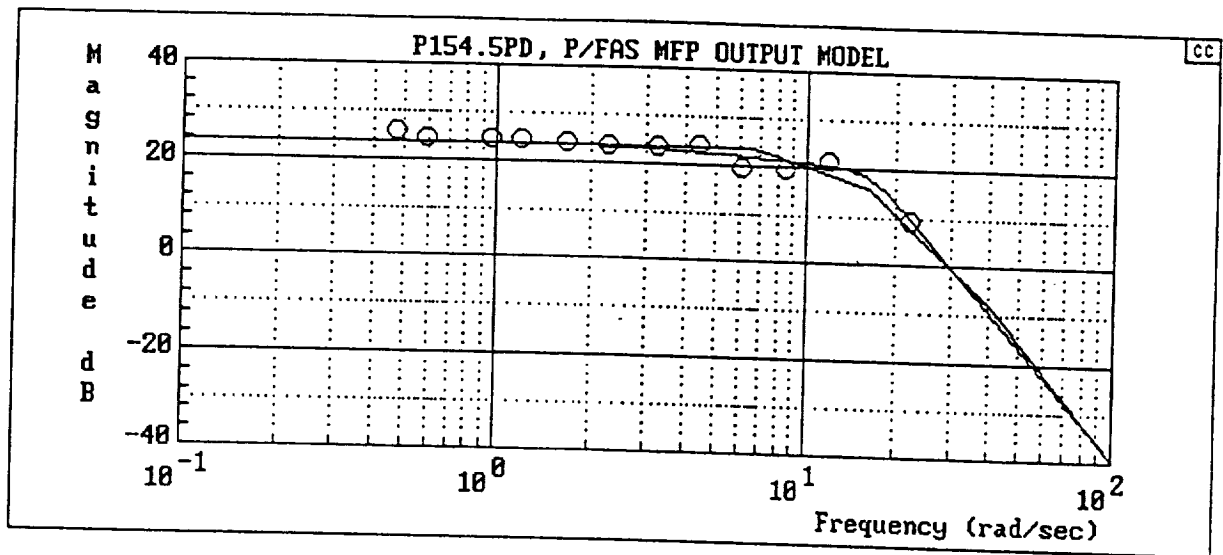
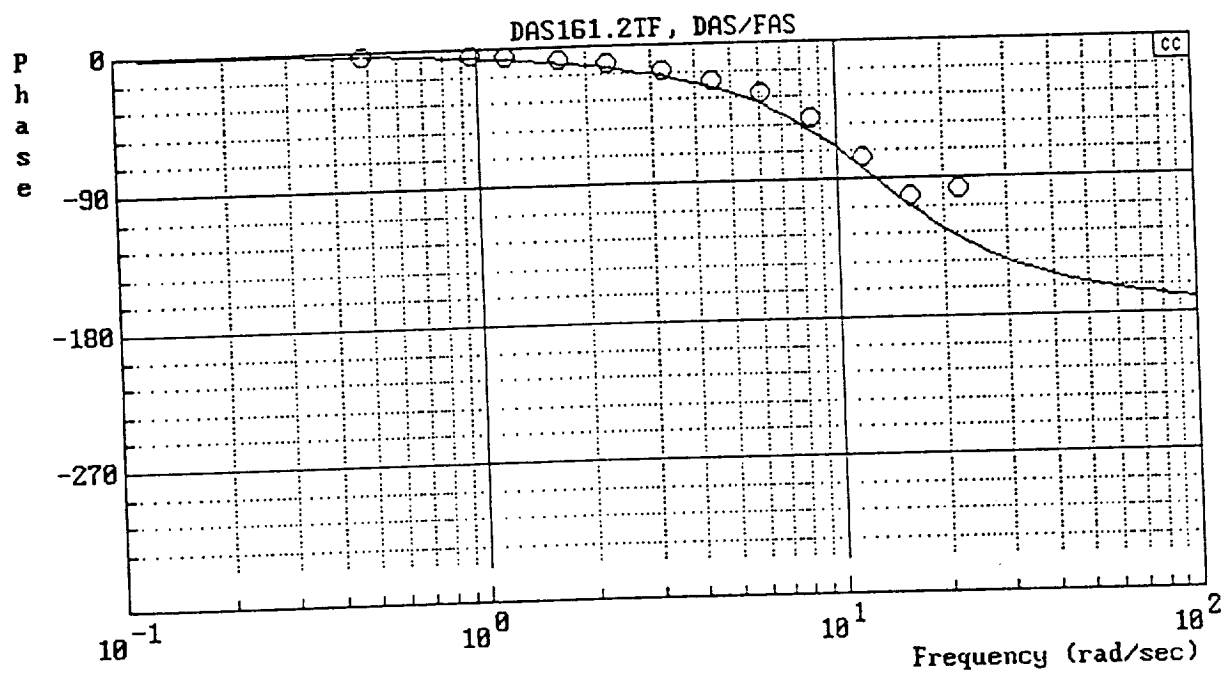$$Y_c = \frac{1099585[-.8660254, 138.2985]}{(6.66667)[.341524, 16.4573] (40)[.8660254, 138.2985]}$$
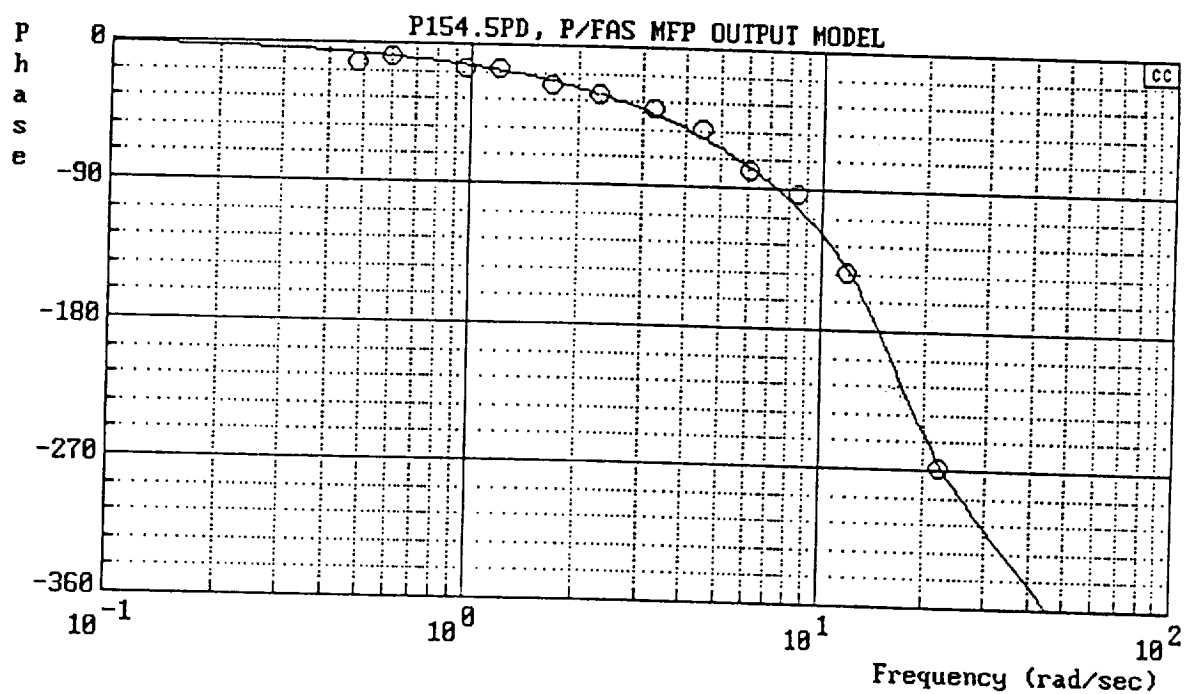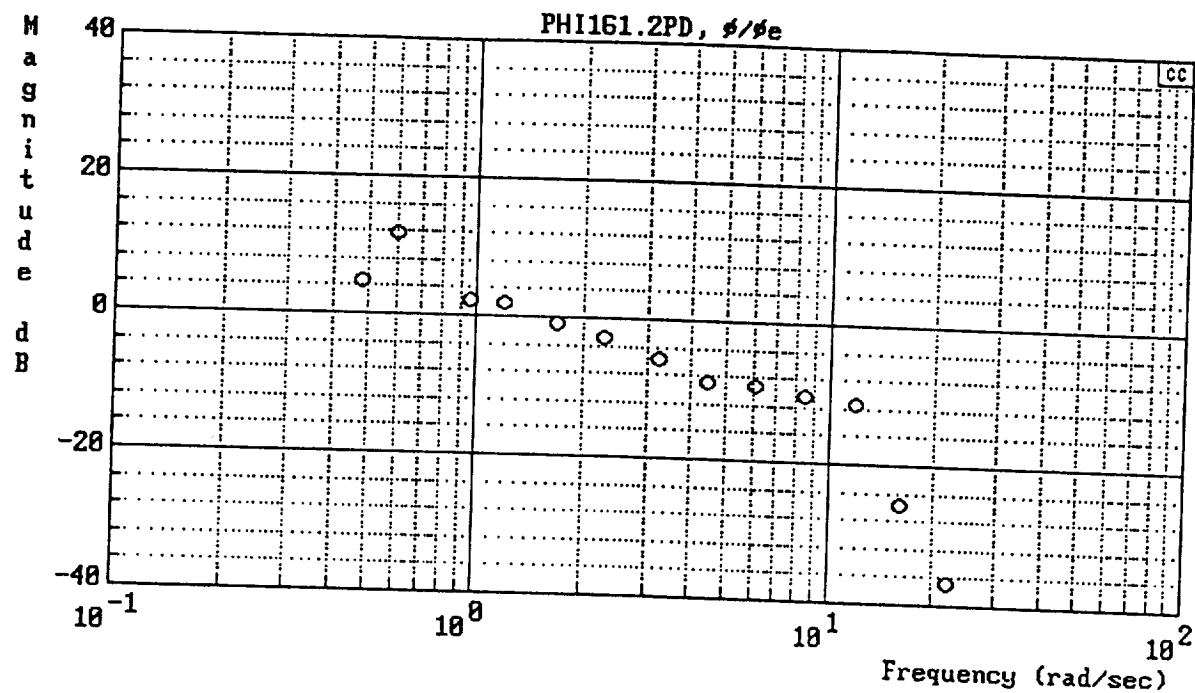

b) Y_c (P/FAS)

Figure B-10. (Continued)

$$Y_{FS} = \frac{16}{[\ .7,\ 8]}$$

c) Y_{FS} (DAS/FAS)

Figure B-10. (Continued)

119

PHI154.5, φ/φe

PHI154.5, φ/φe
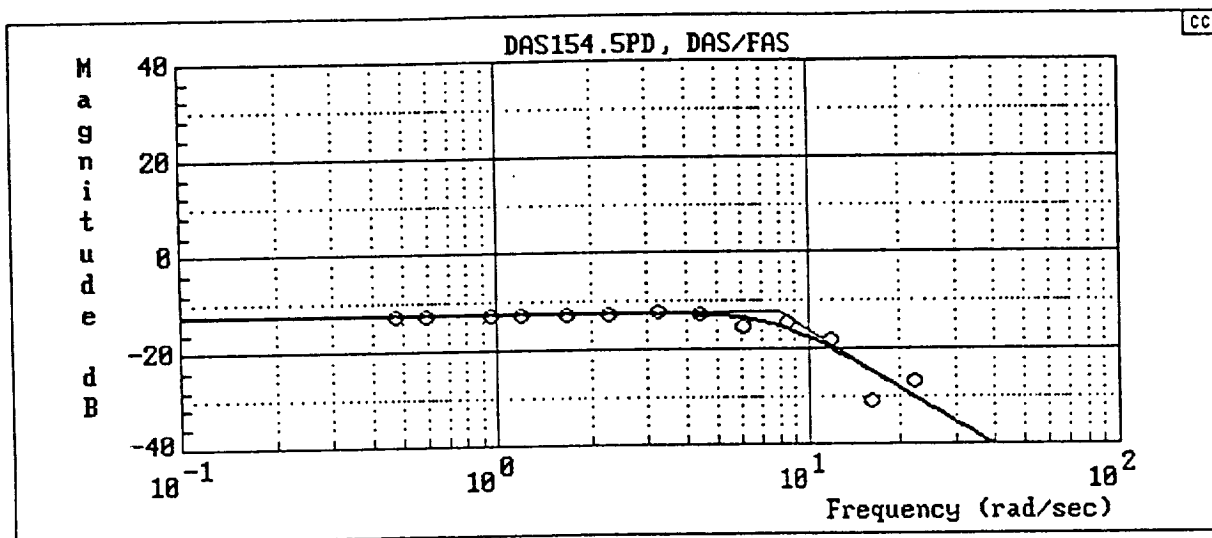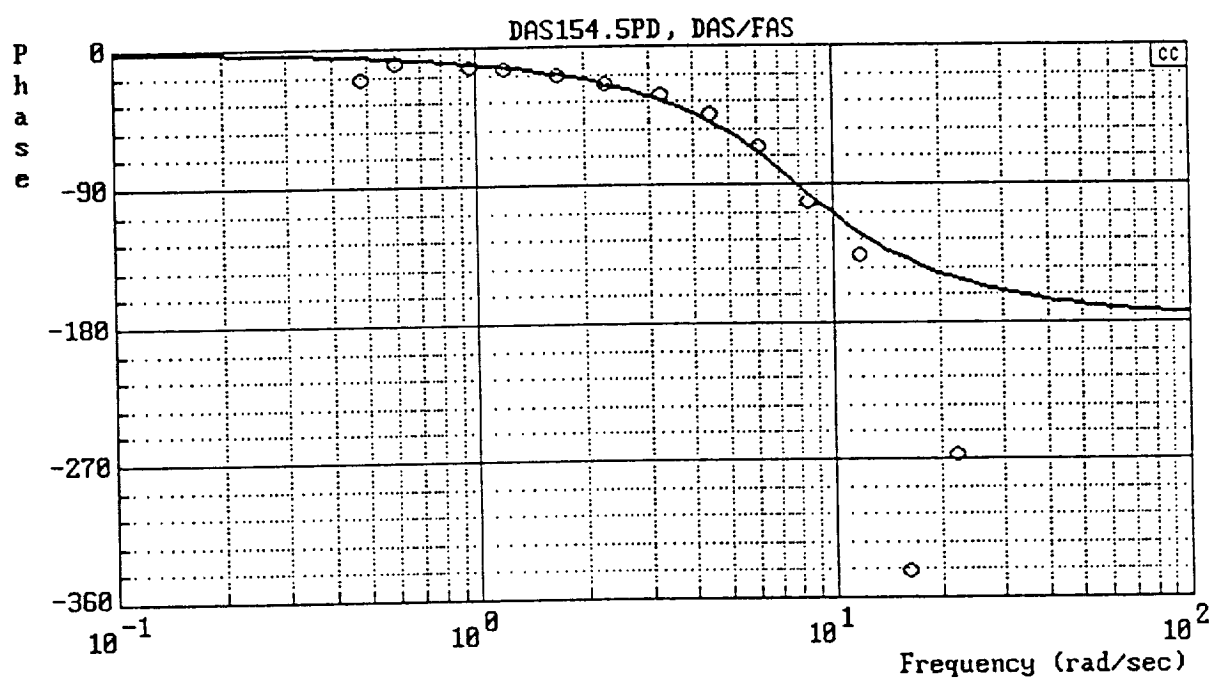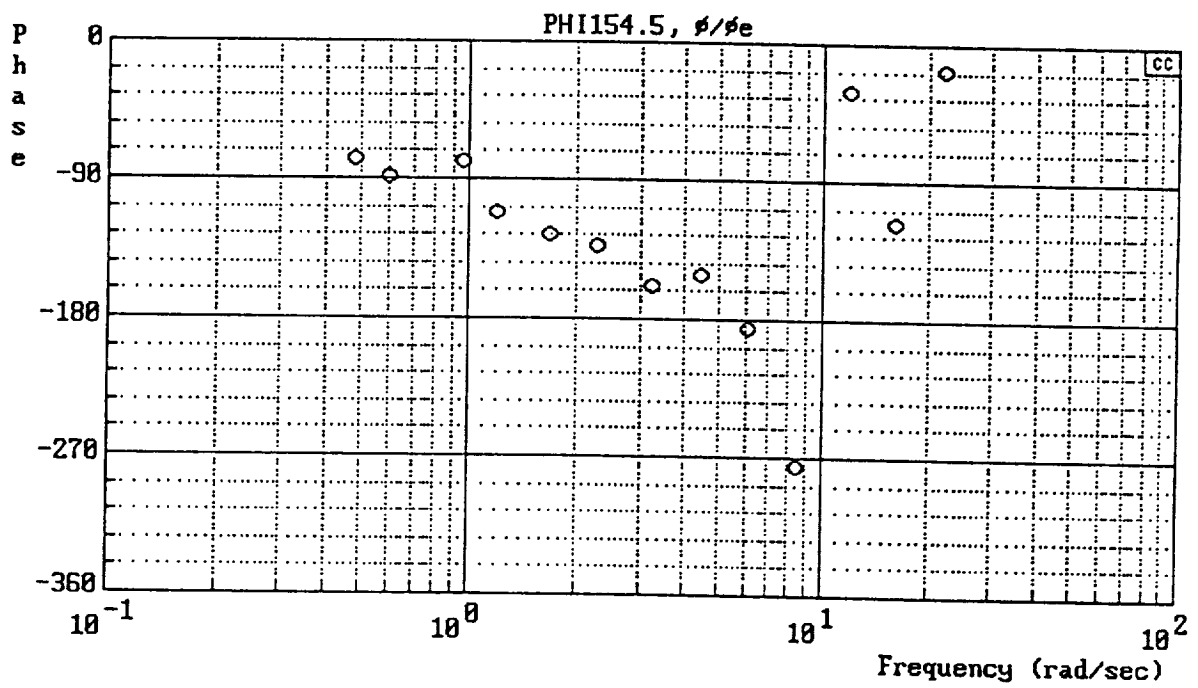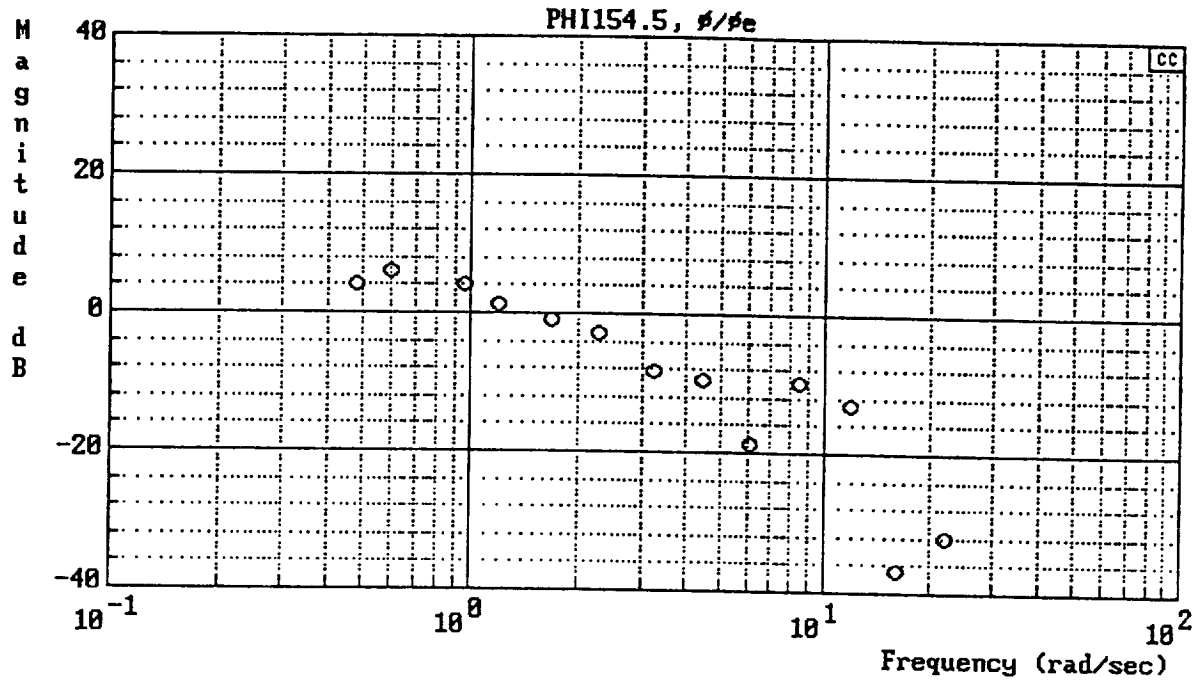
d) $Y_p Y_c$ (PHI/PHIE)

Figure B-10. (Concluded)

120

4156SOS.1

4156SOS.1
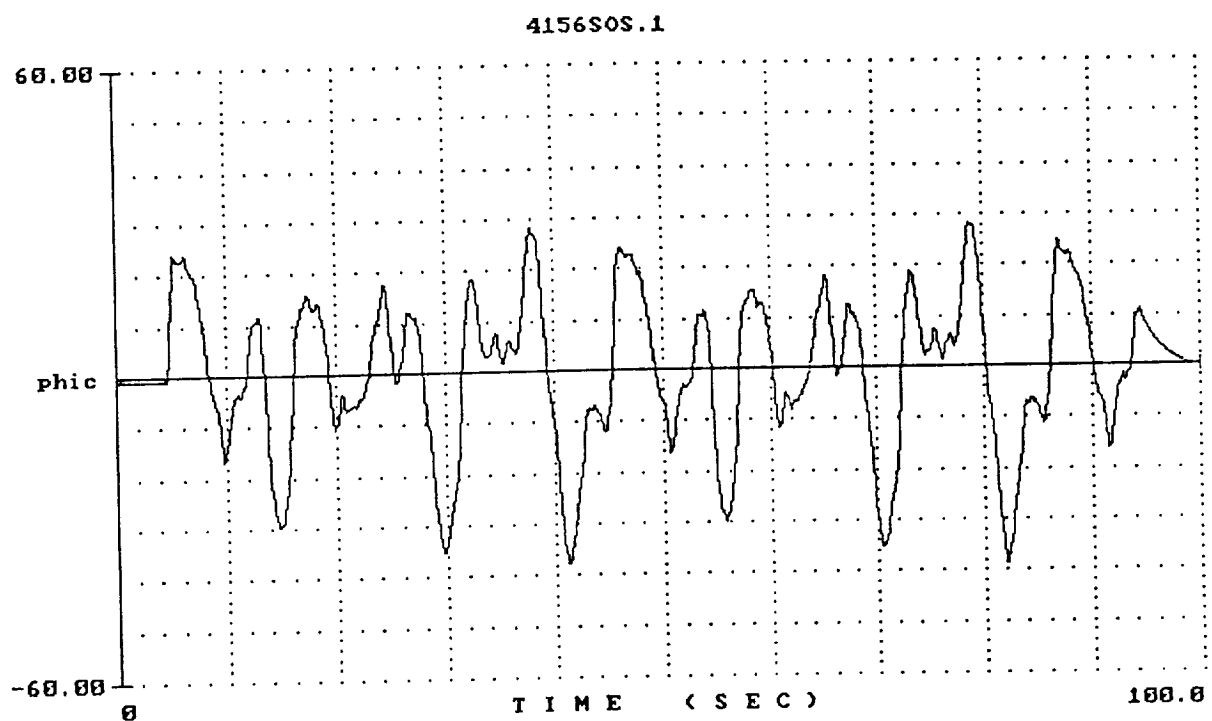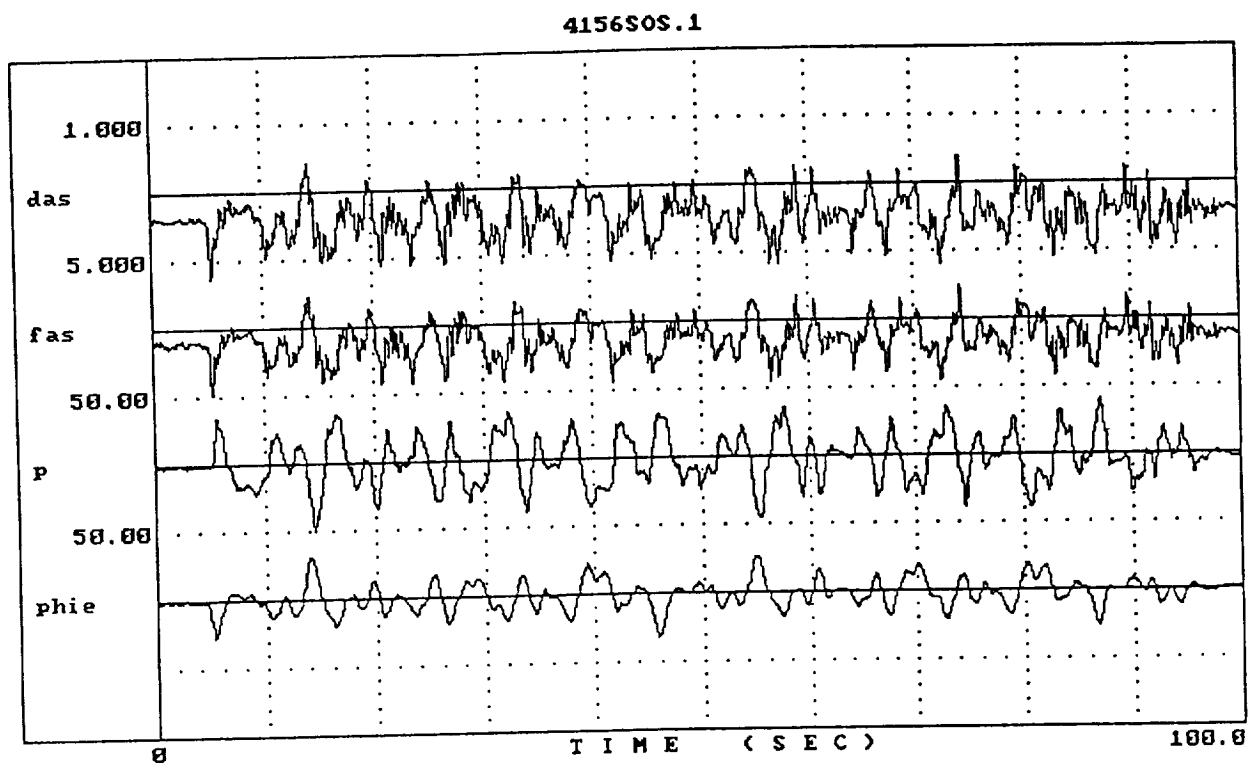
a) Time Histories

Figure B-11. Flight 4156-1

P156.1PD, P/DAS (w/ added time delay)
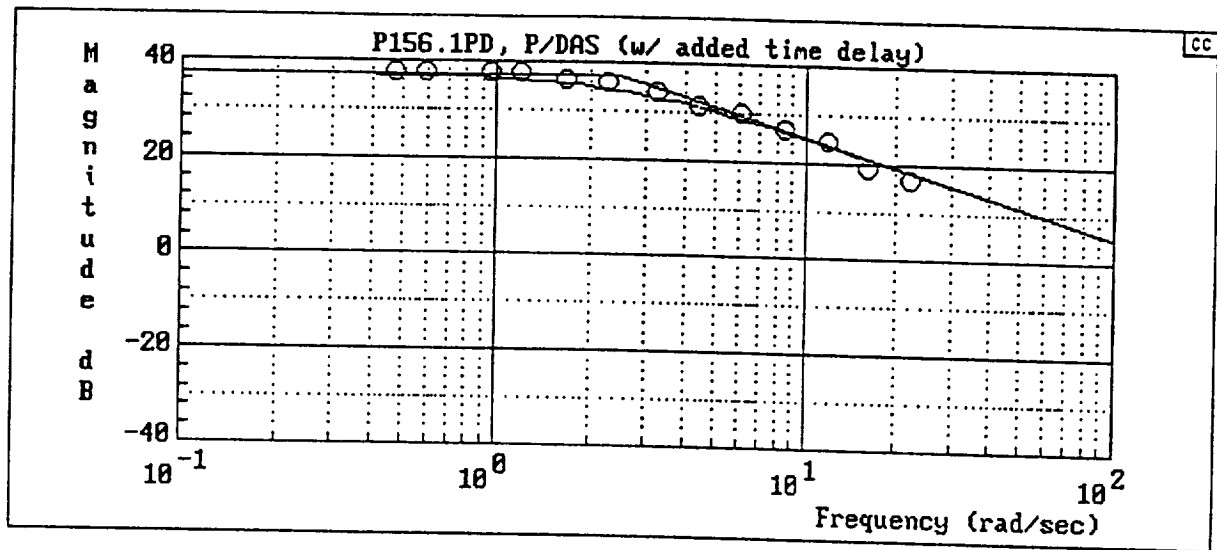
$$Y_c = \frac{180[-.8660254, 43.30127]}{(2.5)[.8660254, 43.30127]}$$

P156.1PD, P/DAS (w/ added time delay)

b) Y_c (P/DAS)

Figure B-11. (Continued)

DAS156.1PD, DAS/FAS

$$Y_{FS} = \frac{169}{[\ .7,\ 26]}$$

DAS156.1PD, DAS/FAS
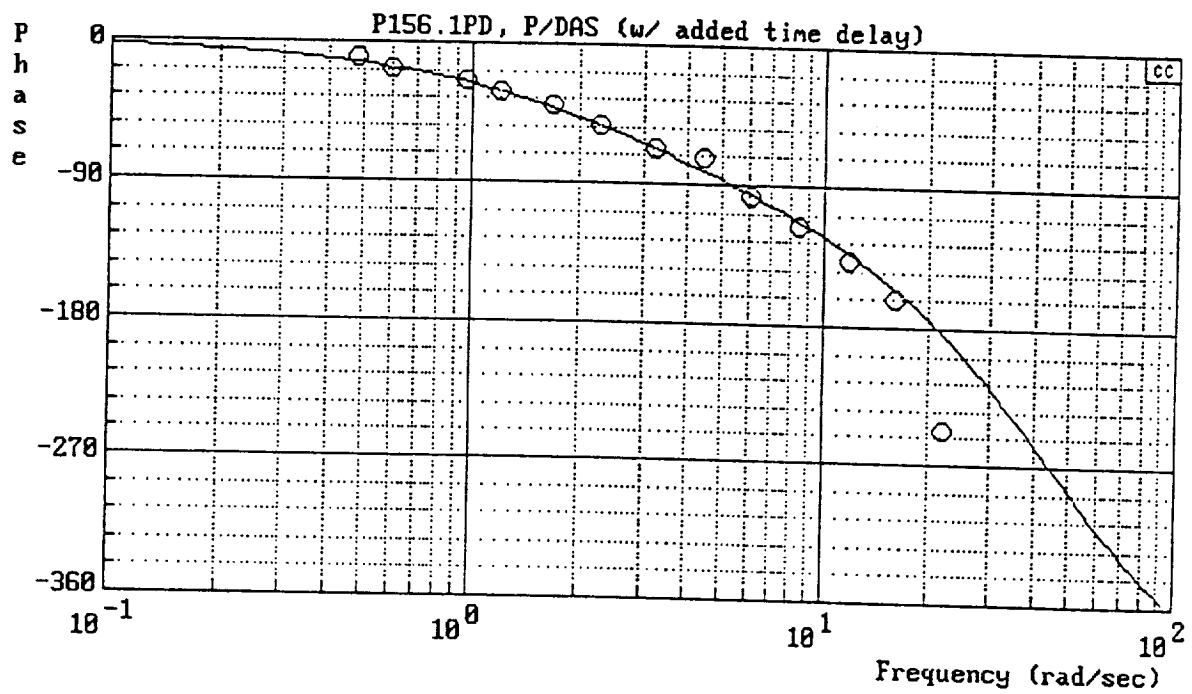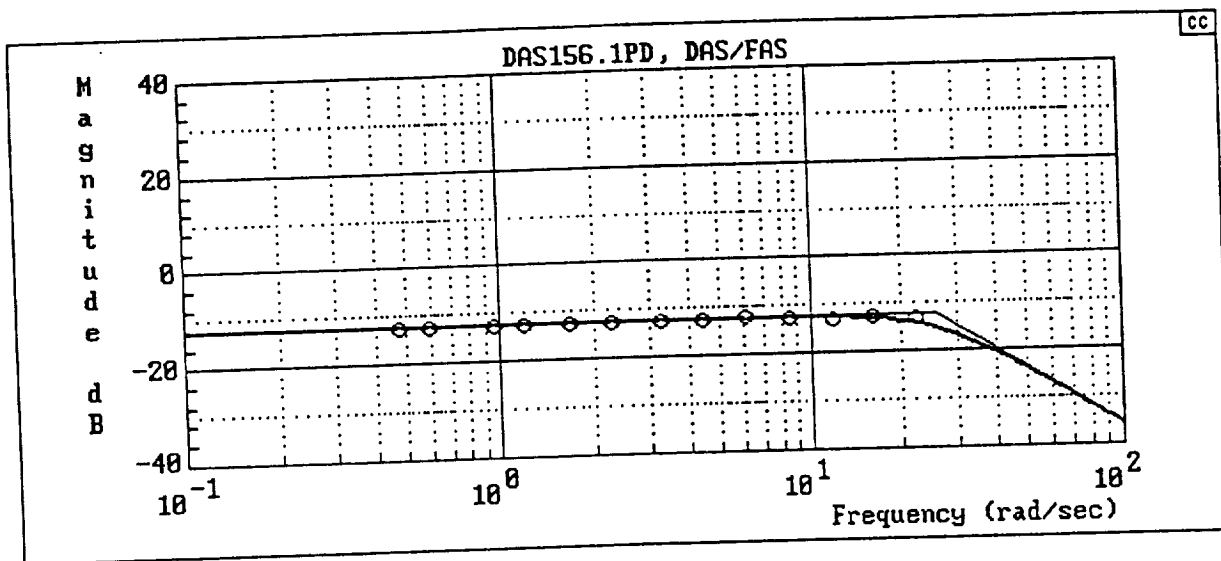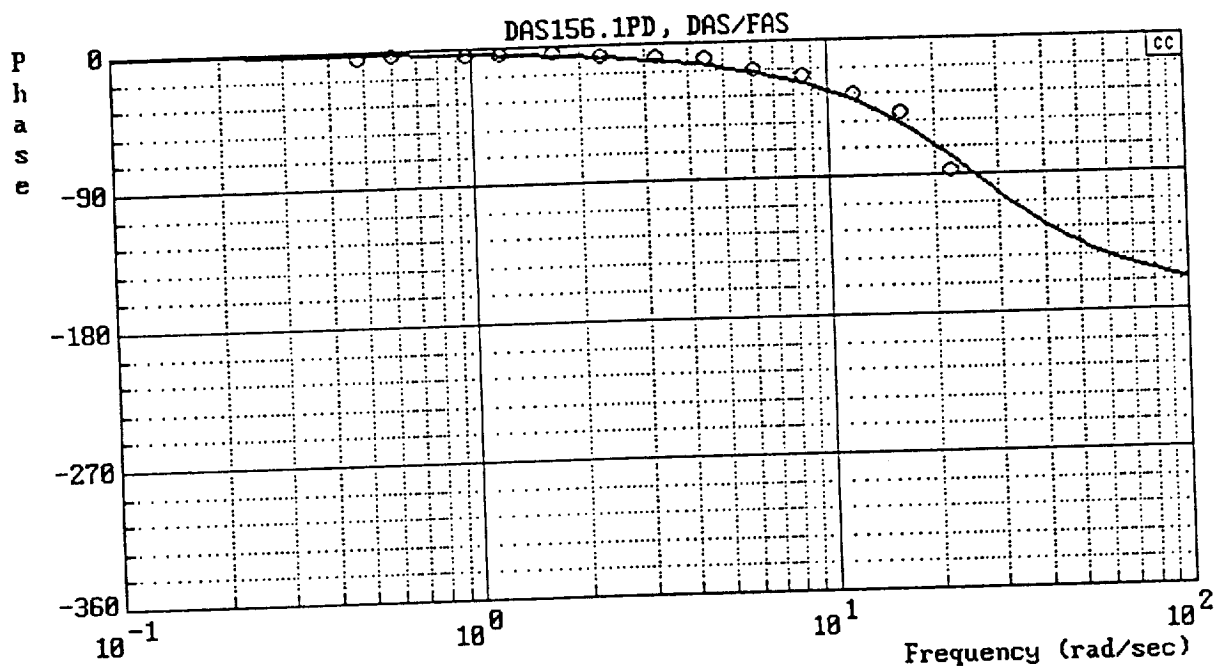
c) Y_{FS} (DAS/FAS)

Figure B-11. (Continued)

PHI156.1PD, ⌀/⌀e

PHI156.1PD, ⌀/⌀e
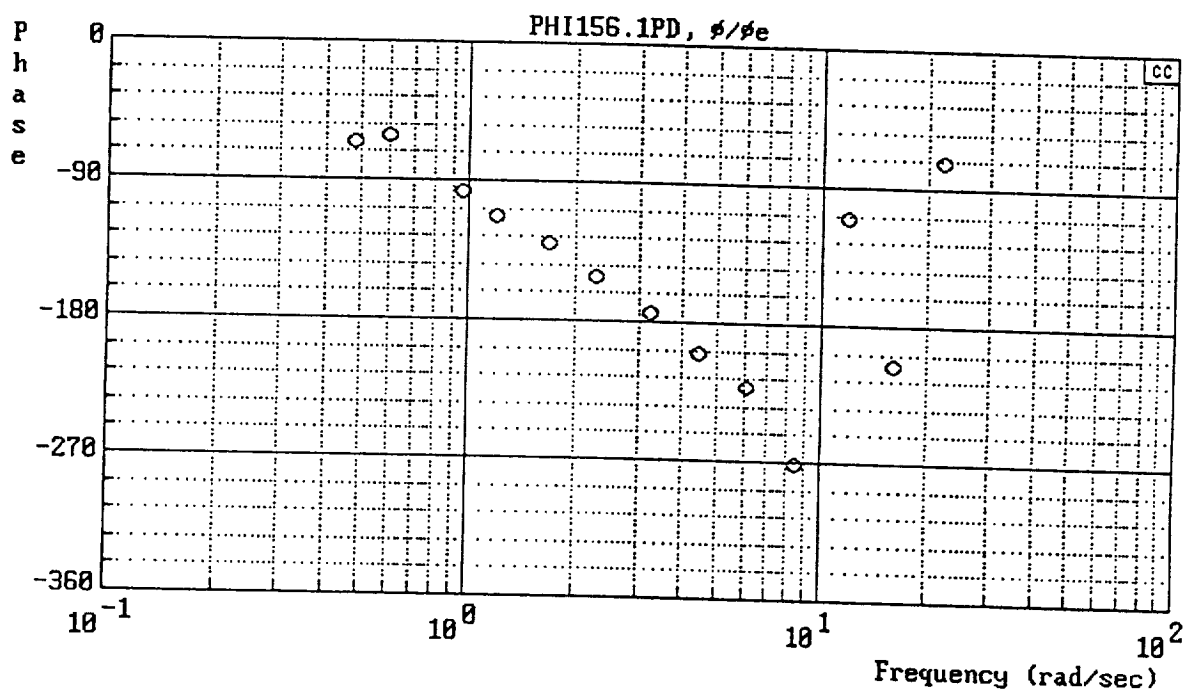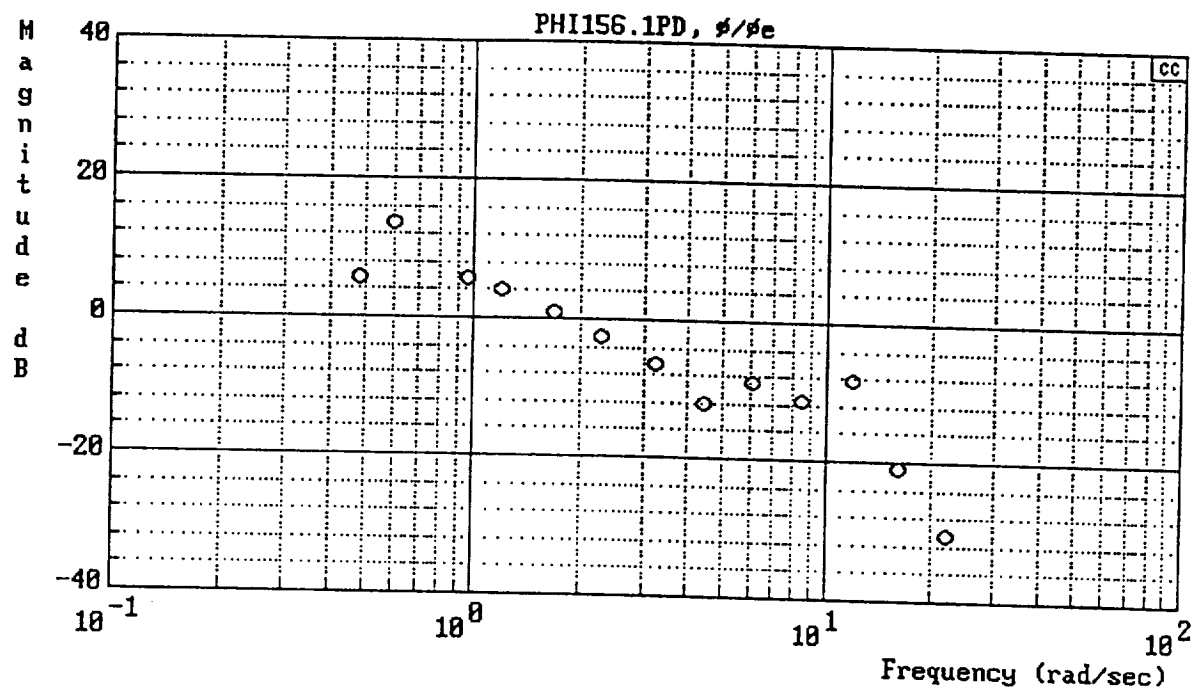
d) $Y_p Y_c$ (PHI/PHIE)

Figure B-11. (Concluded)

4156SOS.2
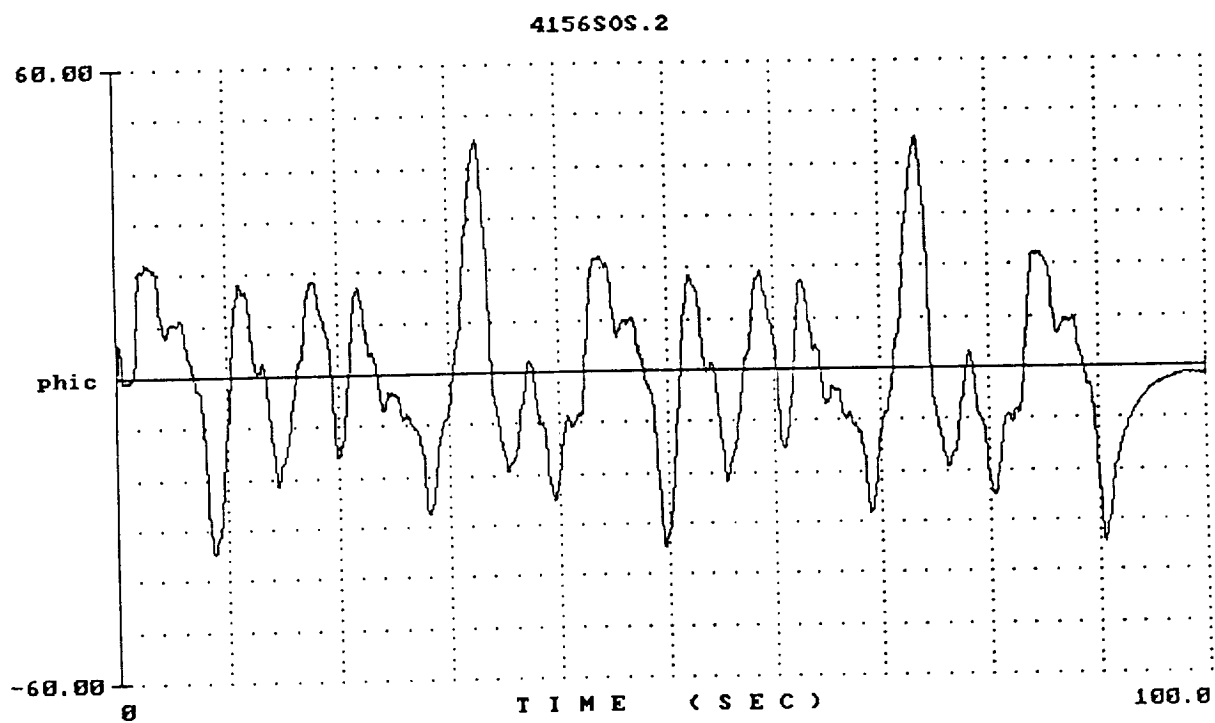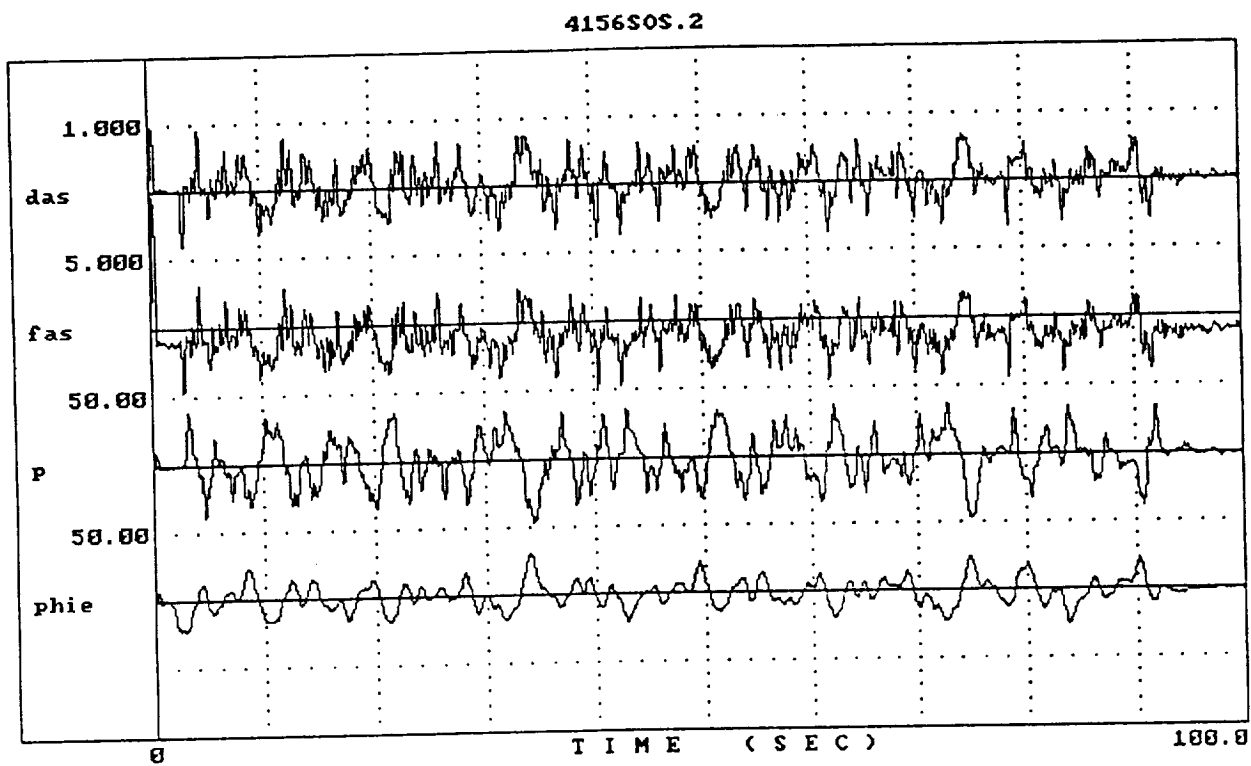
a) Time Histories

Figure B-12. Flight 4156-2

P156.2PD, P/DAS
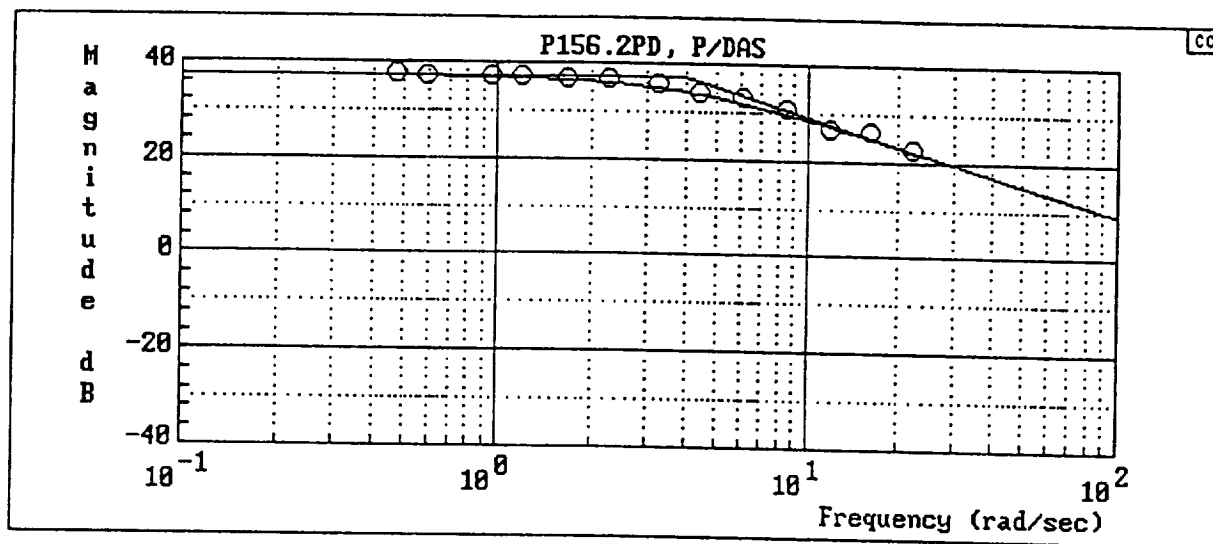
$$Y_c \ = \ \frac{288[-.8660254, \ 86.60254]}{(\ 4)[\ .8660254, \ 86.60254]}$$
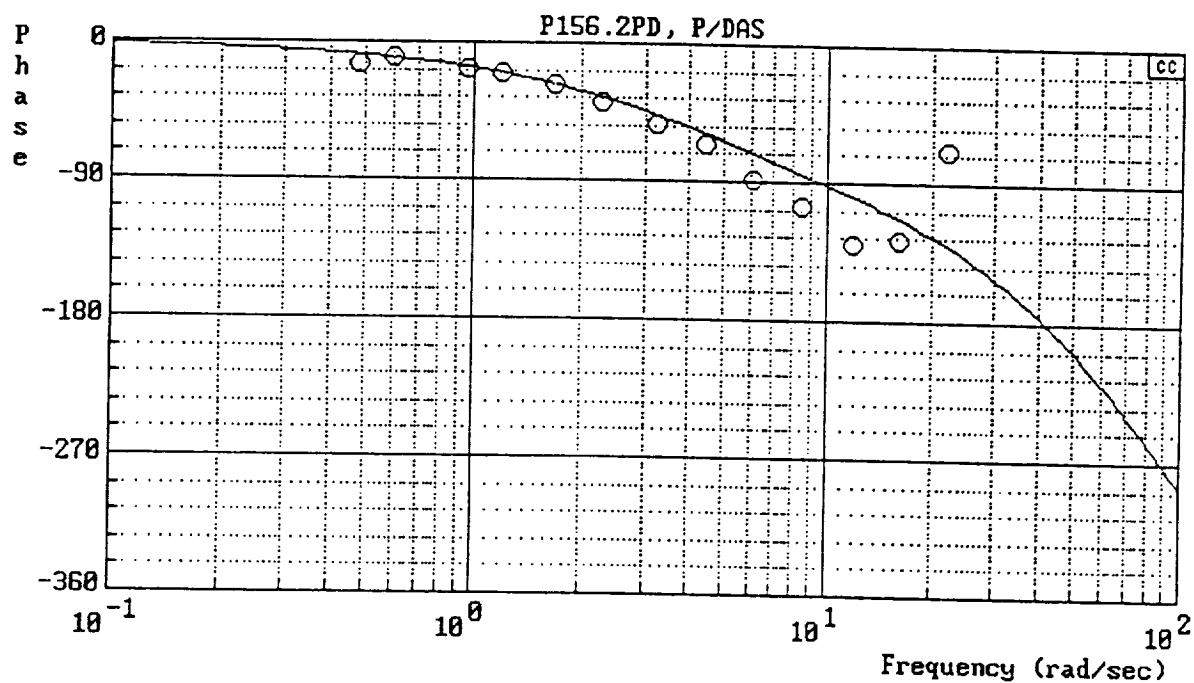
b) Y_c (P/DAS)

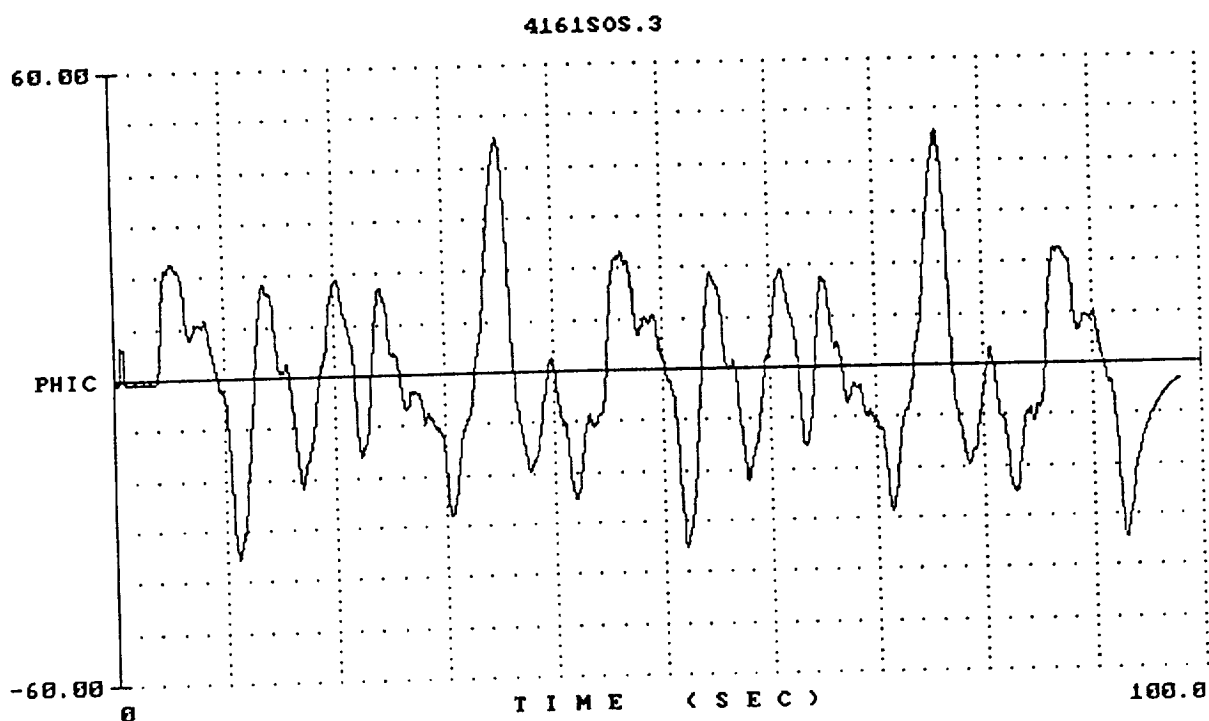Figure B-12. (Continued)
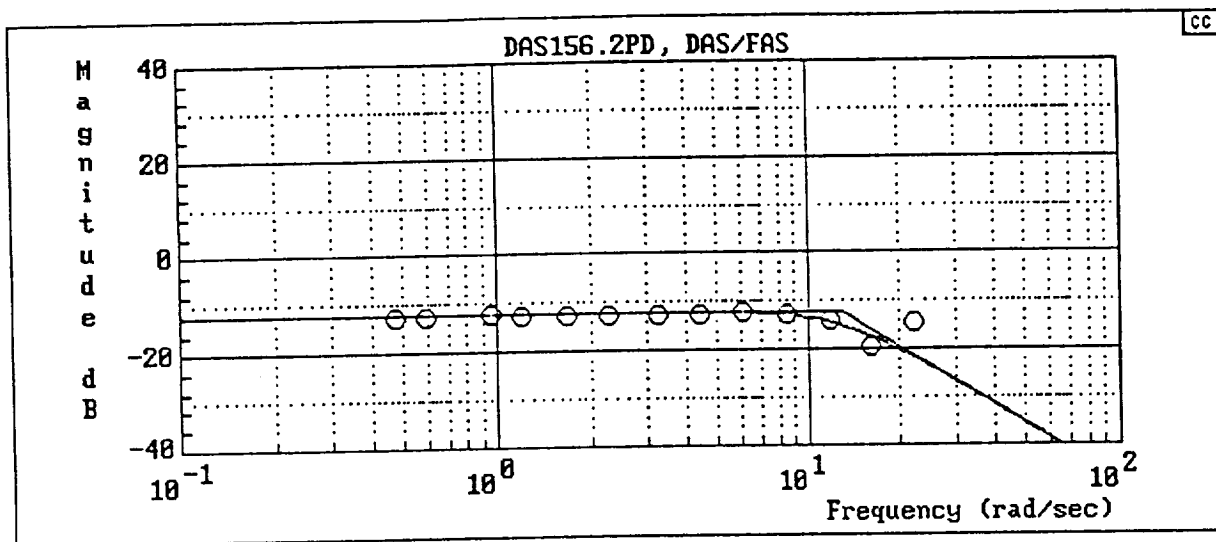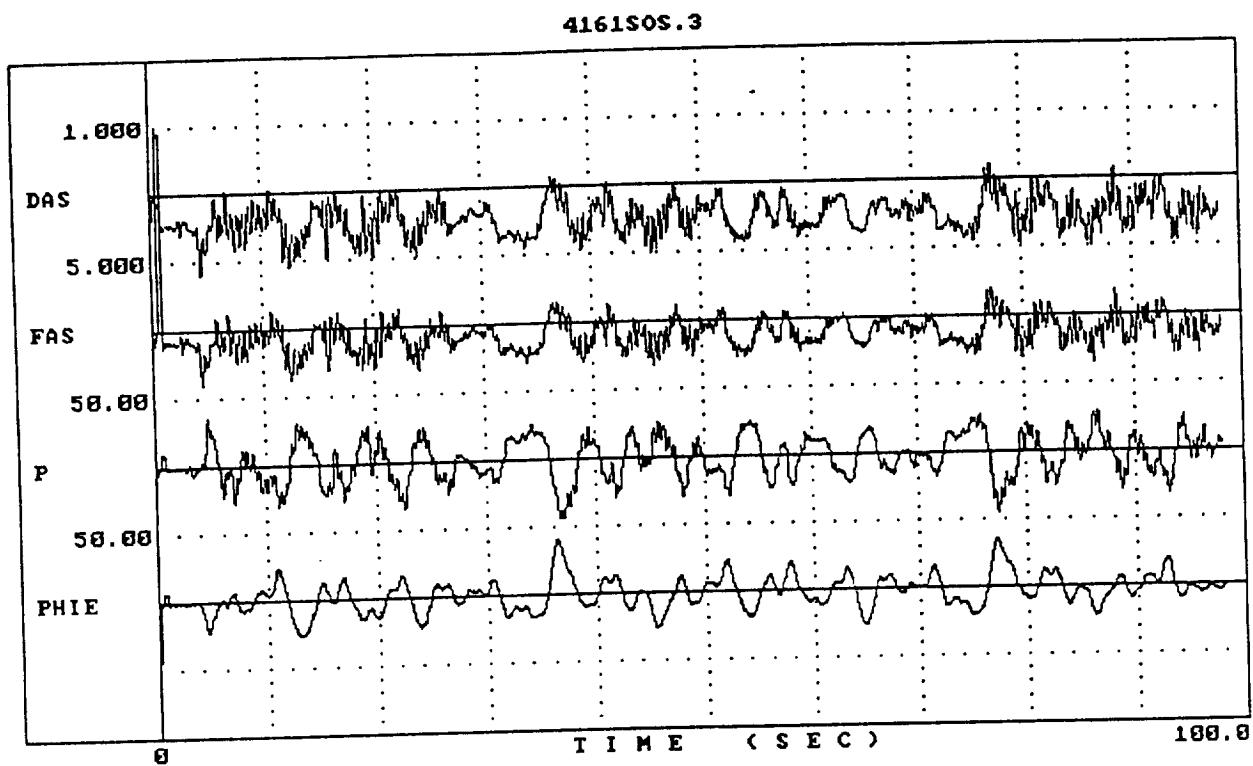
$$Y_{FS} = \frac{42.25}{[\ .7,\ 13]}$$
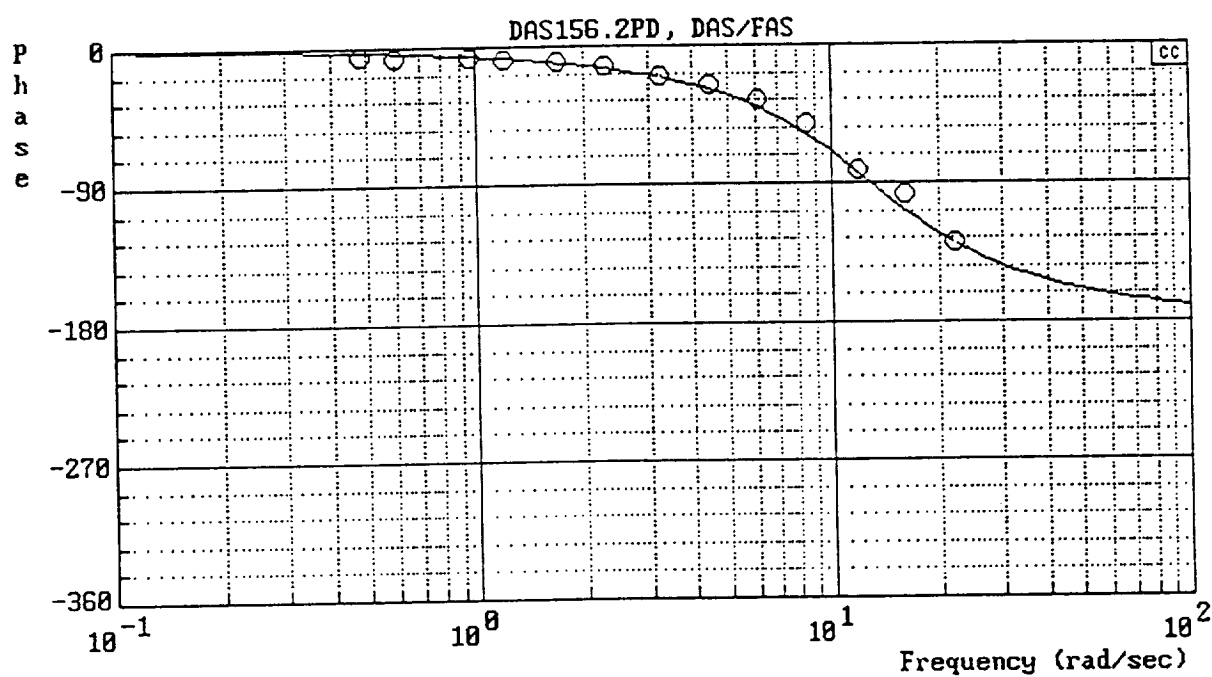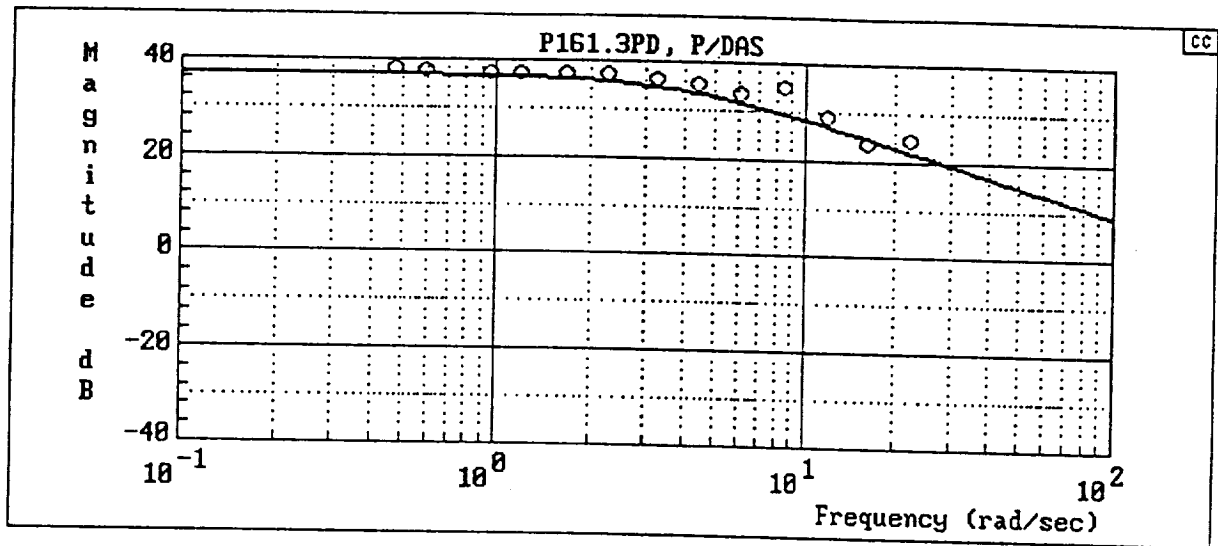

c) Y_{FS} (DAS/FAS)

Figure B-12. (Continued)
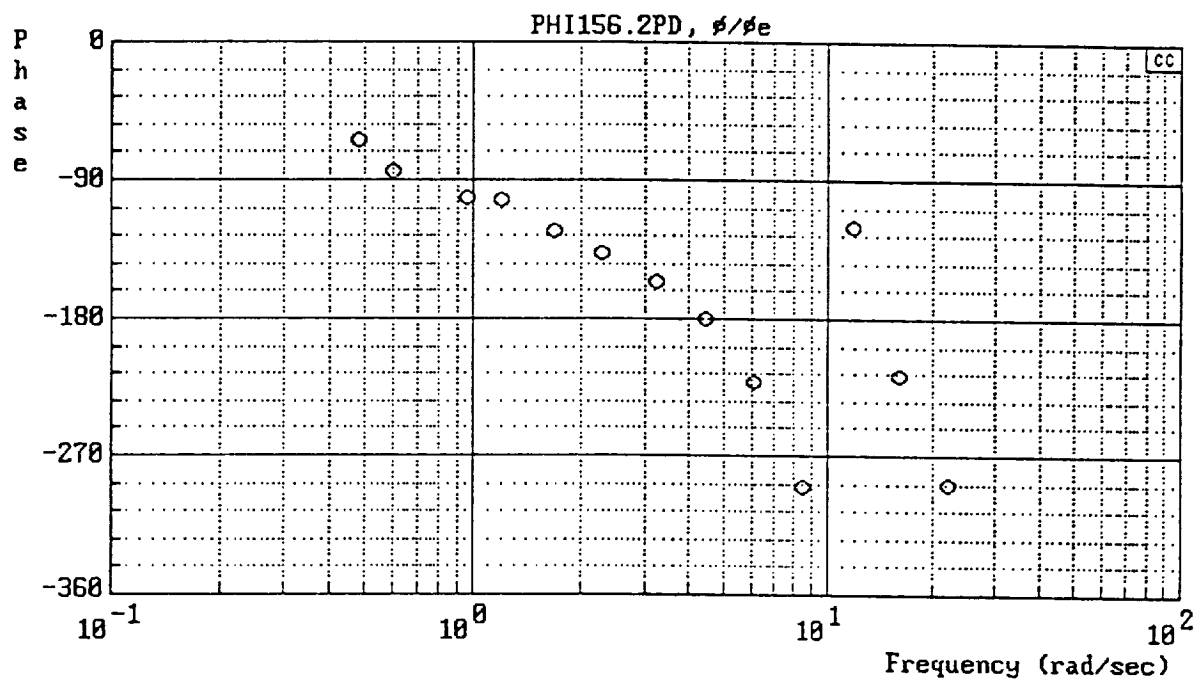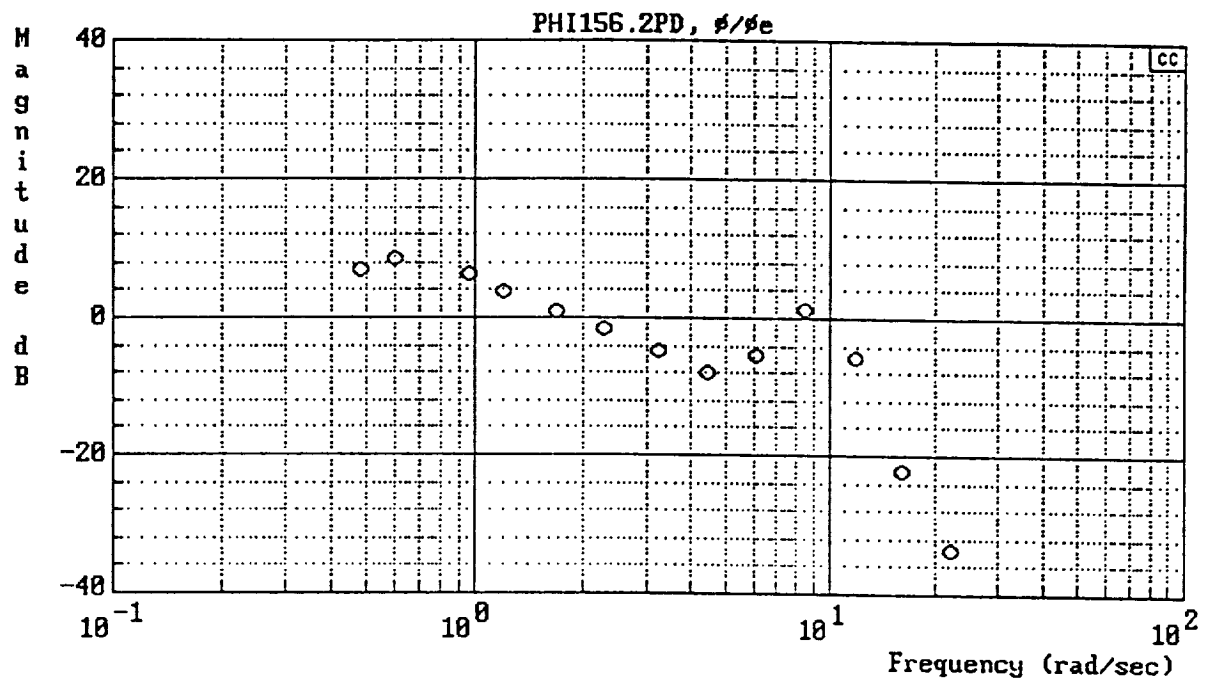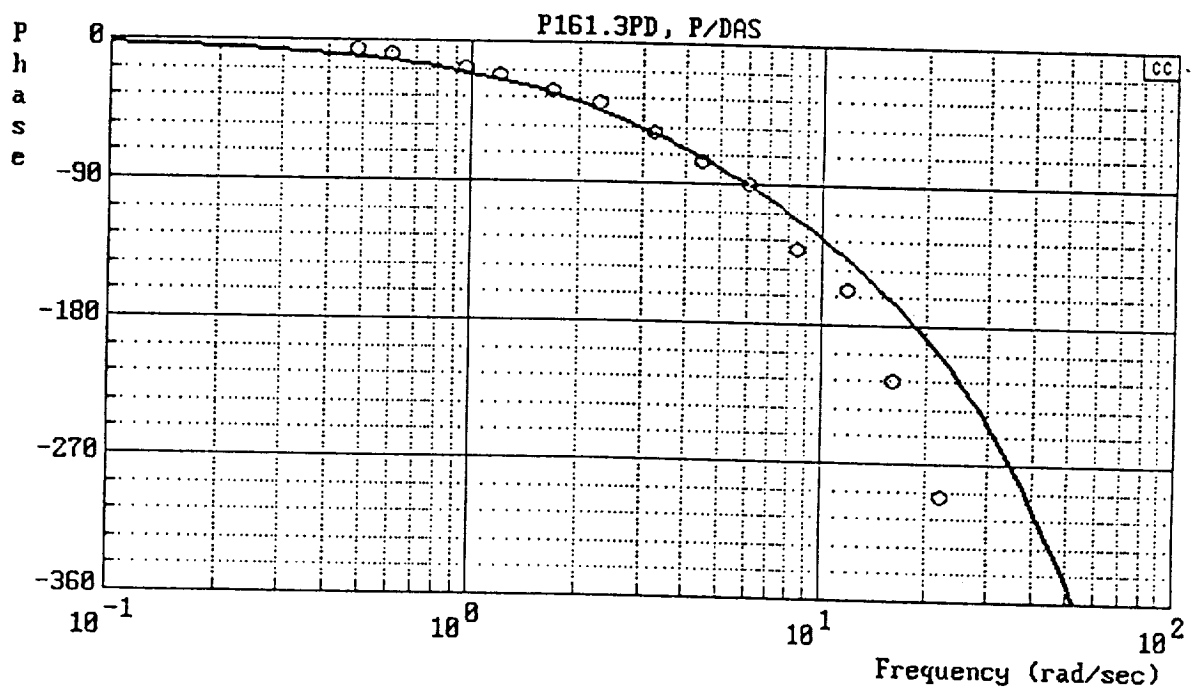
d) Y_pY_c (PHI/PHIE)

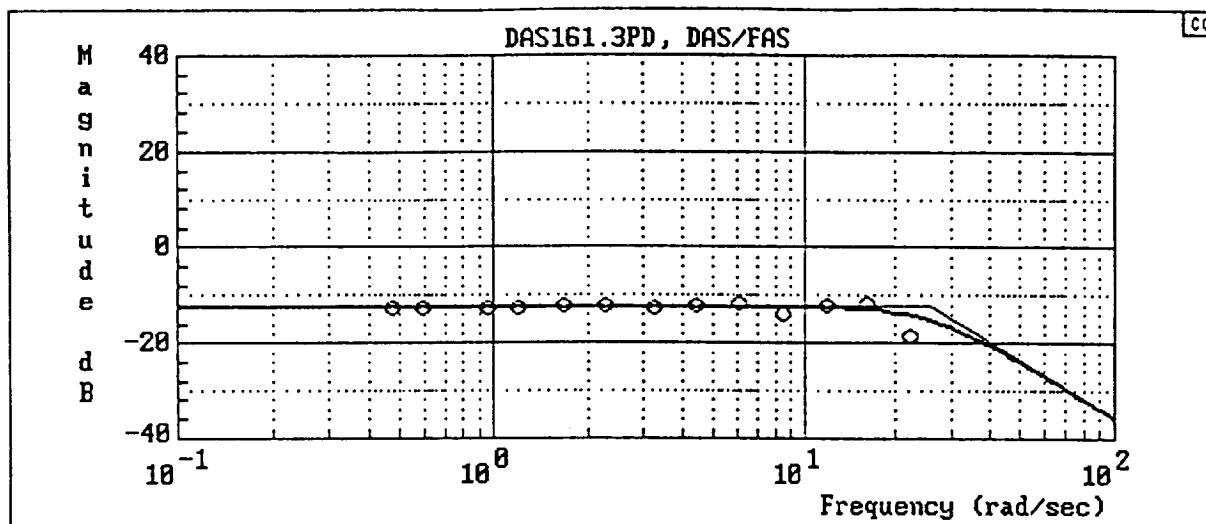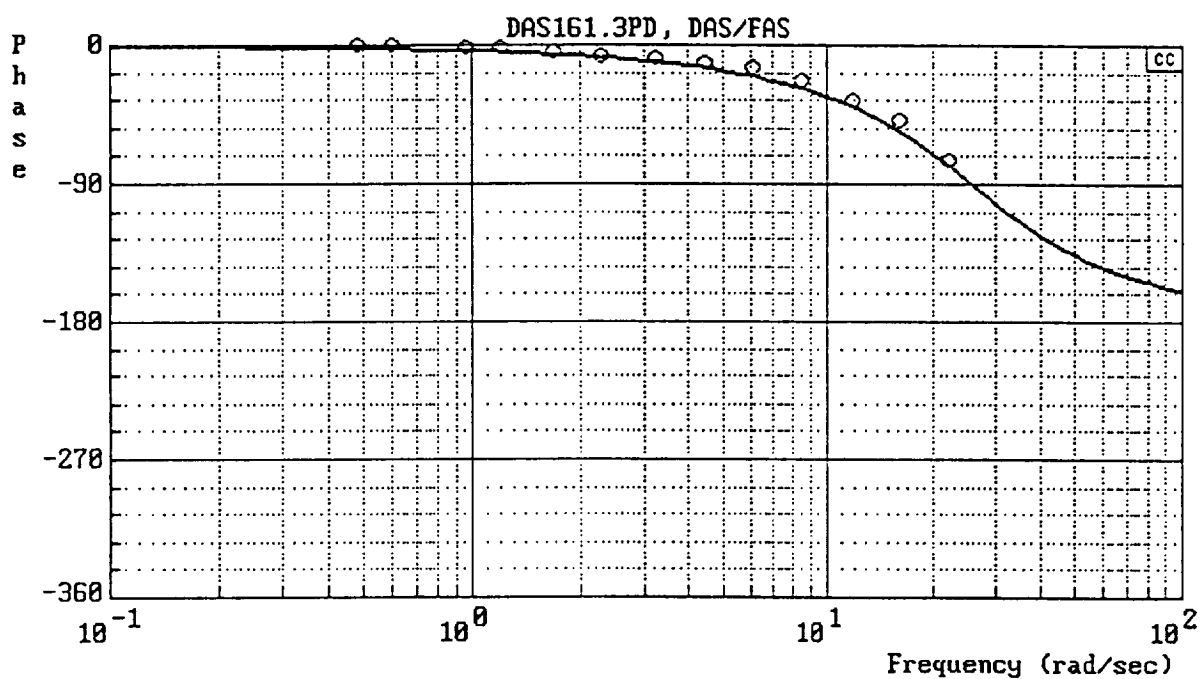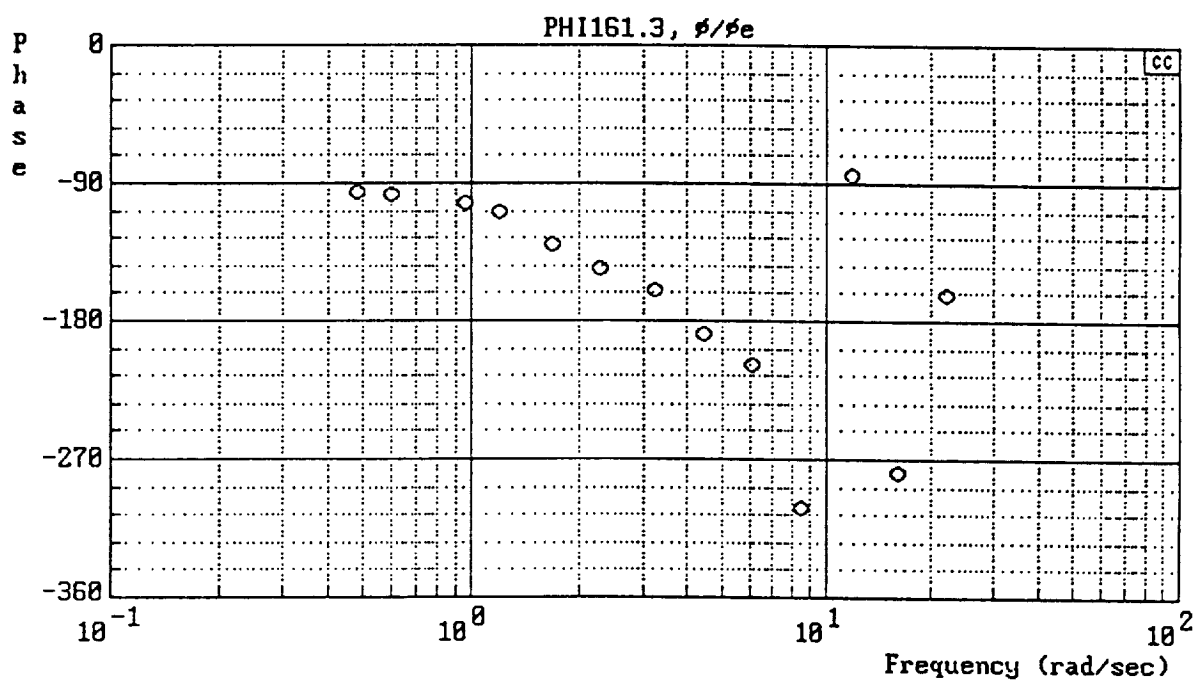Figure B-12. (Concluded)
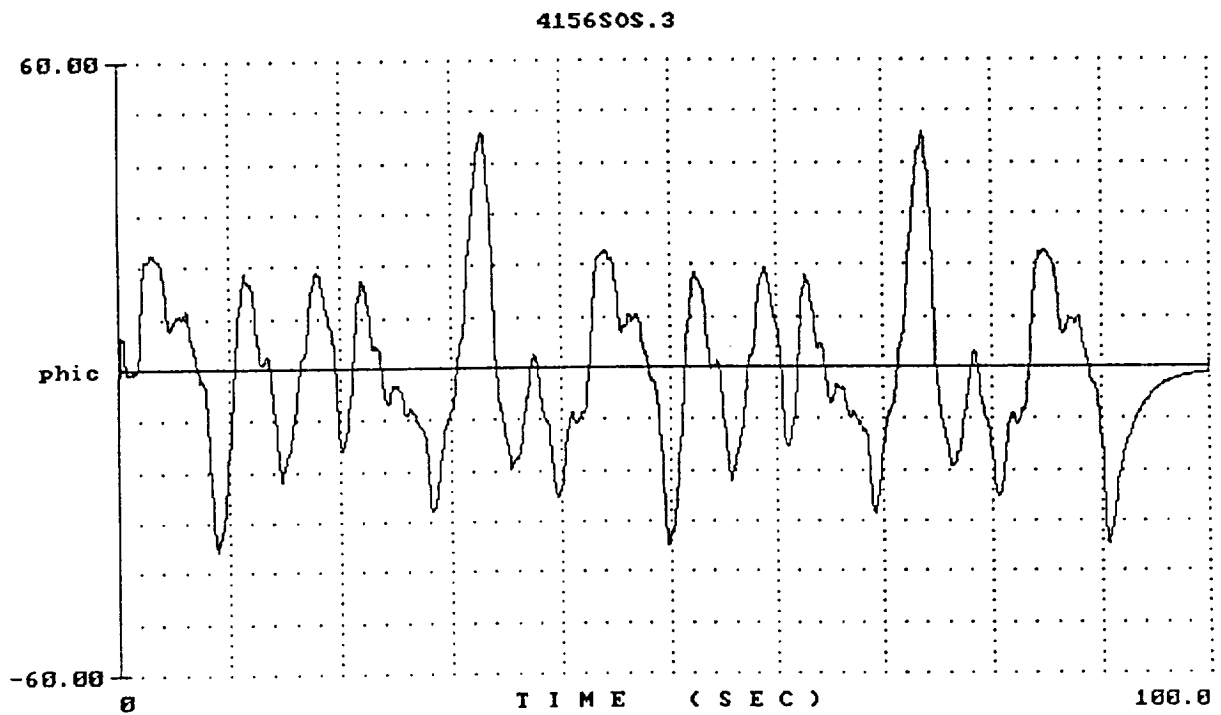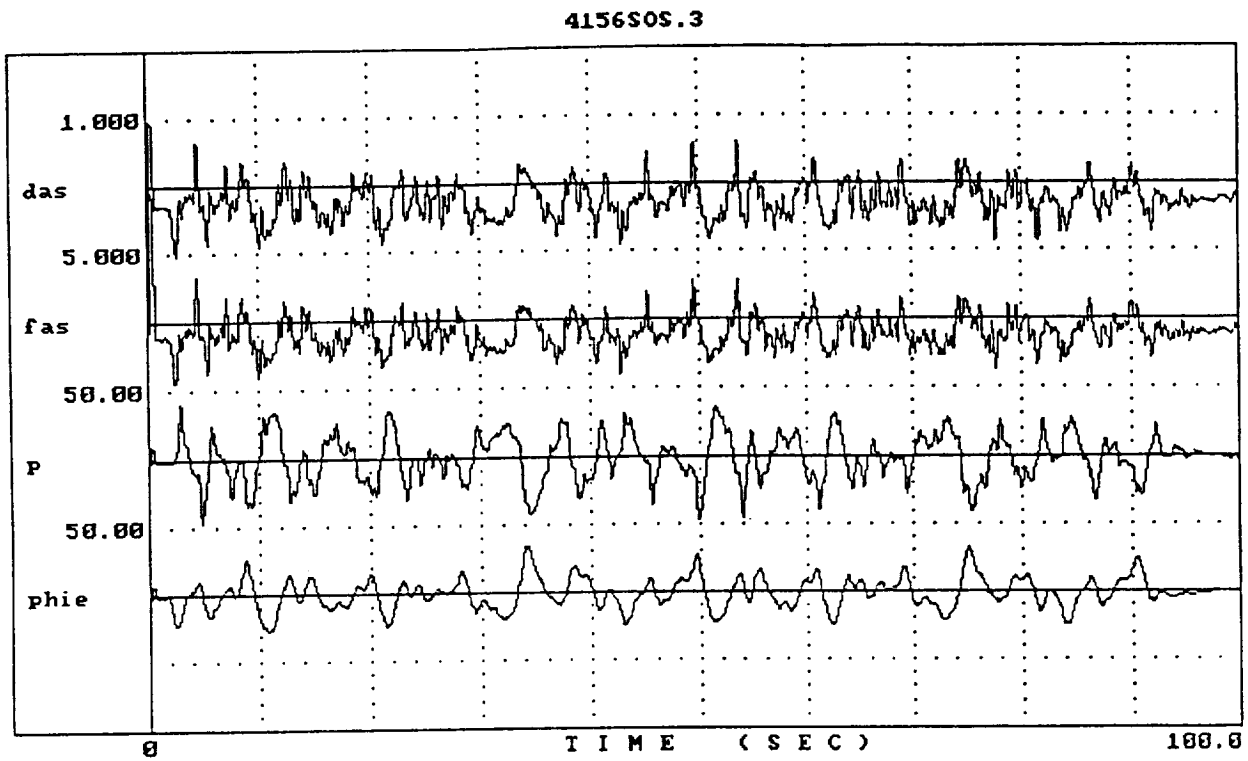
a) Time Histories

Figure B-13. Flight 4156-3
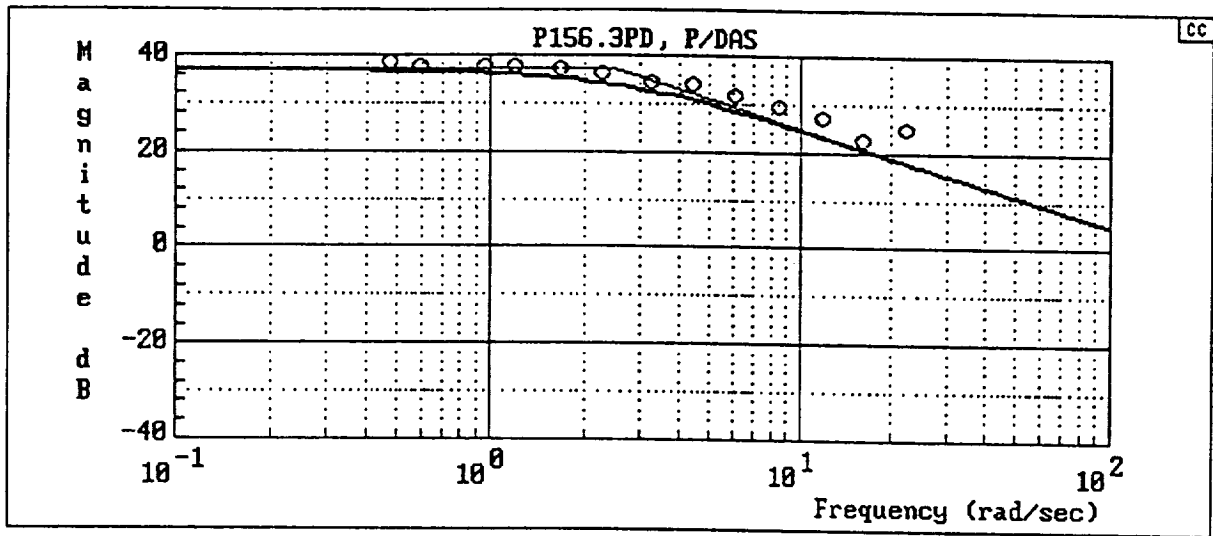
129

P156.3PD, P/DAS

$$Y_c = \frac{180[-.8660254, 62.98367] \; [-.8660254, 86.60254]}{(2.5)[.8660254, 62.98367] \; [.8660254, 86.60254]}$$

P156.3PD, P/DAS

b) Y_c (P/DAS)

Figure B-13. (Continued)

DAS156.3TF, DAS/FAS

$$Y_{FS} = \frac{42.25}{[\ .7,\ 13]}$$

DAS156.3TF, DAS/FAS
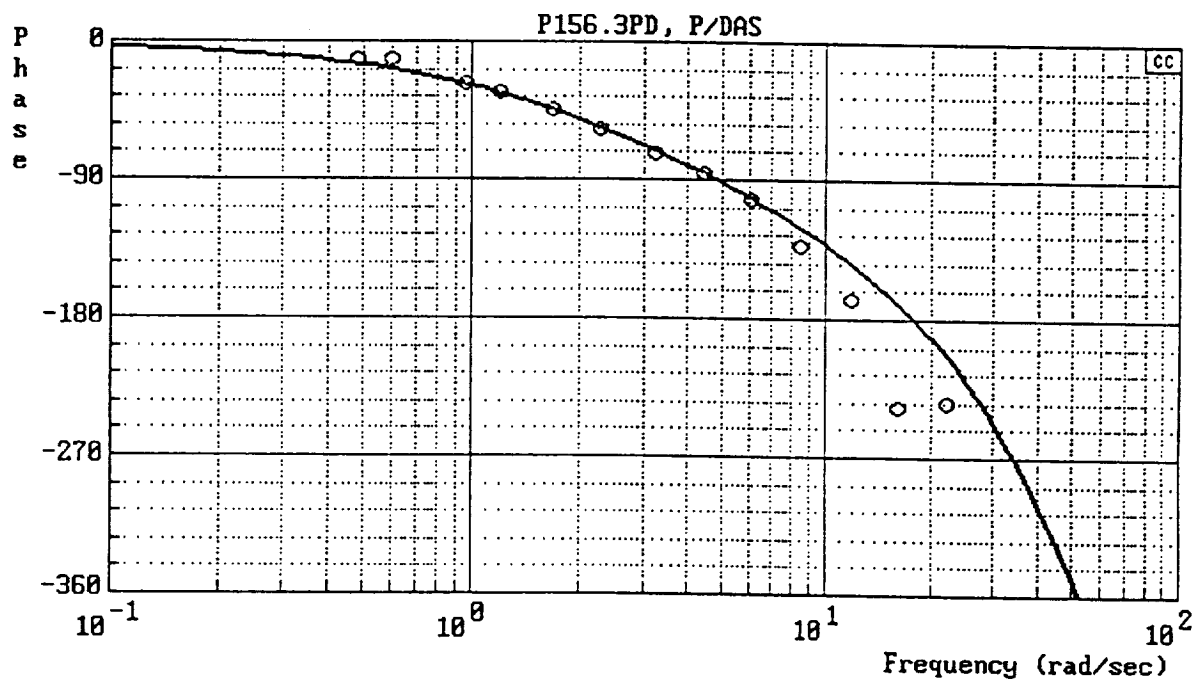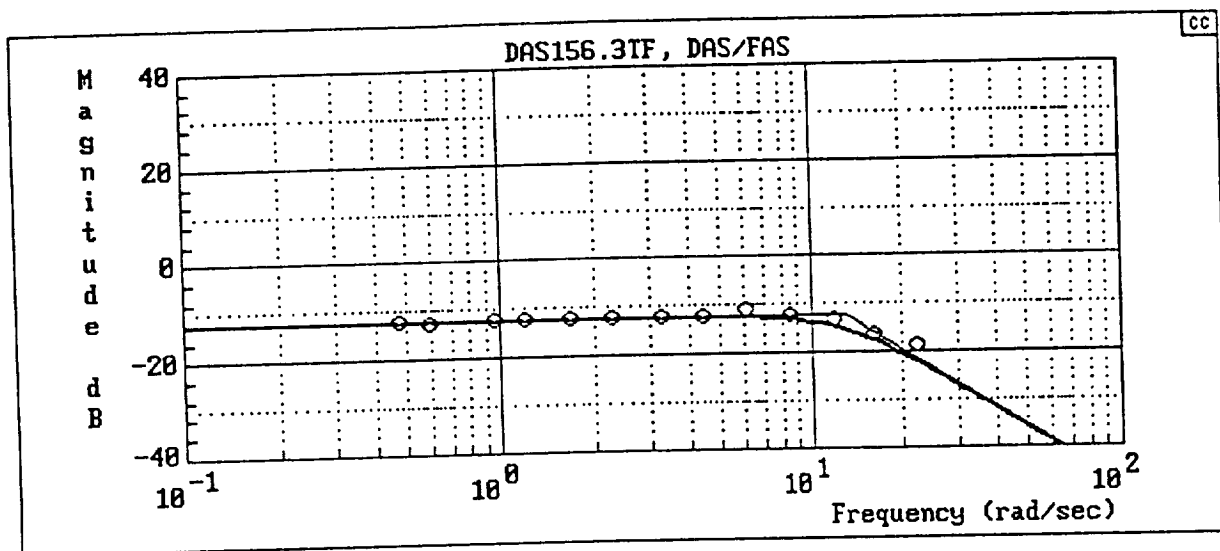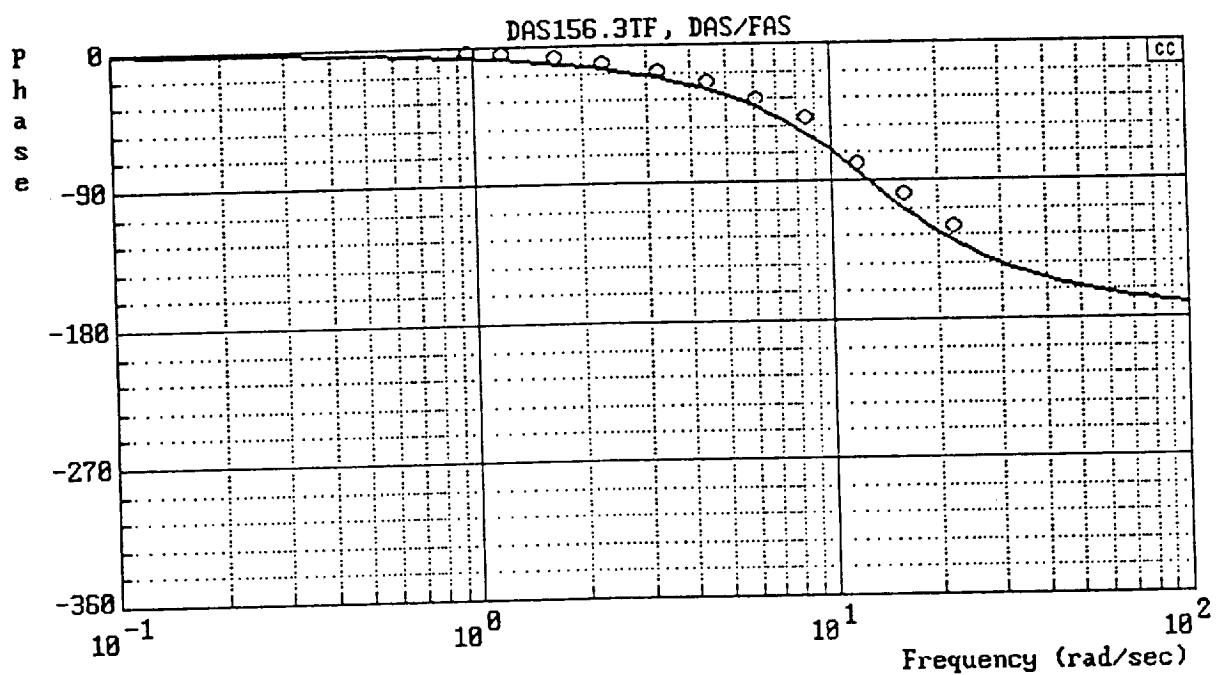
c) Y_{FS} (DAS/FAS)

Figure B-13. (Continued)

131

PHI156.3PD, φ/φe

PHI156.3PD, φ/φe
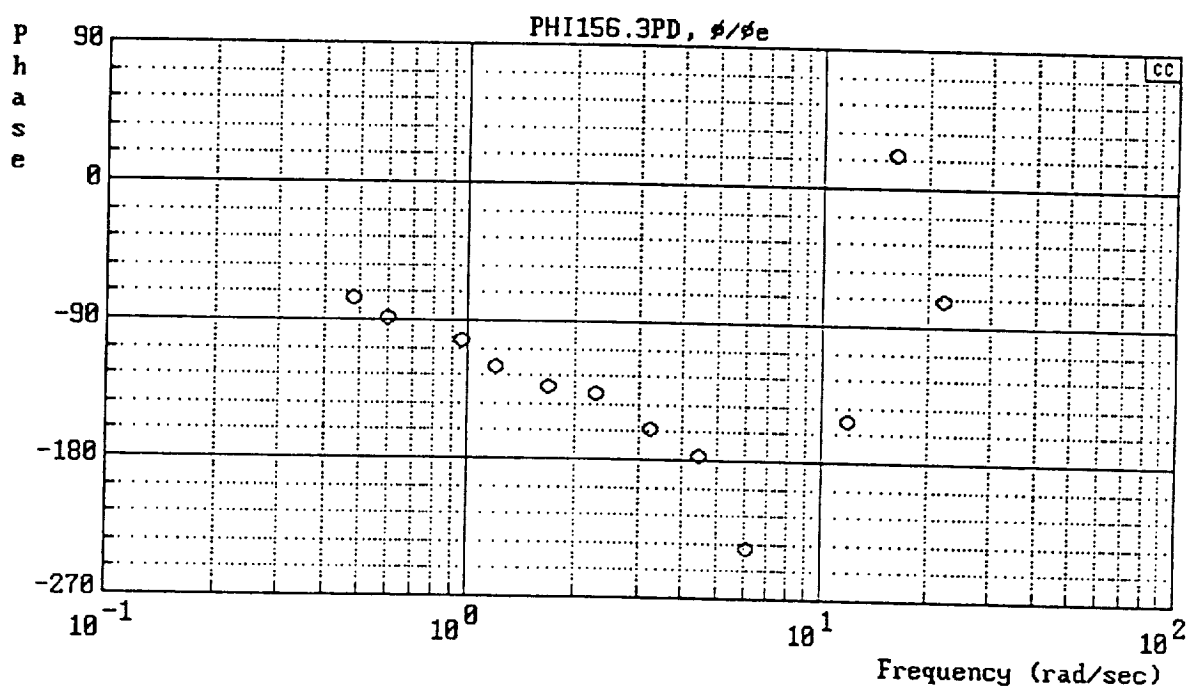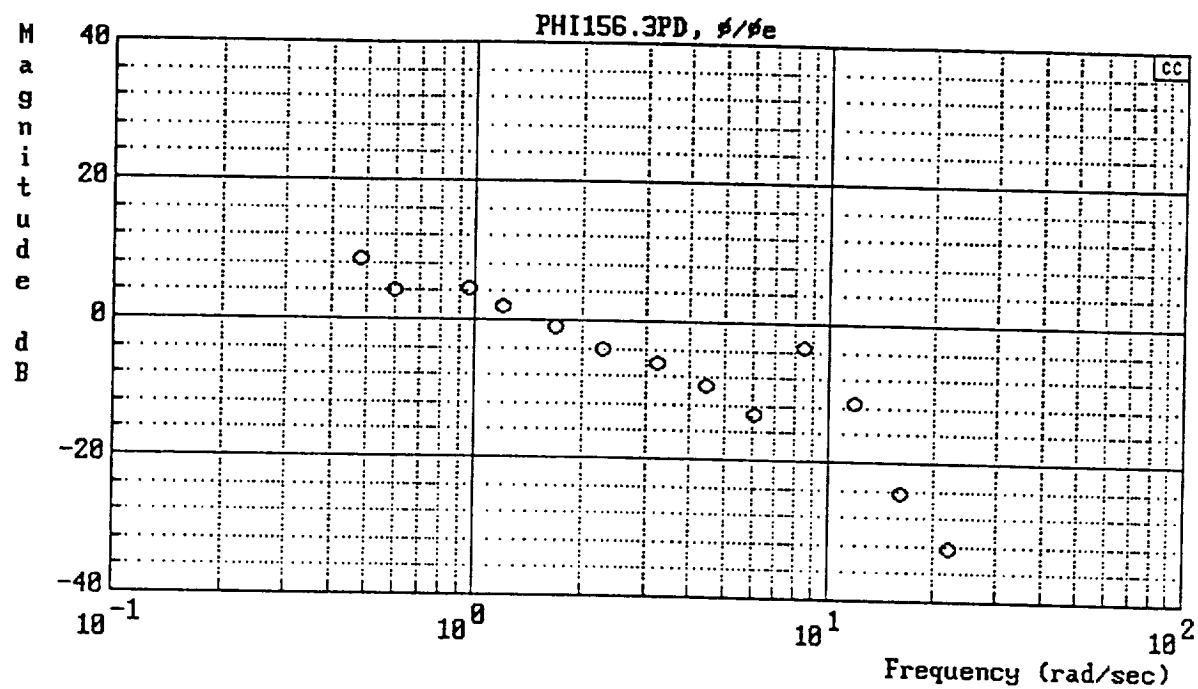
d) $Y_p Y_c$

Figure B-13. (Concluded)

4156SOS.4
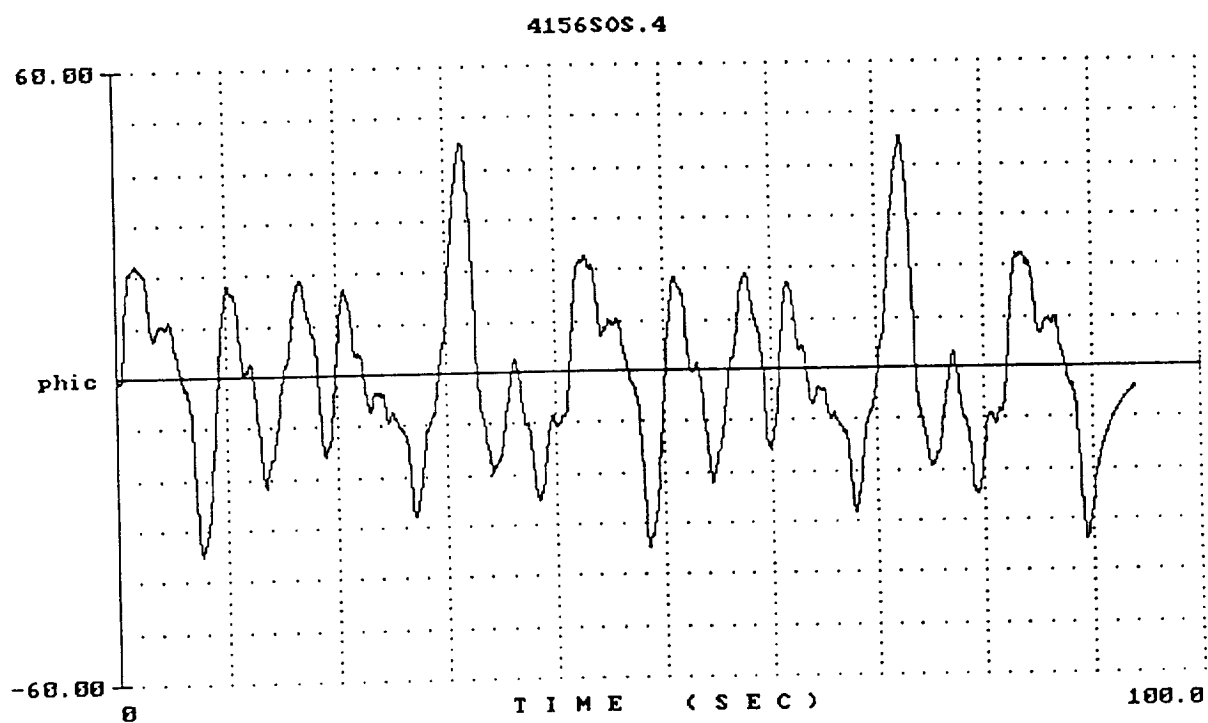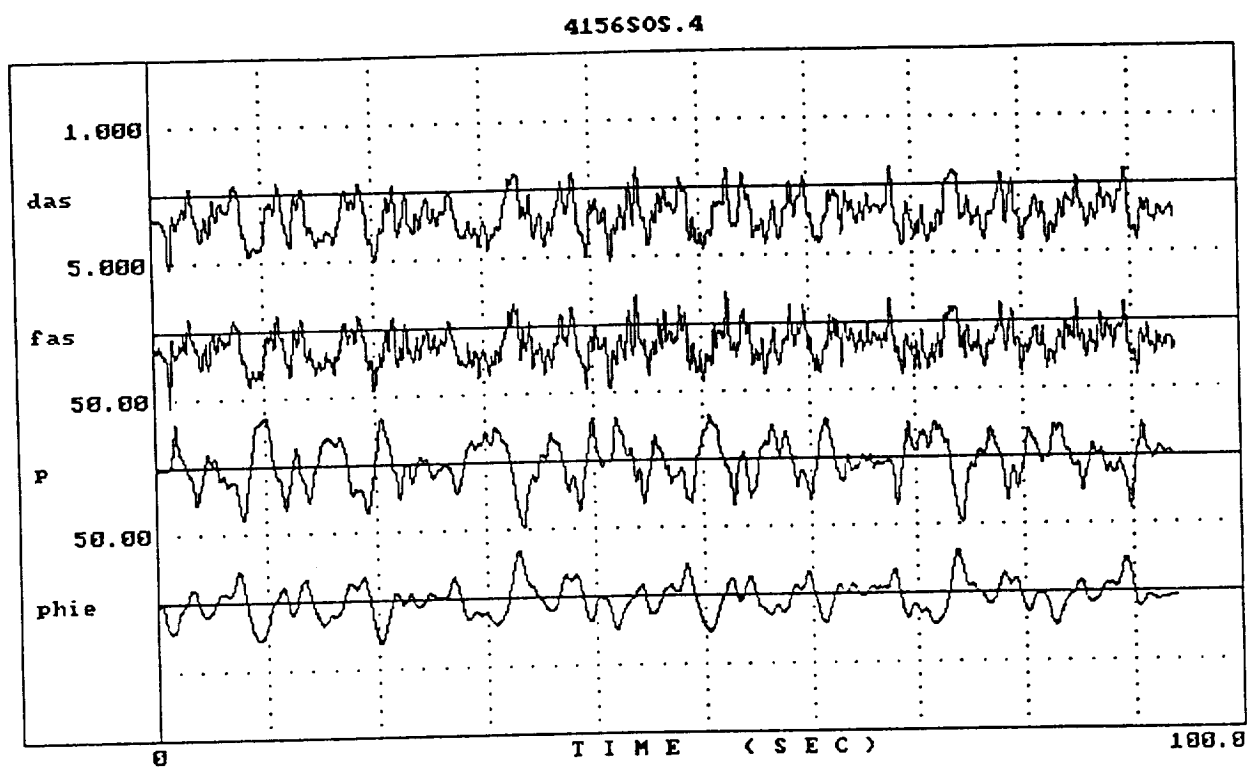
a) Time Histories

Figure B-14. Flight 4156-4

133
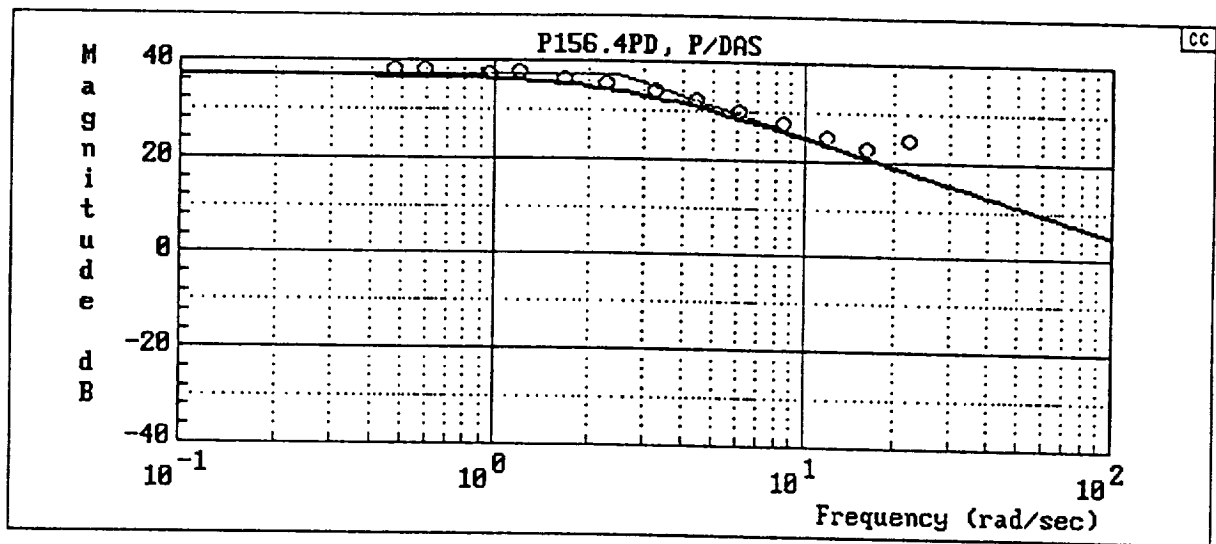
$$Y_c = \frac{180[-.8660254, 86.60254]}{(2.5)[.8660254, 86.60254]}$$

b) Y_c (P/DAS)

Figure B-14. (Continued)

DAS156.4PD, DAS/FAS

$$Y_{FS} = \frac{16}{[\ .7,\ 8]}$$

DAS156.4PD, DAS/FAS
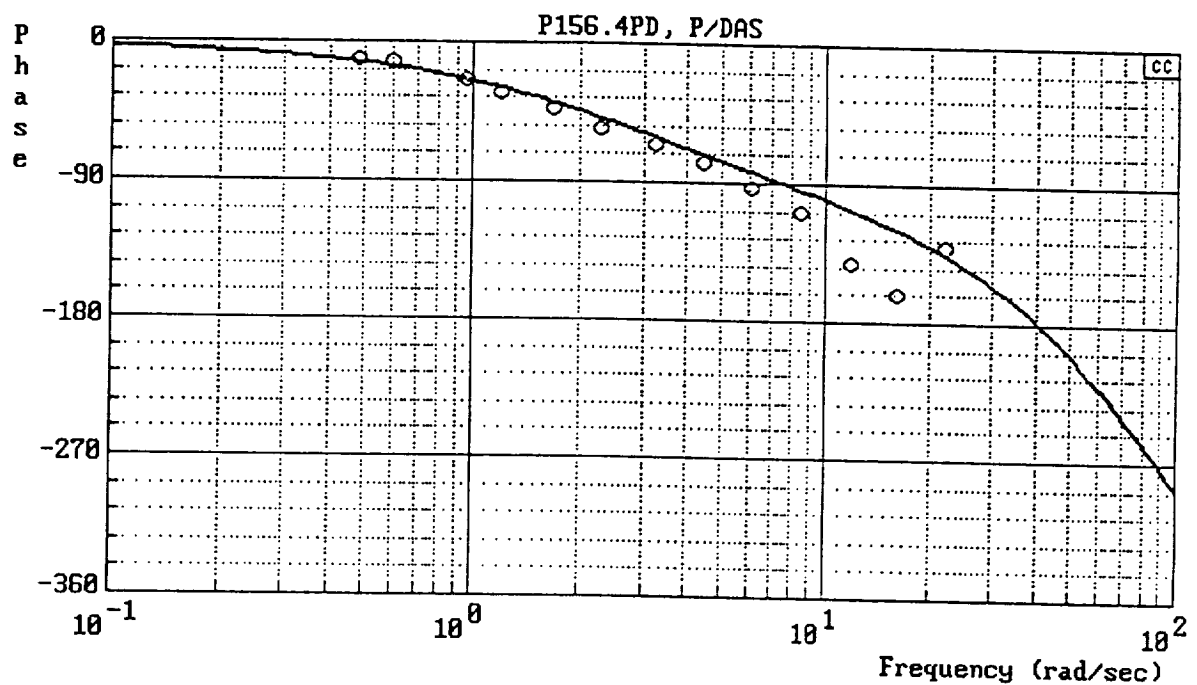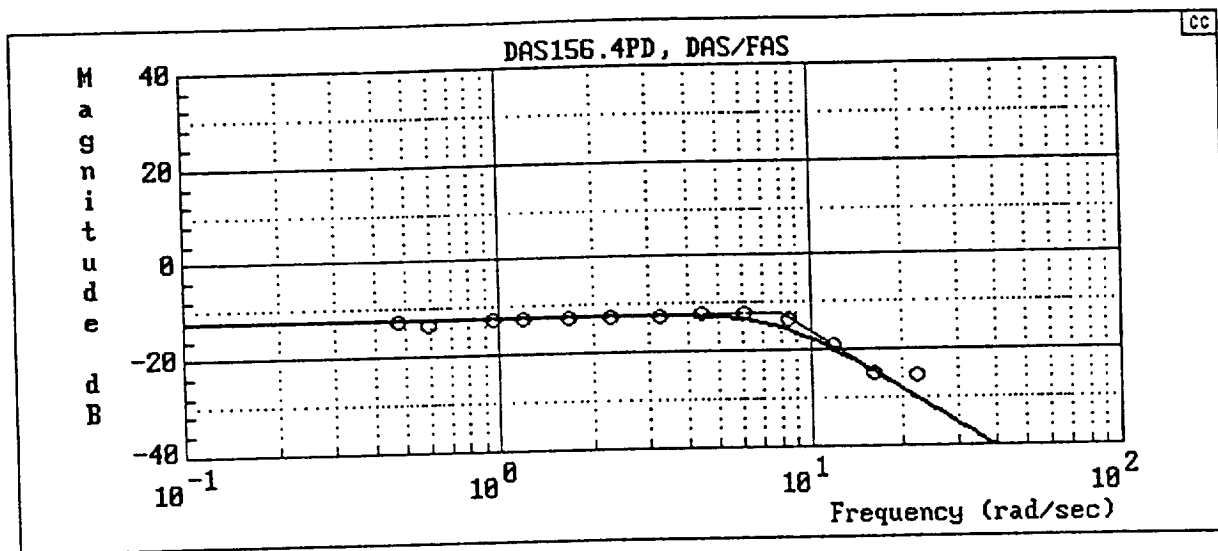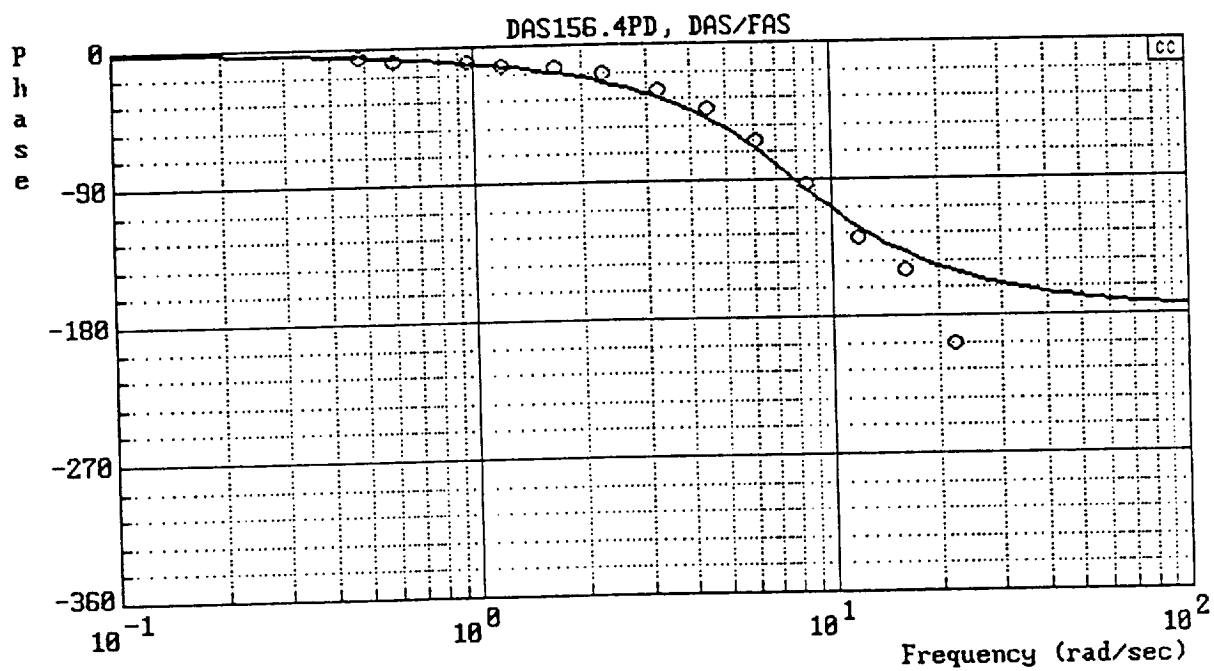
c) Y_{FS} (DAS/FAS)

Figure B-14. (Continued)

135

PHI156.4, ⌀/⌀e

PHI156.4, ⌀/⌀e
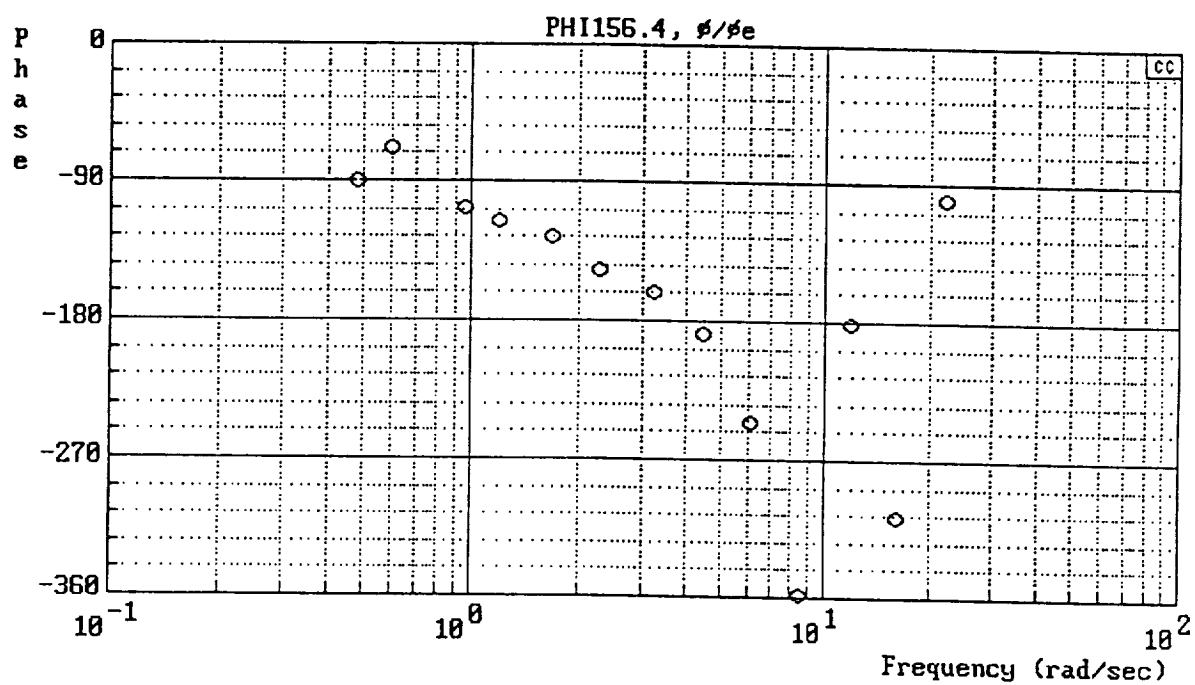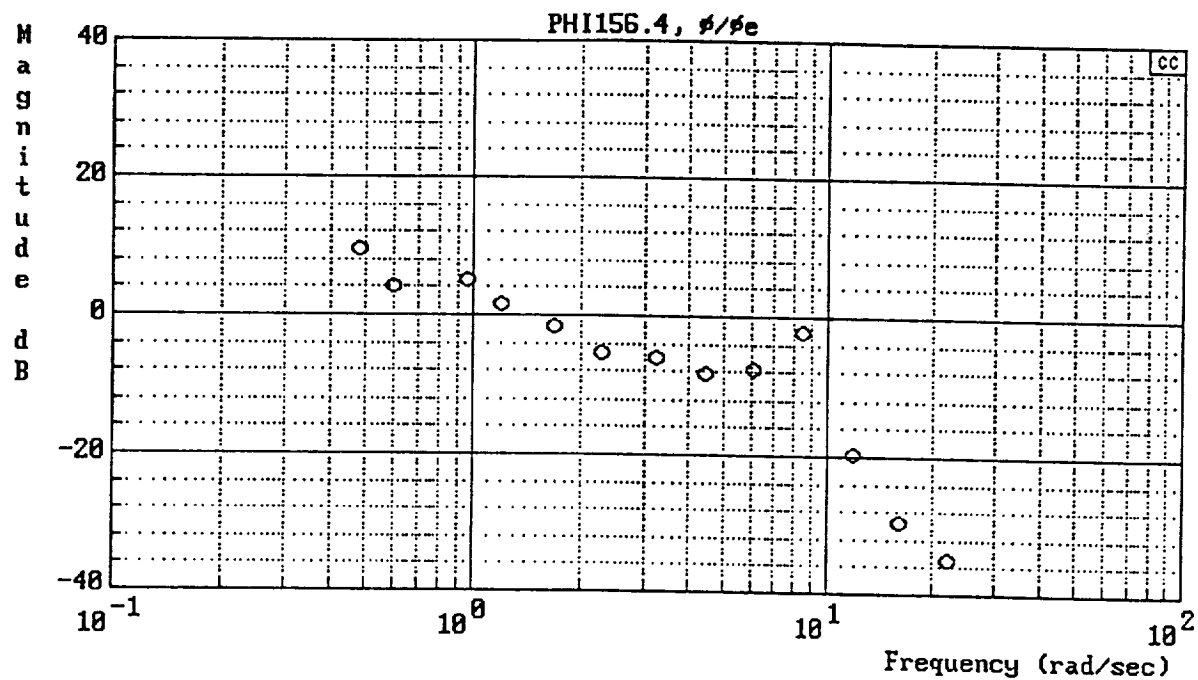
d) $Y_p Y_c$ (PHI/PHIE)

Figure B-14. (Concluded)

136

4159SOS.4

das   1.000

fas   5.000

P   50.00

phie   50.00

TIME (SEC)

0   100.0

4159SOS.4

60.00

phic

-60.00

0   TIME (SEC)   100.0
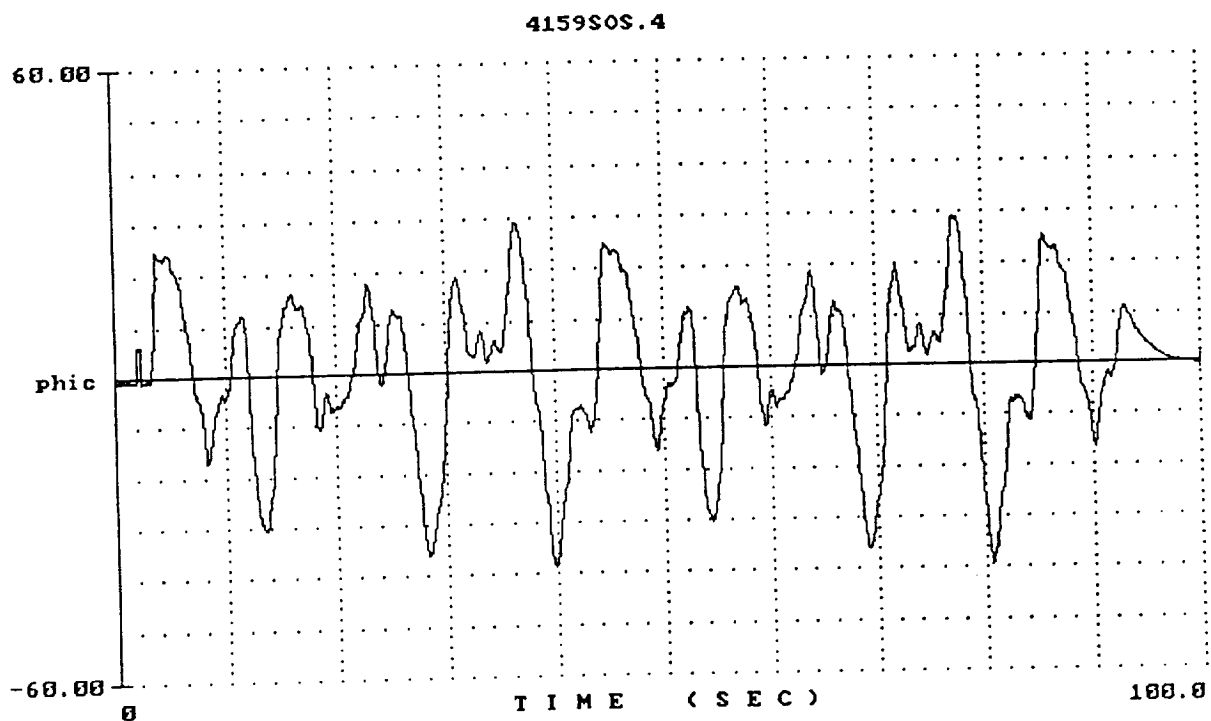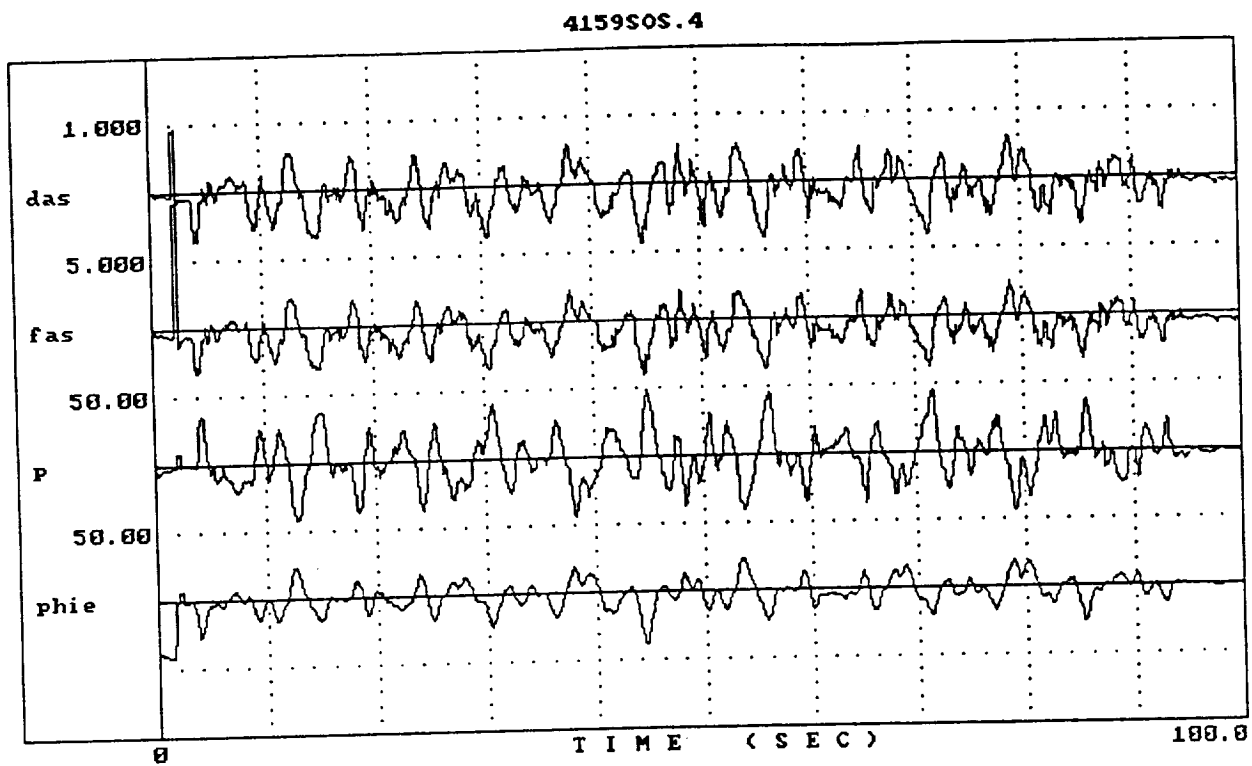
a) Time Histories

Figure B-15. Flight 4159-4
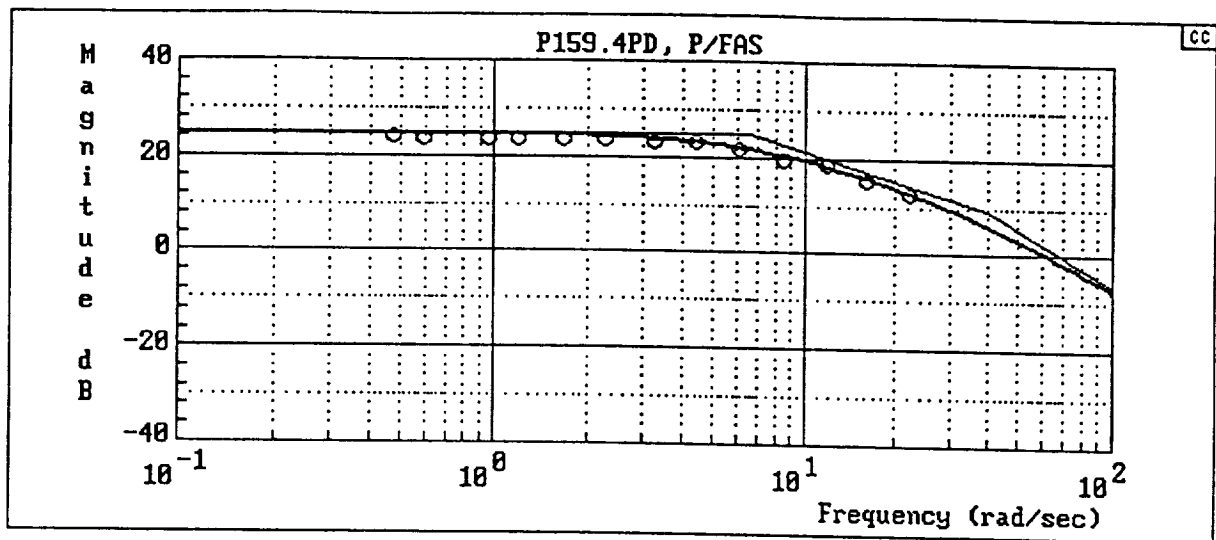
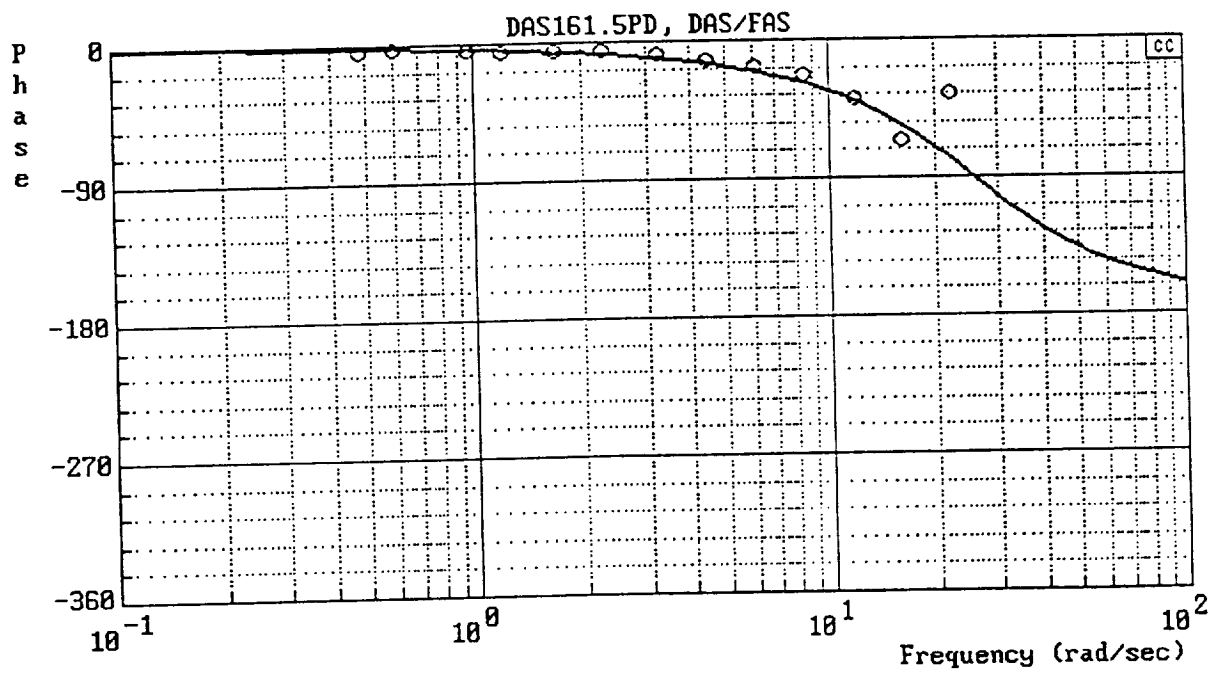$$Y_c = \frac{4802.4[-.8660254, 86.60254]}{(6.67)(40)[.8660254, 86.60254]}$$
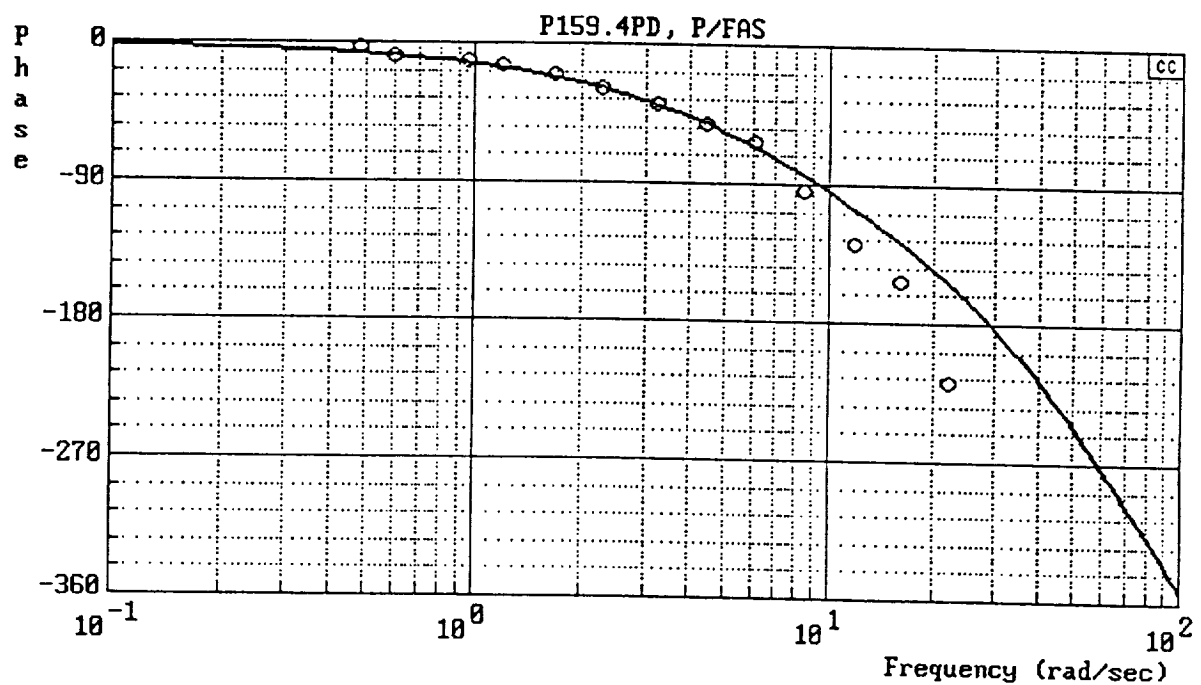
b) Y_c (P/FAS)

Figure B-15. (Continued)

$$Y_{FS} = \frac{169}{[\ .7,\ 26]}$$

c) Y_{FS} (DAS/FAS)

Figure B-15. (Continued)

PHI159.4PD, ϕ/ϕe

PHI159.4PD, ϕ/ϕe
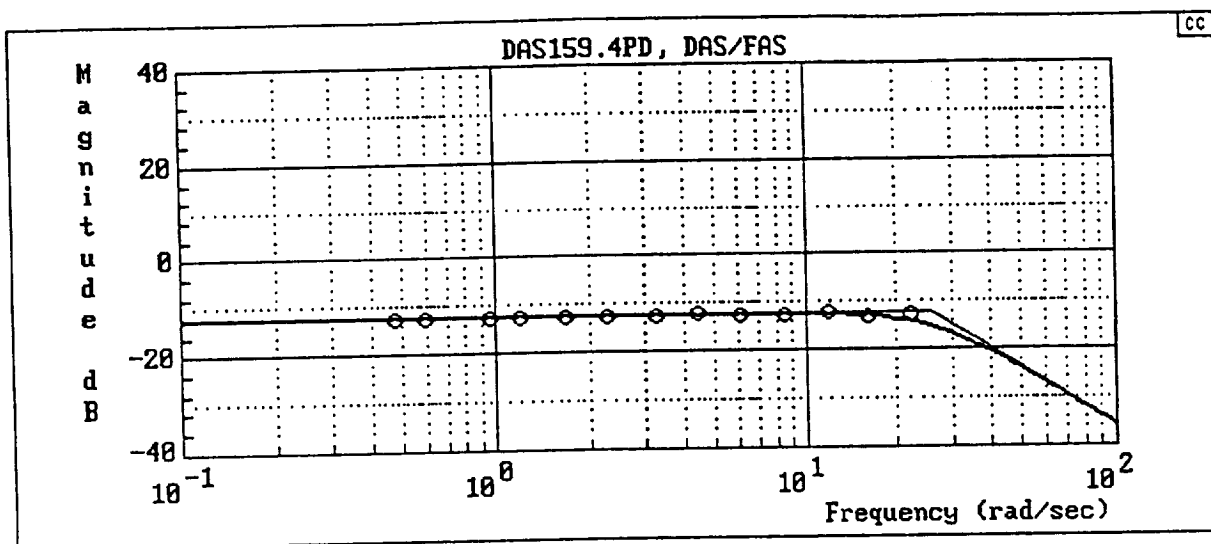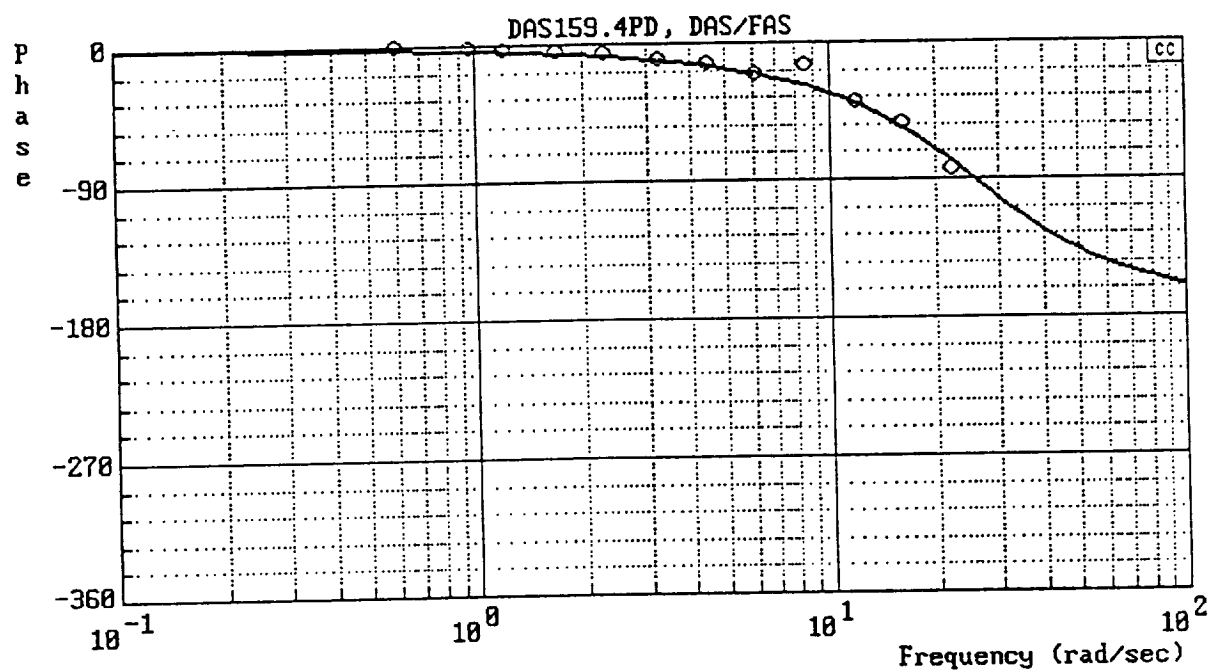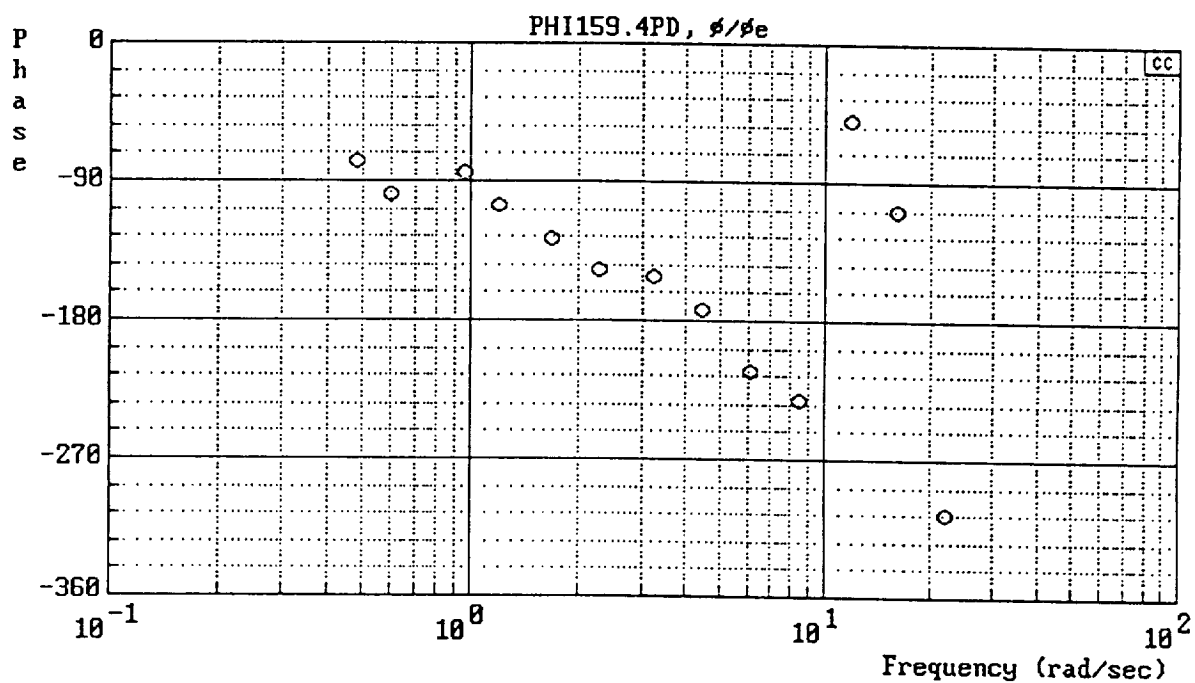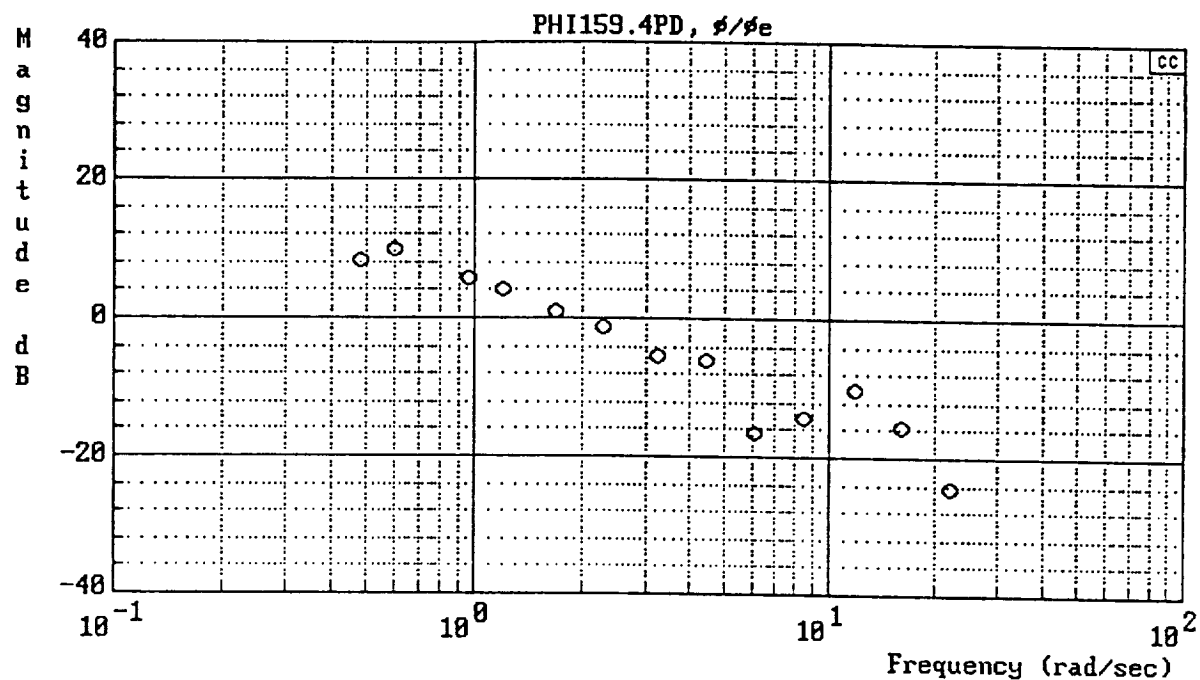
d) Y_pY_c (PHI/PHIE)

Figure B-15. (Concluded)
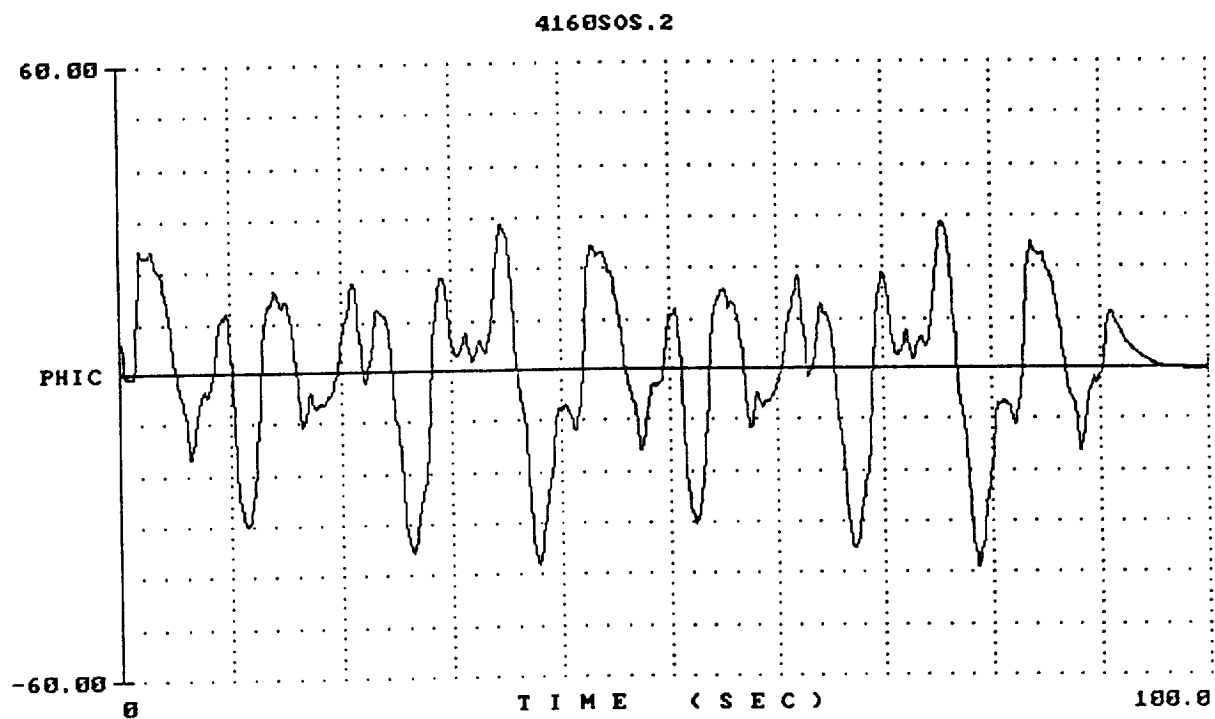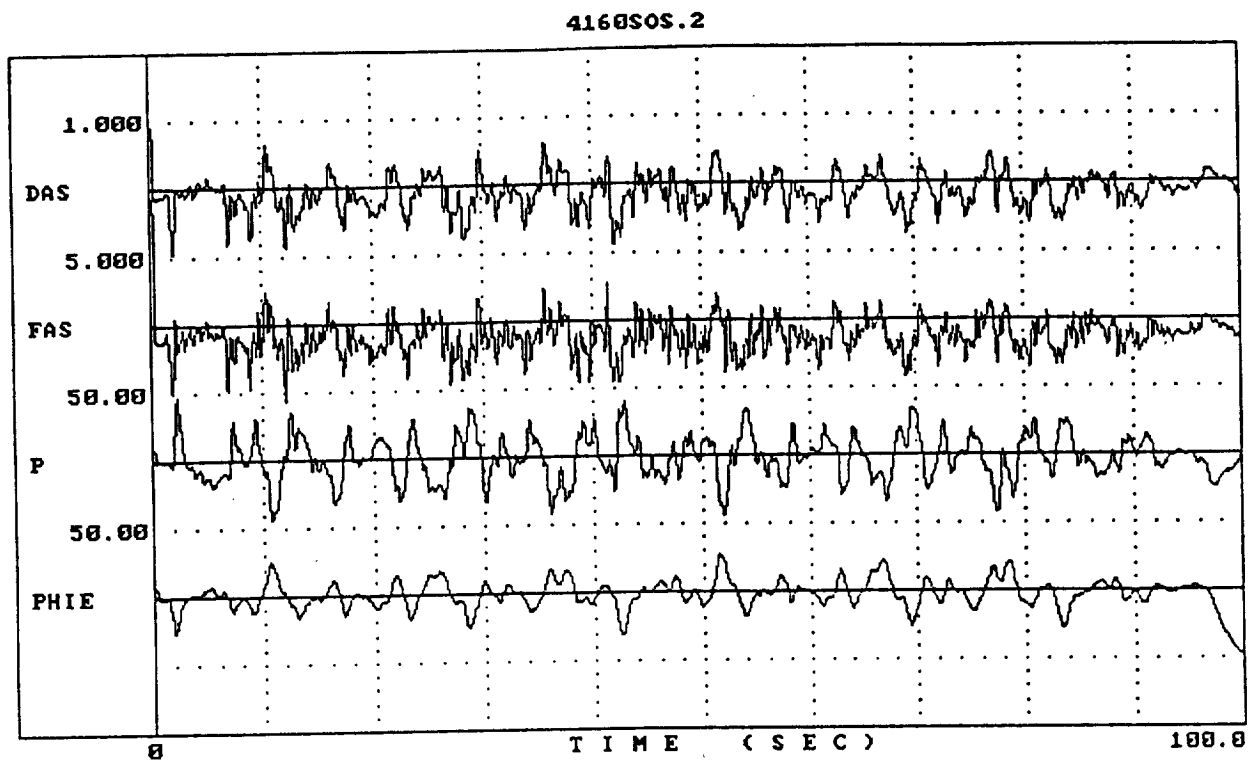
a) Time Histories

Figure B-16. Flight 4160-2

P160.2PD, P/DAS

Magnitude dB vs Frequency (rad/sec)
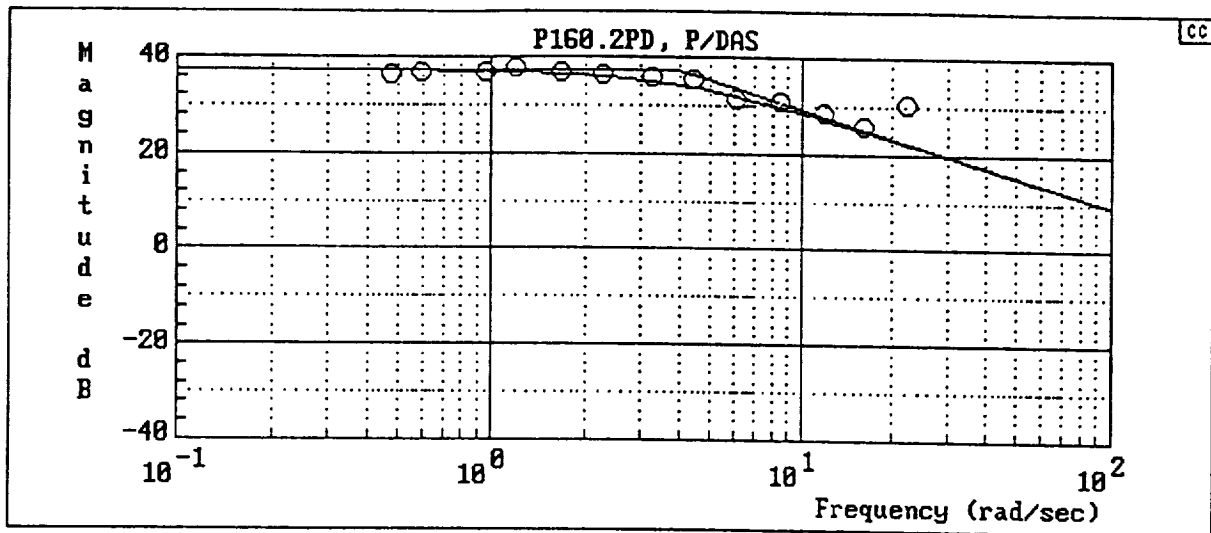
$$Y_c = \frac{288[-.8660254, \ 43.30127]}{(\ 4)[\ .8660254, \ 43.30127]}$$

P160.2PD, P/DAS

Phase vs Frequency (rad/sec)
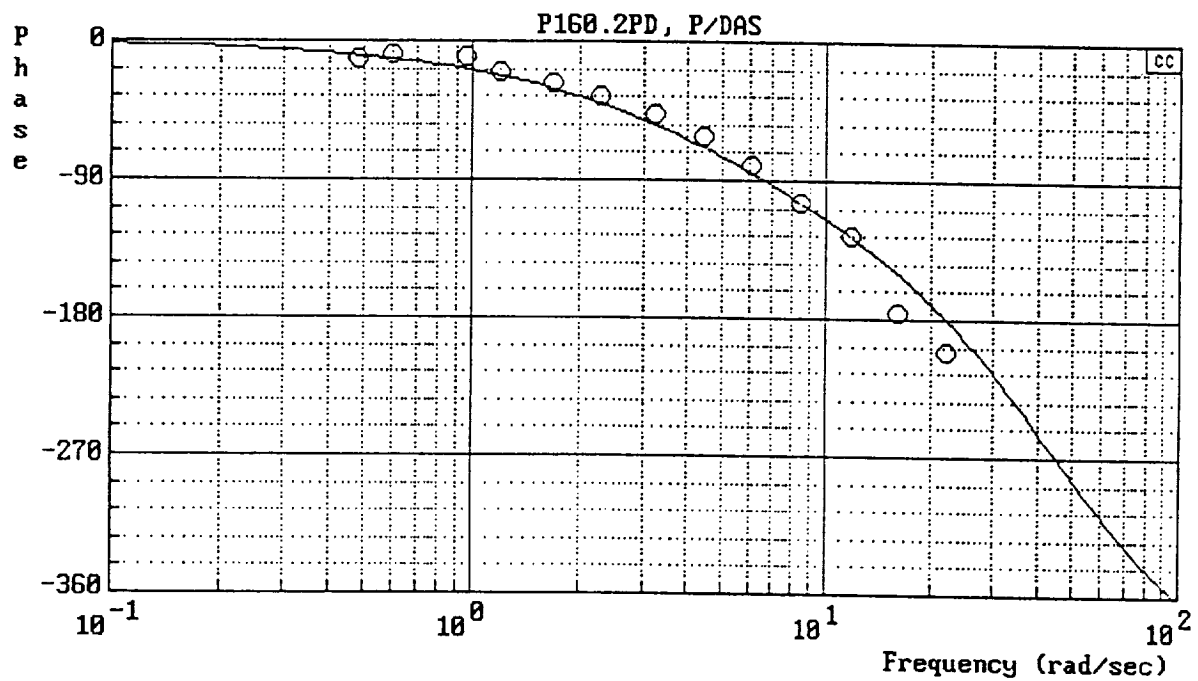
b) Y_c (P/DAS)

Figure B-16. (Continued)

DAS160.2TF, DAS/FAS

$$Y_{FS} = \frac{16}{[.7, 8]}$$

DAS160.2TF, DAS/FAS
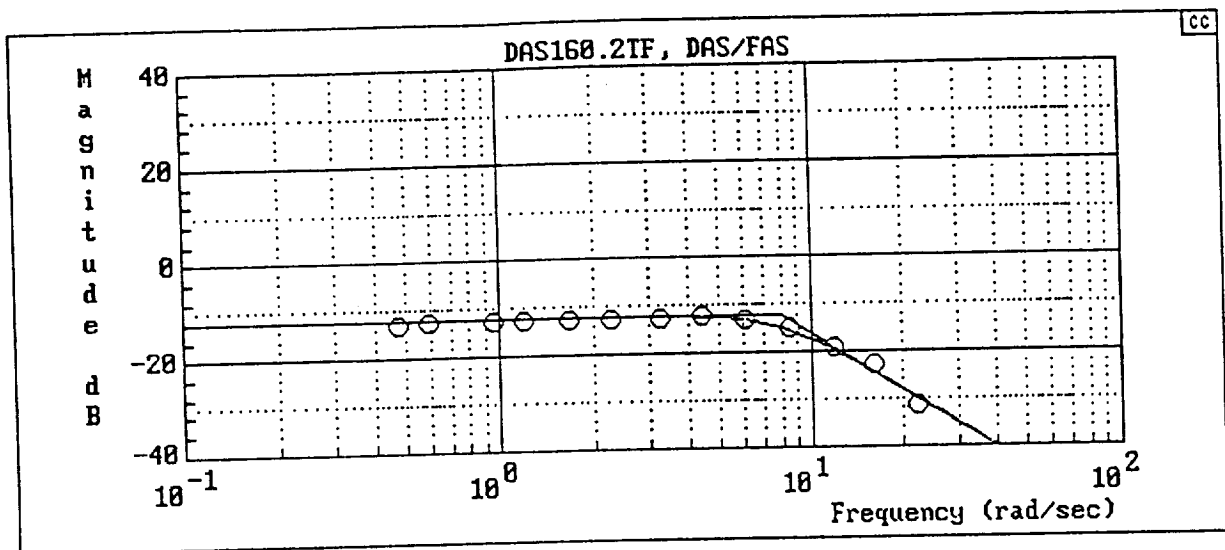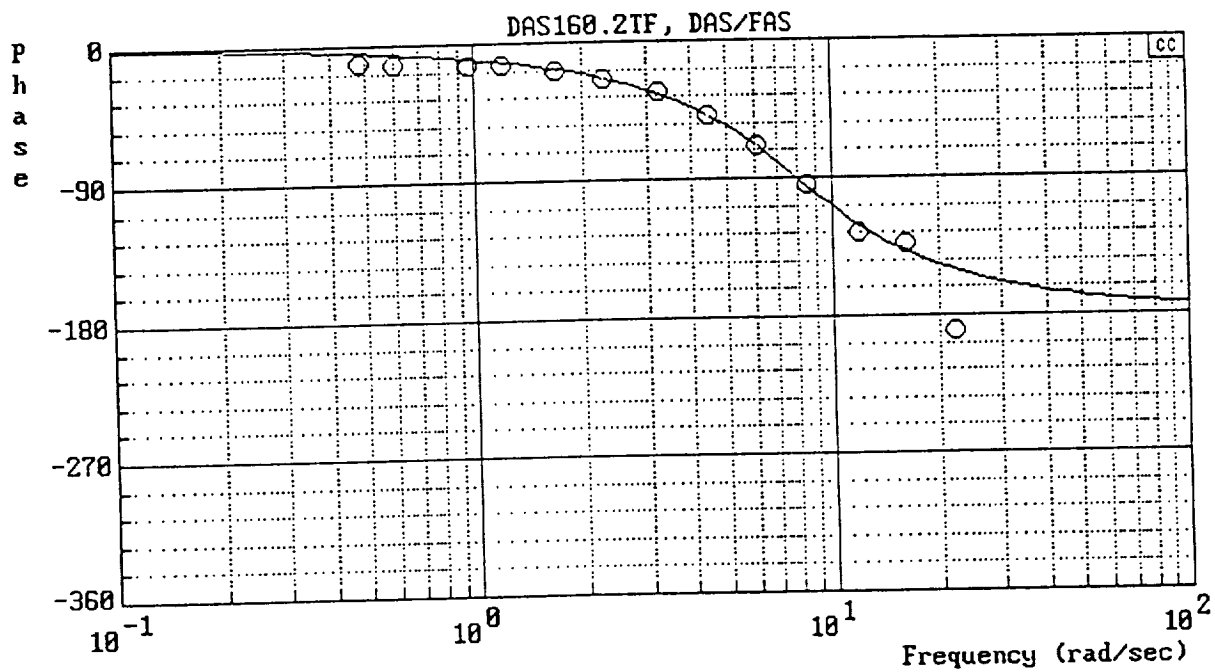
c) Y_{FS} (DAS/FAS)

Figure B-16. (Continued)
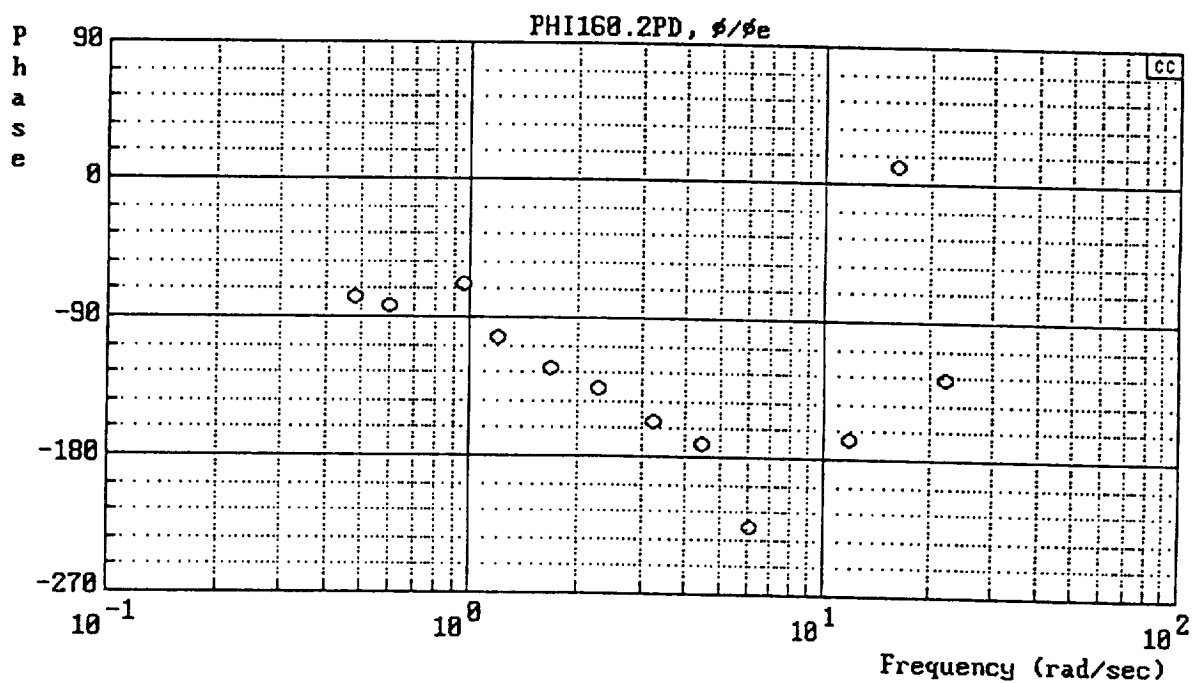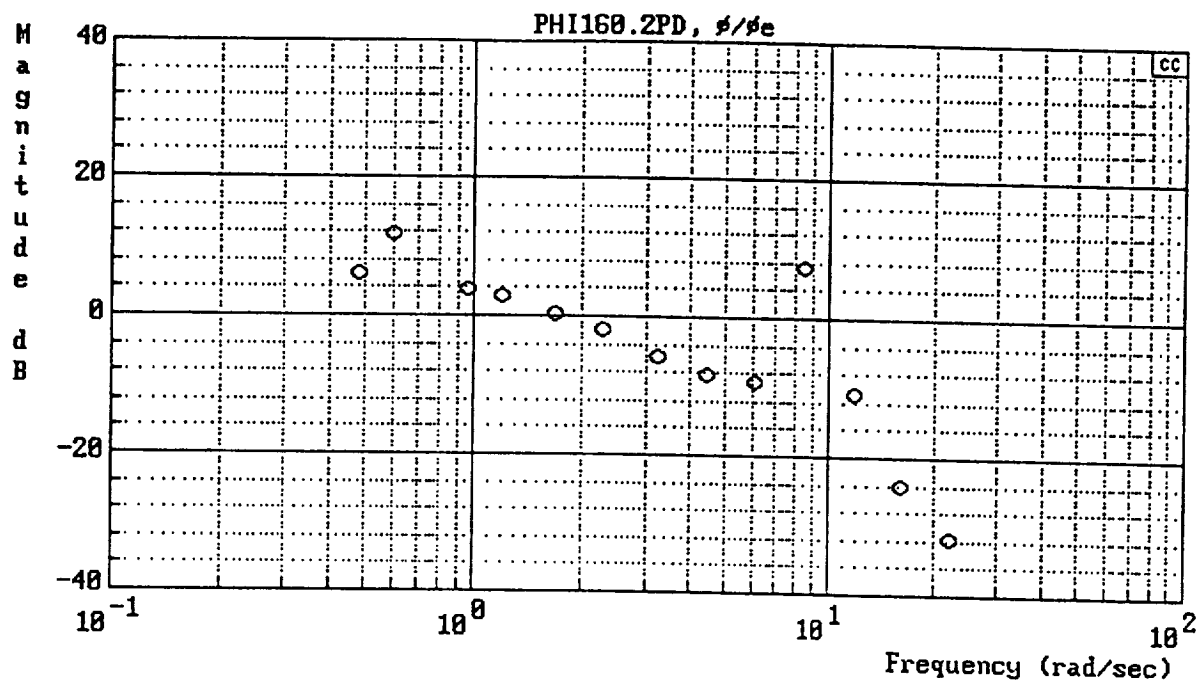
d) $Y_p Y_c$ (PHI/PHIE)

Figure B-16. (Concluded)
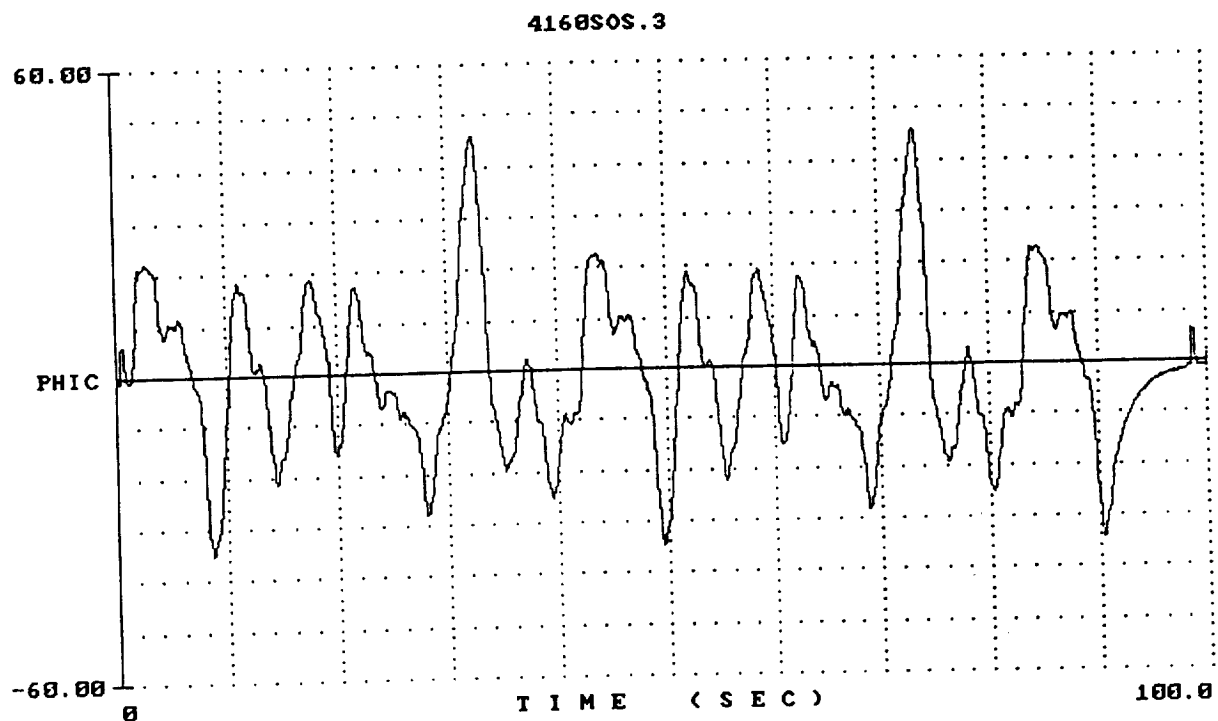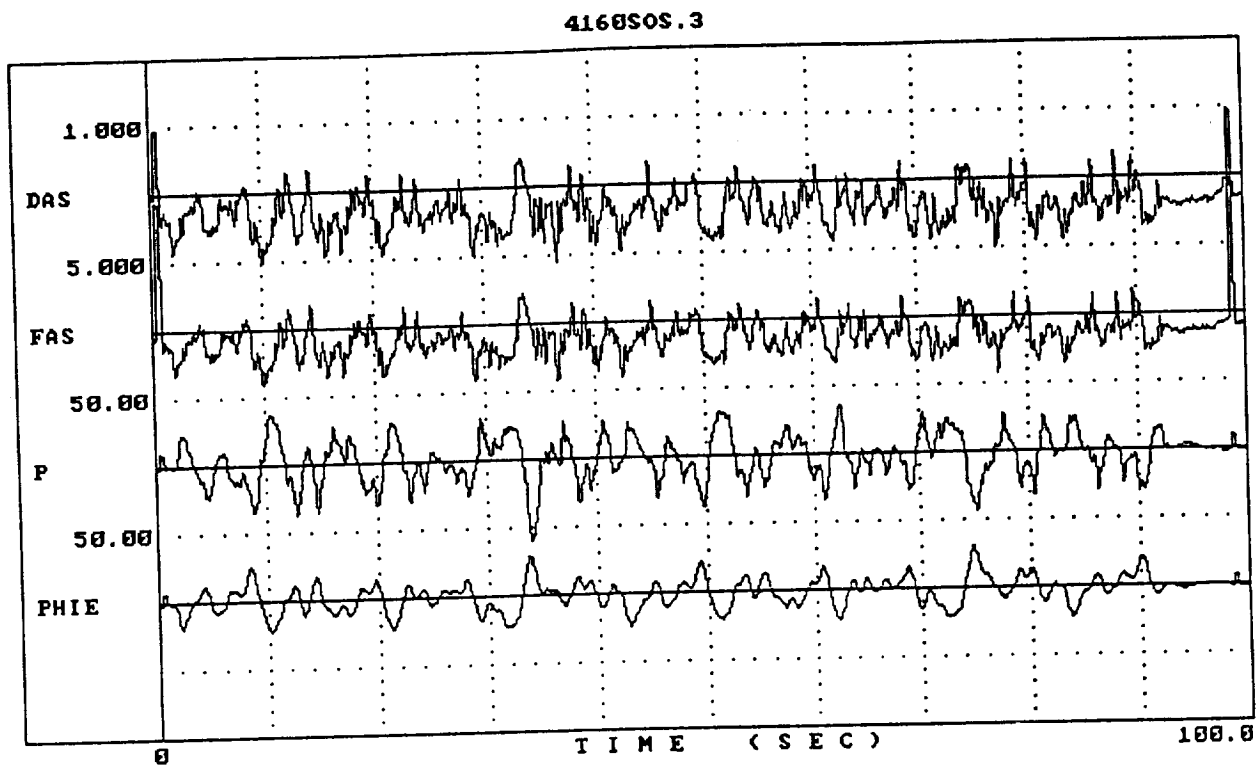
a) Time Histories

Figure B-17. Flight 4160-3

145
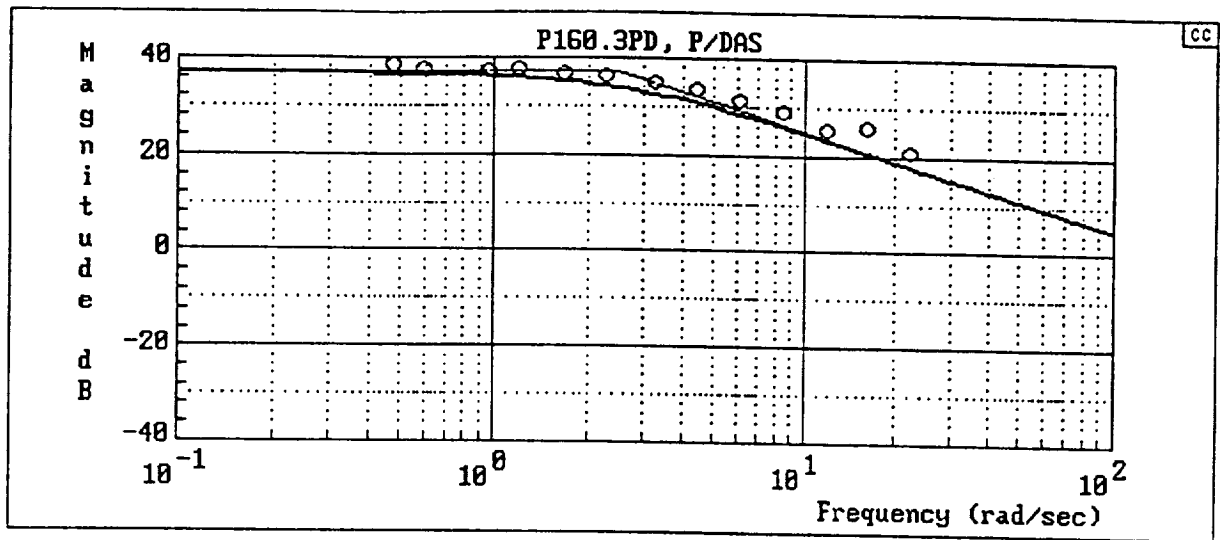
$$Y_c = \frac{180[-.8660254, 62.98367] [-.8660254, 86.60254]}{(2.5)[.8660254, 62.98367] [.8660254, 86.60254]}$$
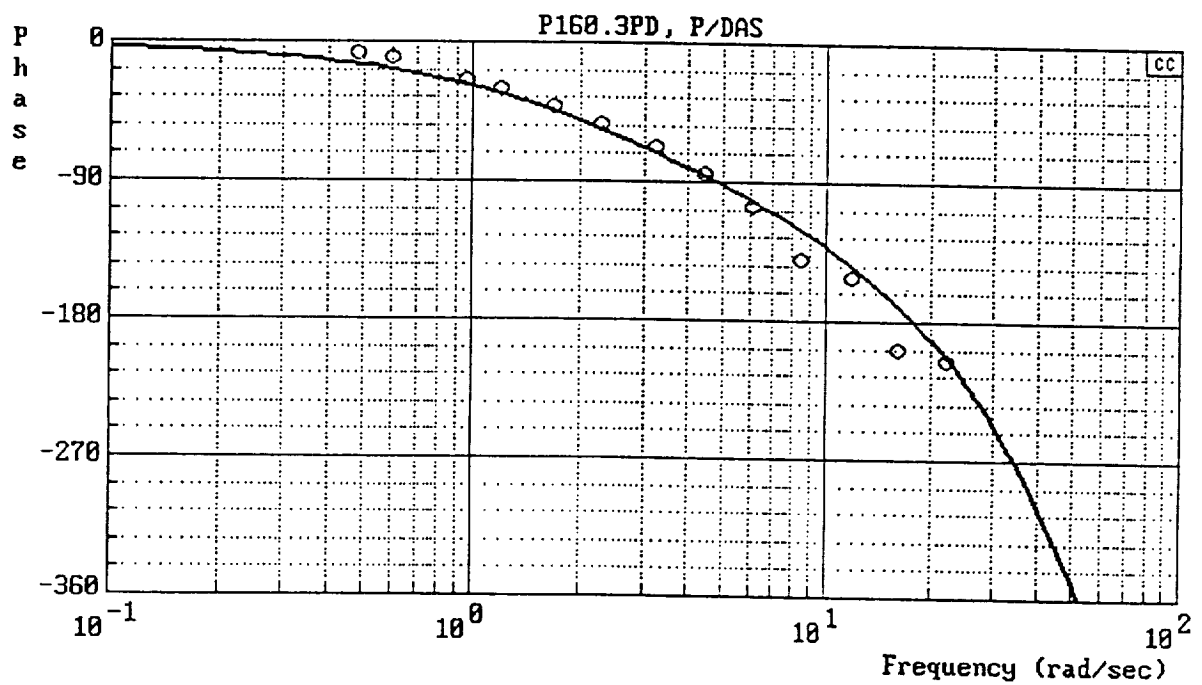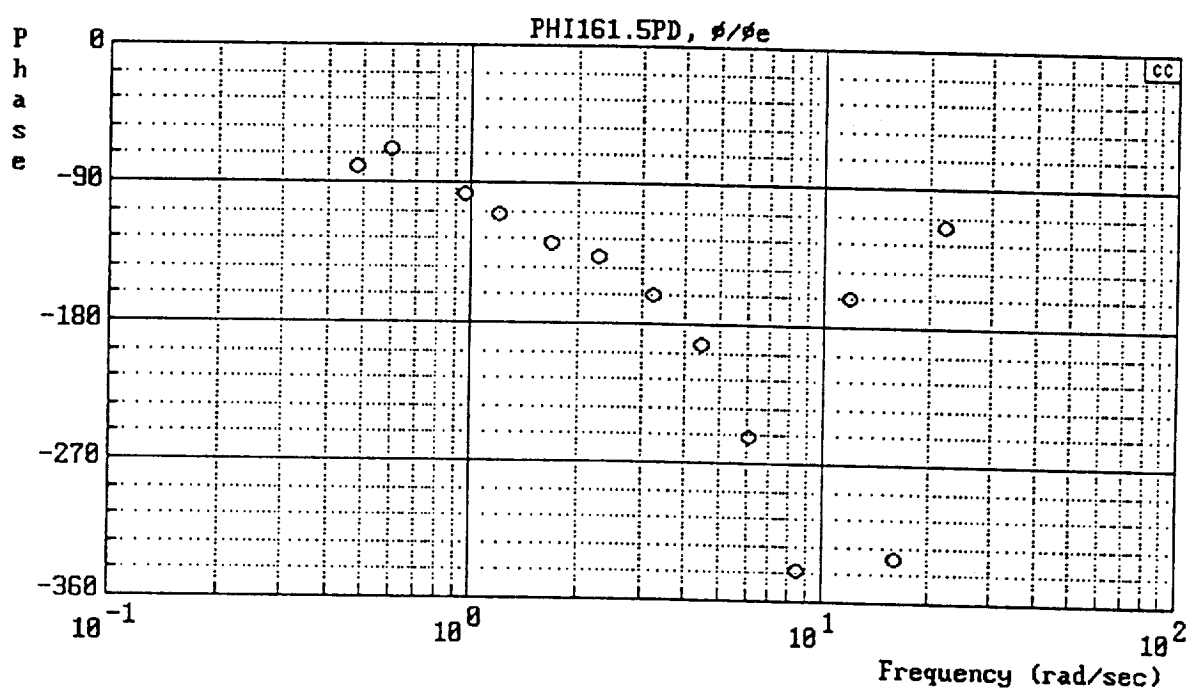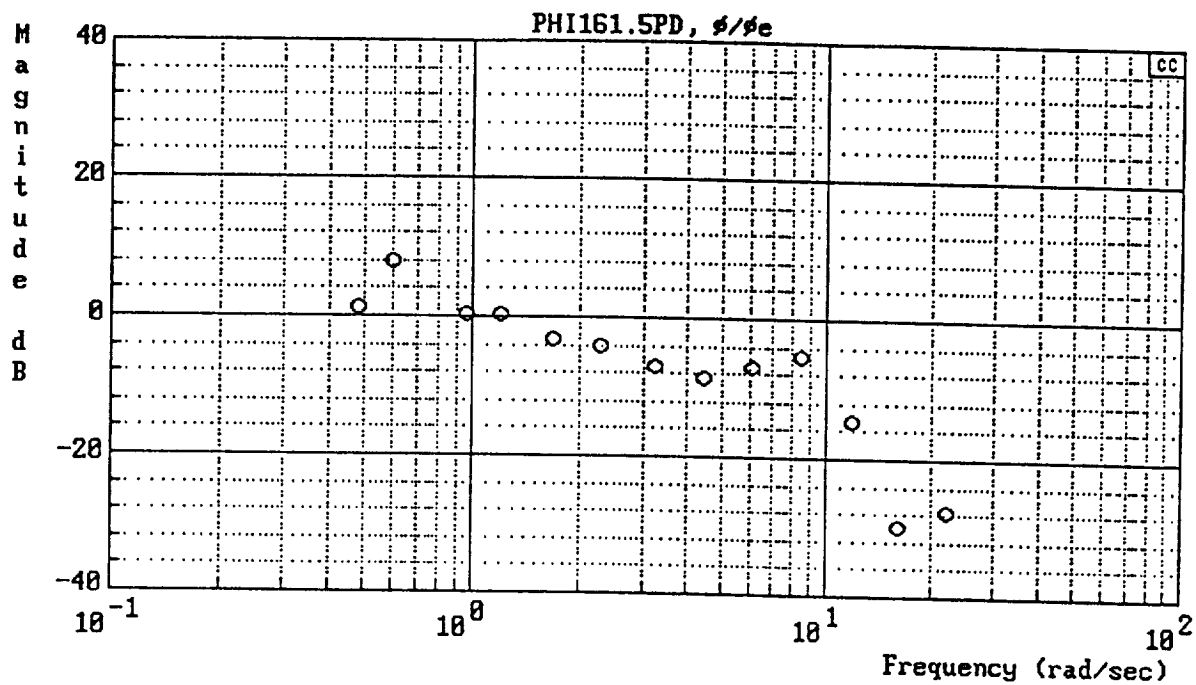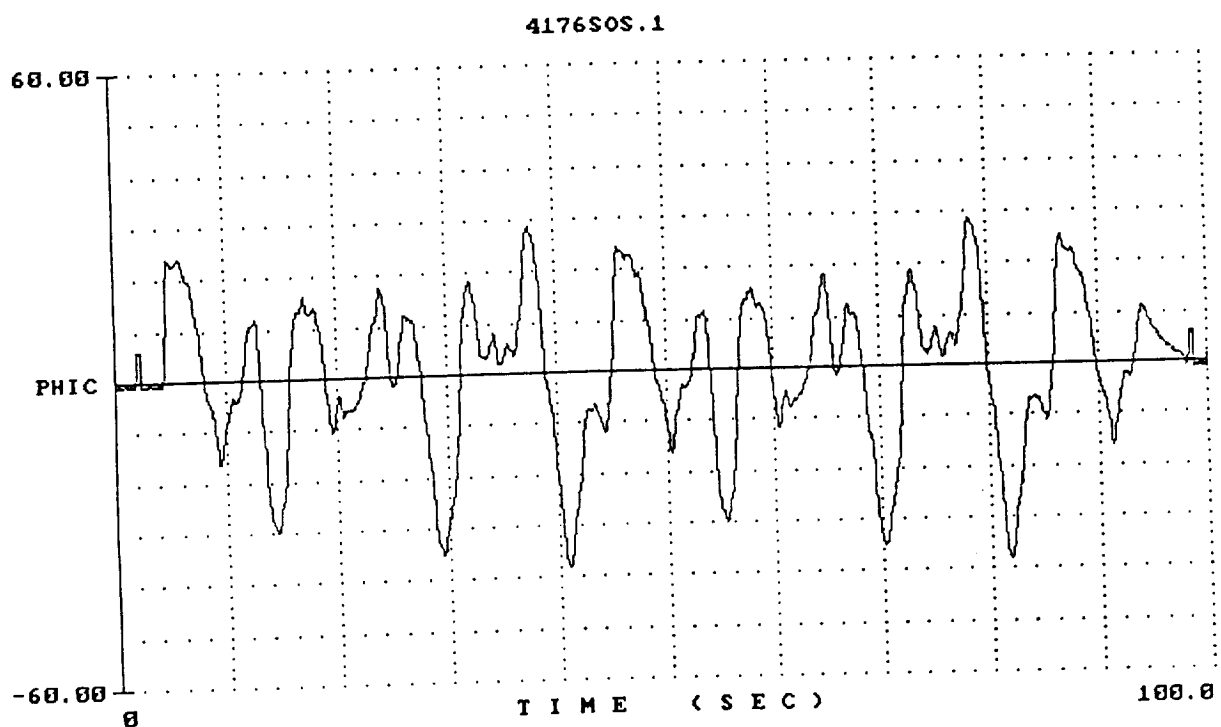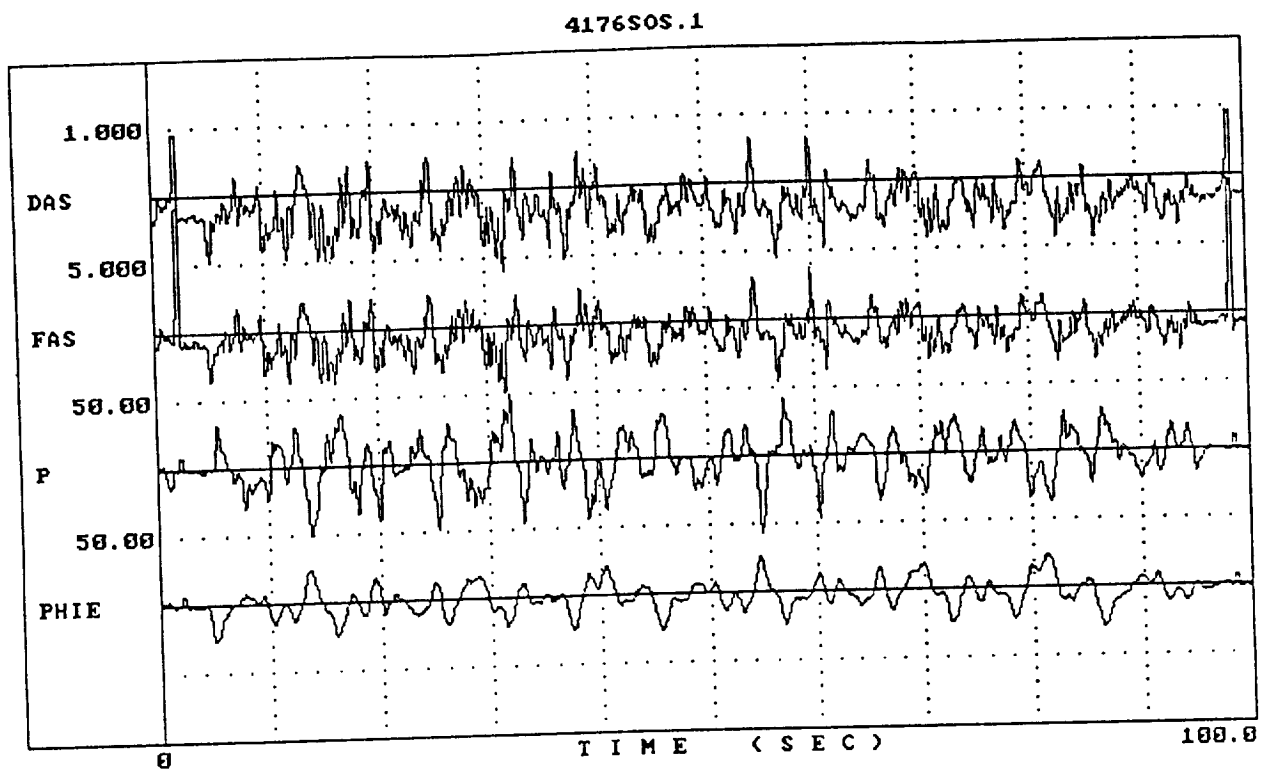

b) Y_c (P/DAS)

Figure B-17. (Continued)

DAS160.3PD, DAS/FAS

$$Y_{FS} = \frac{169}{[\ .7,\ 26]}$$

DAS160.3PD, DAS/FAS
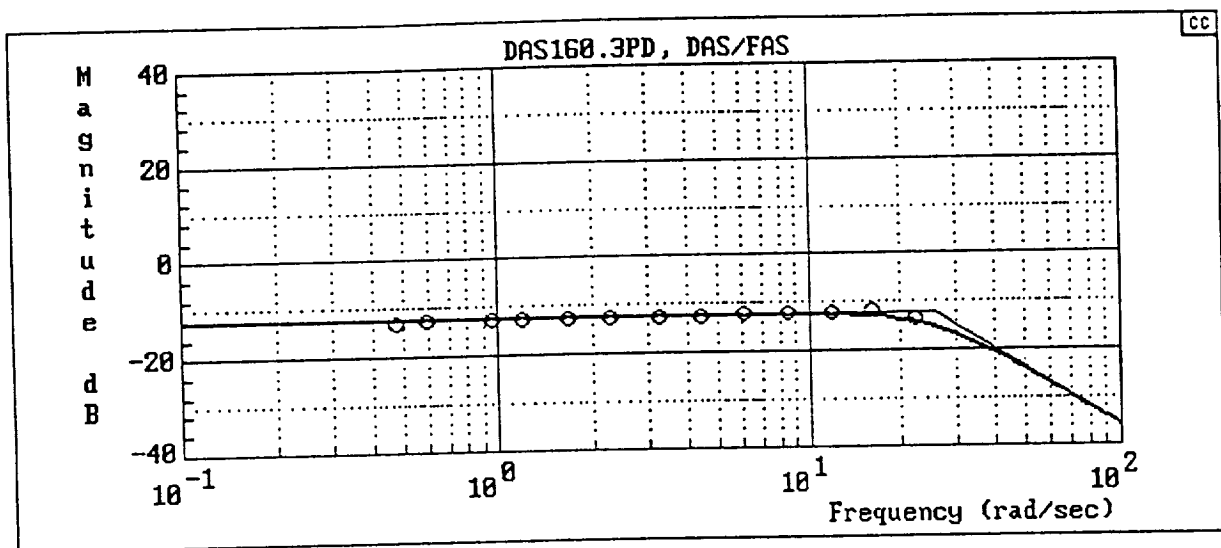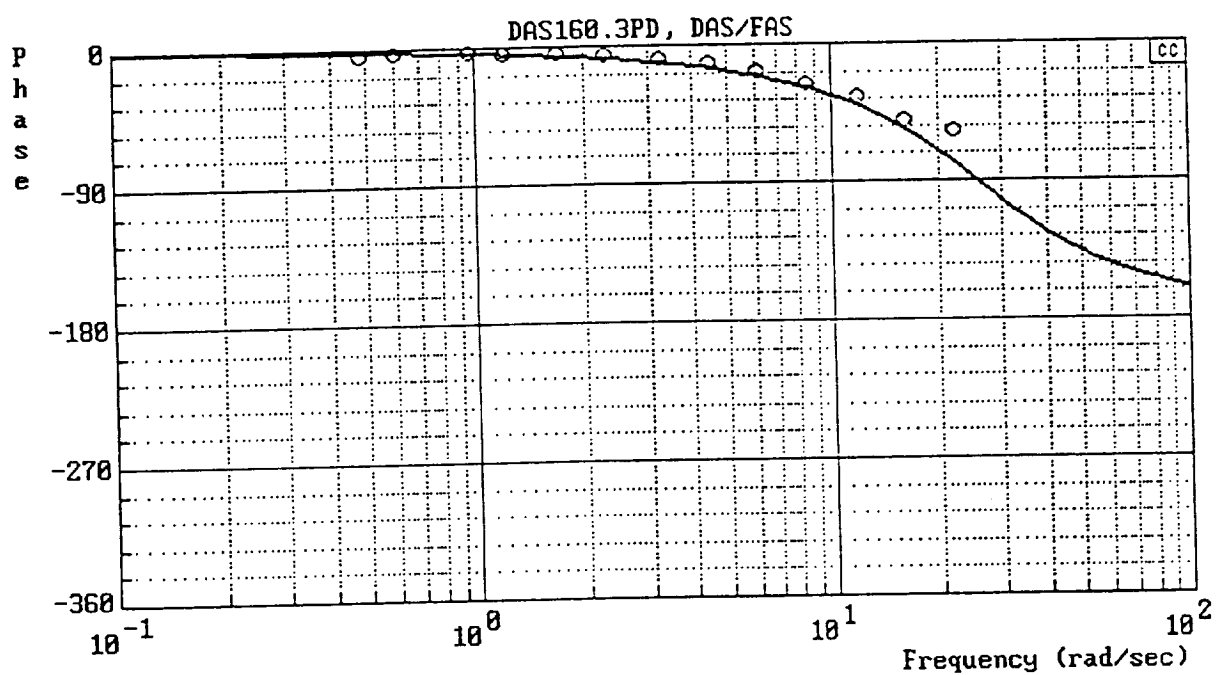
c) Y_{FS} (DAS/FAS)

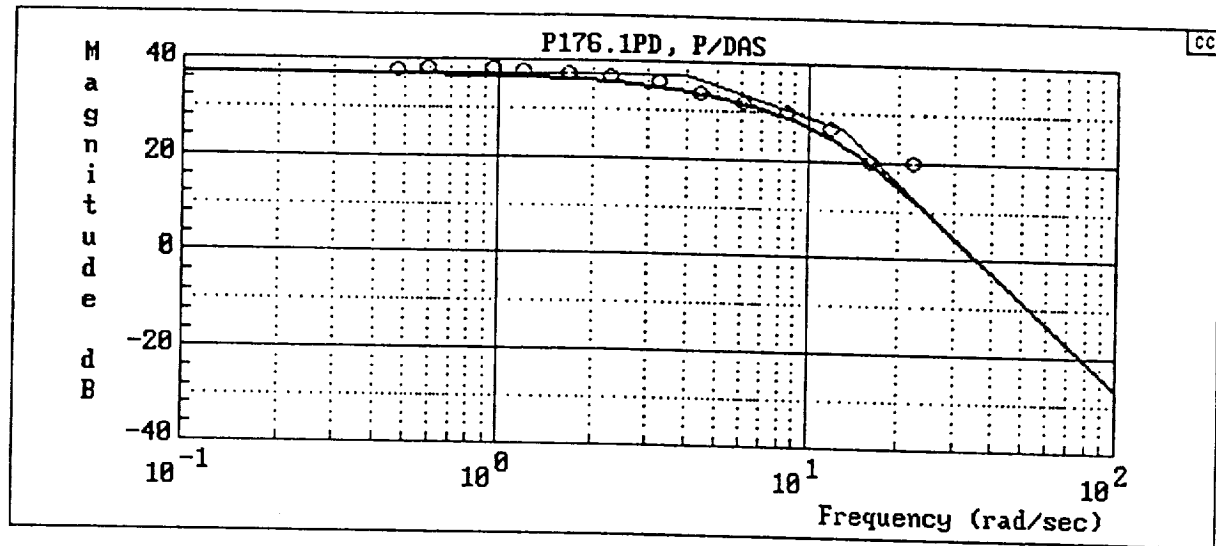Figure B-17. (Continued)

147

PHI160.3PD φ/φe

PHI160.3PD φ/φe
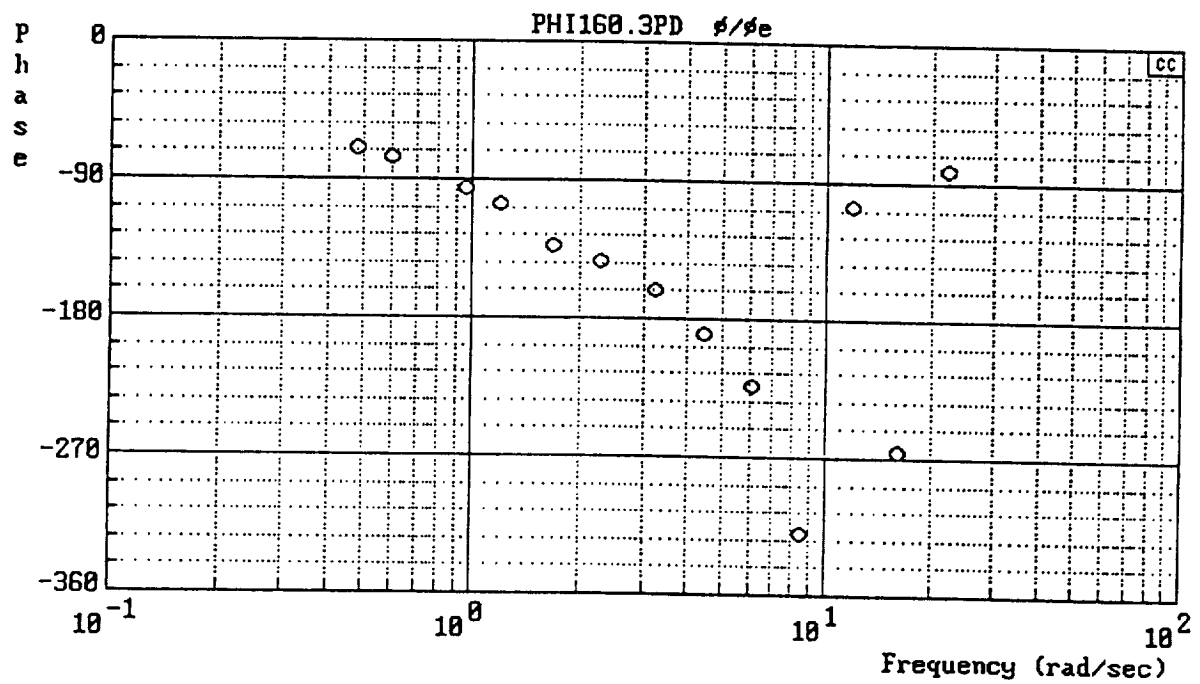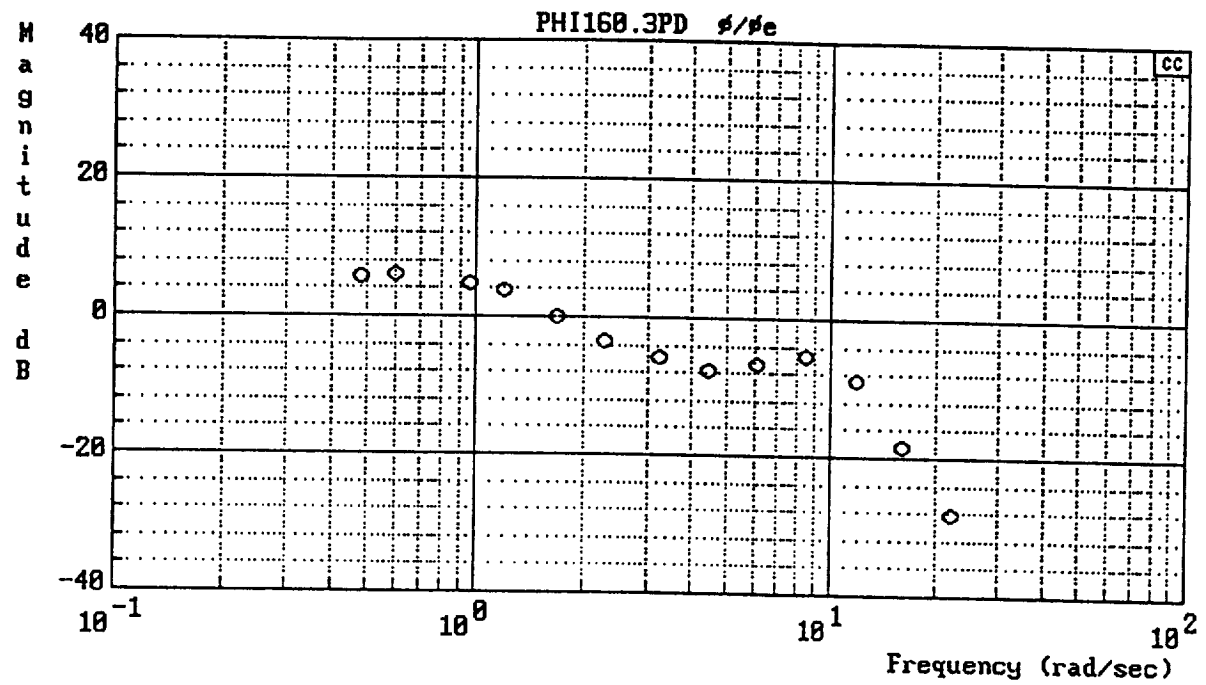
d) Y_pY_c (PHI/PHIE)
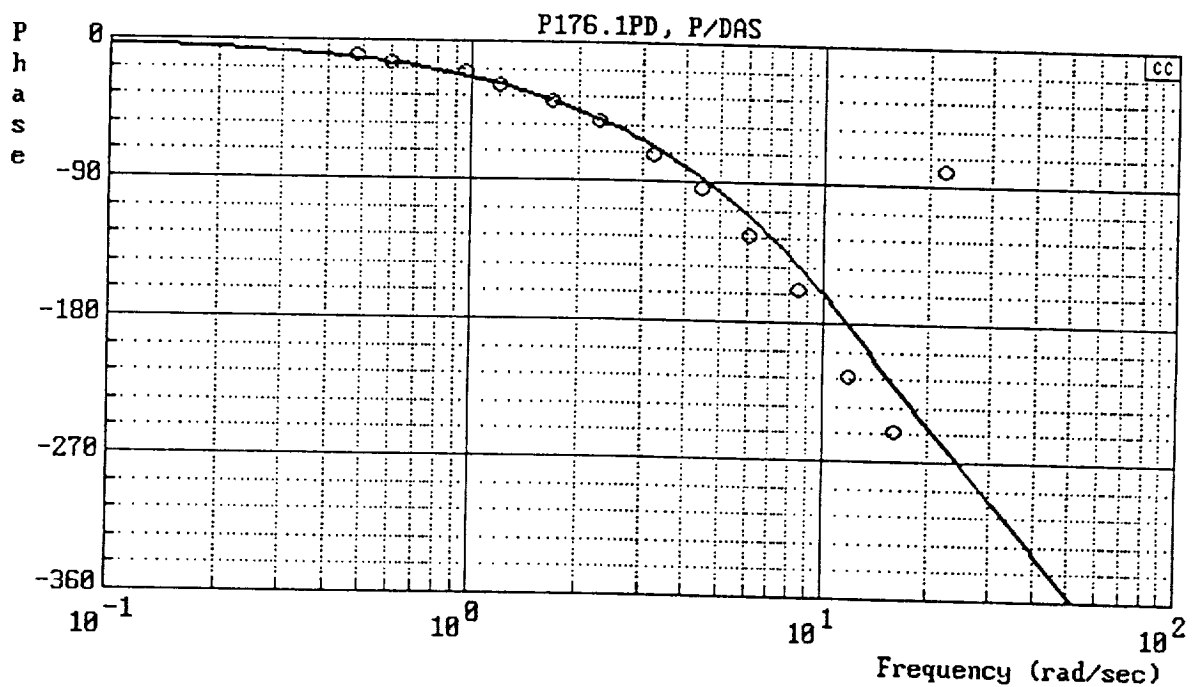
Figure B-17. (Concluded)

148
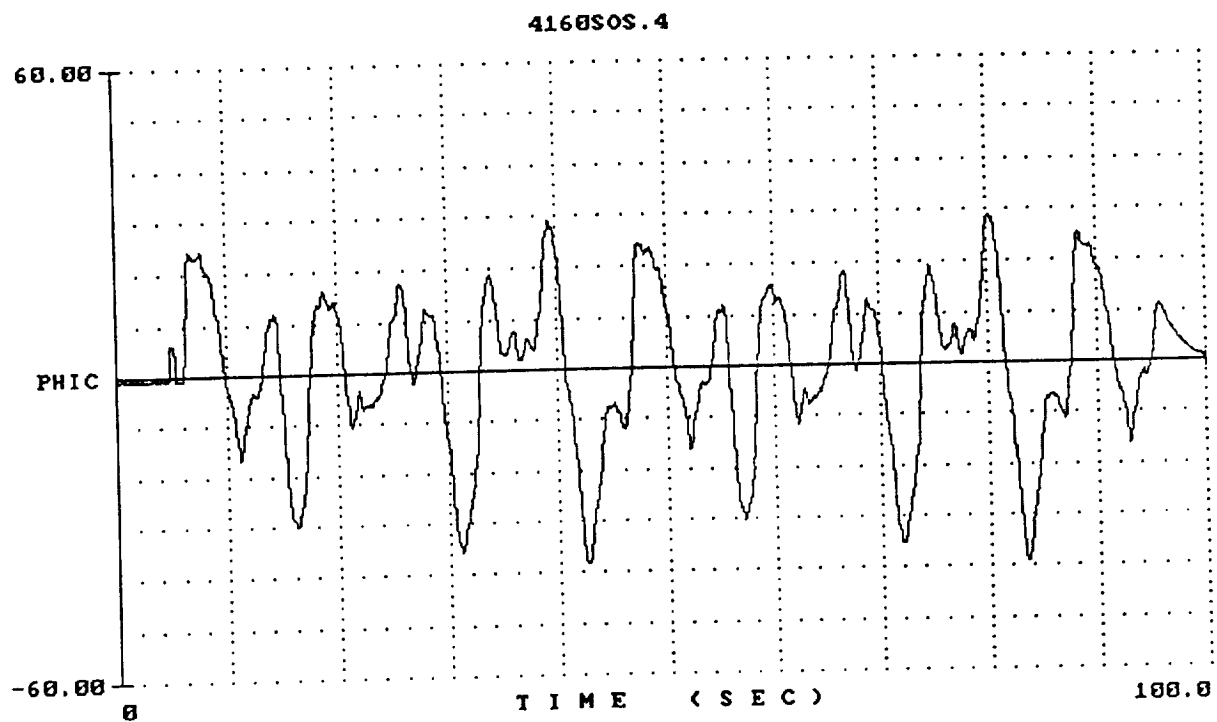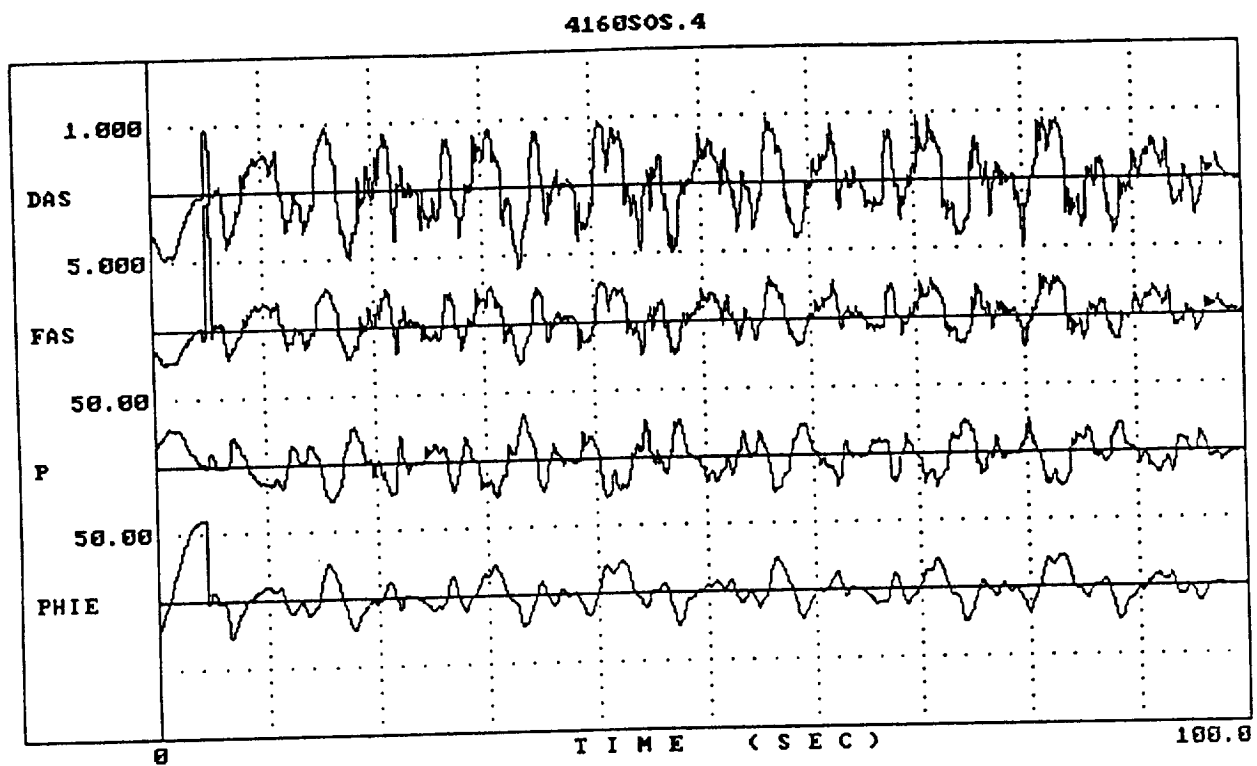
a) Time Histories

Figure B-18. Flight 4160-4
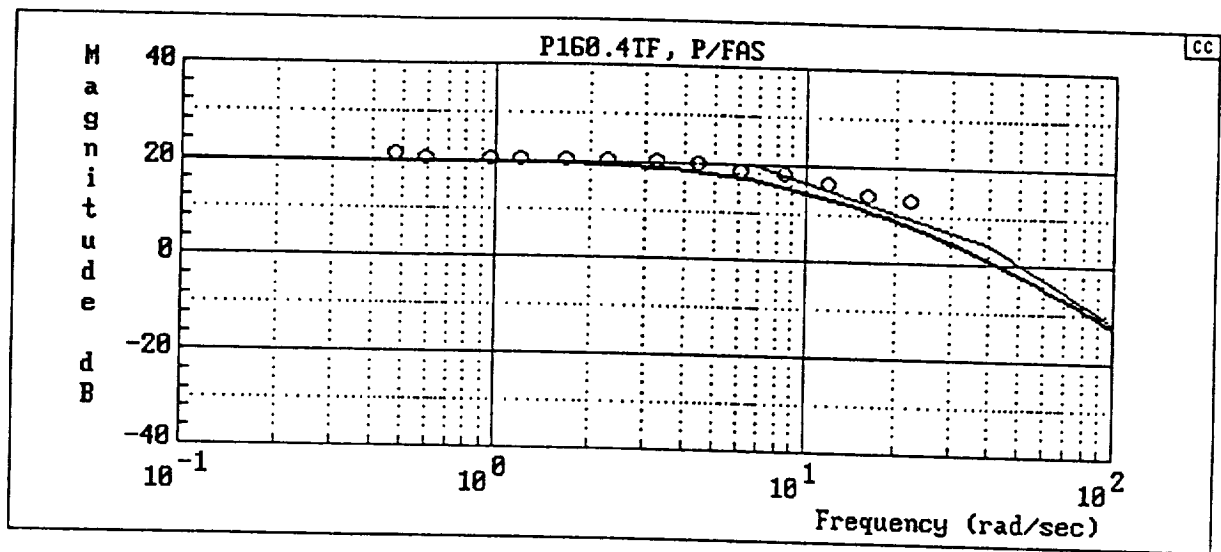
$$Y_c = \frac{2668[-.8660254, \ 86.60254]}{(6.67)(40)[\ .8660254, \ 86.60254]}$$
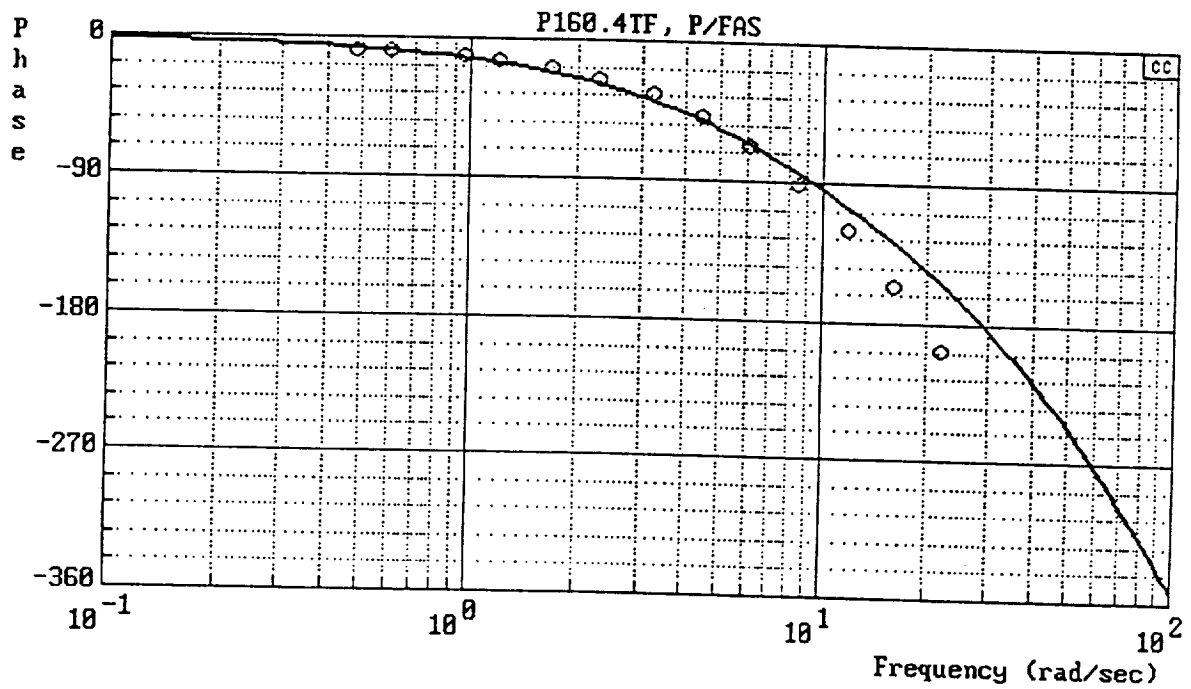
b) Y_c (P/FAS)

Figure B-18. (Continued)

DAS160.4PD, DAS/FAS

$$Y_{FS} = \frac{246.064}{[\ .7,\ 26]}$$

DAS160.4PD, DAS/FAS

c) Y_{FS} (DAS/FAS)

Figure B-18. (Continued)

151

PHI160.4PD ø/øe

Frequency (rad/sec)

PHI160.4PD ø/øe

Frequency (rad/sec)
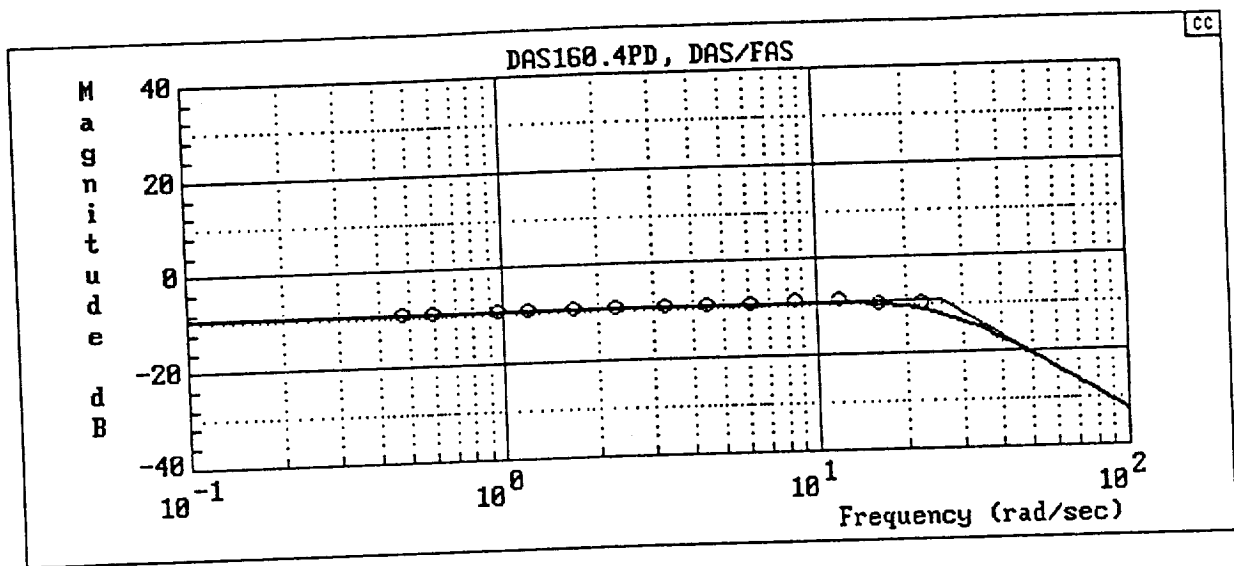
d) Y_pY_c (PHI/PHIE)

Figure B-18. (Concluded)

4160SOS.5

TIME (SEC)

4160SOS.5

TIME (SEC)

a) Time Histories

Figure B-19. Flight 4160-5

P160.5PD, P/FAS

$$Y_c = \frac{120.06[-.8660254, 43.30127]}{(6.67)[.8660254, 43.30127]}$$

P160.5PD, P/FAS

b) Y_c (P/FAS)

Figure B-19. (Continued)

154

DAS160.5TF, DAS/FAS

$$Y_{FS} = \frac{42.25}{[\ .7,\ 13]}$$

DAS160.5TF, DAS/FAS

c) Y_{FS} (DAS/FAS)

Figure B-19. (Continued)

PHI160.5PD, ∮/∮e

PHI160.5PD, ∮/∮e
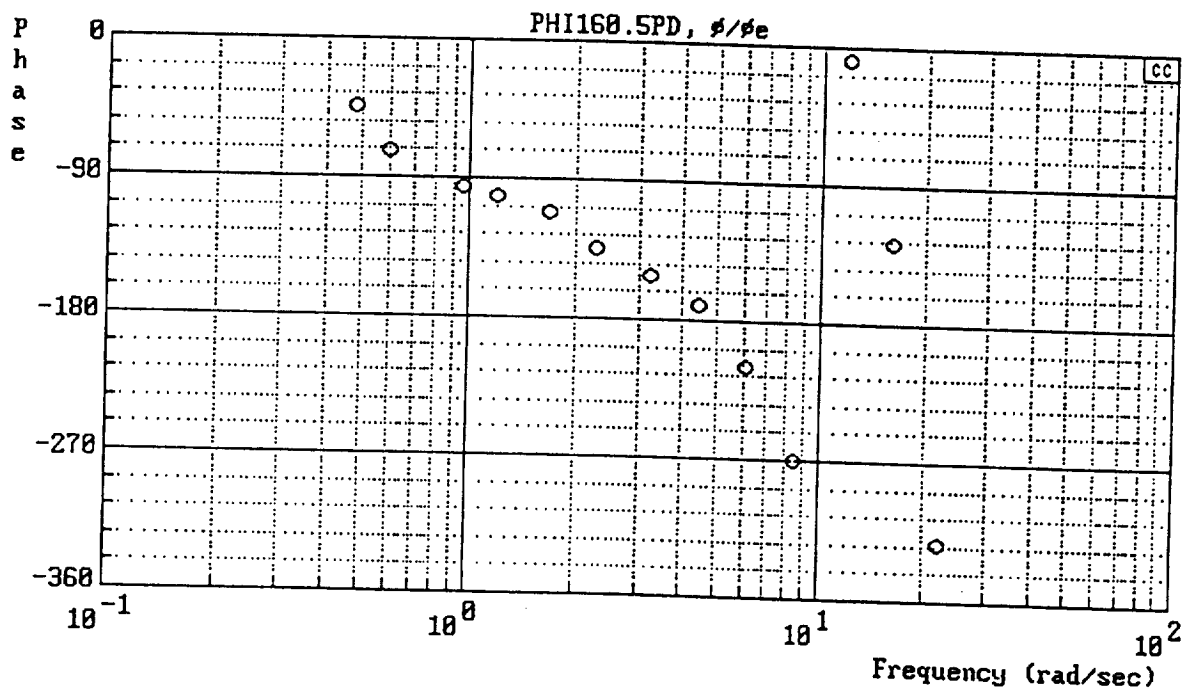
d) Y_pY_c (PHI/PHIE)

Figure B-19. (Concluded)

156

4161SOS.1

4161SOS.1
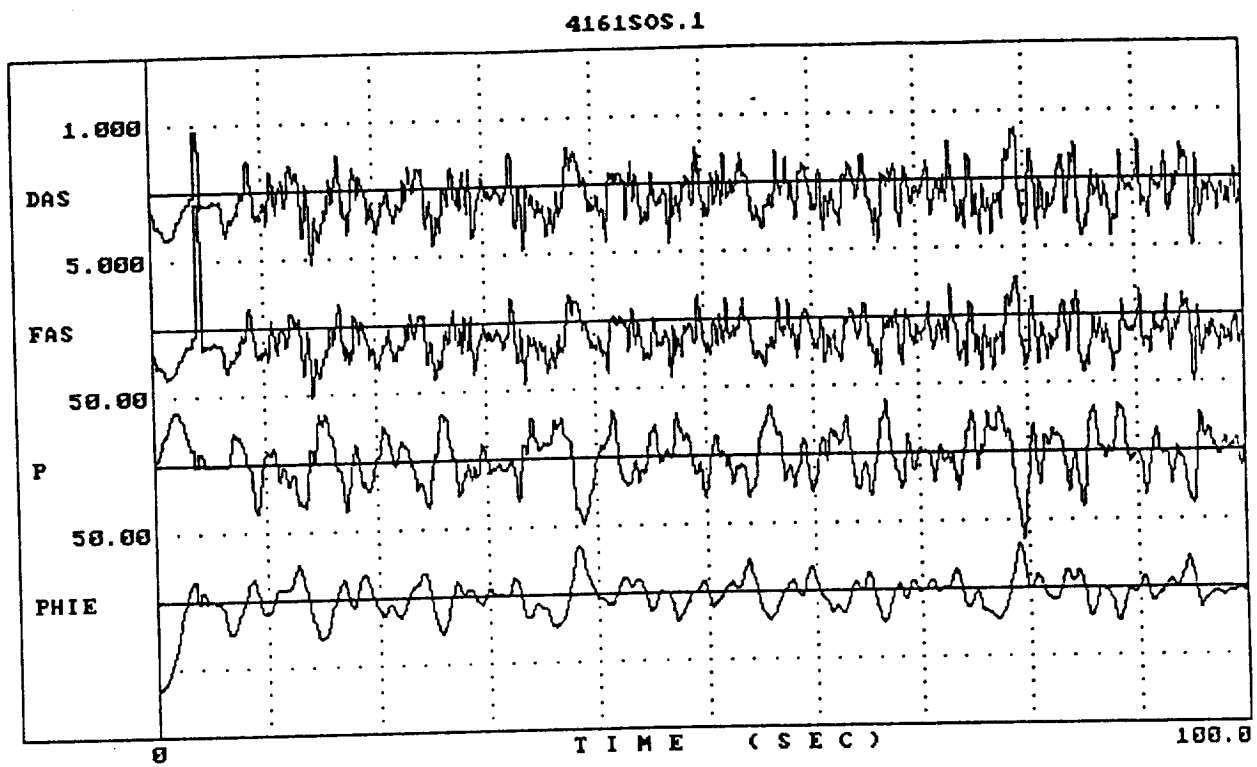
a) Time Histories

Figure B-20.   Flight 4161-1

157
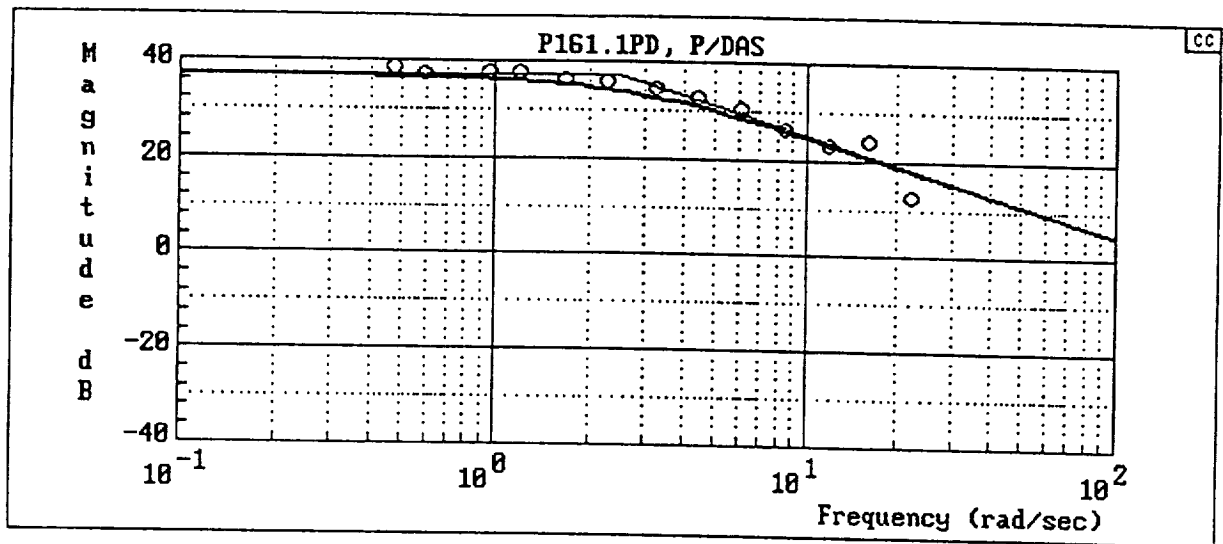
$$Y_c = \frac{180[-.8660254, 31.49183] [-.8660254, 86.60254]}{(2.5)[.8660254, 31.49183] [.8660254, 86.60254]}$$

b) Y_c (P/DAS)

Figure B-20. (Continued)

DAS161.1PD, DAS/FAS

$$Y_{FS} = \frac{169}{[\ .7,\ 26]}$$

DAS161.1PD, DAS/FAS

c) Y_{FS} (DAS/FAS)

Figure B-20. (Continued)

159

PHI161.1PD, ∮/∮e

PHI161.1PD, ∮/∮e
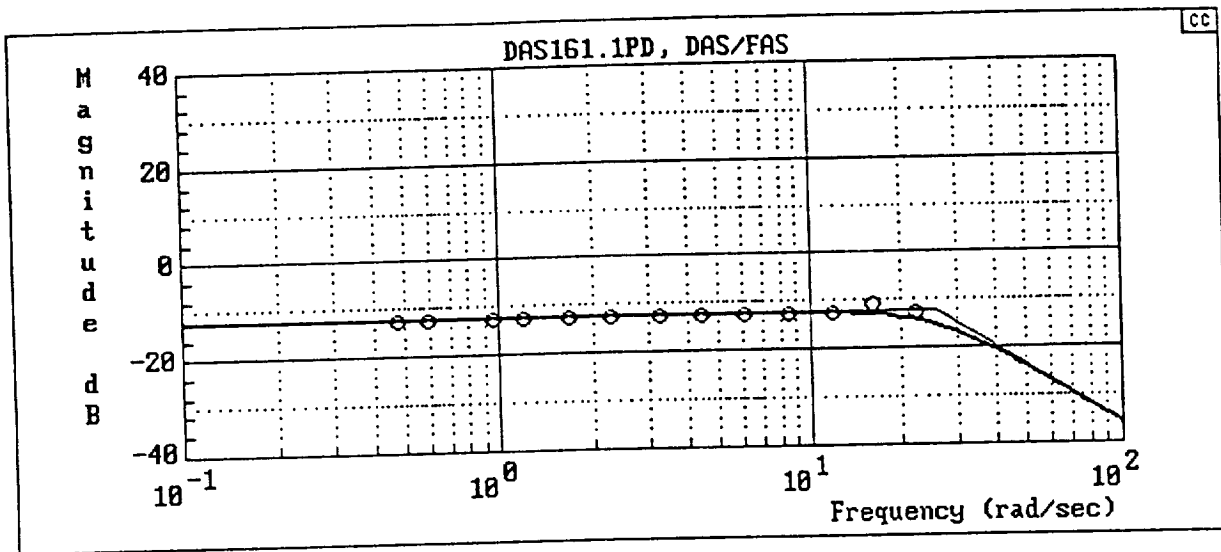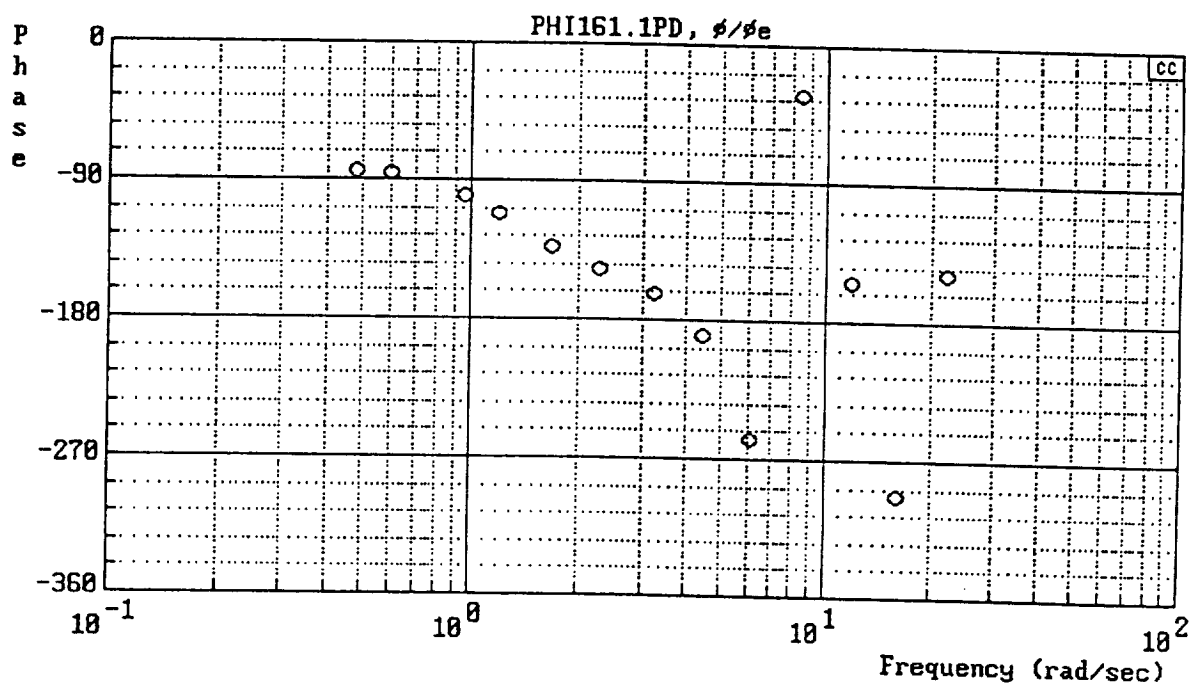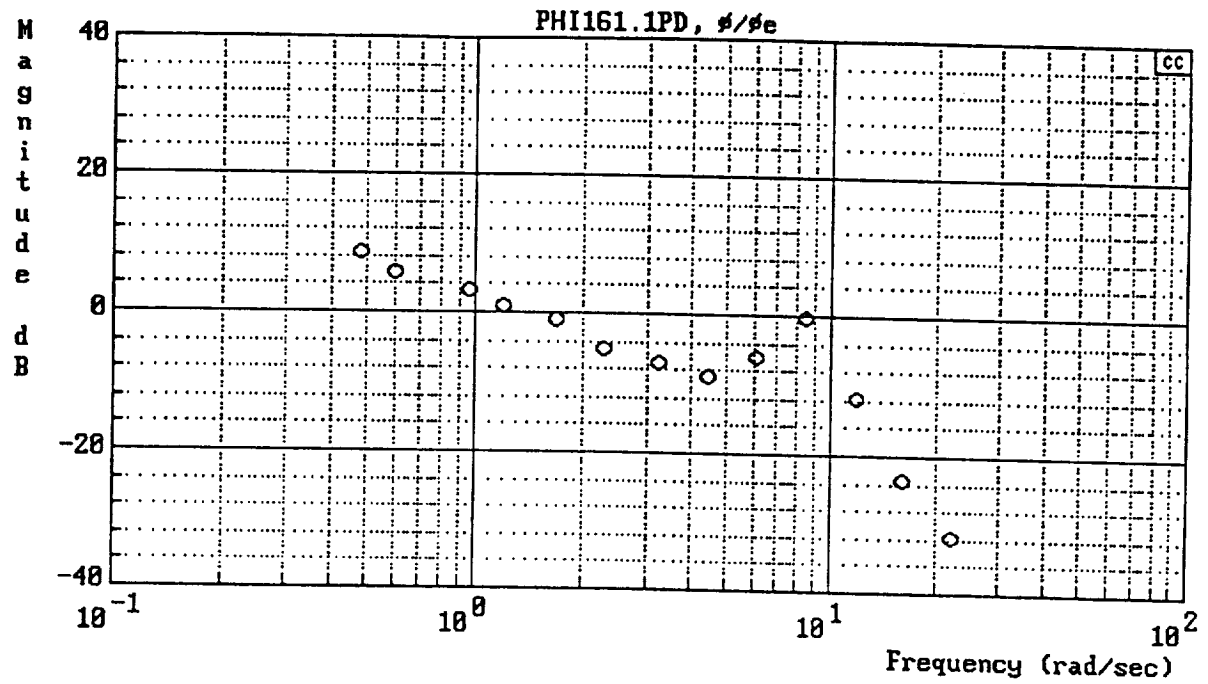
d) $Y_p Y_c$ (PHI/PHIE)

Figure B-20. (Concluded)

160

4161SOS.2

4161SOS.2
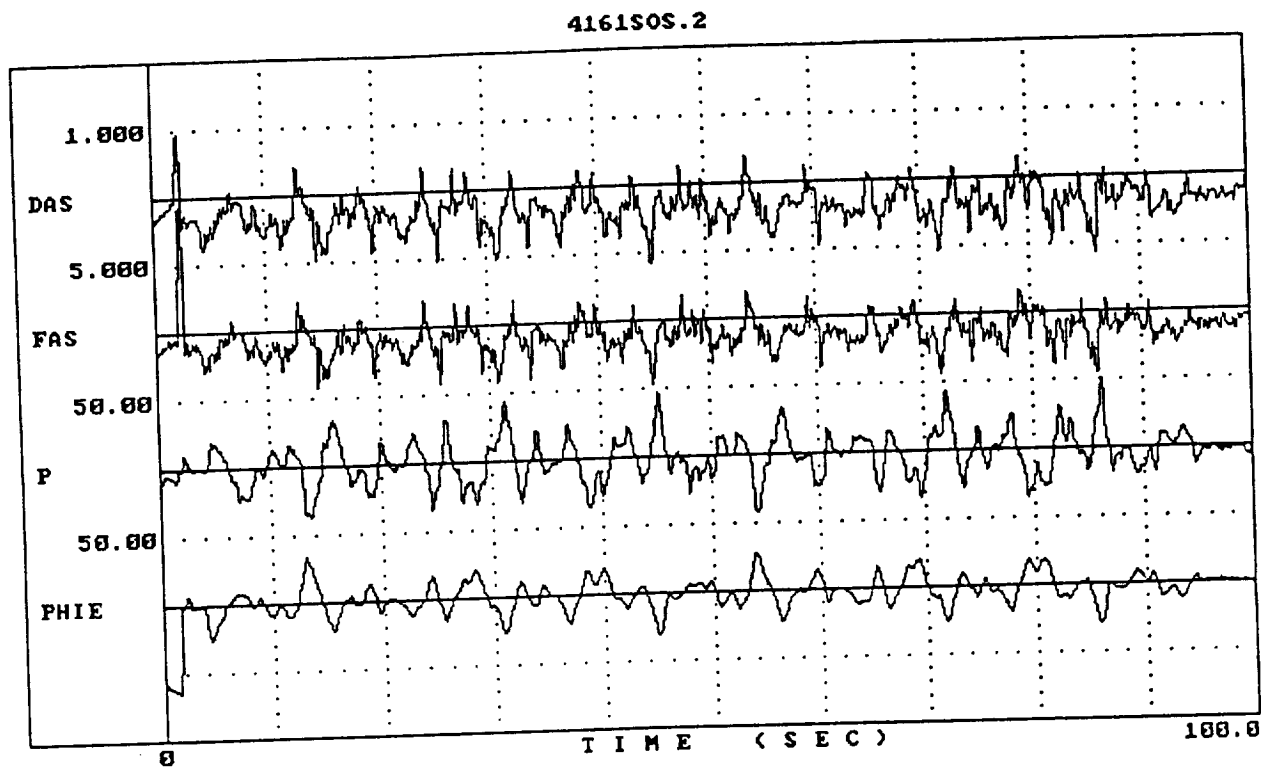
a) Time Histories

Figure B-21. Flight 4161-2
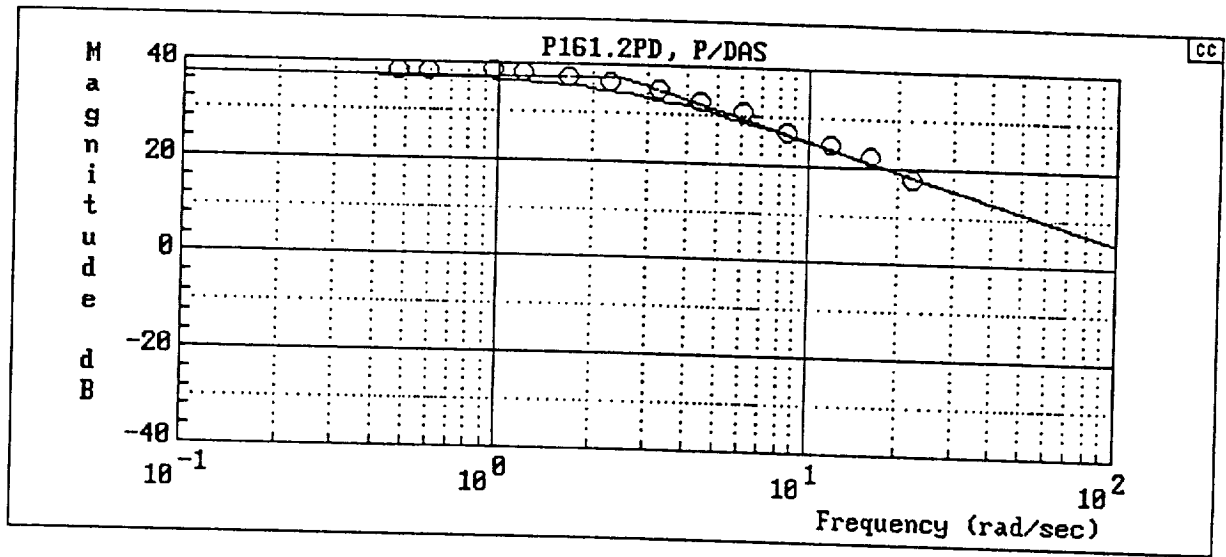
P161.2PD, P/DAS

$$Y_c = \frac{180[-.8660254, 86.60254]}{(2.5)[.8660254, 86.60254]}$$

P161.2PD, P/DAS

b) Y_c (P/DAS)

Figure B-21. (Continued)

DAS161.2TF, DAS/FAS

$$Y_{FS} = \frac{42.25}{[\ .7,\ 13]}$$

DAS161.2TF, DAS/FAS

c) Y_{FS} (DAS/FAS)

Figure B-21. (Continued)

163

PHI161.2PD, ϕ/ϕe

PHI161.2PD, ϕ/ϕe
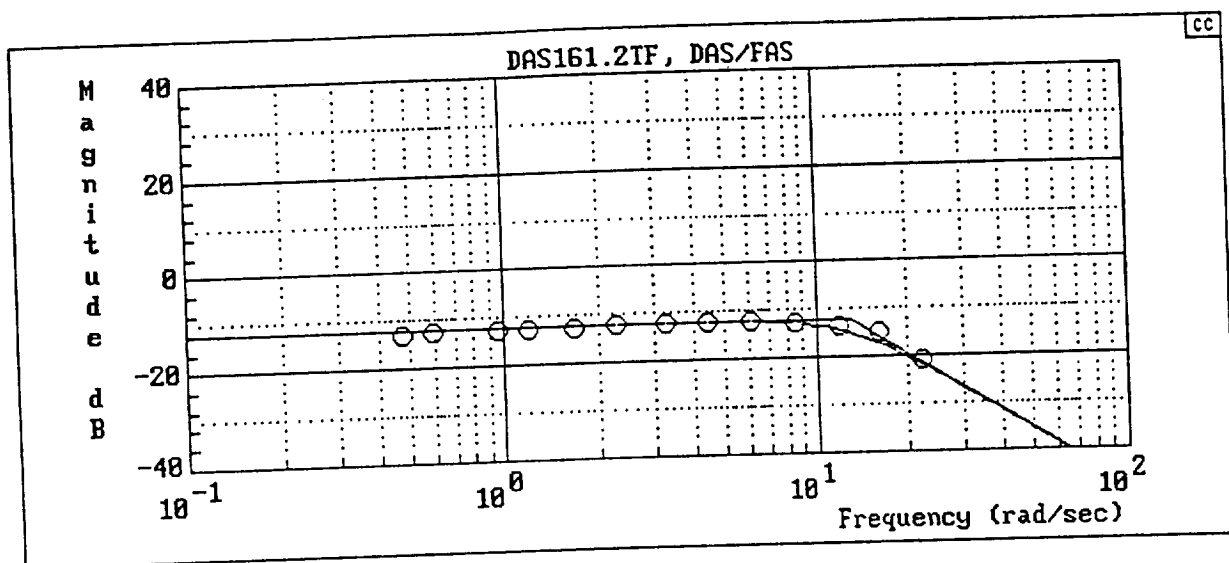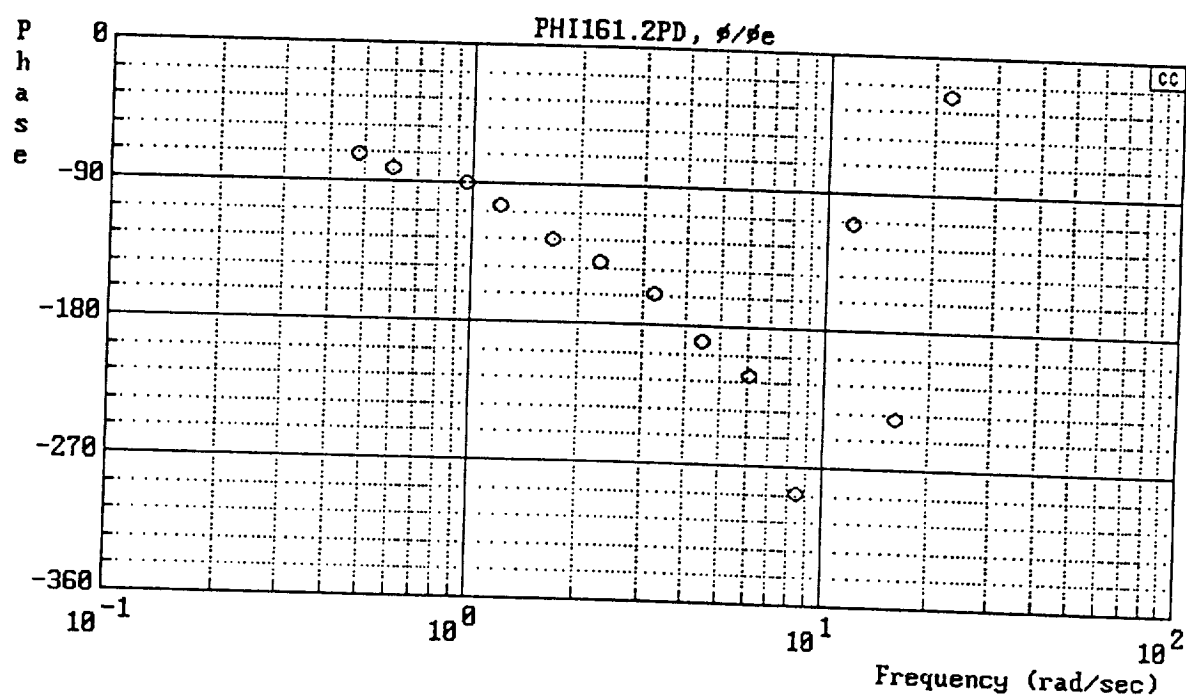
d) $Y_p Y_c$ (PHI/PHIE)

Figure B-21. (Concluded)

a) Time Histories

Figure B-22. Flight 4161-3

P161.3PD, P/DAS

$$Y_c = \frac{288[-.8660254, 62.98367] [-.8660254, 86.60254]}{(4)[.8660254, 62.98367] [.8660254, 86.60254]}$$

P161.3PD, P/DAS

b) Y_c (P/DAS)

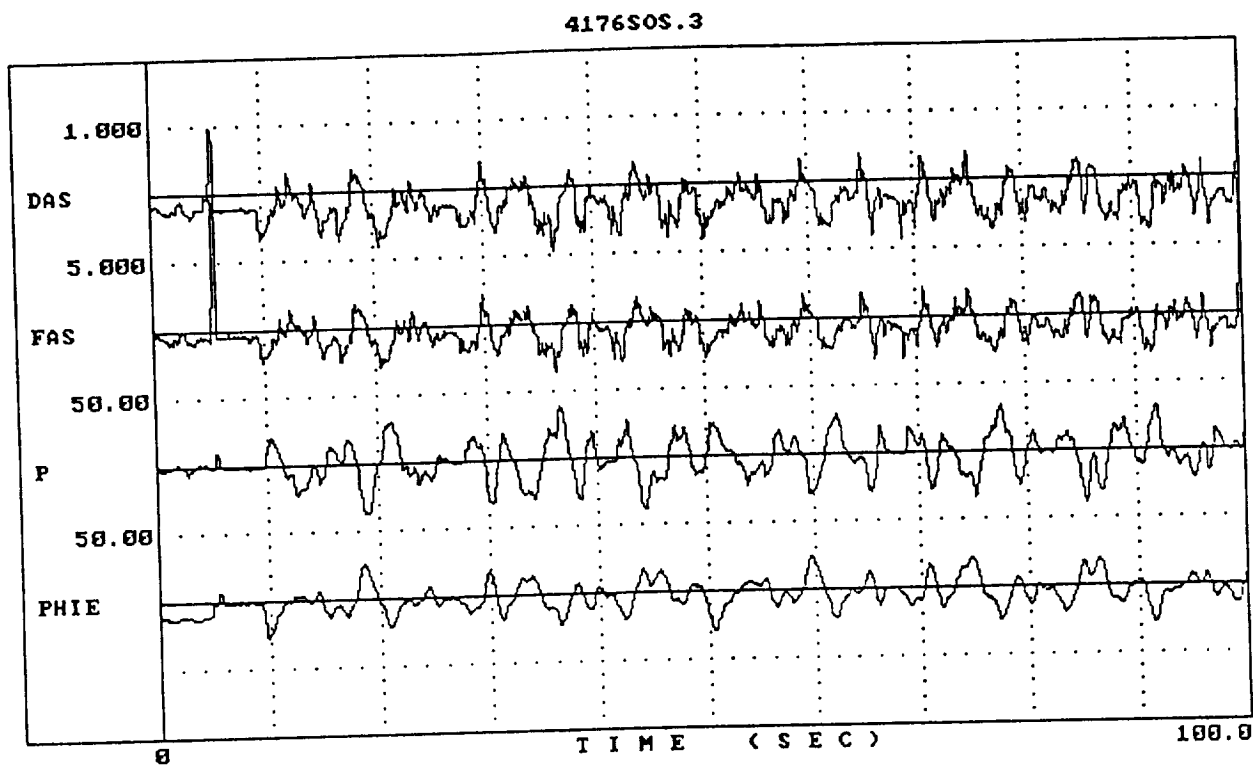Figure B-22. (Continued)

$$Y_{FS} = \frac{169}{[\ .7,\ 26]}$$
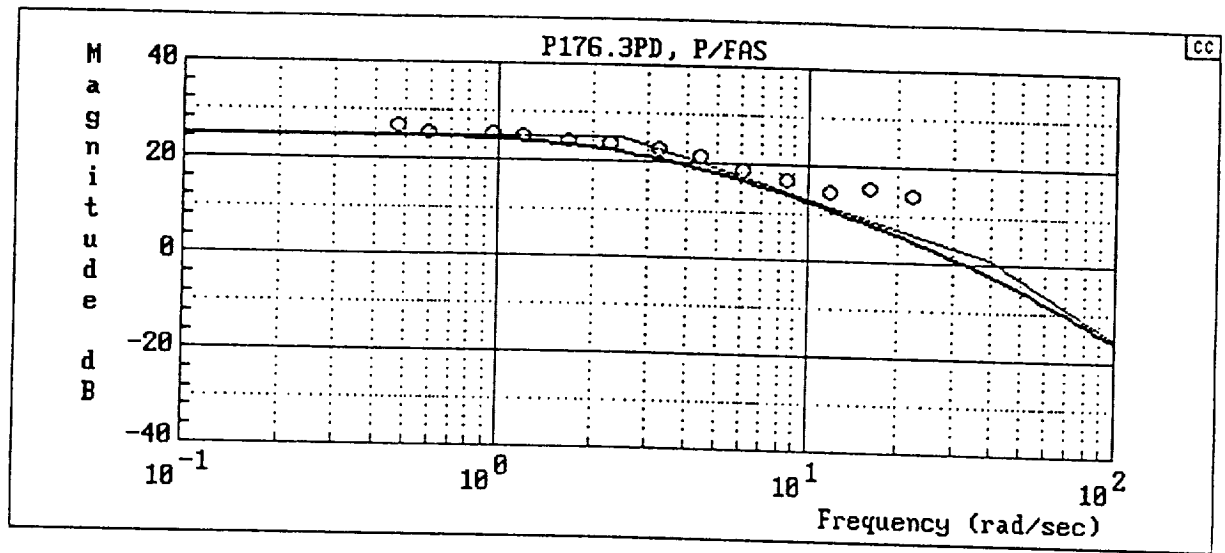

c) Y_{FS} (DAS/FAS)

Figure B-22. (Continued)

167

PHI161.3, ∮/∮e

PHI161.3, ∮/∮e
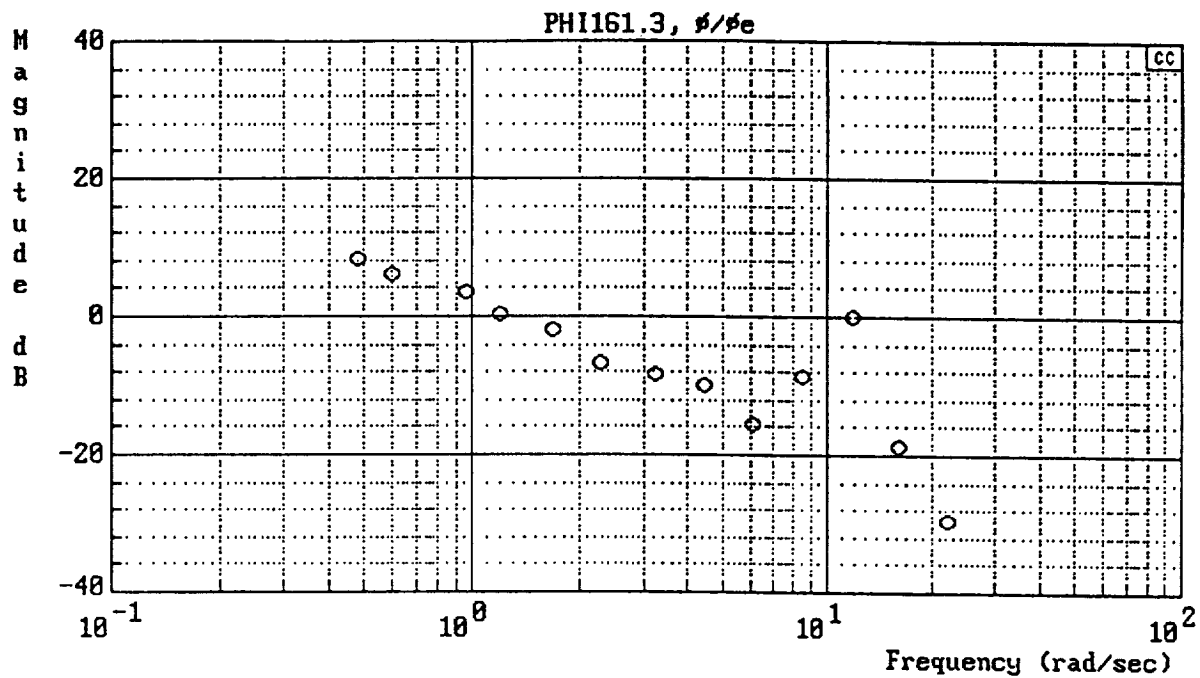
d) Y_pY_c (PHI/PHIE)

Figure B-22. (Concluded)
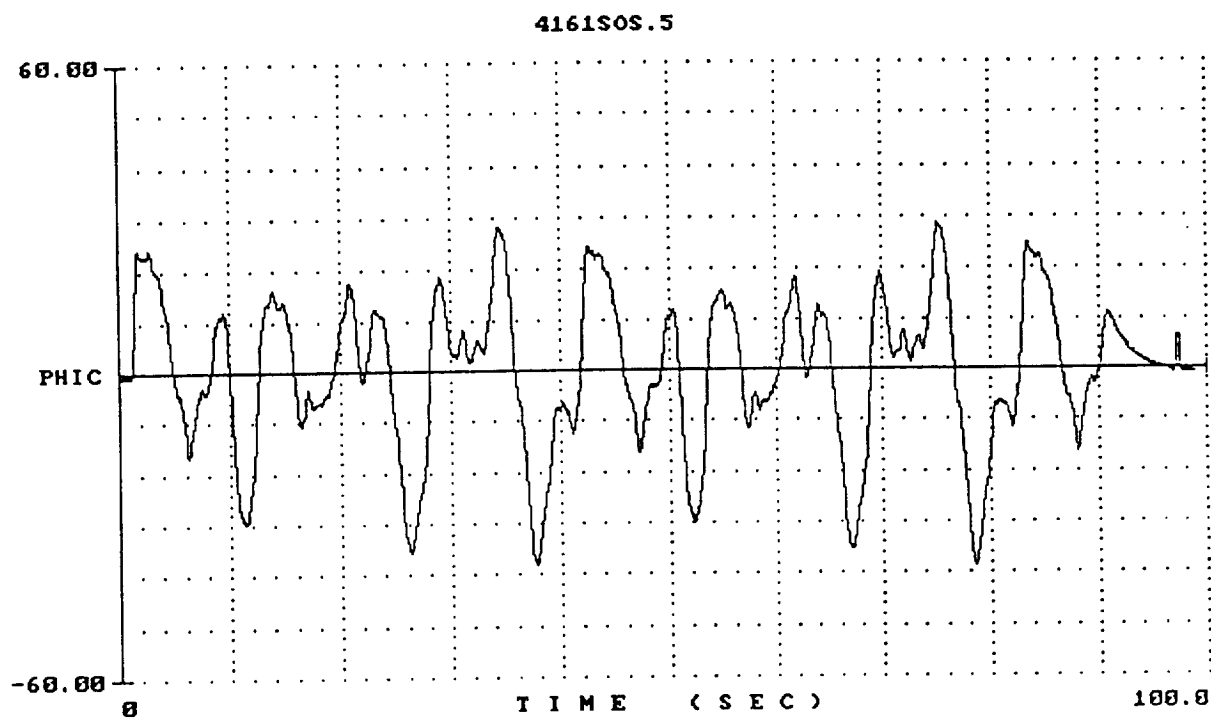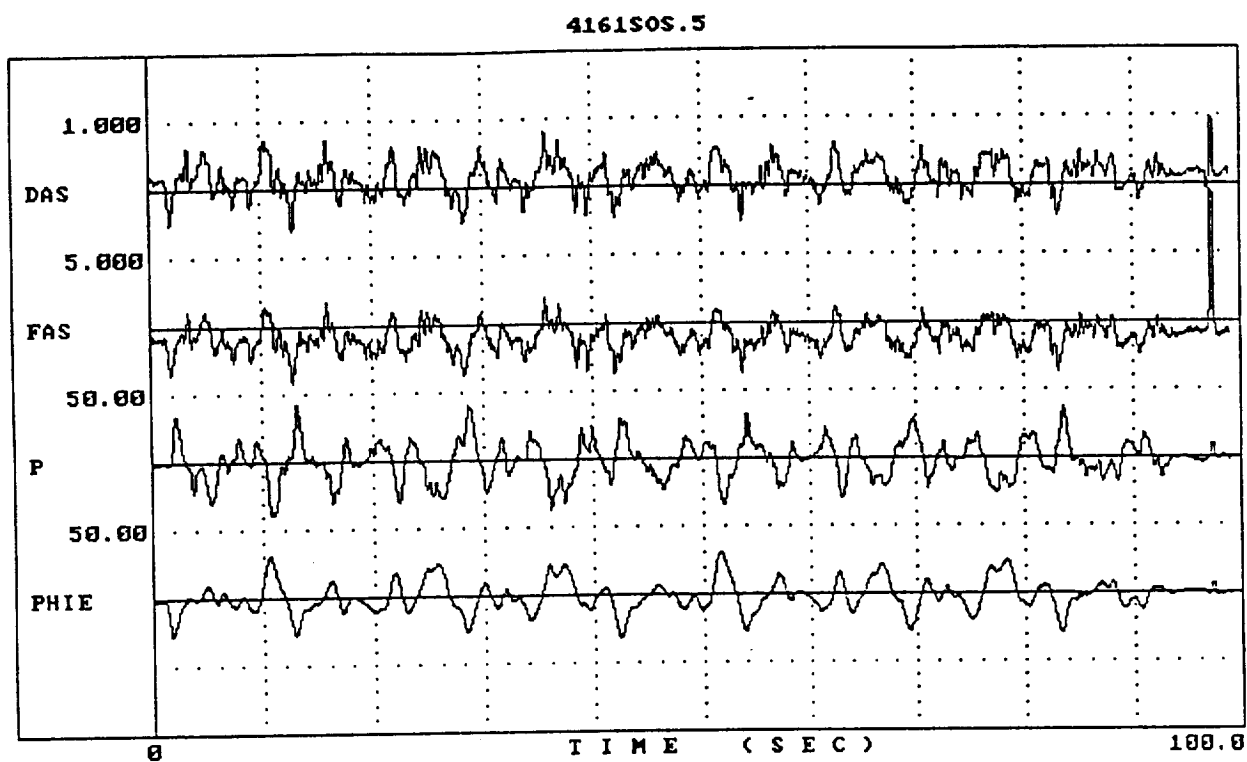
a) Time Histories

Figure B-23. Flight 4161-5

169
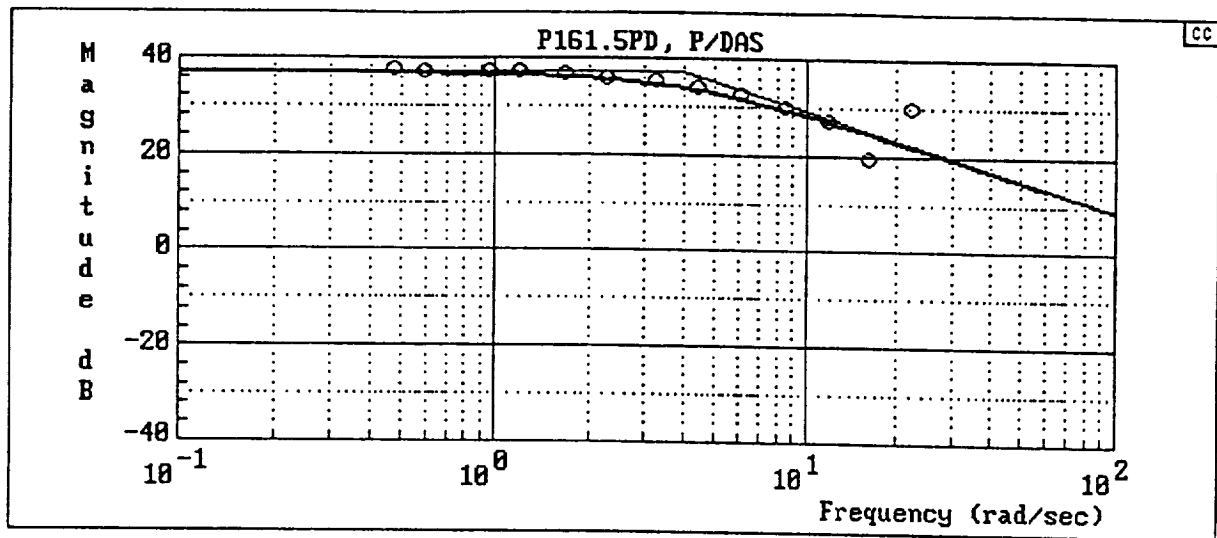
$$Y_c = \frac{288[-.8660254, \ 31.49183] \ [-.8660254, \ 86.60254]}{(\ 4)[\ .8660254, \ 31.49183] \ [\ .8660254, \ 86.60254]}$$
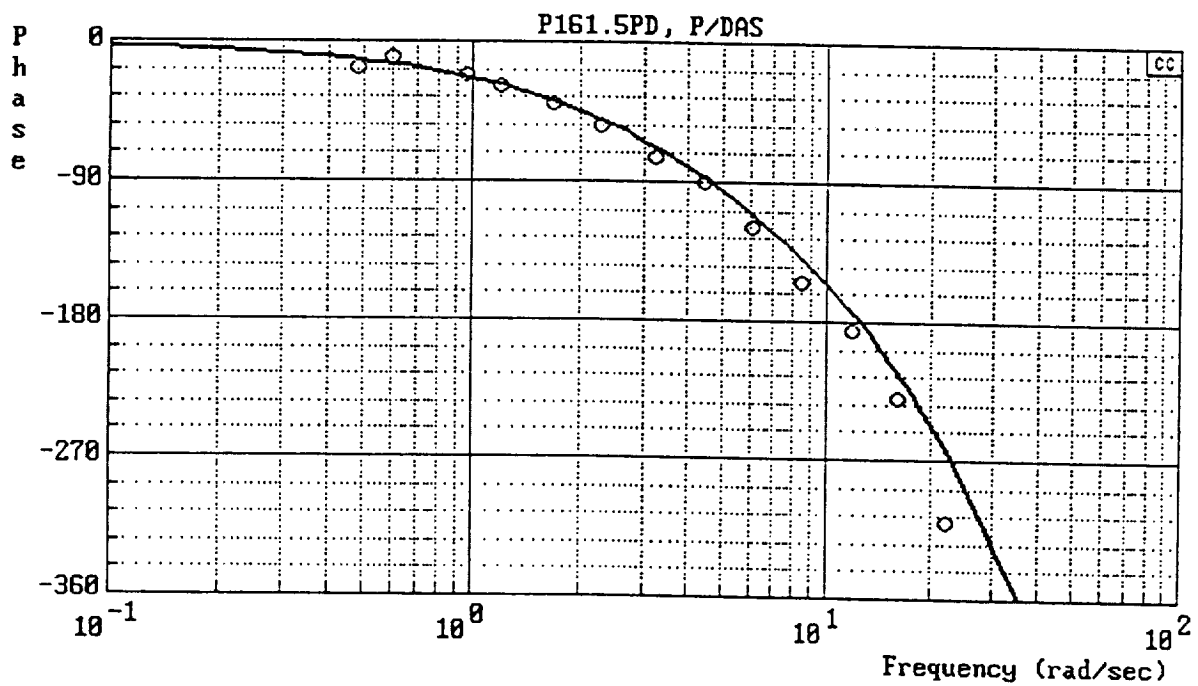
b) Y_c (P/DAS)

Figure B-23. (Continued)

DAS161.5PD, DAS/FAS

$$Y_{FS} = \frac{169}{[\ .7,\ 26]}$$

DAS161.5PD, DAS/FAS

c) Y_{FS} (DAS/FAS)

Figure B-23. (Continued)

171

PHI161.5PD, ∅/∅e

PHI161.5PD, ∅/∅e
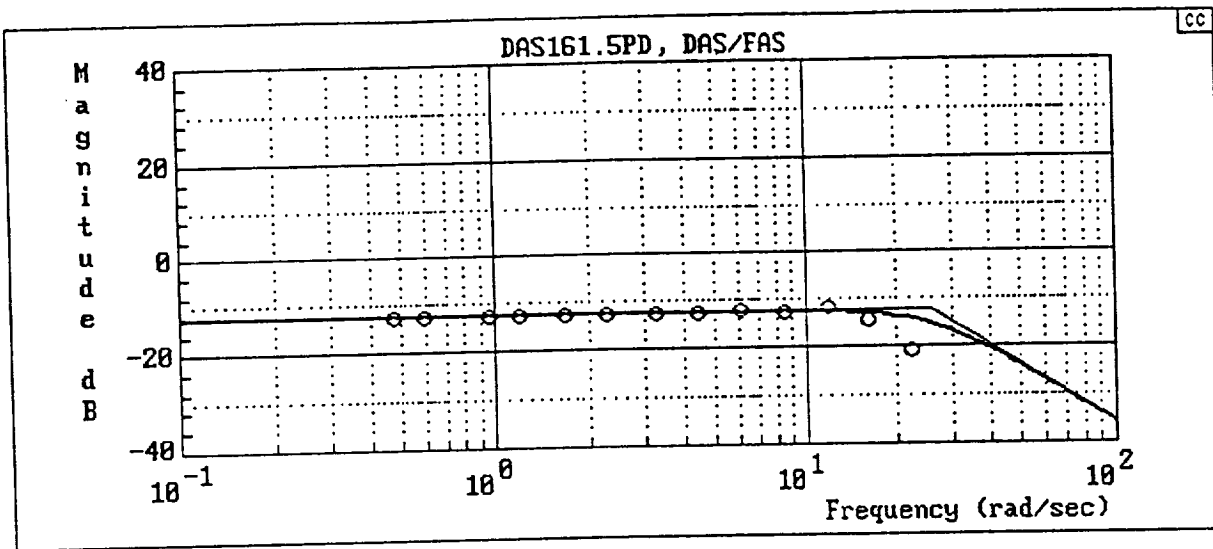
d) $Y_p Y_c$ (PHI/PHIE)
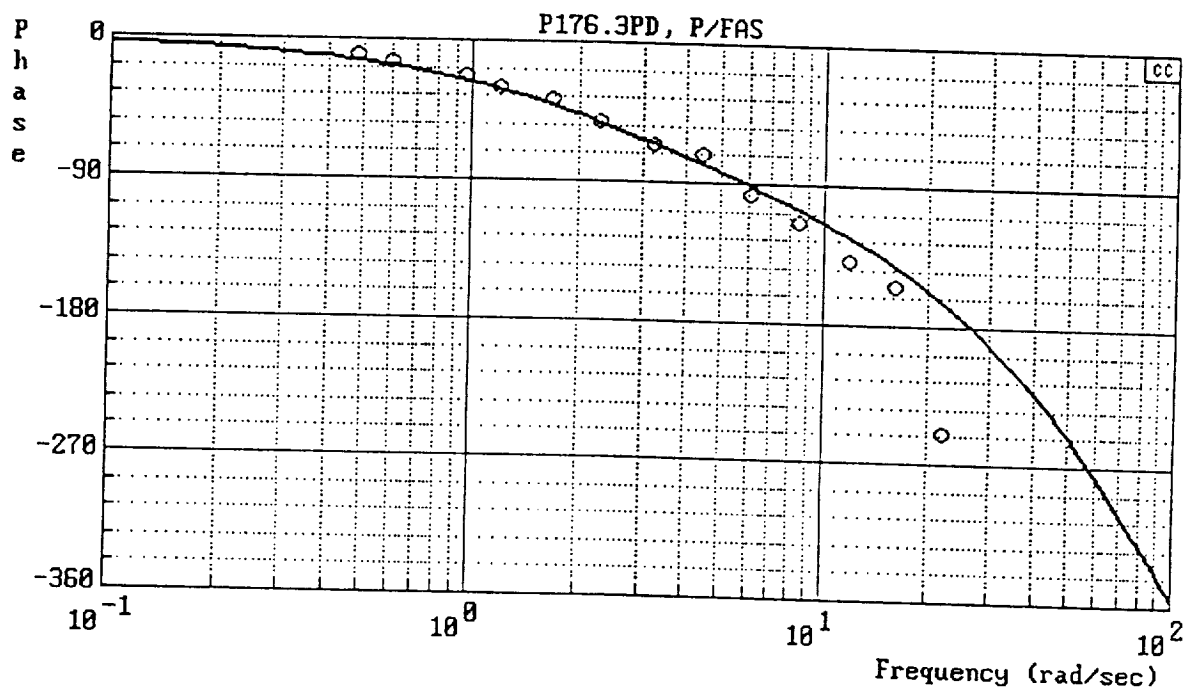
Figure B-23. (Concluded)

4176SOS.1

4176SOS.1

a) Time Histories

Figure B-24. Flight 4176-1

$$Y_c = \frac{48672[-.8660254, 86.60254]}{(4)[.7, 13][.8660254, 86.60254]}$$

b) Y_c (P/DAS)

Figure B-24. (Continued)
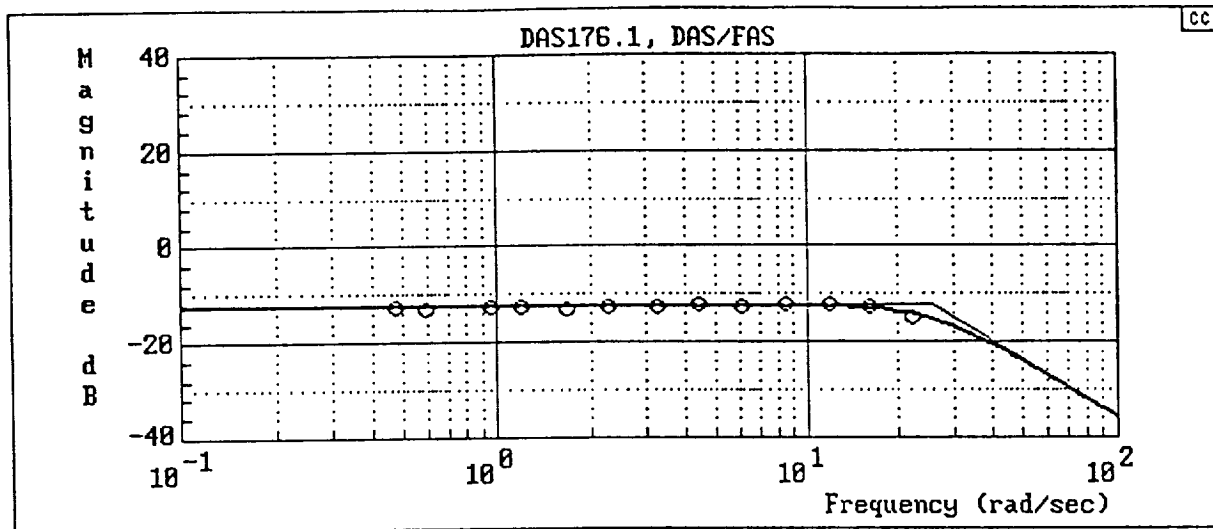
$$Y_{FS} = \frac{169}{[\ .7,\ 26]}$$
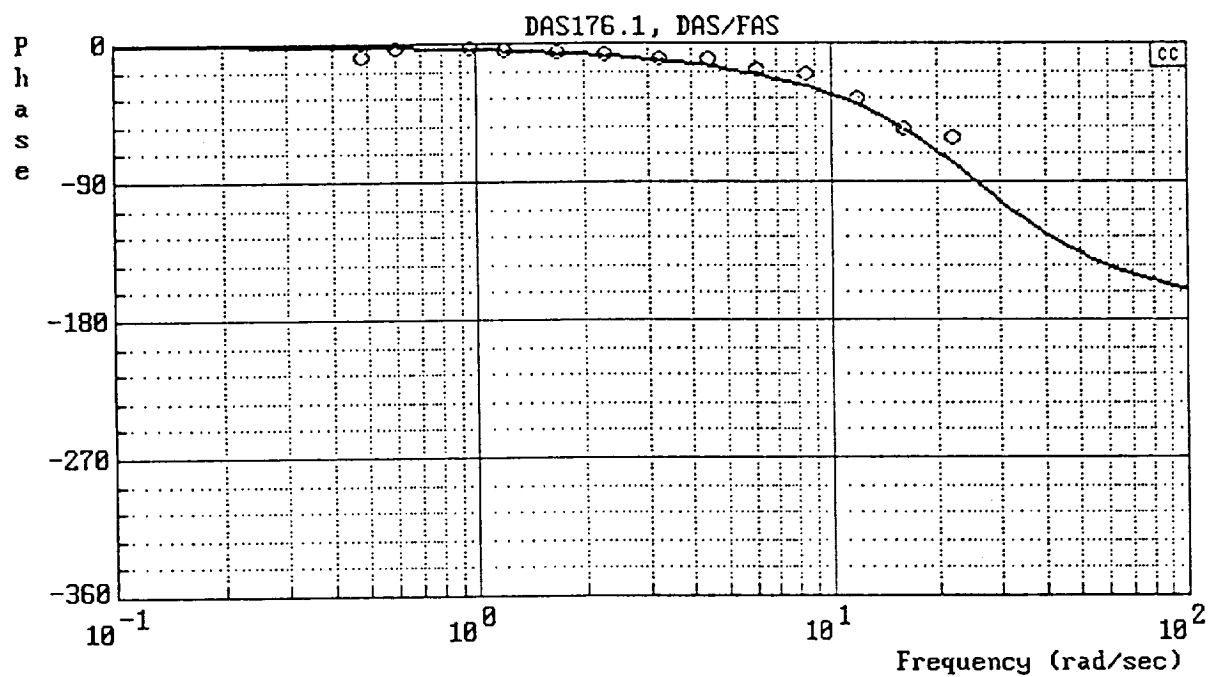
c) Y_{FS} (DAS/FAS)

Figure B-24. (Continued)

175
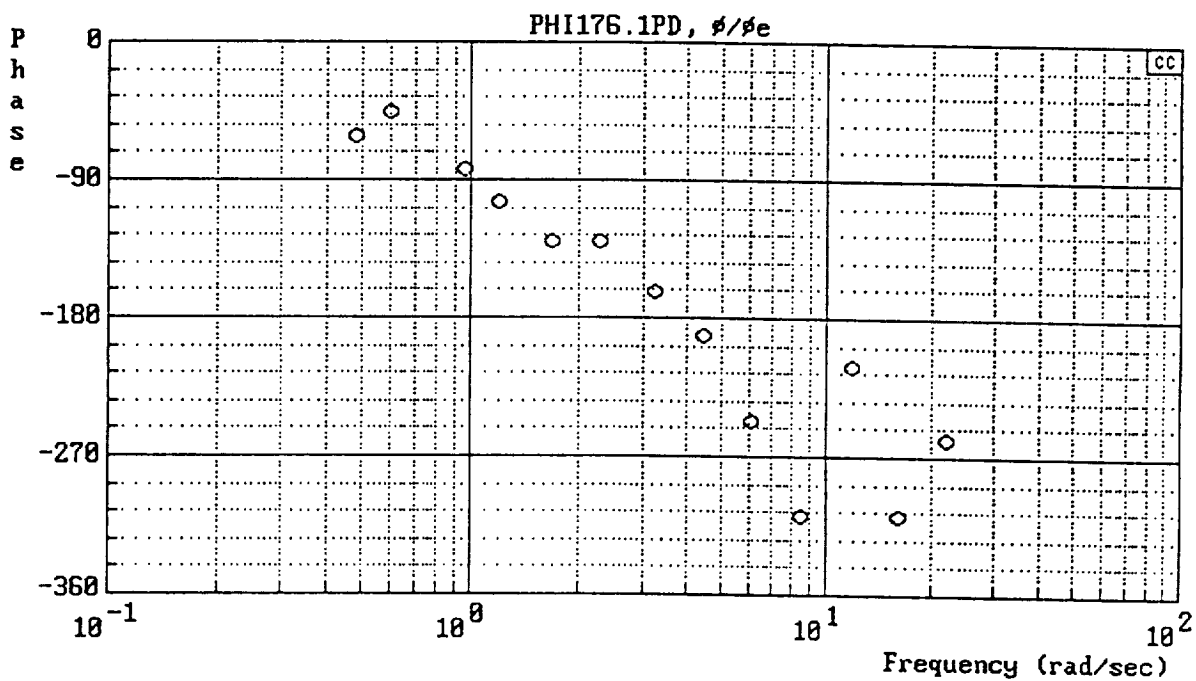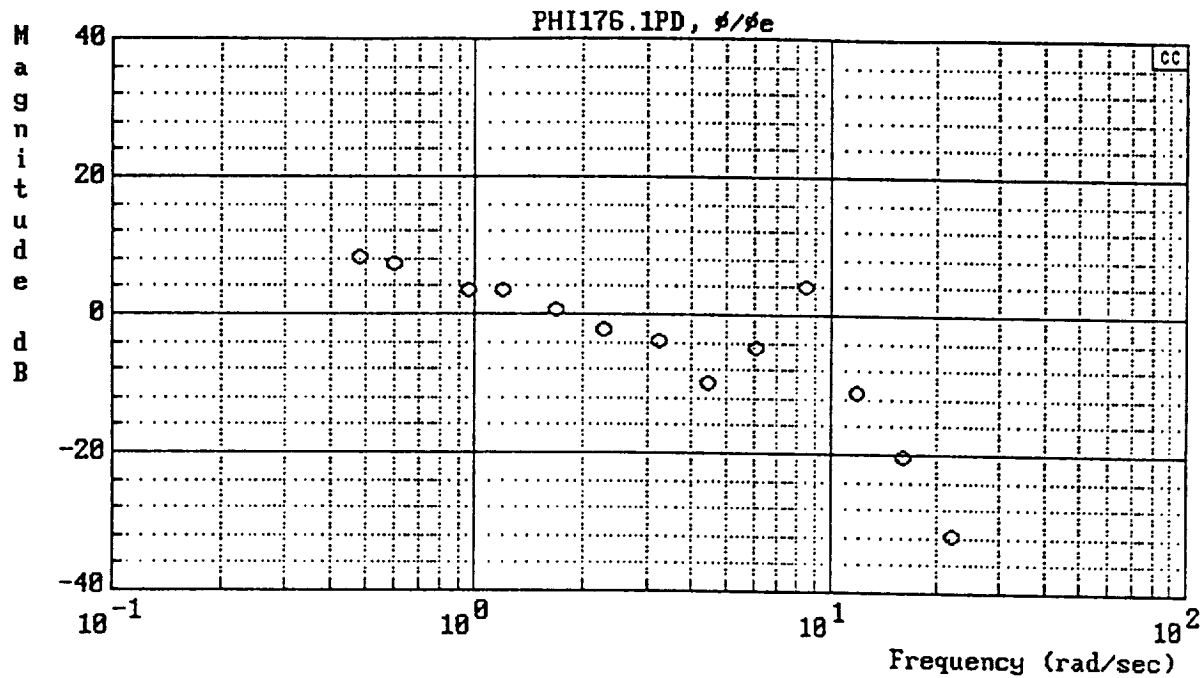
d) Y_pY_c (PHI/PHIE)

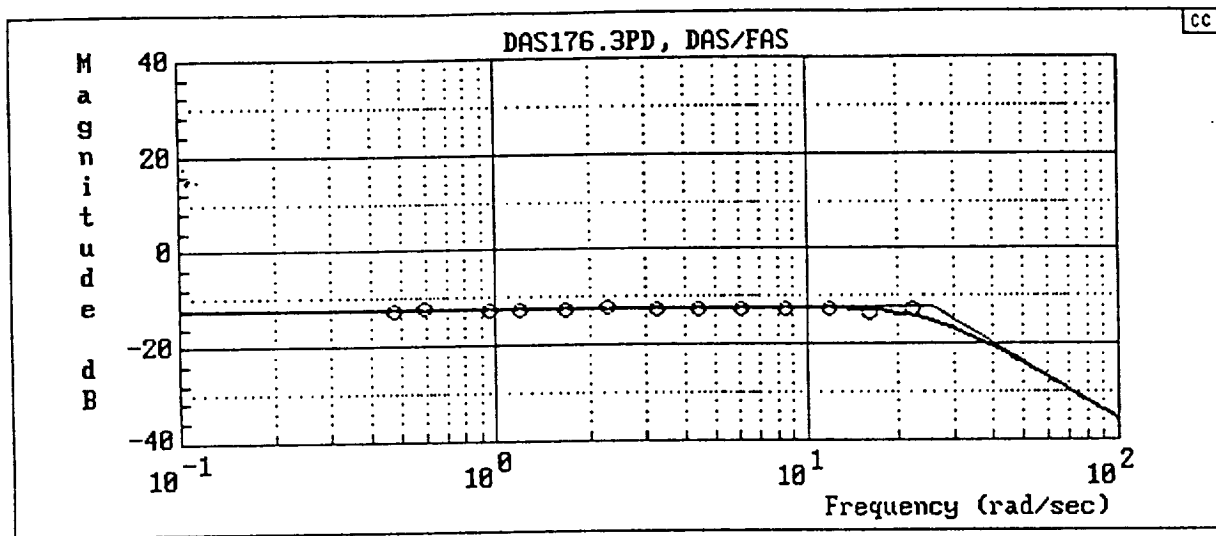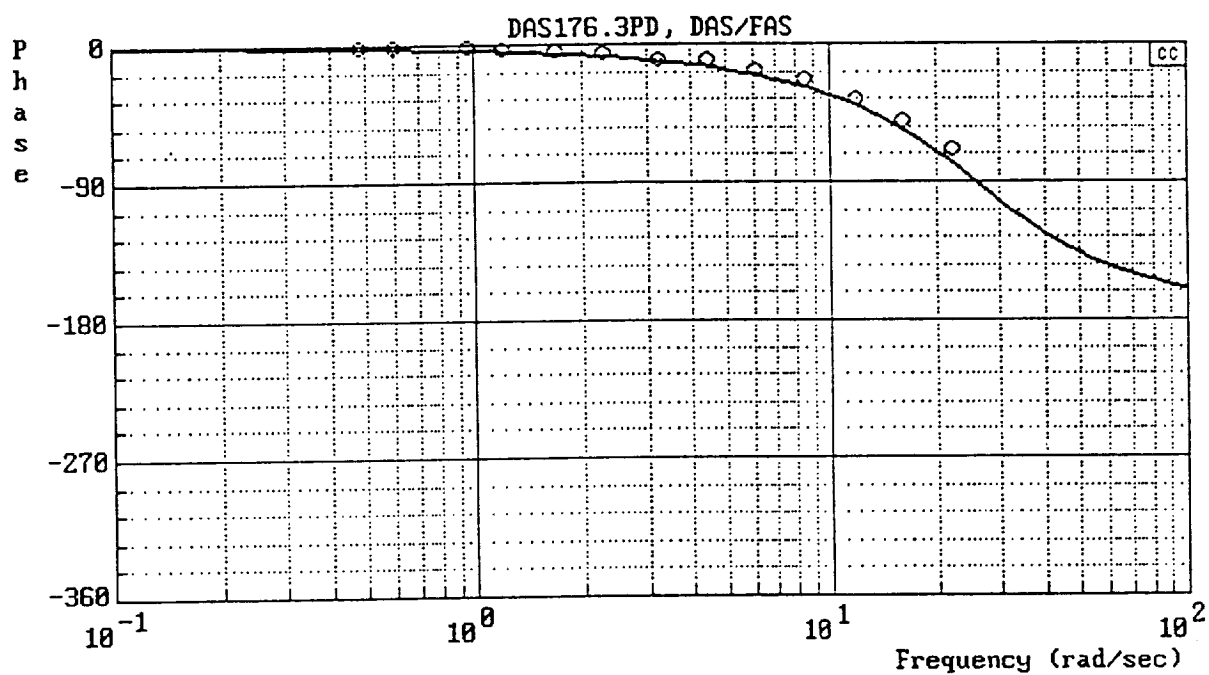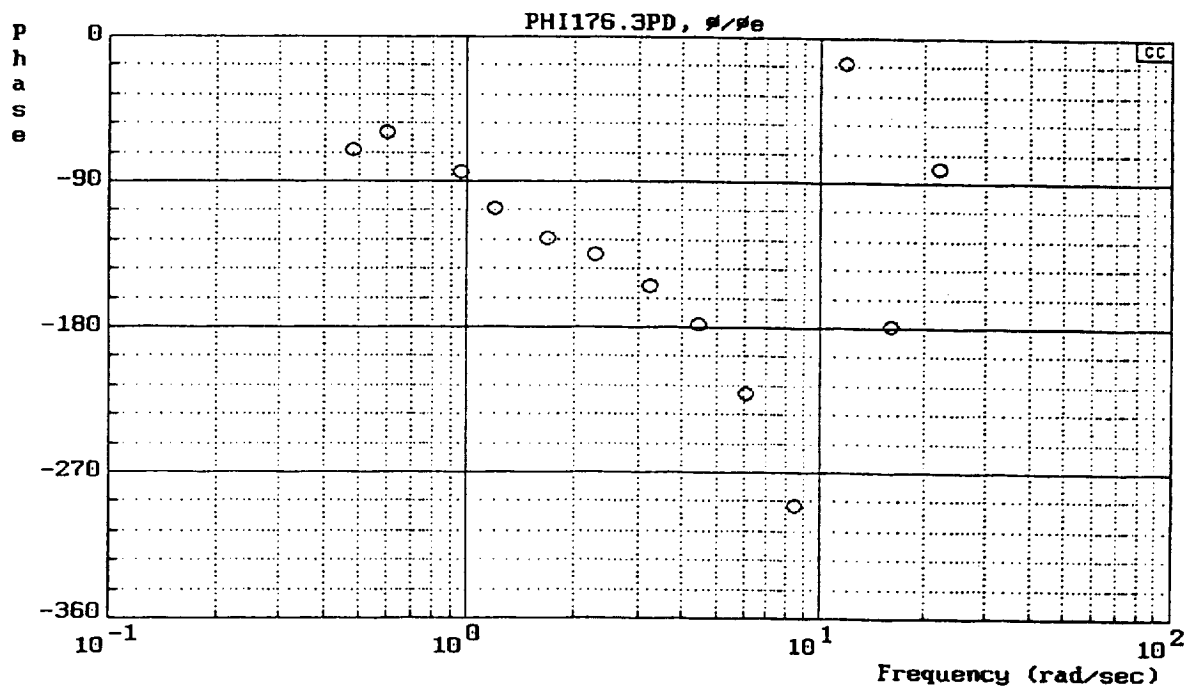Figure B-24. (Concluded)
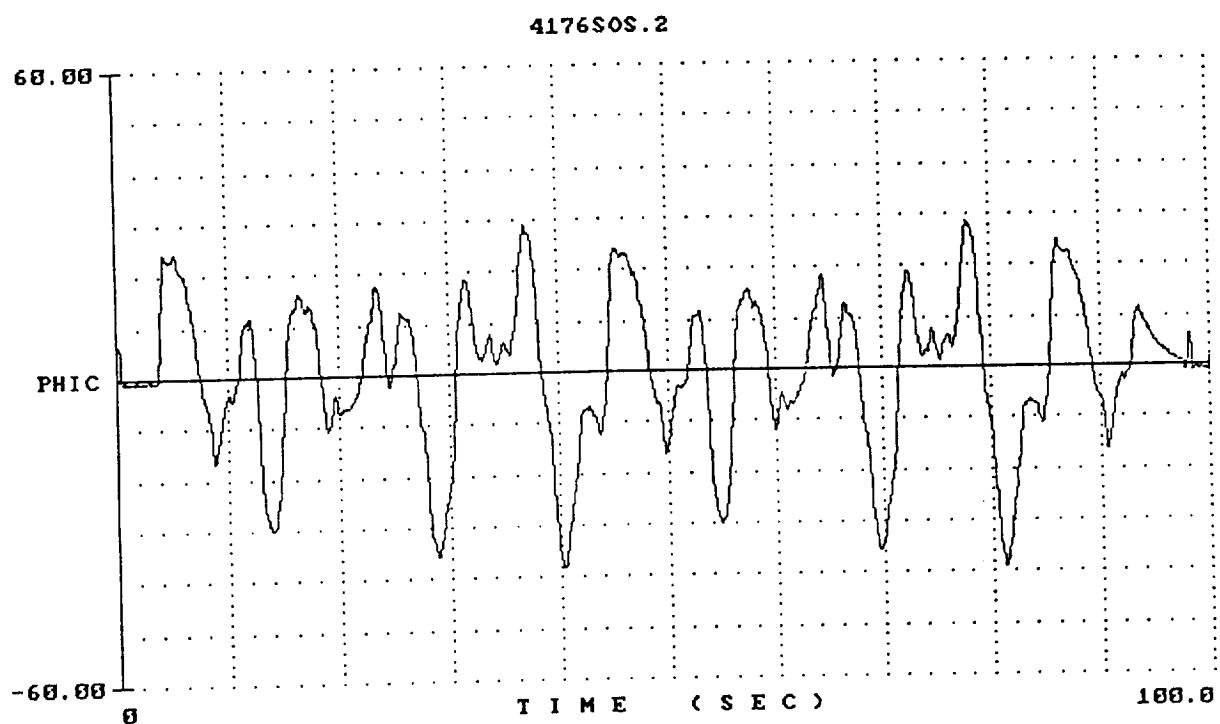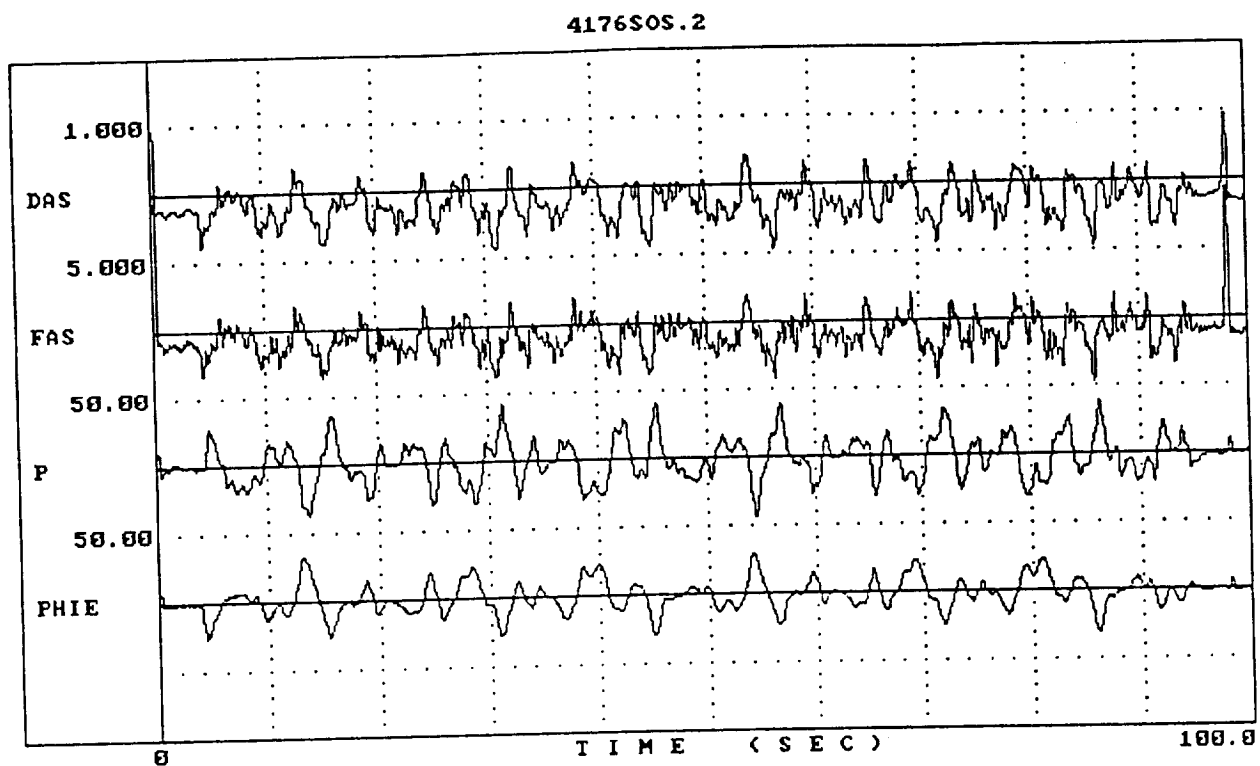
a) Time Histories

Figure B-25. Flight 4176-2

P176.2PD, P/DAS

$$Y_c = \frac{180[-.8660254, 86.60254]}{(2.5)[.8660254, 86.60254]}$$

P176.2PD, P/DAS
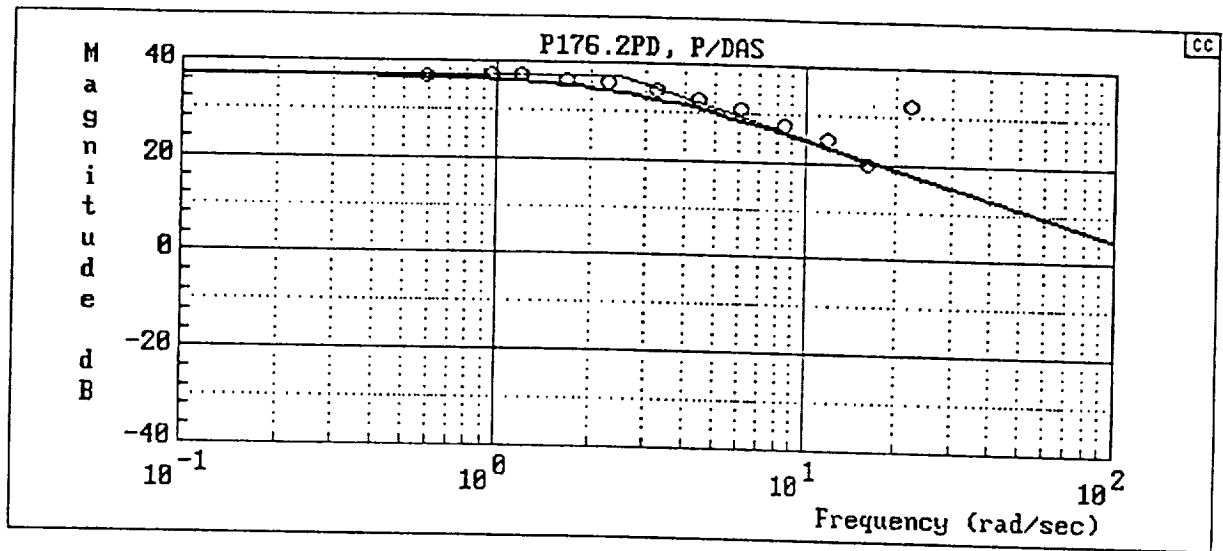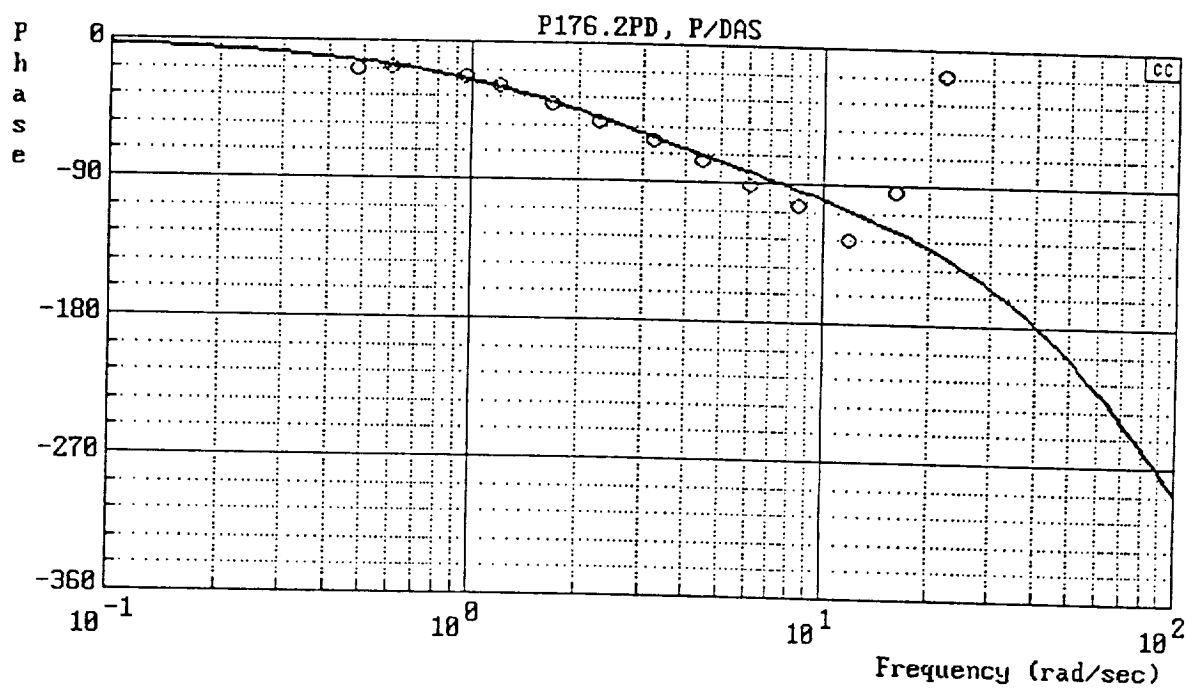
b) Y_c (P/DAS)

Figure B-25. (Continued)
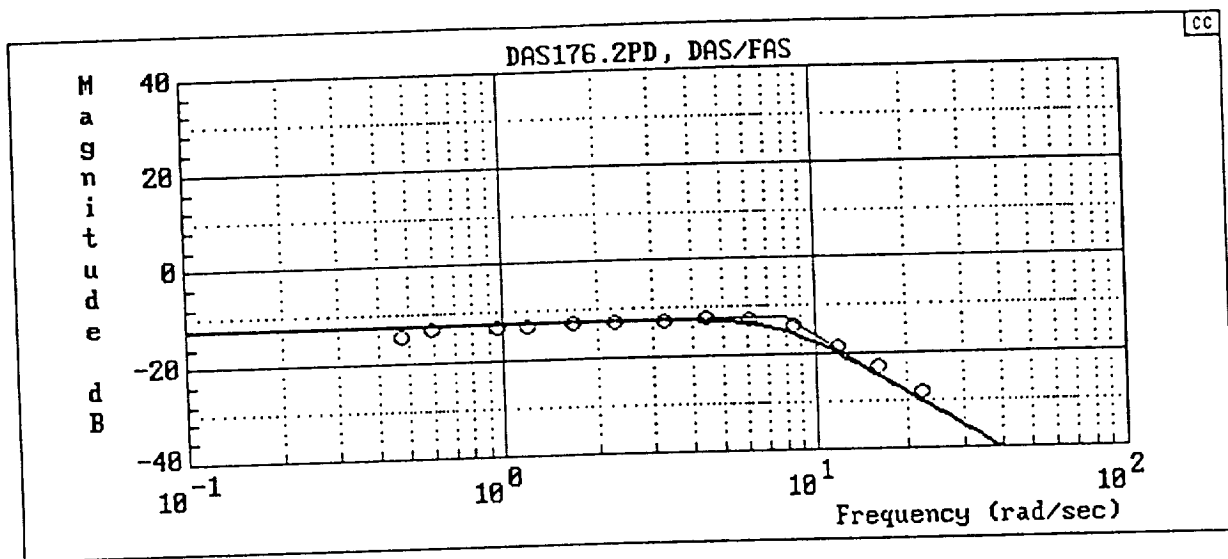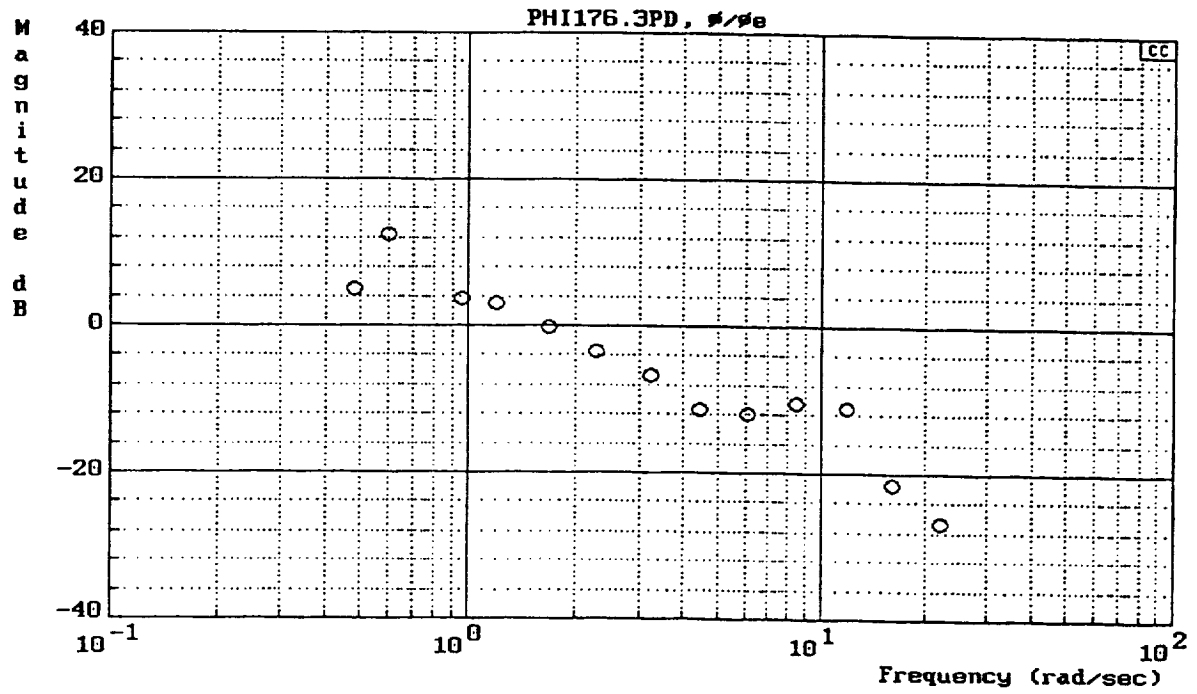
$$Y_{FS} = \frac{16}{[.7, 8]}$$
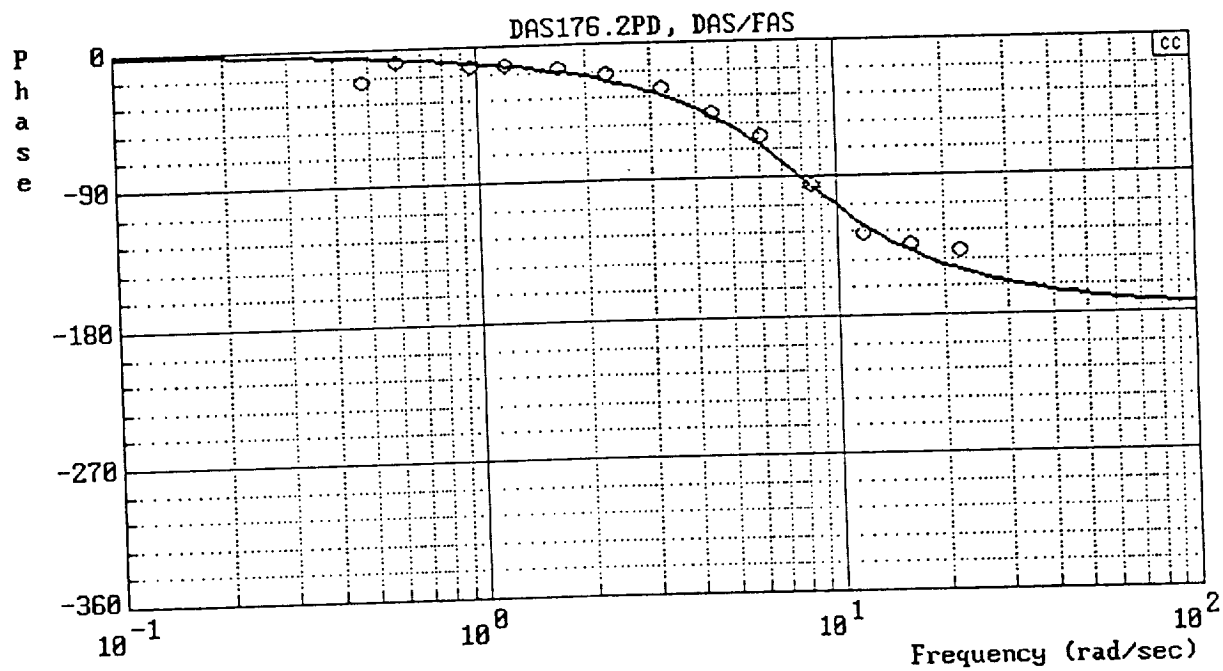
c) Y_{FS} (DAS/FAS)

Figure B-25. (Continued)
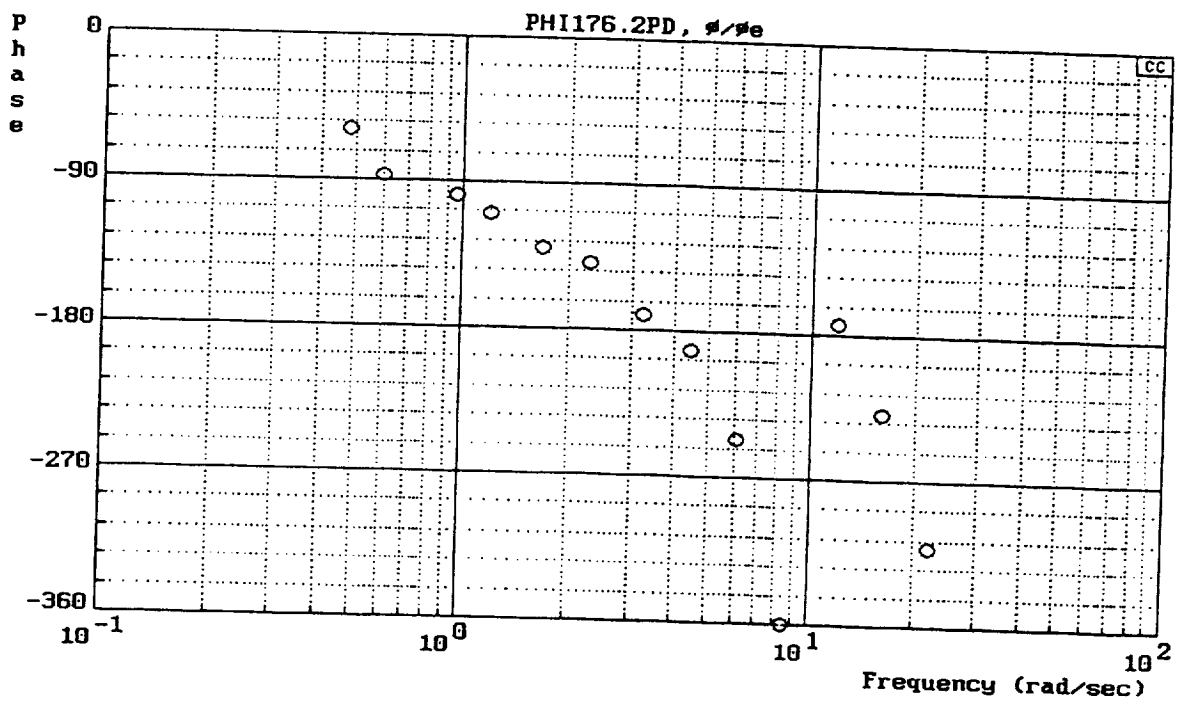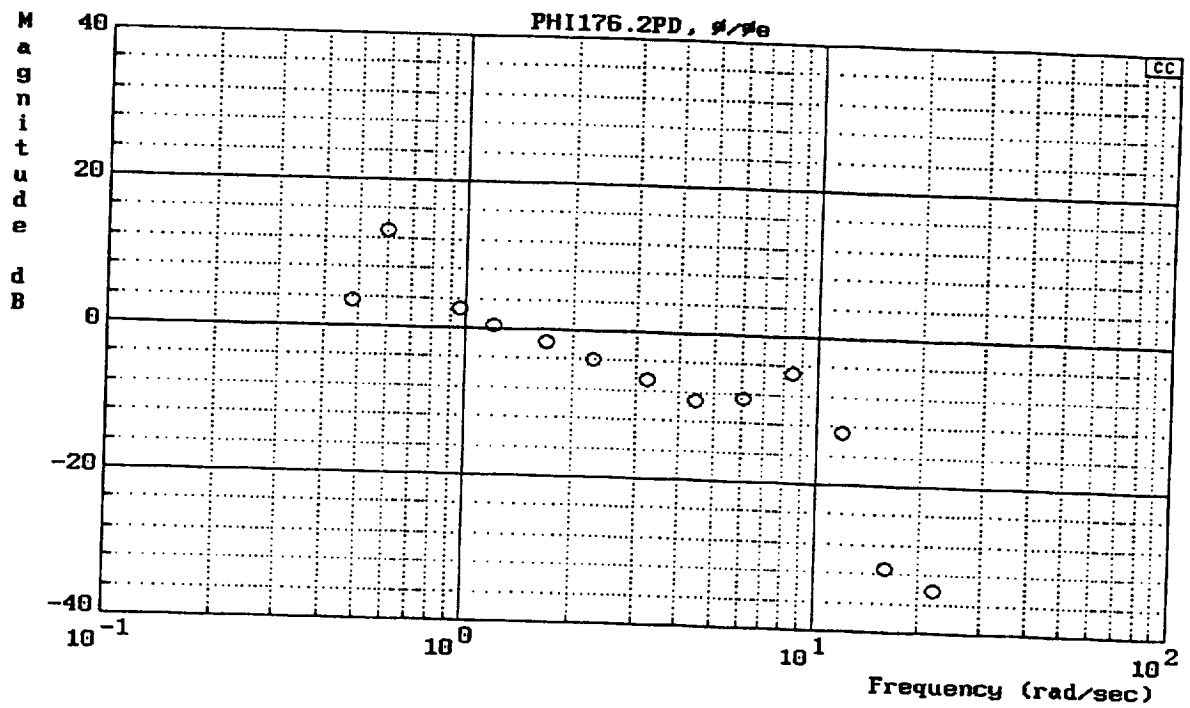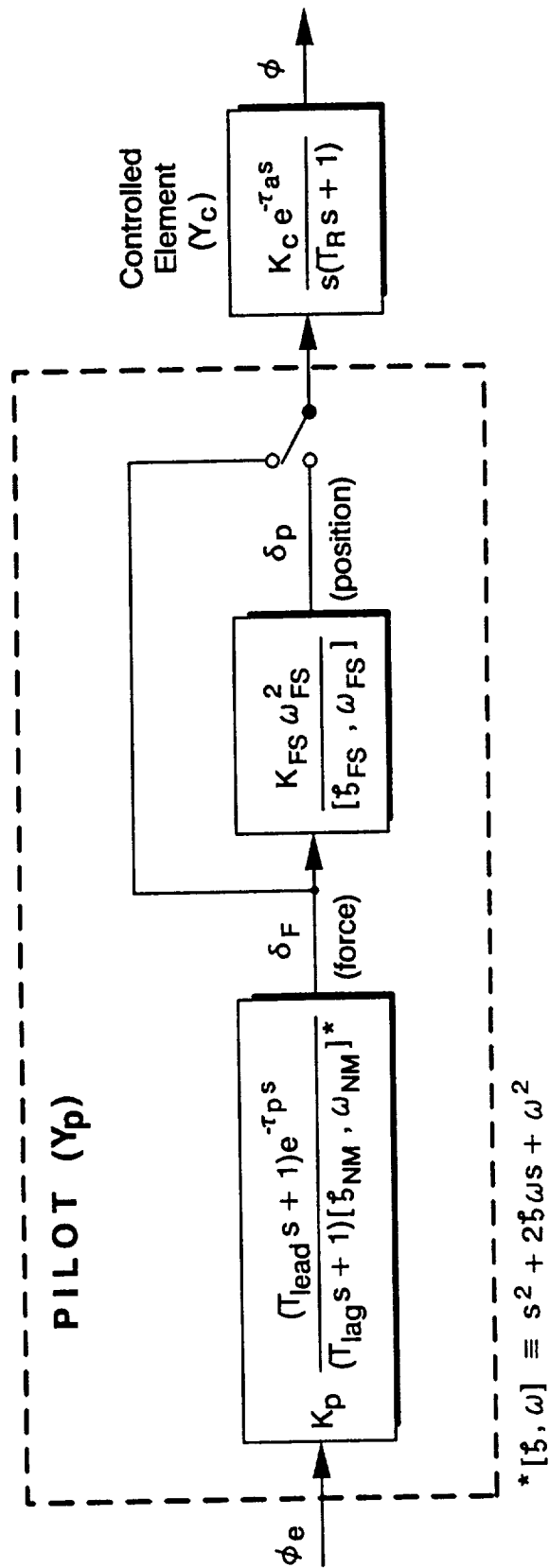
d) $Y_p Y_c$ (PHI/PHIE)

Figure B-25. (Concluded)

4176SOS.3
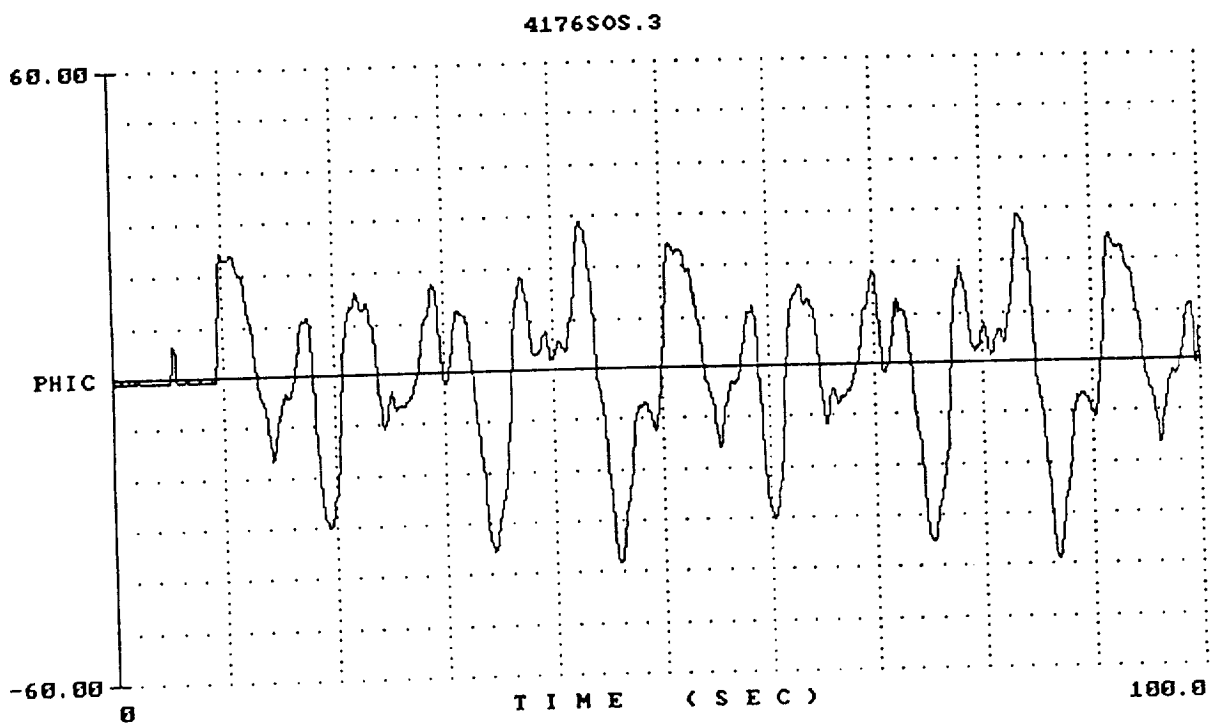
a) Time Histories

Figure B-26. Flight 4176-3

181

P176.3PD, P/FAS

$$Y_c = \frac{1800[-.8660254, 86.60254]}{(2.5)(40)[.8660254, 86.60254]}$$

P176.3PD, P/FAS

b) Y_c (P/FAS)

Figure B-26. (Continued)

DAS176.3PD, DAS/FAS

$$Y_{FS} = \frac{169}{[\ .7,\ 26]}$$

DAS176.3PD, DAS/FAS

c) Y_{FS} (DAS/FAS)

Figure B-26. (Continued)

183

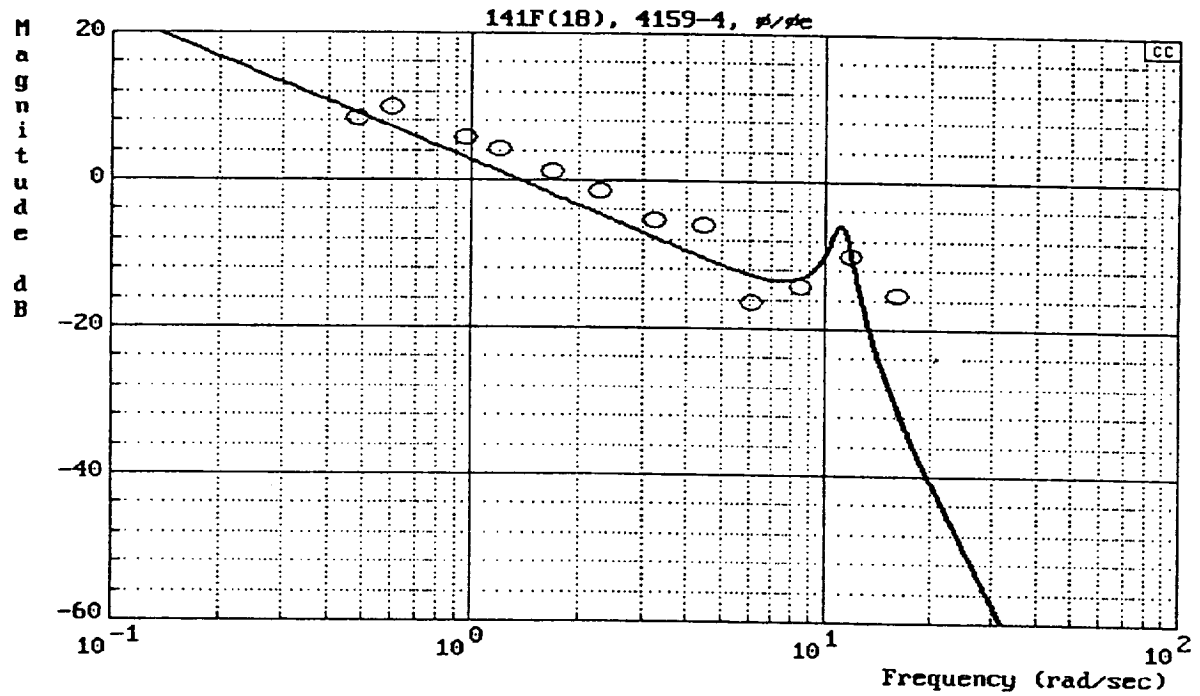d) Y_pY_c (PHI/PHIE)

Figure B-26. (Concluded)

Figure C-1. Open-Loop Pilot/Vehicle Model

$$\frac{\phi}{\phi_e} = \frac{0.0014\,[-0.866,\,28.2][-0.866,\,105](3.36E+7)}{(0)(6.67)[0.0603,\,11.3][0.866,\,28.2](40)[0.866,\,105]}$$
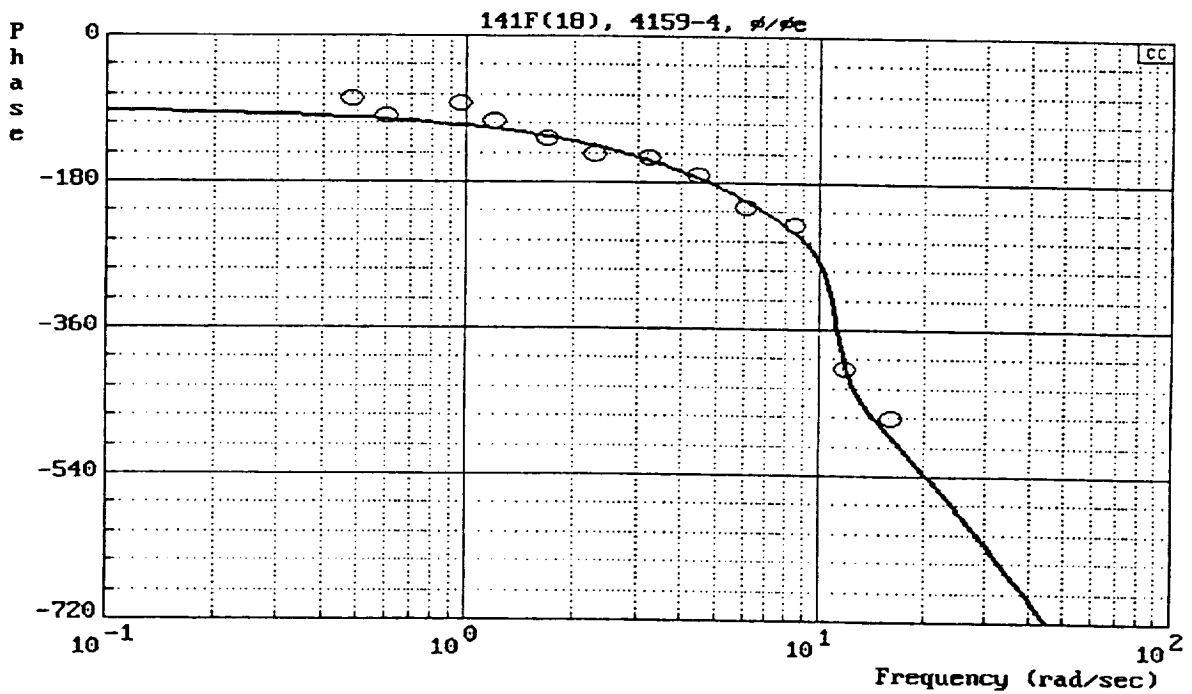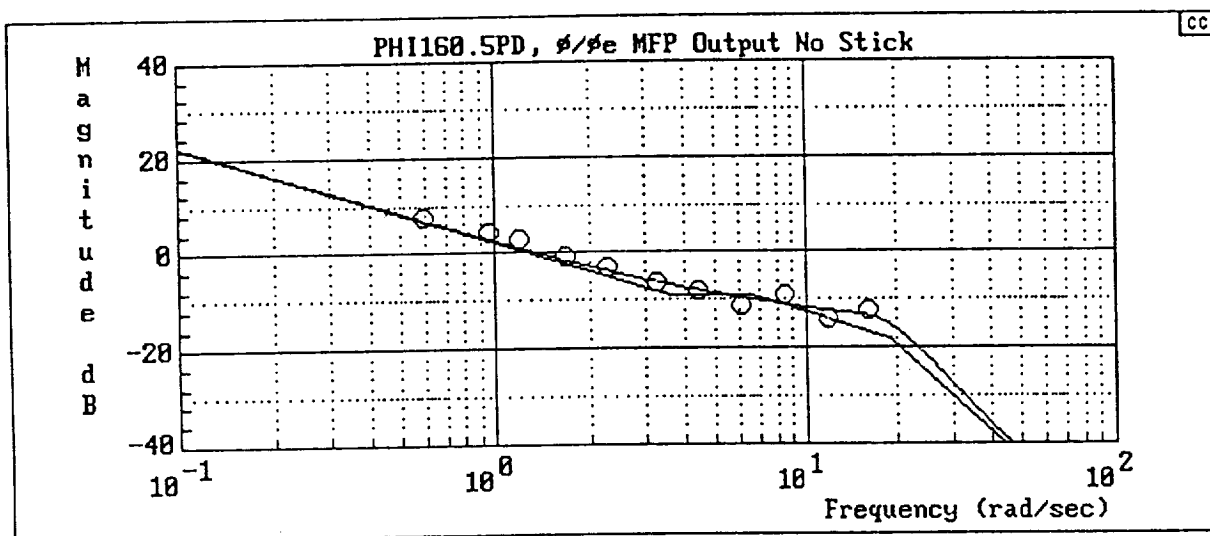

Figure C-2. $Y_p Y_c$ Model/Data Comparison (Flight)
Configuration 141F(18) — Pilot B

PHI160.5PD, φ/φe MFP Output No Stick

$$\frac{\phi}{\phi_e} = \frac{878(\ 3.66)[-.866,\ 12.1]\ [-.866,\ 43.3]}{(\ 8)(\ 6.67)[\ .866,\ 12.1]\ [\ .347,\ 19.1]\ [\ .866,\ 43.3]}$$

PHI160.5PD, φ/φe MFP Output No Stick
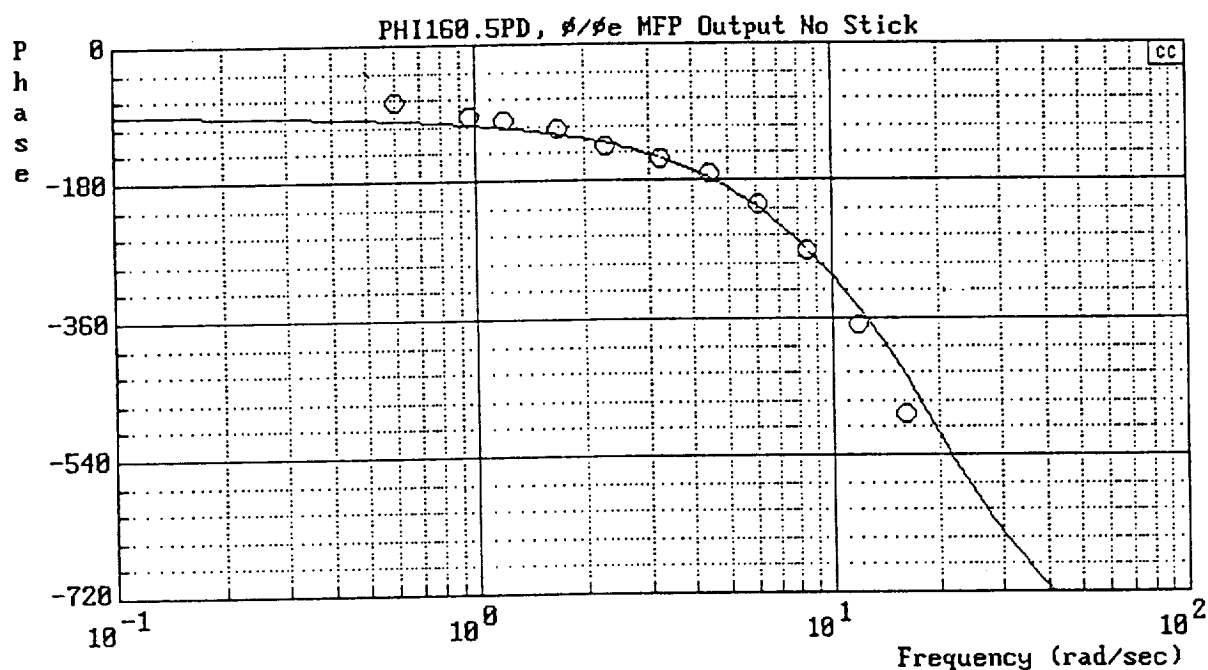
Figure C-3. $Y_p Y_c$ Model/Data Comparison (Flight)
Configuration 142F(18) — Pilot A

143F(18), 4154-5, φ/φc
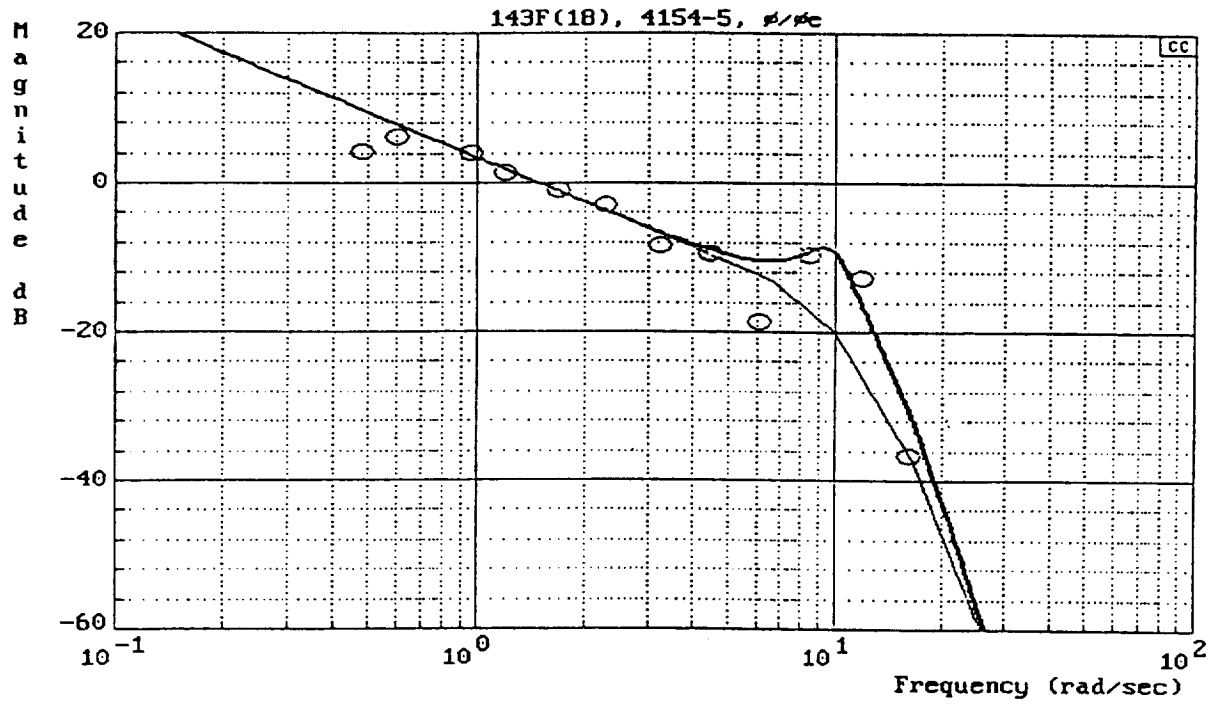
$$\frac{\phi}{\phi_e} = \frac{10656000\ [-0.866,\ 119][-0.866,\ 138]}{(0)(6.67)[0.154,\ 9.92][0.339,\ 16.4](40)[0.866,\ 119][0.866,\ 138]}$$

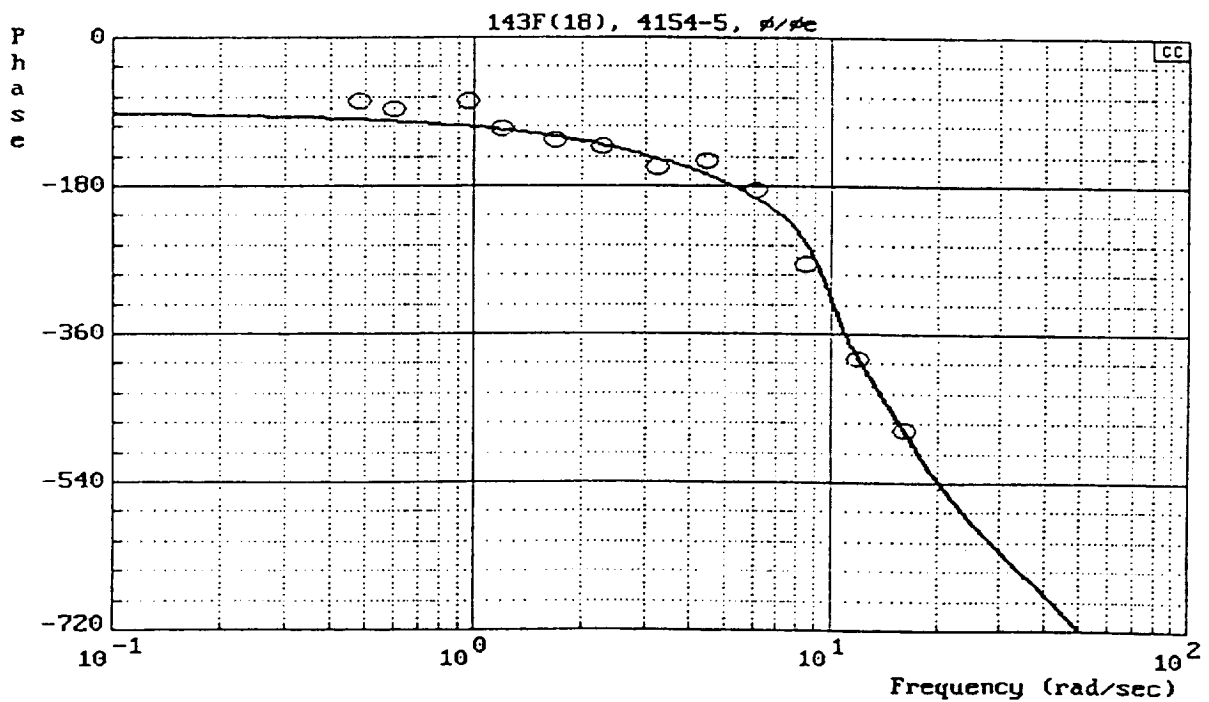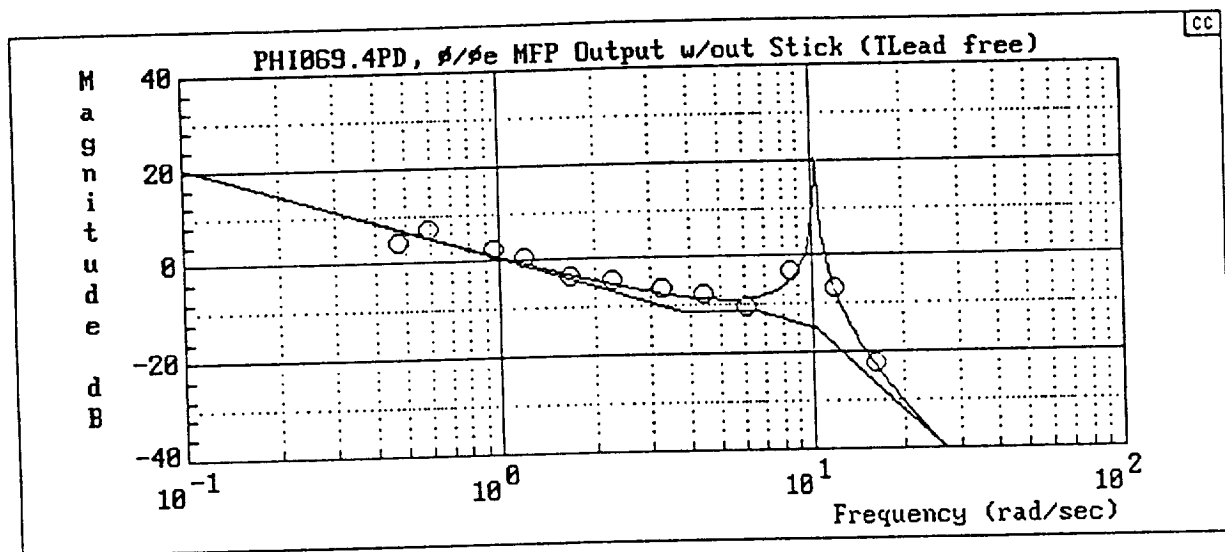143F(18), 4154-5, φ/φc

Figure C-4. $Y_p Y_c$ Model/Data Comparison (Flight)
Configuration 143F(18) — Pilot B

188

PHI069.4PD, φ/φe MFP Output w/out Stick (TLead free)

$$\frac{\phi}{\phi_e} = \frac{8070(3.85)[-.866, 10.2] [-.867, 86.7]}{(0)(6.67)[.866, 10.2] [.00763, 10.4] (40)[.867, 86.7]}$$

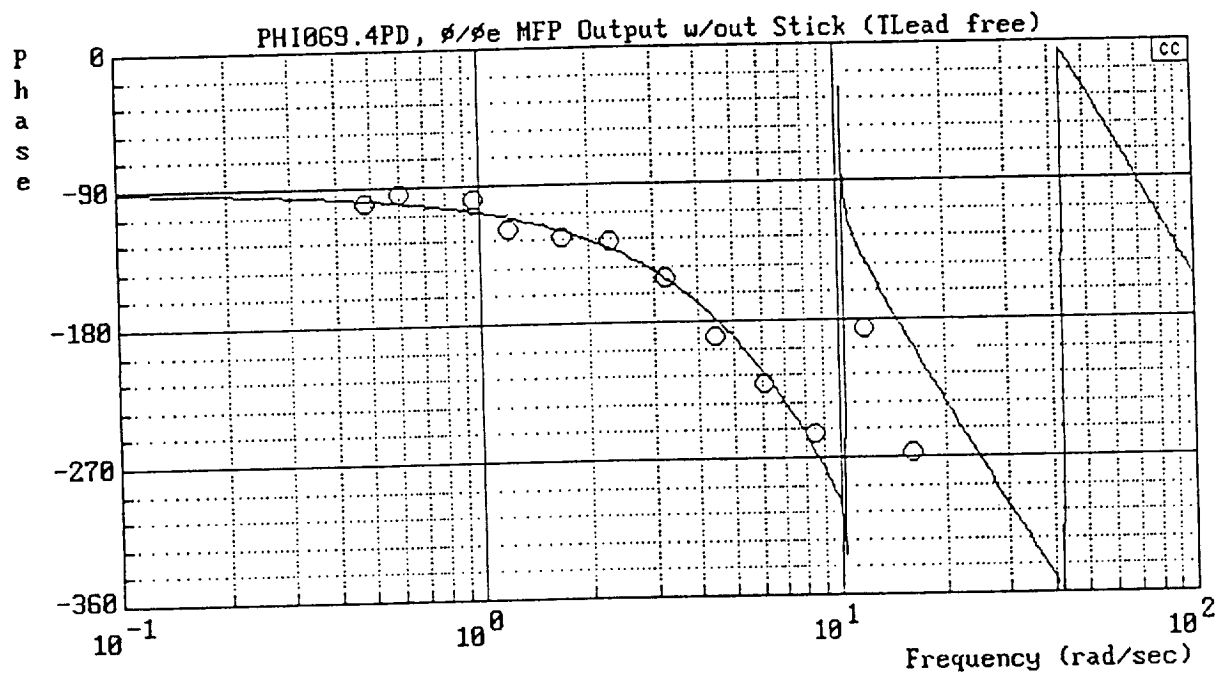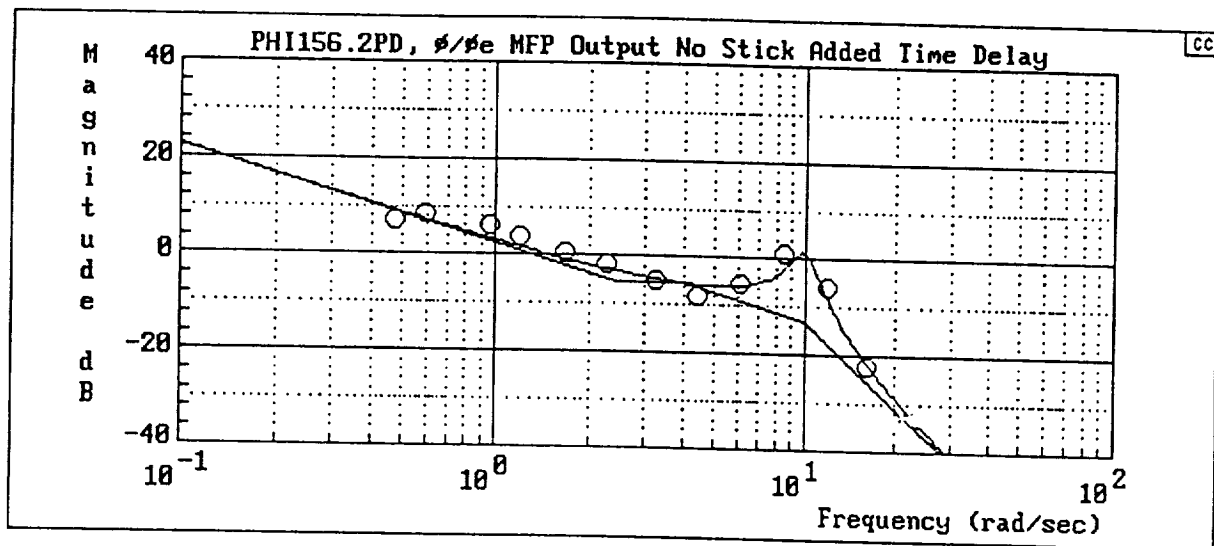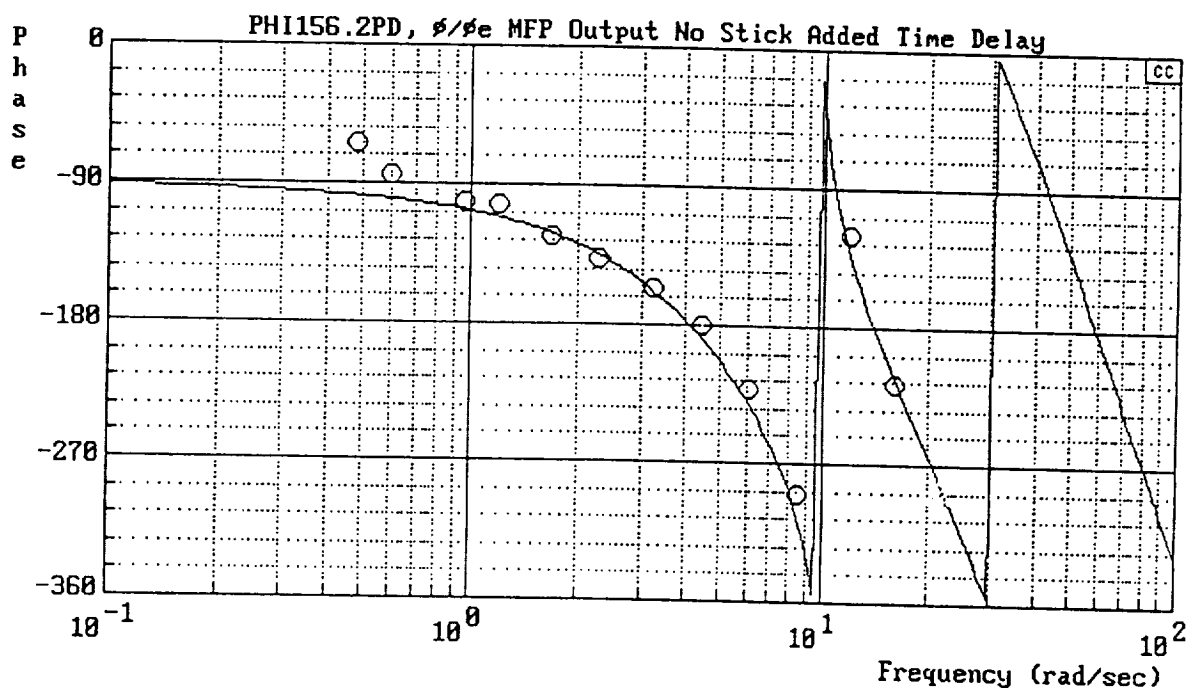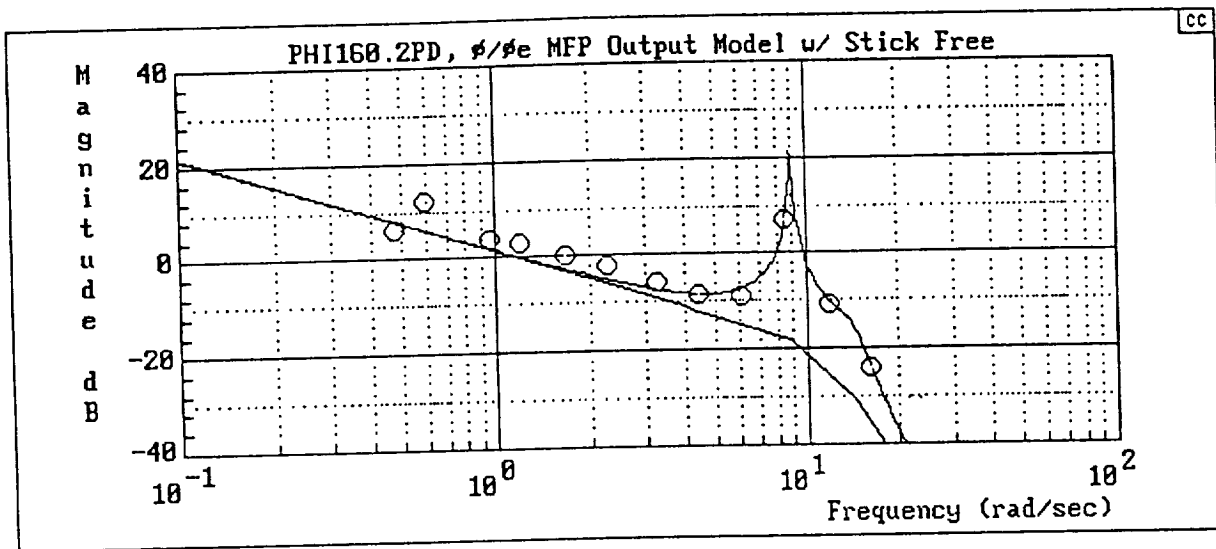PHI069.4PD, φ/φe MFP Output w/out Stick (TLead free)

Figure C-5. $Y_p Y_c$ Model/Data Comparison (Flight)
Configuration 143P(18) — Pilot A

$$\frac{\phi}{\phi_e} = \frac{221(\,2.46)[-.866,\ 10.9]\ [-.866,\ 59.7]\ [-.866,\ 86.6]}{(\,0)(\,4)[\ .0921,\ 9.98]\ [\ .866,\ 10.9]\ [\ .866,\ 59.7]\ [\ .866,\ 86.6]}$$

Figure C-6. $Y_p Y_c$ Model/Data Comparison (Flight)
Configuration 202P(18) — Pilot A

PHI160.2PD, φ/φe MFP Output Model w/ Stick Free

$$\frac{\phi}{\phi_e} = \frac{17500(\ 4.23)[-.866,\ 14.2]\ [-.866,\ 43.3]}{(\ 0)(\ 4)[\ .00889,\ 8.89]\ [\ .148,\ 14.1]\ [\ .866,\ 14.2]\ [\ .866,\ 43.3]}$$

PHI160.2PD, φ/φe MFP Output Model w/ Stick Free
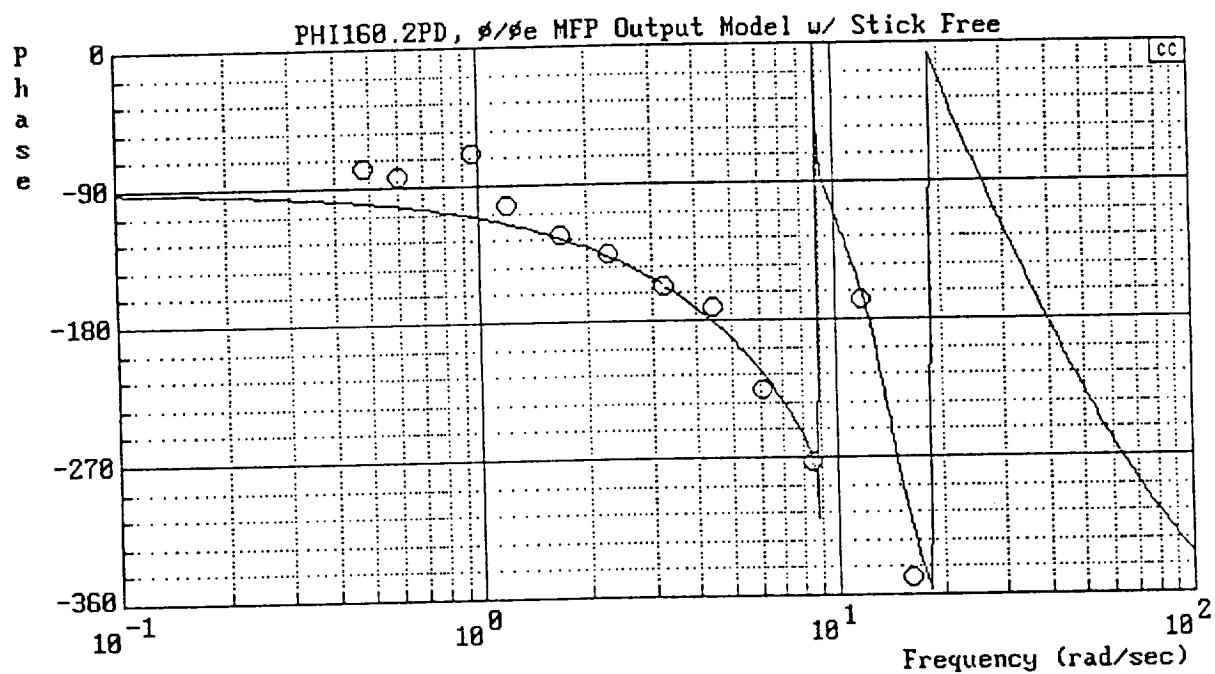
Figure C-7. Y_pY_c Model/Data Comparison (Flight)
Configuration 203P(18) — Pilot A

191

PHI156.1PD, $\phi/\phi e$ MFP Output Model (Vary TLead)

$$\frac{\phi}{\phi_e} = \frac{117(\ 4.69)[-.866,\ 14.2]\ [-.866,\ 43.3]}{(\ 0)(\ 2.5)[\ .0527,\ 10.9]\ [\ .866,\ 14.2]\ [\ .866,\ 43.3]}$$

PHI156.1PD, $\phi/\phi e$ MFP Output Model (Vary TLead)
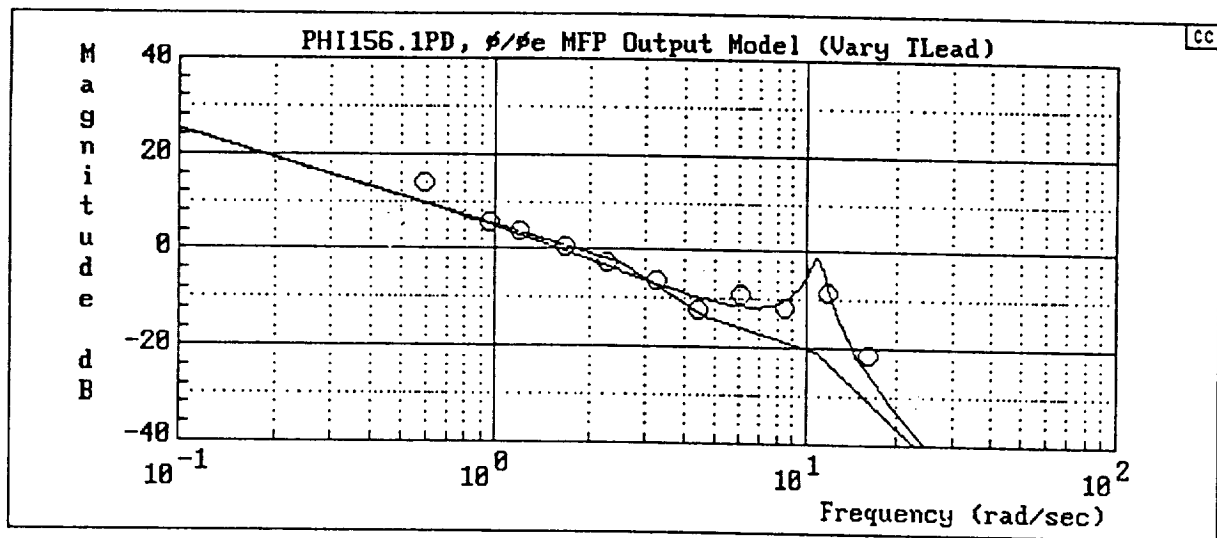
Figure C-8. $Y_p Y_c$ Model/Data Comparison (Flight)
Configuration 301P(18) — Pilot A

PHI176.3PD, ϕ/ϕe MFP Output Model

$$\frac{\phi}{\phi_e} = \frac{8680(\ 2.43)[-.866,\ 15.4]\ [-.866,\ 43.3]}{(\ 0)(\ 2.5)[\ .206,\ 12.6]\ [\ .866,\ 15.4]\ (\ 40)[\ .866,\ 43.3]}$$

PHI176.3PD, ϕ/ϕe MFP Output Model

Figure C-9. $Y_p Y_c$ Model/Data Comparison (Flight)
Configuration 341F(18) — Pilot A

193

PHI161.2PD, $\phi/\phi e$ MFP Output Model No Stick

M
a
g
n
i
t
u
d
e

dB

40

20

0

-20

-40

10^{-1} 10^0 10^1 10^2

Frequency (rad/sec)

$$\frac{\phi}{\phi_e} = \frac{153(1.85)[-.866, 10.6][-.867, 86.7]}{(0)(2.5)[.128, 10.5][.866, 10.6][.867, 86.7]}$$

PHI161.2PD, $\phi/\phi e$ MFP Output Model No Stick

P
h
a
s
e

0

-90

-180

-270

-360

10^{-1} 10^0 10^1 10^2

Frequency (rad/sec)

Figure C-10. $Y_p Y_c$ Model/Data Comparison (Flight)
Configuration 302P(18) — Pilot A

194

PHI127.3PD, φ/φe MFP Output Model No Stick

$$\frac{\phi}{\phi_e} = \frac{9730(2.77)[-.866, 14.8] [-.867, 86.7]}{(0)(2.5)[.311, 12.1] [.866, 14.8] (40)[.867, 86.7]}$$
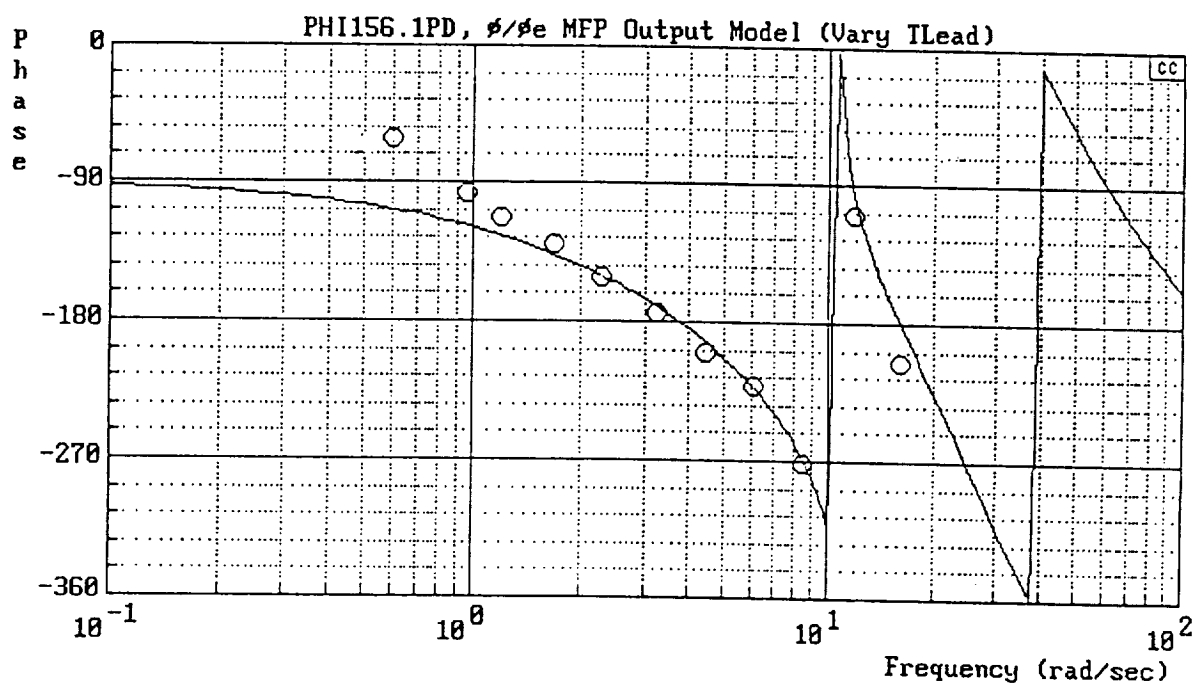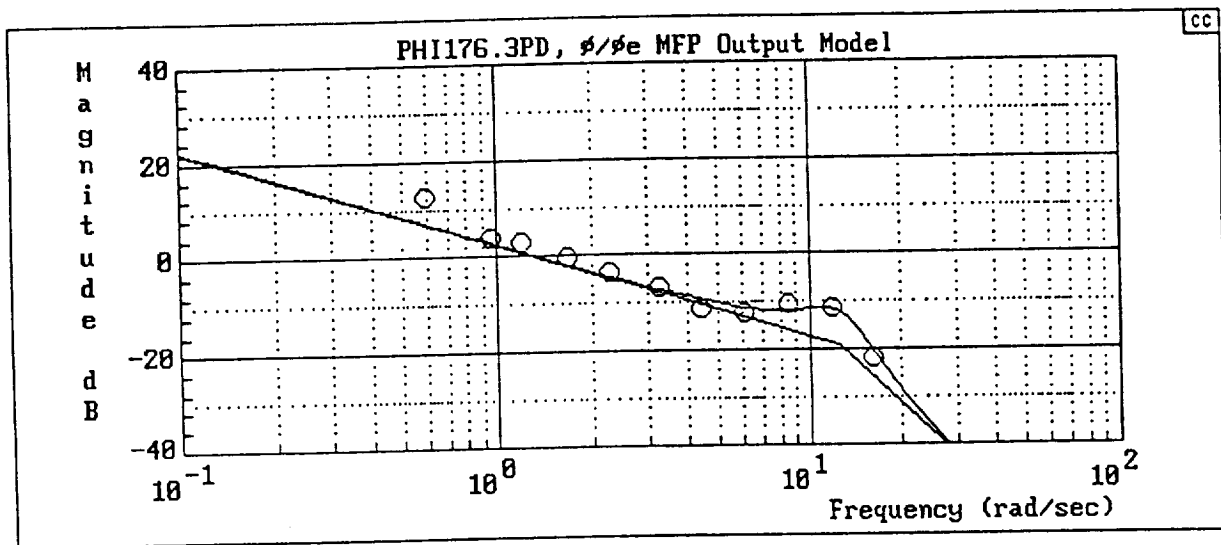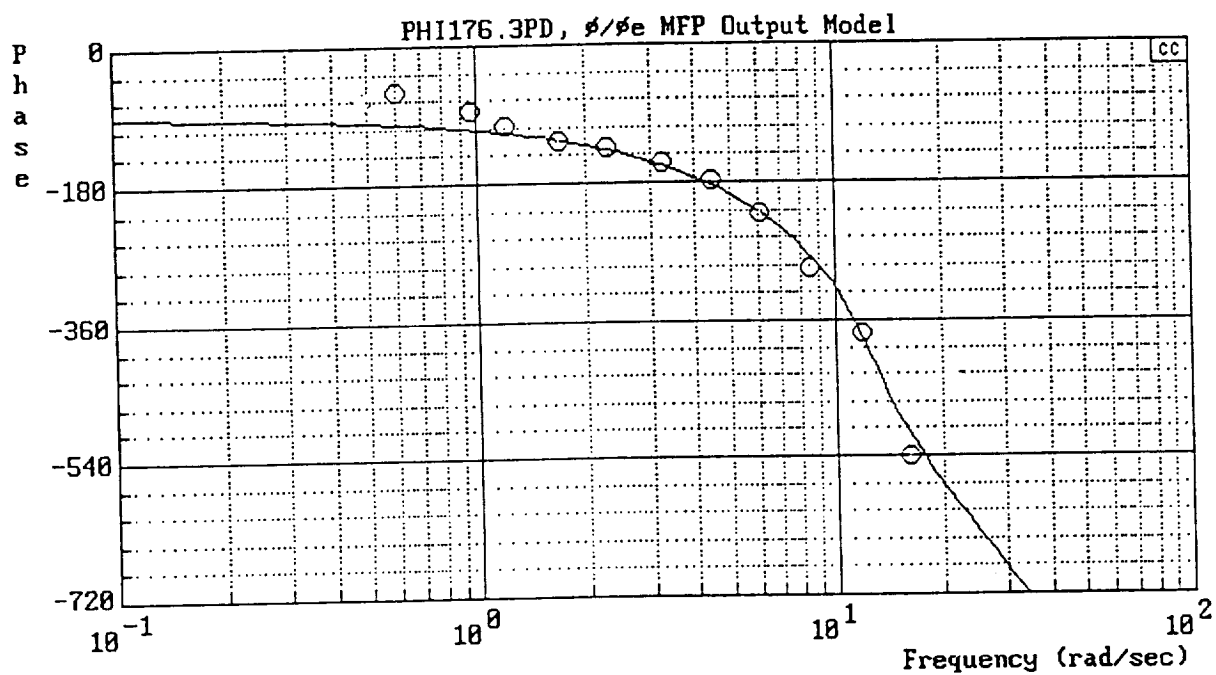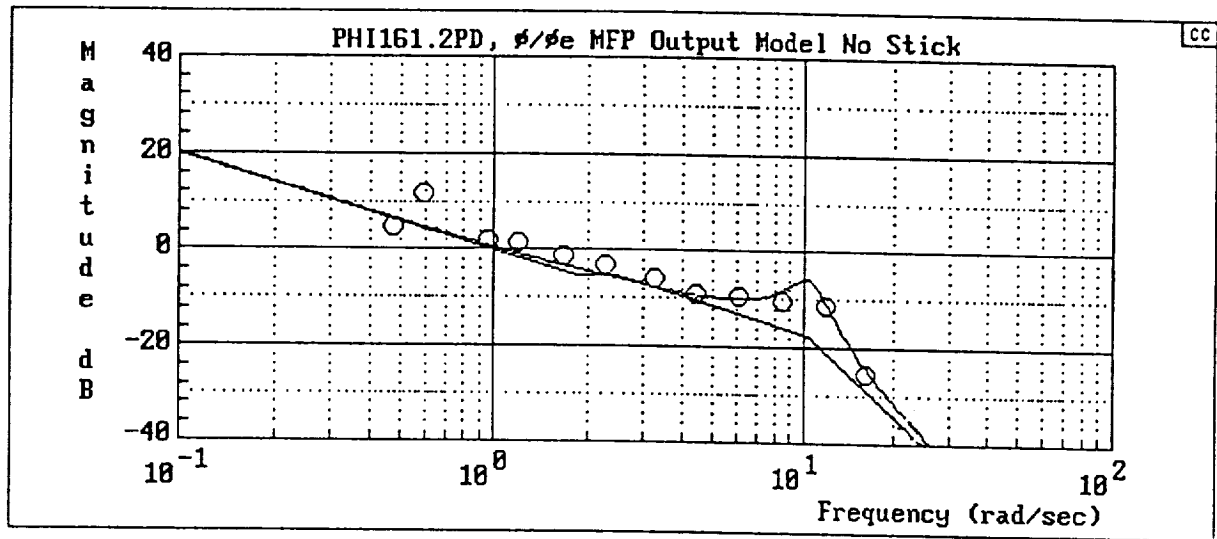

PHI127.3PD, φ/φe MFP Output Model No Stick

Figure C-11. $Y_p Y_c$ Model/Data Comparison (Flight)
Configuration 342F(18) — Pilot C

195

$$\frac{\phi}{\phi_e} = \frac{91.4(\ 2.61)[-.866,\ 10.6]\ [-.866,\ 86.6]}{(\ 0)(\ 2.5)[\ .128,\ 8.54]\ [\ .866,\ 10.6]\ [\ .866,\ 86.6]}$$
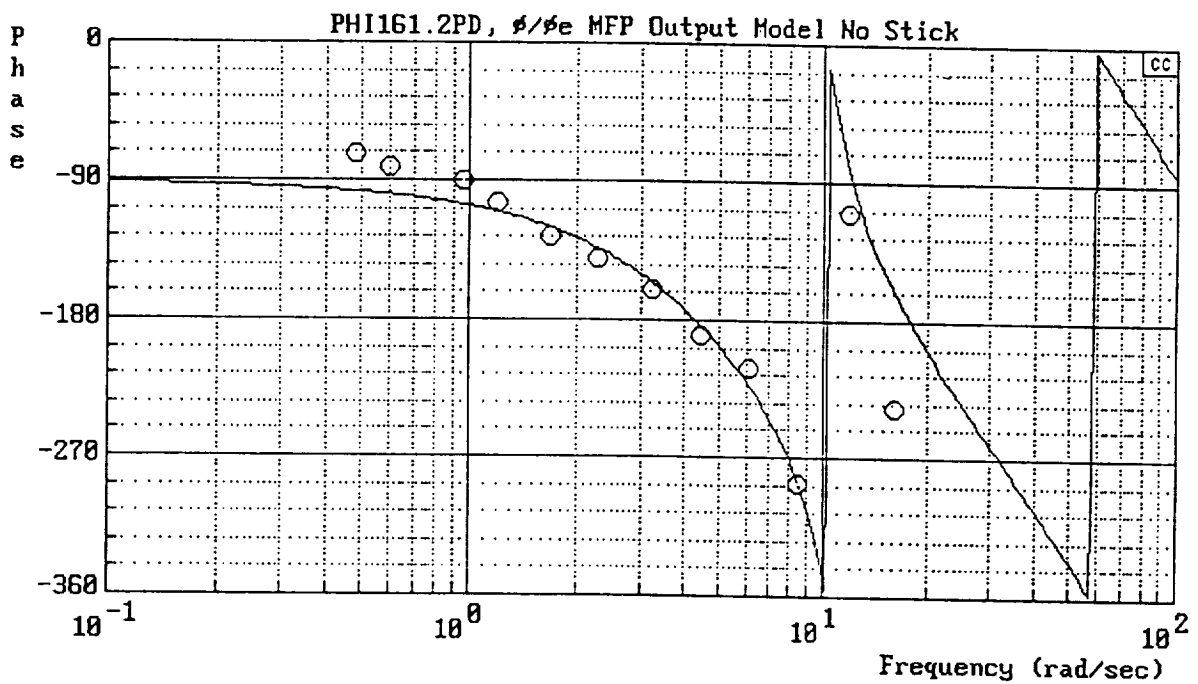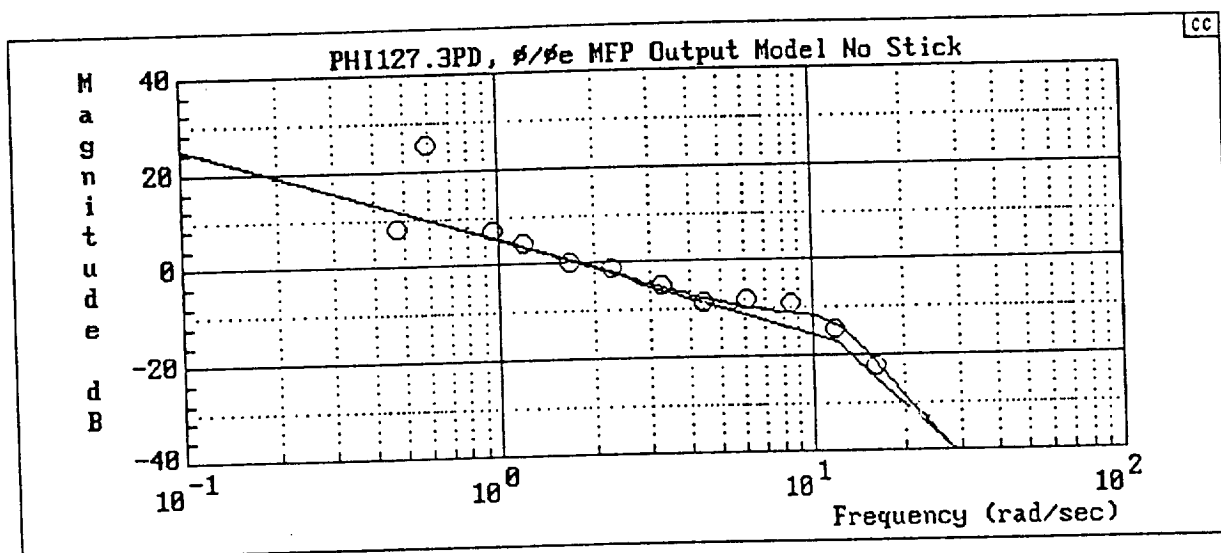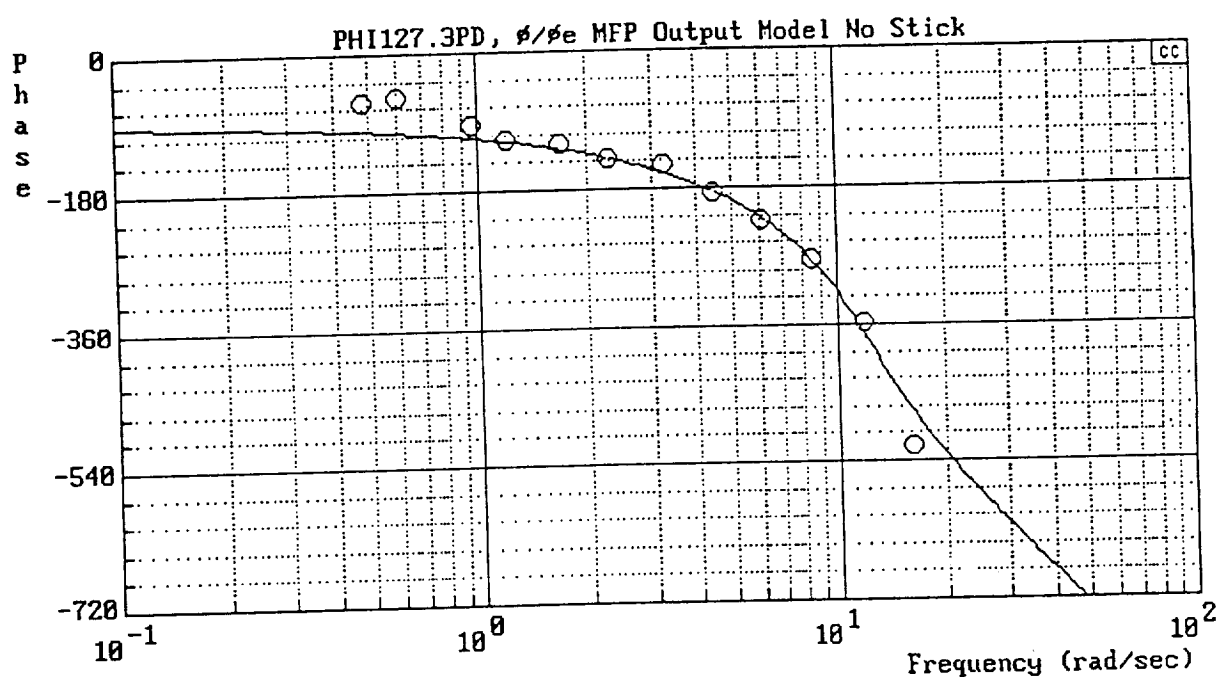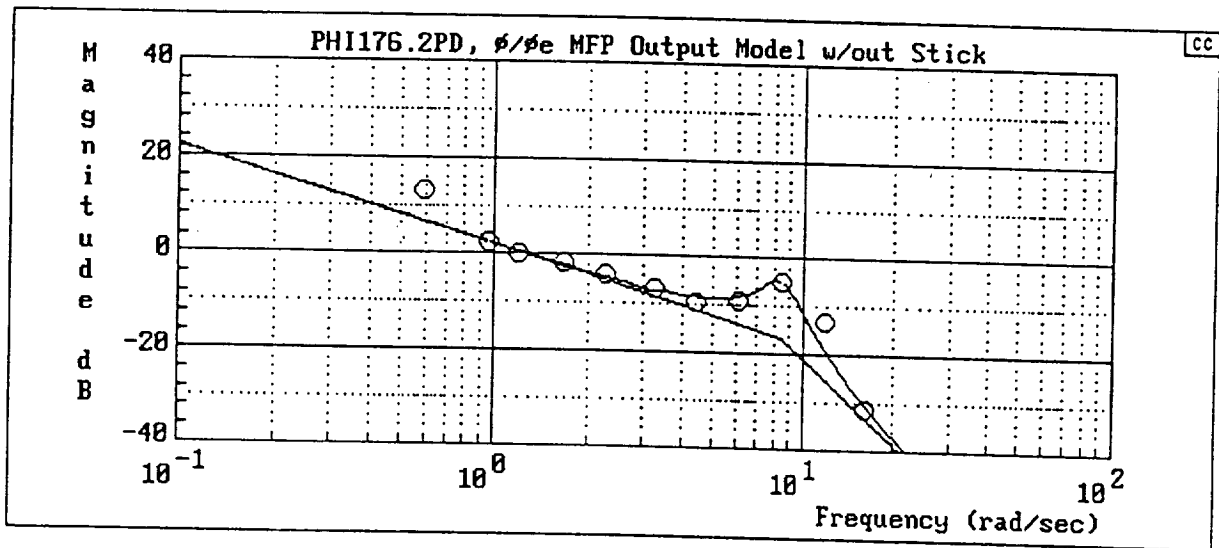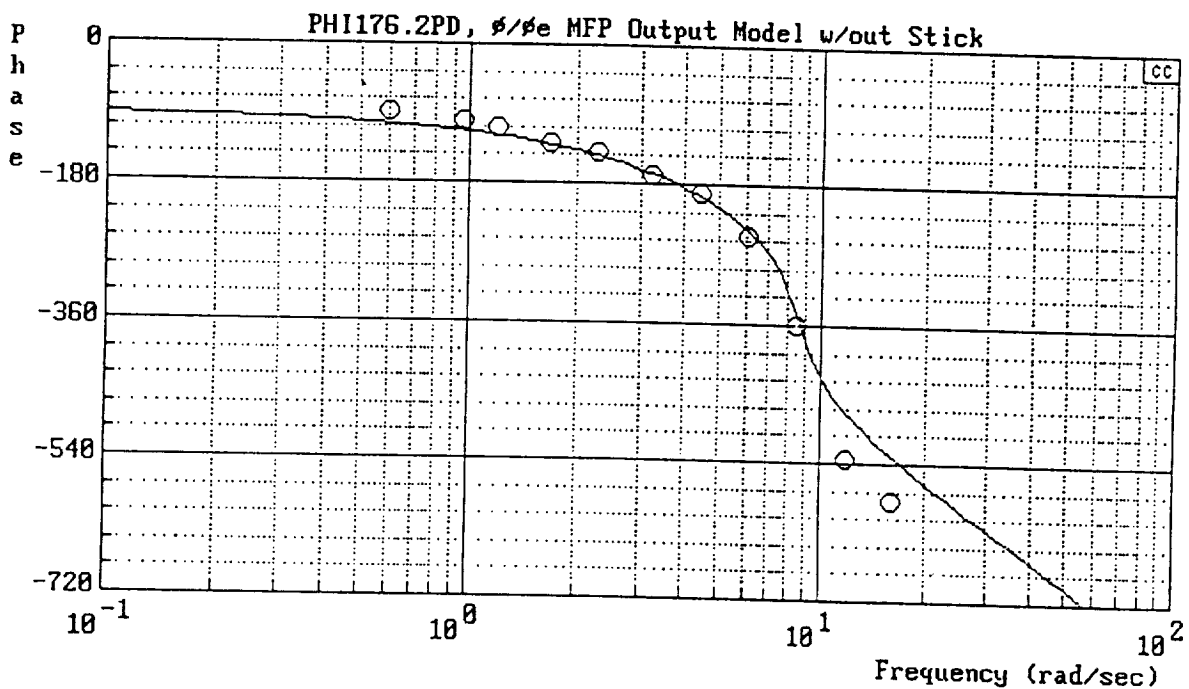

Figure C-12. $Y_p Y_c$ Model/Data Comparison (Flight)
Configuration 303P(18) — Pilot A
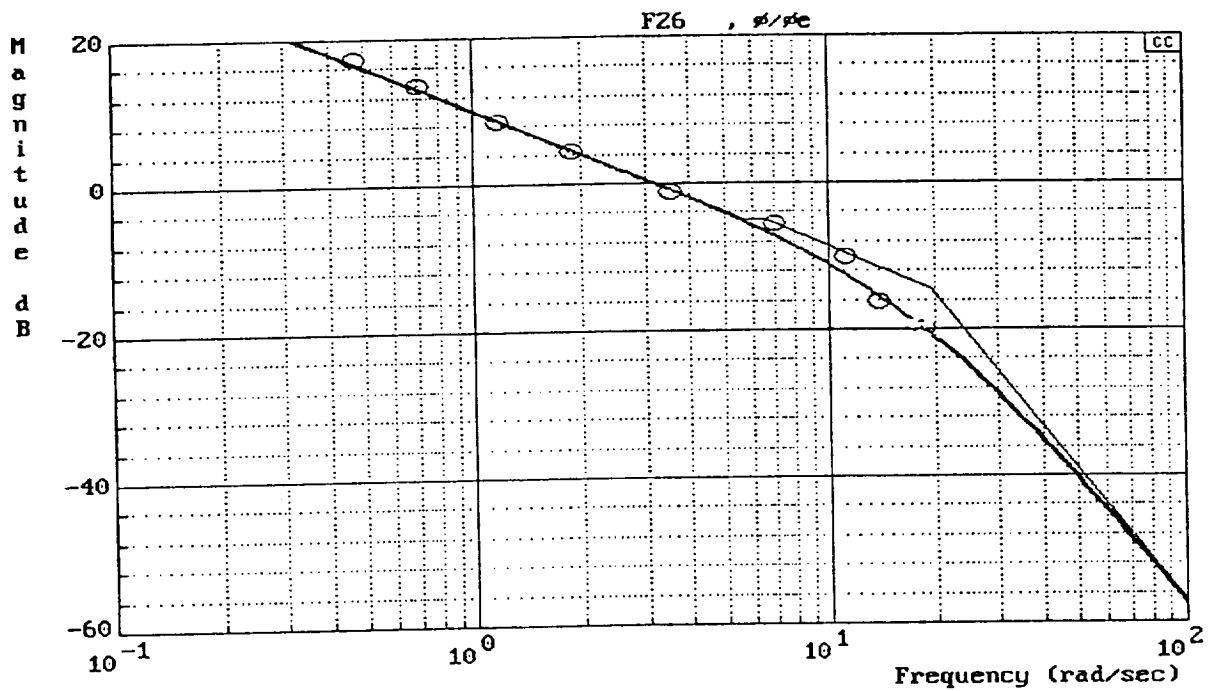
$$\frac{\phi}{\phi_e} = \frac{-1370\ (5.72)[-0.866,\ 12.2][-0.866,\ 105]}{(0)(6.67)[0.866,\ 12.2](-19)(19.3)[0.866,\ 105]}$$

Figure C-13. $Y_p Y_c$ Model/Data Comparison (Fixed-Base)
(Configuration A_2 — Pilot A)

$$\frac{\phi}{\phi_e} = \frac{792\ (4.41)[-0.866,\ 14.4][-0.866,\ 105]}{(0)(6.67)[0.866,\ 14.4][0.184,\ 15.9][0.866,\ 105]}$$

Figure C-14. $Y_p Y_c$ Model/Data Comparison (Fixed-Base)
(Configuration C_2 — Pilot A)

198
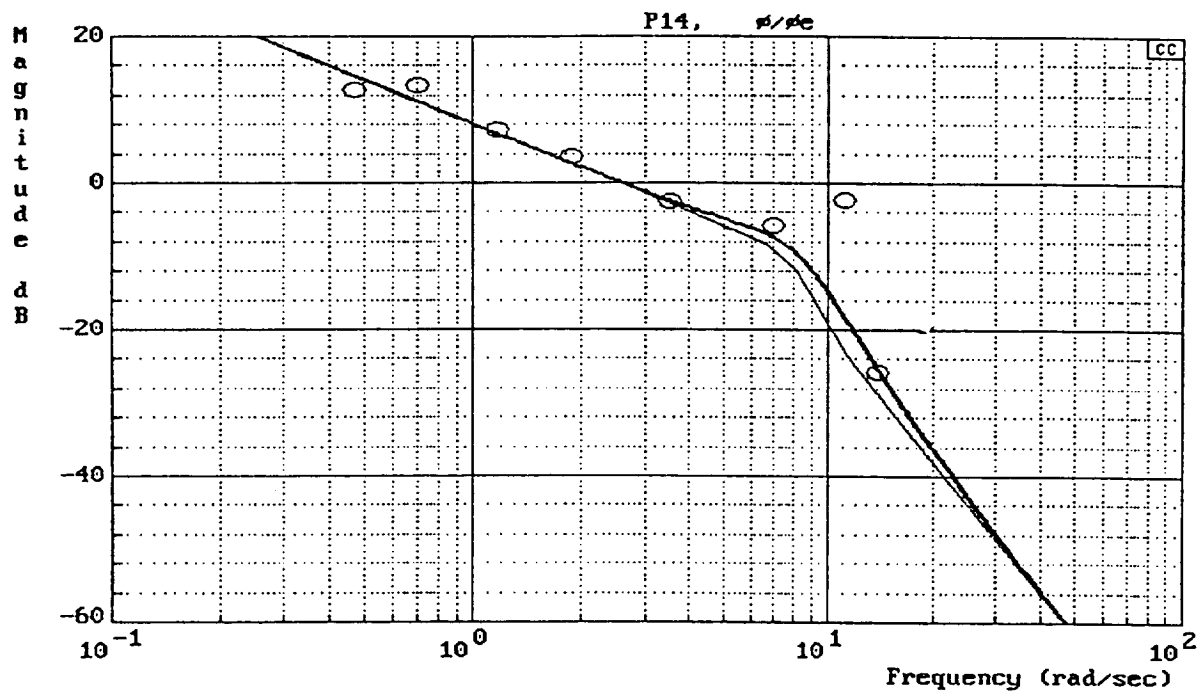
$$\frac{\phi}{\phi_e} = \frac{98.8\ (11.4)[-0.866, 84.5][-0.866,105]}{(0)(6.67)[0.374, 8.11][0.866, 84.5][0.866, 105]}$$
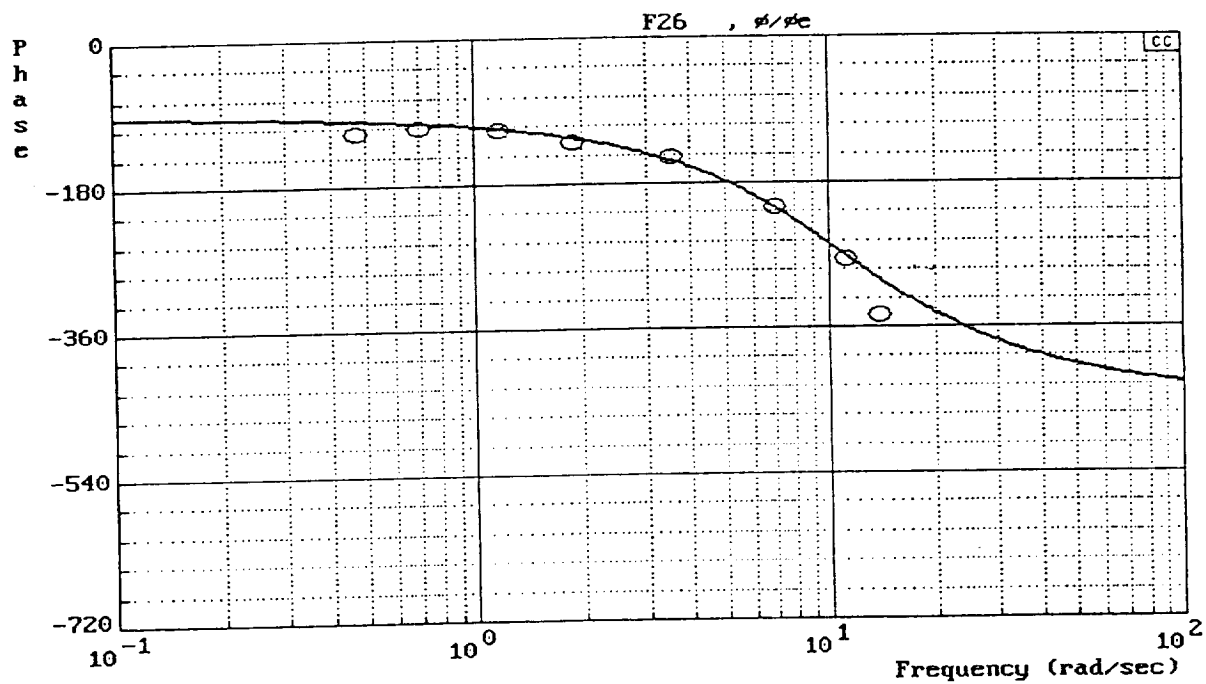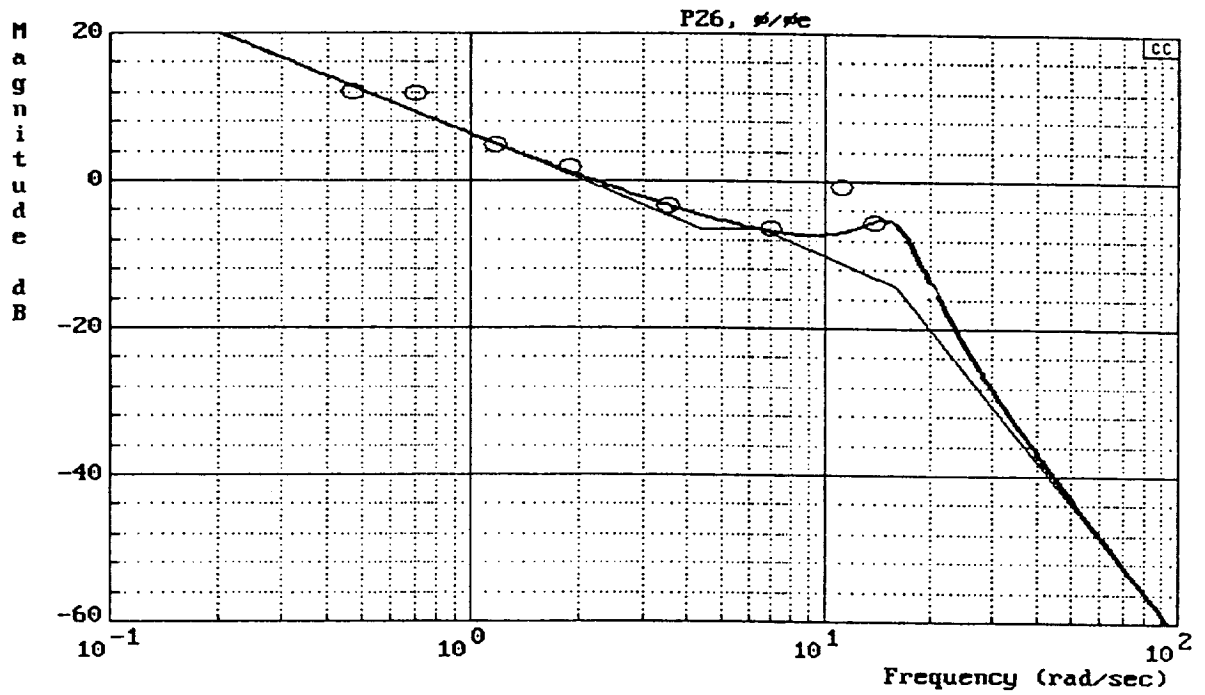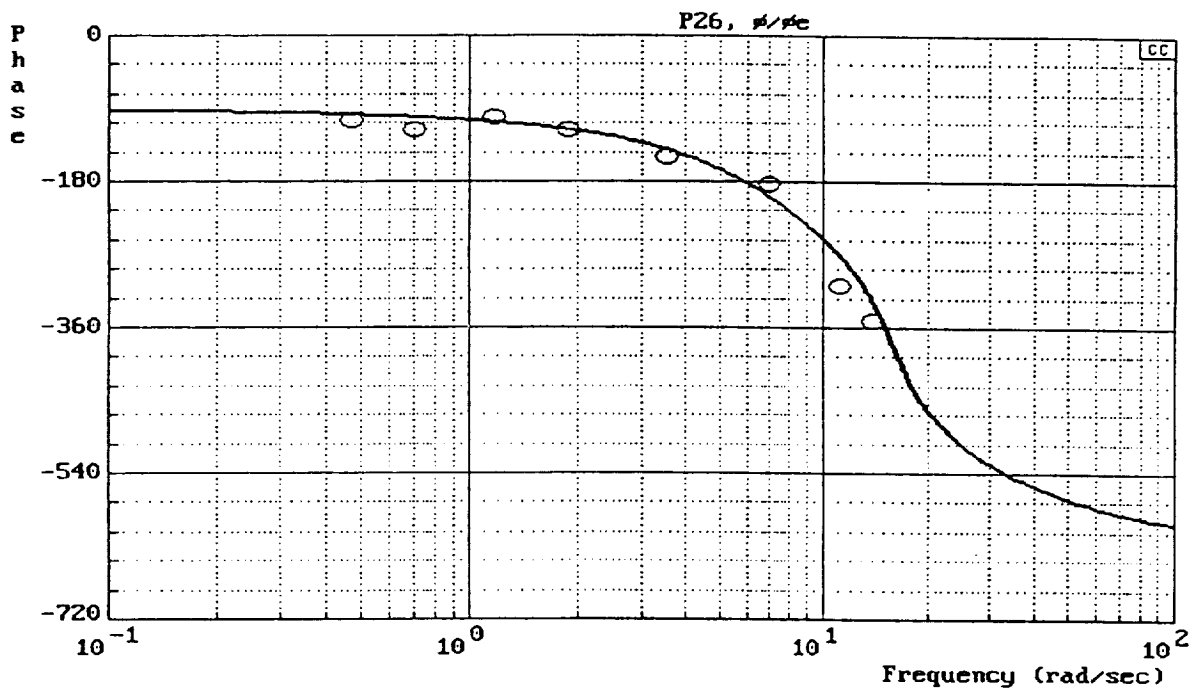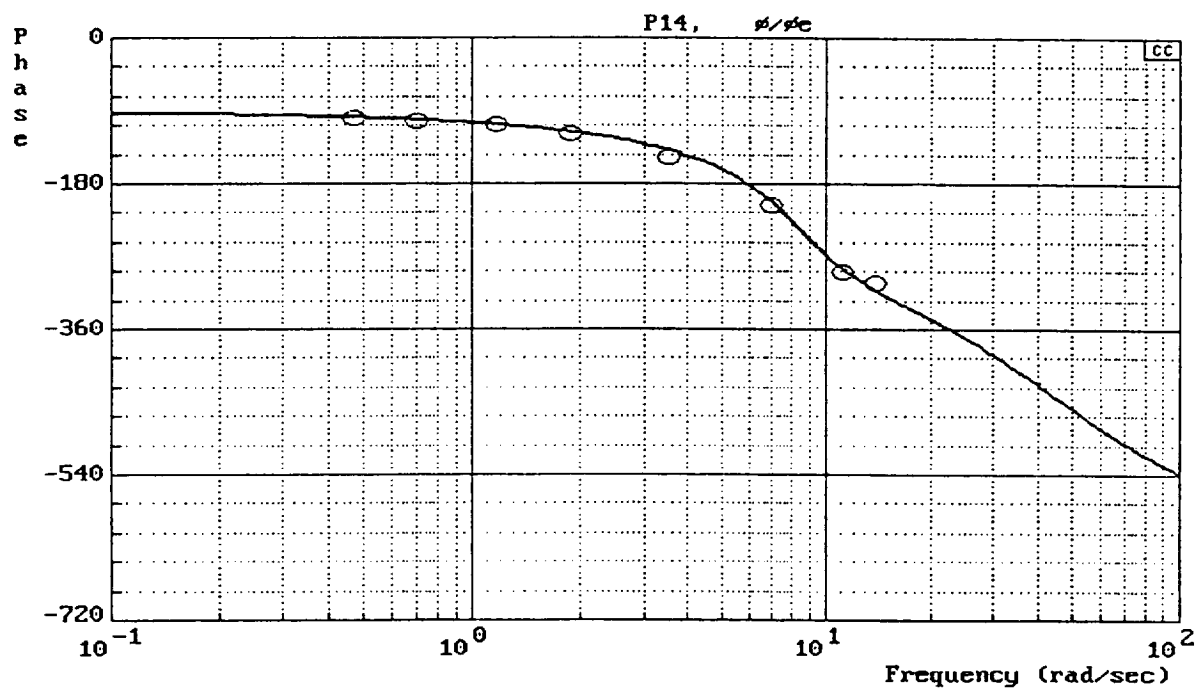

Figure C-15. $Y_p Y_c$ Model/Data Comparison (Fixed-Base)
(Configuration F_2 — Pilot A)
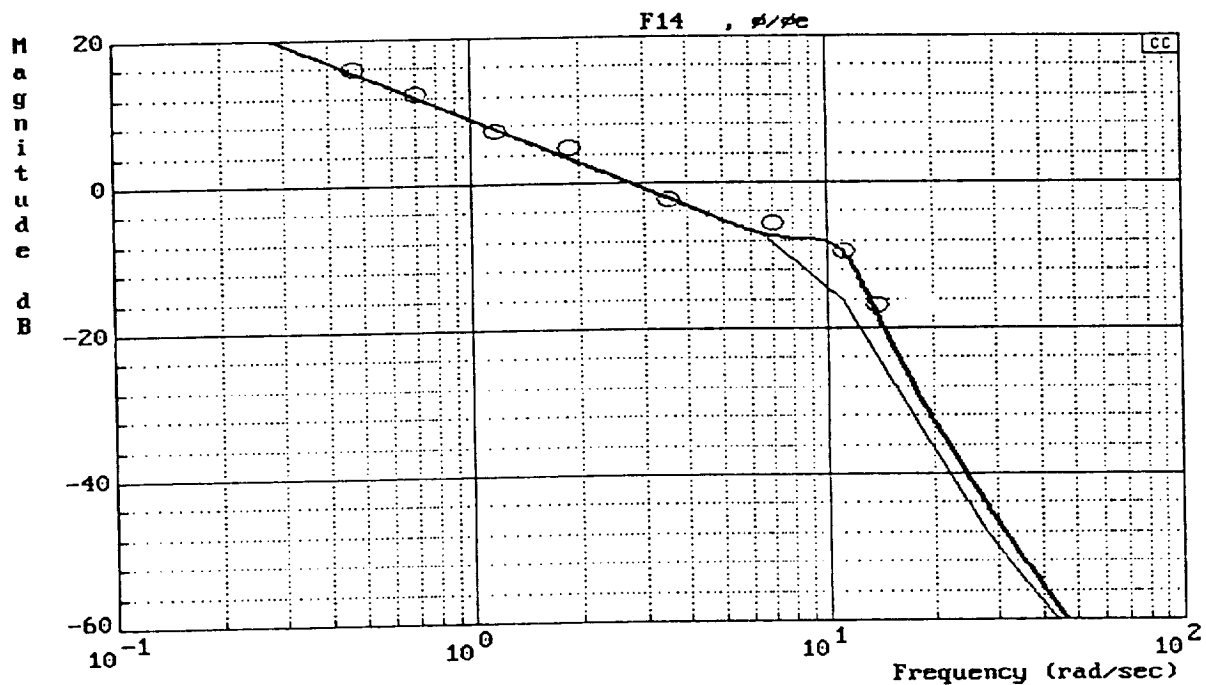
$$\frac{\phi}{\phi_e} = \frac{83.2 \ (27.4)[-0.866, 50.2][-0.866, 105]}{(0)(6.67)[0.211, 11.0][0.866, 50.2][0.866, 105]}$$
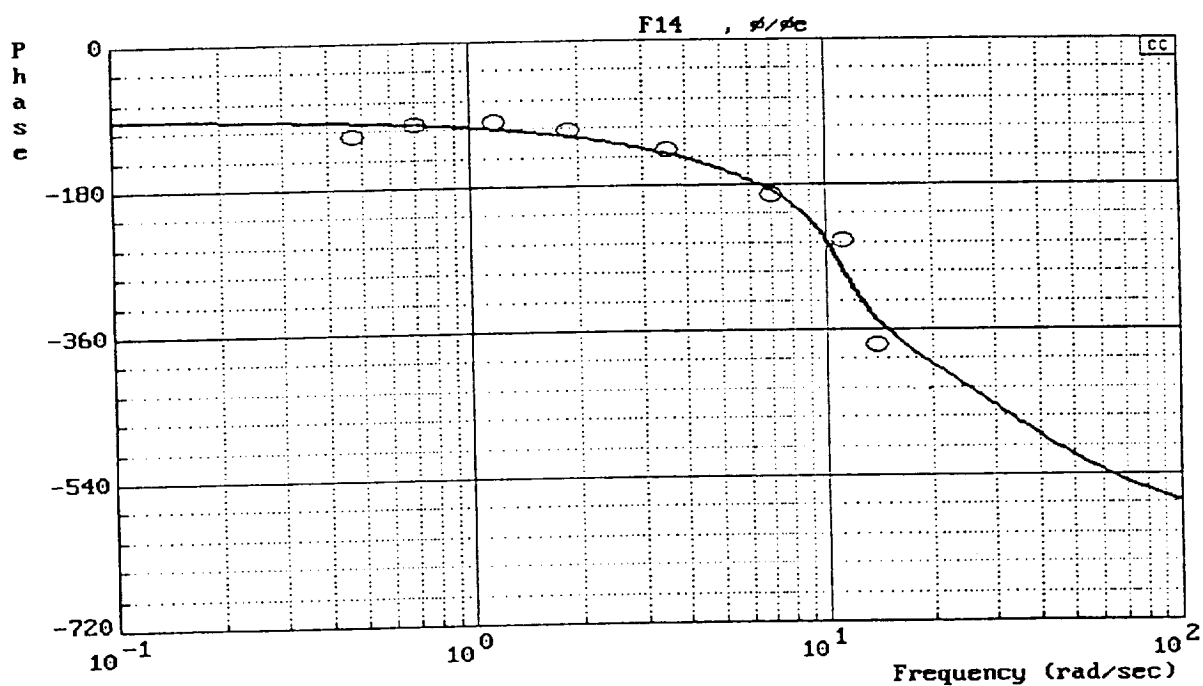
Figure C-16. $Y_p Y_c$ Model/Data Comparison (Fixed-Base)
(Configuration B_2 — Pilot A)

Table C-1. Comparison cases from Smith and Sarrafian (ref. 2) and NASA CR-179445 (ref. 1) — Landing approach.

| ω_{FS} | SMITH & SARRAFIAN | | NASA CR-179445 | | |
	CONF.	HQR(A)	CONF.	HQR(A)	HQR(C)
26	A	2	L201P(10)+55	4,3,3	5
13	B	2	L202P(10)	6	5,6,3
26	C	7,7	L201P(10)+175	-NF-	-NF-
13	D	4,4	L202P(10)+110	-NF-	-NF-
26	E	2,2	L201P(10)	4,2	—
13	F	4	L202P(10)+110	-NF-	-NF-
26	E'	-NF-	L201P(5)	2	2
8	G	-NF-	L203P(10)	4,4	7
8	H	-NF-	L243P(10)	8	7

NOTE: NF = Not Flown

201

Table C-2. Extracted pilot comments for control–response and controller force–displacement variations.

Configuration	Pilot	HQR	Comments
141F(18) (F_{as}/δ_{as} = 4.0 lb/in.)	A	7	Abrupt initial response ... ride qualities are not good ... Initial reponse was really head knocking ... Small amplitude wing rock, ratcheting.
	C	4	Jerky ... Initial response is quick and annoying.
141F(10) (F_{as}/δ_{as} = 4.0 lb/in.)	A	7	Got desired performance but lateral accelerations were unacceptable and require improvement ... extremely sensitive, abrupt airplane. [PIO tendency?] Not in roll attitude ... Try to smooth it down.
	C	3	Still feels sluggish but dynamics are smooth ... Seemed like a long time constant. Not an abrupt response. Predictability was good ... Sluggishness noted for quick tasks.
141F(10) (F_{as}/δ_{as} = 2.75 lb/in.)	A	2	A good, well-rounded airplane. [Roll sensitivity?] About right. When you wanted the response you could get it and it was predictable.
	A	3	In air-to-air, when I first took it, I thought it was going to be a "ratchet" airplane again, but there was something about it that made it quick and precise ... I noticed the stick motions on occasion. It was not objectionable.

202

Table C-3. List of analyzed runs.

Configuration	T_R (sec)	ω_{FS} (rad/sec)	P/F	HQR (SOS)	HQR (over-all)	Pilot	Flight evaluation
241P(18)	0.25	26	P	7	7	A	4069.2
141F(10)	0.15	26	F	7	7	A	4069.3
143P(18)	0.15	8	P	8	8	A	4069.4
343F(18)	0.40	8	F	3	3	B	4079.3
341P(18)	0.40	26	P	5	5	C	4126.1
212P(18)	0.25	13	P	8	8	C	4127.1
143F(18)	0.15	8	F	7	7	B	4154.5
301P(18)	0.40	26	P	3	3	A	4156.1
302P(18)+55	0.40	13	P	7	7	A	4156.3
303P(18)	0.40	8	P	5	5	A	4156.4
141F(18)	0.15	26	F	6	6	B	4159.4
301P(18)+55	0.40	26	P	4	3	A	4160.3
141F(10)	0.15	26	F	2	2	A	4160.4
301P(18)+110	0.40	26	P	7	7	A	4161.1
201P(18)+55	0.25	26	P	7	7	A	4161.3
201P(18)+110	0.25	26	P	6	6	A	4161.5
221P(18)	0.25	26	P	7	7	A	4176.1
341F(18)	0.40	26	F	2	2	A	4176.3
142F(18)	0.15	13	F	5	3	A	4160.5
342P(18)	0.40	13	P	2	2	A	4069.1
212P(18)	0.25	13	P	7	7	C	4126.3
342F(18)	0.40	13	F	2	2	C	4127.3
202P(18)	0.25	13	P	5	5	A	4156.2
203P(18)	0.25	8	P	6	6	A	4160.2
302P(18)	0.40	13	P	2	2	A	4161.2

REPORT DOCUMENTATION PAGE

Form Approved
OMB No. 0704-0188

1. AGENCY USE ONLY *(Leave blank)*	2. REPORT DATE	3. REPORT TYPE AND DATES COVERED
	June 1992	Contractor Report

4. TITLE AND SUBTITLE

Effects of Cockpit Lateral Stick Characteristics on Handling Qualities and Pilot Dynamics

5. FUNDING NUMBERS

C NAS2-12722

WU 505-64-30

6. AUTHOR(S)

David G. Mitchell, Bimal L. Aponso, and David H. Klyde

7. PERFORMING ORGANIZATION NAME(S) AND ADDRESS(ES)

Systems Technology, Inc.
13766 S. Hawthorne Blvd.
Hawthorne, California 90250-7083

8. PERFORMING ORGANIZATION REPORT NUMBER

H-1769

9. SPONSORING/MONITORING AGENCY NAME(S) AND ADDRESS(ES)

Dryden Flight Research Facility
National Aeronautics and Space Administration
Washington, DC 20546-0001

10. SPONSORING/MONITORING AGENCY REPORT NUMBER

NASA CR-4443

11. SUPPLEMENTARY NOTES

This report was prepared for PRC Inc., P.O. Box 273, Edwards, California 93523-0273 by Systems Technology, Inc., under subcontract ATD-90-STI-6401. NASA Technical Monitor was Mary F. Shafer, NASA Dryden Flight Research Facility, P.O. Box 273, Edwards, California 93523-0273. NASA Contracting Officer's Technical Representative for PRC Inc.: Donald C. Bacon, Jr., (805) 258-3484.

12a. DISTRIBUTION/AVAILABILITY STATEMENT

Unclassified — Unlimited
Subject Category 08
Final

12b. DISTRIBUTION CODE

13. ABSTRACT *(Maximum 200 words)*

This report presents the results of analysis of cockpit lateral control feel-system studies. Variations in feel-system natural frequency, damping, and command sensing reference (force and position) were investigated, in combination with variations in the aircraft response characteristics. The primary data for the report were obtained from a flight investigation conducted with a variable-stability airplane, with additional information taken from other flight experiments and ground-based simulations for both airplanes and helicopters. The study consisted of analysis of handling qualities ratings and extraction of open-loop, pilot–vehicle describing functions from sum-of-sines tracking data, including, for a limited subset of these data, the development of pilot models. The study confirms the findings of other investigators that the effects on pilot opinion of cockpit feel-system dynamics are not equivalent to a comparable level of added time delay. The effects on handling qualities ratings are, however, very similar to those of time delay, and until a more comprehensive set of criteria are developed, it is recommended that feel-system dynamics be considered a delay-inducing element in the aircraft response. The best correlation with time-delay requirements was found when the feel-system dynamics were included in the delay measurement, regardless of the command reference. This is a radical departure from past approaches.

14. SUBJECT TERMS

Cockpit lateral stick characteristics; Handling qualities; Feel systems; Describing functions

15. NUMBER OF PAGES

208

16. PRICE CODE

A10

17. SECURITY CLASSIFICATION OF REPORT	18. SECURITY CLASSIFICATION OF THIS PAGE	19. SECURITY CLASSIFICATION OF ABSTRACT	20. LIMITATION OF ABSTRACT
Unclassified	Unclassified	Unclassified	Unlimited